Final Technical Report

Award Number G10AP00086

Sponsors Name: Seismological Society of America

Conference Title: Seismological Society of America's 2010 Annual Meeting in Portland, Oregon

Conference Dates: April 21-23, 2010

Summary of Program:

This year's SSA Annual Meeting included 282 oral presentations and 258 poster presentations distributed among 31 sessions. The meeting was attended by 557 participants from 26 countries. The meeting was preceded by the annual board meeting and committee meetings. Selected results of those meetings were shared with the membership at the annual luncheon, the first day of the meeting. Special presentations were given at the two other luncheons. The Joyner Lecture, a special lecture focusing on the boundary of seismology and engineering, was presented on Thursday night.

The attached PDF contains the following:

- The program schedule (pages 2-32)
- The meeting report including the annual luncheon minutes, the board minutes, awards presentations, and treasurer's report (pages 33-62)
- A list of registrants (Pages 63-73)
- All the meeting abstracts (Pages 74-187)

SSA 2010 Annual Meeting Announcement
Seismological Society of America

Technical Sessions
21–23 April 2010 (Wednesday–Friday)
Portland, Oregon

IMPORTANT DATES	
Meeting Pre-registration Deadline	19 March 2010
Hotel Reservation Cut-Off	29 March 2010
Online Registration Cut-Off	9 April 2010

PROGRAM COMMITTEE

This year's technical program committee is composed of co-chairs Seth Moran (USGS–Cascades Volcano Observatory) and Nick Beeler (USGS–Vancouver), Ivan Wong (Seismic Hazards Group, Oakland CA), Ray Weldon (University of Oregon), Vicki McConnell (DOGAMI), and Anne Trehu (Oregon State University).

MEETING CONTACTS

Technical Program Committee Co-Chairs
Nick Beeler & Seth Moran, 2010Program@seismosoc.org

Abstract Submissions/Logistics
Joy Troyer
Seismological Society of America
510.559.1784
joy@seismosoc.org

Registration
Sissy Stone
Seismological Society of America
510.559.1780
sissy@seismosoc.org

Exhibits
Sarah Karlson
Seismological Society of America
510-559-1783
sarah@seismosoc.org

TECHNICAL PROGRAM

Advances in Seismic Hazard Mapping
Recently much progress has been made in developing informative regional seismic hazard maps that incorporate local as well as regional geologic and geotechnical data. These new maps often rely on a probabilistic characterization of hazard to account for uncertainties and have been developed for soil amplification, liquefaction hazard, and seismic slope instabilities. Also, recent applications of remotely sensed data have improved post-event hazard maps. This session will be used to highlight new approaches in both pre-event seismic hazard maps and post-event seismic hazard surveys.

Conveners: Laurie G. Baise (laurie.baise@tufts.edu), Keith L. Knudsen (keith_knudsen@urscorp.com)

At the Interface Between Earthquake Sciences and Earthquake Engineering in the Pacific Northwest
As the Pacific Northwest comes to grips with the destructive potential of the Cascadia subduction zone and as more active crustal faults are identified, particularly in the Puget Sound region, our understanding of seismic hazards has improved. Greater efforts are being made by both the earth science and engineering communities to insure that new and existing critical and important structures and facilities as well ordinary buildings are capable of withstanding this higher level hazard. Examples of these efforts include the continuing evolution of the USGS National Hazard Maps in the Pacific Northwest and two regional seismic hazard studies for dams being conducted in eastern Washington and British Columbia. This session will focus on recent advances in the earthquake sciences and how

doi: 10.1785/gssrl.81.2.253

they have impacted earthquake engineering practices in the Pacific Northwest. Case histories where state-of-the-art knowledge and procedures are implemented are of particular interest to this session.

Conveners: Ivan G. Wong (ivan_wong@urscorp.com), Arthur D. Frankel (afrankel@usgs.gov)

Building Code Uses of Seismic Hazard Data

The SSA statement of purpose includes the objective to "promote public safety by all practical means." Building codes are one of the most effective means of elevating public safety. This session will focus on the ways in which building code applications use, or could use, seismic hazard data from seismologists and others. Examples include:

- The use of national and regional/urban probabilistic and deterministic hazard maps to develop maps of ground motion intensities for the design of new structures and/or the evaluation/retrofit of existing structures, including buildings,bridges, dams, etc.;
- Site-specific hazard analysis for such structures and others (*e.g.*, nuclear power plants);
- The use of ground motion time histories, whether recorded or simulated; and
- The incorporation of earthquake effects other than ground motion, such as slope instability, liquefaction, total and differential settlement, surface displacement, etc., into building codes

Contributors to the session are encouraged to either present information on current uses of seismic hazard data in building code applications, or to propose future uses that are in line with the SSA objective to promote public safety by all practical means.

Conveners: Nicolas Luco (nluco@usgs.gov), Charles A. Kircher (cakircher@aol.com)

Characterizing the Next Cascadia Earthquake and Tsunami

New insights into the Holocene rupture history of the Cascadia subduction zone, the structure of its forearc, and episodic tremor and slip events located down-dip of the seismogenic zone are redefining source models aimed at characterizing the next megathrust earthquake and tsunami in the Pacific Northwest. This session will feature new research in the fields of geology, seismology and geodesy that have led to improvements in understanding the seismic potential of the Cascadia megathrust. Of particular interest to this session are studies that provide better constraints on the width of the rupture zone, the magnitude of slip, potential fault segmentation and highlight remaining uncertainties. We also encourage submissions that address how new findings can be used to reduce human losses from future megathrust earthquakes and tsunamis, in particular, assessments of seismic and tsunami hazards for mitigation purposes.

Conveners: Rob Witter (rob.witter@state.or.us), Chris Goldfinger (gold@coas.oregonstate.edu)

Deterministic Simulated Ground Motion Records under ASCE 7-10 as a Bridge Between Geotechnical and Structural Engineering Industry

According to new requirements of the American Society of Civil Engineers Standard (ASCE 7-10 Chapter 21 Site-Specific Ground Motion Procedures for Seismic Design), at least five recorded or simulated horizontal ground motion acceleration time histories shall be selected from events having magnitudes and fault distances that are consistent with those that control the Maximum Considered Earthquake. In some cases (*e.g.*, from M6.0 to M8, less than 5 km from the fault zone) there may not be five sets of recorded ground motions that are appropriate, and simulated ground motion would be needed. Based on analytical and numerical simulation for the earthquake rupture propagations ground-motion modeling methods are being increasingly used to supplement the recorded ground-motion database. Unfortunately, there is no official procedure to follow for near-field sites (D < 5 km from the fault) and for determining whether facilities and bridges are considered critical or essential. This presents a paradox: the Building Codes and Standard ASCE/SEI 7-10 requires engineers to provide simulation of ground motion records (Chapter 21), but there is no official procedure for accomplishing this at near-field sites. This paradox should be resolved as soon as possible.

We invite papers that focus on simulating ground motions that satisfy ASCE/SEI 7-10 and address one or more of the following aspects: 1) procedures for simulating horizontal-, vertical-, and torsion-component ground-motion records for planar and nonplanar fault topology within 5 km of a fault zone; 2) comparisons of solutions for different deterministic models; 3) procedures for determining site-specific design ground-motion parameters for landslides and slope stability analyses with time history procedures; 4) site-specific design ground-motion parameters for bridges and essential facilities (with time history procedures) located within 5 km of a fault zone.

Conveners: Alexander Bykovtsev (bykovtsev1@yahoo.com), Walter Silva (pacificengineering@juno.com)

Earthquake Debates

Invited speakers will debate important issues in earthquake science. Such issues include the predictability of earthquakes, the distribution of earthquake sizes on major faults, the role of Coulomb stress change in earthquake triggering, and many others. The predictability debate has been with us for decades and is based on many of the contentious issues debated in this session. Speakers will debate what earthquake prediction really means, how it can be evaluated, and whether it is realistic for scientists to promise progress to funding agencies or the public. The issue of earthquake size is often distilled into two limiting hypotheses: characteristic or Gutenberg-Richter distribution. Does Gutenberg-Richter behavior in a large region imply similar behavior on individual faults, and how do we decide when earthquakes are on individual faults anyway? Earthquakes and stress must (?) influence each other, but how? Do static effects of large earthquakes cause Coulomb stress shadows and bright spots, or do dynamic effects dominate earthquake triggering,

or something else? Other issues like earthquake periodicity, limits on earthquake size, precarious rocks as seismometers, and limits on strong ground motion are equally contentious.

Conveners: Danijel Schorlemmer (ds@usc.edu), David D. Jackson (djackson@ess.ucla.edu), Warner Marzocchi (marzocchi@NOSPAMingv.it), Jeremy D. Zechar (jeremy.zechar@sed.ethz.ch)

Engaging Students and Teachers in Seismology: In Memory of John Lahr

John Lahr was a curious, resourceful, hands-on seismologist who increased understanding of earthquakes, tectonics, and volcanic processes and who inspired teachers and students of all ages to listen to and explore the Earth. This session invites participants to present examples of effective programs, activities and techniques for actively engaging students and the public in seismology in the K-12 and college classroom, and in museums and other learning settings or opportunities. Descriptions of new technologies and ways to bring groups of teachers and students together are particularly encouraged.

Conveners: John Taber (taber@iris.edu), Larry Braile (braile@purdue.edu)

The Evolution of Slow Slip and Tremor in Time and Space

The temporal and spatial resolution with which we can measure slow slip and tremor in Cascadia have sharpened sufficiently that their evolution in time and space can be used as meaningful constraints on models of the underlying causative processes. This session will focus on observations of this evolution within Cascadia and comparisons with other regions, as well as on models that might explain these phenomena. Presentation topics may include the degree to which slow slip and/or tremor events are periodic, whether they propagate continuously or jump, how they start and stop, and at what scales various behaviors apply.

Conveners: Joan Gomberg (gomberg@usgs.gov), Evelyn Roeloffs (evelynr@usgs.gov)

Ground Motion: Observations and Theory

Poster session.

The January 2010 Earthquakes in Haiti and Offshore Northern California: Origins, Impacts and Lessons Learned

On January 10 2010, a magnitude 6.5 earthquake ruptured a fault within the Gorda plate off the coast of Northern California, ending 15 years of relative seismic quiescence on California's North Coast and causing over $40 million in losses in Humboldt County. Three days later, a magnitude 7.0 earthquake occurred near Port-au-Prince, Haiti in an event that is likely to be listed as one of the great earthquake catastrophes of all time. We welcome papers addressing the mechanisms and tectonic settings of these earthquakes, the geotechnical factors, strong motion, remote sensing aspects, and direct observations of the earthquake zones including associated deformation, tsunami, landsliding and other evidence, as well as impacts and implications for regional seismic hazards.

As this session was added after the original submission deadline and the submission deadline for this extended, the abstracts were not ready for publication in this issue. They will be available online by March 15 and published in a later issue of SRL.

Conveners: Lori Dengler, Humboldt State University, Lori.Dengler@humboldt.edu, Chris Goldfinger, Oregon State University, gold@coas.oregonstate.edu, Gavin Hayes, US Geological Survey, ghayes@usgs.gov, Chris Rollins, University of Southern California, chrisrol@usc.edu.

Joint Inversion of Multiple Geophysical Data Sets for Seismic Structure (poster only)

A recent trend in the tomography arena at various scales is the joint inversion of traditionally distinct data sets for improved seismic structure modeling. Combinations of data sets used in these joint inversions have included: resistivity and magnetotelluric data; receiver function and surface wave dispersion observations; teleseismic or local travel times and gravity data; and surface wave velocity and gravity observations. Although multiple geophysical observations have been successfully inverted jointly, many questions about means and methods still remain unanswered.

We invite contributions to this session on simultaneous and/or sequential joint inversion methods for improved tomographic modeling. Of particular interest are studies that highlight novel combinations of data sets, possible relationships between the independent observations and the relative weighting of disparate data sets for successful inversion. Results from reservoir-scale to global-scale are welcome, along with new means to address computational efficiency and robustness of the inversion. To encourage more in-depth discussion, this will be a poster-only session.

Conveners: Monica Maceira (mmaceira@lanl.gov), Haijiang Zhang (hjzhang@mit.edu), Charlotte Rowe (char@lanl.gov)

Magnitude Scaling and Regional Variation of Ground Motion (jointly sponsored by the European Seismological Commission)

Abundant ground-motion data in both the large and small-to-moderate magnitude ranges are now available. These new data allow us to examine the magnitude (and distance) scaling of ground motions and its regional variability over a wide range of magnitudes. These data analysis results have important implications for the use of small and moderate earthquake data to determine or calibrate new ground-motion models and evaluate model applicability, and for the regionalization of global ground motion models in general.

We invite papers related to: 1) the analysis of ground-motion scaling and its regional variations; 2) the applicability of recent empirical models (*e.g.* Next Generation Attenuation (NGA) models) across regions and magnitude/distance ranges; 3) the adjustments of empirical models to specific site conditions or target-region characteristics; 4) the development of new strategies to select ground-motion models for Probabilistic Seismic Hazard Assessment studies; and 5) evaluation of ground motion model predictions against observed ground motions from recent earthquakes.

Conveners: Gail Atkinson (Gmatkinson@aol.com), Fabrice Cotton (fabrice.cotton@obs.ujf-grenoble.fr)

Monitoring for Nuclear Explosions

Seismology has new visibility with policymakers and the general public in the context of current evaluations of the Comprehensive Nuclear-Test-Ban Treaty. Explosion monitoring continues to motivate both innovation and funding in seismology, as it has since Project VELA began in 1959. Infrastructure to improve the monitoring of nuclear explosions has included the WWSSN (1960s to 1980s), the GSN (from 1990) and the International Monitoring System (from 2000). Many fundamental tools now used widely in seismology were developed partly to improve explosion monitoring, including seismic array signal processing, numerical simulation of seismic wave propagation, structure discovery methods such as tomography and receiver functions, and source characterization methods such as moment tensors and coda magnitude. We welcome papers related to all advances in monitoring capability in the last ten years. Such topics include discussion of new data streams and issues of accessibility; new understanding of source physics; assessments of capability; and improvements derived from new methods of analysis such as uses of three-dimensional models and massive data-mining. In addition to papers evaluating routine methods of event detection, association of signals, and event characterization, we welcome special studies of particular data sets, and discussion of monitoring technologies (such as ocean acoustics, infrasound, radiochemistry) that complement seismology.

Conveners: Paul G. Richards (richards@LDEO.columbia.edu), Ola Dahlman (Ola.Dahlman@ctbto.org), Bill Walter (bwalter@llnl.gov), Ray Willemann (ray@iris.edu)

Near-Surface Deformation Associated with Active Faults

This session will focus on imaging, characterizing, and modeling the near-surface expression of active faults using a broad array of geological and geophysical tools. Studies using new remote sensing methods that identify ground deformation (*e.g.*, LiDAR, InSAR), imaging of subsurface deformation (*e.g.*, seismic, radar), geologic mapping studies, and modeling of near-surface deformation above faults are encouraged for this session. Presentations describing methodologies and results from a broad array of tectonic and geologic settings are welcome.

Conveners: Lee M. Liberty (lliberty@boisestate.edu), Thomas L. Pratt (tpratt@ocean.washington.edu)

Numerical Prediction of Earthquake Ground Motion

The last decade has witnessed significant improvements and developments in numerical methods for predicting earthquake ground motion in heterogeneous 3D media. By combining this methodological progress with increasing computational resources, it is becoming technically feasible to calculate realistic seismograms for frequencies of interest in seismic design applications.

The aim of this session is to give an up-to-date view of the capabilities to numerically predict earthquake ground motion, and to identify the challenges in fostering the use of numerical simulation in quantitative seismic hazard assessment.

We invite contributions focused on numerical modeling of earthquake ground motion, in particular on method development, verification and validation, and application to realistic cases. We strongly encourage contributions presenting large-scale simulations in heterogeneous media, possibly including spontaneous rupture, non- linear sediment response, and site-structure interaction.

Conveners: Emmanuel Chaljub (Emmanuel.Chaljub@obs.ujf-grenoble.fr), Steven M. Day (day@moho.sdsu.edu), Peter Moczo (moczo@fmph.uniba.sk)

Operational Earthquake Forecasting

Given the inability to forecast the occurrence of damaging shaking with high certainty and high probability, the application of earthquake forecasting to the evacuation of a large population has never seemed a realistic goal. Despite the large uncertainty over the imminence of a damaging earthquake, some more modest risk mitigation measures may be justified. Just as with other uncertain public threats, such as from pandemic disease or terrorism, prudent risk management may suggest useful societal actions, ranging from enhancing disaster preparedness and emergency response, to the reduction of threat exposure, to informing the public. By gauging the event probability gain associated with observational evidence, cost-benefit analysis can be applied to identify a spectrum of worthwhile mitigating actions. This operational earthquake forecasting bridges the gap between seismology and practical risk decision-making, and addresses the needs of civil authorities responsible for public safety. Just as with inter-disciplinary engineering seismology, this developing field promises to expand into a major branch of seismology.

Contributions to this session would cover time-dependent forecasting models able to run in real-time; review of past real events like the L'Aquila earthquake; comparison of the forecasting capabilities of different models (*e.g.* CSEP); real-time models for loss forecasting; and cost-benefit analysis for specific mitigation actions that may be taken in response to such forecasts.

Conveners: Michael Blanpied (mblanpied@usgs.gov), Gordon Woo (Gordon.Woo@rms.com), Warner Marzocchi (warner.marzocchi@ingv.it)

Quantification and Treatment of Uncertainty and Correlations in Seismic Hazard and Risk Assessments

Multi-location seismic hazard and risk assessments are not complete without proper treatment of uncertainty and correlation. All components of seismic hazard and risk studies, such as seismic source model, ground motion attenuation model, soil amplification model, and vulnerability model, contribute to the uncertainty. Each of these contributing models may have uncertainty in its functional form, as well as in the parameters used in the function. In general, two types of uncertainty can be identified, epistemic (modeling) and aleatory (inherent due to natural variability). Hazard and risk assessments are also affected by correlations in these various types of uncertain-

ties (*e.g.*, spatial correlation in ground motion intensity aleatory uncertainty, and in uncertain model coefficients). Spatial correlations are of particular interest when seismic hazard and risk are being estimated for a group of varying geographic locations. In this session, we will focus on quantification of these uncertainties at various levels (parameter, component, overall model), approaches for quantifying uncertainties, and guidance for uncertainty treatment in future studies.

Conveners: Tuna Onur (tuna.onur@rms.com), Jack Baker (bakerjw@stanford.edu), Chris H. Cramer (ccramer@memphis.edu)

Recent Advances in Source Parameters and Earthquake Magnitude Estimations

Determination of the magnitude of an earthquake is one of the more important tasks of the seismological community. Indeed, accurate magnitude determinations are fundamental for studying the seismic source characteristics and are a primary source parameter input to many other applications (*e.g.*, ShakeMap, earthquake catalogs for seismic hazard studies, etc.). The aim of the session is to gather researchers working in the earthquake source parameter observations and magnitude determination at local/regional and global scale. Contributions presenting results of testing and implementation of new IASPEI standards for the classical empirical magnitudes [such as ML, mb, mb(Lg), mB, MS(20) and MS(BB)] as well as modern physically based scales [such as Mw and Me], of innovative rapid magnitude procedures, of improved calibration functions, and of applications of these magnitudes to seismic hazard assessment and tsunami warning are encouraged.

Conveners: Domenico Di Giacomo (domenico@gfz-potsdam.de), George L. Choy (choy@usgs.gov)

Seismic Hazard Mitigation Policy Development and Implementation

Development and implementation of seismic hazard mitigation policy is complicated, involving seismologists and engineers, social scientists, economists, elected officials, and other stakeholders. In the United States, there is a pressing need for more robust and cost-effective seismic hazard mitigation policies at the national, state, and local level (*i.e.*, county or municipality) to better address seismic risk. Implementation, at the local level is most critical in the United States, as it is most other countries. This special session provides a forum on how to bring seismologists, engineers, federal and state government officials, and private citizens together to develop and implement more effective policies for seismic hazard mitigation and risk reduction at national, state, and local levels. Case histories are especially welcome.

Conveners: Yumei Wang (yumei.wang@dogami.state.or.us), Zhenming Wang (zmwang@uky.edu)

Seismic Imaging: Recent Advancement and Future Directions

Seismic imaging is a powerful tool for geophysicists to probe the Earth's interior. The demand for higher resolution and a broader range of applications is rapidly increasing. This session welcomes contributions from seismic imaging in various scales and application arenas, with special emphasis on recent advances and future directions. Examples include innovations and advances in 3D traveltime tomography, waveform tomography, receiver function mapping, and surface wave inversions. We also encourage case-study papers using seismic imaging to solve real problems. Discussions on the pitfalls, limitations, and artifacts of common seismic imaging methods and potential remedies are most welcomed.

Conveners: Youshun Sun (youshun@mit.edu), Michael Begnaud (mbegnaud@lanl.gov)

Seismic Networks, Analysis Tools, and Instrumentation

Poster session.

Seismic Structure and Geodynamics of the High Lava Plains and Greater Pacific Northwest

The High Lava Plains (HLP) of Oregon has long represented an enigmatic region of massive tectonomagmatism in the Pacific Northwestern United States, with poorly understood relationships to the Columbia River Basalt sequence and the time-progressive tracks of both Newberry and Snake River Plain / Yellowstone rhyolitic volcanism. These events also tie directly to broader-scale mantle dynamics, including ongoing subduction of the Juan de Fuca plate system, extension across most of the Great Basin, and regional instability of lithosphere over a range of spatial scales. To provide new constraints on the structure and dynamics of these terranes, the area has been assaulted over the past 5 years by a host of high-density temporary broadband seismic networks, including EarthScope's USArray Transportable Array, the High Lava Plains Broadband seismic experiment, and several USArray Flexible Array experiments. We encourage contributions to this session that not only address HLP-centered investigations, but also examine the structure and dynamics of the broader Pacific Northwestern United States and surrounding regions.

Conveners: Matthew J. Fouch (fouch@asu.edu), G. Randy Keller (grkeller@ou.edu), David E. James (james@dtm.ciw.edu)

Seismicity and Seismotectonics

Conveners: Diane Doser (doser@utep.edu) and Jeanne Hardebeck (jhardebeck@usgs.gov).

The Seismo-Acoustic Wavefield: Fusion of Seismic and Infrasound Data

The field of seismo-acoustics is flourishing owing to the value of co-located seismic and infrasound arrays that sample both ground- and atmosphere-propagating elastic energy. The fusion of seismic and infrasonic data allows us to uniquely study a broad range of topics including the source physics of geophysical and man-made events, interaction of the atmosphere and lithosphere, source location and characterization, and inversion of atmospheric properties. Seismic sensors deployed near the solid earth atmosphere boundary can be affected by acous-

tic signals and thus the understanding of these interactions are important to seismic noise characterization. We invite abstracts on all aspects of seismo-acoustics, including general studies of infrasound from geophysical and anthropogenic sources that also generate seismic waves.

Conveners: Stephen Arrowsmith (arrows@lanl.gov), Jeff Johnson (jeff.johnson@ees.nmt.edu), Brian Stump (bstump@mail.smu.edu)

Seismologic Methods, Techniques, and Theory

Poster session.

Seismology of the Atmosphere, Oceans, and Cryosphere

Recently, there has been increased interest in Earth's seismic background wavefield and other nontraditional signals. Motivations include: (1) the ambient seismic wavefield can be used in tomographic imaging and seismic interferometry; (2) modern and historical records of microseism (5-25 s period) can be used as proxies for long-term ocean wave climate, which can in turn contribute to global climate studies; (3) increasing quantity, quality, distribution, and geographic coverage of seismic recording has resulted in the discovery of new glaciological, oceanic, and cryospheric signals and dynamic processes. This session welcomes studies that locate and characterize seismic noise/signal from a broad range of environmental and climate related sources. Topics can include characterizing the modal structure of microseismic energy, quantifying temporal variations in microseism properties, and interpreting seismic observations in the context of cryospheric, oceanographic and atmospheric source processes. We also welcome theoretical and numerical simulation studies of relevant seismic source and propagation models in all frequency bands.

Conveners: Daniel McNamara (mcnamara@usgs.gov), Keith Koper (koper@eas.slu.edu), Richard Aster (aster@ees.nmt.edu)

State of Stress in Intraplate Regions

Intraplate earthquakes pose an unexpected hazard for large continental areas. The paradigm for cyclic stress and fault rupture driven by high strain rates at plate boundaries does not seem to be appropriate within plate interiors where measured strain rates are relatively small. Yet, large intraplate earthquakes occur. Session submissions are encouraged that examine the conundrum of intraplate seismicity from observations of seismicity, geodesy, lithospheric rheology, potential fields, and relative and absolute stress measurements. We particularly encourage submissions that assess the progress made in crustal rheology through observational and laboratory experiments that place constraints on the state of stress in continental interiors.

Conveners: Christine Powell (capowell@memphis.edu), Charles Langston (clangstn@memphis.edu)

Statistics of Earthquakes

The purpose of this session is to solicit a wide range of papers concerned with the statistics and statistical physics of earthquakes. Subject matter includes but is not limited to frequency-size statistics, correlations in space-time-magnitude, patterns, forecasting, time series analyses, peaks-over-threshold analyses, record-breaking analyses, detrended fluctuation analyses, first passage time statistics, and similar phenomenology and analyses. Other topics might include reconstruction of paleoevents using statistical analyses, novel statistical methods of forecast validation and testing, and numerical simulations focusing on statistical exploration of simulation catalogs.

Conveners: Donald Turcotte (dlturcotte@ucdavis.edu), John Rundle (rundle@physics.ucdavis.edu), James Holliday (jrholliday@ucdavis.edu), Mark Yoder (yoder@physics.ucdavis.edu)

Subsurface Imaging for Urban Seismic Hazards at the Engineering Scale

Development of realistic seismic hazard maps for urban areas requires comprehensive investigation of faulting, basin geometry, rock properties, stratigraphy, and geotechnical properties. Damaging earthquakes frequently occur on unknown or poorly characterized faults below urban areas, have their energy trapped within poorly imaged sedimentary basins, with shaking further amplified at unexpected places by unknown basin and soil heterogeneity. This session focuses on current practice and future prospects for locating and characterizing faults and detailing basin boundaries and sediment properties with geophysical imaging techniques. Applying these methods to the seismic hazard of urban basins requires adapting techniques from the petroleum and mineral industries, and from crustal studies, to the noisy urban environment and the one-meter to one-kilometer engineering scale of most basins. We invite submission of examples showing how to attain detailed fault and basin characterization and imaging in urban areas with active and passive seismic, electromagnetic, and potential-field methods.

Conveners: John N. Louie (louie@seismo.unr.edu), William J. Stephenson (wstephens@usgs.gov)

Time Reversal in Geophysics

The last decade has seen seismic source studies evolve from event-based observations to the permanent observation of large seismic networks. Recent seismic studies using new arrays and new methods of analysis have led to the recognition of heretofore unnoticed, complex fault motions (*e.g.*, stick-slip to slow maybe diffuse rupture in deeper regions) as well as the recognition of the diversity of processes generating seismic energy (*e.g.*, swarms, glacial earthquakes, background noise, volcanic tremor, non-volcanic tremor, etc.) Key ingredients to determine the processes underlying each observation are locating the origin point, probing source characteristics with a remotely recorded wavefield and producing high-resolution images.

Time Reversal (TR), only requiring synchronized recorded wavefields, is a promising approach for solution of the source location problem. The time reversal recipe, related to the adjoint formulation of the source problem and having empirical justification from laboratory experiments, is also closely

related to seismic migration and interferometry. In comparison, TR focuses on source location and characterization.

Since its re-discovery in acoustics in the 1990s, various schemes have been developed for using time reversal in a range of applications, often very different from the source characterization problem. We seek to gather contributions related to time reversal in its diverse applications and disciplines (*e.g.*, geophysics, material science) in order to offer the opportunity to expose and exchange ideas.

Conveners: Carene Larmat (carene@lanl.gov), Jean-Paul Montagner (jpm@ipgp.jussieu.fr), Kees Wapenaar (C.P.A.Wapenaar@tudelft.nl)

Volcanic Plumbing Systems: Results, Interpretations and Implications for Monitoring

A combination of improved instrumentation, improved network coverage and new techniques has led to an enhanced understanding of the plumbing systems beneath volcanoes, but the paths of magma accumulation and ascent are poorly known at most volcanoes. Because eruptions often begin exclusively with shallow seismicity, the geometry and characteristic behavior of the conduit system should be well known in order to best respond during a volcanic crisis. While many magmatic processes occur aseismically, the increased detection of broadband seismic signals at active volcanoes provides new insights into conduit geometries and processes. We invite papers that give results and interpretations of the plumbing systems beneath volcanoes including source mechanisms, tomography, and precise earthquake locations. We also encourage the presentation of methods and results that elucidate the time-dependent changes that occur within a plumbing system.

Conveners: Weston Thelen (wethelen@ess.washington.edu), Gregory Waite (gpwaite@mtu.edu)

ANNUAL LUNCHEON SPEAKER

Marcia McNutt, Director of the US Geological Survey, will be the President's Invited Speaker at the Annual Luncheon on Wednesday, 21 April.

PUBLIC OUTREACH

IRIS/SSA Distinguished Lecture: Dr. Stephen Malone, past SSA president from the University of Washington Department of Earth and Space Science will present his lecture, "Predicting Earthquakes and Volcanic Eruptions: What Can and Can Not Now Be Done."

This lecture will be held offsite at the Oregon Museum of Science and Industry (OMSI) on Tuesday evening, 20 April 2010.

Town Hall Meeting: "The Big One Is Coming: What Are YOU Going To Do About It?" is the topic of a town hall meeting to raise the awareness of decision-makers and the public on the earthquake hazards and associated risks that face them in the Portland area, western Oregon and the greater Pacific Northwest. Understanding of the magnitude of the earthquake risk in the Pacific Northwest has grown rapidly in recent years and yet progress has been slow to reduce the potential loss of life and impacts on our infrastructure and economy.

Speakers will include Peter Courtney, Oregon State Senate President; George Priest and Yumei Wang of Oregon Department of Geology and Mineral Industries (DOGAMI); Jed Sampson and Carmen Merlo, City of Portland; Craig Weaver, USGS, and Ivan Wong, URS Corp., coordinator of the town hall event.

The meeting will be held Wednesday evening 21 April 2010.

FIELD TRIPS

Both field trips will take place on Saturday, 24 April 2010. *Departure and return times are approximate.*

Portland Geology by Tram, Train, and Foot

Leader: Ian P. Madin, Oregon Dept. of Geology and Mineral Industries.

This trip will take participants on a tour of the geology of Portland by foot, light rail, and aerial tram. We will review the regional and local geologic setting and visit outcrops of most of the local units, including Columbia River Basalt flows, Missoula Flood deposits, and a late Quaternary volcano within the city limits.

This field trip will depart at approximately 8:30 AM and return at approximately 2:30 PM.

Geology and Hazards of Mount Hood, Oregon

Leader: Willie Scott, U.S. Geological Survey, Cascades Volcano Observatory

This all-day tour through the Columbia River Gorge and around Mount Hood will focus on the scenic geology of the Mount Hood region. Final itinerary for the trip will depend on the day's snow and weather conditions. Stops and topics may include regional geology and tectonics, scenic viewpoints and overlooks, giant landslides and ice-age floods in the Columbia River Gorge, past eruptions of Mount Hood, potential hazards from future eruptions, historical seismicity and volcano monitoring of Mount Hood, recent storm-generated debris flows on the volcano, and historic Timberline Lodge at 6,000 feet on the volcano's south flank.

This field trip will depart at approximately 8 a.m. and return at approximately 6 p.m.

MEETING INFORMATION

Registration

You can register for the meeting online at http://www.seismosoc.org/meetings/2010/index.php. The pre-registration deadline is 19 March 2010.

Members receive a discounted registration. Nonmember students can get membership and a student member registration rate for less than the non-member rate. A current copy of

their student ID is required. Online registration closes 9 April 2010. Walk in registrations will be accepted for an additional $25 charge.

Preliminary Schedule

Events will be held at the Portland Marriott Downtown Waterfront Hotel unless otherwise noted.

Tuesday, 20 April
Board of Directors Meeting (9:30 AM–5 PM)
Registration (3 PM–8 PM)
Icebreaker (6 PM–8 PM)
IRIS/SSA Lecture (7 PM–9 PM) at OMSI

Wednesday, 21 April
Technical Sessions (8:30 AM–5:45 PM)
Annual Luncheon (12 PM–2 PM)
Student Reception (5:45 PM-7:30 PM)
Town Hall Meeting (6:45 PM – 8:45 PM)

Thursday, 22 April
Technical Sessions (8:30 AM–5 PM)
Lunch (12 PM–1:15 PM)
Joyner Lecture & Reception (5:15 PM-7:30 PM)

Friday, 23 April
Technical Sessions (8:00 AM–5 PM)
Lunch (12 PM–1:15 PM)

Saturday, 24 April
Field Trips

This schedule is subject to change.

HOTEL INFORMATION

Portland Marriott Downtown Waterfront

Portland's Marriott Downtown Waterfront is an eco-friendly hotel near the Portland Riverplace Marina overlooking the Willamette River. Facilities include indoor pool, whirlpool, fitness center, two restaurants, and the meeting rooms for all the SSA meetings. It is located close to downtown, shops, and restaurants. http://www.marriott.com/hotels/travel/pdxor-portland-marriott-downtown-waterfront/

Please note that there are multiple Marriot hotels in downtown Portland and the names can be confusing. Please be sure you register at the Portland Marriott Downtown Waterfront.

Overview of Technical Program

ORAL SESSIONS

Wednesday, 21 April

	Salon A	*Salon E*	*Salon F*	*Salon G*
8:30–10:00 AM	Building Code Uses of Seismic Hazard Data	Monitoring for Nuclear Explosions	Characterizing the Next Cascadia Earthquake and Tsunami	Magnitude Scaling and Regional Variation of Ground Motion
10:30–NOON	Building Code Uses of Seismic Hazard Data	Monitoring for Nuclear Explosions	Characterizing the Next Cascadia Earthquake and Tsunami	Magnitude Scaling and Regional Variation of Ground Motion
2:15–3:45 PM	Advances in Seismic Hazard Mapping	Monitoring for Nuclear Explosions	The Evolution of Slow Slip and Tremor in Time and Space	Seismic Imaging: Recent Advancement and Future Directions
4:15–5:45 PM	Advances in Seismic Hazard Mapping	Engaging Students and Teachers in Seismology: In Memory of John Lahr	The Evolution of Slow Slip and Tremor in Time and Space	Seismic Imaging: Recent Advancement and Future Directions
6:45–8:45 PM	Town Hall Meeting—Salon E & F			

Thursday, 22 April

	Salon A	*Salon E*	*Salon F*	*Salon G*
8:30–10:00 AM	Operational Earthquake Forecasting	Numerical Prediction of Earthquake Ground Motion	Near-surface Deformation Associated with Active Faults	The Seismo-Acoustic Wavefield: Fusion of Seismic and Infrasound Data
10:30–NOON	Operational Earthquake Forecasting	Numerical Prediction of Earthquake Ground Motion	Near-surface Deformation Associated with Active Faults	The Seismo-Acoustic Wavefield: Fusion of Seismic and Infrasound Data
1:30–3:00 PM	Quantification and Treatment of Uncertainty and Correlations in Seismic Hazard and Risk Assessments	Numerical Prediction of Earthquake Ground Motion	Earthquake Debates	Seismic Structure and Geodynamics of the High Lava Plains and Greater Pacific Northwest
3:30–5:00 PM	Quantification and Treatment of Uncertainty and Correlations in Seismic Hazard and Risk Assessments	Deterministic Simulated Ground Motion Records under ASCE 7-10 as a Bridge between Geotechnical and Structural Engineering Industry	Earthquake Debates	Seismic Structure and Geodynamics of the High Lava Plains and Greater Pacific Northwest
5:15–6:15 PM	Joyner Memorial Lecture —Salon E & F.			

Friday, 23 April

	Salon A	*Salon E*	*Salon F*	*Salon G*
8:00–8:30 AM	The January 2010 Earthquakes in Haiti and Offshore Northern California: Origins, Impacts and Lessons Learned. In Salon E.			
8:30–10:00 AM	Volcanic Plumbing Systems: Results, Interpretations and Implications for Monitoring	Recent Advances in Source Parameters and Earthquake Magnitude Estimations	Subsurface Imaging for Urban Seismic Hazards at the Engineering Scale	State of Stress in Intraplate Regions
10:30–NOON	Volcanic Plumbing Systems: Results, Interpretations and Implications for Monitoring	Recent Advances in Source Parameters and Earthquake Magnitude Estimations	Subsurface Imaging for Urban Seismic Hazards at the Engineering Scale	State of Stress in Intraplate Regions
1:30–3:00 PM	Statistics of Earthquakes	Recent Advances in Source Parameters and Earthquake Magnitude Estimations	Seismology of the Atmosphere, Oceans, and Cryosphere	At the Interface Between Earthquake Sciences and Earthquake Engineering in the Pacific Northwest
3:30–5:00 PM	Statistics of Earthquakes	*Exhibit Hall* Seismicity and Seismotectonics	*Salon I* Time Reversal in Geophysics	Seismic Hazard Mitigation Policy Development and Implementation

POSTER SESSIONS

Exhibit Hall

Wednesday AM
- Engaging Students and Teachers in Seismology: In Memory of John Lahr
- Joint Inversion of Multiple Geophysical Data Sets for Seismic Structure
- Seismic Imaging: Recent Advancement and Future Directions
- Ground Motion: Observations and Theory
- Seismologic Methods, Techniques, and Theory

Wednesday PM
- Numerical Prediction of Earthquake Ground Motion
- Magnitude Scaling and Regional Variation of Ground Motion
- The Seismo-Acoustic Wavefield: Fusion of Seismic and Infrasound Data
- Operational Earthquake Forecasting

Thursday AM
- Characterizing the Next Cascadia Earthquake and Tsunami
- The Evolution of Slow Slip and Tremor in Time and Space
- Monitoring for Nuclear Explosions
- Recent Advances in Source Parameters and Earthquake Magnitude Estimations
- Deterministic Simulated Ground Motion Records under ASCE 7-10 as a Bridge between Geotechnical and Structural Engineering Industry
- Quantification and Treatment of Uncertainty and Correlations in Seismic Hazard and Risk Assessments

Thursday PM
- Near-Surface Deformation Associated with Active Faults
- Advances in Seismic Hazard Mapping

Friday AM
- Statistics of Earthquakes
- Seismology of the Atmosphere, Oceans, and Cryosphere
- Time Reversal in Geophysics
- Seismic Structure and Geodynamics of the High Lava Plains and Greater Pacific Northwest
- Seismicity and Seismotectonics
- Seismic Networks, Analysis Tools, and Instrumentation
- At the Interface Between Earthquake Sciences and Earthquake Engineering in the Pacific Northwest
- Seismic Hazard Mitigation Policy Development and Implementation

Friday PM
- State of Stress in Intraplate Regions
- Volcanic Plumbing Systems: Results, Interpretations and Implications for Monitoring
- Subsurface Imaging for Urban Seismic Hazards at the Engineering Scale
- The January 2010 Earthquakes in Haiti and Offshore Northern California: Origins, Impacts and Lessons Learned

Program for 2010 SSA Annual Meeting

Presenter is indicated in bold.

Wednesday, 21 April—Concurrent SSA Oral Sessions

Time	*Salon A*	*Salon E*	*Salon F*	*Salon G*
	Building Code Uses of Seismic Hazard Data Session Chairs: Charles A. Kircher and Nicolas Luco (see page 284)	**Monitoring for Nuclear Explosions** Session Chairs: Bill Walter, Ola Dahlman, Paul G. Richards, and Ray Willemann (see page 286)	**Characterizing the Next Cascadia Earthquake and Tsunami** Session Chairs: Chris Goldfinger and Rob Witter (see page 288)	**Magnitude Scaling and Regional Variation of Ground Motion** Session Chairs: Fabrice Cotton, Gail Atkinson (see page 291)
8:30	INVITED: The 2008 U.S. National Seismic Hazard Map Applications for Building Codes. **Petersen, M.**, Harmsen, S., Rukstales, K., Luco, N.	INVITED: Comprehensive Test Ban Treaty Is Effectively Verifiable, **Collina, T.**	INVITED: The Landward Limit of Cascadia Great Earthquake Rupture. **Hyndman, R.D.**, Wang, K., Cassidy, J., Kao, H., Mazzotti, S., Dragert, H., Henton, J., Leonard, L., and Rogers, G.	Accurate Predictions of Strong Ground Motion Based on Weak Motion Data: Case Studies from Italy and Japan. Malagnini, L., Akinci, A., Mayeda, K., Herrmann, R.B., Munafo', I.
8:45	INVITED: Project 07—Development of New Ground Motions for Model Building Codes. **Kircher, C.A.**	INVITED: Progress and Achievements in Monitoring Compliance with the Comprehensive Nuclear Test-Ban-Treaty (CTBT). **Zerbo, L.**	INVITED: A Comparison of the Location of Interseismic Locking and Slow Slip Events on the Cascadia Subduction Zone. **Weldon, II, R.J.**, Schmidt, D., Gao, H., Alba, S., and Livelybrooks, D.	Ground-Motion Attenuation Model for Small-To-Moderate Shallow Crustal Earthquakes in California and Its Implications on Regionalization of Ground-Motion Prediction Models. Chiou, B., **Youngs, R.**, Abrahamson, N., and Addo, K.
9:00	(Previous presentation continued)	INVITED: The United States National Data Center for the CTBT. **Woods, M.T.**	INVITED: Segmentation and Probabilities for Cascadia Great Earthquakes based on Onshore and Offshore Paleoseismic Data. **Goldfinger, C.**, Patton, J.R., Morey, A.E., and Witter, R.C.	Comparisons of Ground-Motion Attenuation in Eastern North America versus California. **Atkinson, G.M.**, Assatourians, K., and Nicol, E.A.
9:15	INVITED: New Risk-Targeted Seismic Design Maps for Model Building Codes. Luco, N.	Observed Seismic Technological Advances As Demonstrated During And Following The May 25, 2009 North Korean-Declared Nuclear Test. **Jih, R.-S.**	INVITED: ETS-Delineated Future Rupture of the Cascadia Megathrust. **Melbourne, T.I.**, and Brudzinski, M.	Exploring the Lower Limits of the NGA Using Data from California. **Hellweg, M.**, Darragh, R., and Silva, W.
9:30	INVITED: New Provisions for Peak Ground Acceleration and Vertical Component Design Response Spectra in the 2010 NEHRP Seismic Provisions and ASCE 7-10 Standard. **Crouse, C.B.**, Campbell, K.W., Bozorgnia, Y., Power, M., Anderson, D.G.	INVITED: Seismological Monitoring of the Comprehensive Nuclear Test Ban Treaty. **Sykes, L.R.**	A Continuous Moment Tensor Analysis in the Region of the Mendocino Triple Junction, California. **Guilhem, A.,** Dreger, D.S., and Uhrhammer, R.	An Earthquake Discrimination Scheme to Optimize Ground-Motion Prediction Equation Selection. **Garcia, D.**, Wald, D.J., Allen, T.I., Hayes, G.P., Lin, K.W., and Marano, K.D.

Time	Salon A	Salon E	Salon F	Salon G
9:45	INVITED: Ground Motion Issues Likely to be Addressed in the Next Code Development Cycle. **Hooper, J.D.**	INVITED: Scientific Challenges for Seismic Nuclear Explosion Monitoring. **Zucca, J.J.**	Mapping the Juan de Fuca Slab Beneath the Cascadia Margin. **McCrory, P.A.**, Blair, J.L., and Waldhauser, F.	Comparison of the NGA Models to the Turkish Strong Ground Motion Database: A Preliminary Study. **Gulerce, Z.**, and Abrahamson, N.A.
10:00	Break			
	Building Code Uses of Seismic Hazard Data *(continued)*	**Monitoring for Nuclear Explosions** *(continued)*	**Characterizing the Next Cascadia Earthquake and Tsunami** *(continued)*	**Magnitude Scaling and Regional Variation of Ground Motion** *(continued)*
10:30	Uncertainty in the Risk of Collapse of Code-Designed Structures Due to Uncertainty in the Earthquake Hazard. **Shome, N.**, and Frankel, A.D.	Analysis of the IDC Reviewed Event Bulletin for Detection Capability Estimation of the IMS Primary Seismic Stations. **Kvaerna, T.**, and Ringdal, F.	INVITED: Megathrust Paleogeodesy at the Central Cascadia Subduction Zone. **Horton, B.P.**, Nelson, A., Witter, R., Wang, K., Hawkes, A., Engelhart, S., Sawai, Y.	Next Generation Attenuation (NGA) East Ground Motion Database: Comparing Observations with Current ENA Attenuation Relations. **Cramer, C.H.**, Kutliroff, J.R., and Dangkua, D.T.
10:45	Inealstic Spectral Displacement for the Probabilistic Seismic Hazard Assessment in the Marmara Region, Turkey. **Akkar, S.**, and Akinci, A.	Bayesloc Multiple-Event Location Applied to a Global Data Set. **Myers, S.C.**, and Johannesson, G.	Validating Numerical Tsunami Simulations in Southern Oregon Using Late Holocene Records of Great Cascadia Earthquakes and Tsunamis. **Witter, R.C.**, Zhang, Y.J., Goldfinger, C., Priest, G.R., and Wang, K.	Source Properties, Site Amplification and Crustal Attenuation in Japan from Spectral Analysis of K-and KiK-net Data. **Oth, A.**, Parolai, S., Bindi, D., and Di Giacomo, D.
11:00	Peak and Integral Seismic Parameters of L'Aquila 2009 Ground Motions: Observed vs PSHA and Code provision values. Chiauzzi, L., Masi, A., **Mucciarelli, M.**	A New Look at an Old Discriminant: Ms—mb. **Richards, P.**	Cascadia Supercycles: Energy Management of the long Cascadia Earthquake Series. **Goldfinger, C.**, Witter, R.C., Priest, G.R., Wang, K., and Zhang, Y.J.	"Best Practices" for Using Macroseismic Intensity and Ground Motion to Intensity Conversion Equations for Hazard and Loss Models. **Cua, G.B.**, Wald, D.J., Marano, K., Allen, T., Garcia, D., Gerstenberger, M.C., Worden, C.B.,
11:15	Seismic Loss Estimation Along the North Anatolian Fault Based on Scenario Earthquakes. **Askan, A.**, Erberik, M.A., Ugurhan, B.	Apparent Explosion Moment. **Patton, H.J.**, and Taylor, S.R.	Temporal Clustering and Recurrence of Holocene Paleoearthquakes in the Region of the 2004 Sumatra-Andaman Earthquake. **Patton, J.R.**, Goldfinger, C., Morey, A.E., Erhardt, M., Black, B., Garrett, A.M., Djadjadihardja, Y., and Hanifa, U.	Felt Intensity vs. Instrumental Ground Motion: Why a Difference Between California and Eastern North America at Some Periods? **Dangkua, D.T.**, and Cramer, C.H.

Time	Salon A	Salon E	Salon F	Salon G
11:30	Comparison of Methods for Site Specific Seismic Response Assessment of Shallow and Deep Bedrock Sites. **Ghanat, S.T.**	Regional P/S Methods of Discriminating Explosions from Earthquakes: Applications and Limitations. **Walter, W.R.**, Pasyanos, M.E., Ford, S.R., and Matzel, E.	Characterizing Megathrust Recurrence Probabilities in the Pacific Northwest. Perkins, D., and **Laforge, R.**	VS30 and Kappa from Accelerometric Data Analysis. **Drouet, S.**, Cotton, F., and Guéguen, P.
11:45	Effect of Permafrost on Seismic Site Response and Design Spectrum. **Dutta, U.**, Yang, Z., and Xu, G.	Nuclear Explosion Monitoring R&D Roadmap. Casey, L.R., **Ziagos, J.P.**, and Bell, W.R.	An Analysis of Temporal Clustering of Cascadia Subduction Zone Earthquakes and its Implications to Seismic Hazard. **Wong, I.**, Kulkarni, R., Zachariasen, J., Dober, M., Goldfinger, C., and Lawrence, M.	Ground-Motion at Reference Rock Sites and the Reduction of Uncertainty Related to Site Conditions. **Edwards, B.**, Poggi, V., Faeh, D.
12:00	12:00-2:00 - SSA Annual Meeting—Lower Level			
	Advances in Seismic Hazard Mapping Session Chairs: Keith L. Knudsen and Laurie G. Baise (see page 293)	**Monitoring for Nuclear Explosions** Session Chairs: Bill Walter, Ola Dahlman, Paul G. Richards, and Ray Willemann (see page 295)	**The Evolution of Slow Slip and Tremor in Time and Space** Session Chairs: Evelyn Roeloffs and Joan Gomberg (see page 297)	**Seismic Imaging: Recent Advancement and Future Directions** Session Chairs: Michael Begnaud and Youshun Sun (see page 299)
2:15	May Subsidence Rate Serve as Proxy for Site Effects? Michel, S., **Cornou, C.**, Pathier, E., Menard, G., Collombet, M., Kniess, U., Bard, P.-Y., and Fruneau, B.	Operation of the International Monitoring System Network. Araujo, F., Castillo, J.E., Nikolova, S., The Operations Section of the IDC.	INVITED: Locating ETS Tremors: How? Where? Which? When? and Why? **Kao, H.**, Shan, S.-J., Rosenberger, A., Rogers, G.C., Dragert, H., Klaus, A.J., Wech, A.G., Creager, K.C., Brown, J.R., Beroza, G.C.	Animating the Seismic Wavefield: Exploring the Effects of Solid Earth Heterogeneity on Long-Period Surface Waves. **Lloyd, A.**, and Woodward, R.L.
2:30	Applying Satellite Remote Sensing to Document Liquefaction Failures. **Oommen, T.**, Baise, L.G., Gens, R., Prakash, A., and Gupta, R.P.	Innovative Statistical Data Processing Methods for Automatic Classification of Waveform Data at the CTBTO. Le Bras, R.J., Vaidya, S., Arora, N., and Russell, S.	Spectral Analysis of Tremor Using Beamforming. **Gerstoft, P.**, Zhang, J., Vidale, J., Ghosh, A.,	INVITED: Finite-Frequency Seismic Tomography of Anelastic Structures in East Asia. **Zhao, L.**, Chen, P., Chen, Q.F., and Gaherty, J.B.
2:45	Observations of Pore Pressure Increase in Liquefiable Layers during Strong Shaking at NEES Field Sites. **Seale, S.H.**, and Steidl, J.H.	Geological and Geophysical Applications of On Site Inspection for CTBT Verification. **Sweeney, J.J.**, Hawkins, W.L.	Toward a Unified View of Tremor Distribution in Space and Time. **Ghosh, A.**, Vidale, J.E., Sweet, J.R., Creager, K.C., Wech, A.G., Houston, H.	INVITED: Seismic Tomography and Imaging of the Southern California Crust. Tape, C., Liu, L., Maggi, A., and **Tromp, J.**
3:00	St. Louis Area Earthquake Hazards Mapping Project (SLAEHMP): Hazard Model and Methodology Update. **Cramer, C.H.**	Comparisons of Regional Source Properties of the North Korean Nuclear Explosions and Their Implications. **Hong, T.K.**	Modeling the Pattern of Tremor Migration in Cascadia. **Gershenzon, N.I.**, Bambakidis, G., Hauser, E.C., Creager, K.C.	INVITED: A Global 3D P-Velocity Model of the Earth's Crust and Mantle for Improved Event Location. **Young, C.J.**, Ballard, S., Hipp, J.R., Chang, M.C., Rowe, C.A., and Begnaud, M.L.

Time	Salon A	Salon E	Salon F	Salon G
3:15	A Terrain-based Vs30 Estimation Map of the Contiguous United States. **Yong, A.**, Hough, S.E., Braverman, A., and Iwahashi, J.	Seismic Simulations of Recent DPRK Nuclear Explosions Including the Effects of Free Surface Topography and 3D Structure. **Rodgers, A.J.**, Petersson, N.A., and Sjogreen, B.	Segmentation of Non-Volcanic Tremor Activity along the Cascadia Subduction Zone. **Farahbod, A.M.**, Calvert, A.J.	Full-3D Waveform Tomography for Southern California. **Chen, P.**, Lee, E., Jordan, T.H., and Maechling, P.J.
3:30	Exploring the Proximity of Ground-Motion Models Using High-Dimensional Visualization Techniques. **Scherbaum, F.**, Kuehn, N., Ohrnberger, M., and Koehler, A.	An Analysis of Seismic Characteristics of the 25 May 2009 North Korean Underground Nuclear Test. **Murphy, J.R.**, Kohl, B.C., Bennett, T.J., Israelsson, H.G.	Low Frequency Earthquakes from Tremor in Subduction Zones. **Brown, J.R.**, Beroza, G.C.,	Full-wave Ambient Noise Tomography of the Northern Cascadia. **Shen, Y.**, and Zhang, W.
3:45	Break			
	Advances in Seismic Hazard Mapping *(continued)*	**Engaging Students and Teachers in Seismology: In Memory of John Lahr** Session Chairs: John Taber and Larry Braile (see page 301)	**The Evolution of Slow Slip and Tremor in Time and Space** *(continued)*	**Seismic Imaging: Recent Advancement and Future Directions** *(continued)*
4:15	A Comprehensive Model to Include the Effects of Near-Fault Ground Motions in Probabilistic Seismic Hazard Analysis. **Baker, J.W.**, and Shahi, S.K.	John Lahr's Lasting Impact on the IRIS E&O Program. **Taber, J.J.**, Bravo, T.K., Hubenthal, M., Johnson, J., McQuillan, P., Toigo, M., and Welti, R.	The Background Hum of a Plate Boundary: Developing a Detailed Catalog of Tremor Activity Along 150 Kilometers of the South-Central San Andreas Fault, 2001–Present. **Shelly, D.R.**	Can We Improve Q Estimates by Using a New "Geometrical Spreading" Model? **Jiakang, X.**
4:30	Assessing the Seismic Hazard of Lake Maracaibo, Northwestern Venezuela. **Wong, I.**, Zachariasen, J., and Dober, M.	A Decade of Earthquake Monitoring with an Educational Seismograph. **Braile, L.W.**	INVITED: Spatial and Temporal Evolution of Long Term Slow Slip Events in the Guerrero Gap, Mexico. Radiguet, M., **Cotton, F.**, Vergnolle, M., Valette, B., Kostoglodov, V., Cotte, N., Pathier, E., and Shapiro, N.	INVITED: Eikonal Tomography: Surface Wave Tomography by Phase-Front Tracking Across a Regional Broad-Band Seismic Array. **Lin, F.**, Ritzwoller, M.H., and Snieder, R.
4:45	Probabilistic Seismic Hazard Assessment for Central Manila, Philippines. **Mote, T.I.**, Koo, R., Manlapig, R.V., and Zamora, C.	The Quake-Catcher Network: Bringing Seismology to Homes and Schools. **Lawrence, J.F.**, Cochran, E.S., Saltzman, J., Christensen, C.M., Hubenthal, M., and Chung, A.I.	INVITED: Documenting Transient Slip Events in Cascadia with Geodesy: Working Towards a Catalog of Slow Slip Events. **Schmidt, D.A.**, and Gao, H.	Seismic Wave Gradiometry Using the Wavelet Transform: Potential Application to Surface Wave Inversions Using USArray. **Poppeliers, C.**
5:00	Comparison of Seismicity of the Dead Sea Fault and San Andreas Faults. **Kutliroff, J.K.**,	Seismological Education and Outreach at a College Football Game: An Experiment to Record Crowd-Related Seismicity. **Nies, A.**, Haney, M.M., Zollweg, J., and the Boise State Football Seismology Team.	Comparison of Five Northern Washington Episodic Tremor and Slip Events. **Houston, H.B.**, Delbridge, B.G., Wech, A.G., and Creager, K.C.	Influence of Velocity Anisotropy on an Accuracy of Microearthquake Locations. **Chesnokov, E.M.**, and Krasnova, M.A.

Time	Salon A	Salon E	Salon F	Salon G
5:15	Non-Ergodic PSHA—Example. **Walling, M.A.**, and Abrahamson, N.A.	Translating Seismology into Simple Animations: A Powerful Learning Tool for Earth-science Educators. **Johnson, J.**, Bravo, T.K., and Butler, R.F.	Slow Slip Phenomena Not So Phenomenal? Peng, Z., and **Gomberg, J.**	INVITED: Imaging with Scattered Teleseismic Waves: Data, Method and Application to the Hellenic Subduction Zone. **Pearce, F.D.**, and Rondenay, S.
5:30	Testing the Plausibility of Anthropogenic versus Seismogenic Causes of the Rotation of a Lycien Sarcophagus in Pınara, SW-Turkey. **Hinzen, K.-G.**, Schreiber, S., and Yerli, B.	Teachable Moments: Capturing the Power of an Earthquake to Teach about Seismology. **Bravo, T.K.**, Butler, R.F., and Johnson, J.,	Slow Slip and Dynamic Rupture from Competition Between Dilatant Stabilization and Thermal Pressurization. **Segall, P.**, and Bradley, A.	Investigating the Limits of Ray-Based Global Surface-Wave Tomography. **Hjorleifsdottir, V.**, Dalton, C.A., Ekstrom, G.
6:45	Town Hall Meeting—Salon E & F (see page 260)			

Wednesday, 21 April—Morning Poster Sessions

Engaging Students and Teachers in Seismology: In Memory of John Lahr (see page 302)

1. Temblor: Simplifying Earthquake Visualization. **Powers, P.M.**
2. Introduction to Earthquake Focal Mechanisms Using Seismographs in Schools Data. **Levasseur, D.**, and Ford, S. R.
3. Teachers Involved in Expeditionary Seismology: The TIES that Bind. **Boyd, D.**, Dillon, T., Arratia, M., Ringgold Middle School, Rio Grande City, Tx Usa; Weart, Mote, A., Myrick, M., Ohman, S., Theis, H., Pulliam, J., Grand, S.P., Ellins, K., and Olson, H.
4. Networking in Educational Seismology: The IRIS Seismographs in Schools Program. **Bravo, T.K.**, Braile, L.W., Hubenthal, M., Taber, J., Toigo, M., and Wyatt, K.
5. Teachers on the Leading Edge: An Earth Science Teacher Professional Development Program Featuring Pacific Northwest Geologic Hazards. Butler, R.F., Granshaw, F., Butler, R.F., Groom, R., Hedeen, C., **Johnson, J.**, Magura, B., Pratt-Sitaula, B., Thompson, D., and Whitman, J.

Joint Inversion of Multiple Geophysical Data Sets for Seismic Structure (see page 303)

6. A Probabilistic Framework for the Joint Inversion of Multiple Datasets. Hauser, J., Dyer, K.M., **Pasyanos, M.E.**, Bungum, H., Faleide, J.I., and Clark, S.A.
7. Testing Joint Inversion of Travel Times and Gravity Data for Imaging of Western Colombia: Trade-offs and Sensitivities. **Rowe, C.A.**, Dionicio, L.V., Maceira, M., and Zhang, H.
8. Tomographic Imaging of the Upper Mantle beneath the Colorado Rocky Mountains from Simultaneous Joint Inversion of Teleseismic Body Wave Residuals and Bouguer Gravity. **MacCarthy, J.K.**, Aster, R.C., Hansen, S.M., and Dueker, K.G.
9. Joint Inversion of Seismic and Magnetotelluric Data in the Parkfield Region of California Using the Cross-Gradient Constraint. **Bennington, N.L.**, Thurber, C.H., Bedrosian, P., and Zhang, H.
10. Joint Inversion of InSAR and Seismic Waveform Data for the Finite-fault Solution of the 21 February 2008 Wells, Nevada Earthquake. **Ford, S.R.**, Dreger, D.S., and Ryder, I.
11. Joint Inversion of Rayleigh Wave Ellipticity and Spatial Autocorrelation Measurements. **Hobiger, M.**, Cornou, C., Le Bihan, Endrun, B., Renalier, F., Di Giulio, G., Savvaidis, A., Wathelet, M., and Bard, P.-Y.

Seismic Imaging: Recent Advancement and Future Directions (see page 305)

12. Characterization of the Closely-Spaced Earthquakes along the North Anatolian Fault Zone, NW Turkey. **Bulut, F.**, Bohnhoff, M., Ellsworth, W.L., and Dresen, G.
13. SORD as a Computational Platform for Earthquake Simulation, Source Imaging, and Full 3D Tomography. **Wang, F.**, Ely, G.P., and Jordan, T.H.
14. The Crustal and Uppermost Mantle Structure of Iran from 3D Seismic Tomography. **Sun, Y.**, Zeng, X., and Toksoz, M.N.
15. Seattle Basin Shear-Velocity Model from Noise Correlation Rayleigh Waves. **Delorey, A.A.**, and Vidale, J.E.
16. Testing Global 3D Travel Time Prediction for Earthquake Location. **Begnaud, M.**, Ballard, S., Rowe, C., Young, C., Steck, L., and Hipp, J.
17. Global 3-D P-Wave Tomography with Teleseismic and Regional Travel Time Prediction Capabilities. **Simmons, N.A.**, Myers, S.C., and Johannesson, G.
18. Determination and Validation of Regional 3-D Crust and Upper Mantle Vp and Vs Models and Their Tectonic Implications—Case Example from the Taiwan Region. **Chiu, J.M.**, Kim, K.H., Huang, B.S., Chen, K.C., Liang, W.T., Yen, H.Y., and Pujol, J.

Ground Motion: Observations and Theory (see page 306)

19. Experimental Evidence of Inhomogeneous P Wave at Very Low Strain. **Marcellini, A.**, Tento, A., and Daminelli, R.
20. Response Spectra of Probable Ground Motions for Nonlinear Analysis of Systems. **Malhotra, P.K.**
21. Strong Motion Recordings and Residual Displacements: What Are We Actually Recording in Strong Motion Seismology? **Graizer, V.**
22. 'Domitoring': First Results of the Seismic Surveillance of Cologne Cathedral. **Hinzen, K.-G.**, Fleischer, C., and Schock-Werner, B.

Seismologic Methods, Techniques, and Theory (see page 307)

23. Seismological Attenuation Coefficient and Q. **Morozov, I.B.**
24. Wave Equations in Nonlinear Elastic Anisotropic Randomly Inhomogeneous Media. **Chesnokov, E.M.**, Kukharenko, Y.A., and Goncharuk, S.
25. Smoothing-Free Earthquake Source Inversion: Physically-Guided Regularization in Finite Fault Modeling. **Song, S.**, and Somerville, P.
26. Determining the Focal Mechanisms of Earthquakes in Southern California by Full Waveform Modeling. **Busfar, H.A.**
27. Multiwavelet Seismic Wave Gradiometry: Application to the Glendora Array, Sullivan, IN, USA. **Poppeliers, C.**
28. A Bayesian Method for Single-Station Identification of Local and Regional Earthquake. **Ebel, J.E.**
29. Toward Using Eccentric Mass Shakers for Active Seismic Monitoring. **Niu, F.**, Silver, P., and Nigbor, R.
30. Thermal Anomalies Identification and Analysis of Several Earthquakes in Sichuan, China. **Zhao, J.**, Zhang, W., Wang, W., Yan, G., and Mu, X.

Wednesday, 21 April—Afternoon Poster Sessions

Numerical Prediction of Earthquake Ground Motion (see page 308)

31. Numerical Modeling of 3D Wave Propagation in the Grenoble Valley (French Alps) with Special Reference to the Duration Observed for Local Seismic Events. **Chaljub, E.**, Cornou, C., and Tsuno, S.
32. Euroseistest Numerical Simulation Project: Comparison with Local Earthquake Recordings for Validation. **Chaljub, E.**, Bard, P.Y., Hollender, F., Theodulidis, N., Moczo, P., Tsuno, S., Kristek, J., Cadet, H., and Bielak, J.
33. High-Frequency Generation in k^{-2} Kinematic Source Model. Causse, M.C., **Laurendeau, A.L.**, Cotton, F.C., and Mai, M.M.
34. Modeling of Scattering from the Pacific Trench of Mexico Excited by Teleseismic Body Waves. **Dominguez-Ramirez, L.**, Sanchez-Sesma, F., and Davis, P.
35. Numerical Analysis of Earthquake Ground Motion in the Mygdonian Basin, Greece: Comparison of 2D Wave Propagation in Linear and Nonlinear Media. **Bonilla, L.F.**, Gelis, C., Foerster, E., Mariotti, C., Pecker, A., Steinitz, B., Bard, P.Y., Tsuno, S., Hollender, F., Pitilakis, K., and Makra, K.
36. Stable Discontinuous Staggered Grid in the 4th-order Finite-difference Modeling of Seismic Ground Motion. **Kristek, J.**, Moczo, P., and Galis, M.
37. Seismic Wavefield Generated by SH Line Sources in Two Quarter Spaces with Scatterers Distributed around the Bimaterial Interface. **Benites, R.A.**, and Ben-Zion, Y.
38. Numerical Modeling of Earthquake Ground Motion in the Mygdonian Basin, Greece: Verification of the 3D Numerical Methods. **Moczo, P.**, Kristek, J., Franek, P., Chaljub, E., Bard, P.-Y., Tsuno, S., Iwata, T., Iwaki, A., Priolo, E., Klin, P., Aoi, S., Mariotti, C., Bielak, J., Taborda, R., Karaoglu, H., Etienne, V., and Virieux, J.
39. Formulation and Implementation of the Spectral Element Method (SEM) for Elastodynamic Problems. **Meza-Fajardo, K.C.**, and Papageorgiou, A.S.
40. Moderate Earthquake Ground Motion Validation in the San Francisco Bay Area. **Dreger,D.S.**, Kim, A., and Larsen, S.
41. Nonstandard FDTD Scheme for Computation of Elastic Waves. **Takenaka, H.**, Jafargandomi, A
42. Studying the Effect of Fault Roughness on Strong Ground Motion. **Shi, Z.**, and Day, S.
43. A Stochastic Earthquake Ground-Motion Prediction Model for the United Kingdom. **Rietbrock, A.**, Strasser, F., and Edwards, B.
44. The Big Ten Earthquake Scenarios for Southern California. **Ely, G.P.**, Jordan, T.H., Maechling, P., Olsen, K.B., Day, S.M., Minster, J.-B., Graves, R.W., Bielack, J., Taborda, R., Beroza, G., Ma, S., Cui, Y., Urbanic, J., and Callaghan, S.
45. 2D P-SV Nonlinear Investigations of Basin-Edge Amplification. **O'connell, D.R.H.**, Liu, P.C., and Bonilla, L.F.
46. The SCEC-USGS Rupture Dynamics Code Comparison Exercise. **Harris, R.A.**, Barall, M., Archuleta, R., Andrews, D.J., Dunham, E., Aagaard, B., Ampuero, J.P., Cruz-Atienza, V.M., Dalguer, L., Day, S., Duan, B., Ely, G., Gabriel, A., Kaneko, Y., Kase, Y., Lapusta, N., Ma, S., Noda, H., Oglesby, D., Olsen, K., Roten, D., and Song, S.
47. Long Period ($T > 0.8s$) Strong Ground Motion Simulations along the Wasatch Front. **Moschetti, M.P.**, Ramirez-Guzman, L., and Bielak, J.
48. Effect of Some Key Parameters on Directivity of Near-fault Ground Motions Derived from a Homogeneous Strike-Slip Fault Modeling. **Hu, J.**, and Xie, L.
49. The Dynamics of Fault Stepovers with Rate-State Friction. **Ryan, K.**, and Oglesby, D.D.

Magnitude Scaling and Regional Variation of Ground Motion (see page 312)

50. Accelerometer Housing as a Cause of Variation of Recorded Ground Motion: The Example of the L'Aquila (Italy) 2009 Earthquake. Ditommaso, R., and **Mucciarelli, M.**

51. Ground Motion in Northen Sicily (Italy). **D'amico, S.**, Mercuri, A., Malagnini, L., Herrmann, R.B., and Akinci, A.
52. Towards Regional Ground Motion Models on the Eastern North Anatolian Fault Zone. **Ugurhan, B.**, and Askan, A.
53. Source Scaling Relationship for M4.6-M7.6 Earthquakes in Taiwan Orogenic Belt. Yen, Y.-T., and **Ma, K.-F.**
54. Empirical Characterization of Ground Motion Processes in Japan, and Comparison to Other Regions. **Ghofrani, H.**, and Atkinson, G.M.
55. Ground Motions from the 29 September 2009 Samoa M8.0 Earthquake and Aftershocks. **McNamara, D.**, Meremonte, M., Leeds, A., Fox, J., Petersen, M., and Gee, L.
56. Ground-Motion Prediction Equations for Eastern North America from a Hybrid Empirical Method. Pezeshk, S., **Zandieh, A.**, and Tavakoli, B.
57. Investigating the Regional Dependence of Ground-Motion Models from an Information-Theoretic Perspective. Delavaud, E., **Scherbaum, F.**, Kuehn, N., and Allen, T.
58. A Hierarchical Global Ground Motion Model to Take into Account Regional Differences. **Kuehn, N.M.**, Scherbaum, F., Riggelsen, C., and Allen, T.
59. New Attenuation Relationship for Far Field Earthquakes Caused by Dip Slip Mechanism. **Adnan, A.B.**, Meldi, S., Masyhur, I.
60. Energetic and Enervated Earthquakes: Real Scatter in Apparent Stress and Implications for Ground Motion Prediction. **Baltay, A.S.**, Prieto, G.A., Ide, S., and Beroza, G.C.
61. Surface and Borehole Estimates of Single-Station Standard Deviation. **Rodriguez-Marek, A.**, Bonilla, L.F., and Cotton, F.

The Seismo-Acoustic Wavefield: Fusion of Seismic and Infrasound Data (see page 314)

62. Seismo-acoustic Investigation at Mt. Etna Volcano: the Case Study of November 16, 2006. Sciotto, M., Cannata, A., Privitera, E., Di Grazia, G., **Gresta, S.**, and Montalto, P.
63. Low Frequency Sound from Earthquakes: What Can We Uniquely Learn from Seismo-Acoustics? **Arrowsmith, S.**, Hartse, H., Whitaker, R., and Burlacu, R.
64. Robust Detection and Location of Infrasound and Seismo-Acoustic Events. **Arrowsmith, S.**, Whitaker, R., Modrak, R., and Anderson, D.
65. Monitoring of Micro-Seismicity Using the Temporal Seismo-Acoustic Network in Eastern Coastal Area of the Korean Peninsula. **Jeon, J.**, and Che, I.
66. Comparing Coupled and Separated Finite-Difference Calculations of Seismo-Acoustic Wave Propagation. **Chael, E.P.**, Aldridge, D.F., Preston, L., and Symons, N.P.
67. The HUMBLE REDWOOD Seismic/Acoustic Coupling Experiments: Joint Inversion for Yield Using Seismic, Acoustic and Crater Data. **Foxall, B.**, Marrs, R., Lenox, E., Reinke, R., Seastrand, D., Bonner, J., Mayeda, K., and Snelson, C.
68. The Utilization of Portable Seismic Stations and a Small-Size Infrasound Array for Characterizing Local Seismicity along Coastal Areas in Korea. **Che, I.Y.**, and Jeon, J.S.
69. Lessons Learned from the Design, Installation and Operation of Seismo-Acoustic Arrays. **Hayward, C.T.**, Stump, B.W., Kubacki, R., and Golden, P.
70. The Los Alamos Seismo-Acoustic Research Center. Arrowsmith, S., **Roberts, P.**, Baker, D., Stead, R., and Whitaker, R.

Operational Earthquake Forecasting (see page 316)

71. CSEP: Preliminary Results of the New Zealand Earthquake Forecast Testing Center. **Gerstenberger, M.C.**, Christophersen, A., and Rhoades, D.A.
72. A New Generic Model for Aftershock Decay in Earthquake Forecasting. **Christophersen, A.**, and Gerstenberger, M.C.
73. Earthquake Early Warning: Update on Prospective Users' Perspectives. **Savage, W.U.**, Nishenko, S.P., and Johnson, T.B.
74. An Intermediate-Term Attenuation Precursor to the 2004 Parkfield Earthquake: Was It Fluid Driven? **Chun, K.-Y.**, Yuan, Q.-Y., and Henderson, G. A.
75. Earthquakes Prediction: Proper and Non-Proper Seismicity, Their Relations with Geophysical Fields' Precursors. **Kerimov, I.G.**, and Kerimov, S.I.
76. Multidisciplinary Approach for Atmospheric Earthquake Precursors Validation. **Ouzounov, D.P.**, Pulinets, S.A., Liu, J.Y., Hattori, K., Parrot, M., Taylor, P., and Kafatos, M.
77. Instrumentally Recorded Precursors for the 24 May 2006, Mw=5.4, Morelia Fault Earthquake Sequence, in Mexicali Valley, Baja California, Mexico. Sarychikhina, O., **Glowacka, E.**, Vázquez, R., Munguía, L., Farfán, F., and Díaz de Cossío Batani, G.

Thursday, 22 April—Concurrent SSA Oral Sessions

Time	*Salon A*	*Salon E*	*Salon F*	*Salon G*
	Operational Earthquake Forecasting Session Chairs: Gordon Woo, Michael Blanpied, and Warner Marzocchi (see page 317)	**Numerical Prediction of Earthquake Ground Motion** Session Chairs: Emmanuel Chaljub, Peter Moczo, and Steven M. Day (see page 319)	**Near-Surface Deformation Associated with Active Faults** Session Chairs: Lee M. Liberty and Thomas L. Pratt (see page 323)	**The Seismo-Acoustic Wavefield: Fusion of Seismic and Infrasound Data** Session Chairs: Brian Stump, Jeff Johnson, and Stephen Arrowsmith (see page 326)
8:30	Operational Earthquake Forecasting and Risk Management. **Woo, G.**	INVITED: High Frequency Ground Motion from Spontaneous Ruptures on Rough Faults. **Dunham, E.M.**, and Kozdon, J.E.	Crustal Deformation Modeling in the Central United States. **Boyd, O.S.**, Zeng, Y., Frankel, A.D., and Ramirez-Guzman, L.	The Seismo-Acoustic Wavefield: A New Paradigm in Studying Geophysical Phenomena. **Arrowsmith, S.**, Stump, B., Johnson, J., and Drob, D.
8:45	INVITED: Prospects for Operational Earthquake Forecasting. **Jordan, T.H.**	Accurate and Stable Treatment of Nonlinear Fault Boundary Conditions with Higher-Order Finite Difference Methods. **Kozdon, J.E.**, Dunham, E.M., and Nordström, J.	Recurrent Eocene and Quaternary Uplift Above the Southwestern Blytheville Arch, Arkansas: Is It Contributing to the Formation of Lake St. Francis? **Williams, R.A.**, Stephenson, W.J., Pratt, T.L., and Odum, J.K.	INVITED: Harmonic Tremor on Active Volcanoes: Seismo-acoustic Wavefields. **Lees, J.M.**, and Johnson, J.B.
9:00	Development of an Official Operational Earthquake Forecast for California (UCERF3 by the ongoing WGCEP). **Field, E.H.**	Dynamic Modeling of Mw 7.0 or Larger Earthquakes on the Sierra Madre–Cucamonga Fault System in Los Angeles: Effects of Inelastic Off-Fault Response. **Ma, S.**, Day, S.M.	Evidence for One or More Major Late-Quaternary Earthquakes and Surface Faulting in the East Tennessee Seismic Zone. **Vaughn, J.D.**, Obermeier, S.F., Hatcher, R.D., Howard, C.W., Mills, H.H., and Whisner, S.C.	Seismo-Acoustic Signals Produced by the Rapidly Inflating Santiaguito Lava Dome, Guatemala. **Johnson, J.B.**, and Lees, J.M.
9:15	INVITED: Operational Earthquake Forecasting in Italy. **Marzocchi, W.**	Dynamic Ground Motion in Fault Stepovers with Material Contrasts. **Lozos, J.C.**, Oglesby, D.D., and Brune, J.N.	Seismic Potential of the Pishin/Mach Shear Zone in Northern Baluchistan, Pakistan. **Kakar, D.M.**, Szeliga, W., Bilham, R.,	INVITED: Probing the Atmosphere and Atmospheric Sources with the USArray. **Hedlin, M.A.H.**, Drob, D., Walker, K., De Groot-and Hedlin, C.D.
9:30	Development of an Earthquake Impact Scale for use with the USGS PAGER System. **Wald, D.J.**, Marano, K.D., Jaiswal, K.S., Hearne, M., and Bausch, D.	Ground Motion from Dynamic Ruptures on the Wasatch Fault Embedded in a 3-D Velocity Structure. **Liu, Q.**, Archuleta, R.J., and Smith, R.B.	Creep on the Ornach-Nal Fault, India's Western Boundary with Asia. **Bilham, R.**, Szeliga, W., and Lodi, S.	Atmospheric Measurements with the USArray Transportable Array. **Busby, R.W.**, Woodward, R., Hafner, K., Hedlin, M., and Vernon, F.
9:45	Are Mitigation Actions Warranted? The Case of the 2009 L'Aquila Earthquake. **Van Stiphout, T.**, Wiemer, S., and Marzocchi, W.	Ground Motion Predictions from 0–10 Hz for M7 Earthquakes on the Salt Lake City Segment of the Wasatch Fault, Utah. **Roten, D.**, Olsen, K.B., Pechmann, J.C., Cruz-Atienza, V.M., and Magistrale, H.	Probabilistic Estimates of Surface Slip including the Effects of Creep and Afterslip. **Aagaard, B.T.**, Lienkaemper, J.L., and Schwartz, D.P.	INVITED: Seismo-acoustic Studies in the European Arctic. **Gibbons, S.J.**, and Ringdal, F.
10:00	Break			

Time	Salon A	Salon E	Salon F	Salon G
	Operational Earthquake Forecasting (*continued*)	**Numerical Prediction of Earthquake Ground Motion** (*continued*)	**Near-Surface Deformation Associated with Active Faults** (*continued*)	**The Seismo-Acoustic Wavefield: Fusion of Seismic and Infrasound Data** (*continued*)
10:30	Tobago 2011—A Prospective Case for Operational Earthquake Forecasting. **Latchman, J.L.**, and Aspinall, W.P.	Calibration of Simulated Motions from Spontaneous Rupture Models Relative to NGA Ground Motion Prediction Equations. **Seyhan, E.**, Star, L.M., Graves, R.W., and Stewart, J.P.	Slip Partitioning in Oblique Fault Systems. Nunley, M., **Oglesby, D.D.**, and Bowman, D.	INVITED: The Seismo-Acoustic Boundary Layer. **Langston, C.A.**
10:45	Testing and Evaluating Operational Earthquake Forecasts. **Schorlemmer, D.**, Jordan, T.H., Jackson, D.D., and the CSEP Working Group.	INVITED: Efficient Simulation of Anelastic Wave Propagation by the Octree-based Finite Element Method—An Improved Approach. **Bielak, J.**, Karaoglu, H., and Taborda, R.	GPS Constraints on Deformation and Fault Slip Rates in the Back Arc of the Cascadia Subduction Zone from Northern California to Central Oregon. **Thatcher, W.**	Seismic and Acoustic Waves Generated by an Exploding Meteoroid. **Evers, L.G.**, and Dost, B.
11:00	Time-Dependent Earthquake Forecasts Based on Smoothed Seismicity and Rate-And-State Friction. **Helmstetter, A.**, and Werner, M.	On Accuracy of the Numerical Schemes in Media With a Large P-wave to S-wave Speed Ratio. **Moczo, P.**, Kristek, J., Pazak, P., Galis, M., and Chaljub, E.	Possible Late Quaternary Folding and Faulting Along Umtanum Ridge, Yakima Fold and Thrust Belt, Washington. **Sherrod, B.L.**, Blakely, R.J., Barnett, E.A., and Knepprath, N.	INVITED: Source Signature and Propagation Path Effects from Topography on Local Seismic-Acoustic (Infrasound) Data. **McKenna, M.H.**, Lester, A.P., McKenna, J.R., Anderson, T.S., Kopenhoeffer, K., Gibson, R., and McComas, S.
11:15	Automated Calculation of Post-Earthquake Damage State Exceedance Probabilities Considering the Threat of Aftershocks. **Gerstenberger, M.C.**, Luco, N., Uma, S.R., and Ryu, H.	Numerical Prediction of Long-Period Earthquake Ground Motion in Japan. **Koketsu, K.**, Miyake, H., Hikima, K., Hayakawa, T., Suzuki, H., and Watanabe, M.	Geometry and Rupture History of the Seattle Fault Zone, Washington State, from Modeling of Late Holocene Land-level Changes. **Pratt, T.L.**	Detection of Short Time Transients From Spectrograms Using Scan Statistics. **Taylor, S.R.**, Arrowsmith, S.J., and Anderson, D.N.
11:30	Early Aftershocks Statistics: First Results of Prospective Test of Alarm-Based Model (EAST) and Setting a Frequency-Based Model. **Shebalin, P.**, Narteau, C., Holschneider, M., and Scholrlemmer, D.	Accurate Prediction of Ground Motion Using an hp-adaptive Discontinuous Galerkin Finite-Element Method. **Etienne, V.**, Chaljub, E., Virieux, J., and Operto, S.	Active Thrusting within the Himalayan Orogenic Wedge in the Kashmiri Himalaya. Gavillot, Y.G., **Meigs, A.M.**, Hebeler, A.H., Yule, J.D., Madden, C., Malik, M.M., Yeats, R.Y., and Kaericher, M.K.	Infrasound Network Design for Recovering Near-Surface Atmospheric Structure. **Marcillo, O.E.**, and Johnson, J.B.
11:45	Using Simple Models for Fast, Robust Results. **Holliday, J.R.H.**, and Rundle, J.B.R.	Efficient Parallel Seismic Simulations Including Topography and 3-D Material Heterogeneity on Locally Refined Composite Grids. **Petersson, N.A.**, and Rodgers, A.	Characterizing Very Slow Faults in an Active Pull-Apart Setting, Vienna Basin, Austria. **Decker, K.**, and Hintersberger, E.	Seismo-Acoustic Signals from a Semi-Urban Environment. **Lewkowicz, J.**, Bonner, J.L., Leidig, M., and Britton, J.M.

Time	Salon A	Salon E	Salon F	Salon G
12:00	Lunch			
	Quantification and Treatment of Uncertainty and Correlations in Seismic Hazard and Risk Assessments Session Chairs: Chris H. Cramer, Jack Baker, and Tuna Onur (see page 328)	**Numerical Prediction of Earthquake Ground Motion** (*continued*)	**Earthquake Debates** Session Chairs: Danijel Schorlemmer, David D. Jackson, Jeremy D. Zechar, and Warner Marzocchi (see page 330)	**Seismic Structure and Geodynamics of the High Lava Plains and Greater Pacific Northwest** Session Chairs: David E. James, G. Randy Keller, and Matthew J. Fouch (see page 331)
1:30	Non-Stationary Path Effects in Portfolio Loss Computation. **Walling, M.A.**, Luco, N., and Ryu, H.	Euroseistest Verification and Validation Project: An International Effort to Evaluate Ground Motion Numerical Simulation Relevance. **Hollender, F.**, Manakou, M., Bard, P.-Y., Chaljub, E., Raptakis, D., Pitilakis, K., Tsuno, and S.	Invited: A Discussion of Elastic Rebound, Earthquake Recurrence and Characteristic Earthquakes. **Ellsworth, W.L.**, and Weldon II, R.J.	Seismic Imaging of Remnant Slabs, Slab Gaps and Problematic Plumes in the Pacific Northwest. **James, D.E.**, Fouch, M.J., Roth, J.B., and Carlson, R.W.
1:45	Impacts of Earthquake Hazard Uncertainties on Probabilistic Portfolio Loss Risk Assessment. **Molas, G.L.**, Onur, T., Bryngelson, J., and Shome, N.	Amplification and Attenuation in Southern California Basins Extracted from Ambient Seismic Field Analysis. **Denolle, M.**, Beroza, G., Prieto, G., and Lawrence, J.	Invited: Reply to Ellsworth and Open Discussion. **Weldon, II, R.J.**	Invited: Seismic Evidence for Fossil Subduction and Small-Scale Convection Beneath the Northwestern U.S. **Schmandt, B.**, and Humphreys, E.
2:00	Updated Computation of Probability Distributions of Regional Annual Losses for Seismic Design Alternatives in Memphis, Tennessee. **Ryu, H.**, Luco, N., Karaca, E., and Walling, M.	Invited: Elastic Model Up-Scaling for the Elastic Wave Equation Based on Non-Periodic Homogenization. **Capdeville, Y.**, Guillot, L., and Marigo, J.-J.	Invited: A Discussion of Elastic Rebound, Earthquake Recurrence and Characteristic Earthquakes. **Weldon, II, R.J.**, and Ellsworth, W.L.	Invited: Lithosphere-Asthenosphere Interaction Beneath the Pacific Northwest From the Integrated Analysis of Body and Surface Waves. **Obrebski, M.**, Allen, R., Porritt, R., Pollitz, F., and Hung, S.-H.
2:15	A Bayesian Ground Motion Model for Estimating the Covariance Structure of Ground Motion Intensity Parameters. **Kuehn, N.M.**, Riggelsen, C., Scherbaum, F., and Allen, T.	Invited: Numerical Insights of 2D-PSV Nonlinear Basin Response Analyses. **Bonilla, L.F.**, Gelis, C., and Liu, P.C.	Invited: Reply to Weldon and Open Discussion. **Ellsworth, W.L.**	Invited: Surface Wave Constraints on the Causes of High Lava Plains Volcanism. **Wagner, L.S.**, Fouch, M.J., Long, M.D., James, D.E., and Forsyth, D.
2:30	Spatial Correlation of Earthquake Ground Response Spectra: Measurement Techniques and Implications for Regional Infrastructure Risk. **Baker, J.W.**, and Jayaram, N.	Invited: Quantifying the Risk Posed to Tall Steel Frame Buildings in Southern California from Earthquakes on the San Andreas Fault. Mourhatch, R., Siriki, H., and **Krishnan, S.**	Invited: The Case for Gutenberg-Richter Scaling on Faults. **Page, M.T.**, Felzer, K.R., Weldon II, R.J., Biasi, G.P., Alderson, D.L., and Doyle, J.C.	Invited: Regional Electrical Conductivity of the Pacific Northwestern U.S. from EMScope. **Egbert, G.D.**, Schultz, A., and Fouch, M.J.

Time	Salon A	Salon E	Salon F	Salon G
2:45	The CyberShake Project: Full-Waveform Probabilistic Seismic Hazard Calculations for Southern California. **Graves, R.**, Callaghan, S., Small, P., Mehta, G., Milner, K., Juve, G., Vahi, K., Field, E., Deelman, E., Okaya, D., Maechling, P., and Jordan, T.	Site Effects in Nonlinear Structural Performance Predictions. **Li, W.**, and Assimaki, D.	INVITED: Reply to Page and Open Discussion. **Schwartz, D.P.**	INVITED: Raytrace Models from the High Lava Plains (HLP) Controlled-source Experiment. **Cox, C.M.**, Keller, G.R., Harder, S.H., and Klemperer, S.
3:00	Break			
	Quantification and Treatment of Uncertainty and Correlations in Seismic Hazard and Risk Assessments (*continued*)	**Deterministic Simulated Ground Motion Records under ASCE 7-10 as a Bridge Between Geotechnical and Structural Engineering Industry** Session Chairs: Alexander Bykovtsev and Walter Silva (see page 334)	**Earthquake Debates** (*continued*)	**Seismic Structure and Geodynamics of the High Lava Plains and Greater Pacific Northwest** (*continued*)
3:30	An Empirical Perspective on Uncertainty in Earthquake Ground Motions. **Atkinson, G.M.**	INVITED: Requirements for Development of Acceleration Time Histories per ASCE 7-10 Standard. **Crouse, C.B.**	INVITED: Do Large Earthquakes on Faults Follow a Gutenberg-Richter or Characteristic Distribution?: A Characteristic View. **Schwartz, D.P.**	INVITED: P-to-S Receiver Function Imaging of the Crust Beneath the High Lava Plains of Eastern Oregon. **Eagar, K.C.**, Fouch, M.J., James, D.E., and Carlson, R.W.
3:45	Intra-Event Uncertainty of Long-Period Ground Motions For Large Earthquakes With Southeast-Northwest Rupture Direction on the Southern San Andreas Fault. **Olsen, K.B.**, Day, S.M., Dalguer, L.A., Cui, Y., Maechling, P., Jordan, T., Chourasia, A., and Okaya, D.	INVITED: On the Sensitivity of Near-Source Ground Motions to Heterogeneity of Fault Ruptures. **Rowshandel, B.**	INVITED: Reply to Schwartz and Open Discussion. **Page, M.**	An Integrated Analysis of Lithospheric Structure in the High Lava Plains region: Preliminary Observations. **Keller, G.R.**, Okure, M., Wallet, B., and Cox, C.
4:00	Empirical Testing of Probabilistic Seismic Hazard Estimates. **Albarello, D.**, D'Amico, V., and Mucciarelli, M.	INVITED: A Consideration of Uncertainty when Selecting Near-Source Ground Motions for Design. **Olsen, A.H.**, Heaton, and T.H.	INVITED: Applications of Earthquake Simulators to Assessments of Earthquake Probabilities. **Dieterich, J.**, and Richards-Dinger, K.	Crustal Stress Indicators for Southwest British Columbia: What Controls Faulting in the Crust? **Balfour, N.J.**, Cassidy, J., and Dosso, S.
4:15	Uncertainty in Probabilistic Fault Displacement Hazard Analysis. **Moss, R.E.S.**, and Travasarou, T.	INVITED: Structural Effects of Earthquake Vertical Ground Motions. **Sprague, H.O.S.**	INVITED: Reply to Dieterich and Open Discussion. **Michael, A.J.**	Coulomb Stress Interactions among M≥6 Earthquakes in the Gorda Deformation Zone and on the Mendocino Fracture Zone, Cascadia Megathrust and Northern San Andreas Fault. **Rollins, J.C.R.**, and Stein, R.S.S.

Time	Salon A	Salon E	Salon F	Salon G
4:30	A First Attempt to Constrain Reliability and Measurement Error Associated with Expert Opinion and Judgment in Interpreting Paleoseismic Data. **Grant Ludwig, L.**, and Runnerstrom, M.G.	INVITED: Earthquake Source Statistics Including Variability of Slip for Simulation-Based Ground Motion Prediction. **Song, S.**, Somerville, P., and Graves, R.	INVITED: Barriers to the Use of Physics-Based Seismicity Simulators in Seismic Hazards Assessments. **Michael, A.J.**	Upper Mantle Anisotropy Beneath the High Lava Plains: Linking Upper Mantle Dynamics to Surface Tectonomagmatism. Long, M.D., **Fouch, M.J.**, Wagner, L.S., and James, D.E.
4:45	Possible Explanations for Discrepancies Between Precario0usly Balanced Rocks and 2008 Hazard Maps. **Brune, J.**, Purvance, M., Anooshehpoor, R., Anderson, J., Grant-Ludwig, L., Rood, D., and Kendrick, K.	INVITED: Deterministic Simulated Ground Motion (SGM) Records under ASCE 7-10 as a Bridge between Geotechnical and Structural Engineering Industry. **Bykovtsev, A.S.**	INVITED: Reply to Michael and Open Discussion. **Dieterich, J.H.**	The Mantle Flow Field Beneath Western North America. **Fouch, M.J.**, and West, J.D.
5:15	Joyner Lecture: Progress and Controversy in Seismic Hazard Mapping. **Frankel, A**. (see page 334).			

Thursday, 22 April—Morning Poster Sessions

Characterizing the Next Cascadia Earthquake and Tsunami (see page 335)

1. An Evaluation of Tsunami Evacuation Options of Padang, West Sumatra, Indonesia. **Cedillos, V.**, Deierlein, G.G., Henderson, J.S., Ismail, F.A., Syukri, A., Toth, J., Tucker, B.E., and Wood, K.R.
2. Reconciling Recurrence Interval Estimates, Southern Cascadia Subduction Zone. **Patton, J.R.**, and Leroy, T.H.
3. Cascadia Tremor and Its Megathrust Implications. **Wech, A.G.**, and Creager, K.C.
4. HAZUS Analyses of 15 Earthquake Scenarios in the State of Washington. **Terra, F.M.**, Wong, I.G., Frankel, A., Bausch, D., Biasco, T., and Schelling, J.D.
5. The National Science Foundation American Reinvestment and Recovery Act Cascadia Initiative. **Jackson, M.**, Woodward, R., and Toomey, D.
6. The 17 November, 2009 Haida Gwaii (Queen Charlotte Islands), British Columbia, Earthquake Sequence. **Cassidy, J.F.**, Rogers, G.C., Brillon, C., Kao, H., Mulder, T., Dragert, H., Bird, and A.L., Bentkowski, W.

The Evolution of Slow Slip and Tremor in Time and Space (see page 336)

7. Imaging Shallow Cascadia Structure with Ambient Noise Tomography. **Porritt, R.W.**, Allen, R.M., Shapiro, N.M., Boyarko, D.C., Brudzinski, M.R., O'Driscoll, L., Zhai, Y., Humphreys, E.D., and Levander, A.R.
8. PBO Strainmeter Measurements of Cascadia Slow Slip and Tremor Events, 2005–2010. Hodgkinson, K., **Mencin, D.**, Henderson, B., Borsa, A., Gallaher, W., Gottlieb, M., Johnson, W., Van Boskirk, and Jackson, M.
9. Constraints on Aseismic Slip During and Between Northern Cascadia Episodic Tremor and Slip Events from Plate Boundary Observatory Borehole Strainmeters. **Roeloffs, E.A.**, and McCausland, W.A.
10. Cascadia Slow slip Events Found in Water Level Changes at Tidal Stations. **Alba, S.K.M.**, Weldon II, R.J., Livelybrooks, D., and Schmidt, D.A.
11. On the Temporal Evolution of an ETS Event along the Northern Cascadia Margin. **Dragert, H.**, Wang, K., and Kao, H.
12. Tectonic Tremor Near the Calaveras Fault Triggered by Large Teleseisms. **Aguiar, A.C.**, Brown, J.R., and Beroza, G.C.
13. Tidal Triggering of LFEs near Parkfield, CA. **Thomas, A.T.**, Burgmann, R.B., and Shelly, D.R.
14. Investigating Low Frequency Impulsive Events at Slumgullion Landslide. **Macqueen, P.**, Gomberg, J., Schulz, W., Bodin, P., Foster, K., Kean, J., and Creager, K.
15. The Seismic Story of the Nile Valley Landslide - Foreshocks, Mainshocks, and Aftershocks. Allstadt, K., **Vidale, J.**, Thelen, W., Sarikhan, I., and Bodin, P.

Monitoring for Nuclear Explosions (see page 338)

16. Recent Fundamental Advances in Seismic Monitoring. **Willemann, R.J.**
17. Towards Continental Scale Regional Phase Amplitude Tomography. **Phillips, W.S.**, Yang, X., and Stead, R.J.
18. Station Set Residual: Event Classification Using Historical Distribution of Observing Stations. Procopio, M.J., **Lewis, J.E.**, and Young, C.J.

19. IMS Seismic Stations Instrumentation Challenges. **Starovoit, Y.O.**, and Grenard, P.
20. ISC Contribution to Monitoring Research. **Storchak, D.A.**, Bondár, I., Harris, J., and Gaspà, O.
21. Comprehensive Nuclear Test Ban Treaty (CTBT) Monitoring in the Context of the National Data Centre Preparedness Exercise (NPE). **Coyne, J.**, Kitov, I., Krysta, M., Becker, A., Brachet, N., and Mialle, P.
22. Crust and Upper Mantle Tomography using Pn, Pg, Sn, and Lg Phases for Improved Regional Seismic Travel Time Prediction. **Myers, S.C.**, Begnaud, M.L., Ballard, S., Pasyanos, M.E., Phillips, W.S., Ramirez, A.L., Antolik, M.S., Hutchenson, K.D., Dwyer, J.J., Rowe, C.A., and Wagner, G.S.
23. A New Approach for Improved Epicenter Location of Regional Earthquakes Using a Sparse Remote Network. **Song, F.**, Fehler, M.C., Toksöz, M.N., and Lee, W.
24. Toward an Empirically-based Parametric Explosion Spectral Model. **Ford, S.R.**, and Walter, W.R.
25. Modeling Rg from the HUMBLE REDWOOD II Experiment: A Blind Test for Yield and Depth of Burial Estimation. **Bonner, J.L.**, Reinke, R., Lenox, E., Foxall, B., and Mayeda, K.
26. Analysis of Repeated Explosions at Degelen Mountain in the Semipalatinsk Test Site, Kazakhstan. **Stroujkova, A.**, and Bonner, J.L.
27. Exploring the Limits of Waveform Correlation Event Detection as applied to Three Earthquake Aftershock Sequences. **Carr, D.B.**, Resor, M.E., and Young, C.J.
28. Automatic Hydroacoustic Phase Identification using a Two-Stage Neural Net. **Salzberg, D.**, Dysart, P., and Lockwood, M.
29. Routine Infrasound Event Detection and Location at the IDC. Brachet, N., Mialle, P., Bittner, P., and **Given, J.**
30. Theoretical and Experimental Developments in Ground to Ground Infrasound Propagation. **Waxler, R.**, Talmadge, C.L., Drob, D., Chunchuzov, I., Hetzer, C., Assink, J., Blom, P., and Di, X.
31. What InSAR Can Tell Us About Underground Nuclear Explosions: A Decade of Experience. **Vincent, P.**, and Buckley, S.M.

Recent Advances in Source Parameters and Earthquake Magnitude Estimations (see page 342)

32. Moment Magnitudes in the Middle East from Regional Coda Wave Envelopes. **Gok, R.**, Mayeda, K., Pasyanos, M.E., Matzel, E., Rodgers, A.J., and Walter, W.R.
33. Temporal and Spatial Variations of Local Magnitudes in Alaska and Aleutians and Calibration with Moment Magnitudes. **Ruppert, N.A.**, and Hansen, R.A.
34. New Developments in Earthquake Monitoring in Switzerland. **Olivieri, M.**, Clinton, J., Deichmann, N., Husen, S., and Giardini, D.
35. Seismic Quality Factor and Source Parameters of the Baikal Rift System Earthquakes. **Dobrynina, A.A.**, Chechelnitsky, V.V., Chernykh, E.N., and Sankov, V.A.
36. A General Method to Estimate Earthquake Moment and Magnitude Using Regional Phase Amplitudes. **Pasyanos, M.E.**
37. Detailed Results and Validations of the SCARDEC Method. Ferreira, A.M.G., **Vallée, M.**, and Charléty, J.

Deterministic Simulated Ground Motion Records under ASCE 7-10 as a Bridge Between Geotechnical and Structural Engineering Industry (see page 343)

38. Invited: Deterministic Simulations of Nonlinear Vibration of Viscoelastic Elements in Thin-Walled Constructions with Variable Rigidity. **Abdikarimov, R.A.**
39. Invited: Deterministic Calculation of Dynamic Stability of Viscoelastic Elements in Thin-Walled Constructions with Variable Rigidity. **Abdikarimov, R.A.**, and Khodzhaev, D.A.
40. Invited: Simulated Ground-Motion (SGM) Procedure with Time History Analysis for Bridges, High-Rise Buildings and Essential Facilities Located within 5 km of a Fault Zone. **Bykovtsev, A.S.**
41. Invited: Site Specific Seismic Investigation (SSSI) for Large Landslides in Santa Barbara and Ventura Counties, California. **Bykovtsev, A.S.**
42. Invited: Deterministic Calculation of Nonlinear Vibrations of Viscoelastic Orthotropic Cylindrical Panels with Concentrated Masses. **Khodzhaev, D.A.**
43. Invited: Addressing Surface Faulting at Caltrans Bridges. **Merriam, M.**, and Yashinsky, M.
44. Invited: Detection and Identification of Seismic Phases on Engineered Structures. **Baker, M.R.**

Quantification and Treatment of Uncertainty and Correlations in Seismic Hazard and Risk Assessments (see page 344)

45. Ground Motion Uncertainty in ShakeMap Constrained by Observations, Prediction Equations, and Empirical Studies. **Worden, C.B.**, Wald, D.J., Lin, K., and Cua, G.
46. A Generalised Conditional Intensity Measure Approach and Holistic Ground Motion Selection. **Bradley, B.A.**, University of Canterbury, Christchurch, New Zealand, brendon.bradley@canterbury.ac.nz
47. Estimating Epistemic Uncertainty in the Location and Magnitude of Historical Earthquakes. **Bakun, W.H.**, Gomez Capera, A.A., and Stucchi, M.

Thursday, 22 April—Afternoon Poster Sessions

Near-Surface Deformation Associated with Active Faults (see page 345)

48. What Is the Effective Number of Parameters in a Fault Slip Model? **Funning, G.J.**
49. Revisiting Surface Rupture Mapping of the 2002 M7.9 Denali Fault Earthquake with LiDAR. **Haeussler, P.J.**, Labay, K., Schwartz, D.P., and Seitz, G.G.

50. Spatial and Temporal Variability of Submarine Landslide Deposits Triggered by Megathrust Earthquakes at Port Valdez, Alaska. **Ryan, H.F.**, Haeussler, P.J., Lee, H.J., Parsons, T., and Sliter, R.W.
51. A Tunnel Runs through It—An inside View of the Thrust-Faulted Portland Hills, Oregon. **Wells, R.**, Walsh, K., Peterson, G., Fleck, R., Beeson, M., Evarts, R., Burns, S., Blakely, R., and Duvall, A.
52. Shallow Crustal Structure in the South Georgia Rift near the Epicenter of the 1886 Charleston, South Carolina Earthquake. **Beale, J.N.**, Buckner, and Chapman, M.C.
53. Determining Earthquake Recurrence Over the Past 3 - 4 Events on the Southern Santa Cruz Mountains Section of the San Andreas Fault. **Streig, A.R.**, and Dawson, T.E.
54. Late Quaternary Shortening and Earthquake Chronology of an Active Fault in the Kashmir Basin, Northwest Himalaya. **Madden, C.**, Trench, D., Meigs, A., Ahmad, B., Bhat, M.I., and Yule, J.D.
55. Middle Holocene surface rupture of the Riasi fault, Kashmir, India. **Hebeler, A.**, Yule, J.D., Madden, C., Malik, M., Meigs, A., Gavillot, Y., and Kaericher, M.
56. Timing and Magnitude of Late Quaternary Paleoearthquakes on the South Kochkor Thrust fault, central Tien Shan, Kyrgyz Republic. **Weldon, L.M.**, Djumabaeva, A., Abdrakhmatov, K., Weldon, II, R.J., and Bemis, S.
57. Tracing Active Faulting in the Inner Continental Borderland, Southern California, Using New High-Resolution Seismic Reflection and Bathymetric Data. **Conrad, J.E.**, Ryan, H.F., and Sliter, R.W.
58. The San Andreas Fault Zone Directly Offshore Pacifica and Daly City, California: Complex Deformation and Previously Unmapped Structures. **Ross, S.L.**, Ryan, H.F., Chin, J.L., Sliter, R.W., Conrad, J.E., Dartnell, P., Edwards, B.E., Phillips, E.L., and Wong, F.L.
59. Measurement of Apparent Offset and Interpretation of Paleoslip: A Case Study from the San Andreas Fault in the Carrizo Plain. **Akciz, S.O.**, Grant-Ludwig, L., Zielke, O., and Arrowsmith, J.R.
60. A Re-evaluation and Comparison of Paleoseismic Earthquake Dates for the Pallett Creek Site on the Southern San Andreas Fault. **Biasi, G.P.**, and Scharer, K.M.
61. Insights into Active Deformation of Southern Prince William Sound, Alaska from New High-Resolution Seismic Data. **Finn, S.P.**, Liberty, L.M., Haeussler, P.J., and Pratt, T.L.
62. PFLOW: A 3-D Numerical Modeling Tool for Calculating Fluid-Pressure Diffusion from Coulomb Strain. **Wolf, L.W.**, Lee, M.-K., Meir, A.J., and Dyer, G.

Advances in Seismic Hazard Mapping (see page 348)

63. Preliminary Geological Site Condition Map of Korea. **Kang, S.**, and Kim, K.-H.
64. Assessment of Seismic Hazard for Jordan: A Sensitivity Study with Respect to Different Seismic Source and Magnitude Recurrence Models. **Yilmaz, N.**, and Yucemen, M.S.
65. Field Reconnaissance and Response to the M=7.6 Padang, Indonesia Earthquake. **McGarr, A.**, and Mooney, W.D.
66. Seismic Hazard Assessment of Georgia, Taking into Account Local Site Conditions with Emphasis on Tbilisi Urban Area. Elashvili, M., **Javakhishvili, Z.**, Godoladze, T., and Jorjiashvili, N.
67. Dissemination and Visualization of Digital Geotechnical Data Associated with the 1995 Hyogo-ken Nanbu Earthquake in Kobe, Japan. Thompson, E.M., Tanaka, H., **Baise, L.G.**, Tanaka, Y., and Kayen, R.
68. A Kinematic Fault Network Model of Crustal Deformation for California and Its Application to the Seismic Hazard Analysis. **Zeng, Y.**, Shen, Z.-K., and Petersen, M.D.
69. The Importance of Detailed Geologic Mapping in Regional Seismic Slope Stability Assessment. **Abramsonward, H.**, Apel, T., Gray, B.T., and Bozkurt, S.B.
70. Estimating 5% Damped Response Spectra at Shallow Soil Sites in the Central United States. **Woolery, E.**, Street, R., and Paschall, A.
71. Key Science Issues in the Intermountain West for the Next Version of the U.S. National Seismic Hazard Maps. **Harmsen, S.C.**, Petersen, M.D., Haller, K.M., and Lund, W.R.
72. Constraints on Ground Accelerations Inferred from Unfractured Hoodoos near the Garlock Fault, California. **Anooshehpoor, R.**, Brune, J.N., Purvance, M.D., and Daemen, J.K.
73. Dating Precariously Balanced Rocks Using Be-10 With Numerical Models. Rood, D.H., Balco, G., Purvance, M., Anooshehpoor, R., Brune, J., **Grant Ludwig, L.**, and Kendrick, K.

Time	*Salon A*	*Salon E*	*Salon F*	*Salon G*
8:00	Field Observations of the Mw 7.0 Haiti Earthqauke of January 12, 2010. **Mooney, W.D.** In Salon E (see page 262).			
	Volcanic Plumbing Systems: Results, Interpretations and Implications for Monitoring Session Chairs: Gregory Waite and Weston Thelen (see page 350)	**Recent Advances in Source Parameters and Earthquake Magnitude Estimations** Session Chairs: Domenico Di Giacomo and George L. Choy (see page 352)	**Subsurface Imaging for Urban Seismic Hazards at the Engineering Scale** Session Chairs: John N. Louie and William J. Stephenson (see page 356)	**State of Stress in Intraplate Regions** Session Chairs: Charles Langston and Christine Powell (see page 359)
8:30	INVITED: Seismic Monitoring at Cascade Range Volcanoes: What We've Learned, Where We Are, Where We Need To Be. **Moran, S.C.**, Malone, S.D., Murray, T.L., Oppenheimer, D.H., and Thelen, W.A.	INVITED: IASPEI Standard Magnitudes At The U.S. Geological Survey/National Earthquake Information Center. **Dewey, J.W.**, Bryan, C.J., Buland, R.P., and Benz, H.M.	New Technique to Invert 1-D Soil Structure Based on the Site Information with Similar Amplification Characteristics. **Kawase, H.**, and Kuribayashi, K.	State of Stress in Central and Eastern North America Seismic Zones. **Mazzotti, S.**, Townend, J.
8:45	INVITED: Real-Time Tracking of Earthquake Swarms at Redoubt Volcano, 2009. **West, M.E.**, and Thompson, G.	Estimating Source Parameters of Small-To-Medium Sized Earthquakes Using a Multi-Objective Optimisation Approach. **Heyburn, R.**, Bowers, D., and Fox, B.	Shear-wave Velocity Model of the Santiago de Chile Basin Derived from Ambient Noise Measurements for Simulations of Ground Motion. **Pilz, M.**, Parolai, S., Picozzi, M., and Zschau, J.	Seismogenic Yield Stresses in an Intraplate Region Estimated Using Laboratory Friction Experiments to Interpret Earthquake source Parameters. **McGarr, A.**, Boatwright, J.
9:00	Precursory Seismicity to the November 21, 2008 Eruption at Nevado del Huila Volcano, Colombia. **McCausland, W.A.**, Cardona, C.E., White, R.A., and Santacoloma, C.	Application of Regional Body-Wave Magnitude Scales to Earthquakes in a Continental Margin. **Hong, T.K.**, and Lee, K.	Estimating Dynamic Strain Amplitudes Beneath Mobile Shakers. **Menq, F.-Y.**, Cox, B., and Stokoe, K.H.	Passive Margin Earthquakes as Indicators of Intraplate Deformation. **Wolin, E.**, and Stein, S.
9:15	Investigating Volcanic Plumbing Systems through "Inversion" of Seismologically-Determined Crustal Stress Fields. **Roman, D.C.**	Automatic Computation of Moment Magnitudes for Small Earthquakes and the Scaling of Local to Moment Magnitude. **Edwards, B.**, Allmann, B., Clinton, J., and Faeh, D.	INVITED: Earthquakes in Southern Nevada Project: A Summary of Findings to Date. **Snelson, C.M.**, Taylor, W.J., Luke, B., and Said, A.	Reservoir-Triggered Seismicity in the Canadian Shield. **Lamontagne, M.**, and Manescu, D.
9:30	Inflation and Rheology of the Submarine Campi Flegrei Magma Systems Using Long Water Pipe Tiltmeters. **Bilham, R.**, Romano, P., and Scarpa, R.	Regional Variations in Apparent Stress Scaling From Coda Envelopes. **Mayeda, K.**, and Malagnini, L.	INVITED: Analysis of High-Resolution P-Wave Seismic Imaging Profiles Acquired through Reno, Nevada, for Earthquake Hazards Assessment. **Frary, R.N.**, Stephenson, W.J., Louie, J.N., Odum, J.K., Maharrey, J.Z., Dhar, M.S., Kent, R.L., and Hoffpauir, C.G.	On the New Madrid Strain Rate/Release Discrepancy: Reexamining the Observational Underpinnings of Sacred Exotic COws. **Hough, S.E.**, and Page, M.

Time	Salon A	Salon E	Salon F	Salon G
9:45	Evolution of the Lateral Conduit System at Kilauea Volcano during the Early Stages of the Pu'u O'o Eruption. **Colella, H.V.**, and Dieterich, J.H.	Comparisons of Different Teleseismic Magnitude Estimates from Global Earthquake Datasets and Assessment of Influence of Site and Propagation Effects. **Di Giacomo, D.**, Parolai, S., Bormann, P., Saul, J., Bindi, D., Wang, R., and Grosser, H.	INVITED: Seismic, Geotechnical, and Earthquake Engineering Site Characterization. **Yilmaz, O.**, Eser, M., and Berilgen, M.	INVITED: Earthquake Focal Mechanisms and Stress Estimates in the New Madrid Seismic Zone. **Horton, S.P.**, and Johnson, G.
10:00	Break			
	Volcanic Plumbing Systems: Results, Interpretations and Implications for Monitoring (*continued*)	**Recent Advances in Source Parameters and Earthquake Magnitude Estimations** (*continued*)	**Subsurface Imaging for Urban Seismic Hazards at the Engineering Scale** (*continued*)	**State of Stress in Intraplate Regions** (*continued*)
10:30	INVITED: Volcano Monitoring with Continuous Seismic Correlations: Examples Using Ambient Noise and Volcanic Tremor. **Haney, M.M.**	INVITED: A Report Card on Real-Time Estimators of Seismic Sources. **Okal, E.A.**	A Case Study for Seismic Zonation in Municipal Areas. **Yilmaz, O.**, Eser, M., and Berilgen, M.	The Relationship Between Intrusions and Earthquakes in the New Madrid Seismic Zone as an Indicator of Stress Concentration. **Powell, C.A.**, and Langston, C.A.
10:45	Noise Tomography and Green's Function Estimates on Erebus Volcano, Antarctica. **Chaput, A.J.**, Aster, R.C., and Kyle, P.R.	Developing Real-Time Magnitude Estimation Using a Damped Predominant Period Function, Tpd, Applied to Data from the Hellenic Seismological Broadband Network (Operated by the Institute of Geodynamics, National Observatory of Athens, NOA). Lodge, A., Boukouras, K., **Rietbrock, A.**, and Melis, N.	Interferometric Multichannel Analysis of Surface Waves (IMASW). **O'Connell, D.R.H.**, and Turner, J.P.	Seismicity and Crustal Structure of the Eastern Tennessee Seismic Zone from Gravity and Magnetic Data Modeling. **Arroucau, P.**, Vlahovic, G., and Powell, C.A.
11:00	Pulsatile Loading of Redoubt Volcano, Alaska. **Denlinger, R.P.**, West, M.E., and Diefenbach, A.	Rapid Centroid Moment Tensor (CMT) Inversion in 3D Earth Structure Model for Earthquakes in Southern California. **Lee, E.**, Chen, P., Jordan, T.H., and Maechling, P.J.	Constraints on the Near Surface Seismic Velocity Structure of the Wasatch Front Region, Utah, from Sonic Log Analyses. **Pechmann, J.C.**, Jensen, K.J., and Magistrale, H.	Mesozoic-Cenozoic Structure at the Epicenter of the 1886 Charleston, South Carolina Earthquake. **Chapman, M.C.**, and Beale, J.N.
11:15	Initial Results from a Temporary Seismic Array in Katmai National Park, Alaska: Velocity and Attenuation Models. **Murphy, R.A.**, Thurber, C.H., Prejean, S.G.	Characteristics of the Earthquake Environment Inferred from Global Variations in Modern Magnitudes. **Choy, G.L.**, and Kirby, S.H.	INVITED: Preliminary Results from a Multi-Method Approach for Acquiring Shear-Wave Velocity Data in the Portland and Tualatin Basins, Oregon. **Odum, J.K.**, Stephenson, W.J., Maharrey, J.Z., Frary, R.N., and Dart, R.L.	The Mt Narryer Fault: the Source of Australia's Largest Earthquake? **Hengesh, J.V.**, and Whitney, B.B.

Time	Salon A	Salon E	Salon F	Salon G
11:30	Crustal Structure and Magma Plumbing of Newberry Volcano: A P-Wave Tomography Study. **Beachly, M.W.**, Hooft, E.E.E., Toomey, D.R., Waite, G.P., and Durant, D.T.	Toward a Moment Magnitude Catalog for Earthquake Hazard Assessment in Eastern Canada. **Bent, A.L.**	INVITED: Optimized Velocities and PSDM in the Reno Basin. **Kell-Hills, A.M.**, Pullammanappallil, S., Louie, J.N., Cashman, P., and Trexler, J.	A Seismic Investigation of the Rio Grande Rift: the Role of Edge-Driven Convection in Continental Rifting. **Rockett, C.V.**, Pulliam, J., and Grand, S.P.
11:45	Two-dimensional P-wave Velocity Model of Ross Island, Antarctica: Preliminary Results. **Maraj, S.**, Snelson, C.M., Kyle, P., Aster, R.C.	INVITED: Tsunami Early Warning Using Earthquake Rupture Duration and Predominant Period: The Importance of Length and Depth of Faulting. **Lomax, A.** and Michelini, A.	Mt. Rose Fan Failure Plane: Low Angle Normal Fault or Landslide? **Kell-Hills, A.M.**, Sarmiento, A., Ashcroft, T., Louie, J.N., Kent, G., Wesnousky, S., and Pullammanappallil, S.	Seismic Anisotropy and Crustal Thickness of Eastern Flank of the Rio Grande Rift. **Pulliam, J.**, Barrington, T., Xia, Y., Grand, S.P., Boyd, D., Dillon, T., Arratia, M., and Weart, C.
12:00	Lunch			
	Statistics of Earthquakes Session Chairs: Donald Turcotte, James Holliday, John Rundle, and Mark Yoder (see page 361)	**Recent Advances in Source Parameters and Earthquake Magnitude Estimations** (*continued*)	**Seismology of the Atmosphere, Oceans, and Cryosphere** Session Chairs: Daniel McNamara, Keith Koper, and Richard Aster (see page 363)	**At the Interface Between Earthquake Sciences and Earthquake Engineering in the Pacific Northwest** Session Chairs: Arthur D. Frankel and Ivan G. Wong (see page 364)
1:30	Evaluating Earthquake Predictions on Laboratory Experiments and Resulting Strategies for Predicting Natural Earthquake Recurrence. Kilgore, B., and **Beeler, N.M.**	INVITED: Recent Developments in Source Inversion by Using the W-phase. **Rivera, L.**, Duputel, Z., and Kanamori, H.	INVITED: Storms, Infragravity Waves and Possible Sources of the Earth's Vertical and Horizontal Hum. **Romanowicz, B.A.**, Dolenc, D., and Rhie, J.,	INVITED: A SSHAC Level 3 Probabilistic Seismic Hazard Analysis for British Columbia. **McCann Jr, M.W.**, and Addo, K.
1:45	The Effect of Censored Time, Space and Magnitude Data on Earthquake Clustering Statistics. **Wang, Q.**, and Jackson, D.	Rapid Determination of Large Earthquakes Moment Magnitude, Focal Mechanism, and Source Time Functions Inferred from Body-Wave Deconvolution. **Vallée, M.**, Charléty, J., Ferreira, A.M.G., Delouis, B., and Vergoz, J.	INVITED: Atmosphere -> Ocean Waves -> Seismic Signals: Solid Earth - Climate Connections. **Bromirski, P.D.**	Seismic Hazard in Western Canada from Global Positioning System vs. Earthquake Catalogue Data. **Mazzotti, S.**, Leonard, L.J., Cassidy, J.C., Rogers, G., and Halchuk, S.
2:00	Activation vs. Quiescence: Which is the Precursory Signal for the Next Large Earthquake? **Rundle, J.B.**, Holliday, J.R., Turcotte, D.L., Tiampo, K.F., and Klein, W.	Ms vs. Mw for Italian Earthquakes: Focus on the L'Aquila Earthquake Series. **Bonner, J.L.**, Herrmann, R.B., Malagnini, L., and Stroujkova, A.	Global Trends in Microseism Intensity from the 1970s to Present. **Aster, R.C.**, McNamara, D.E., Bromirski, P.D.	INVITED: Key Scientific Issues in the Pacific Northwest for the Next Version of the U.S. National Seismic Hazard Maps. **Petersen, M.D.**, and Frankel, A.D.

Time	Salon A	Salon E	Salon F	Salon G
2:15	Regional Seismicity as a Flow of Clusters: A Case Study in California. **Zaliapin, I.**, and Bautista, J.	Source Parameters of Nanoseismicity Recorded at Mponeng Deep Gold Mine, South Africa: Implications for Scaling Relationships. **Kwiatek, G.**, Plenkers, K., Dresen, G., and the Jaguars Group.	INVITED: Probing Microseism Origin and Earth Structure via Array Analysis of *P* Waves from Storms. **Zhang, J.**, Gerstoft, P., Shearer, P.M., and Bromirski, P.D.	INVITED: Site Response and Sedimentary Basin Effects in the Portland, Oregon Region. **Frankel, A.D.**, Carver, D.L., and Norris, R.D.
2:30	Parkfield Repeating Earthquakes Are Neither Time- nor Slip-Predictable. **Rubinstein, J.L.**, and Ellsworth, W.L.	Empirical Relations Between Radiated Seismic Energy and Source Dimension. Chesnokov, E.M., **King, J.**, and Abaseyev, S.S.	On the Composition of Earth's Short-Period Seismic Noise Field. **Koper, K.D.**, Seats, K., and Benz, H.M.	Impacts to Oregon's Critical Energy Infrastructure Hub. **Wang, Y.**
2:45	When Geomorphology Discriminates Between Occurrence Probability Models. **Fitzenz, D.D.**, Ferry, M.A., and Jalobeanu, A.	Further Development of the Cepstral Stacking Method (CSM) for Accurate Determinations of Focal Depths for Earthquakes and Explosions. **Alexander, S.S.**, and Cakir, R.	Seismic Observations of Seasonal Sea-Ice Cycles in Alaska. **McNamara, D.**, and Koper, K.	INVITED: Seismic Source Characterization of the Yakima Fold Belt and its Implications to Seismic Hazard. **Wong, I.**, Zachariasen, J., Thomas, P., Youngs, R., Hanson, K., Swan, B., Perkins, B., and McCann, M.
3:00	Break			
	Salon A	*Exhibit Hall*	*Salon I*	*Salon G*
	Statistics of Earthquakes (*continued*)	**Seismicity and Seismotectonics** Session Chairs: Diane Doser and Jeanne Hardebeck (see page 365)	**Time Reversal in Geophysics** Session Chairs: Carene Larmat, Jean-Paul Montagner, and Kees Wapenaar (see page 367)	**Seismic Hazard Mitigation Policy Development and Implementation** Session Chairs: Yumei Wang and Zhenming Wang (see page 368)
3:30	Epistemic Uncertainty in California-Wide Synthetic Seismicity Simulations. **Pollitz, F.F.**	Finite Fault Kinematic Rupture Model of the 2009 Mw 6.3 L'Aquila Earthquake from Joint-Inversion of Strong Motion, GPS and InSAR Data. **Yano, T.**, Shao, G., Liu, Q., Ji, C., and Archuleta, R.J.	Time Reversal Source Localization of Long-Duration Signals in a Laboratory Sample with Implications to Earth Processes. Anderson, B.E., **Ulrich, T.J.**, Guyer, R.A., and Johnson, P.A.	INVITED: What Earthquake Engineers Need Seismologists to Contribute. **Poland, C.D.P.**
3:45	Earthquake Statistics of Synthetic Seismicity for Northern California Using Virtual California. **Yikilmaz, M.B.**, Turcotte, D.L., Yakovlev, G., Rundle, J.B., and Kellogg, L.H.	Pronounced sP Phases Recorded at Regional Distances in Southwestern Japan: Modeling and Implications. **Hayashida, T.**, Tajima, F., and Mori, J.	Time Reverse Modeling of Low-Frequency Tremor Signals. **Steiner, B.**, Saenger, E.H., Artman, B., Witten, B., and Schmalholz, S.M.	INVITED: Seismic Policy Development and Implementation in Kentucky. **Cobb, J.**
4:00	Distinguishing Tectonic Categories of Earthquakes in the EEPAS Forecasting Model. **Rhoades, D.A.**, Somerville, P.G., Dimer de Oliveira, F., and Thio, H.K.	Spatial Distribution of Stress along the Interplate Boundary in Hokkaido Northern Japan. **Ghimire, S.**, and Tanioka, Y.	Time Reversal Applied to Location of San Andreas Triggered Tremor. **Larmat, C.**, Johnson, P.A., and Guyer, R.A.	INVITED: New "Courtney Grants" to Seismically Strengthen Community Infrastructure in Oregon: What about Other States? **Wang, Y.**

	Salon A	Exhibit Hall	Salon I	Salon G
4:15	Numerical Models of Aftershocks, with 3D Heterogeneous Stress, Rate-State Friction, and Coulomb Stress: Comparisons with the Landers, Denali, and Loma Prieta Earthquakes. **Smith, D.E.**, and Dieterich, J.H.	Investigating the Source of Seismic Swarms Along the Eastern End of the Puerto Rico Trench. **Mintz, H.E.**, Pulliam, J., Lopez Venegas, A.M., Ten Brink, U., and Von Hillebrandt-Andrade, C.	INVITED: Time Reversal Source Imaging and GRiD MT Monitoring with W-Phase. **Tsuruoka, T.**, Kawakatsu, K., and Rivera, R.	History of Seismic Provisions in the Building Code of Arkansas. **Ausbrooks, S.M.**
4:30	Forecasts of Repeating Microearthquakes near Parkfield, California. **Zechar, J.D.**, and Nadeau, R.M.	A New Method for Identifying Triggered Seismicity. **Magee, A.C.**, Fouch, M.J., and Clarke, A.B.	INVITED: The Gap between Theory and Practice for Seismic Interferometry for the Earth. **Snieder, R.**, Slob, E., and Wapenaar, K.	Impacts of the 2009 Samoa Tsunami and Earthquake. **Dengler, L.A.**, Brandt, J., Ewing, L., Irish, J., Jones, C., and Lazrus, H.
4:45	Analysis of Spatial Variations in Magnitude of Completeness of JAGUARS Catalog ($-5 < M < -1$) Recorded in the Mponeng Deep Gold Mine in South Africa. **Plenkers, K.**, Schorlemmer, D., Kwiatek, G., and the Jaguars-Group	Asymmetric Properties of Early Aftershocks on Faults in California. **Zaliapin, I.**, and Ben-Zion, Y.	INVITED: Earthquake Source Modeling using Time-Reversal or Adjoint Methods. **Hjorleifsdottir, V.**, Liu, Q., and Tromp, J.	Discussion

Friday, 23 April—Morning Poster Sessions

Statistics of Earthquakes (see page 369)

1. Darned Lies and Circular Statistics? **Anderson, D.N.**, Arrowsmith, M.D., and Taylor, S.R.
2. Separating Aftershocks from Background Seismicity Using Record-Breaking Intervals. **Yoder, M.R.**, Turcotte, D.L., and Rundle, J.B.
3. Initiation and Propagation of Earthquake Rupture. Gran, J.D., Yakovlev, G., Turcotte, D.L., and Rundle, J.B.

Seismology of the Atmosphere, Oceans, and Cryosphere (see page 369)

4. First Observations From the NEPTUNE Canada Seismograph Network. **Rogers, G.C.**, Meldrum, R.D., Mulder, T.L., Baldwin, R., and Rosenberger, A.
5. Investigating Source Locations for Body Wave Energy in Ambient Seismic Noise. **Pyle, M.L.**, and Koper, K.D.
6. Seismic Noise Polarization at Stations in the Central United States. **Hawley, V.**, and Koper, K.D.
7. An Explicit Relationship Between Time-Domain Noise Correlation and Spatial Autocorrelation (SPAC) Results and Application to Microseism Directionality. **Tsai, V.C.**, Moschetti, M.P., and McNamara, D.E.
8. Temporal Icequake Investigation and Location at Mount Erebus, Antarctica. **Knox, H.A.**, Aster, R.C., and Kyle, P.R.
9. Hydro Acoustics in Tsunami Warning. **Salzberg, D.**

Time Reversal in Geophysics (see page 371)

10. Time Reversal and Cross-Correlations Techniques - the Normal Mode Approach. **Montagner, J.-P.**, Larmat, C., and Phung, H.
11. Revealing Source and Path Sensitivities of Basin Guided Waves by Time-Reversed Simulations. **Roten, D.**, Day, S.M., and Olsen, K.B.
12. Looking inside a Subducting Slab Using Source-Side Seismic Interferometry. **Matzel, E.M.**
13. Imaging the Rupture of the September 2009 M8.1 Samoan Outer Rise Earthquake and a Triggered Aftershock on the Plate Interface. **Hutko, A.**, Lay, T., and Koper, K.
14. Rupture Imaging of Recent Large Earthquakes in South America via Backprojection of Teleseismic P-waves. **Sufri, O.**, Xu, Y., and Koper, K.D.

Seismic Structure and Geodynamics of the High Lava Plains and Greater Pacific Northwest (see page 372)

15. Rayleigh Wave Phase Velocity Dispersion Analysis in the High Lava Plains, Oregon. **Feng, H.S.**, and Beghein, C.
16. Crustal and Lithosphere Structure of the Pacific Northwest with Ambient Noise Tompgraphy. **Gao, H.**, Humphreys, E., Yao, H., and Hilst, R.
17. Preliminary Model of the Juan de Fuca Slab. **Chu, R.**, Sun, D., and Helmberger, D.V.
18. The 2006–2010 Maupin, Oregon Earthquake Swarm. **Braunmiller, J.**, Williams, M., Trehu, A.M., and Nabelek, J.

Seismicity and Seismotectonics (see page 372)

19. Broadband Source Mechanism Modeling of Recent Earthquakes in Calabria, Southern Italy. **D'Amico, S.**, Orecchio, B., Presti, D., Gervasi, A., Guerra, I., Neri, G., Zhu, L., and Herrmann, R.
20. Crustal Structure of the Iranian Plateau and Surounding Region. **Priestley, K.**, Rham, D., and Acton, C.
21. Modeling of Three-Dimensional Regional Velocity Structure Using Wide-Angle Seismic Data from the Hi-CLIMB Experiment in Tibet. **Griffin, J.D.**, Nowack, R.L., Tseng, T.L., and Chen, W.P.
22. Seismotectonic Environment of Some Enervated Earthquakes Along the Sumatra Subduction Zone. **McCann, W.R.**, and Choy, G.L.
23. A Study of Seismicity, Earthquake Source Processes, and Fault Interactions in the Region Between the Denali and Fairweather-St. Elias Fault Systems, Southeast Alaska and Northwest Canada. **Doser, D.I.**, Escudero, C.R., Rodriguez, H.
24. Seismic Reflection Images of the Central California Coast Ranges and the Tremor Region around Cholame from Reprocessing of Industry Seismic Reflection Profile "SJ-6." **Gutjahr, S.**, and Buske, S.
25. Finite-Source Parameters and Scaling of Micro-Repeating Earthquakes at Parkfield. Dreger, D.S., Nadeau, R.M., Kim, A., **Statz-Boyer, P.**, and Acevedo-Cabrera, A.
26. Landers Off-Fault Aftershocks are Well-Aligned with the Background Stress Field, Contradicting the Hypothesis of Highly-Heterogeneous Crustal Stress. **Hardebeck, J.L.**
27. The Earthquakes of August 3, 2009 in the Canal de Ballenas Region, in the Gulf of California, Mexico. **Castro, R.R.**, Valdes, C.M., Shearer, P., Wong, V.M., Astiz, L., Vernon, F., Perez-Vertti, A., and Mendoza, A.
28. Foreshock Sequence of the 2008 Mw 5.0 Mogul-Somersett, Nevada, Earthquake. **Smith, K.D.**, Von Seggern, D.H., Anderson, J.G.
29. P-Wave Slowness Anomalies across USArray Determined by Limited-Aperture Beam Forming. **Sawyer, R.L.**, and Poppeliers, C.
30. Lateral Crustal Velocity Variations across the Andean Foreland in San Juan, Argentina from the JHD Analysis. **Asmerom, B.B.**, Chiu, J.M, Pujol, J., and Smalley, R.

Seismic Networks, Analysis Tools, and Instrumentation (see page 375)

31. A Software Toolbox for Systematic Evaluation of Seismometer-Digitizer System Responses. **Bonner, J.L.**, Buland, R., Herrmann, R.B., Stroujkova, A., Leidig, M.R., and Ferris, A.
32. Guidelines for Standardized Testing of Broadband Seismometers and Accelerometers. Hutt, C.R., Evans, J.R., Followill, F., **Nigbor, R.L.**, and Wielandt, E.
33. NetQuakes—A New Approach to Urban Strong Motion Seismology. **Luetgert, J.H.**, Hamilton, J.C., and Oppenheimer, D.H.
34. How Low Can You Go? Exploring the Capabilities of Low-Cost Accelerometers. **Chung, A.I.**, Lawrence, J.F., Prieto, G.A., Kohler, M.D., and Cochran, E.S.
35. ShakeNet: A Tiered Wireless Accelerometer Network for Rapid Deployment in Civil Structures. Mishra, N., Hao, S., **Kohler, M.**, Govindan, R., and Nigbor, R.
36. The Central U.S. Seismic Observatory (CUSSO). **Wang, Z.**, McIntyre, J., and Woolery, E.W.
37. Arizona Integrated Seismic Network: A New Era in Seismology for Arizona. Brumbaugh, D.S., Arrowsmith, J.R., Beck, S.L., Diaz, M., Fouch, M.J., **Hodge, B.E.**, and Zandt, G.
38. ANSS Quake Monitoring System (AQMS) at the Pacific Northwest Seismic Network. **Hartog, R.**, Kress, V., Bartlett, T., and Bodin, P.
39. EMERALD: Software for Managing Large Seismic Data Sets. **West, J.D.**, Fouch, M.J., and Arrowsmith, J.R.
40. The New Data Product Development Effort within the IRIS DMS. **Bahavar, M.**, Hutko, A.R., and Trabant, C.
41. Real-Time Double-Difference Location and Monitoring of Fine-Scale Seismic Properties. **Waldhauser, F.**, and Schaff, D.
42. Chasing Aftershocks with Subspace Detectors. **Harris, D.B.**, and Dodge, D.A.

At the Interface Between Earthquake Sciences and Earthquake Engineering in the Pacific Northwest (see page 377)

43. Development of Ground Motions for Scoggins Dam Seismic Retrofit. **Zafir, Z.**
44. Vertical Escape Options Needed to Transform Tsunami Safety. Wang, Y., Raskin, J., Boyer, M.M., Moncada, J., Straus, S., Yeh, H., and **Yu, K.**
45. Seismic Monitoring at the Alaskan Way Viaduct in Seattle, Washington. **Delorey, A.A.**, and Vidale, J.E.

Seismic Hazard Mitigation Policy Development and Implementation (see page 378)

46. Developing Seismic Hazard Maps for Policy Applications in Kentucky. **Wang, Z.**
47. Earthquake Safety Initiative for Rural Communities in Western China. **Yuan, Z.X.**, Wang, L.M., and Wang, Z.M.

Friday, 23 April—Afternoon Poster Sessions

State of Stress in Intraplate Regions (see page 378)

48. Are Recent Earthquakes near Greenbrier, Arkansas Induced by Waste-Water Injection? **Horton, S.P.**, and Ausbrooks, S.M.
49. Preliminary Results for the Detection of Non-volcanic Tremor in the New Madrid Seismic Zone Using a Phased Array. Langston, C.A., **Deshon, H.R.**, Horton, S., and Withers, M.

50. Analysis of Recent Earthquakes in Cleburne, Texas. **Howe, A.M.**, Hayward, C.T., Stump, B.W., and Frohlich, C.
51. Observation of Microearthquake Sequences in the Haicheng, Liaoning, China. **Kim, G.Y.**, and Shin, J.-S.
52. Relocation of the 20 January 2007 ML 4.8 Odaesan Earthquake Sequence. **Kim, K.-H.**, Kang, S., and Park, Y.
53. Seismicity of Stable Continental Regions (SCRs): Correlation of Earthquake Locations, Magnitudes, and Mmax with Deep Lithospheric Structure. **Ritsema, J.**, and Mooney, W.D.
54. The North American Upper Mantle: Density, Composition, and Evolution. **Mooney, W.D.**, and Kaban, M.K.
55. Source Parameters of the April 18, 2008 (Mw 5.2) Mount Carmel, Illinois Earthquake Sequence. **Ayele, S.T.**, Horton, S., and Powell, C.

Volcanic Plumbing Systems: Results, Interpretations and Implications for Monitoring (see page 380)

56. An Integrated Analysis of Low-Frequency Seismicity at Fuego Volcano, Guatemala. **Waite, G.P.**, Lyons, J.J., and Nadeau, P.A.
57. Return to Lo`ihi: Cross-correlation Analysis of the 1996 Earthquake Swarm at Lo`ihi Submarine Volcano, Hawai`i. **Caplan-Auerbach, J.**, and Thurber, C.H.
58. Halloween 2009 Earthquake Swarm Near Sunset Crater National Monument, Arizona. **Hodge, B.E.**, and Brumbaugh, D.S.
59. Tracking Long Period Earthquakes Beneath Mammoth Mountain, California. **Shelly, D.R.**, Hill, D.P., and Pitt, A.M.
60. Analysis of a "New" Seismic Dataset from the 1980 Eruption of Mount St. Helens. **Thelen, W.A.**, Malone, S.D.
61. Statistical Analysis of Seismicity Beneath Alaskan Volcanoes. **Junek, W.N.**
62. Oscillation of Fluid-filled Cracks Triggered by Degassing of CO2 due to Leakage Along Wellbores: Field Observations of a Single Force Source Process. **Bohnhoff, M.**, and Zoback, M.D.

Subsurface Imaging for Urban Seismic Hazards at the Engineering Scale (see page 381)

63. Superficial 3-D Basin Structural Model in Grenoble, France, Evaluated by Geophysical and Geological Data. **Tsuno, S.**, Cornou, Collombet, M., Menard, G., and Bard, P.-Y.
64. Cross-Constraints between Station Delays, Gravity, and Reflection for the Reno-area Basin Floor, Nevada. **Dhar, M.S.**, Thompson, M., Kell-Hills, A., Louie, J.N., Smith, K.D., and Widmer, M.C.
65. Surface Geophysics for Emergency Microzonation: The L'Aquila Earthquake Example. **Gallipoli, M.R.**, Mucciarelli, M., and Albarello, D.
66. Seismic Characterization of the Sites of the Italian Accelerometric Network. Foti, S., Parolai, S., Albarello, D., Milana, G., Mucciarelli, M., Puglia, R., Maraschini, M., Bergamo, P., Comina, C., Tokeshi, K., Picozzi, M., Di Giacomo, D., Strollo, A., **Pilz, M.**, Milkereit, R., Bauz, R., Lunedei, E., Pileggi, D., Bindi, D.
67. Shallow-Seismic Site Characterizations of Near-Surface Geology at 20 Strong-Motion Stations in Washington State. **Cakir, R.**, Walsh, T.J., Maffucci, C.M., Perreault, J., and Burton, K.
68. Characterization of Shallow Seismic Velocity Structure in Southwestern Utah Using Spatial Autocoherence. **Huang, S.**, Pankow, K.L., and Thorne, M.S.
69. Site Characterization in Northwestern Turkey Based on Spatial Autocorrelation Technique: A Comparative Study on Site Hazard Estimation. Asten, M., **Askan, A.**, Ekincioglu, E.E., Sisman, F.N., and Ugurhan, B.
70. Site Effect Assessment in Bishkek (Kyrgyzstan) Using Earthquake and Noise Recording Data. Parolai, S., Orunbayev, S., Bindi, D., Strollo, A., Usupayev, S., Picozzi, M., **Di Giacomo, D.**, Augliera, P., D'alema, E., Milkereit, C., Moldobekov, B., and Zschau, J.
71. Shallow Seismic and Geotechnical Site Surveys at the Turkish National Grid for Strong-Motion Seismograph Stations. **Yilmaz, O.**, Savaskan, E., Bakir, S., Yilmaz, T., Eser, M., Akkar, S., and Tuzel, B.
72. Comparison of Shear-Wave Velocity Depth Profiles from Downhole and Surface Seismic Experiments. **Yilmaz, O.**, Eser, M., Sandikkaya, A., Akkar, S., Bakir, S., and Yilmaz, T.
73. Absolute Site Response from L'Aquila Earthquake. **Mercuri, A.**, Malagnini, L., and Herrmann, R.B.

The January 2010 Earthquakes in Haiti and Offshore Northern California: Origins, Impacts and Lessons Learned (see page 384)

74. Shaking, Ground Effects, and Human Response to the Mw 6.5 Northern California Earthquake of January 10, 2010. **Dengler, L.A.**, Bazard, D., Cashman, S.M., Hemphill-Haley, E., Hemphill-Haley, M., Kelsey, H., McPherson, R., and Tillinghast, S.

As this session was added after the original submission deadline and the submission deadline for this extended, the abstracts were not ready for publication in this issue. They will be available online by March 15 and published in a later issue of SRL.

2010 SSA Annual Meeting Report

Portland, Oregon
21–23 April 2010

The 2010 Annual Meeting of the Seismological Society of America was held at the Portland Marriott Downtown Waterfront Hotel in Portland, Oregon, 21–23 April 2010. The program committee co-chairmen were Seth Moran of the USGS Cascades Volcano Observatory and Nick Beeler of USGS Vancouver. They were assisted by program committee members Ivan Wong of the Seismic Hazards Group at URS Corporation in Oakland, CA; Ray Weldon of University of Oregon; Vicki McConnell of the Oregon Department of Geology and Mineral Industries (DOGAMI); and Anne Trehu of Oregon State University.

Official attendance at SSA 2010 totaled 557 participants and would have been record-setting if the eruption of Iceland's Eyjafjallajokul volcano hadn't stranded 41 registered attendees in Europe and prevented them reaching Portland. Among the 2010 conference participants were 101 nonmembers (18% of all attendees), 40 Oregonians (31 more than at SSA 2009, which was held in Monterey, California), 176 Californians (75 fewer than at SSA 2009), 98 people from outside the United States (representing 25 countries), 97 students, 13 exhibiting organizations with 19 people staffing their booths, 7 travel-grant recipients, and 9 SSA staff members. In a follow-up survey, 100% of respondents had positive things to say about the 2010 program.

SSA 2010 began with the traditional ice breaker on Tuesday evening, 20 April, where seismologists and friends enjoyed reconnecting with colleagues and making new acquaintances amid cocktails and hors d'oeuvres.

The formal program began Wednesday 21 April and it included 540 scheduled presentations: 282 oral presentations and 258 poster presentations distributed among 31 sessions.

The sessions included the following topics: Advances in Seismic Hazard Mapping; At the Interface Between Earthquake Sciences and Earthquake Engineering in the Pacific Northwest; Building Code Uses of Seismic Hazard Data; Characterizing the Next Cascadia Earthquake and Tsunami; Deterministic Simulated Ground Motion Records under ASCE 7-10 as a Bridge Between Geotechnical and Structural Engineering Industry; Earthquake Debates; Engaging Students and Teachers in Seismology: In Memory of John Lahr; The Evolution of Slow Slip and Tremor in Time and Space; Ground Motion: Observations and Theory; The January 2010 Earthquakes in Haiti, Offshore Northern California, and Chile: Origins, Impacts and Lessons Learned; Joint Inversion of Multiple Geophysical Data Sets for Seismic Structure; Magnitude Scaling and Regional Variation of Ground Motion (jointly sponsored by the European Seismological Commission); Monitoring for Nuclear Explosions; Near-Surface Deformation Associated with Active Faults; Numerical Prediction of Earthquake Ground Motion; Operational Earthquake Forecasting Quantification and Treatment of Uncertainty and Correlations in Seismic Hazard and Risk Assessments; Recent Advances in Source Parameters and Earthquake Magnitude Estimations; Seismic Hazard Mitigation Policy Development and Implementation; Seismic Imaging: Recent Advancement and Future Directions; Seismic Networks, Analysis Tools, and Instrumentation; Seismic Structure and Geodynamics of the High Lava Plains and Greater Pacific Northwest; Seismicity and Seismotectonics; The Seismo-Acoustic Wavefield: Fusion of Seismic and Infrasound Data; Seismologic Methods, Techniques, and Theory; Seismology of the Atmosphere, Oceans, and Cryosphere; State of Stress in Intraplate Regions; Statistics of Earthquakes; Subsurface Imaging for Urban Seismic Hazards

at the Engineering Scale; Time Reversal in Geophysics; and Volcanic Plumbing Systems: Results, Interpretations and Implications for Monitoring; SSA President Rick Aster presided over the SSA Annual Luncheon on Wednesday 21 April and reported that the state of the Society—financial and otherwise—is one of good health.

Aster also presided over the presentation of four awards: the Harry Fielding Reid Medal (also known as the SSA Medal) for Paul Richards; the Charles F. Richter Early Career Award to Karen Felzer; the Frank Press Public Service Award to Art Frankel; and the Bruce Bolt Award to David Boore. Marcia McNutt, director of the U.S. Geological Survey, was the President's Invited Speaker at the annual luncheon. (For more details of the 2010 Annual Luncheon, including the names of those to be honored with awards at the 2011 Annual Meeting, see the Minutes of the 2010 Annual Luncheon, included in this annual report on page 818.)

That evening SSA 2010 hosted "The Big One is Coming: What Are You Going to Do about It?" a town hall meeting to raise the awareness among decision-makers and the public about the earthquake hazards and associated risks that face them in the Portland area, western Oregon, and the greater Pacific Northwest. The event featured a keynote talk by seismic safety advocate and Oregon Senate President Peter Courtney. Also on Wednesday evening, the conference hosted a well-attended student reception at Champion's Sports Bar, located in the conference hotel.

On Thursday 22 April, invited speaker Jofi Joseph, senior advisor to the U.S. undersecretary of state for arms control and international security, presented the luncheon address, "The Obama Administration and CTBT Ratification," remotely from Washington DC.

On Thursday evening, Art Frankel, a senior scientist with USGS Seattle, delivered the 2010 Joyner Lecture, "Progress and Controversy in Seismic Hazard Mapping."

Two field trips were offered on Saturday 24 April. The first, "Portland Geology by Tram, Train, and Foot," was led Ian P. Madin of the Oregon Department of Geology and Mineral Industries. The 16 participants visited outcrops of most of the local geologic units, including Columbia River Basalt flows, Missoula Flood deposits, and a late Quaternary volcano within the city limits.

The second field trip was to Mount Hood, led by Willie Scott of the USGS Cascades Volcano Observatory. The 32 participants on this all-day tour through the Columbia River Gorge and around Mount Hood took in regional geology and tectonics, scenic overlooks, giant landslides and ice-age floods, past eruptions of Mount Hood, and other related points of interest.

A special thanks to sponsors of the SSA 2010 Annual Meeting, the program committee members, the SSA staff, and all of the volunteers who contributed to making the 2010 SSA Annual Meeting a success.

Minutes of the 2010 Business Meeting
21 April 2010

The 2010 Business Meeting of the Seismological Society of America was held during the annual luncheon on Wednesday, 21 April 2010. The business meeting was part of the SSA's 104th Annual Meeting, held 21–23 April 2010, at the Portland Marriott Downtown Waterfront Hotel in Portland, Oregon.

SSA President Rick Aster opened the business meeting by welcoming members and their guests and acknowledging the remarkable sequence of seismic and volcanic events in Haiti, Chile, Mexico, and Iceland that had already occurred this year. He reminded the audience of SSA's statement of purpose, in particular its mission to help people understand that earthquakes are dangerous chiefly because we don't take adequate precautions against their effects.

Aster noted that the 2010 Annual Meeting had drawn nearly record-breaking attendance, despite more than 40 registrants who were prevented from attending by Iceland's volcanic eruption. He then recognized those who worked on the 2010 meeting, especially Program Co-Chairmen Seth Moran and Nick Beeler; program committee members Ivan Wong, Ray Weldon, Vicki McConnell, and Anne Trehu; and field trip leaders Ian P. Madin and Willie Scott. He also recognized the SSA's retiring board members Roland Bürgmann, Bill Ellsworth, and John Anderson.

Aster announced that the 2010 IRIS/SSA Distinguished Lectures were ongoing and still available to communities interested in hosting lectures this year. He acknowledged the two 2010 lecturers: Steve Malone, "Predicting Earthquakes and Volcanic Eruptions—What Can and Can't Be Done"; and Brian Stump, "Science and Politics in a Nuclear Era."

He named the 2010 Travel Grant Award Winners: Wei Li, Carrie Rockett, Hunter Knox, Julien Chaput, Shaun Finn, and Luis Dominguez-Rameriz, as well as the International Travel Grant awardee, Din Muhammad Kakar of Pakistan. He then introduced the SSA staff. Aster noted that the Society will be able to award more travel grants as donations increase to the Student Travel Fund.

Aster reported briefly on the Society board meeting held the day previous, noting the following:

- Membership is up by 3.5% and the Society remains financially healthy despite the economic downturn.
- Incoming BSSA Editor Diane Doser and outgoing BSSA Editor Andy Michael are working together on the transition.
- SRL Editor Luciana Astiz has announced that she will leave that position at the end of the year and the Society is now seeking her successor. Former SRL Editor Sue Hough, former SSA President Mike Fehler, and SSA Board Member David Wald are heading the search.
- *BSSA* and *SRL* are thriving.
- The SSA board approved the management and use of the Kanamori Fund for international and domestic student and professional support for travel and publications.
- The board is encouraging SSA members with connections to the European Seismological Commission to help the Society move forward with student, professional, and program exchanges.
- A special request for members to participate in the upcoming election of four new board members as well as nominations for awards and key committees.

(Complete minutes of the board meeting start on page 827 of this annual report.)

Aster announced that evening's student reception as well as the town hall meeting scheduled on the topic, "The Big One Is Coming: What Are YOU Going to Do about It?" co-sponsored by the Oregon Seismic Safety Policy Advisory Commission, the Cascadia Region Earthquake Working Group, and the Federal Emergency Management Agency. He noted that Jofi Joseph, senior advisor to undersecretary of state for arms control and international security at the state department would speak on nuclear proliferation as Thursday's Distinguished Luncheon Speaker; and that Art Frankel would deliver the Joyner Lecture Thursday evening. He offered special thanks to SSA 2010 Annual Meeting sponsors Bechtel, GeoTech Instruments, Kinemetrics, Pacific Gas & Electric, Nanometrics, Refraction Technology, Weston Geophysical, and the USGS Earthquake Hazards and Volcanic Hazards programs.

Aster reported that the 2011 Annual Meeting will be held 13–16 April 2011 in Memphis, Tennessee, and that Chuck Langston and Beatrice Magnani of the University of Memphis are program co-chairmen, and that the 2012 meeting likely will be in southern California.

He announced that at the 2011 Annual Meeting in Memphis, the 2010 Harry Fielding Reid Medal, also known as the SSA Medal, will be awarded to Tatiana Rautian, most recently of the Lamont Doherty Earth Observatory, Columbia University; the Frank Press Award for Public Service will be awarded to Hugo Yepes of Instituto Geophysico Ecuador; and the Richter Early Career Award will be awarded to Zhigang Peng of Georgia Tech.

David M. Boore of the USGS in Menlo Park was presented with this year's Bruce Bolt Medal, which is a coordinated honor of SSA, the Consortium of Organizations for Strong Motion Observation Systems (COSMOS), and the Earthquake Engineering Research Institute (EERI). Aster also acknowledged Boore's long service to SSA, in part as editor of BSSA. (See excerpts of Boore's nomination on page 823 of this Annual Report.)

Karen Felzer of the USGS Pasadena was presented with this year's Charles F. Richter Award Early Career Award, com-

doi: 10.1785/gssrl.81.5.818

plete with a plaque and a check funded by the Joyner Fund. (See excerpts of Felzer's nomination on page 823 of this Annual Report.)

Art Frankel of the USGS Seattle received this year's Frank Press Public Service Award, which honors outstanding contributions to the advancement of public safety or public information relating to seismology. He received a plaque noting his award. (See excerpts of Frankel's nomination on page 824 of this Annual Report.)

Jim Brune read the citation for the award of the 2009 SSA Medal to Paul Richards of Lamont-Doherty Earth Observatory, Columbia University. (The complete citation and reply is printed beginning on page 820 of this report.)

USGS Director Marcia McNutt gave the President's Invited Address entitled, "My View of the USGS Earthquake Hazards Program after My 30-year Hiatus."

President Aster made his closing remarks and adjourned the annual business meeting.

The complete program of the 2009 Annual Meeting was published in *SRL* volume 81, number 2. The proceedings and reports of the meeting, including awards citations, are published in this issue of *SRL* (volume 81, number 5).

Harry Fielding Reid Medal Citation for Paul Richards

It is a great honor and great pleasure for me to present the citation for Paul Richards to receive the Reid Medal of the Seismological Society of America, our highest honor. I suppose in general the qualifications required for receiving our medal are that the recipient be outstandingly talented and use that talent outstandingly well. In the case of this year's medalist there is no question. His great talents were recognized early on, and his subsequent career is powerful testimony to his dedicated and elegant use of that talent. To quote from his nominators: "Paul Richards has been one of most influential contributors to theoretical and observational seismology over the past three decades."

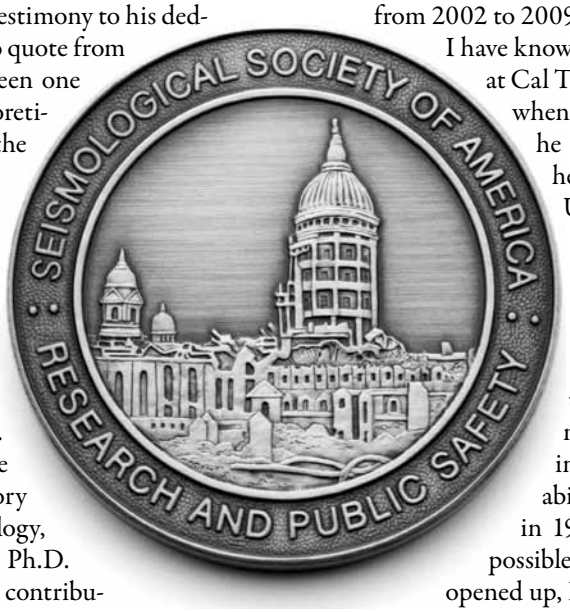

Paul was born in Cirencester, Gloucestershire, England, an undergraduate of Peterhouse, University of Cambridge, and he was a State Scholar. He won the college Mathematics prize and the Essay prize in Physics. He obtained his B.A. in Mathematics from the University of Cambridge. From 1965 to 1970 Paul was a graduate student at the Seismological Laboratory of the California Institute of Technology, obtaining an M.S. in Geology and a Ph.D. in Geophysics. His thesis was titled "A contribution to the theory of high frequency elastic waves, with applications to the shadow boundary of the Earth's core." From 1970 to 1971 he was an Assistant Research Geophysicist at the Institute of Geophysics and Planetary Physics, University of California at San Diego. In 1971 he went to Lamont-Doherty Geological Observatory of Columbia University, becoming professor in 1979, and Mellon Professor of the Natural Sciences in 1987.

Recognition of Paul's contributions has come from many organizations. To cite a few:

- He was a Sloan Foundation Research Fellow, American Editor of the Geophysical Journal of the Royal Astronomical Society, recipient in 1977 of the James B. Macelwane Award of the American Geophysical Union, and a MacArthur Fellow in 1981. He was a member of the Red Team advising the U.S. Arms Control and Disarmament Agency on capability of the U.S. to verify compliance with the Comprehensive Test Ban Treaty.
- He was honored as Harold Jeffreys Lecturer of the Royal Astronomical Society in 1999 on the subject: Earth's Inner Core—Discoveries and Conjectures, and recipient of the 2006 Leo Szilard Lectureship Award from the American Physical Society for work on seismic monitoring of a test ban treaty.
- In 2008 he was elected Fellow of the American Academy of Arts and Sciences.
- In our Society he has served on the Board of Directors from 2002 to 2009.

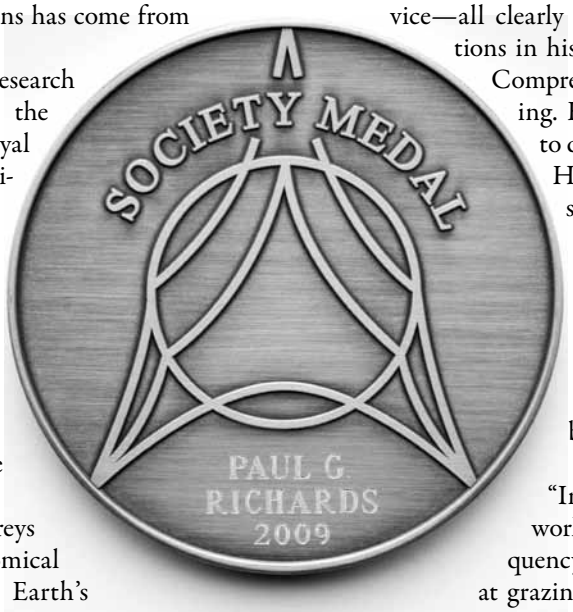

I have known Paul since he was a graduate student at Cal Tech. We overlapped from 1965 to 1970 when, after getting a Masters in Geology, he completed his Ph.D. After Cal Tech he spent a post-doc with me at IGPP-UCSD, where I got to appreciate his abilities even further. He worked on, and quickly solved a problem relative to using sonobouys to record earthquakes in the ocean. Paul seemed to me humbly surprised by his own abilities—in quantitative, analytical, and mathematical insight, and in physical intuition. I was so impressed with Paul's abilities that when, on a visit to Lamont in 1970, I was asked for an evaluation of possible candidates for a position that had just opened up, I unhesitatingly recommended Paul as the most promising seismologist. I am happy to say that Paul has more than satisfied my expectations for his future.

Paul has made numerous outstanding contributions to quantitative seismology, seismological aspects of the Comprehensive Test Ban Treaty, the structure of the earth's inner core, earthquake and explosion source physics, national and international political aspects of arms control, and highest quality scientific reviewing and professional service—all clearly documented with his many publications in his Curriculum Vitae. His work on the Comprehensive Test Ban has been outstanding. He did not suffer easily any attempts to distort the science for political reasons. His widespread cooperation with other scientists is clearly indicated by the number of high-level co-authors on his publications. He has not hesitated to work constructively with others when that was to the advantage of the science, and, because of his unselfish personality, students and colleagues have been eager to work with him.

I quote again from nominators: "Important insights developed in [h]is work include the detailed effects of frequency dependence and tunneling of waves at grazing incidence to discontinuities, exhib-

ited in the strong frequency dependence of compressional waves in the outer core multiply reflected from the core-mantle boundary. In 2005, using high quality waveform doublets, Paul and co-authors confirmed the temporal change of waves through the inner core by about a tenth of a second per decade. The discovery has been dubbed as one of the most important discoveries in the last century and thrust deep earth research into the front pages of the world-wide media and the views of the general public."

Another quote: "Paul's service contributions have been as outstanding as those in research. He has been intensively committed to serving the cause of nuclear disarmament and non-proliferation, serving on national committees advising on the monitoring of the Comprehensive Test Ban Treaty, serving as a visiting fellow at the U.S. Arms Control and Disarmament Agency, and contributing to national reports on treaty verification problems. Paul's continuing commitment in this area has included seminar visits to many universities and colleges and the establishment of a regular course on Weapons of Mass Destruction at Columbia University."

Last, but definitely not least, the Aki and Richards textbook *Quantitative Seismology* has been, to quote from nominators: "truly a bible for seismology. It has been one of most authoritative references and textbooks for researchers and students worldwide."

In summary, based on his contributions in science, education and public service, Paul eminently deserves being awarded the Reid Medal of the Seismological Society of America.

James N. Brune
21 April 2010

▲ SSA Medal awardee Paul Richards.

Harry Fielding Reid Medal Response

To President Rick Aster, to members of the SSA, and guests: I express my amazement, and my sincere thanks, for the honor bestowed on me today.

This was a total surprise to me when I first heard of it, at the icebreaker last year; one that brings me great pleasure—to have the work I have done in my professional life be recognized in this way.

I thank Jim Brune, not just for a generous citation, but for the guidance he has given me since 1965, when we began a student-advisor relationship at Caltech. I had just arrived with a pure mathematics degree from England and knew almost nothing about geology or geophysics. He and Clarence Allen put me to work reading seismograms, in a project that looked for unusual microseismicity on the San Andreas. But we didn't find it. Then Jim suggested what became a thesis topic, with help from Charles Archambeau—the behavior of *P*-waves and *S*-waves near the core shadow boundary. I looked at hundreds of seismograms, but every patch of the core-mantle boundary seemed to behave differently, so it was a theoretical study. No data. And then, as a another great service, as a representative of the Pasadena Quaker Meeting, Jim Brune signed the legal papers recognizing my marriage in 1968 to Jody—who is here, with our daughter Gillian, and son-in-law Grisha.

During the ups and downs of my professional life, the good days and the difficult ones, my family has provided a sanity check, and the frame of reference for what I try to do. I thank you, my beloved ones.

After Caltech, in a junior research job at U.C. San Diego, Freeman Gilbert encouraged me to tackle something different from my thesis, and I solved a self-similar problem in shear crack theory. But still I wasn't using data.

In 1971, Jody and I left San Diego with our three-week-old son Mark for what has been a career at Columbia University—at Lamont, a place that has a formidable reputation for data gathering, and where at last I learned to grapple with observations.

I was in the right place at the right time when John Filson wanted help running the American office of what was then the Geophysical Journal of the Royal Astronomical Society. That editorial work for seven years was a terrific education.

Another piece of good fortune was being asked in 1975 by Kei Aki to co-author a textbook, which was blessed with his insight and good timing, as seismology moved in the 1980s to new levels of quantitative capability—with the spread of digital broadband high-dynamic-range stations. Our book is still in print, now as a paperback that came out last year.

It was through students including John Anderson, George Choy, Vernon Cormier, and Bill Menke, that I learned about

practical realities of strong ground motion, of tunneling, and whispering galleries. It was through Won-Young Kim, Vitaly Khalturin, and Tanya Rautian, that progress was made using regional seismograms to discriminate between explosions and earthquakes—with opportunities to apply these new methods especially to events in Central Asia and East Asia.

In the mid-1990s Xiaodong Song came as a post-doc to Lamont, and our discovery of seismological evidence that the inner core of the Earth rotates faster than the mantle and crust was the most exciting time of my professional life. I'd been thinking about it for years, with no progress. But then everything came together in a three-week period in early 1996, from having the right idea—to use transmitted waves—through Xiaodong's finding the data and making the measurements, to sending off a manuscript to *Nature*. The inner core is a Moon-sized object at the center of our planet, but it's almost 60 times nearer to us than the Moon. And whereas the Moon keeps the same face to us, the inner core does not—it rotates with respect to us at a rate that can be detected in a human lifetime. Xiaodong was able to document a systematic change in the 20-minute travel-time of a *P*-wave traversing the Earth via the inner core. The change was about one part in a hundred thousand, per year. Ken Creager improved on our original interpretation of the observations; and my student Jian Zhang—and others, including Xiaodong—found doublets that provided evidence a hundred times stronger than we had in our original paper, though due to Xiaodong's careful work we had obtained the right rate of travel-time change for the path we studied in 1996.

This was "precision seismology," where the scientific payoff came from arrival-time changes measured to better than a hundredth of a second. So, now I'm really wedded to data; and precision seismology is needed too in the hugely effective new methods for locating earthquakes. I've had adventures there with Won-Young Kim, David Schaff, Felix Waldhauser, Mark Fisk, and Relu Burlacu; and Felix and David are now doing what I regard as some of the most important work in all of seismology with their studies of terabyte-sized archives of waveforms, using hundreds of thousands of events in the past, as a resource to locate most of today's events in California, a few minutes after they occur, to within a few hundred meters.

To conclude: I wrote theoretical papers at first, and was then fortunate to find colleagues who got me into practical applications and data analysis. I'm glad that Lynn Sykes and I are now writing together.

In our profession as seismologists, we can be fortunate that there *is* such a range of good work to do: the intellectual challenges of various theories and sorting out important ideas; the terabytes of high-quality data sets to be interpreted; and the applications to hazard mitigation, and (I hope) to nuclear arms control.

I am so glad I was guided into seismology, and the community of seismologists; and I greatly appreciate the company I've found.

Paul Richards
21 April 2010

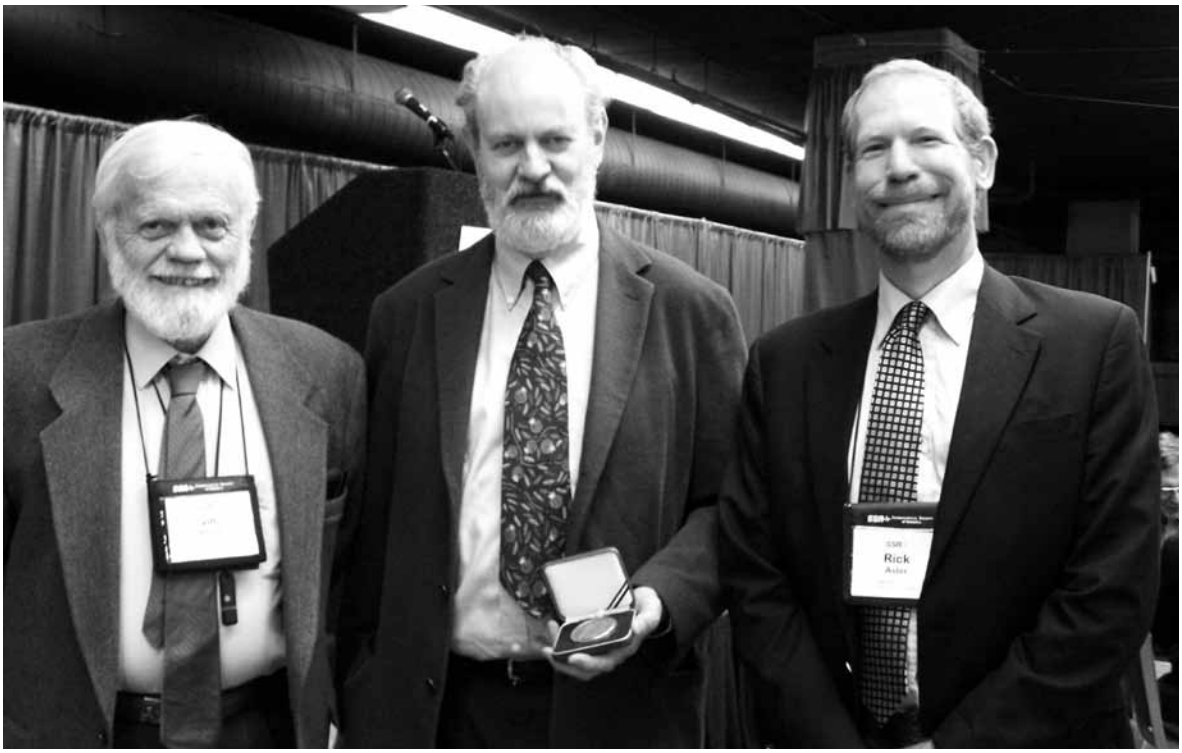

▲ Jim Brune, Paul Richards, and SSA President Rick Aster. Brune presented the citation for Reid Medal honoree Richards at the annual luncheon.

Bruce Bolt Medal Award to David M. Boore

The Bolt Medal is an honor coordinated by SSA, the Consortium of Organizations for Strong Motion Observation Systems (COSMOS), and the Earthquake Engineering Research Institute (EERI) that recognizes individuals whose accomplishments involve promotion and use of strong-motion earthquake data and whose leadership in the transfer of scientific and engineering knowledge into practice or policy has led to improved seismic safety.

In presenting the Bolt medal to David. M. Boore, SSA President Rick Aster read the following:

Boore's work has advanced the understanding of strong-motion seismology. Focusing primarily on strong ground motion, Boore's work has influenced seismic building standards and improved seismic safety in the U.S. and around the world. During his career, Boore has focused on the prediction of strong ground shaking, both from analysis of observed data and from simulations.

▲ Bolt Medal awardee David Boore.

While Boore was not the first researcher to pursue ground motion prediction equations (GMPEs), he has been on the forefront of improving prediction equations. Between 1982 and 2008, one can find at least 20 highly cited and otherwise significant publications published by Boore on GMPEs that delve into critical issues for the central and eastern United States, extensional regimes, subduction zones and other regions of the world including Taiwan, Turkey and Europe. Efforts throughout Boore's career have had profound effects on seismic design.

It's a great pleasure to present the COSMOS/EERI/SSA Bolt Medal to Dave Boore.

Charles F. Richter Early Career Award Commendation to Karen Felzer

SSA President Rick Aster read the following before presenting the Richter Award to Karen Felzer:

In her relatively young career, Karen Felzer has produced transformative and sometimes valuably controversial research by utilizing statistical approaches to tackle tough seismological questions. Her oft-cited work has constructively challenged previously held theories and reshaped the way earthquake physics is understood.

While completing her doctoral work at Harvard, Felzer produced three publications that focused on a statistical approach to earthquake clustering and provided a clearer view of how earthquake sequences work. She confirmed earlier work by others that foreshock-mainshock pairs are, statistically, simply cases where an aftershock is larger than the initial event. This led her to conclude that robust and useful calculations can be made of the probability that a given earthquake will be followed by a larger earthquake across a given time and distance using these empirical aftershock statistics. During here post-doc work, Felzer documented that studies of aftershock rates are often confounded by the inclusion of background events, which is a particular problem as one looks for distant aftershocks. Felzer has also been a key contributor to the Working Group on California Earthquake Probabilities. Among other contributions, she created a uniform, long-term seismicity catalog and then used this catalog to estimated expected seismicity rates. The drills developed for the Great Southern California ShakeOut relied on aftershock scenarios that Felzer produced.

▲ Richter awardee Karen Felzer.

It's a great pleasure to present the 2009 Charles Richter Early Career Award to Karen Felzer.

Frank Press Public Service Award Commendation to Art Frankel

The Frank Press Public Service Award honors outstanding contributions to the advancement of public safety or public information relating to seismology. SSA President Rick Aster read the following before presenting the Press Award to Art Frankel:

Since being tasked with leading an update to national seismic hazard maps for the USGS in 1993, Art Frankel has contributed significantly to improved public policy, building codes and earthquake safety across the United States.

The national seismic hazard maps that Frankel and USGS colleagues developed under his leadership were the first to be used directly in the seismic provisions of building codes. Within three years, Art had led the development of new national seismic hazard assessments based on hazard values for about 150,000 gridded sites nationwide. Frankel not only expanded the scientific methodology behind the maps, he also established and carried out essential consensus-building procedures for gathering expert opinion and feedback to ensure confidence in the process and for spurring improved communication between the seismology and engineering communities.

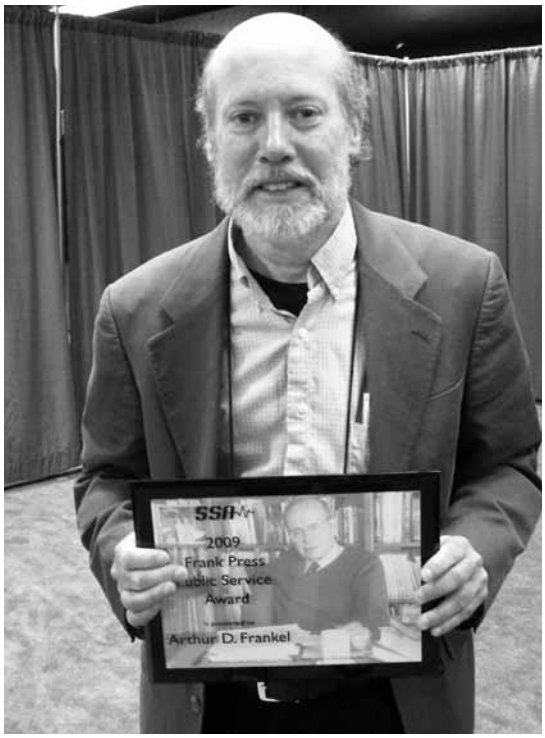

▲ Press awardee Art Frankel

The national seismic hazard maps developed through Art's efforts draw upon a wide body of results from geological research and earthquake monitoring supported by the National Earthquake Hazards Reduction Program. The hazard maps are used as the definitive basis for seismic design maps, which are in turn used in the seismic safety elements of model building codes adopted by more than 20,000 cities, counties, and communities in the U.S. Frankel has also further applied his research and leadership skills in developing finer scale, urban hazard maps that take into account site conditions and other local geologic features.

The work of Frankel and colleagues has provided the basis for a new standard of building codes nationwide that are promoted by FEMA and other organizations. In recent years, Frankel has turned over the reins of the national hazard project and focused on developing techniques for urban and regional seismic hazard assessments that account for soil conditions and nonlinear site response, three-dimensional basin effects and fault rupture directivity. In this work he has focused, most appropriately for this meeting of the SSA, on the Seattle and Portland areas.

It's a great pleasure to present the 2009 Frank Press Award to Art Frankel.

2010 SSA Student Presentation Awards

The SSA Student Presentation Awards recognize excellence in student poster presentations or talks at the annual meeting. This year the award is given to up to 15% of the number of students presenting at the annual meeting whose presentations meet absolute criteria that cover the quality of both content and presentation. The 2010 SSA Student Presentation Awards were given based on evaluation by the Student Award subcommittee, made up of Thomas Pratt (chair), Elizabeth Barnett, Chris Cramer, Lee Liberty, Morgan Moschetti, Justin Rubenstein, Lara Wagner, Ray Willeman, and Lorraine Wolf. From among a total of about 80 student presentations at the 2010 SSA Annual Meeting, the subcommittee chose the following 12 for recognition:

Biniam Beyene Asmerom
University of Memphis Center for Earthquake Research and Information
Lateral Crustal Velocity Variations in the Andean Foreland in San Juan, Argentina, Determined with the JHD Analysis and 3D P and S Velocity Inversion, B. B. Asmerom, J.-M. Chiu, J. Pujol, and R. Smalley

Shaun Finn
Boise State University
Insights into Active Deformation of Southern Prince William Sound, Alaska, from New High-Resolution Seismic Data, S. P. Finn, L. M. Liberty, P. J. Haeussler, and T. L. Pratt

Annemarie Baltay
Stanford University
Energetic and Enervated Earthquakes: Real Scatter in Apparent Stress and Implications for Ground Motion Prediction, A. S. Baltay; G. Prieto, S. Ide, and G. C. Beroza

Abhijit Ghosh
University of Washington Seattle
Toward a Unified View of Tremor Distribution in Space and Time, A. Ghosh, J. E. Vidale, J. R. Sweet, K. C. Creager, A. G. Wech, and H. Houston

Kevin Eagar
Arizona State University
P-to-S receiver function imaging of the crust beneath the High Lava Plains of Eastern Oregon, K. C. Eagar, M. J. Fouch, D. E. James, R. W. Carlson, and the High Lava Plains Seismic Working Group

Jessica Griffin
Purdue University
Modeling of Three-Dimensional Regional Velocity Structure Using Wide-angle Seismic Data from the Hi-CLIMB Experiment in Tibet, J. D. Griffin, R. L. Nowack, T. L. Tseng, W. P. Chen

Nicolas Kuehn
University of Potsdam
A Bayesian Ground Motion Model for Estimating the Covariance Structure of Ground Motion Intensity Parameters, N. M. Kuehn, C. Riggelsen, F. Scherbaum, and T. I. Allen

Frederick Pearce
Massachusetts Institute of Technology
Imaging with Scattered Teleseismic Waves: Data, Method, F. D. Pearce and S. Rondenay

Jonathan MacCarthy
New Mexico Institute of Mining and Technology
Tomographic Imaging of the Upper Mantle beneath the Colorado Rocky Mountains from Simultaneous Joint Inversion of Teleseismic Body Wave Residuals and Bouguer Gravity, J. K. MacCarthy, R. C. Aster, S. M. Hansen, and K. G. Dueker

Brandon Schmandt
University of Oregon Eugene
Seismic Evidence for Fossil Subduction and Small-scale Convection beneath the Northwestern U.S., B. Schmandt and E. Humphreys

Christopher Madden
Oregon State University Corvallis
Late Quaternary Shortening and Earthquake Chronology of an Active Fault in the Kashmir Basin, Northwest Himalaya, C. Madden, D. Trench, A. Meigs, S. Ahmad, M. I. Bhat, and J. D. Yule

Amanda Thomas
University of California Berkeley
Tidal Triggering of LFEs near Parkfield, CA, A. T. Thomas, R. Bürgmann, and D. Shelly

Minutes of the Meeting of the Board of Directors

20 April 2010
Mount Hood Room, Downtown Waterfront Marriott
Portland, Oregon

2009–2010 BOARD MEETING (retiring Board)

The 2009–2010 Board of Directors of the Seismological Society of America met in Portland Oregon on 20 April 2010. President Rick Aster called the meeting to order at 9:34 AM. Present at roll call were Vice-President Christa von Hillebrandt-Andrade, Directors Roland Bürgmann, Steven Day, Bill Ellsworth, Art Frankel, Robert Graves, Woody Savage, Brian Tucker, Dave Wald and Mary Lou Zoback.

Also present were Secretary Keith Knudsen, Treasurer Mitch Withers, Executive Director Susan Newman, *Bulletin of the Seismological Society of America* Editor Andrew Michael, *Seismological Research Letters* Editor Luciana Astiz; and Directors-Elect Steven Day, Tom Jordan, Lisa-Grant Ludwig. Others leaders in attendance during all or part of the meeting included Publications Committee Chair John Ebel, Government Relations Committee Chair Stu Nishenko, Annual Meeting Program Committee Co-Chair Seth Moran and incoming BSSA Editor Diane Doser. Staff and consultants present during parts of the meeting included Operations Director Joy Troyer, BSSA Managing Editor Carol Mark, SRL Managing Editor Mary George, and Government Affairs Director of Federal Affairs Elizabeth Duffy.

The board approved the minutes of the Board of Directors' meeting on 7 April 2009 as published in SRL and minutes from a Board conference 15 July 2009 as distributed by email and included with the agenda.

REPORTS OF OFFICERS

President Aster welcomed the new Board members and conveyed the regrets of retiring Director John Anderson, on sabbatical in Japan, and Director-Elect Klaus Hinzen, unable to travel due to the eruption of Eyjafjallajökull Volcano. Over forty annual meeting pre-registrants cancelled because of the volcano. Record attendance at the meeting was still anticipated and press interest was high. Aster reported that overall it had been a very successful year. He reviewed the Strategic Issues that the Board had previously identified to guide the discussion.

Secretary Knudsen referenced the written Secretary's Report. The Secretary's report was approved and will be printed in SRL as an attachment to these minutes (page 830). Knudsen reported that the Executive Committee now approves organizational goals for the year following the April Board meeting and expressed his thanks to the staff.

Treasurer Withers reported on the audited financial statements and reviewed graphs of historical assets, income and expenditures. The fiscal health of the society remains strong and income was higher than expenses. Withers was asked about the financial impact of policy changes on color figures income. He noted that the impact will not be felt until after June 2011. The Treasurer's report was accepted and ordered printed in SRL (see page 832).

REPORTS OF STANDING COMMITTEES AND EDITORS

Roland Bürgmann reported that the Audit Committee had reviewed the audited financial statements and Management Letter with auditor Hilary Crosby in a conference call on 15 April and were satisfied that SSA financial management is in good shape. Minor issues identified in the Auditor's Management Letter do need to be resolved. The Board voted to accept the Report of the Auditor. It also voted to accept the auditor's Management Letter and direct the staff to resolve the issues raised.

The Executive Committee actions were included in the Secretary's report.

The Management Committee report by Secretary Knudsen noted that the Committee had finalized an update of the Employee Handbook and completed a second year of the new performance review process for the Executive Director.

Publications Committee Chair John Ebel submitted a written report on publications activities and reported orally on decisions made at the morning breakfast meeting. The Committee's major activity during the year was the very successful search for a new BSSA Editor. The process of transition from Andy Michael to Diane Doser has already begun and should be complete by summer. In October, SRL Editor Luciana Astiz asked the Society to begin a search for her replacement. A Search Committee consisting of Sue Hough, Mike Fehler and David Wald has been formed. The Publications Committee also discussed the best timing for installing electronic submission for SRL. Although the budget anticipated waiting until the new editor was in place the Committee felt that it should be ready for the new editor.

BSSA Editor Andy Michael reported that beginning with the June issue, authors may submit color figures to the online edition and have them printed in black and white. It is still too soon to judge the implications of this on finances and the quality of figures in the print journal. He noted that the current procedure for electronic supplements is unusual, some authors find it onerous and recommended that a task force be appointed to review it.

SRL Editor Luciana Astiz reported that submissions to SRL continue to increase and the annual volume was the largest to date. A special section dedicated to earthquake early warning included a pamphlet prepared by the Japan Meteorological

Agency on what to do in an earthquake. Translations of the poster into seven languages are posted on the SSA website.

The Board voted to accept the written reports from the Publications Committee, the BSSA Editor and the SRL Editor and place them on file.

Stu Nishenko, chair of the Government Relations Committee, reported that it had been an active year due to reauthorization of the National Earthquake Hazards Reduction Program and more interest in nuclear monitoring. He noted that several officers and directors had participated in these efforts as well. He submitted a written report detailing a number of Committee activities including letters and visits to legislators, co-sponsoring Congressional briefings, and participating in several coalitions to support key agencies. The Board accepted the written report from the Government Relations Committee.

Brian Tucker, Chair of the Honors Committee, presented the Committee's report. Some issues arose in the nomination process this year that should be discussed. One was the timing of the nominations for the COSMOS/EERI/SSA Bolt Medal. October 1 is the current deadline for nominations. The current deadline requires a Board call to ratify the decision at a very busy time of year. The Board agreed to recommend to the joint committee on the Bolt Medal that the deadline be moved to 1 Sept. It also agreed that there should be a regular SSA Board conference call in October and that the representatives to the Joint Committee on the Bolt Medal should be a subcommittee of the Honors Committee. Tucker noted that his term and the terms of the Honors Committee subcommittee chairs expire this year and he agreed to stay on as a member of the committee to assist. The Board agreed to accept the written report of the Honors Committee and place it on file.

REPORTS OF TASK COMMITTEES

Mitch Withers reported on the discussions of the ad hoc **Committee to Revise the Investment Policy,** which was formed to draft a new investment policy that may be less conservative than the current policy, if appropriate. The committee submitted a report to the Executive Committee in September 2009 recommending an expansion of investment options, with decisions delegated to the Management Committee. The Executive Committee noted that this was beyond the charge to that committee. The Executive Committee recommended to the Board that a standing Investment Committee be formed. The Board voted to accept the report of the task Committee to Revise the Investment Policy, discharge the Committee with thanks, and consider a standing committee under New Business.

Seth Moran, Co-Chair of the Program Committee for the 2010 Meeting, reported that it appeared that the meeting would draw record attendance for a meeting of SSA, even though travel from Europe was curtailed. Moran co-chaired the program committee with Nick Beeler and having co-chairs worked well. He recommended that SSA's guidelines for rejecting abstracts be reviewed, and that in the future, SSA announce that abstract deadlines be strictly enforced. A number of special challenges were encountered, including the growth of the meeting and the necessity to add a late session due to late-breaking earthquakes. The Board approved a resolution expressing appreciation for the 2010 Program Committee: co-chairs Seth Moran (USGS Cascades Volcano Observatory) and Nick Beeler (USGS Vancouver), Ivan Wong (Seismic Hazards Group, URS Corporation, Oakland CA), Ray Weldon (University of Oregon), Vicki McConnell (DOGAMI), and Anne Trehu (Oregon State University).

STAFF REPORT

The Board accepted Executive Director Newman's written report on **Staff Activities** for the year ending 31 January 2010 and the new system for setting annual goals. Operations Director Joy Troyer presented the **membership report**. She reported that membership is up 3.5%; 68% of members now elect to receive the electronic edition of BSSA; 54% get SRL electronically. A list of **lapsed members** was distributed and board members asked the staff to personally contact several people on the list. The board passed a motion that we advise members who have not paid dues for 2009 or 2010 of their status and drop them from the membership rolls if no response is received within 60 days after notification.

REPORTS OF SECTIONS AND AFFILIATED ORGANIZATIONS

Susan Newman reported that the **Eastern Section** met 4–6 October 2009 at the Lamont Campus of Columbia University, in Palisades, New York. The 2010 meeting will be held 17–19 October at Boston College.

Newman also referred to brief written reports on SSA affiliations with the American Geological Institute, the Earthquake Engineering Research Institute (EERI) the Geological Society of America, and IRIS.

Christa von Hillebrandt-Andrade, SSA's representative to the Committee on the IRIS/SSA Lectureship, asked the Board to ratify the Committee's selection of 2011 Lecturers. It did so unanimously.

Woody Savage, SSA's representative to the American Association for the Advancement of Science (AAAS) reported on discussions of how to increase the number of seismologists nominated for AAAS Fellow.

Savage also reported on the cooperation with the Consortium of Organizations for Strong Motion Observation Systems (COSMOS) and EERI regarding the Bruce Bolt Medal. The award recognizes individuals worldwide whose accomplishments involve the promotion and use of strong-motion earthquake data and whose leadership in the transfer of scientific and engineering knowledge into practice or policy has led to improved seismic safety. The second recipient of the medal will be David M. Boore. He will be recognized by each of the three organizations that co-sponsor the award and he will receive the award at the SSA Annual Luncheon.

CLOSING MOTIONS, retiring board:

The Board approved a resolution expressing **appreciation to retiring Directors John Anderson, Roland Bürgmann and Bill Ellsworth** for their excellent contributions to SSA leadership.

The Board approved **a consent agenda of routine motions** that have been incorporated in these minutes as appropriate.

The 2009–2010 Board adjourned and the 2010–2011 Board was called to order.

2010-2011 BOARD MEETING (continuing Board)

A roll call of the 2010–2011 Board showed all Directors present except for Klaus Hinzen. Retiring Director Roland Bürgmann left the meeting.

COMMITTEE ASSIGNMENTS

Committee Rosters were reviewed and additional appointments discussed. John Ebel noted that he had chaired the Publications Committee since 2002 and it was time for a change. Lisa Grant Ludwig agreed to chair the Honors Committee and work with Tucker to populate it after the meeting. Tom Jordan agreed to chair a new standing Investment Committee. Aster said that appointing a Board Nominating Committee and finalizing the roster of all committees should be a priority during and after the annual meeting.

UNFINISHED BUSINESS

Ellsworth and Aster presented a written report with a draft mission statement for the **Kanamori Fund.** After considerable discussion, the following motion passed unanimously:

"The Kanamori Fund will support the professional development of students, seismologists and earthquake engineers including:

- subsidized dues for international student and professional colleagues
- travel support to SSA meetings for international colleagues, international and U.S. students and young professionals
- editorial assistance for international colleagues for publication in SSA journals"

A committee will be formed to move forward with a plan for fund raising. Ellsworth, Jordan and Tucker agreed to serve and others will be added.

There was a brief discussion of Hinzen's written report on **cooperation with the European Seismological Commission**. Several proposals for continued cooperation had been put forth by ESC. Wald agreed to participate in a call after the meeting. The board favored continuing joint sessions at each meeting on a year-to-year basis. Specific proposals for travel grants for students to participate in each of the two meetings would also be favorably considered.

NEW BUSINESS

In Executive Session, the Board considered nominations for the 2010 awards, which will be presented at the 2011 meeting. As a result of those deliberations, the 2010 **Reid Medal** will be awarded to Tatiana Rautian. Zhigang Peng will be the recipient of the **Richter Award**. Hugo Yepes will be awarded the **Frank Press Public Service Award**.

Newman reported that the next meeting will be **17–20 April in Memphis, Tennessee**. Aster has asked Charles Langston and Beatrice Magnani to co-chair the Program Committee. Space has been reserved for a Public Forum.

The staff is pursuing plans to hold the **2012 meeting in San Diego,** California.

The board approved the proposed **budget** for the fiscal year ending 31 January 2010, with the understanding that a revision to accommodate costs of an SRL online submission system would be provided at a later date.

The meeting adjourned at 6:22 PM.

Report of the Secretary and Actions of the Executive Committee For the Period April 2009 to March 2010

During the past fiscal year, ending January 31, 2010, the Seismological Society of America published seven issues of Volume 99 of the Bulletin of the Seismological Society of America (BSSA) totaling 3,533 pages. Issue 2B, published in May 2009, was a special issue on Rotational Seismology and Engineering Issues. The Society also published volume 80, numbers 2 through 6 and volume 81, number 1, of Seismological Research Letters (SRL), totaling 1080 pages. Both journals published significantly more content than last year, as indicated by the number of pages published.

The 104rd Annual Meeting was held in Monterey California from April 8 to 10. Approximately 550 attendees participated in the meeting. Many thanks to the Program Committee: Marcia McLaren (Chair), Greg Beroza, Susan Hough, and Joe Litehiser. Minutes of the meeting were printed on page 832 of SRL, volume 80, number 5. The meeting program with abstracts was published prior to the meeting in SRL volume 80, number 2.

Abstracts for the 2010 Annual Meeting in Portland appeared in SRL volume 81, number 2, and were mailed to members in March. There are 27 special sessions and 4 general sessions, for a total of 31 sessions. 540 abstracts were submitted.

The Society continues to be blessed with an excellent and professional Headquarters staff. Susan Newman (Executive Director) and Joy Troyer (Operations Director), both operating out of the office in El Cerrito that the Society has occupied for more than 20 years, continued in their positions. Sissy Stone is their Administrative Assistant and Sarah Karlson serves as the Membership Coordinator. In recent years, the Society has been relying heavily on freelance and consultant help. The following contract/freelance team members continued in their roles: Bo Orloff (IT support and website enhancements), Carol Mark (BSSA Managing Editor), Mary George (SRL Managing Editor), Nan Broadbent (media liaison), Elizabeth Duffy (Federal Affairs Office, Washington DC representation), Miranda Beasley (accounting services), and Joyce Novicky-Martinez (annual meeting coordination). The change made a couple of years ago in which Headquarters staff takes on greater responsibilities in planning annual meetings has contributed to the recent string of well organized meetings, and appreciative organizing committees.

The Executive Committee consists of President Rick Aster, Vice President Christa von Hillebrandt-Andrade, and Secretary Keith Knudsen. The Executive Committee's role is to serve on behalf of the Board of Directors and make those decisions requiring action between meetings of the Board. Mitch Withers, the Treasurer, is consulted on many matters. This year the Executive Committee took the following actions:

- Approved organizational goals for the year, based on actions taken at the April board meeting and discussions with the Management Committee and Executive Director.
- Reviewed applications for travel grants for the Portland annual meeting. The committee decided to award grants to: Din Muhammad Kakar, Wei Li, Corrie Neighbors, Carrie Rockett, Hunter Knox, Julien Chaput, Shaun Finn, and Luis Dominguez-Rameriz. This support is available due, in part, to the generous gift of a member in 2006 that started the fund
- Discussed recommendations made by an ad hoc Investment committee appointed in April of 2009, and proposed actions for full-board discussion at the 2010 board meeting.
- Approved a revision of the Employee Handbook, acting on recommendations from the Management Committee.

At a Board meeting in July, the Board voted to change the journal of record for BSSA from the print edition to the online edition.

Several Society members served an important role as members of the Nominating Committee for candidates for the 2010 Board of Directors. These committee members included Susan Beck (Chair), Gail Atkinson, Susan Bilek, Jim Dolan, and Miaki Ishii.

The total number of members and subscriptions this year was 3111, an increase of only 2 over last year (Figure 1). The number of members is up by 3.5% this year, but subscriptions decreased by nearly 10%. Although this was the third year for the new membership category "Developing Countries", the number of members in this category rose considerably this year (from 5 to 41) due to a change in the definition to include all countries except those identified as "High-income Economies". We continue to move graduating students into the "Transitional" membership category (29 transfers this year, 69 current members in this category), thus helping us to retain these members after graduation. Free membership (with electronic access to journals) for first-time members was once again offered to student attendees at the AGU fall meeting, with 73 students signing up for this benefit. The number of members opting to receive only the electronic version of BSSA continues to increase. 68% of our membership no longer receives a hard copy of the Bulletin. This is the third year that SRL has been available electronically and 57% of members no longer receive a hard copy.

Keith L. Knudsen
Secretary

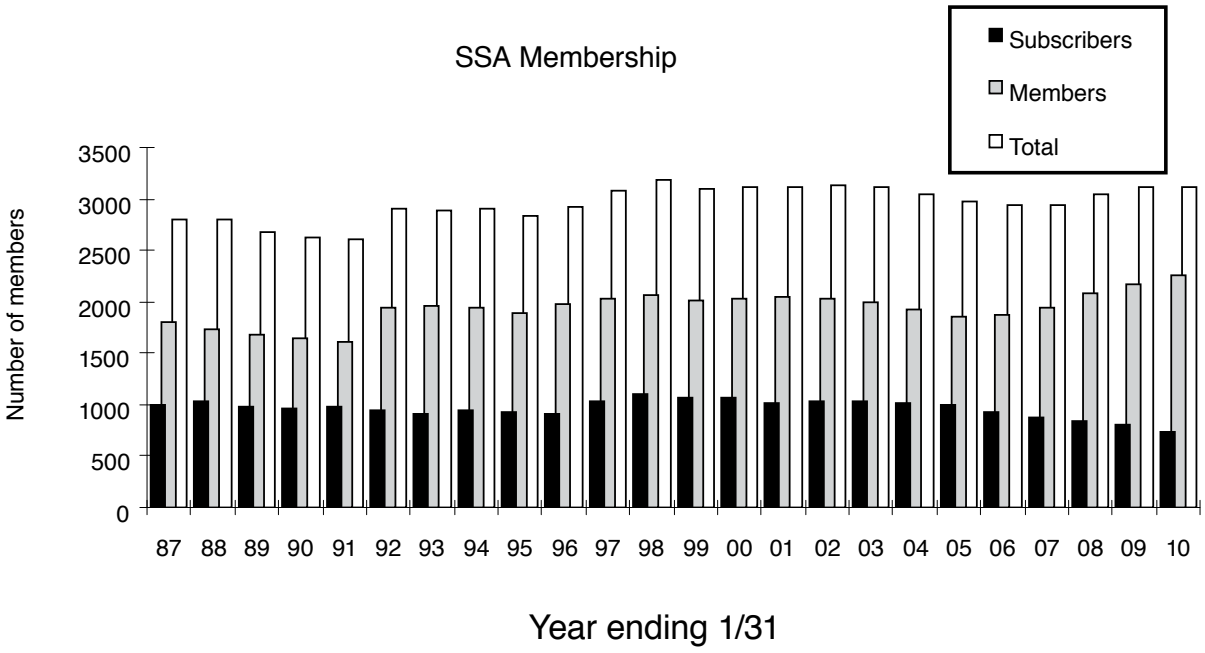

▲ **Figure 1.** SSA members (primarily regular and student) and subscribers (primarily institutions and libraries) for recent fiscal years. The annual total includes Corporate membership (12 members) and EERI Associate memberships (122 members).

Treasurer's Report

The Society again had an excellent financial year. Investment losses are down relative to last year and publication revenues are up. The annual meeting continues to grow and was the primary source of the increase last year. As of the fiscal year end on January 31, 2010, our net assets stood at $1,530,005—an increase of $158,434 over the previous fiscal year end. Net assets are total assets minus any liabilities; liabilities were $116,655 at the end of the fiscal year. The history of the society's net assets is shown in Figure 1. The Consumer Price Index (CPI) from the Commerce Department of the federal government was used to correct the raw dollar amounts to an inflation-adjusted series in this figure, with the average CPI for 2009 as the normalization value. The line labeled "net assets adj." is then the truer picture of the society's assets.

A $26,704 increase in the Joyner fund provided essentially the sole growth in the Society's investments. Investments are detailed in note 6 of the audit report. It is becoming increasingly difficult in the current market to find reasonable investments that conform to the SSA investment policy. We anticipate this situation to change pending approval of the Officer's recommendation to the Board of the new policy.

Figures 2 and 3 show the history of the income and expenses of the society—again with adjustments for the CPI. We had a larger than estimated increase in income than expenses this past fiscal year, reflecting the tradition of conservative budget estimates. Income and Expenses for FYE 1/2010 were $1,713,115 and $1,554,681 respectively. This represents an increase in income of $232,987 (16% over FYE 1/2009) and an expense increase of $107,088 (7.4%).

We were again able to finalize the audit report prior to the Board meeting and anticipate as of the writing of this report that it will be approved by the Audit Committee during a conference call scheduled for April 15. Subject to Audit Committee approval, the report again concludes that the financial statements provided by the SSA "present fairly, in all material respects, the financial position of the Seismological Society of America…in conformity with accounting principles generally accepted in the United States of America."

Mitch Withers

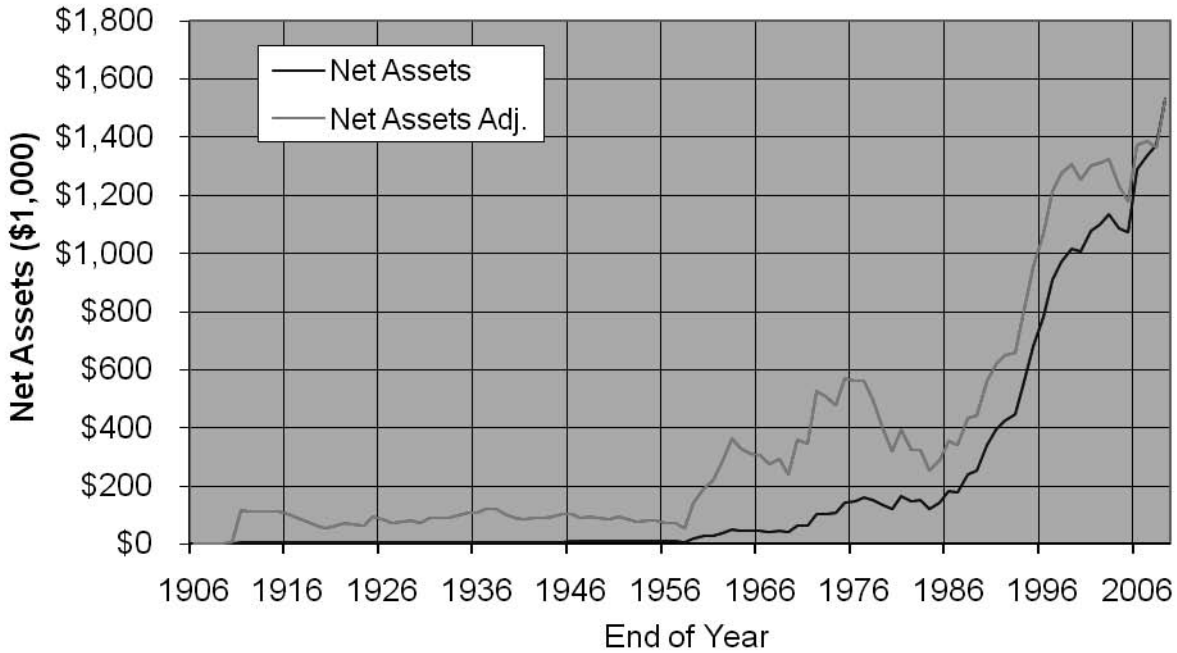

▲ **Figure 1.** History of the net assets of the Seismological Society of America through the end of FYE 1/31/2010. The "adj" curve takes into account inflation using the consumer price index from the Bureau of Labor Statistics (http://www.bls.gov/data) normalized to 2009.

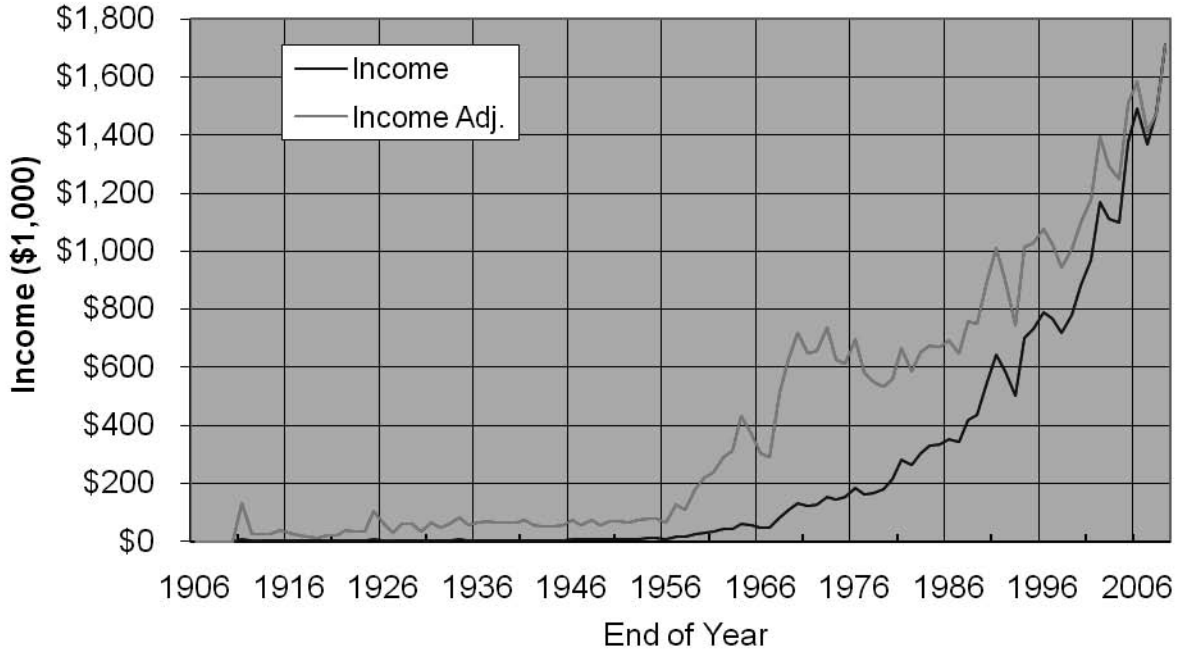

▲ **Figure 2.** History of the income of the Seismological Society of America through the end of FYE 1/31/2010. The "adj" curve takes into account inflation as in Figure 1.

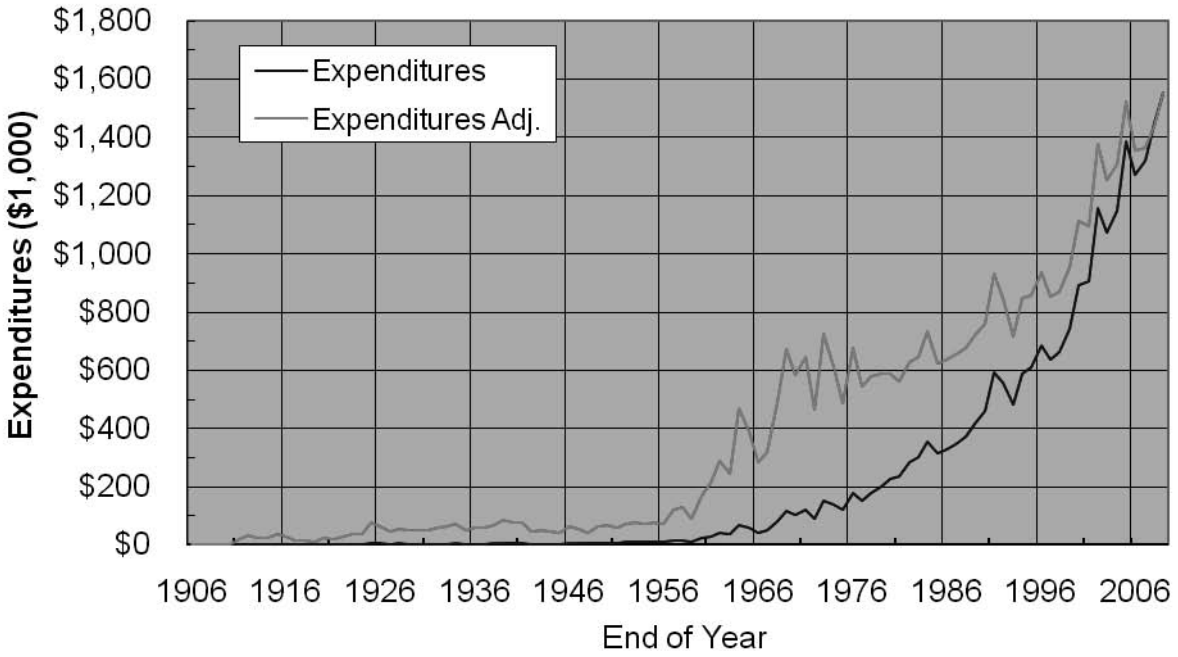

▲ **Figure 3.** History of the expenditures of the Seismological Society of America through the end of FYE 1/31/2010. The "adj" curve takes into account inflation as in Figure 1.

Seismological Society of America

FINANCIAL STATEMENTS

January 31, 2010 and 2009

CROSBY & KANED
Certified Public Accountants

Dedicated to Nonprofit Organizati

SEISMOLOGICAL SOCIETY OF AMERICA

CONTENTS

CROSBY & KANEDA
Certified Public Accountants

Dedicated to Nonprofit Organizations

Latham Square Building
1611 Telegraph Ave. Suite 318
Oakland, CA 94612-2151
Tel: 510 · 835 · CPAS (2727)
Fax: 510 · 835 · 5711
e-mail: info@ckcpa.biz

INDEPENDENT AUDITORS' REPORT

Board of Directors
Seismological Society of America
El Cerrito, California

We have audited the accompanying statement of financial position of Seismological Society of America (a nonprofit California corporation) as of January 31, 2010 and 2009, and the related statements of activities, cash flows, and functional expenses for the years then ended. These financial statements are the responsibility of the Organization's management. Our responsibility is to express an opinion on these financial statements based on our audits.

We conducted our audits in accordance with auditing standards generally accepted in the United States of America. Those standards require that we plan and perform the audit to obtain reasonable assurance about whether the financial statements are free of material misstatement. An audit includes examining, on a test basis, evidence supporting the amounts and disclosures in the financial statements. An audit also includes assessing the accounting principles used and significant estimates made by management, as well as evaluating the overall financial statement presentation. We believe that our audit provide a reasonable basis for our opinion.

In our opinion, the financial statements referred to above present fairly, in all material respects, the financial position of Seismological Society of America as of January 31, 2010 and 2009, and the changes in its net assets and its cash flows for the years then ended in conformity with accounting principles generally accepted in the United States of America.

Crosby + Kaneda

Certified Public Accountants
Oakland, California
March 17, 2010

Seismological Society of America
Statement of Position
January 31, 2010 and 2009

	2010	2009
Assets		
Current Assets		
Cash and cash equivalents	$ 890,879	$ 904,681
Accounts receivable, net of allowance for doubtful accounts of $26,993 and $24,033 respectively	77,401	53,335
Prepaid expenses	1,031	1,461
Total current assets	969,311	959,477
Investments (Note 3)	667,084	465,985
Property and equipment, net (Note 4)	9,180	7,275
Deposits	1,085	1,085
Total Assets	$ 1,646,660	1,433,822
Liabilities and Net Assets		
Liabilities		
Accounts payable and accrued expenses	$ 61,511	$ 23,485
Deferred page charges	36,309	21,986
Deferred conference registration	15,940	14,170
Advance postage	2,895	2,610
Total liabilities	116,655	62,251
Commitments (Note 5)		
Net Assets		
Unrestricted		
Undesignated	1,285,886	1,167,375
Designated (Note 6)	244,119	204,196
Total net assets	1,530,005	1,371,571
Total Liabilities and Net Assets	$ 1,646,660	$ 1,433,822

See Notes to the Financial Statements

Seismological Society of America
Statement of Activities
For the Years Ended January 31, 2010 and 2009

	2010	2009
Revenue and Support		
Contributions	$ 18,260	$ 19,865
Dues	218,640	205,990
Publications	1,181,346	1,071,520
Annual meeting	233,076	223,996
Interest and dividends	14,231	34,143
Realized gain	754	-
Unrealized gain (loss)	37,117	(77,830)
Other	9,691	2,444
Total Revenue and Support	1,713,115	1,480,128
Expenses		
Program services	1,001,461	919,973
General and administrative	553,220	527,620
Total Expenses	1,554,681	1,447,593
Change in Net Assets	158,434	32,535
Net Assets, beginning of year	1,371,571	1,339,036
Net Assets, end of year	$ 1,530,005	$ 1,371,571

See Notes to the Financial Statements

3

Seismological Society of America

Statement of Cash Flow

For the Years Ended January 31, 2010 and 2009

	2010	2009
Cash flows from operating activities:		
Change in net assets	$ 158,434	$ 32,535
Adjustments to reconcile change in net assets to		
net cash provided (used) by operating activities:		
Depreciation	6,630	3,664
Realized gain	(754)	-
Unrealized (gain) loss	(37,117)	77,830
Changes in assets and liabilities:		
Accounts receivable	(24,066)	2,645
Prepaid expenses	430	9
Accrued payable and accrued expenses	38,026	(40,333)
Deferred page charges	14,323	(2,614)
Funds held for others	-	1,752
Advance postage	285	(6,022)
Deferred conference registration	1,770	(8,530)
Net cash provided by operating activities	157,961	60,936
Cash flows from investing activities:		
Sales and redemption of investments	100,000	300,000
Purchase of investments	(263,228)	(13,065)
Purchase of fixed assets	(8,535)	(4,295)
Net cash provided (used) by investing activities	(171,763)	282,640
Net change in cash	(13,802)	343,576
Cash and cash equivalents, beginning of year	904,681	561,105
Cash and cash equivalents, end of year	$ 890,879	$ 904,681

See Notes to the Financial Statements

Seismological Society of America
Statement of Functional Expenses
For the Years Ended January 31, 2010 and 2009

	2010			2009		
	Program	Management and administrative	Total	Program	Management and administrative	Total
Salaries	$	$ 227,491	$ 227,491	$	$ 238,923	$ 238,923
Pension		21,920	21,920		16,033	16,033
Employee benefits		26,336	26,336		7,672	7,672
Payroll taxes		19,106	19,106		18,385	18,385
Total personnel	-	294,853	294,853	-	281,013	281,013
Accounting and legal		20,200	20,200		19,665	19,665
Office expenses		52,615	52,615	17,300	32,811	50,111
Occupancy		53,171	53,171	7,839	58,346	66,185
Printing and publications	397,812		397,812	333,402	15,574	348,976
Travel	19,696	12,152	31,848	28,562	6,276	34,838
Conferences and meetings	145,124	907	146,031	147,067	2,586	149,653
Bad debt	60,839	7,191	68,030		4,390	4,390
Depreciation		6,630	6,630		3,664	3,664
Professional services	377,990	69,684	447,674	378,139	82,938	461,077
Dues and subscriptions		6,526	6,526	5,951	1,223	7,174
Bank charges		24,596	24,596	-	19,850	19,850
Miscellaneous		4,695	4,695	1,713	1,004	2,717
Total expenses	$ 1,001,461	$ 553,220	$ 1,554,681	$ 919,973	$ 529,340	$ 1,449,313

See Notes to the Financial Statements

NOTE 1: NATURE OF ACTIVITIES

The Seismological Society of America (the Society) is a nonprofit organization dedicated to the advancement of the science and practice of seismology and related sciences. An organization, the Eastern Section of the Seismological Society of America (ESSA), is a separate legal entity and is not included in these financial statements.

NOTE 2: SIGNIFICANT ACCOUNTING POLICIES

Basis of Accounting

The accompanying financial statements have been prepared on the accrual basis of accounting in accordance with generally accepted accounting principles.

Basis of Presentation

The Society reports information regarding its financial position and activities according to three classes of net assets: unrestricted net assets, temporarily restricted net assets, and permanently restricted net assets. The Society has no temporarily or permanently restricted net assets.

Revenue Recognition

Contributions are recognized as revenue when received or unconditionally promised. Contributions are recorded as unrestricted, temporarily restricted, or permanently restricted support depending on the existence and/or nature of any donor restrictions.

All donor-restricted contributions are reported as increases in temporarily or permanently restricted net assets, depending on the nature of the restriction. When a restriction expires (that is, when a stipulated time restriction ends or purpose restriction is accomplished), temporarily restricted net assets are reclassified to unrestricted net assets and reported in the statement of activities as net assets released from restrictions.

Deferred revenue

Dues, including unconditional promises to give, are recognized as revenue in the period received. Conditional promises to give are not recognized until they become unconditional, that is when the conditions on which they depend are substantially met.

Income Taxes

The Internal Revenue Service and the California Franchise Tax Board have determined that the Society is exempt from federal and state income taxes under Internal Revenue Code Section 501 (c) (3) and the California Revenue and Taxation Code Section 23701(d).

Donated Services

Donated services are recognized as contributions if the services (a) create or enhance nonfinancial assets or (b) require specialized skills, are performed by people with those skills, and would otherwise be purchased by the Society.

Cash and Equivalents

For purposes of the statement of cash flows, the Society considers all cash and other highly liquid investments with maturities of three months or less to be cash equivalents. At January 31, 2010 and 2009, the Society had $492,850 and $531,325 respectively in money market funds in one financial institution. The amount did not exceed the Securities Investor Protection Corporation insurance limit.

Fair Value of Financial Instruments

The fair values of financial instruments represent the quoted marked prices for similar assets or liabilities in active markets.

Estimates

The preparation of financial statements in conformity with generally accepted accounting principles requires management to make estimates and assumptions that affect certain reported amounts and disclosures. Accordingly, actual results could differ from those estimates.

Property and Equipment

All acquisitions of property and equipment in excess of $500 and all expenditures for repairs and maintenance, renewals, and betterments that materially prolong the useful lives of assets are capitalized. Property and equipment are stated at cost or, if donated, at the approximate fair value at the date of donation. Depreciation is computed using the straight-line method over the estimated useful lives on the property and equipment.

Functional Allocation of Expenses

The costs of providing the various programs and activities have been summarized on a functional basis in the statement of activities. Accordingly, certain costs have been allocated among the programs and supporting services benefited.

Reclassifications

Certain accounts in the prior year financial statements have been reclassified for comparative purposes to conform with the presentation in the current-year financial statements.

NOTE 3: INVESTMENTS

Investments are long-term and carried at market value. Investments consist of the following at January 31:

	2010	2009
Mutual funds	$ 203,914	$ 155,000
Certificates of deposit	249,413	-
Fixed income	213,757	310,985
Total	$ 667,084	$ 465,985

Fixed income investments were liquidated at maturity and are included in cash and cash equivalents.

NOTE 4: PROPERTY AND EQUIPMENT

Property and equipment consist of the following at January 31:

	2010	2009
Furniture and equipment	$ 73,160	$ 69,083
Less accumulated depreciation	(63,980)	(61,808)
Total	$ 9,180	$ 7,275

NOTE 5: COMMITMENTS

Operating Leases

The Society leases office space and storage space under an operating lease with a five-year term expiring in June 30, 2013.

Minimum payments due under this lease as of January 2010 are as follows for the years ending January 31:

2011	$ 35,400
2012	35,400
2013	35,400
Total	$ 106,200

Rent expense for the years ended January 31, 2010 and 2009 were $34,301 and $31,805 respectively.

Note 6: Board Designated Funds

Funds received or designated by the Board of Directors for specific purposes are accounted for separately from those available for the general operations of the Society. The Life Membership fund, established prior to 1930, represents all moneys received for life memberships for permanent investment, the income from which may be expended at the discretion of the Board.

The William B. Joyner Memorial Fund was established in 2002 upon receipt of an initial gift from May Lou Joyner. It may be used at the discretion of the Board, (in consultation with the Joyner Fund Committee) for activities that encourage communication between seismology and earthquake engineering.

As of January 31, 2010, the balances of board designated funds were as follows:

				Life Membership		
	Joyner Memorial Fund	Student Travel Fund	Kanamori Fund	Accumulated Income	Permanent Investment	Total Designated
January 31, 2009	$ 101,506	$ 8,269	$ 50,817	$ 29,749	$ 13,855	$ 204,196
Additions/(Transfers)	10,750	85	-	-	-	10,835
Unrealized gain	26,704	-	-	-	-	26,704
Interest/Dividends	2,352	4	9	1	18	2,384
January 31, 2010	$ 141,312	$ 8,358	$ 50,826	$ 29,750	$ 13,873	$ 244,119

As of January 31, 2009, the balances of board designated funds were as follows:

				Life Membership		
	Joyner Memorial Fund	Student Travel Fund	Kanamori Fund	Accumulated Income	Permanent Investment	Total Designated
January 31, 2008	$ 136,922	$ 7,196	$ -	$ 29,212	$ 13,855	$ 187,185
Additions/(Transfers)	10,466	1,060	50,009	-	-	61,535
Unrealized loss	(48,419)	-	-	-	-	(48,419)
Interest/Dividends	2,537	13	808	537	-	3,895
January 31, 2009	$ 101,506	$ 8,269	$ 50,817	$ 29,749	$ 13,855	$ 204,196

NOTE 7: EMPLOYEE BENEFITS

For the year ended January 31, 2010 and 2009, the Society contributed a maximum of 9% of each employee's salary to the employees' retirement plan consisting of tax-shelter annuities underwritten by the Teachers Insurance and Annuity Association-College Retirement Equities Fund, in accordance with Section 403(b) of the Internal Revenue Code. As a condition of employment, all employees are required, unless alternate coverage is held, to participate in the health insurance program. The Society also contributes a maximum of 8% of each employee's salary to the health insurance program. Any excess premium becomes deductible from the employee's monthly pay on a pre-tax basis. For the year ended January 31, 2010 and 2009, The Society incurred $21,920 and $16,033 respectfully for retirement expense.

2010 SSA Annual Meeting
Attendance List

Registration Type	Which Day	First Name	Last Name
SSA Member Preregistration		Brad	Aagaard
SSA Member Preregistration		Robert	Abbott
SSA Member Preregistration		Norman	Abrahamson
SSA Member Preregistration		Hans	AbramsonWard
SSA Member Preregistration		Azlan	Adnan
Student Member Preregistration		Ana	Aguiar
SSA Member Registration		Jon	Ake
Student Nonmember Registration		Linda	Alatik
Student Member Registration		Sequoia	Alba
SSA Member Preregistration		Clarence	Allen
SSA Member Preregistration		Jean-Paul	Ampuero
Nonmember Preregistration		Larry	Anderson
SSA Member Preregistration		Rasool	Anooshehpoor
SSA Member Preregistration		David	Applegate
SSA Member Preregistration		Ralph	Archuleta
SSA Member Preregistration		Pierre	Arroucau
SSA Member Preregistration		Stephen	Arrowsmith
SSA Member Registration		Marie	Arrowsmith
SSA Member Preregistration		Aysegul	Askan
Student Member Preregistration		Biniam	Asmerom
SSA Member Preregistration		Richard	Aster
SSA Member Preregistration		Luciana	Astiz
SSA Member Preregistration		Gail	Atkinson
SSA Member Preregistration		Scott	Ausbrooks
Student Member Preregistration		solomon	Ayele
SSA Member Preregistration		Manochehr	Bahavar
SSA Member Preregistration		Laurie	Baise
SSA Member Preregistration		Jack	Baker
Nonmember Preregistration		Mark	Baker
SSA Member Preregistration		William	Bakun
Student Member Preregistration		Natalie	Balfour
SSA Member Preregistration		Sanford	Ballard
Student Member Preregistration		Annemarie	Baltay
Member or Non-Profit Exhibitor		Mary	Baranowski
Nonmember Registration		Elizabeth	Barnett
SSA Member Preregistration		Noel	Barstow
SSA Member Preregistration		Laurel	Bauer
Student Nonmember Preregistration		Jennifer	Bautista
Student Member Preregistration		Matthew	Beachly
SSA Member Preregistration		Jacob	Beale
SSA Member Preregistration		Bruce	Beaudoin
Non-Member For Profit Exhibitor		Nick	Beeler
Student Member 1-day Registration	Weds 21 April	Jeff	Beeson
SSA Member Preregistration		Michael	Begnaud
SSA Member Preregistration		Sean	Bemis
SSA Member Preregistration		Yehuda	Ben-Zion
Nonmember Preregistration		Rafael	Benites
Student Member Preregistration		Ninfa	Bennington
SSA Member Registration		Allison	Bent
SSA Member Registration		Gregory	Beroza
SSA Member Preregistration		Glenn	Biasi
SSA Member Preregistration		Jacobo	Bielak

2010 SSA Annual Meeting
Attendance List

Registration Type	Which Day	First Name	Last Name
SSA Member Registration		Roger	Bilham
SSA Member Preregistration		Selena	Billington
SSA Member Preregistration		Michael	Blackford
SSA Member Preregistration		Michael	Blanpied
SSA Member Preregistration		Marco	Bohnhoff
Nonmember Registration		Maiclaire	Bolton
SSA Member Preregistration		Jessie	Bonner
SSA Member Preregistration		David	Boore
SSA Member Preregistration		Adrian	Borsa
SSA Member Preregistration		Oliver	Boyd
Nonmember Registration		David	Boyd
SSA Member Preregistration		Brendon	Bradley
SSA Member Registration		Lawrence	Braile
SSA Member Preregistration		Tammy	Bravo
SSA Member Preregistration		Nan	Broadbent
SSA Member Preregistration		Thomasq	Brocher
SSA Member Registration		Peter	Bromirski
Student Member Preregistration		Justin	Brown
SSA Member Preregistration		Jim	Brune
SSA Member Preregistration		Carol	Bryan
Student Member Preregistration		Jesse	Buckner
SSA Member Preregistration		Roland	Burgmann
SSA Member Preregistration		Relu	Burlacu
SSA Member Preregistration		Robert	Busby
Student Member Preregistration		Hussam	Busfar
SSA Member 1-day Preregistration	Thurs 22 April	Alexander	Bykovtsev
SSA Member 1-day Preregistration	Fri 23 April	Recep	Cakir
SSA Member Preregistration		Kenneth	Campbell
SSA Member Preregistration		Jacqueline	Caplan-Auerbach
SSA Member Preregistration		Dorthe	Carr
SSA Member Preregistration		Jerry	Carter
SSA Member Preregistration		John	Cassidy
SSA Member Preregistration		Raul	Castro
Nonmember Preregistration		Veronica	Cedillos
SSA Member Preregistration		Eric	Chael
SSA Member Preregistration		Martin	Chapman
Student Member Registration		Julien	Chaput
SSA Member Registration		Il young	Che
SSA Member Preregistration		Po	Chen
SSA Member Preregistration		Evgeni	Chesnokov
SSA Member Preregistration		Jer-Ming	Chiu
SSA Member Preregistration		George	Choy
Student Nonmember Preregistration		Risheng	Chu
SSA Member Preregistration		Kin-Yip	Chun
Student Member Registration		Angela	Chung
SSA Member Preregistration		LLoyd	Cluff
Nonmember Preregistration		James	Cobb
Student Member Preregistration		Harmony	Colella
Nonmember 1-day Registration	Weds 21 April	Tom	Collina
SSA Member Registration		Clive	Collins
Nonmember Preregistration		James	Conrad
Student Member Preregistration		catherine	Cox

2010 SSA Annual Meeting
Attendance List

Registration Type	Which Day	First Name	Last Name
SSA Member Preregistration		Chris	Cramer
SSA Member Preregistration		Juliet	Crider
SSA Member Registration		C.B.	Crouse
Student Nonmember Preregistration		Sebastiano	D'Amico
SSA Member Preregistration		Anton	Dainty
Student Member Preregistration		Donny	Dangkua
Nonmember 1-day Preregistration	Weds 21 April	Paul	Davis
SSA Member Preregistration		Timothy	Dawson
SSA Member Preregistration		Steven	Day
Student Nonmember Preregistration		Brent	Delbridge
Nonmember 1-day Registration	Weds 21 April	Daniel	Delgado
Student Member Preregistration		Andrew	Delorey
SSA Member Preregistration		Lori	Dengler
SSA Member Preregistration		Roger	Denlinger
Student Member Preregistration		Marine	Denolle
SSA Member Preregistration		Heather	DeShon
Nonmember Registration		Robert	Detrick
Nonmember Preregistration		Stephanie	Devlin
SSA Member Preregistration		James	Dewey
Student Member Preregistration		Mahesh	Dhar
Student Member 1-day Preregistration	Fri 23 April	Domenico	Di Giacomo
Member or Non-Profit Exhibitor		Rick	Dielman
Nonmember Preregistration		James	Dieterich
Student Member 1-day Registration	Thurs 22 April	Marcin	Dombrowski
Student Member Preregistration		Luis	Dominguez-Ramirez
SSA Member Preregistration		Diane	Doser
Nonmember Preregistration		Timothy	Draelos
SSA Member Preregistration		Douglas	Dreger
SSA Member Preregistration		Elizabeth	Duffy
SSA Member Preregistration		Eric	Dunham
SSA Member Preregistration		Utpal	Dutta
Student Member Preregistration		Kevin	Eagar
SSA Member Preregistration		John	Ebel
SSA Member Preregistration		Benjamin	Edwards
SSA Member 1-day Registration	Thurs 22 April	Gary	Egbert
SSA Member Preregistration		Leo	Eisner
SSA Member Preregistration		William	Elliott
SSA Member Preregistration		William	Ellsworth
SSA Member Registration		Geoffrey	Ely
Nonmember Preregistration		Ryan	Emmitt
Member or Non-Profit Exhibitor		Kim	English
SSA Member Preregistration		John	Evans
SSA Member Preregistration		Zijun	Fang
Student Member Preregistration		Amir Mansour	Farahbod
SSA Member Preregistration		Karen	Felzer
Student Member Preregistration		Helen	Feng
SSA Member Preregistration		Edward	Field
SSA Member Preregistration		John	Filson
Student Member Preregistration		Shaun	Finn
SSA Member Preregistration		Delphine	Fitzenz
SSA Member Preregistration		Sean	Ford
SSA Member Preregistration		Matthew	Fouch

2010 SSA Annual Meeting
Attendance List

Registration Type	Which Day	First Name	Last Name
SSA Member Preregistration		Bill	Foxall
SSA Member Preregistration		Arthur	Frankel
Student Member Preregistration		Roxanna	Frary
SSA Member Preregistration		Gareth	Funning
Nonmember Registration		Maria Rosaria	Gallipoli
Student Member Preregistration		Haiying	Gao
SSA Member Preregistration		Daniel	Garcia
Nonmember Preregistration		Cynthia	Gardner
Student Nonmember 1-day Registration	Weds 21 April	Amy	Garrett
SSA Member Preregistration		Mary	George
SSA Member Preregistration		Naum	Gershenzon
SSA Member Preregistration		Matthew	Gerstenberger
Nonmember Preregistration		Peter	Gerstoft
Student Member 1-day Registration	Weds 21 April	Simon	Ghanat
SSA Member Preregistration		Subesh	Ghimire
Student Member Preregistration		Hadi	Ghofrani
Student Member Preregistration		Abhijit	Ghosh
SSA Member Preregistration		Ewa	Glowacka
Member or Non-Profit Exhibitor		Charlotte	Goddard
SSA Member Registration		Rengin	Gok
SSA Member Registration		Chris	Goldfinger
SSA Member Preregistration		Joan	Gomberg
SSA Member Preregistration		Vladimir	Graizer
SSA Member Preregistration		Lisa	Grant Ludwig
SSA Member Preregistration		Robert	Graves
SSA Member Preregistration		Brian	Gray
SSA Member Preregistration		Nick	Gregor
Nonmember Registration		Patrick	Grenard
Student Member Preregistration		Jessica	Griffin
SSA Member Preregistration		Roland	Gritto
Student Member Preregistration		Aurélie	Guilhem
SSA Member Preregistration		Zeynep	Gulerce
Nonmember Preregistration		Peter	Haeussler
SSA Member Preregistration		Katrin	Hafner
Nonmember Registration		Joshua	Handler
SSA Member Preregistration		Matthew	Haney
SSA Member Preregistration		Thomas	Hanks
SSA Member Preregistration		Roger	Hansen
Nonmember Preregistration		Philip	Harben
SSA Member Preregistration		Jeanne	Hardebeck
Nonmember 1-day Registration	Thurs 22 April	Stephen	Harmsen
SSA Member Preregistration		Ruth	Harris
SSA Member Registration		David	Harris
SSA Member Preregistration		Darren	Hart
SSA Member Preregistration		Renate	Hartog
Nonmember Registration		Robert	Hatcher, Jr.
Nonmember Preregistration		Ward	Hawkins
Student Member Preregistration		Veronica	Hawley
SSA Member Preregistration		Takumi	Hayashida
SSA Member Registration		Gavin	Hayes
SSA Member Preregistration		Chris	Hayward
SSA Member Registration		Elizabeth	Hearn

2010 SSA Annual Meeting
Attendance List

Registration Type	Which Day	First Name	Last Name
Student Nonmember Preregistration		Aaron	Hebeler
Nonmember Preregistration		Michael	Hedlin
SSA Member Preregistration		Margaret	Hellweg
SSA Member Preregistration		David	Hill
SSA Member Preregistration		Barry	Hirshorn
SSA Member Registration		Vala	Hjorleifsdottir
Nonmember 1-day Preregistration	Fri 23 April	Brendan	Hodge
Nonmember Preregistration		James	Holliday
SSA Member Preregistration		Tae-Kyung	Hong
SSA Member Registration		Emilie	Hooft
SSA Member Preregistration		Stephen	Horton
SSA Member Preregistration		Susan	Hough
Nonmember Preregistration		Heidi	Houston
Student Nonmember Preregistration		Ashley	Howe
Nonmember Preregistration		Jinjun	Hu
Nonmember Registration		Gene	Humphreys
Nonmember 1-day Registration	Weds 21 April	Maria	Husband
Nonmember Registration		Musa	Hussein
SSA Member Preregistration		Alexander	Hutko
Nonmember Preregistration		Roy	HYNDMAN
SSA Member Preregistration		David	Jackson
SSA Member Preregistration		David	James
Nonmember Registration		Jeong Soo	Jeon
SSA Member Registration		Rongsong	Jih
SSA Member Preregistration		Jeffrey	Johnson
Member or Non-Profit Exhibitor		Claire	Johnson
SSA Member Preregistration		Jenda	Johnson
SSA Member Preregistration		Thomas	Jordan
Student Member Preregistration		William	Junek
SSA Member Preregistration		Din	Kakar
Nonmember 1-day Registration	Thurs 22 April	Erol	Kalkan
Student Member Preregistration		Deborah	Kane
SSA Member Preregistration		Honn	Kao
Student Member Registration		Haydar	Karaoglu
SSA Member Preregistration		Sarah	Karlson
SSA Member Preregistration		Hiroshi	Kawase
SSA Member Preregistration		Armen	Kazarian
Student Member Registration		Annie	Kell
SSA Member Registration		George	Keller
SSA Member 1-day Registration	Weds 21 April	Hong	Kie
SSA Member Registration		Geun Young	Kim
Student Member Preregistration		Jeremy	King
Student Member Preregistration		Hunter	Knox
SSA Member Preregistration		Keith	Knudsen
SSA Member Preregistration		Monica	Kohler
SSA Member Preregistration		Kazuki	Koketsu
SSA Member Preregistration		Keith	Koper
Nonmember Preregistration		Jeremy	Kozdon
SSA Member Preregistration		Swaminathan	Krishnan
SSA Member Preregistration		Richard	Kromer
Student Member Preregistration		Jerome	Kutliroff
SSA Member Preregistration		Roland	LaForge

2010 SSA Annual Meeting
Attendance List

Registration Type	Which Day	First Name	Last Name
SSA Member Preregistration		Maurice	Lamontagne
SSA Member Preregistration		Charles	Langston
SSA Member Preregistration		Joan	Latchman
Nonmember Preregistration		Alexis	Lavine
SSA Member Preregistration		Jesse	Lawrence
Nonmember Preregistration		Ronan	Le Bras
SSA Member 1-day Preregistration	Weds 21 April	P	Leahy
Student Member Preregistration		En-Jui	Lee
SSA Member Preregistration		Selina	Lee
Student Nonmember Preregistration		Ya-Ting	Lee
SSA Member Preregistration		Richard	Lee
SSA Member Preregistration		Jonathan	Lees
Nonmember Registration		Elizabeth	Lenox
Nonmember 1-day Registration	Weds 21 April	David	Levasseur
Nonmember 1-day Preregistration	Thurs 22 April	Jennifer	Lewis
SSA Member Preregistration		Jim	Lewkowicz
SSA Member Preregistration		Wei	Li
SSA Member Preregistration		Lee	Liberty
Nonmember Preregistration		Robert	Lillie
Nonmember Preregistration		Fan-Chi	Lin
SSA Member Preregistration		Jian	Lin
SSA Member Preregistration		Joe	Litehiser
Student Member Preregistration		Qiming	Liu
Student Nonmember Preregistration		Andrew	Lloyd
SSA Member Registration		Andrew	Lockhart
SSA Member Preregistration		Anthony	Lomax
SSA Member Preregistration		John	Louie
Student Member Preregistration		Julian	Lozos
SSA Member Preregistration		Nicolas	Luco
SSA Member Preregistration		James	Luetgert
SSA Member Preregistration		Shuo	Ma
SSA Member Preregistration		Kuo-Fong	Ma
Student Member Preregistration		Jonathan	MacCarthy
SSA Member Preregistration		Monica	Maceira
Student Member 1-day Preregistration	Thurs 22 April	Patricia	MacQueen
Student Member Registration		Christopher	Madden
Nonmember Registration		Ian	Madin
SSA Member Preregistration		Harold	Magistrale
SSA Member Preregistration		Stphen	Malone
Student Member Preregistration		Shoba	Maraj
SSA Member Preregistration		Kristin	Marano
Student Member Preregistration		Omar	Marcillo
SSA Member Preregistration		Carol	Mark
SSA Member Preregistration		James	Marrone
SSA Member Preregistration		Warner	Marzocchi
Nonmember Preregistration		Larry	Mastin
SSA Member Preregistration		Eric	Matzel
SSA Member Preregistration		Kevin	Mayeda
Nonmember Preregistration		Stephane	Mazzotti
SSA Member Preregistration		William	McCann
SSA Member Preregistration		Jill	McCarthy
SSA Member Registration		Wendy	McCausland

2010 SSA Annual Meeting
Attendance List

Registration Type	Which Day	First Name	Last Name
Nonmember Registration		Vicki	McConnell
Nonmember Preregistration		Patricia	McCrory
SSA Member Preregistration		Art	Mcgarr
Member or Non-Profit Exhibitor		Robin	McGuire
SSA Member Preregistration		Jeff	McGuire
Nonmember 1-day Registration	Fri 23 April	Cecilia	McHugh
SSA Member Preregistration		Mihan	McKenna
SSA Member Preregistration		Marcia	McLaren
SSA Member Preregistration		Daniel	McNamara
Nonmember 1-day Registration	Weds 21 April	Marcia	McNutt
SSA Member Preregistration		Bob	McPherson
SSA Member Preregistration		Andrew	Meigs
SSA Member Registration		Tim	Melbourne
SSA Member Preregistration		David	Mencin
Student Member Registration		Lingsen	Meng
Nonmember Preregistration		Farn-Yuh	Menq
Student Member Preregistration		Dara	Merz
SSA Member Preregistration		Andrew	Michael
SSA Member Preregistration		Jeffrey	Miller
Student Member Preregistration		Hallie	Mintz
Student Nonmember 1-day Registration	Fri 23 April	Nilesh	Mishra
SSA Member Preregistration		Gilbert	Molas
SSA Member Preregistration		Walter	Mooney
SSA Member Preregistration		Seth	Moran
SSA Member Preregistration		Igor	Morozov
Nonmember Preregistration		Morgan	Moschetti
SSA Member Registration		Timothy	Mote
SSA Member Registration		Marco	Mucciarelli
SSA Member Preregistration		John	Murphy
Student Member Registration		Rachel	Murphy
SSA Member Preregistration		Mark	Murray
SSA Member Preregistration		Stephen	Myers
SSA Member Registration		John	Nabelek
SSA Member Registration		Robert	Nadeau
SSA Member Preregistration		Susan	Nava
SSA Member Preregistration		Susan	Newman
Student Nonmember Preregistration		Andrew	Nies
SSA Member Preregistration		Robert	Nigbor
Nonmember Registration		Svetlana	Nikolova
SSA Member Preregistration		Stu	Nishenko
Member or Non-Profit Exhibitor		Eddie	Nishimori
SSA Member Preregistration		Fenglin	Niu
Nonmember Preregistration		David	Nyland
SSA Member Preregistration		Marleen	Nyst
SSA Member Registration		Daniel	O'Connell
Nonmember Preregistration		Mathias	Obrebski
SSA Member Preregistration		Jack	Odum
SSA Member Preregistration		David	Oglesby
SSA Member 1-day Preregistration	Fri 23 April	Emile	OKAL
Nonmember Preregistration		Anna	Olsen
SSA Member Preregistration		KimB	Olsen
Member or Non-Profit Exhibitor		Lani	Oncescu

2010 SSA Annual Meeting
Attendance List

Registration Type	Which Day	First Name	Last Name
SSA Member Preregistration		Tuna	Onur
Nonmember Preregistration		Thomas	Oommen
SSA Member Preregistration		David	Oppenheimer
SSA Member Preregistration		Morgan	Page
SSA Member Preregistration		Kristine	Pankow
SSA Member Preregistration		Gerassimos	Papadopoulos
SSA Member Preregistration		Michael	Pasyanos
SSA Member Preregistration		Howard	Patton
Student Member Preregistration		Jason	Patton
Student Member Preregistration		Frederick	Pearce
Nonmember 1-day Registration	Thurs 22 April	Grant	Pease
SSA Member Preregistration		James	Pechmann
SSA Member Preregistration		Mark	Petersen
Nonmember 1-day Registration	Thurs 22 April	Gary	Peterson
Nonmember Preregistration		Anders	Petersson
SSA Member Registration		William	Phillips
Student Member 1-day Preregistration	Fri 23 April	Marco	Pilz
SSA Member Preregistration		Arben	Pitarka
SSA Member Preregistration		Chris	Poland
SSA Member Preregistration		Fred	Pollitz
SSA Member Preregistration		Christian	Poppeliers
Student Member Preregistration		Robert	Porritt
SSA Member Preregistration		Lawrence	Porter
SSA Member Preregistration		Christine	Powell
SSA Member Preregistration		Peter	Powers
SSA Member Registration		Thomas	Pratt
SSA Member Preregistration		Keith	Priestley
Student Member Preregistration		Rafael	Pujols
SSA Member Preregistration		Jay	Pulliam
SSA Member Preregistration		Moira	Pyle
SSA Member Preregistration		Richard	Quittmeyer
Member or Non-Profit Exhibitor		Horst	Rademacher
Student Nonmember Preregistration		Shahid	Ramzan
SSA Member Registration		Robert	Reinke
SSA Member Preregistration		Leon	Reiter
SSA Member Preregistration		Megan	Resor
SSA Member Preregistration		David	Rhoades
SSA Member Preregistration		Paul	Richards
Nonmember Preregistration		Luis	Rivera
Student Member Preregistration		Carrie	Rockett
Member or Non-Profit Exhibitor		James	Roddey
SSA Member Preregistration		Arthur	Rodgers
SSA Member Registration		Adrian	Rodriguez-Marek
SSA Member Registration		Evelyn	Roeloffs
SSA Member Preregistration		Garry	Rogers
SSA Member Preregistration		Alan	Rohay
Student Member Preregistration		John	Rollins
SSA Member Preregistration		Diana	Roman
SSA Member 1-day Preregistration	Fri 23 April	Barbara	Romanowicz
Nonmember Registration		Dario	Rosidi
Student Member Preregistration		Zachary	Ross
SSA Member Preregistration		Stephanie	Ross

2010 SSA Annual Meeting
Attendance List

Registration Type	Which Day	First Name	Last Name
Nonmember Preregistration		Daniel	Roten
SSA Member Registration		Badie	Rowshandel
SSA Member Preregistration		Justin	Rubinstein
SSA Member Preregistration		John	Rundle
SSA Member Preregistration		Natalia	Ruppert
SSA Member Preregistration		Holly	Ryan
Student Member Registration		Kenny	Ryan
Nonmember Preregistration		Hyeuk	Ryu
SSA Member Registration		David	Salzberg
SSA Member Preregistration		William	Savage
Student Member Preregistration		Rebecca	Sawyer
Student Member Preregistration		Brandon	Schmandt
SSA Member Preregistration		David	Schmidt
SSA Member Preregistration		Kimberly	Schramm
SSA Member Registration		Frederick	Schult
SSA Member Preregistration		Hans	Schwaiger
SSA Member Preregistration		David	Schwartz
Student Nonmember Preregistration		Mariangela	Sciotto
SSA Member Preregistration		Sandra	Seale
SSA Member Preregistration		Paul	Segall
SSA Member 1-day Registration	Thurs 22 April	Gordon	Seitz
Student Member Preregistration		Emel	Seyhan
Student Member Registration		Ali	Shahbazian
SSA Member Registration		Peter	Shebalin
SSA Member Preregistration		David	Shelly
SSA Member Preregistration		Yang	Shen
SSA Member Preregistration		Brian	Sherrod
SSA Member Preregistration		Zheqiang	Shi
SSA Member Preregistration		Nilesh	Shome
Nonmember 1-day Preregistration	Weds 21 April	Dennis	Sigrist
SSA Member 1-day Registration	Fri 23 April	Gerald	Simila
SSA Member Preregistration		Nathan	Simmons
Nonmember Preregistration		Ray	Sliter
SSA Member Preregistration		Ken	Smith
SSA Member Preregistration		Deborah	Smith
SSA Member Registration		Catherine	Snelson
Nonmember 1-day Preregistration	Fri 23 April	Roelof	Snieder
Student Member Preregistration		Fuxian	Song
SSA Member Preregistration		Seok Goo	Song
Member or Non-Profit Exhibitor		Edelvays	Spassov
SSA Member Registration		John	Stamatakos
SSA Member Preregistration		Jamison	Steidl
SSA Member Preregistration		William	Stephenson
Student Member Preregistration		Pamela	Stewart
SSA Member Preregistration		Michael	Stickney
SSA Member Preregistration		Sissy	Stone
Student Member Preregistration		Ashley	Streig
SSA Member Preregistration		Anastasia	Stroujkova
SSA Member Preregistration		Brian	Stump
Nonmember Registration		Feng	Su
Student Member Preregistration		Oner	Sufri
SSA Member Preregistration		LYNN	SYKES

2010 SSA Annual Meeting
Attendance List

Registration Type	Which Day	First Name	Last Name
SSA Member Preregistration		John	Taber
Nonmember Preregistration		Deanne	Takasumi
SSA Member Preregistration		Hiroshi	Takenaka
SSA Member 1-day Registration	Weds 21 April	Carl	Tape
Nonmember Preregistration		Behrooz	Tavakoli
SSA Member Preregistration		Steven	Taylor
SSA Member 1-day Preregistration	Weds 21 April	Ta-liang	Teng
SSA Member Preregistration		Fabia	Terra
Nonmember Preregistration		Wayne	Thatcher
SSA Member Preregistration		Weston	Thelen
Student Member Preregistration		Amanda	Thomas
Nonmember Registration		Glenn	Thompson
Member or Non-Profit Exhibitor		Gene	Traverse
SSA Member Preregistration		Joy	Troyer
Nonmember Preregistration		Victor	Tsai
SSA Member Preregistration		Hiroshi	Tsuruoka
SSA Member Registration		Brian	Tucker
SSA Member Preregistration		Donald	Turcotte
Nonmember 1-day Preregistration	Weds 21 April	Althea	Turner
Student Member Registration		Beliz	Ugurhan
Student Member Preregistration		Fabio	Upegui Botero
SSA Member Preregistration		Martin	Vallée
SSA Member Preregistration		Thomas	van Stiphout
SSA Member Preregistration		Karl	Veith
SSA Member Preregistration		John	Vidale
SSA Member Preregistration		Paul	Vincent
SSA Member Preregistration		Christa	von Hillebrandt-Andrade
SSA Member Preregistration		Lara	Wagner
SSA Member Preregistration		Gregory	Waite
SSA Member Preregistration		David	Wald
SSA Member Preregistration		Felix	Waldhauser
Nonmember 1-day Preregistration	Weds 21 April	Kyle	Walker
SSA Member Preregistration		Melanie	Walling
SSA Member Preregistration		William	Walter
SSA Member Preregistration		Zhenming	Wang
Nonmember Preregistration		Yumei	Wang
Student Member Preregistration		Qi	Wang
Student Member Registration		Feng	Wang
Nonmember Preregistration		Roger	Waxler
SSA Member Preregistration		Craig	Weaver
SSA Member Preregistration		Spahr	Webb
Student Nonmember Registration		Aaron	Wech
SSA Member Preregistration		Elise	Weldon
SSA Member Preregistration		Ray	Weldon
SSA Member Preregistration		Ray	Wells
SSA Member Preregistration		Donald	Wells
Student Member Preregistration		John	West
SSA Member Preregistration		Michael	West
SSA Member Preregistration		Robert	White
SSA Member Preregistration		Robert	Williams
SSA Member Preregistration		Chesley	Williams
SSA Member Preregistration		Mitchell	Withers

2010 SSA Annual Meeting
Attendance List

Registration Type	Which Day	First Name	Last Name
SSA Member Preregistration		Robert	Witter
SSA Member Preregistration		Lorraine	Wolf
Student Member 1-day Preregistration	Fri 23 April	Emily	Wolin
SSA Member Preregistration		Ivan	Wong
SSA Member Preregistration		Mark	Woods
SSA Member Registration		Bradley	Woods
SSA Member Preregistration		Robert	Woodward
SSA Member Preregistration		Edward	Woolery
Nonmember Preregistration		Charles	Worden
SSA Member Preregistration	Weds 21 April	Jiakang	Xie
SSA Member Preregistration		Xiaoning	Yang
Student Member Preregistration		Tomoko	Yano
SSA Member Preregistration		Robert	Yeats
Student Member Preregistration		Mehmet	Yikilmaz
SSA Member Preregistration		OZ	YILMAZ
SSA Member Preregistration		Mark	Yoder
SSA Member Preregistration		Alan	Yong
SSA Member Preregistration		Christopher	Young
SSA Member Registration		Robert	Youngs
Nonmember 1-day Registration	Fri 23 April	Qi Song	Yu
Nonmember Preregistration		Zhongxia	Yuan
SSA Member Preregistration		Doug	Yule
SSA Member Registration		Zia	Zafir
Nonmember Preregistration		Ilya	Zaliapin
Student Nonmember Preregistration		Arash	Zandieh
SSA Member Preregistration		Yuehua	Zeng
SSA Member Preregistration		Jian	Zhang
SSA Member Preregistration		Li	Zhao
Nonmember Preregistration		John	Ziagos
SSA Member Preregistration		Mary Lou	Zoback
SSA Member Registration		John	Zucca

Building Code Uses of Seismic Hazard Data

Oral Session · Wednesday 8:30 AM, 21 April · Salon A
Session Chairs: Charles A. Kircher and Nicolas Luco

The 2008 U.S. National Seismic Hazard Map Applications for Building Codes

PETERSEN, M., U.S. Geological Survey, Golden, CO USA, mpetersen@usgs.gov; HARMSEN, S., U.S. Geological Survey, Golden, CO USA, harmsen@usgs.gov; RUKSTALES, K., U.S. Geological Survey, Golden, CO USA, rukstales@usgs.gov; LUCO, N., U.S. Geological Survey, Golden, CO USA, luco@usgs.gov

The 2008 U.S. National Seismic Hazard maps incorporated several new models and datasets including: new and revised fault source models; NGA, CEUS, and subduction-interface ground-motion prediction models, updated seismicity catalogs and estimates of uncertainties; UCERF 2.0 model for California; and recommendations from WSSPC on the Intermountain West. Ground shaking changed by 30 % at several sites across the conterminous U.S. The hazard maps have been adopted as the basis for building code maps in the 2009 NEHRP Recommended Provisions, 2010 ASCE Standard, and 2012 IBC. For the building code maps we also developed deterministic median hazard maps that are used to limit the design ground motions over some active faults. These maps were prepared using the same weighted ground motion prediction equations and mean characteristic earthquake magnitudes that were applied in the probabilistic maps. We are now considering the next update of the maps that will be due in 2013–2014. We will hold a user workshop in 2012 or 2013 to discuss products that would be helpful for the engineering community in mitigating earthquake risk. Some of the issues that may be considered include: (1) Spectral periods in design codes - Should a series of maps ranging from 0.1 s to 5.0 s spectral accelerations be used directly in building codes? (2) Soils maps—Which Vs30 maps should be developed and how can we translate ground-motion prediction equations to appropriate Vs30 levels? How do these soil maps compare with amplifying the 760 m/s maps using the NEHRP factors? (3) Directivity—How should directivity be incorporated into maps? (4) Time dependence—Should renewal or clustering recurrence models be incorporated in hazard maps? (5) Ground-motion parameter—Should we make maps for maximum component ground, that are applied in the building codes, as well as geometric mean ground motions?

Project 07—Development of New Ground Motions for Model Building Codes

KIRCHER, C.A., Kircher & Associates, Palo Alto CA USA, cakircher@aol.com

Over a decade has passed since seismic design procedures and ground motions were established (by Project 97) and adopted for use in the NEHRP Recommended Provisions. These procedures and related ground motion maps (prepared by the USGS) are now widely used in model building codes, including ASCE/SEI 7-05, 2006 IBC and 2007 CBC.

Questions have arisen concerning the conservative nature of the procedures and maps, especially with respect to those areas of the nation with low to moderate seismic risk (central and eastern United States). Further, advancements in the earth science have occurred, including development of new ground motion relations for the western United States by the PEER NGA project. Thus, it is both timely and appropriate to reassess the design procedures and to update the ground motion maps, incorporating current scientific information.

Accordingly, Project 07, a cooperative BSSC-FEMA-USGS effort, similar to that which resulted in the 1997 procedures, developed improvements to seismic design procedures and ground motion maps that are now part of the 2009 NEHRP Recommended Provisions and ASCE 7-10. This presentation will highlight the work of Project 07 and describe the technical basis for the new ground motions of model building codes.

New Risk-Targeted Seismic Design Maps for Model Building Codes

LUCO, N., USGS, Golden, CO, nluco@usgs.gov

Through collaboration between the U.S. Geological Survey and the Building Seismic Safety Council (with funding from the Federal Emergency Management Agency), the probabilistic basis for the ground-motion amplitudes used in designing new buildings in the U.S. has recently undergone a significant conceptual shift. In the 2000–2009 triennial editions of the International Building Code (IBC)—as well as their referenced editions of the American Society of Civil Engineers (ASCE) standard entitled "Minimum Design Loads for Buildings and Other Structures"—the probabilistic ground motions for design purposes are equated to uniform-hazard spectral response accelerations (SRAs) for a ground-motion exceedance probability of 2% in 50 years. For most U.S. locations, these probabilistic SRAs have been the ground motions used for design, governing over parallel deterministic SRAs that are also considered. This will still be the case in the 2012 IBC (as it is in the 2010 update of the ASCE standard), except there the probabilistic ground motions will be computed as "risk-targeted" SRAs. Risk-targeted ground motions are defined as those which, when used to design buildings according to the IBC (or the ASCE standard) are expected to result in buildings having a collapse probability of 1% in 50 years. Whereas the previous uniform-hazard definition of probabilistic ground motions for design took only a single point from each seismic hazard curve for a location (namely the ground motion corresponding to the 2%-in-50-year exceedance probability), the new risk-targeted definition utilizes the entire hazard curve. As a result, risk-targeted design ground motions account for differences between shapes of hazard curves in, for example, portions of the Pacific Northwest and the rest of the western U.S., as well as portions of the central and eastern U.S.

New Provisions for Peak Ground Acceleration and Vertical Component Design Response Spectra in the 2010 NEHRP Seismic Provisions and ASCE 7-10 Standard

CROUSE, C.B., URS Corp., Seattle, WA, cb_crouse@urscorp.com; CAMPBELL, K.W., EQECAT, Beaverton, OR, kcampbell@eqecat.com; BOZORGNIA, Y., PEER, UC Berkeley, Berkeley, CA, yousef@berkeley.edu; POWER, M., AMEC Geomatrix, Oakland, CA, maury.power@amec.com; ANDERSON, D.G., CH2M Hill, Bellevue, WA, Donald.anderson@ch2m.com

New provision for computing peak ground acceleration (PGA) for soil liquefaction and stability evaluations have been introduced in Section 11.8.3 of the 2010 NEHRP Seismic Provisions and the ASCE 7-10 standard. Provisions for obtaining vertical component design response spectra will appear as a separate Chapter in the 2010 NEHRP provisions, and as an appendix in the ASCE 7-10 standard. The PGA provisions consist of maps of the Maximum Considered Earthquake (MCE), geometric mean, horizontal component, bedrock PGA, plus a site-coefficient (F_{PGA}) table to convert the bedrock PGA value to one corresponding to another site class. The coefficients in the table are identical to the Fa site coefficients in Table 11.4-1 of the NEHRP and ASCE 7 documents. Sections were added to Chapter 21 of ASCE 7-10 for the site-specific determination of PGA. The procedures in these sections are similar to those for response spectra in Chapter 21 of ASCE 7-05. The deterministic lower limit PGA (in g unit) is set at 0.5 F_{PGA}. Of particular note is the requirement that liquefaction must now be evaluated for the MCE, rather than the design earthquake, as currently required in ASCE 7-05. Equations for computing vertical component design response spectra are based on Bozorgnia and Campbell (2004) and Campbell and Bozorgnia (2003). Each equation, which defines a segment of the vertical response spectrum, is a function of the short period, horizontal component, spectral response acceleration parameter, S_{DS}, and a coefficient C_V, which depends on the mapped MCE bedrock spectral response parameter, S_S, and the site class. The equations provide more accurate vertical response spectra than those derived from simple vertical-to-horizontal component ratios of 1/2 or 2/3, which appear in a number of seismic provisions.

Ground Motion Issues Likely to be Addressed in the Next Code Development Cycle

HOOPER, J.D., Magnusson Klemencic Assoicates, Seattle, Washington, USA, jhooper@mka.com

Development efforts over the past several years, beginning with Project 07, a cooperative BSSC-FEMA-USGS effort, resulted in the update to the seismic design procedures and ground motion maps that are now part of the 2009 NEHRP Recommended Seismic Provisions for New Buildings and Other Structures (Provisions) and ASCE/SEI 7-10 Minimum Design Load for Buildings and Other Structures (ASCE 7-10). ASCE 7-10 was adopted for use in the 2012 International Building Code (IBC) at the International Code Council's (ICC) Structural Committee Hearings held in October, 2009. Most state and local jurisdictions will adopt the 2012 IBC by 2013.

Notable changes to the seismic design procedures resulted in the development of risk-target ground motions, the use of the maximum response direction for design and changes to the response-history scaling procedures. The details of these and other new seismic design procedures will be presented by others.

The next provisions update cycle for the 2014 NEHRP Provisions kicked off at the BSSC Annual Meeting/Workshop in January, 2010. The major focus of the workshop was to identify "Issue Teams" for the upcoming cycle. Numerous issues were discussed and several Issue Teams were formed, two of which relate specifically to seismic design/ground motions: (1) Improving Existing Seismic Performance Factors and (2) Response-history Analysis and Ground Motion Scaling.

The specifics of the scope of these issue teams as they relate to ground motions, and their use in guidelines, standards and codes, will be presented.

Uncertainty in the Risk of Collapse of Code-Designed Structures Due to Uncertainty in the Earthquake Hazard

SHOME, N., Risk Management Solutions, 7015 Gateway Blvd, Newark, CA 94560, nilesh@stanfordalumni.org; FRANKEL, A.D., US Geological Survey, University of Washington, Dept of Earth and Space Sciences, PO Box 351310, Seattle, WA 98195, afrankel@usgs.gov

Recently, building codes are being developed to achieve a uniform probability of collapse of 1% in 50 years by developing a methodology to compute a "risk-targeted ground motion". The calculation of this ground motion, however, has been carried out using the mean hazard curves, neglecting the uncertainty in the estimation of hazard. The mean hazard curve, which is calculated by the National Seismic Hazard Mapping project, considers both the aleatory and the epistemic variability. Logic trees are used to characterize the epistemic variability, which is uncertainty attributable to incomplete knowledge about a phenomenon. Epistemic uncertainty is reflected in a range of variable models (*e.g.*, a range characteristic magnitudes), multiple expert interpretations (*e.g.*, different moment-area relationships), and statistical uncertainty (*e.g.*, different b-values). The hazard calculations are performed following all the possible branches through the logic trees, each analysis producing a single hazard curve showing ground motion against annual frequency of exceedance and the mean hazard curve is obtained by combining all the hazard curves for all the branches based on the weights along all the component branches. The results from each of the possible branches help to define the uncertainty in the hazard curve. The information of uncertainty of the hazard curve has been used to estimate the uncertainty in the collapse probability. The uncertainty in the collapse probability has been calculated at three sites in California: 1) San Francisco, which is dominated by the Type-A faults, 2) Los Angeles, which is dominated by Type-B faults and 3) Sacramento which is dominated by the gridded seismicity. The results at these sites help to demonstrate the variation in the uncertainty of probability of collapse as well as quantify the uncertainty of hazard at different locations.

Inelastic Spectral Displacement for the Probabilistic Seismic Hazard Assessment in the Marmara Region, Turkey

AKKAR, S., METU, Ankara/Turkey, sakkar@metu.edu.tr; AKINCI, A., INGV, Rome/Italy, akinci@ingv.it

Probabilistic seismic hazard analyses for the Bolu region of interest as well as for the entire Marmara region are performed for PGV (as a tunnel seismic assesment parameter) and for inelastic spectral displacement (as a viaduct seismic assessment parameter). The present study is carried out under the framework of the "Assessment and Reduction of Seismic Risk to Large Infrastructural Systems" project where the Bolu region case study was chosen because of the very high level of earthquake hazard to the recent construction of infrastructures. The use of inelastic spectral displacement for the hazard assessment would yield more realstic results for engineering purposes as it directly relates structural performance with the damage sustained by the structure. This type of analysis is done for the first time in Turkey. The use of inelastic spectral displacement hazard maps all around the world has recently started and in that sense the outcomes of this study will contribute significantly to the relevant literature. In our study, for the seismic source model we incorporate both smoothed historical seismicity over the area and geological information on faults. We have used ground motion prediction equations by Akkar and Bommer (2007) as an European model and recent NGA one by Boore and Atkinson (2008). The inelastic spectral displacements are obtained (a) by modifying the elastic spectral displacement estimations of above two GMPEs through the empirical expression of Tothong and Cornell (2006), (b) by modifying the PGV estimations of above two GMPEs through the empirical expression of Akkar and Kucukdogan (2008). The results show that the use of PGV for estimating inelastic spectral displacements for their implementation in probabilistic hazard maps yields comparable results to those obtained by modifying the elastic spectral displacements by some empirical factors. Thus, PGV can be a robust tool for preparing quick nonlinear hazard maps in the vicinity of active faults.

Peak and Integral Seismic Parameters of L'Aquila 2009 Ground Motions: Observed vs PSHA and Code Provision Values

CHIAUZZI, L., Basilicata University, Potenza Pz Italy; MASI, A., Basilicata University, Potenza Pz Italy; MUCCIARELLI, M., Basilicata University, Potenza Pz Italy.

The Mw=6.3 L'Aquila earthquake occurred April 6th, 2009 caused widespread damage in the Abruzzo region (Central Italy). The epicentre of the mainshock was localized very close to the urban centre of L'Aquila, capital town of the region, at distance less than 10 km. It was the strongest earthquake recorded in Italy providing ground motion recordings from accelerometric stations placed on the surface projection of the seismogenic fault. This area (as the rest of Italian territory) was recently re-classified according to a new PSHA estimate derived on the basis of PGA only, substituting the previous classification based on PGA, Housner Intensity (IH) and macroseismic intensity. Three independent studies carried out before the quake, based on time-dependent models, zonation-free approaches and observed site seismic history, already claimed for a possible underestimation of the expected PGA. Analysis has now been performed in terms of peak (PGA, PGV, PGD) and integral (IH) seismic parameters on the recorded accelerograms. PGA recorded values are higher than code values for seismic actions with return period (Tr) up to 2475 years, even considering possible effects due to site amplification. A previous study using the same catalogue, attenuation and logic tree for L'Aquila requires Tr=10.000 years to match the observed values. Concerning IH, code values remain generally lower than expected for Tr=475 years, whilst they are remarkably higher considering Tr=2475 years. The non-parametric analysis of the site seismic histories returns for the observed VIII-IX MCS a Tr of the order of 300 years. We thus think that PGA alone is an insufficient intensity measure to provide reliable PSHA estimates to be implemented in building codes.

Seismic Loss Estimation Along the North Anatolian Fault Based on Scenario Earthquakes

ASKAN, A., Middle East Technical University, Ankara, Turkey, aaskan@metu.edu.tr; ERBERIK, M.A., Middle East Technical University, Ankara, Turkey, altug@metu.edu.tr; UGURHAN, B., Middle East Technical University, Ankara, Turkey, ugurhan@metu.edu.tr

Despite the high damage potential of earthquakes, it is possible to identify, estimate and reduce the resulting structural, social and economic losses during potential major seismic activities. Current methodologies for seismic loss estimation involve the following key steps: seismic hazard estimation, site response analyses and building vulnerability assessment. Seismic hazard estimation techniques traditionally employ existing ground motion prediction equations. However, in regions of high seismicity with sparse seismic recordings or large earthquakes with long return periods, it is essential to employ ground motion simulations along with region-specific site response and building vulnerability estimation. In this study, we present our initial attempts towards an integrated seismic loss estimation approach which takes geophysical, geotechnical, and building information into account to estimate potential seismic losses by employing fragility functions. We present results in the form of spatial distribution of ground motion intensity parameters, synthetic ground motion prediction equations, and building fragility curves based on synthetic time histories obtained from finite-fault simulations of large earthquakes on the North Anatolian Fault Zone (Turkey).

Comparison of Methods for Site Specific Seismic Response Assessment of Shallow and Deep Bedrock Sites

GHANAT, S.T., Arizona State University, Tempe, Arizona, USA, sganat@aol.com

In current U.S. design practice, the effect of local soil conditions on seismic site response is generally accounted for based upon a seismic hazard analysis conducted for a reference site condition and National Earthquake Hazard Reduction Program (NEHRP) developed site factors based upon (Vs30), the shear wave velocity over the top 30 meters of the site. The site factors are used to adjust the Peak Ground Acceleration, spectral acceleration at 0.2 second termed the short period spectral acceleration (Ss) and the spectral acceleration at 1 second (S1) for local site conditions. The adjusted values are then used to develop a site specific design spectrum. The adequacy of the NEHRP site factors at sites with a shallow impedance contrast (shallow bedrock sites) and at deep soil sites have been evaluated directly using Next Generation Attenuation (NGA) relationships in a seismic hazard analyses and by performing one-dimensional frequency domain site response analysis with an equivalent linear soil model. The equivalent linear analyses were conducted on three representative columns consisting of 30, 60, and 500 meters of soil on top of a bedrock half space using a suite of five time histories. The suite of time histories was selected as representative of a magnitude 6.7 earthquake on a reverse fault at a distance of 19 km from the reference site (median peak horizontal ground acceleration of 0.25g). The spectra obtained from these analyses were compared to spectra devel-

oped using NEHRP site factors. Results of the comparison suggest that the use of NEHRP site factors may not be appropriate for either sites with a sharp impedance contrast, or for the sites with bedrock at great depths. Results of the comparison also indicate that the NGA relationships are capable of accounting for site-specific response effects for deep soil sites but not for shallow bedrock sites.

Effect of Permafrost on Seismic Site Response and Design Spectrum

DUTTA, U., University of Alaska Anchorage, Anchorage, AK, USA, afud@uaa.alaska.edu; YANG, Z., University of Alaska Anchorage, Anchorage, AK, USA, afzy@uaa.alaska.edu; XU, G., State of Alaska DOT&PF, Juneau, AK, USA, gang.xu@alaska.gov

Permafrost extensively exists in the seismically active interior of Alaska. The high shear wave velocity of the permafrost along with relatively low velocity unfrozen soils both above and below it induces anomalous velocity structure in the soil. The main aim of this study is to understand the ground motion characteristics due to such anomalous shear wave velocity structure. The seismic site response for one of such site in Fairbanks, AK has been used for this purpose. One-dimensional equivalent linear analysis method was used to propagate hazard consistent input bedrock motions through the soil column for different hazard levels. Spectral acceleration of 5% damped response spectra have been computed for the soil layer in the frequency range of 0.01–10.0 Hz. Parametric studies have been conducted to assess the spectral response of the soil by varying thicknesses and shear wave velocities of the permafrost and depth of the bedrock to understand the permafrost effect on site response. The results show that the depth to the top of the permafrost layer with respect to the bedrock depth affect the peak ground acceleration and the predominant frequency of the response. It has also been observed that the shear wave velocity of the unfrozen layer present above the permafrost layer influence the seismic response significantly. The analysis of results clearly indicates that it may not always be conservative to ignore the effect of high velocity permafrost layer in the seismic design in the cold region. Current seismic code does not have exclusive provision to account for the effect of permafrost layer in the seismic design.

Monitoring for Nuclear Explosions

Oral Session · Wednesday 8:30 AM, 21 April · Salon E
Session Chairs: Bill Walter, Ola Dahlman, Paul G. Richards, and Ray Willemann

Comprehensive Test Ban Treaty Is Effectively Verifiable

COLLINA, T., Arms Control Association, Washington, DC, U.S.A., tcollina@armscontrol.org

The goal for any treaty monitoring regime is to provide effective verification. It is generally recognized that no verification system gives absolute assurances. Effective verification means that any attempts to cheat in ways that could threaten U.S. national security must be uncovered in a timely manner. Describing this concept in the context of the Intermediate Nuclear Forces (INF) Treaty, Ambassador Paul Nitze said, "If the other side moves beyond the limits of the treaty in any militarily significant way, we would be able to detect such violation in time to respond effectively and thereby deny the other side the benefit of the violation."

If Comprehensive Test Ban Treaty (CTBT) parties know the Treaty is effectively verifiable, cheating would be deterred because: 1) the potential gains of a nuclear test that might escape detection would be small (not militarily significant), and 2) the potential costs would be high in terms of international reaction and the possibility of sanctions and military measures in response. The goal of the CTBT verification regime is to deter violations by convincing potential cheaters that the risks and costs of cheating outweigh any plausible benefits. The effectiveness of the regime can be evaluated by reviewing the properties of the global alarm system, the response of the system to the North Korean tests, the effectiveness of the system against plausible cheating scenarios, and the types of tests that are militarily significant.

Progress and Achievements in Monitoring Compliance with the Comprehensive Nuclear Test-Ban-Treaty (CTBT)

ZERBO, L., CTBTO, Vienna, Austria, lassina.zerbo@ctbto.org

Since the CTBT was opened for signature in 1996, the Preparatory Commission of the CTBTO has worked towards implementing the verification regime called for by the Treaty. The initial International Monitoring System (IMS) network consisted mostly of capable legacy stations (from an earlier prototype) for the seismic, hydro-acoustic, infrasound and radionuclide technologies.

The IMS network was extended to the point where about 80% of the seismic networks (40 primary and 90 auxiliary stations) are now certified to IMS standards as well as 10 hydro-acoustic and 41 infrasound stations (90 and 70% complete); in addition 59 radionuclide particulate stations and ten laboratories are certified (74 and 60% complete) and 24 radionuclide noble gas stations are sending data to the International Data Centre (IDC.)

Progress has been made in the network calibration for seismic location and magnitude, surface-wave processing, and analysis tools. In hydro-acoustics, the use of the 6 hydrophone triads has been optimized. Infrasound processing has made considerable advances to the point where data from improved sensors are routinely automatically processed, reviewed and published.

CTBT verification relies on fusion of the waveform data with that from the radionuclide sensors. Over the past 10 years, the measurement sensitivity has increased for both particulate and noble gas (Xenon) radionuclides. The noble gas systems were at the prototype stage in 2000 and have improved nearly ten-fold in detection capability. Finally, the interpretation of radionuclide and waveform data requires sophisticated atmospheric transport modelling to relate the observations to a common origin.

The CTBT is ultimately verified by its Member States, and an important activity of the organization is to provide the data and tools to the States and to train their representatives to making informed decisions.

The United States National Data Center for the CTBT

WOODS, M.T., AFTAC/TTR, Patrick AFB FL USA, mwoods@aftac.gov

The Air Force Technical Applications Center (AFTAC), which has monitored the Limited Test Ban Treaty, the Threshold Test-Ban Treaty, and the Peaceful Nuclear Explosion Treaty, has been designated by the Office of the Secretary of Defense as the U.S. National Data Center for monitoring the Comprehensive Test Ban Treaty (CTBT). As such, AFTAC hosts a complete data processing system encompassing computer hardware, software, and databases for geophysical monitoring. In addition to a continuous analysis pipeline, it includes a test bed on which new algorithms and techniques can be tested in an operational setting. After rigorous evaluation, the most promising techniques can then be integrated into operational data analysis.The broad seismological research community plays a critical role in this activity, as it is primarily from the focused efforts of universities and industry that such techniques are gleaned. In this paper we shall describe the evaluation and integration procedures, and highlight some of the research efforts that have been successfully integrated. We shall clarify the relationship between the U.S. NDC and the principal explosion monitoring research program jointly funded by the Air Force Research Laboratories and the Department of Energy. We shall also discuss the relationships of the U.S. NDC with other Government agencies, such as the Office of the Secretary of Defense and the Department of State's Bureau of Verification, Compliance, and Implementation.

Observed Seismic Technological Advances As Demonstrated During And Following The May 25, 2009 North Korean-Declared Nuclear Test

JIH, R.-S., Department of State / VCI Bureau, Washington DC, U.S.A., jihrs@state.gov

The 80%-complete International Monitoring Systems (IMS) met general expectations for the North Korean-announced 2nd nuclear test on May 25, 2009. The IDC SEL bulletin, which is based on exclusively IMS data, along with the USGS/NEIC bulletin, were among the first that became available to the VCI Bureau users for preliminary assessment. As far as detection is concerned, USGS, AFTAC, and IMS all performed very well. While regional P/S ratios using solely IMS and IRIS broadband seismographs nearby suggest discrimination to be straightforward in this case, discrimination using the traditional mb:Ms presented a nontrivial difficulty, as in October 2006, and thereby suggests that empirical formulae or procedures established for one test site may not be categorically transported to another without careful adjustment and careful validation. That is, region-specific calibration would be required. Multiple seismic research teams, including LDEO, UK Blacknest (UK NDC), KIGAM (ROK NDC), SAIC, and SUNYSB, have all independently derived a high-precision spatial separation of two kilometers between the 2009 and 2006 events, based on a variety of relative location techniques. Of interest is an innovative depth estimation procedure proposed by Murphy *et al.*, matching the prediction by the Mueller-Murphy source scaling model with the observed spectral ratios of the two explosions at common stations. This approach led to well-constrained depths as well as yields for the two events - a judicious utilization of the Mueller-Murphy model that exploits the nearly common propagation paths between multiple events in close vicinity. All these advances in seismic verification technology are significant and relevant. Some of these could be readily transitioned to operation, some would require follow-up research to quantify the associated uncertainty. It is interesting to witness growing bilateral cooperation among some Northeastern Asian countries, a step toward a "seismic neighborhood watch".

Seismological Monitoring of the Comprehensive Nuclear Test Ban Treaty

SYKES, L.R., Lamont-Doherty Earth Observatory, Palisades NY 10964 USA, sykes@ldeo.columbia.edu

Renewed interest in the CTBT led to recent studies in which seismic monitoring is a key issue: the ISS Conference in Vienna and a 2010 report by the National Academy of Sciences on progress during the last 10 years. I chaired a sub-committee on Seismology for the NAS study. I give my views on progress made in seismic verification since 2000. No country that signed the CTBT has tested since 1996. The North Korean explosion of 2006 was well located and identified even though its yield was about 0.5 kiloton. The use of high-frequency seismic waves at regional distances for discriminating earthquakes from nuclear explosions is a major advance that has been applied to areas near the Novaya Zemlya, Lop Nor, Indian and North Korean test sites. Novaya Zemlya is now monitored down to magnitude 2 to 2.5, corresponding to a yield of a tamped explosion of 5 to 16 tons (not kilotons) and fully decoupled tests of 100 to 630 tons at 90% confidence. A lower confidence level likely would be appropriate for an evader not wanting to be detected. That could reduce the above yields by a factor of about 2.5. Because salt is not present in appreciable thickness at Novaya Zemlya, decoupled tests would have to be in hard rock. The database of decoupled nuclear tests is very slight although that concept of muffling is 50 years old. Another major advance is the availability of digital seismic records from thousands of stations in near real time. Problem seismic events that are difficult to identify with routine analyses, are fewer and of lower magnitude than 10 years ago. Moment-tensor solutions are more powerful because they use more of the seismogram than the older Ms-mb method. They are now available worldwide down to about magnitude 5 and for several test sites down to magnitude 4. Clear dilatational first motions that are observed at regional distances identify events as earthquakes.

Scientific Challenges for Seismic Nuclear Explosion Monitoring

ZUCCA, J.J., Lawrence Livermore National Lab, Livermore, CA, USA, zucca2@llnl.gov

In the 1990s as the U.S. prepared to enter the negotiations for the Comprehensive Test Ban Treaty there were critical technical challenges facing the seismic monitoring community. In order to achieve the lower monitoring thresholds required for the CTBT, regional phases needed to be integrated into event solutions with teleseismic phases. The relatively large regional-phase travel time residual errors needed to be accounted for and new regional discriminants needed to be developed. Source-specific station correction approaches using ground truth events eventually evolved into the Regional Seismic Travel Time model. This effort was coupled with broader frequency empirical studies tied to an active field program to understand regional explosion signals. This work has led to dramatic improvements in our ability to monitor worldwide for nuclear testing. That said, seismic nuclear explosion monitoring faces further significant challenges. We still do our best monitoring where we have well-characterized ground truth events. To extend our monitoring capability we need to move from being primarily empirical to being physics-based. We need to be able to predict the broad features of the seismic waveform for an arbitrary source/receiver pair and compare with the data. Major advances in the seismic community's ability to develop integrated earth models and calculate full-waveform 3D synthetic seismograms over the last ten years are beginning to enable this capability. Supercomputing allows new approaches to developing stochastic earth models that better represent uncertainties. This capability needs to be coupled with a new field program that explores the explosion source so that the absolute excitation of P and S waves can be predicted for an arbitrary geologic environment. These challenges are a fertile research ground.

This work performed under the auspices of the U.S. Department of Energy by Lawrence Livermore National Laboratory under Contract DE-AC52-07NA27344.

Analysis of the IDC Reviewed Event Bulletin for Detection Capability Estimation of the IMS Primary Seismic Stations

KVAERNA, T., NORSAR, Kjeller, Norway, tormod@norsar.no; RINGDAL, F., NORSAR, Kjeller, Norway, frode@norsar.no

We have investigated the IDC Reviewed Event Bulletin (REB) for the time period 1 January 2000 to 15 July 2009 to quantify the event detection capability of individual primary seismic stations of the International Monitoring System (IMS). For a specific target area, we can obtain estimates of the detection threshold of a given station by considering the ensemble of REB reported events in the area, and downscaling each event magnitude with the observed SNR at the station. However, there are some problem areas associated with this procedure such as:

- Possible biases in the REB magnitudes caused by non-detections
- Skewness in the distribution of threshold estimates, also caused by non-detections
- The validity of using the signal-to-noise ratio for downscaling the event magnitude

We address these issues by dividing the events into a binned global grid system and introduce a maximum likelihood estimation procedure to compensate for the presence of non-detections. A major result of this study is a quantification and ranking of the IMS primary seismic stations based on their capability to detect events. For each station, source regions with noticeable signal amplitude focusing effects (bright spots) and defocusing effects can be identified and quantified. We apply this information to calculate updated global detection capability maps for the IMS primary seismic network, both the current capability using existing stations and the projected capability once the network is completed.

Future work will focus on estimating region-specific station corrections and the associated standard deviations and investigate approaches to combining the region-specific station corrections and the detection thresholds in order to provide dynamic checking of the validity of individual phases associated with events defined in the automatic phase association processing at the IDC.

Bayesloc Multiple-Event Location Applied to a Global Data Set

MYERS, S.C., Lawrence Livermore National Lab., Livermore, CA, smyers@llnl.gov; JOHANNESSON, G., Lawrence Livermore National Lab., Livermore, CA, gardar@llnl.gov

We extend the Bayesloc multiple-event location algorithm for application to global data sets. Bayesloc is a formulation of the joint probability function for multiple-event location parameters that includes hypocenters, travel time corrections, pick precision, and phase labels. Stochastic priors may be input for any of the Bayesloc parameters. Markov chain Monte Carlo sampling is used to draw samples from the joint probability distribution. The data set is selected from the LLNL database, which is a collection of bulletins, as well as over 100,000 LLNL picks. In this application, events with the most picks are selected to produce an even geographic distribution. Data selection is done independently for a number of depth bins, each depth bin spanning 50 km. To this data set we add a number of explosion events, some with known origin times, and earthquakes that are accurately located with a local network. Preliminary relocation results without any prior constraints place epicenters within ~8 km of known locations on average. Much of the improvement in location accuracy is attributed to dynamic assessment data precision, which factors into data weights. Location accuracy will improve when location priors are used. Of arrivals labeled P, Pn, and PcP, ~93%, ~90%, and 96% are properly labeled with probability > 0.9, respectively. Incorrect phase labels are frequently reassigned to another phase, but many arrivals are confidently determined to be erroneous. P and Pn residual standard deviation with respect to the ak135 model are dramatically reduced from 3.45 seconds to 1.01 seconds. Accurate locations, phase label reassignment that includes data culling, and overall data consistency make Bayesloc data sets ideal for tomographic studies. Prepared by LLNL under Contract DE-AC52-07NA27344, LLNL-ABS-422253.

A New Look at an Old Discriminant: Ms—mb

RICHARDS, P., Lamont-Doherty Earth Observatory, Palisades, NY, USA.

The Ms—mb discriminant was discovered more than forty years ago, and was a key method for distinguishing between earthquakes and explosions in the era of teleseismic monitoring. It is still useful (old discriminants never die), though now it competes with methods based on regional signals. We understand why it works well for sources large enough that body waves (from earthquakes) are radiated incoherently. But why does it work so well when source dimensions are small enough for the resulting body waves to be coherent? This paper reviews answers given over several decades, most recently by Patton and Taylor (GRL, 2008), who took a new look at plausible non-isotropic terms in the moment tensor representation of an underground nuclear explosion, and showed that they act to suppress surface waves, *i.e.* they reduce Ms. Their method is extended in two ways: (1) by allowing for a more general type of shear faulting; and (2) by discussing effects on body waves as well as surface waves—finding cases where the non-isotropic terms proposed by Patton and Taylor can enhance mb.

Apparent Explosion Moment

PATTON, H.J., Los Alamos National Laboratory, Los Alamos NM USA, patton@lanl.gov; TAYLOR, S.R., Rocky Mountain Geophysics, Los Alamos NM USA, srt-rmg@comcast.net

A tenet of explosion source theory is that seismic moment M_t is proportional to the steady-state level of the reduced displacement potential. Measurements M_I of explosion moment have long been interpreted as estimates of M_t. Assuming incompressibility of the inelastic region, the steady-state level is proportional to the volume V of the cavity created by vaporization and pressurization of materials around the point of energy release. Thus M_t is the moment of the volumetric source associated with cavity creation. New source models incorporating free-surface interactions and shock-wave rebound predict V and volume U created by rapid changes in shear and bulk moduli in the medium over the shot point. The notion of apparent explosion moment M_x includes volumetric source contributions from V and U. A

compensated linear vector dipole (CLVD) is used to represent the non-volumetric source component. K is a measure of steady-state strength M_{CLVD} with respect to M_x. Moment tensor inversion results of NTS explosions show that K steadily decreases with yield, approaching values near 1.0 for highest yield shots. A value of 1.0 implies $M_{CLVD} = 0$ and, by inference, small U. Our hypothesis is that the force of spall slapdown is great enough at high yields to crush the tuff matrix, reducing U while V remains intact. Slapdown at low yields is not great enough to do so, leaving both V and U unaffected. We test the hypothesis by comparing measurements M_I with estimates of M_t based on relationships of V and velocity models for Pahute Mesa, including reduced coupling effects above the water table. The results support the hypothesis and the conclusion that measurements M_I are composed of two volumetric components: V due to the explosion itself and U related to nonlinear processes occurring above the explosion.

Regional P/S Methods of Discriminating Explosions from Earthquakes: Applications and Limitations

WALTER, W.R., Lawrence Livermore National Lab., Livermore, CA, USA, bwalter@llnl.gov; PASYANOS, M.E., LLNL, Livermore, CA, USA, pasyanos1@llnl.gov; FORD, S.R., LLNL, Livermore, CA, USA, ford17@llnl.gov; MATZEL, E., LLNL, Livermore, CA, USA.

Ratios of regional P/S seismic wave amplitudes at sufficiently high frequency (~2–16 Hz) have demonstrated an excellent ability to discriminate nuclear explosions from nearby earthquakes everywhere they have been tested, including the 2006 and 2009 North Korean tests. Regional P/S can operate on smaller magnitude events than the older Ms:mb technique, as Ms can be difficult to measure for explosions less than around mb 4. With path correction techniques such as multiphase attenuation tomography (Pasyanos *et al.*, 2009) regional P/S discriminants can be successfully used over broad and complex areas (*e.g.* Pasyanos and Walter, 2009). However an important limitation to applying the technique occurs when, for a given path, the S-wave amplitudes are blocked or attenuated below the background noise due to Earth structural complexity. Because the absence of S-waves can indicate an explosion source, it is critical to establish for a given path that S-waves would have been observed had the source been an earthquake. We are making use of earthquake source spectral models and attenuation tomography results to map out by magnitude for a given station where regional P/S will work as a discriminant. Such calibrations are an important part of effectively using P/S ratios to identify explosions. We demonstrate the creation and use of these maps in the Middle East and the Korea-Japan region using recent regional multiphase tomography results. In addition there remain questions about possible limitations for P/S discrimination due to magnitude dependent behavior, with small explosions requiring higher frequencies to discriminate than the larger ones. There are also possible limitations to discriminating uncontained and ripple-fired mining and industrial chemical blasts from earthquakes. We explore these limitations as well, adding additional examples in the western U.S.

Nuclear Explosion Monitoring R&D Roadmap

CASEY, L.R, DOE/NNSA/NA-22, Washington, DC, Leslie.Casey@nnsa.doe.gov; ZIAGOS, J.P., DOE/NNSA/NA-22, Washington, DC, John.Ziagos@nnsa.doe.gov; BELL, W.R., DOE/NNSA/NA-22, Washington, DC, Randy.Bell@nnsa.doe.gov

This talk reviews research and development highlights and accomplishments (https://na22.nnsa.doe.gov/mrr) as well as future research directions of the Ground-based Nuclear Explosion Monitoring R&D (GNEM R&D) program within the National Nuclear Security Administration's Office of Nuclear Detonation Detection, NA-222. GNEM R&D's mission is "...to develop, demonstrate, and deliver advanced technologies and systems to operational monitoring agencies to fulfill US monitoring requirements and policies for detecting, locating, and identifying nuclear explosions."* Work sponsored by GNEM R&D and collaborators is conducted by world-class scientists and engineers in national laboratories, universities, and private industry. In the past ten years, significant progress has been made in detection, location and identification with substantial improvements yet possible. There is increasing interest in GNEM R&D technology particularly in light of its relevance to the Comprehensive Nuclear Test Ban Treaty. GNEM R&D direction is captured in roadmaps: waveform technologies, including seismic, hydroacoustic, and infrasound and radionuclide monitoring. The roadmaps have the same four areas: source physics, signal propagation, sensors, and signal analysis. Within each area illustrative R&D themes, program metrics, and future R&D directions will be presented. The goals of the R&D program are to: perform innovative scientific research, deliver capability-enhancing technologies to monitoring agencies and to motivate and nurture human capital to meet future monitoring challenges.

**Nuclear Explosion Monitoring Research and Engineering Program Strategic Plan,* DOE/NNSA/NA-22-NEMRE-2004, https://na22.nnsa.doe.gov/cgi-bin/prod/nemre/index.cgi?Page=Strategic+Plan

Characterizing the Next Cascadia Earthquake and Tsunami

Oral Session · Wednesday 8:30 AM, 21 April · Salon F
Session Chairs: Chris Goldfinger and Rob Witter

The Landward Limit of Cascadia Great Earthquake Rupture

HYNDMAN, R.D., Geological Survey of Canada, Sidney, BC Canada, rhyndman@nrcan.gc.ca; WANG, K., Geological Survey of Canada, Sidney, BC Canada, kwang@nrcan.gc.ca; CASSIDY, J., Geological Survey of Canada, Sidney, BC Canada, jcassidy@nrcan.gc.ca; KAO, H., Geological Survey of Canada, Sidney, BC Canada, hkao@nrcan.gc.ca; MAZZOTTI, S., Geological Survey of Canada, Sidney, BC Canada, smazzotti@nrcan.gc.ca; DRAGERT, H., Geological Survey of Canada, Sidney, BC Canada, hdragert@nrcan.gc.ca; HENTON, J., Geological Survey of Canada, Sidney, BC Canada, jhenton@nrcan.gc.ca; LEONARD, L., Geological Survey of Canada, Sidney, BC Canada, lleonard@nrcan.gc.ca; ROGERS, G., Geological Survey of Canada, Sidney, BC Canada, grogers@nrcan.gc.ca

The dominant control for megathrust shaking intensity at near-coastal cities is the landward, downdip extent of rupture. It represents the source closest approach and, with along-strike length, constrains the maximum magnitude. The updip limit and wave propagation factors are also important for shaking and tsunami generation. Some downdip estimates are for past rupture, some for the "locked" zone, and some for downdip limits to seismic behaviour. Bases for estimating downdip rupture extent include: (1) Modeled paleoseismic coastal subsidence, and the 1700 tsunami. (2) Locked/transition zones from modelling geodetic deformation. (3) Seismic behaviour limits from downdip temperatures, change in seismic reflection character downdip, and the ETS updip limit (with some offset). The limits to coseismic rupture and the interseismic "locked" zone from geodetic data are not identical because of the deformation time dependence. The rates of rupture are also important, *i.e.*, seismic rupture, slower tsunamogenic slip, and slower long-term slip detected geodetically. A related issue is the nature and relationship of postseismic and interseismic slip and viscous relaxation. Although the differences among the estimates are important, most give similar extents, *i.e.*, the principal rupture displacement occurs offshore beneath the outer continental shelf, and the majority of events appear to rupture most of the seismogenic region, *i.e.*, M9. Unresolved questions include: Vertical interseismic models that involve several poorly constrained parameters, the relationship between coseismic rupture distribution and interseismic locking from geodetic data and from ETS distributions, and uncertainties in the depth to the megathrust.

A Comparison of the Location of Interseismic Locking and Slow Slip Events on the Cascadia Subduction Zone

WELDON, II, R.J., Dept. of Geological Sciences, University of Oregon, Eugene, OR, USA, ray@uoregon.edu; SCHMIDT, D., Dept. of Geological Sciences, University of Oregon, Eugene, OR, USA, das@uoregon.edu; GAO, H., Dept. of Geological Sciences, University of Oregon, Eugene, OR, USA; ALBA, S., Dept. of Geological Sciences, University of Oregon, Eugene, OR, USA; LIVELYBROOKS, D., Dept. of Physics, University of Oregon, Eugene, OR, USA.

We determine the distribution of interseismic locking and slip associated with ETS events along the Cascadia subduction zone interface using historical leveling, tide gauges, and continuous GPS data sets. To determine locking, we convert the horizontal deformation from GPS to strain and model the contraction rate parallel to the local convergence direction to isolate the subduction-related deformation from the clockwise rotation of western Oregon. Horizontal contraction rates are greatest at the coast and diminish inland, with local maximums of ~100 nanostrain/yr observed in Washington and the CA/OR border region, but ~50 nanostrain/yr for the central OR coast. Near the coast, sparse GPS stations relative to the steep deformation gradient likely result in minimum strain rate values. Vertical deformation is inferred from historical leveling and tidal data (vertical GPS provides minimal constraint). We anchor the leveling estimates of relative uplift into an absolute reference frame by using a weighted least-squares adjustment that accounts for errors in both the tidal and leveling data. The horizontal and vertical deformation fields are consistent and dominated by strain accumulation related to a locked zone near the coast. Slow slip events are mapped by performing a time-dependent inversion of transient surface displacements inferred from the GPS time series. The distribution of slip on the plate interface compares well with the distribution of non-volcanic tremor sources located by Boyarko and Brudzinski (in press).

The down dip distribution of locking is more variable than the distribution of the zone of slow slip. In Washington and the CA/OR border region the locked, transition, and slow slip zones appear to be contiguous along the plate interface. In central Oregon, the locked and transition zones are distinctly shifted up-dip from the region of slow slip and tremor.

Segmentation and Probabilities for Cascadia Great Earthquakes based on Onshore and Offshore Paleoseismic Data

GOLDFINGER, C., Oregon State University, Corvallis, OR, gold@coas.oregonstate.edu; PATTON, J.R., Oregon State University, Corvallis, OR, jpatton@coas.oregonstate.edu; MOREY, A.E., Oregon State University, Corvallis, OR, morey@coas.oregonstate.edu; WITTER, R.C., Oregon Dept of Geol. & Min. Ind., Newport, OR, rob.witter@dogami.state.or.us

Analysis of offshore and onshore paleoseismic data suggest at least four seismic segments operating in the Holocene on the Cascadia margin. Along the northern margin, we find a consistent earthquake recurrence averaging ~ 500–530 years. The central Oregon to northern California margin comprises at least three segments that include all of the northern ruptures and ~ 22 smaller events of restricted latitude range that are correlated between multiple sites. At least two northern California sites probably also record numerous small sedimentologically or storm triggered turbidites during the early Holocene. The four segments include 19 full or nearly full -length ruptures; 1 or 2 ruptures comprising the southern 50–70% of the margin, and 20 smaller southern margin ruptures in two smaller segments during the Holocene. The shorter extents and thinner turbidites of the southern margin correspond well with timing and spatial extents interpreted from the onshore paleoseismic record. 41 events define a Holocene recurrence for the southern Cascadia margin of ~240 years. Time-independent probabilities for segmented ruptures range from 7–9% in the next 50 years for full margin ruptures, to ~18% in 50 years for a southern segment rupture. Time dependent failure analysis suggests the probability of an event by 2060 of ~25% for the northern margin and ~80% for the southern margin. The long paleoseismic record also indicates a pattern of clustered earthquakes that includes 4–5 cycles that are more robust in the later Holocene. Probabilities would markedly change for the northern margin if the event were a significant gap or cluster in a clustered model. Probabilities change little for the southern margin where no temporal clustering is apparent. The next Cascadia event is most likely to be a segmented rupture along one or both of the southern segments.

ETS-Delineated Future Rupture of the Cascadia Megathrust

MELBOURNE, T.I., CWU, Ellensburg/WA/USA, tim@geology.cwu.edu; BRUDZINSKI, M., MUO, Miami/OH/USA, brudzimr@muohio.edu

A suite of 15 Episodic Tremor and Slip (ETS) events imaged between 1997 and 2008 along the northern Cascadia subduction zone suggests future coseismic rupture will extend to 25 km depth, or ~60 km inland of the Pacific coast, rather than stopping offshore at 15 km depth. An ETS-derived coupling profile accurately predicts GPS-measured interseismic deformation of the overlying North American plate, as measured by ~50 continuous GPS stations across western Washington State. When extrapolated over the 550-year average recurrence interval of Cascadia megathrust events, the coupling model also replicates the pattern and amplitude of coseismic coastal subsidence inferred from previous megathrust earthquakes here. For only the Washington State segment of the Cascadia margin, this seismogenic zone translates into an Mw=8.9 earthquake, with significant moment release close to its metropolitan centers.

Outside of Washington State, the rapid expansion of GPS and seismic networks along the arc have enabled identification of nearly 40 isolated ETS events from 1992 through 2009. GPS offsets inverted for slip show moment magnitudes ranging from 5.9 (smallest resolvable with GPS) to 6.8, and typically 2–3 cm of slip. A comparison of geodetic moment estimates with tremor analyses of nearly 30 well-recorded events over a ten-year period yields a highly linear relationship between moment release, as estimated from GPS, and total duration of non-volcanic tremor, as summed from regional seismic arrays. All Cascadia events detected since 1997 for which geodetic and seismic data are available, which collectively span the Cascadia arc from northern California to Vancouver Island, Canada, release moment during tremor at a rate of 5.3 ± 0.4 x 1023 dyne-cm per hour of recorded tremor. This empirical ETS moment rate enables mapping the depth extent of the megathrust seismogenic zone throughout the arc and the quantification of the hazards it poses to its major metropolitan centers.

A Continuous Moment Tensor Analysis in the Region of the Mendocino Triple Junction, California

GUILHEM, A., Berkeley Seismological Lab, Berkeley, CA USA, aurelie@seismo.berkeley.edu; DREGER, D.S., Berkeley Seismological Lab, Berkeley, CA USA, dreger@seismo.berkeley.edu; UHRHAMMER, R., Berkeley Seismological Lab, Berkeley, CA USA, bob@seismo.berkeley.edu

In the goal of more efficiently monitoring the Mendocino Triple Junction, which is the most seismically active region of Northern California where a variety of anomalous seismic events occurs including repeating earthquakes, slow/low-stress-drop earthquakes, and non-volcanic tremors, in addition to typical inter- and intra-plate seismic activity we are developing an automatic scanning of continuous long-period (> 20 sec) broadband seismic records following the method proposed by Kawakatsu (1998) and implemented by Tsuruoka et al (2009).

We continuously perform the cross-correlation of Green's functions and every 2 seconds invert for the seismic moment tensor for sources distributed over a spatial grid of about 5,000 virtual sources (~ every 20 km). The algorithm automatically detects, locates, and determines the scalar seismic moment and focal mechanism once a defined threshold of fit between data and synthetics is reached.

The power of this method is that it offers the possibility of rapidly identifying any seismic events occurring in the region especially large damaging and potentially tsunamigenic earthquakes along the Cascadia subduction zone within the time it takes for the complete low-frequency wavefield, including surface waves, to propagate through the network.

We are implementing two parallel running algorithms: one focusing on the small to moderate (Mw ≤ 7) earthquakes by scanning data filtered between 20 and 50 sec period and on large, potentially tsunamigenic events (Mw ≥ 8) with data filtered between 100 and 200 sec period. We present tests for the two algorithms and we show that we can identify small to great earthquakes thanks to such a scanning that provides the complete earthquake information in realtime using a single stage of processing, and for this reason it will be faster and more reliable than the current in-cascade procedures.

Mapping the Juan de Fuca Slab Beneath the Cascadia Margin

MCCRORY, P.A., US Geological Survey, Menlo Park/CA/USA, pmccrory; BLAIR, J.L., US Geological Survey, Menlo Park/CA/USA, lblair@usgs.gov; WALDHAUSER, F., Lamont-Doherty Earth Observatory, Palisades/NY/USA, felixw@ldeo.columbia.edu

An accurate map of the Cascadia plate boundary is essential for developing realistic seismic hazard assessments. We have updated our model of Juan de Fuca (JdF) slab geometry beneath the Cascadia subduction margin with depth control from recent studies of double-differenced (DD) hypocenter locations, and velocity models based on active and passive source experiments. However, mismatches both within and between these data types illuminate remaining uncertainties on the location and geometry of the slab.

Seismic velocity models based primarily on S-wave data depict JdF crust up to 10 km shallower beneath Washington (WA) and Vancouver Island (VI) than P-wave models. Does this reflect model uncertainties, or are the two data types mapping different structures? To date, baseline comparisons of P- and S-wave models that employ equivalent initial velocity parameters are lacking.

Could oceanic terranes accreted during previous subduction regimes mimic the JdF plate in the subsurface? Such tectonic complexities hamper efforts to directly compare Cascadia velocity models with those developed in subduction settings such as Japan or Alaska.

If shallow slab seismicity beneath WA and VI occurs mainly in JdF mantle, our slab model could shift upwards as much as 5 km. Where DD hypocenters resolve double seismic zones beneath California, we can identify the JdF Moho, thus delineate a complex geometry that suggests buckling of the JdF plate. The DD method offers the potential to better map the arched slab geometry beneath PS and VI as well. A more accurate slab model will provide a crucial tool for investigating links between slab geometry and rates of seismic moment release.

Resolving the source of mismatches in depth control is critical for efforts to estimate shaking hazard from subduction earthquakes. Development of a community or consensus seismic velocity model is a key first step.

Megathrust Paleogeodesy at the Central Cascadia Subduction Zone

HORTON, B.P., University of Pennsylvania, bphorton@sas.upenn.edu; NELSON, A., USGS, ; WITTER, R., DOGMI, ; WANG, K., University of Victoria, ; HAWKES, A., WHOI, ; ENGELHART, S., University of Pennsylvania, ; SAWAI, Y., Geological Survey of Japan.

Our research will test various hypotheses that explain how strain accumulates along the great megathrust fault between continental and oceanic plates at the Cascadia subduction zone, and is then suddenly released during great (magnitude 8 to 9) earthquakes on the fault. We measure subduction-zone strain indirectly by inferring coastal land-level changes from small changes in relative sea level. This new information about how the Cascadia plate boundary deforms will help us understand deformation at other plate boundaries and improve assessments of earthquake and tsunami hazards in central western North America.

The wetland sediments fringing estuaries at the Cascadia subduction zone harbor a unique record of plate-boundary earthquakes during the past 5000 years. However, the precision of past measurements of land-level changes at Cascadia is low (errors of >±0.5 m), the measurements are spatially limited, and they span only fractions of complete cycles of subduction zone strain accumulation and release. This makes past measurements insufficient for determining which hypotheses of

plate-boundary deformation are most valid. We aim to re-dress this deficiency by applying recently developed statistical transfer functions to microfossils, such as foraminifera and diatoms, collected from Cascadia estuarine sediments. Similar studies of sea-level change on other continents have obtained an unprecedented vertical resolution of ±0.1–0.3 m.

Validating Numerical Tsunami Simulations in Southern Oregon Using Late Holocene Records of Great Cascadia Earthquakes and Tsunamis

WITTER, R.C., Oregon Dept of Geology, Newport, OR, rob.witter@dogami.state.or.us; ZHANG, Y.J., Oregon Health & Science Univ, Beaverton, OR, yinglong@stccmop.org; GOLDFINGER, C., Oregon State University, Corvallis, OR, gold@coas.oregonstate.edu; PRIEST, G.R., Oregon Dept of Geology, Newport, OR, george.priest@dogami.state.or.us; WANG, K., Geological Survey of Canada, Sidney, BC, Canada, kwang@nrcan.gc.ca

Marine and coastal paleoseismic evidence for Cascadia subduction earthquakes imply a range of rupture scenarios that provide model inputs for tsunami simulations. 41 turbidites from submarine channels along the length of the margin define a mean Holocene recurrence of ~530 yr for ruptures ≥800-km-long and ~240 yr for southern Cascadia earthquakes that ruptured 3 shorter segments. Coastal paleoseismic records spanning the past ~7000 yr include 13 tsunami deposits archived in Bradley Lake in southern Oregon. We test the smallest Cascadia tsunami scenarios capable of reaching the lake for consistency with paleoseismic data.

Earthquake scenarios employ either: 1) regional rupture with slip distribution symmetrically tapering to zero up and down dip; or 2) regional rupture diverting slip onto an offshore splay fault. Maximum slip in each scenario varies as the product of selected recurrence intervals and the convergence rate. Using the hydrodynamic model SELFE, we ran >50 tsunami simulations on numerical grids that reflect inferred changes in coastal paleotopography.

Simulating the 1700 tsunami requires earthquake slip equivalent to ≥400 yr of convergence using the regional symmetric slip model. Augmenting uplift with a splay fault reduces the recurrence time to 360 yr—still longer than the 174 to 341 yr range of paleoseismic intervals that correlate with tsunami deposits in the lake. Earlier tsunamis, likely smaller than the 1700 wave, probably followed the largest earthquakes when the shoreline migrated to its most landward position due to subsidence and coastal erosion. Tsunami simulations with these conditions require a minimum recurrence of 280 yr. Other factors like seafloor acceleration or extreme tides may account for the smallest Cascadia tsunamis that reached the lake. Alternatively, these small events may release stored strain from previous earthquake cycles.

Cascadia Supercycles: Energy Management of the long Cascadia Earthquake Series

GOLDFINGER, C., Oregon State University, Corvallis, OR, gold@coas.oregonstate.edu; WITTER, R.C., Oregon Dept. of Geology, Newport, OR, rob.witter@dogami.state.or.us; PRIEST, G.R., Oregon Dept. of Geology, Newport, OR, george.priest@dogami.state.or.us; WANG, K., Geological Survey of Canada, Sidney, BC, Canada, kwang@nrcan.gc.ca; ZHANG, Y.J., Oregon Health & Science Univ, Beaverton, OR, yinglong@stccmop.org

The Holocene Cascadia earthquake series affords uncommon opportunities to examine recurrence models, clustering and long term strain history. We attempt to address the issue of energy management over multiple earthquake cycles through the temporal record of interseismic intervals and a proxy for magnitude of the earthquakes. Plate convergence between earthquakes is assumed to increase elastic strain energy in proportion to interevent time. We propose that coseismic energy may be modeled as proportional to the mass of turbidites triggered in seismic shaking. We infer that turbidite mass is a suitable proxy for energy release because of its consistency along strike at multiple sites. We scale turbidite mass (energy release) to balance plate convergence (energy gain) to generate a 10ka energy time series for Cascadia. The pattern reveals that the earthquake clusters apparent in the time series have variable behavior. Cluster 4 (~10000–8800 BP) maintains an even energy state before falling to a low after large event T16. Cluster 3 (~8200–5800 BP) climbs steadily in energy state until large event T11 drops it to another low. Cluster 2 (~4800–2500 BP) climbs then falls to a low after T6. Cluster 1 (~1600–300 BP) slowly declines from T5 to T1. What is apparent is that some events release less while others release more energy than available from plate convergence (slip deficit). Those that are larger may have borrowed stored energy from previous cycles. Cycle variations may explain mismatches between deformation models based on interevent times in the last 4600 years and coastal paleoseismic data. During that time, a long series of 8 earthquakes comprise a decline in energy state, yet some produced outsized tsunami relative to plate convergence alone. We suggest these events may be using energy from a previous peak at the time of T8, ~ 3400 years prior.

Temporal Clustering and Recurrence of Holocene Paleoearthquakes in the Region of the 2004 Sumatra-Andaman Earthquake

PATTON, J.R., Oregon State University, COAS, Corvallis/OR/USA, jpatton@coas.oregonstate.edu; GOLDFINGER, C., Oregon State University, COAS, Corvallis/OR/USA, gold@coas.oregonstate.edu; MOREY, A.E., Oregon State University, COAS, Corvallis/OR/USA, morey@coas.oregonstate.edu; ERHARDT, M., Oregon State University, COAS, Corvallis/OR/USA, gosar951@yahoo.com; BLACK, B., Oregon State University, COAS, Corvallis/OR/USA, blackbra@onid.orst.edu; GARRETT, A.M., Oregon State University, COAS, Corvallis/OR/USA, amymonicagarrett@googlemail.com; DJADJADIHARDJA, Y., Bandan Penghajian Dan Penerapan, Jakarta/Indonesia, iyung24@yahoo.com; HANIFA, U., Bandan Penghajian Dan Penerapan, Jakarta/Indonesia, udrekh@gmail.com

Earthquakes and tsunamis are some of the most deadly natural disasters, with the 26 December 2004 Sumatra-Andaman earthquake and tsunami responsible for the deaths of nearly a quarter of a million people. Knowledge about the earthquake cycle, through many cycles, is fundamental to understanding both the societal risk and the nature of the seismogenic process. Recurrence of great earthquakes (7.25 ka, years before present, BP, 1950) is estimated based on turbidite stratigraphy (representing earthquake events) correlated between 49 deep sea sediment cores in the region of the 2004 rupture. We apply criteria developed in Cascadia, Japan, and in Sumatra thus far to discriminate such events from those triggered by other mechanisms by testing the turbidite stratigraphy for synchronous triggering of turbidity currents between sedimentologically isolated basin core sites and deeper trench sites using radiocarbon, multiple proxies and ash stratigraphy.

Nineteen turbidites are interpreted to have been triggered during strong ground shaking from earthquakes over the past ~7,250 years. The youngest turbidite is most likely the result of the 2004 earthquake. Calibrated probability density function peak ages for events 4–13 are 640±60, 800±70, 1190±100, 1500±90, 1600±80, 2090±70, 2750±60, 3910±80, 4480±80, 4830±60 years BP and events 15–19 are 5150±110, 5460±110, 5720±100, 6540±80, and 7230±70 years BP. The turbidite record is also compatible with the developing onshore record of paleoearthquakes in Aceh, Thailand, Sumatra, and the Andaman Islands, but the terrestrial record is less complete. The recurrence interval (RI) estimate for earthquakes in the 2004 rupture region for the last 7.25 ka is 390±60 years. The recurrence pattern appears to include significant clustering through the Holocene, with three apparent clusters, and two gaps of 700–1000 years.

Characterizing Megathrust Recurrence Probabilities in the Pacific Northwest

PERKINS, D., US Geological Survey, Golden, CO, perkins@usgs.gov; LAFORGE, R., Fugro William Lettis Associates, Golden, CO, r.laforge@fugro.com

We show that the times between dated megathrust events of Goldfinger (2009) can be represented by a series of Gaussian intervals. Given the postulated dates, we thereby estimate the time-dependent probability of megathrust events off the coast of Washington and off the coast of northern California, assuming no clustering is occurring. By randomization tests we evaluate the significance of regressions of time intervals or rupture lengths on the previous interval or rupture length. We demonstrate through similar tests that observation of the lengths of rupture of these events is not homogeneous in time.

By several methods we also estimate (a) the probability that the observed sequences of apparent clustering arise from random intervals, (b) the probability that a clustered sequence having uncertain dates can fail to exhibit that clustering, and, through these probabilities, (c) a Bayesian probability that the observed clustering is true clustering behavior rather than a statistical accident.

An Analysis of Temporal Clustering of Cascadia Subduction Zone Earthquakes and its Implications to Seismic Hazard

WONG, I., URS Corporation, Oakland, CA USA, ivan_wong@urscorp.com; KULKARNI, R., URS Corporation, Oakland, CA USA; ZACHARIASEN, J., URS Corporation, Oakland, CA USA; DOBER, M., URS Corporation, Oakland, CA USA; GOLDFINGER, C., OSU, Oceanic and Atmospheric Sci, Corvallis, OR USA; LAWRENCE, M., British Columbia Hydro & Power, Burnaby, BC CAN.

Several investigators have suggested that full-length ruptures along the Cascadia subduction zone exhibit temporal clustering. Goldfinger *et al.* (in press) observes a repeating pattern of clustered earthquakes that may be interpreted as 4–5 Holocene cycles of 2–5 earthquakes each separated by unusually long intervals in the turbidite record. We performed statistical analyses on the turbidite event record to test the temporal clustering model, calculate time-dependent recurrence intervals, and evaluate its implications to hazard. Assuming the turbidite record reflects a complete record of full rupture **M** ~9 megathrust events, we used a Monte Carlo simulation

to determine if the turbidite recurrence intervals follow an exponential distribution consistent with a Poisson (memoryless) process. The Poisson hypothesis was rejected at a statistical significance level of 0.05.

We performed a "cluster analysis" on 20 randomly simulated catalogs of 18 events, using ages with uncertainties from the turbidite dataset, to assess whether the events occur in clusters. Results indicate 13 catalogs exhibit statistically significant clustering behavior, yielding a probability of clustering of 13/20 or 0.65. Most (70%) of the 20 catalogs contain 2 or 3 closed clusters and the current cluster T1-T5 appears consistently in all catalogs. The appearance of older clusters varied among the catalogs, likely due to larger uncertainties in their ages. The consistent occurrence of the same recent clusters suggests that clustering of recent events is stable despite the uncertainty in ages. Analysis of the 13 catalogs that manifest clustering indicates the probability that at least one more event will occur in the current cluster is 0.82. Last, we calculated time-dependent equivalent recurrence intervals; the median intracluster interval was 260 yrs, and the intercluster interval was 1759 yrs.

Magnitude Scaling and Regional Variation of Ground Motion

Oral Session · Wednesday 8:30 AM, 21 April · Salon G
Session Chairs: Fabrice Cotton, Gail Atkinson

Accurate Predictions of Strong Ground Motion Based on Weak Motion Data: Case Studies from Italy and Japan

MALAGNINI, L., Ist. Naz. Geofisica Vulcanologia, Rome, Italy, luca.malagnini@ingv.it; AKINCI, A., Ist. Naz. Geofisica Vulcanologia, Rome, Italy, aybige.akinci@ingv.it; MAYEDA, K., Weston Geophysical Corporation, Lexington, MA, USA, kmayeda@yahoo.com; HERRMANN, R.B., Saint Louis University, St. Louis, MO, USA, rbh@eas.slu.edu; MUNAFO', I., Ist. Naz. Geofisica Vulcanologia, Rome, Italy, irene.munafo@ingv.it

Recent papers have recognized the importance of weak-motion-based investigations of wave propagation, pointing out strong regional variations. Other studies demonstrated the existence of complex source scaling in various tectonic environments. At the same time, the use of weak-motion data for deriving region-specific ground motion predictive equations (GMPEs) for large earthquakes is controversial, and a large part of the seismological community still thinks in terms of boringly self-similar sources, and of negligible variations in regional wave propagation. As a result, we tend to use only GMPEs derived from global data sets of strong ground motion recordings.

For predicting the ground motions induced by small-to-moderate-size events (Mw between 4.5 and 6), global GMPEs may be inadequate. For example, peak motions are carried around by distance- and magnitude-dependent dominant frequencies, and thus the PGAs induced by events with Mw between 4.5 and 6 undergo a much more severe attenuation with distance than the PGAs of the large events (Mw 7, 7+). Moreover, global GMPEs are from heterogeneous databases from various tectonic environments, and may introduce biases in the seismic hazard due to small-to-moderate-size earthquakes. These events may be very important for Mediterranean countries like, among many, Italy, Turkey, or Greece, where moderate-size earthquakes may pose a great threat to ancient buildings and poor constructions.

In the present study, we present compelling results for the validity of our approach from the recent l'Aquila earthquake of April 6, 2009. In this case we used a weak-motion based regional GMPE, together with the specific source scaling obtained from a recent coda-based technique, and successfully fit the observed ground motions. Similar results were obtained for recent Japanese events.

Ground-Motion Attenuation Model for Small-To-Moderate Shallow Crustal Earthquakes in California and Its Implications on Regionalization of Ground-Motion Prediction Models

CHIOU, B., California Department of Transpo, Sacramento, CA USA, Brian_Chiou@dot.ca.gov; YOUNGS, R., AMEC Geomatrix, Oakland, CA USA, bob.youngs@amec.com; ABRAHAMSON, N., Pacific Gas and Electric, San Francisco, CA USA, NAA3@earthlink.net; ADDO, K., BC Hydro and Power Authority, Burnaby, BC Canada, Kofi.Addo@bchydro.com

This paper presents the development of a ground-motion prediction model for small-to-moderate magnitude crustal earthquakes ($3 \le M \le 5.5$) using data from the California ShakeMap systems. Our goal is to provide an empirical model that can be confidently used in the investigation of ground-motion difference between California and other active tectonic regions, such as the Pacific Northwest and British Columbia, Canada, where the bulk of ground-motion data from shallow crustal earthquakes is in the small-to-moderate magnitude range. This attenuation model is developed as a small-magnitude extension of the Chiou and Youngs NGA model (CY2008). We observe, and incorporate into this model, a regional difference in median amplitude between central and southern California earthquakes. The strength of the regional difference diminishes with increasing spectral period. More importantly, it is magnitude dependent and becomes insignificant for $M \ge 6$ earthquakes, as indicated by the large-magnitude California data used in CY2008. Altogether, these findings have important implications on the practice of utilizing regional differences in ground motion observed in small-to-moderate earthquakes to infer the regional differences expected in large earthquakes, including the NGA model applicability in active tectonic regions outside California.

Comparisons of Ground-Motion Attenuation in Eastern North America versus California

ATKINSON, G.M., Univ. of Western Ontario, London, Ont., gmatkinson@aol.com; ASSATOURIANS, K., Univ. of Western Ontario, London, Ont., kassatou@uwo.ca; NICOL, E.A., Univ. of Western Ontario, London, Ont.

Previous empirical studies of ShakeMap databases for California, for earthquakes of **M** <5.5, show that ground-motion attenuation is different in southern vs. northern California, and that it is steeper than expected at short distances (decaying significantly faster than 1/R) (Atkinson and Morrison, 2009 BSSA). In this study, we examine in greater detail the attenuation characteristics of ground motions in California, and compare this behavior with that of motions in eastern North America (ENA), making direct amplitude comparisons for events of similar magnitude. The comparisons are facilitated by use of the recently-compiled ShakeMap database of Chiou and Youngs (2010 Earthquake Spectra), that allows the influence of site effects on the motions for California to be explicitly considered. Within 70 km of the earthquake source, ground motions in California in the frequency range from 1 to 3.3 Hz appear to have similar attenuation characteristics to those in ENA. Eastern motions become significantly slower in their attenuation (relative to California) at larger distances, and typically show more pronounced 'Moho bounce' effects. Point-source stochastic simulations are used to infer and compare basic source excitation parameters across the regions.

Exploring the Lower Limits of the NGA Using Data from California

HELLWEG, M., Berkeley Seismological Laboratory, Berkeley, CA, USA, peggy@seismo.berkeley.edu; DARRAGH, R., Pacific Engineering and Analysis, El Cerrito, CA, USA, pacificengineering@juno.com; SILVA, W., Pacific Engineering and Analysis, El Cerrito, CA, USA, pacificengineering@juno.com

The NGA relationships were calculated using data from large earthquakes. As part of the effort to migrate the use of these relationships to the Central and Easter United States, it is necessary to explore their behavior at low magnitudes. We use a dataset of small-to-moderate events (M>3) events from California. With data from these events, we investigate the capacity of the NGA regressions to predict ground motion for small earthquakes and explore the scaling of small magnitudes against the NGA models. We also study the dependence of standard deviation and other important parameters on magnitude.

An Earthquake Discrimination Scheme to Optimize Ground-Motion Prediction Equation Selection

GARCIA, D., U.S. Geological Survey, Golden, CO., danielgarcia@usgs.gov; WALD, D.J., U.S. Geological Survey, Golden, CO., wald@usgs.gov; ALLEN, T.I., Geoscience Australia, Canberra, ACT., Australia, trevor.allen@ga.gov.au; HAYES, G.P., U.S. Geological Survey, Golden, CO., ghayes@usgs.gov; LIN, K.W., U.S. Geological Survey, Golden, CO., klin@usgs.gov; MARANO, K.D., U.S. Geological Survey, Golden, CO., kmarano@usgs.gov

Regionalization of ground-motion prediction equations (GMPEs) has become an important issue in strong-motion seismology and for some related tools recently developed, from Probabilistic Seismic Hazard Analyses (PSHA) to Early Warning Systems, ShakeMaps, and Earthquake Rapid Response Systems. In all cases, the tectonic regime and the type of earthquake under consideration are crucial prerequisites needed to produce accurate results. This is especially true for the Global ShakeMap and Prompt Assessment of Global Earthquake for Response (PAGER) systems of the US Geological Survey, where the estimation of ground shaking and human and economical losses, generated in the aftermath of potentially damaging global earthquakes, strongly depends on the correct classification of the event and the chosen GMPE associated to it. Although some global regionalization efforts have been done in the context of seismic hazard studies, they are mainly focused on determining the possible earthquakes that can take place in a particular region. Following the approach proposed for the GEM project, we present a new earthquake discrimination procedure to determine in near-real time the type of earthquake among different tectonic regimes and their corresponding event classes. This method makes use of the source parameters available from the USGS National Earthquake Information Center in the minutes following an earthquake and of cri-

teria developed for each tectonic regime to give the best estimation of the type of event. The scheme is validated against a large database of historical and recent earthquakes. Though developed primarily to assess the selection of GMPEs in Global ShakeMap operations, we anticipate other uses for this strategy, particularly those that require automated GMPE assignments, such as real-time processing systems or analyses involving large quantities of events (namely PSHA).

Comparison of the NGA Models to the Turkish Strong Ground Motion Database: A Preliminary Study

GULERCE, Z., Middle East Technical University, Ankara, Turkey, zyilmaz@metu.edu.tr; ABRAHAMSON, N.A., Pacific Gas and Electricity, San Francisco, CA, USA, naa3@earthlink.net

The objective of this ongoing study is to evaluate the regional differences between the worldwide based NGA ground motion models and available Turkish strong ground motion data. Turkish strong ground motion data may show a divergence from the NGA model predictions since only six earthquakes from Turkey out of a total of 173 earthquakes were included in NGA data base (Chiou et al, 2008). A strong motion data base using parameters consistent with the NGA ground motion models (Abrahamson *et al.*, 2008) is developed by including strong motion data from earthquakes occurred in Turkey with at least three recordings per earthquake. The data set consists of 333 earthquakes with magnitudes from 2.0–7.6 and includes 90 earthquakes with magnitude over 5.0. The rupture distances range from 2 to 300 km. VS30 values were estimated for each station and range from about 180 to 900 m/s. The depth to rock (Z1.0 and Z2.5) parameters are not available for any ground motion station, therefore these parameters are estimated using the available VS30 values. The depth to top of the rupture values in the selected data set goes up to 30 km, providing a broader range of depths than was available in the NGA data set. Average horizontal component ground motion is computed for response spectral values at periods of 0.0, 0.2, 0.5, 1.0, and 3.0 seconds using the GmrotI definition consistent with the NGA models (Boore et al, 2006). A random-effects regression with a constant term only is used to evaluate the systematic differences in the average level of shaking. Plots of the residuals are used to evaluate the differences in the magnitude, distance, site amplification, and depth scaling between the Turkish data set and the NGA models.

Next Generation Attenuation (NGA) East Ground Motion Database: Comparing Observations with Current ENA Attenuation Relations

CRAMER, C.H., CERI, University of Memphis, Memphis, TN, USA, ccramer@memphis.edu; KUTLIROFF, J.R., CERI, University of Memphis, Memphis, TN, USA, jkutlrff@memphis.edu; DANGKUA, D.T., CERI, University of Memphis, Memphis, TN, USA, dtdngkua@memphis.edu

The U.S. Nuclear Regulatory Commission has funded our initial effort of developing an eastern North America database of ground motions, which so far has focused on collecting data for M > 4 earthquakes in the CEUS and southeast Canada, mostly since January 1, 2000. We selected 24 events with moment magnitudes of M 4.0 and greater between 25N and 55N latitude and 65W and 100W longitude. In addition we have added data from the 2008 M5.2 Mt. Carmel, Illinois earthquake and three M4 aftershocks. More data from M<4 ENA earthquakes will be added in 2010. Initial comparisons to current ENA ground motion attenuation relations provide insights as to the future trend of ground motion prediction equations for M<6. Moderate sized earthquakes, such as the 2002 Mw5.0 Au Sable Forks, 2005 Mw4.7 (Mn 5.4) Riviere du Loup, and 2008 Mw5.2 Mt. Carmel earthquakes, suggest current ENA relations on average predict similar levels of ground motion at short periods (PGA and 0.2s Sa) and over predict long period ground motions (1.0s), particularly at distances less than 100 km. Unfortunately, there are no observations available for M>6 earthquakes in ENA, so future ENA ground motion prediction equations will remain model based for now. However, alternative magnitude determinations for the same event can vary by 0.2 magnitude units, which can affect attenuation interpretations and comparisons significantly. Issues to be addressed while developing the NGA East ground motion database include proper assigning of event magnitude, examination for radiation/source effects, and limited availability of station Vs data to help identify soil amplification.

Source Properties, Site Amplification and Crustal Attenuation in Japan from Spectral Analysis of K-and KiK-net Data

OTH, A., European Center for Geodynamics, Walferdange, Luxembourg, adrien.oth@ecgs.lu; PAROLAI, S., GFZ Potsdam, Potsdam, Germany, parolai@gfz-potsdam.de; BINDI, D., GFZ Potsdam, Potsdam, Germany, INGV Milano, Milano, Italy, bindi@gfz-potsdam.de; DI GIACOMO, D., GFZ Potsdam, Potsdam, Germany, domenico@gfz-potsdam.de

Japan is one of the regions with highest seismic activity in the world and, at the same time, one of the most densely instrumented countries. Following the highly destructive Kobe earthquake in 1995, two strong motion networks, K-net and KiK-net, have been deployed, recording earthquakes in and around Japan on a continuous basis. In addition, the KiK-net sites are equipped with borehole sensors. This wealth of accelerometic data, covering a large range of magnitudes (ranging from about 3 to 8), makes these datasets highly valuable for obtaining new insights into highly debated topics, such as the scaling of seismic sources and issues regarding site response estimation.

We analyze a dataset of about 2200 earthquakes recorded at more than 1000 K- and KiK-net stations with the generalized inversion technique (GIT) in order to separate site response, source spectra and attenuation characteristics. Data has been selected in order to provide an appropriate input to the inversion, after having quantified the influence of down going propagation in the borehole. Initial results from the GIT inversion indicate that the spectral amplitudes at frequencies larger than about 5 Hz, in contrast to general expectation, show a slower decay with distance than the lower frequencies within the first 100–150 km. A first comparison of surface and borehole recordings for the KiK-net data shows that this effect can be mainly attributed to strong amplification effects and generation of high-frequency surface waves at observation sites with high velocity contrasts at shallow depth. We then use the combined information from borehole and surface data to derive site amplification functions and seismic attenuation characteristics and investigate source scaling in Japan.

"Best Practices" for Using Macroseismic Intensity and Ground Motion to Intensity Conversion Equations for Hazard and Loss Models

CUA, G.B., Swiss Seismological Service, ETH, Zurich, Switzerland, georgia.cua@sed.ethz.ch; WALD, D.J., United States Geological Survey, Golden, Colorado, wald@usgs.gov; MARANO, K., United States Geological Survey, Golden, Colorado, kmarano@usgs.gov; ALLEN, T., Geoscience Australia, Canberra, Australia, Trevor.Allen@ga.gov.au; GARCIA, D., United States Geological Survey, Golden, Colorado, danielgarcia@usgs.gov; GERSTENBERGER, M.C., GNS Science, Lower Hutt, New Zealand, m.gerstenberger@gns.cri.nz; WORDEN, C.B., United States Geological Survey, Golden, Colorado, cbworden@usgs.gov

Macroseismic shaking intensity is a necessary input parameter for empirical and semi-empirical loss models. Macroseismic data quantifies shaking and damage from past events and is thus crucial for calibrating seismic hazard models. In addition, they are often used to relate shaking hazard to incurred losses. There are two approaches to predicting shaking intensity. Direct intensity prediction equations (IPE) use a single-step approach to predict intensity as a function of predictor variables such as magnitude, distance, and site amplification. Alternatively, a two-step approach applying ground motion prediction equations (GMPEs) and ground motion to intensity conversion equations (GMICE) is often used. A GMICE is necessary if Next Generation Attenuation-type (NGA) GMPEs are to be used in intensity-based loss models. Our goal is to determine, on a global scale, how to best predict shaking intensity, taking into account tectonic regime, earthquake magnitude, and default GMPEs for a given region. To this end, we compared the performance of the IPE and GMPE-GMICE approaches in predicting the observed intensities in the ShakeMap Atlas dataset, which contains intensity and ground motion observations from significant global earthquakes since 1973. We also derived a new global GMICE for shallow crustal regimes based on a joint ground motion-intensity dataset using datasets from various regions. Preliminary results indicate that what have been previously interpreted as regional variations in GMICE may in fact be a sampling effect, since region-specific datasets are typically based on low to moderate intensity observations, and that a joint dataset combining data from various regions is necessary to characterize GMICE behavior over the intensity range of interest. Results from this study will be incorporated into the Global Earthquake Model (GEM) and global ShakeMap efforts.

Felt Intensity vs. Instrumental Ground Motion: Why a Difference Between California and Eastern North America at Some Periods?

DANGKUA, D.T., CERI - University of Memphis, Memphis/TN/US, dtdngkua@memphis.edu; CRAMER, C.H., CERI - University of Memphis, Memphis/TN/US, ccramer@memphis.edu

Dangkua and Cramer (2009) examined the differing conclusion between Kaka and Atkinson (2004) and Atkinson and Kaka (2007) concerning whether one empirical relationship is applicable to both eastern North America (ENA) and California. Dangkua and Cramer found that the blast recorder data of Street *et al.* (2005) was different from the rest of the CUS data and biased the comparisons. They also found strong differences at longer periods. In this paper we add intensity vs. ground motion data from the 2008 M5.2 Mt. Carmel, IL earthquake to the CUS data of Atkinson and Kaka (2007), which consists of datasets for both the CUS and California. We also add the data from 2005 M5.0 Riviere du Loup earthquake, including recently released strong motion data, to the Canadian data of Kaka and Atkinson (2004). For each dataset the median of ground motion

values at each MMI level and their 95% confidence limits are calculated for peak ground velocity (PGV), peak ground acceleration (PGA) and spectral acceleration (Sa) at 0.3 s, 1.0 s and 2.0 s. PGA has the smallest difference among these data sets and 2.0 s Sa has the largest. The California median value is relatively higher than the CUS and Canada for PGV and 1.0 s and 2.0 s Sa. Based on the median values and its uncertainty, we combine all datasets for PGA in order to determine a predictive relationship between intensity vs. ground motion. The CUS and Canada are combined together for PGV, 1.0 s Sa and 2.0 s Sa, while the CUS is separated from Canada and California for 0.3 s Sa. Eastern North America has a different spectral shape than California, particularly at intermediate periods (~1.0 s) where ENA spectral amplitudes are reduced (Atkinson, 1993), which can explain the longer period difference we see. Finally, log-linear fit of MMI to the median values of ground motion is use to determine predictive relationships.

VS30 and Kappa from Accelerometric Data Analysis

DROUET, S., LGIT, Grenoble/France, st_drouet@yahoo.fr; COTTON, F., LGIT, Grenoble/France, fabrice.cotton@obs.ujf-grenoble.fr; GUÉGUEN, P., LGIT, Grenoble/France, pgueg@obs.ujf-grenoble.fr; CNRS, LCPC, UJF.

We investigate recordings from weak to moderate earthquakes, magnitudes ranging between about 3 and 5, recorded by the French Accelerometric Network. S-waves spectra are modeled as a product of source, propagation and site terms. An inversion procedure of large data sets of multiple earthquakes recorded at multiple stations allows us to separate the three contributions. Source parameters such as moment magnitude, corner frequency and stress drop are estimated for each earthquake. Moment magnitudes (M_w) are linearly correlated with local magnitudes (M_L) in the 3–5 magnitude range but when magnitude increases M_w becomes lower than M_L. Stress drops are found to be regionally dependent as well as magnitude dependent, and range from about 1 bar to several hundreds of bars. The attenuation parameters show that, at the scale of the national French territory, variations of attenuation do exist. Site transfer functions are also computed giving the level of amplification at different frequencies with respect to the response of a generic rock site characterized by an average 30 meters S-wave velocity (v_{s30}) of 2000 m/s. From these site terms, we compute the high-frequency fall-off parameter K modeled as $\exp(-\pi Kf)$ (with f the frequency) for all the stations. We also determine the v_{s30} for the rock stations by comparison of the site transfer functions with the ratios between the responses of generic rock sites with different v_{s30} values. We finally show the K-v_{s30} relationship for 21 rock stations compared with data coming from other regions.

Ground-Motion at Reference Rock Sites and the Reduction of Uncertainty Related to Site Conditions

EDWARDS, B., Swiss Seismological Service, Zurich, Switzerland., edwards@sed.ethz.ch; POGGI, V., Swiss Seismological Service, Zurich, Switzerland., poggi@sed.ethz.ch; FAEH, D., Swiss Seismological Service, Zurich, Switzerland., faeh@sed.ethz.ch

A critical aspect of the formulation of predictive ground-motion equations (GMPEs), whether empirical or stochastic, is the parameterisation of site amplification and the definition of a reference rock condition. Propagation of seismic energy through the uppermost crust is known to significantly amplify ground-motion at the surface. Often the parameterisation of this phenomenon is achieved through the correlation of simple site characterisation parameters such as NEHRP class, or Vs30, to amplification. However, for a particular site class or Vs30, observed site amplification can vary significantly. We present a combined empirical-theoretical approach to define both a reference velocity profile and site-specific amplification for use with GMPEs based on the quarter-wavelength approximation. The method physically relates average quarter-wavelength velocity classes to frequency-dependent amplification, such that the reference bedrock velocity profile can be directly defined in relation to expected amplification characteristics. We compare 20 quarter-wavelength velocity profiles from seismic station locations in Switzerland with amplification functions obtained from spectral modelling. In an application of the method, the resultant reference amplification is removed from a large Swiss weak-motion dataset. A combined grid-search and direct minimisation approach are then used to define stress-drop and attenuation characteristics including a depth dependent Q model and consideration of amplification due to Moho reflections. The resulting model facilitates the simulation of ground-motion using the stochastic method. We compare pseudo response spectral acceleration (PSA) from the Swiss foreland region with our rock-reference model. It is shown that the use of site specific amplification functions based on the derived reference condition significantly reduces the uncertainty of predictions when compared to pseudo response spectral acceleration, PGA and PGV.

Advances in Seismic Hazard Mapping

Oral Session · Wednesday 2:15 PM, 21 April · Salon A

Session Chairs: Keith L. Knudsen and Laurie G. Baise

May Subsidence Rate Serve as Proxy for Site Effects?

MICHEL, S., LGIT, Grenoble,France, michels@obs.ujf-grenoble.fr; CORNOU, C., LGIT, Grenoble,France, cecile.cornou@obs.ujf-grenoble.fr; PATHIER, E., LGIT, Grenoble, France, erwan.pathier@obs.ujf-grenoble.fr; MENARD, G., EDYTEM, Chambery,France, gilles.menard@univ-savoie.fr; COLLOMBET, M., Geolithe, Grenoble, France, marielle.collombet@yahoo.fr; KNIESS, U., LGIT, Grenoble, France, ulrich.kniess@obs.ujf-grenoble.fr; BARD, P.-Y., LGIT, Grenoble, France, bard@obs.ujf-grenoble.fr; FRUNEAU, B., Laboratoire G2I, Marne-la-Vallee, France.

There is a growing interest to incorporate site effects in seismic hazard estimates (*e.g.* shaking maps, earthquake scenario, insurance models). The current practice is to use for site classification the average shear-wave velocity in the upper 30 meters (Vs30). Since site conditions are usually not known with the appropriate spatial coverage, a growing attention is paid to proxies. Recently, Wald and Allen (2007) proposed to use as a proxy for Vs30 the surface topography: a large slope is related to rock or stiff soil, while a small slope testify of soft soils. Cadet *et al.* (2008) proposed the use of resonance frequencies with or without information on the shallow shear-wave velocity as an alternative for site classification. Recent studies have shown the ability of INSAR Permanent Scatterer approach to densely map present-day ground motion in urban area with a millimetric precision for relative average annual displacement rate. Except anthropogenic causes (pumping, underground infrastructure), the long-term subsidence is caused by compaction of sediments due to increasing overburden. Since both resonance periods and subsidence rate increase with thickness and softness of soil, both data should be correlated. We test this simple idea on Grenoble city which is located in a valley filled with thick late quaternary deposits and for which all necessary data are available: SAR images, resonance frequencies, bedrock depth, shear-wave velocities, geotechnical and geological drillings, levelling data. Results show that subsidence rates (d), ranging from 0 to −6 mm/year, are linearly correlated with the resonance periods (T) through the following regression law: $d\ (mm/an) = -0.36\ T\ (s) - 1$. The linear correlation between subsidence rate and bedrock depth together with analysis of geotechnical drillings indicate that subsidence is mostly caused by compaction of the entire sedimentary column.

Applying Satellite Remote Sensing to Document Liquefaction Failures

OOMMEN, T., Tufts University, Medford, MA 02155, USA., thomas.oommen@tufts.edu; BAISE, L.G., Tufts University, Medford, MA 02155, USA., laurie.baise@tufts.edu; GENS, R., University of Alaska Fairbanks, Fairbanks, AK 99775, USA., rgens@alaska.edu; PRAKASH, A., University of Alaska Fairbanks, Fairbanks, AK 99775, USA., anupmaprakash@gmail.com; GUPTA, R.P., Indian Institute of Technology, Roorkee, UA-247667, India., rp.rpgesfes@gmail.com

Historically, earthquake induced liquefaction is known to have caused extensive structural and lifeline damage around the world. Documenting these instances of liquefaction is extremely important to help earthquake professionals to better evaluate design procedures, and enhance their understanding of liquefaction processes. Currently, after an earthquake event, field-based mapping of liquefaction remains sporadic due to inaccessibility, and difficulties in identifying and mapping large aerial extents. Researchers have used change detection using remotely sensed pre- and post-event satellite images to assist field reconnaissance. However, general change detection is only a first step in developing effective field reconnaissance strategies for liquefaction due to the inherent assumption that all the change observed results from liquefaction.

We hypothesize that as liquefaction occurs in saturated granular soils due to an increase in pore pressure, the liquefaction related terrain changes should have an associated increase in soil moisture with respect to the surrounding non-liquefied regions. Mapping the increase in soil moisture using pre- and post-event images that are sensitive to soil moisture is suitable for identifying areas that have undergone liquefaction. However, often only coarse resolution pre- and post-event images are available after an earthquake event making detailed mapping difficult. Therefore, synergistic use of multisensor and multispectral remote sensing images will improve post-liquefaction reconnaissance mapping. We verify this by using supervised change detection on fine resolution post-event images with Support Vector Machine (SVM) using training instance derived from coarser image. The results indicate that satellite remote sensing can be an integral part in strategizing post-earthquake response and reconnaissance as well as for regionally documenting liquefaction failures.

Observations of Pore Pressure Increase in Liquefiable Layers during Strong Shaking at NEES Field Sites

SEALE, S.H., Institute for Crustal Studies, UCSB Santa Barbara, CA 93106, sandy@crustal.ucsb.edu; STEIDL, J.H., Institute for Crustal Studies, UCSB Santa Barbara, CA 93106, steidl@crustal.ucsb.edu

The Wildlife Liquefaction Array (WLA) and the Garner Valley Downhole Array (GVDA) have been recording ground motions and pore pressure from earthquakes for more than a decade. Both sites have liquefaction potential, with silty clay layers at the surface over layers of saturated silty sand. The sites have accelerometers located at the surface and in boreholes at various depths within and below the liquefiable layers. Multiple pressure transducers are also located within the soft near-surface layers. The two sites are producing a large data set that includes records from earthquakes in the magnitude 4 to 7 range, with peak accelerations of ~10%g, where nonlinear response becomes important. At these acceleration levels, we see pore pressure start to build up in the saturated layers at both WLA and GVDA. We observe a sudden increase in pore pressure associated with the first arrival of the S-wave, followed by a slow decay back to the pre-event level. The pore pressure increase in most cases is largest at the top of the saturated layers. Four events from the Obsidian Buttes swarm of August 2005 produced this effect at WLA. Five events since 1999 have caused the jump in pore pressure at GVDA. The 30 December 2009 M5.8 event in Baja California, Mexico, also produced increased pore pressure at the WLA site. These data are very interesting because they show the increase in pore pressure in a liquefiable layer and represent the onset of nonlinear material behavior. Using the accelerometer data, we will show analysis of the correlation between the pore pressure response and the incident ground motion excitation. In particular the particle motions and stress-strain regime responsible for generating the excess pore pressure. This analysis is helping to improve our understanding of the physical process that drives liquefaction and nonlinear soil response.

St. Louis Area Earthquake Hazards Mapping Project (SLAEHMP): Hazard Model and Methodology Update

CRAMER, C.H., CERI, University of Memphis, Memphis, TN, USA, ccramer@memphis.edu

SLAEHMP is a multi-year, multi-contributor project to develop seismic hazard maps for the greater St. Louis area that include the effects of local geology. In preparation for generating seismic hazard maps for SLAEHMP and with funding from U.S. Geological Survey, the seismic hazard model has been updated to the 2008 national seismic hazard model and a more efficient hazard calculation methodology has been implemented and applied to generating less detailed St. Louis regional probabilistic seismic hazard maps. Currently, hazard calculations with the effects of site geology are made by calculating both the hazard and the site amplification distribution every time a change is made in the soil model. I have implemented a methodology (Lee, 2000) whereby the hard-rock hazard curves and site amplification distributions are calculated separately and combined probabilistically at the end. Both the new and old methodologies differ from the engineering practice of applying NEHRP soil factors to firm-rock ground motion estimates by being completely probabilistic and site-geology specific. Thus, with the new approach, hazard curves need to be calculated only once, as a standard hazard model is used. Changes and updates in site amplification distributions can then be made and applied to the existing hard-rock hazard curves, which offers a factor of 5 or more in computational savings. A more regional hazard assessment of the St. Louis area has been performed using regional reference profiles from the project (Karadeniz, 2007) and soil thickness values from Soller and Packard, 1998. This will facilitate an improved general understanding of seismic hazard in the region in the short-term, and provide a quantitative means of documenting the improvements provided by urban hazard maps over the regional maps in the long-term.

A Terrain-based Vs30 Estimation Map of the Contiguous United States

YONG, A., U.S. Geological Survey, Pasadena, CA - U.S.A., yong@usgs.gov; HOUGH, S.E., U.S. Geological Survey, Pasadena, CA - U.S.A., hough@usgs.gov; BRAVERMAN, A., JPL-Caltech, Pasadena, CA - U.S.A., amy.braverman@jpl.nasa.gov; IWAHASHI, J., GSI - Japan, Tsukuba-shi Ibaraki, Japan, iwahashi@gsi.go.jp

As an extension of recent efforts to develop a site characterization map for California based on multiple parameters, such as topographic, geologic and geotechnical data, we are developing a Vs30 map for the contiguous U.S. Like the California map, the U.S. Vs30 map is derived using an automated classification method (Iwahashi and Pike, 2007) that relies on taxonomic criteria (slope gradient, local convexity and surface texture) developed from geomorphometry to identify 16 terrain types from a 1-km spatial resolution (SRTM30) digital elevation model. In developing the predictive site characterization map of California, Yong *et al.* (2009) apply statistically rigorous methods to infer the correlation of observed Vs30 values with terrain units. To evaluate the utility of this approach, Yong *et al.* (2009) compare these correlations with those from recently developed models based on geologic mapping (Wills *et al.*, 2000) and topographic slope (Wald and Allen, 2008). The terrain-based site characterization map is found to yield the best correlation with available Vs30 estimates, with a typical standard deviation of 128 m/s, compared to 142 m/s and 192 m/s for the topography-based and geology-based models, respectively. We further compare the terrain-based Vs30 estimates to 1-Hz amplification factors estimated from a joint inversion of Southern California Seismic Network data, and find a statistically significant association. On the basis of these results, we develop our U.S. map by applying the same terrain classification approach and adopting the same Vs30 values determined for each terrain type in California. Although our database of Vs30 estimates outside of California is currently too sparse to permit a rigorous validation of the terrain-based site characterization model, we anticipate that a newly initiated effort to perform shear-wave velocity measurements at Advanced National Seismic System station sites will aid in the evaluation of our approach in the near future.

Exploring the Proximity of Ground-Motion Models Using High-Dimensional Visualization Techniques

SCHERBAUM, F., University of Potsdam, Potsdam/Germany, fs@geo.uni-potsdam.de; KUEHN, N., University of Potsdam, Potsdam/Germany, Nicolas.Kuehn@geo.uni-potsdam.de; OHRNBERGER, M., University of Potsdam, Potsdam/Germany, Matthias.Ohrnberger@geo.uni-potsdam.de; KOEHLER, A., University of Oslo, Oslo/Norway, andreas.kohler@geo.uio.no

Logic trees have become a popular tool to capture epistemic uncertainties in seismic hazard analysis. They are commonly used by assigning weights to models on a purely descriptive basis (nominal scale). This invites creating unintended inconsistencies regarding the weights on the corresponding hazard curves. On the other hand, for human experts it is difficult to confidently express degrees-of-beliefs in particular numerical values. Here we demonstrate for ground-motion models how the model and the value-based perspectives can be partially reconciled by using high-dimensional information-visualization techniques. For this purpose we use Sammon's mapping and self-organizing mapping to project ground-motion models onto a two-dimensional map (an ordered metric set). Here they can be evaluated jointly according to their proximity in predicting similar ground motions, potentially making the assignment of logic tree weights consistent with their ground motion characteristics without having to abandon the model based perspective.

A Comprehensive Model to Include the Effects of Near-Fault Ground Motions in Probabilistic Seismic Hazard Analysis

BAKER, J.W., Stanford University, Stanford/CA/USA; SHAHI, S.K., Stanford University, Stanford/CA/USA.

Pulse-like near-fault ground motions resulting from directivity effects are a special class of ground motions that are particularly challenging to characterize for seismic performance assessment. These motions contain a 'pulse' in the velocity time history of the motion, typically in the direction perpendicular to the fault rupture, and generally occur at locations near the fault where the earthquake rupture has propagated towards the site. It has been observed that these motions have, on average, larger elastic spectral acceleration values at moderate to long periods. To account for this effect in probabilistic seismic hazard analysis (PSHA), we have developed several data-constrained predictive models for the occurrence and impact of velocity pulses in the near fault environment. The models are used to perform an example PSHA for a near-fault site with and without accounting for directivity effects, to examine the impact of directivity. The results will be of use in identifying potential amplification of design spectra due to directivity, and will aid in selection of appropriate ground motions for dynamic structural analysis. The results are also compared to results from the widely used model of Somerville et al (1997), and the distinctions and advantages of the approach proposed here are described.

Assessing the Seismic Hazard of Lake Maracaibo, Northwestern Venezuela

WONG, I., URS Corporation, Oakland, CA USA, ivan_wong@urscorp.com; ZACHARIASEN, J., URS Corporation, Oakland, CA USA; DOBER, M., URS Corporation, Oakland, CA USA.

Venezuela is located in a seismically active, tectonically complex region containing three major strike-slip faults and the South Caribbean Deformed Belt (SCDB). Since 1610, 21 earthquakes of approximately **M** 6 (or MM intensity VIII) and larger have been documented in western Venezuela and northern Columbia. The sources of seismicity in Venezuela are mainly shallow crustal faults. The 1894 "Great Venezuela" moment magnitude (**M**) 8.2 earthquake, which occurred along the Bocono fault southeast of Lake Maracaibo, is one of the largest crustal earthquakes observed worldwide. The SCDB is not fully understood, but may be the source of megathrust and the Wadati-Benioff zone earthquakes.

In a probabilistic seismic hazard analysis (PSHA) of a site north of Lake Maracaibo, we considered 16 active faults within about 200 km of the site. Little

previous detailed work has been conducted to assess the paleoseismic history or earthquake potential of most of these faults. We used a recent Quaternary fault database for Venezuela compiled by Audemard *et al.* (2000).

The 650-km-long Oca-Ancon fault system is the closest fault to the site, about 7 km away. It has well-developed late Quaternary and Holocene geomorphic expression, but its slip rate is poorly constrained. We used a preferred slip rate of 2 mm/yr, ranging to 5 mm/yr in the west, decreasing eastward. Maximum magnitude estimates range from **M** 6.7 to 7.8.

Few strong motion records exist in Venezuela; we used the Next Generation Attenuation (NGA) relationships for the crustal seismic sources as well as recent subduction zone attenuation models. The probabilistic PGA hazard for a soil site condition (V_S30 400 m/sec) ranged from about 0.3 to 0.5 g for a 2,475-year return period. Hazard is dominated by the Oca-Ancon fault system. These hazard levels are comparable to those along coastal California.

Probabilistic Seismic Hazard Assessment for Central Manila, Philippines

MOTE, T.I., Arup, Sydney, NSW, Australia, tim.mote@arup.com; KOO, R., Arup, Hong Kong, raymond.koo@arup.com; MANLAPIG, R.V., Arup, Manila, Philippines; ZAMORA, C., Arup, Manila, Philippines.

A probabilistic seismic hazard assessment (PSHA) has been carried out for central Manila in the Philippines.

Manila is located in an area of high seismicity related to an active tectonic setting characterized by two converging subduction zones and related transform faulting. On the average, Manila has been shaken by a damaging earthquake approximately every 15 years over the last 300 years.

A source model was developed from an interpretation of the geologic/tectonic setting and earthquake catalog within 500km surrounding central Manila. The diverse tectonic setting is reflected in the complexity of the PSHA model, which includes crustal fault sources, subduction zone intraslab and interface sources and areal source zones.

The dominant seismic source contributing to the hazard within the study is the Marikina Valley Fault System, a major strike slip fault system running through metropolitan Manila with Holocene activity. Other active seismic sources affecting the study area include the Manila Trench plate interface to the west, the East Luzon Trough plate interface to the northeast, and the Philippine Fault Zone to the east. Lesser seismogenic structures modelled include the Lubang Fault and Mindoro-Aglubang Fault.

Ground motions were computed across the study area using the recently developed Next Generation Attenuation Relationships for shallow crustal earthquakes and appropriate subduction zones attenuation relationships. The calculated bedrock horizontal peak ground acceleration (PGA) and response spectra for 50%, 10% and 2% chance of being exceeded in the next 50 years (equivalent to 72, 475 and 2,475 years return period) is modelled across the study area and contour maps of ground motions are developed to support engineering design.

Comparison of Seismicity of the Dead Sea Fault and San Andreas Faults

KUTLIROFF, J.K., CERI - University of memphis, Memphis, TN, USA, jkutlrff@memphis.edu

Earthquake forecasts for the segments of the San Andreas Fault (SAF) can be transferred to segments of the Dead Sea Fault (DSF) that show similar seismicity, increasing the accuracy of earthquake forecasts for the DSF. Both show a comparable correlation between fault offset and rate of earthquakes (Begin and Steinitz, 2005) as well as variations in seismicity for regions over each fault (Wesnousky, 1990; Hamiel *et al.*, 2009). Each transform has a bend which has been the site of at least one large earthquake in historical time. The faults differ most distinctively in their relative motion. The right lateral strike slip SAF has a relative motion between the two sides of 48 mm/yr compared with the 4 mm/yr relative motion of the left lateral strike slip DSF. The 500 km of the southern section of the SAF and its associated fault system generates earthquakes of magnitude ≥ 6.5 at an average rate of one every 3.3 years, compared with a damaging earthquake averaging every 80 years generated on the DSF. The larger number of earthquakes on the SAF, allows for more accurate earthquake forecasts on the SAF than is possible on the DSF. Establishing a relation between seismicity of regions on the SAF and the earthquake forecast and transferring it to regions of relative similar seismicity of the DSF and adjusting for scaling due to the different rates of motion, permits an earthquake forecast for the DSF with the accuracy of that on the SAF.

Non-Ergodic PSHA—Example

WALLING, M.A., U.S.G.S., Golden/CO/USA, mwalling@usgs.gov; ABRAHAMSON, N.A., P.G.E, San Francsico/CA/USA, naa2@pge.com

A method is developed for probabilistic seismic hazard analysis (PSHA) without the ergodic assumption accounting for the impacts on both the median and aleatory standard deviation of the ground-motion model. Impacts of the removal of the ergodic assumption on both the intra-event and inter-event residuals are addressed. A strong motion data set from Taiwan with multiple recordings at each site and multiple earthquakes within small regions is used to quantify the separation of the aleatory variability from the systematic source, path, and site effects. Systematic site effects are accommodated by scale factors at each site. Systematic source and path effects are more complicated because they are spa- tially correlated. Models of the spatial covariance functions of the systematic source and path effects of the Taiwan data set are developed to capture the spatial correlation of the systematic effects and are then used to generate stochastic spatial simulations of the spatial correlations of the path and source effects for applications to other regions. Example hazard calculations show that there can be up to a factor of four increase in epistemic uncertainty of the hazard when the ergodic assumption is removed if there is no site-specific data. The method developed here to remove the ergodic assumption provides a framework that shows the benefits of installing instrumentation to record site-specific data and using analytical models of the path-specific wave propagation and site-specific site response effects to estimate source-, path-, and site-specific ground motions models to reduce the epistemic uncertainty in the systematic effects.

Testing the Plausibility of Anthropogenic versus Seismogenic Causes of the Rotation of a Lycien Sarcophagus in Pınara, SW-Turkey

HINZEN, K.-G., Cologne University, Cologne, Germany, hinzen@uni-koeln.de; SCHREIBER, S., Cologne University, Cologne, Germany, stephan.schreiber@uni-koeln.de; YERLI, B., Ruhr-University Bochum, Bochum, Germany, baris.yerli@rub.de

A Lycien sarcophagus located in the ancient city of Pınara, southwest Turkey, shows a clockwise rotation of 5.37° with respect to its North-South oriented foundation. Considering the seismotectonic potential of the area, this rotation has been attributed to earthquake ground motion before. We present a 3D model of the sarcophagus constructed out of 10 million points from a 3D laser scan. This sarcophagus shows a crater in the eastern side of the coffin, which was most probably caused by the detonation of an explosive charge during looting. As the direction of the rotation agrees with the sense expected from the blast, the question arises whether the rotation has a natural or an anthropogenic cause. With a rigid block model we studied the feasibility of two alternative sources as the cause for the rotation of the coffin: an explosion and earthquake ground motion. Scaled recorded ground motions from local earthquakes and a strong motion record from the recent L'Aquila, Italy, earthquake were used to study the sarcophagus dynamic reactions. The geometry of the structure requires large ground motion amplitudes to initiate rocking. Rocking is necessary to produce rotation around the vertical axis by translational movements. The size of the explosion is back calculated from the crater size and compared to the duration and amplitude of an impulse necessary to rotate the coffin. The minimal rotations which result from all earthquake simulations and the plausible explosion charge necessary to rotate the coffin by the observed amount suggest that looting was the probable cause of the misalignment of coffin and base.

Monitoring for Nuclear Explosions

Oral Session · Wednesday 2:15 PM, 21 April · Salon E

Session Chairs: Bill Walter, Ola Dahlman, Paul G. Richards, and Ray Willemann

Operation of the International Monitoring System Network

ARAUJO, F., CTBTO, Vienna, Austria, fernando.araujo@ctbto.org; CASTILLO, J.E., CTBTO, Vienna, Austria, jorge.enrique.castillo@ctbto.org; NIKOLOVA, S., CTBTO, Vienna, Austria, Svetlana.NIKOLOVA@ctbto.org; The Operations Section of the IDC: E. Abaya, K. Aktas, T. Assef, T. Daly, W. Drexler, D. Giordanino, J. Guerrero, D.Han, M. Johnson, A. Klafas, B. Kiema, M. Malakhova, G. Mponela, R. Otsuka, M. Singute, H. Stangel, A. Tait, C. Taylor.

The IMS is a globally distributed network of monitoring facilities using sensors from four technologies. It is designed to detect the seismic and acoustic waves produced by nuclear test explosions and the subsequently released radioactive isotopes. Monitoring stations transmit their data to the IDC in Vienna, Austria, over a global private network known as the Global Communications Infrastructure (GCI).

In order to satisfy the strict data and network availability requirements of the IMS Network, the operation of the facilities and the GCI are managed by IDC Operations. IDC Operations has three functions: the first is to ensure proper operation of the stations, the second to ensure proper operation of the GCI, and the third, handled by the IDC Operations Centre is to provide network oversight and incident management.

At the core of the IDC Operations Centre are a series of tools for: monitoring the IMS network, troubleshooting incidents, communicating with internal and

external stakeholders, and reporting. As the operational requirements of the IMS network continue to expand, including potential entry-into-force of the Treaty, the tools and procedures of the IDC Operations Centre will need to evolve. An overview of the tools currently in use at the IDC Operations Centre as well as those under development will be presented. This will include an outline of the IDC's strategy for operations and its dependence on entities both inside and outside the CTBTO.

Innovative Statistical Data Processing Methods for Automatic Classification of Waveform Data at the CTBTO

LE BRAS, R.J., CTBTO, Vienna, Austria, ronan.lebras@ctbto.org; VAIDYA, S., Lawrence Livermore National Labs, Livermore, CA, USA, vaidya1@llnl.gov; ARORA, N., UC Berkeley, Berkeley, CA, USA, nimar@cs.berkeley.edu; RUSSELL, S., UC Berkeley, Berkeley, CA, USA, russell@cs.berkeley.edu

The facilities making up the Comprehensive Nuclear-Test-Ban Treaty's (CTBT) International Monitoring System (IMS) collect approximately 10 gigabytes of seismic, hydroacoustic, infrasound data daily. The IDC automatic processing system sifts through the data and publishes a series of Standard Event Lists (SELs). The events in the final list, SEL3, are carefully examined by a team of highly trained professional analysts before they are published in a Reviewed Event Bulletin (REB). In the process of putting together the REB, analysts discard roughly half of the SEL3 events and make many more corrections, including the addition of events missed by the automatic system. We tapped the potential of the fast evolving statistical machine learning techniques to assess their application for improving automatic event classification. The 2009 International Scientific Studies (ISS) meetings, organized by the CTBTO, first demonstrated the use of automatic algorithms to find patterns in the SELs in order to better classify events as "true" (*i.e.* the event will be retained by the analyst and finally reported) or "false" (the event will be discarded). It was shown that event detection accuracy could be improved from 62% to 85%, lowering the false event rate from 38% to 15%. Another type of study investigates potential improvements in the identification of seismic and acoustic phases based on extracted waveform features and previous statistical patterns is also showing promise. A third category of studies investigated the use of vertically integrated methods involving feedback mechanism to use posterior information to refine the previous steps of processing and shows a promising 6% gain in obtaining true events. We present the most current results of these investigation efforts which promise to improve on the automatic results and free analyst time for higher value-added tasks.

Geological and Geophysical Applications of On Site Inspection for CTBT Verification

SWEENEY, J.J., Lawrence Livermore National Lab, Livermore/CA/USA, sweeney3@llnl.gov; HAWKINS, W.L., Los Alamos National Laboratory, Los Alamos/NM/USA, whawkins@lanl.gov

Most of the presentations in this session deal with monitoring for detection of underground nuclear explosions with an obvious emphasis on seismic methods. On-site inspections are another important aspect of verification of the Comprehensive Nuclear Test Ban Treaty (CTBT) that relies heavily on geologic and geophysical investigations. The objective is to apply methods that are effective while at the same time minimally intrusive. We present a general overview of the on-site inspection (OSI) provisions of the CTBT, specifying the allowed techniques and the timeline for their application. In addition to radiological measurements and aerial and ground-based visual observational methods, CTBT OSI relies on many geophysical methods, including ground and airborne magnetic surveys, multispectral imaging, ground penetrating radar, electrical conductivity methods, and passive and active seismic methods. The search area for an OSI is mostly defined by uncertainty in the location of a suspect event detected by the International Monitoring System (IMS) and can be as large as 1000 km^2. Thus OSI methods are fundamentally divided into general survey methods to narrow the search area and more concentrated survey methods to look for evidence of an underground explosion and try to pinpoint its location within an area of several km^2. We will focus on the particular challenges of the application of active and passive seismic methods for the later, narrowed search where the emphasis is on detection and characterization of the explosion damage zone. *Prepared under LLNL contract DE-AC52-07NA27344.*

Comparisons of Regional Source Properties of the North Korean Nuclear Explosions and Their Implications

HONG, T.K., Yonsei University, Seoul, South Korea.

Seismic analyses based on regional waveforms receive increasing attention for discrimination and investigation of moderate-size underground nuclear explosions (UNEs). North Korea conducted two UNE tests in 9 October 2006 and 25 May 2009. The Noth Korean UNEs were well observed by dense regional seismic networks in Korea, China and Japan. The epicentral locations of the UNEs are very close, which allows us to investigate the source properties of the North Korea UNEs by comparing the source parameters of the two UNEs. The source parameters of the UNEs are investigated using source-spectral inversions of regional phases. The corner frequencies and overshoot parameters are determined. The apparent moments of high-frequency regional phases of the 2009 UNE are estimated to be about 5 times greater than those of the 2006 UNE. The North Korean UNEs are well discriminated from natural earthquakes using P/S spectral ratios. The S waves from the North Korean UNEs show weaker overshooting feature in the spectra than the P waves. The shear-wave features are compared with those from UNEs of other test sites. We discuss about the shear-wave excitation mechanisms from the observations.

Seismic Simulations of Recent DPRK Nuclear Explosions Including the Effects of Free Surface Topography and 3D Structure

RODGERS, A.J., LLNL, Livermore, CA, USA, rodgers7@llnl.gov; PETERSSON, N.A., LLNL, Livermore, CA, USA, andersp@llnl.gov; SJOGREEN, B., LLNL, Livermore, CA, USA, sjogreen2@llnl.gov

We report results of numerical simulations of ground motions from the recent nuclear explosions in the Democratic People's Republic of Korea (DPRK) including the effects of free surface topography and three-dimensional (3D) volumetric structure. Motions from shallow explosions are strongly impacted by topography, especially when the wavelengths are comparable to the scale of topographic features. We show that the very rugged terrain in the vicinity of the DPRK test area strongly impacts the emerging wavefield using high-resolution (8 Hz) elastic finite difference simulations including topography. Specifically, we show that strong S-waves are generated when the direct P-wave is normally incident on steep slopes. We also investigated the effect of topographic roughness on ground motions and found that when the scale of topography includes features as short as 2–5 km there can be dramatic effects on the response across the body-wave discrimination frequency band 0.5–8.0 Hz. Topographic scattering tends to increase amplitudes of S-waves in the near-source region, suggesting that high-frequency P/S discriminants for explosions may be biased towards the earthquake populations. However, we do not yet know how these S-waves propagate to long-range. Further work will seek to understand the propagation mode of energy emerging from the source region with topographic scattering. In order to understand observed long-period regional waveforms we performed larger scale simulations at lower resolution using both finite difference and spectral element method simulations including free surface topography and 3D crustal and uppermost mantle structure. The observed regional long-period waveforms at several stations clearly show an apparent Love that is generated near the source. Simulations are being performed to investigate the excitation of this wave, whether due to source or propagation effects and to understand how unmodeled propagation effects may bias source estimates.

An Analysis of Seismic Characteristics of the 25 May 2009 North Korean Underground Nuclear Test

MURPHY, J.R., SAIC, McLean, VA, John.R.Murphy@saic.com; KOHL, B.C., SAIC, Louisville, CO, Benjamin.C.Kohl@saic.com; BENNETT, T.J., SAIC, McLean, VA, Theron.J.Bennett@saic.com; ISRAELSSON, H.G., SAIC, McLean, VA, Hans.G.Israelsson@saic.com

On May 25, 2009 North Korea conducted a second underground nuclear test in the same area as their 2006 test. We have analyzed available short-period seismic data to define accurate locations, depths and yields for these two nuclear tests. In order to determine accurate locations for the events, we made precise arrival time measurements at 35 stations that recorded both explosions with good signal to noise ratios. The location of the 2006 explosion was held fixed at the previously determined preferred location and the relative location of the 2009 explosion was estimated using a variety of relative location algorithms. All of the relative location techniques yielded similar results, indicating that the 2009 test was conducted ~2 km WNW of the 2006 test. These relative seismic locations were integrated with local topographic data and satellite imagery to define what we believe to be very reasonable and accurate locations for these two explosions. The corresponding source depths cannot be reliably determined using the available arrival time data or the observed, narrowband network-averaged teleseismic P wave spectral data. Consequently, we have implemented a new approach using broadband P wave spectral ratios of the two explosions at common regional stations to obtain estimates of the corresponding source spectral ratios. The resulting network-averaged spectral ratio was then compared with theoretical Mueller/Murphy based source spectral ratios to estimate best-fitting source depths and associated yields. The results of this analysis indicate that the two explosions could not have been detonated at any common depth in the plausible 100 to 800 m range; and, in fact, the observed spectral ratio data are best fit by source depths of about 200 m for the 2006 test and 550 m for the 2009 test. The corresponding yield estimate for the 2009 explosion is then found to be ~4.6 kt.

The Evolution of Slow Slip and Tremor in Time and Space

Oral Session · Wednesday 2:15 PM, 21 April · Salon F
Session Chairs: Evelyn Roeloffs and Joan Gomberg

Locating ETS Tremors: How? Where? Which? When? and Why?

KAO, H., Geological Survey of Canada, Sidney, BC, Canada, hkao@nrcan.gc.ca; SHAN, S.-J., Geological Survey of Canada, Sidney, BC, Canada, sshan@nrcan.gc.ca; ROSENBERGER, A., Geological Survey of Canada, Sidney, BC, Canada, arosenberger@nrcan.gc.ca; ROGERS, G.C., Geological Survey of Canada, Sidney, BC, Canada, grogers@nrcan.gc.ca; DRAGERT, H., Geological Survey of Canada, Sidney, BC, Canada, hdragert@nrcan.gc.ca; KLAUS, A.J., University of Washington, Seattle, WA, aklaus@u.washington.edu; WECH, A.G., University of Washington, Seattle, WA, wech@uw.edu; CREAGER, K.C., University of Washington, Seattle, WA, kcc@ess.washington.edu; BROWN, J.R., Stanford University, Stanford, CA, jrbrown5@stanford.edu; BEROZA, G.C., Stanford University, Stanford, CA, beroza@stanford.edu

The discovery of episodic tremor-and-slip (ETS) opens the gate to a detailed understanding of seismogenic processes in subduction zones. Recent reports of slow slips and non-volcanic tremors in places other than young subduction zones further promise that ETS may hold the key to comprehending the brittle–ductile transition in general. One of the fundamental issues in the ETS study is to determine the locations where tremors are taking place. Several methodologies have been developed over the years for such a purpose. Although the results of different methods have many features in common, some differences are apparent and demand thorough investigations. In this study, we focus on an ETS episode that occurred in mid-Vancouver Island. An improved version of the source-scanning algorithm (ISSA) incorporating an efficient ground motion analyzer to separate the P energy from S is applied to construct the tremor catalogue. To facilitate a fair and meaningful comparison, the same waveform dataset is processed by two other methods, namely the cross-correlation method using waveform envelopes and the autocorrelation method that identifies low-frequency earthquakes within tremor signals. Preliminary results suggest some similarities and differences among the tremor catalogues produced by each method. The found similarities and differences will be analyzed to better understand the strength, weakness, uncertainties, effectiveness and possible improvements of each method. Our results will also shed light on the optimal way to establish the ETS tremor catalogue.

Spectral Analysis of Tremor Using Beamforming

GERSTOFT, P., UCSD, La Jolla/CA/USA, gerstoft@ucsd.edu; ZHANG, J., UCSD, La Jolla/CA/USA, gerstoft@ucsd.edu; VIDALE, J., University of Washington, Seattle, Washington, USA, seismoguy@mac.com; GHOSH, A., University of Washington, Seattle, Washington, USA, aghosh.earth@gmail.com

We employ frequency domain beamforming to obtain spatio-temporal spectral estimates of Non-volcanic tremor. Using an array of 70 stations deployed on Big Skidder Hill, WA, where we focus on 6–15 May when the tremor activity was strongest. By shooting rays up from the plate boundary potential source locations are found as they best match the beamformer output. An advantage of such an approach is that all the information in the time series are used for giving a more detailed map of the frequency dependent source locations. The tremor was observable up to 25 Hz and the decay in power seems to best follow an exponential decay. While different frequencies can radiate simultaneously from different patches they often tend to come from the same patch.

Toward a Unified View of Tremor Distribution in Space and Time

GHOSH, A., University of Washington, Seattle WA USA, aghosh.earth@gmail.com; VIDALE, J.E., University of Washington, Seattle WA USA; SWEET, J.R., University of Washington, Seattle WA USA; CREAGER, K.C., University of Washington, Seattle WA USA; WECH, A.G., University of Washington, Seattle WA USA; HOUSTON, H., University of Washington, Seattle WA USA.

The recent discovery of slow slip and nonvolcanic tremor (NVT) challenges our understanding of fault dynamics. Episodic tremor and slip (ETS) refers to the remarkably periodic slow-slip events and associated NVT activity in Cascadia that recurs every 14.5 months or so. ETS events occur in the transition zone, and each such event transfers stress to the updip locked part of the subduction fault, making it a step closer to the big megathrust earthquake. Hence, it is important to comprehend the physical processes, and state of stress that control this phenomenon.

We captured the May 2008 ETS event in Washington, USA, with a small-aperture dense seismic array. We developed and applied a novel beam-backprojection method to detect and locate tremor. This technique reveals four times more tremor duration during weak tremor episode, and gives unprecedented resolution in relative tremor location, compared to an envelope cross-correlation method. We track tremor minute-by-minute using the beam-projection method, and map spatiotemporal tremor distribution over various time scales. Over the short time scale of several minutes, tremor shows rapid, continuous, slip-parallel migration with a velocity of ~50 km/hr. Over time scale of several hours, slip-parallel tremor bands sweep Cascadia along-strike from south to north with a velocity of ~10 km/day. Finally, over time scale of several days, tremor activity develops distinct moment patches that coincide with geodetic slip patch on the plate interface. We integrate these varied and intriguing observations over different time scales, strive to explain their relationship, explore possible physical models, and present a unified picture of tremor distribution in space and time.

Modeling the Pattern of Tremor Migration in Cascadia

GERSHENZON, N.I., Wright State University, Dayton, OH, USA, naum.gershenzon@wright.edu; BAMBAKIDIS, G., Wright State University, Dayton, OH, USA, gust.bambakidis@wright.edu; HAUSER, E.C., Wright State University, Dayton, OH, USA, ernest.hauser@wright.edu; CREAGER, K.C., University of Washington, Seattle, WA, USA, kcc@ess.washington.edu

Regular earthquakes generally propagate at speeds comparable to the shear-wave speed and scale such that the amount of slip is proportional to fault length. A second class of phenomena, collectively called slow earthquakes, have very different scaling [*e.g.* Ide et al, 2007]. We propose a model that is consistent with scaling relations observed in northern Cascadia episodic tremor and slip (ETS) events. In particular, tremor duration appears to be proportional to both seismic moment and to the square of fault length. These imply that the amount of slip, which is of order cms for the largest events, is nearly independent of seismic moment. Tremors are observed to migrate in the strike direction with a low velocity of 10 km/day and simultaneously zip back and forth in the relative plate-motion direction with high velocity (~100 km/h). The latter has only been observed during the few days that the May 2008 ETS passed directly below a temporary 84-station seismic array, but is inferred to happen elsewhere as well. Fault dynamics can be described by the Frenkel-Kontorova model [Gershenzon et al, 2009]. This model predicts the formation of inelastic waves, each wave consisting of moving dislocations, generated at the boundary between two plates. Here the term dislocation is analogous to an edge dislocation in crystal materials. The only difference is in the size of the periodic substrate. For plate surfaces it is the distance between two microasperities. The passage of one dislocation along a fault is equivalent to the relative displacement of the plates by one substrate length. If this length were a few cm it could explain the apparent independence of amount of slip on fault size. A moving dislocation radiates seismic energy, in particular tremors. The along-strike versus slip-direction migration speeds could be described in terms of dislocation movement.

Segmentation of Non-Volcanic Tremor Activity along the Cascadia Subduction Zone

FARAHBOD, A.M., Simon Fraser University, Burnaby/BC/Canada, amirf@sfu.ca; CALVERT, A.J., Simon Fraser University, Burnaby/BC/Canada, acalvert@sfu.ca

Location of non-volcanic tremors along the Cascadia subduction zone between southern Vancouver Island and Northern California during slow slip events between 2003 and 2006 reveals five independent regions of activity. This trend is in some aspects different from the large-scale pattern of areas of high and low earthquake seismicity along the margin. The greatest earthquake activity is found in southern Cascadia beneath northwestern California and in the northern Cascadia mainly in the Puget Sound region, while Oregon experiences a relatively low number of events. For tremors, high level of activity in the south extends from northern California to the California-Oregon border region and in the north from Puget Sound to Vancouver Island. Although tremor activity in central Cascadia is less than either the north or south, a considerable number of tremors can be located but the lowest number of events observed in the southern Washington and central Oregon. By measuring amplitudes at so called reference stations, *i.e.* those with the lowest noise level and highest record quality, in all five segments during the episodes of tremor activity it was clear that the largest tremor are of the same order of magnitude along the subduction zone. The origin times and hypocenters of all tremors were estimated using the Source-Scanning Algorithm. Located tremors are well confined between the 20 km and 50 km depth contours of the Cascadia subduction interface. Using the source-scanning algorithm, estimated tremor depths cover a wide range, but the majority of the well-located events occur at depths between 20 km and 40 km. Although it is difficult to recognize tremor migration patterns in the regions of low activity, migration along the strike of the subduction interface is most common.

Low Frequency Earthquakes from Tremor in Subduction Zones

BROWN, J.R., Stanford University, Stanford, CA, jrbrown5@stanford.edu; BEROZA, G.C., Stanford University, Stanford, CA, beroza@stanford.edu

Recent studies suggest that deep tremor in multiple subduction zones consists of swarms of low frequency earthquakes (LFEs) that occur as shear slip on the plate

interface. Three hours of tremor during the September 2005 slow slip event in the northern Cascadia subduction zone is composed of a LFE swarm in southern Vancouver Island between 30–45 km where modeled temperatures in the subducting oceanic crust reach 400–500 degrees C; conditions favorable for dehydration of hydrous minerals in oceanic basalt in subduction zones. Tremor in SW Japan exhibits similar behavior. The LFEs in both regions are also located in vicinity of geodetically constrained slow slip. In contrast, previous studies of tremor in other subduction zones yield different results. Unlike Cascadia or SW Japan, LFEs from tremor in Costa Rica occur where modeled temperatures of the plate interface are much cooler and spatially offset from the slow slip patch. Meanwhile, tremor in south-central Alaska has been shown to occur in a cooler subduction zone but the depth errors of tremor locations preclude a definitive relationship to the slow slip. In this study we compare multiple regions and episodes of tremor in order to understand this phenomenon on a broader level. As our previous studies have shown, we are able to employ a running autocorrelation technique to snapshots of tremor to extract LFEs- and in some cases ordinary earthquakes- for a more detailed picture of plate interface seismicity.

The Background Hum of a Plate Boundary: Developing a Detailed Catalog of Tremor Activity Along 150 Kilometers of the South-Central San Andreas Fault, 2001-Present

SHELLY, D.R., U.S. Geological Survey, Menlo Park, CA, USA, dshelly@usgs.gov

Tremor occurs frequently beneath much of the south-central San Andreas fault (SAF) and can be detected at least 75 km in either direction along the fault at seismic stations near Parkfield, CA. Tremor activity is concentrated in the lower crust, below the maximum depth of regular earthquakes, and appears to consist of a rapid-fire sequence of small earthquakes (sometimes called "low frequency earthquakes" or LFEs).

Here, I present a detailed catalog of tremor activity in this region, developed using a multi-channel matched filter with 88 waveform templates. Each template is derived from a stack of multiple similar LFEs. I detect more than 500,000 individual tremor-forming LFEs since mid-2001. Because this method relies on the shape and timing of waveforms across multiple stations, rather than amplitudes, it permits identification of tremor with amplitudes extending below the background noise level and automatically distinguishes tremor from other similar-looking sources, such as T-phases from teleseismic earthquakes and fault zone drilling noise.

Stacks of hundreds of similar events from each tremor family reveal clear P and S body waves, even on analog surface stations of the Northern California Seismic Network (NCSN). These body wave arrival times constrain tremor locations to beneath the surface expression of the SAF. While most activity is concentrated in the lower crust at ~22–26 km, tremor as shallow as 17 km occurs beneath the Parkfield segment itself, where activity is greatly elevated in the months following the 2004 earthquake. At the same time, tremor behaves similarly beneath the creeping and locked sections NW and SE, respectively, of Parkfield. The extensive event catalog derived from this study provides a wealth of possibilities for future study, including tremor migration and triggering by teleseismic waves and tides (Thomas *et al.*, this meeting).

Spatial and Temporal Evolution of Long Term Slow Slip Events in the Guerrero Gap, Mexico.

RADIGUET, M., LGIT Université J. Fourier CNRS, Grenoble, France, mathilde.radiguet@obs.ujf-grenoble.fr; COTTON, F., LGIT Université J. Fourier CNRS, Grenoble, France, fabrice.cotton@obs.ujf-grenoble.fr; VERGNOLLE, M., LGIT Université J. Fourier CNRS, Grenoble, France, mathilde.vergnolle@obs.ujf-grenoble.fr; VALETTE, B., LGIT Université J. Fourier CNRS, Chambéry, France, Bernard.Valette@univ-savoie.fr; KOSTOGLODOV, V., Instituto de Geofísica UNAM, Mexico, vladi@servidor.unam.mx; COTTE, N., LGIT Université J. Fourier CNRS, Grenoble, France, nathalie.cotte@obs.ujf-grenoble.fr; PATHIER, E., LGIT Université J. Fourier CNRS, Grenoble, France, erwan.pathier@ujf-grenoble.fr; SHAPIRO, N., Institut de Physique du globe, Paris, France, nshapiro@ipgp.jussieu.fr

Recent geodetic observations allowed to detect slow slip events (SSE) in several subduction zones worldwide. These events are characterized by an important variability (in terms of duration, migration, recurrence time), and the physical mechanisms responsible for their occurrence are still unclear.

Two of the largest recorded SSE occurred in 2002 and 2006 in the Guerrero subduction zone (Mexico). These events were recorded by 8 and 15 continuous GPS stations respectively, and gave us a good opportunity to constrain the characteristics of large SSEs. The 2006 SSE record especially allow a detailed study of the spatial and temporal evolution of slip at depth.

We inverted the cumulative GPS displacements to find the distribution of slip on the subduction interface during the 2002 and 2006 SSEs. Both events show significant slip in the bottom of the seismogenic zone and in the transition zone. The slip distribution obtained by inversion is consistent with the surface deformation observed by InSAR (data are available for the 2006 SSE).

For the 2006 SSE, we modeled the spatial and temporal evolution of slip by inverting the GPS time series. We assumed a functional form for the slip function, and we inverted for the slip amplitude, the initiation time and the duration, using a linearized least-square inversion procedure. The rupture initiated at a depth of 40 km (transition zone), in the western part of the Guerrero gap, and propagated with an average velocity of 1.2 km/day (with regional variations). The rise time (duration of slip in each cell) is about 170 days and the total duration of the event is 11–12 months.

These characteristics help us discuss the physical mechanisms responsible for SSE occurrence. We discuss the characteristics of the large Mexican SSEs, in comparison with others SSEs worldwide, and their relations with non-volcanic tremors in the Mexican subduction zone and the geometry of the subduction zone.

Documenting Transient Slip Events in Cascadia with Geodesy: Working Towards a Catalog of Slow Slip Events

SCHMIDT, D.A., University of Oregon, Eugene, OR, das@uoregon.edu; GAO, H., University of Oregon, Eugene, OR.

The geodetic network in the Pacific Northwest has recorded numerous, repeating slow slip events on the Cascadia Subduction zone over the past decade. This event sequence provides the opportunity to examine spatial and temporal patterns in rupture history and explore the segmentation of the plate interface. We have compiled a catalog of slow slip events in Cascadia that includes 17 of the largest slow slip events from 1998 to the present. Slip histories for individual events are inferred from time-dependent inversions of continuous GPS time series using the Extended Network Inversion Filter. Of the 17 best resolved events, 11 slip patches are centered in northwestern Washington, 5 slip patches are located in southwestern Washington and northwestern Oregon, and 1 slip patch is resolved in Oregon. Moment magnitudes range from 6.1 to 6.7. We compare our results to the slip histories inferred by other studies, evaluate the spatial and temporal completeness of the catalog, and establish thresholds for detecting events using GPS. The non-uniform distribution of continuous GPS stations results in variable slip resolution on the plate interface. Limited station coverage south of Portland restricts our analysis of pre-2008 events primarily to events on the northern half of the subduction zone. Using events from our catalog along with slow slip events recorded on other subduction zones, we compile statistics on source parameters, such as magnitude, propagation rate, rupture dimension, and stress drop, which can be used to constrain proposed models of the source mechanics. Scaling relationships are compared between slow slip events and traditional earthquakes. We find some scaling laws to be consistent between slow slip events and earthquakes. But other scaling relationships, such as rupture velocity versus seismic moment, appear to differ.

Comparison of Five Northern Washington Episodic Tremor and Slip Events

HOUSTON, H.B., University of Washington, Seattle, WA, heidi.houston@gmail.com; DELBRIDGE, B.G., University of Washington, Seattle, WA, brent2d@uw.edu; WECH, A.G., University of Washington, Seattle, WA, wech@uw.edu; CREAGER, K.C., University of Washington, Seattle, WA, kcc@ess.washington.edu

We examine the spatio-temporal evolution of tremor in five major ETS in Northern Washington from 2004 to 2009 with Mw 6.5 to 6.7. Tremor was located by cross correlation of 5-minute envelopes of vertical short-period seismograms from regional stations (Wech and Creager, 2008). The combined catalogs contain ~110 days of strong tremor and ~16000 tremor locations.

All five episodes share the tendency to propagate primarily northwestward and somewhat up-dip as they cross the broad arch in the subducting plate under the NE Olympic Peninsula. However, each episode also shows some development of a southward-propagating arm, a feature that was most developed in the 2004, 2005, and 2009 episodes. To assess along-strike ETS propagation velocities, we projected tremor locations onto a straight line fit to the 2007 ETS epicenters. Along-strike tremor propagation velocities achieved during the five episodes vary from 7 to 12 km/day over periods of at least 3 days. Higher velocities tend to occur in the 2007 ETS, later in an ETS, and in the southward propagating arms of ETS.

A new feature was revealed by our scrutiny of the spatio-temporal progression of tremor: back-propagating tremor—tremor bursts that zip quickly back through the region that has already tremored. They last 5 to 13 hours and tend to occupy elongate regions along strike in map view. Their propagation velocities are about 100 km/day (4 km/hr), about ten times faster than those of the slow along-strike progression of ETS (7 to 12 km/day), but much slower than the relatively rapid up- and down-dip streaks of tremor (about 50 km/hr) recently found by Ghosh *et al.* None of these velocities/processes is well understood. We speculate that fluid pressure fluctuations can move back through a previously-ruptured region faster than they can advance through a region that has not yet tremored and slipped.

Slow Slip Phenomena Not So Phenomenal?

PENG, Z., Georgia Inst. of Techn., Atlanta/GA/USA, zpeng@gatech.edu; GOMBERG, J., US Geological Survey, Seattle/WA/USA, gomberg@usgs.gov

Slow slip phenomena at plate boundaries have revealed new understanding about how faults accommodate plate motions. We examine these phenomena in a broader context and conclude that they may not be so phenomenal after all. Slow slip phenomena include geodetic and seismic observations, indicative of quasi-static and dynamic fault slip, respectively. Seismic slow slip signals such as tremor, low and very-low frequency earthquakes with sources primarily at depths below the locked zone have been only recently identified, but seismic signals with similar characteristics are not new; examples documented decades ago include those from slow and tsunami earthquakes, and glaciers. Recent GPS data have revealed quasi-static slow slip phenomena also originating from below the locked zone, but quasi-static slip events with the same features also have long been recognized elsewhere. Moreover, the coupling of quasi-static and seismic slip events has been documented in many settings, such as afterslip and aftershocks and quasi-static slip and earthquake swarms.

The moment of the quasi-static slip events almost always exceeds that of the seismic slip, suggesting that the latter are secondary and 'triggered' by the quasi-static deformation. This inference and the hypothesis that slow slip phenomena reflect mechanics common to many faults are consistent with observations of duration and moment presented in Ide *et al.* (2007), which we have augmented to include many of the aforementioned observations. We re-examine the bimodal scaling and implied binary failure modes (*e.g.* fast and slow) inferred in Ide *et al.* (2007). The addition of new data begins to fill the gap between the slow and fast populations for durations <~250 seconds and emphasizes the fact that the bimodal inference requires extrapolation across a large observational gap (between durations ~250 s to ~50,000 s).

Slow Slip and Dynamic Rupture from Competition Between Dilatant Stabilization and Thermal Pressurization

SEGALL, P., Stanford University, Stanford, CA, USA, segall@stanford.edu; BRADLEY, A., Stanford University, Stanford, CA, USA, ambrad@stanford.edu

Slow-slip events (SSE) appear to occur in zones of high pore-pressure, p. We suggest that at low effective normal stress (Sn) dilatancy stabilizes velocity weakening faults, while at high Sn thermal pressurization overwhelms dilatancy leading to dynamic rupture (DR). We present 2D simulations that include rate-state friction, dilatancy, and heat and pore-fluid flow. Fault behavior is controlled by frictional a/b, W/h* (W = width of weakening region, h* = critical nucleation length), dilatancy and shear heating efficiencies.

We examine full-space models with uniform properties, loaded by v_plate and locked up-dip. For nominal properties, a/b = 0.9, W/h*=30, and Sn = 1 MPa we find a series of propagating SSE stabilized by dilatancy-induced decreases in p. SSE driven by down-dip slip, as well as faster (but quasi-static) events that relax the accumulated stress both occur. At Sn = 3 MPa we find both SSE and DR. Following a DR, steady slip propagates into the locked zone; after some time SSE initiate and propagate further updip. Ultimately faster slip-rates induce thermal pressurization and DR. At Sn = 100 MPa we observe only DR.

Half-space models with depth variable friction and low Sn below ~25 km exhibit both SSE and DR. Following a DR the quasi-linear transition between locked and steadily sliding regions migrates up-dip. After some time SSE initiate, and migrate up-dip into the locked fault; slip and moment rates generally (but not monotonically) increase with time. If the velocity-weakening/low Sn zone is big enough DR nucleate there and propagate both up and down dip, including into the velocity strengthening region. These models emphasize that the depth dependence of Sn as well as friction control slip behavior, can be compared to geodetic data, and have implications for the down-dip extent of megathrust ruptures.

Seismic Imaging: Recent Advancement and Future Directions

Oral Session · Wednesday 2:15 PM, 21 April · Salon G
Session Chairs: Michael Begnaud and Youshun Sun

Animating the Seismic Wavefield: Exploring the Effects of Solid Earth Heterogeneity on Long-Period Surface Waves

LLOYD, A., Pennsylvania State University, State College, PA, USA, ajl5000@psu.edu; WOODWARD, R.L., IRIS, Washington, D.C., USA, woodward@iris.edu

Subtle variations in seismic wave speed and amplitude can be observed directly in animated visualizations of the seismic wavefield that are generated using data from the Transportable Array (TA) component of EarthScope's USArray. The TA is a dense network of approximately 400 seismic stations slowly traversing the contiguous US from west to east. TA stations are separated by roughly 70 km; as such this allows long-period seismic energy to be animated as coherent propagating waves. In most such visualizations created to-date, the data are portrayed in a simple point-wise manner that emphasizes the smooth, coherent structure of the wave field. Such visualizations are a direct demonstration of real-world wave propagation, and are an excellent education and outreach tool. However, to focus on wavefield effects introduced by heterogeneity of the solid Earth, we create a "surface" by contouring the data at each time step. The contoured images are combined into a movie that provides an insightful and captivating animated visualization of the seismic wavefield. Using such visualizations of surface waves from teleseismic events we can directly observe the effects of heterogeneity and generate residuals with respect to waves propagating through a homogenous Earth. By combining the residuals of multiple events a crude tomography model is constructed and is visually compared to formal tomography models of the western United States in order to confirm that the heterogeneity of the solid Earth is truly being observed in the animations.

Finite-Frequency Seismic Tomography of Anelastic Structures in East Asia

ZHAO, L., Institute of Earth Sciences, Academia Sinica, Taipei 11529, Taiwan, zhaol@earth.sinica.edu.tw; CHEN, P., Dept. of Geology and Geophysics, University of Wyoming, Laramie, WY 82071, USA, pchen@uwyo.edu; CHEN, Q.F., Inst. Earthquake Science, China Earthquake Administration, Beijing 100036, China, chenqf@seis.ac.cn; GAHERTY, J.B., Lamont-Doherty Earth Observatory, Palisades, NY 10964, USA, gaherty@ldeo.columbia.edu

Finite-frequency seismic tomography provides a unified approach to the interpretation of observed frequency-dependent phase and amplitude anomalies in terms of perturbations in the earth's elastic and anelastic parameters. Recent developments in both computational seismology and high-performance computing have also enabled us to enhance our efficiency in obtaining tens of thousands of measurements of phase and amplitude anomalies, computing their three-dimensional sensitivity kernels, and inverting the anomalies for high-resolution images of the earth's structure. In this study, we conduct a regional finite-frequency tomography of the anelastic shear-wave structure in the upper mantle under East Asia. Frequency-dependent traveltime and amplitude anomalies of body and surface waves in the frequency band of 0.01Hz–0.05Hz are measured from regional earthquakes recorded at the IRIS Global Seismic Network (GSN) stations as well as the broadband stations of the China Digital Seismic Network (CSN). These traveltime and amplitude anomalies are jointly inverted for elastic and anelastic perturbations so as to properly account for the influences of both the intrinsic attenuation and the focusing/defocusing by elastic heterogeneities on the amplitudes. We have also implemented the LSQR inversion algorithm on a CPU-GPU hybrid cluster to improve the efficiency of our inversion scheme.

Seismic Tomography and Imaging of the Southern California Crust

TAPE, C., Harvard University, Cambridge, MA, USA, carltape@fas.harvard.edu; LIU, L., University of Toronto, Toronto, ON, Canada, liuqy@physics.utoronto.ca; MAGGI, A., University of Strasbourg, Strasbourg, France, alessia@unistra.fr; TROMP, J., Princeton University, Princeton, NJ, USA, jtromp@princeton.edu

We iteratively improve a three-dimensional tomographic model of the southern California crust using numerical simulations of seismic wave propagation based on a spectral-element method (SEM) in combination with an adjoint method. The initial 3D model is provided by the Southern California Earthquake Center. The dataset comprises three-component seismic waveforms (*i.e.*, both body and surface waves), filtered over the period range from 2 s to 30 s, from 143 local earthquakes recorded by a network of 203 stations. Time windows for measurements are automatically selected by the FLEXWIN algorithm. The misfit function in the tomographic inversion is based on frequency dependent multitaper traveltime differences. The gradient of the misfit function and related finite-frequency sensitivity kernels for each earthquake are computed using an adjoint technique. The kernels are combined using a source subspace projection method to compute a model update at each iteration of a gradient-based minimization algorithm. The inversion involved 16 iterations, which required 6800 wavefield simulations. The new crustal model is described in terms of independent shear and bulk-sound wavespeed variations. It exhibits strong heterogeneity, including local changes of ±30% with respect to the initial 3D model. The model reveals several features that relate to geologic observations, such as sedimentary basins, exhumed batholiths, and contrasting lithologies across faults. The quality of the new model is validated by quantifying waveform misfits of full-length seismograms from 91 earthquakes that were not used in the tomographic inversion. The new model provides more accurate synthetic seismograms that will benefit seismic hazard assessment.

A Global 3D P-Velocity Model of the Earth's Crust and Mantle for Improved Event Location

YOUNG, C.J., Sandia National Laboratories, Albuquerque, NM, cjyoung@sandia.gov; BALLARD, S., Sandia National Laboratories, Albuquerque, NM; HIPP, J.R., Sandia National Laboratories, Albuquerque, NM; CHANG, M.C., Sandia National Laboratories, Albuquerque, NM; ROWE, C.A., Los Alamos National Laboratory, Los Alamos, NM; BEGNAUD, M.L., Los Alamos National Laboratory, Los Alamos, NM.

Using high-quality 3D Earth models should result in more accurate seismic event locations. To test this hypothesis, we have developed a global P wave velocity model of the Earth's crust and mantle using seismic tomography.

Our model is derived from the latest version of the Ground Truth (GT) catalog of P and Pn travel time picks assembled by Los Alamos National Laboratory. To prevent over-weighting due to ray path redundancy and to reduce the compational burden, we cluster rays to produce representative rays. Reduction in the total number of ray paths is > 30%.

The model is represented using the variable resolution tessellation developed by Ballard *et al.* (2009), with a modification to allow much higher resolution crustal information. For our starting model, we use a simplified 2 layer crustal model derived from the Crust 2.0 model over a uniform AK135 mantle. Sufficient damping is used to reduce velocity adjustments so that ray path changes between iterations are small. We regularize using progressive grid refinement, refining the grid only around areas with significant velocity changes from the starting model. Our approach produces a smooth, multi-resolution model with node density appropriate to both ray coverage and the velocity gradients required by the data. This scheme is computationally expensive, so we use a distributed computing framework developed by Sandia National Laboratories, providing us with 300+ processors.

We evaluate the effectiveness of our model by analyzing travel time residual variance reduction globally, by station, by region, and for a set of 42 well-characterized low GT events. Resolution of our model is determined using standard techniques, and we compare it with a model we derived using the openly-available EHB catalog data.

Full-3D Waveform Tomography for Southern California

CHEN, P., Dept. of Geology and Geophysics, Laramie, WY, U.S.A., pochengeophysics@gmail.com; LEE, E., Dept. of Geology and Geophysics, Laramie, WY, U.S.A., elee8@uwyo.edu; JORDAN, T.H., Dept. of Earth Sciences, Los Angeles, CA, U.S.A.; MAECHLING, P.J., Dept. of Earth Sciences, Los Angeles, CA, U.S.A.

We are automating our full-3D waveform tomography (F3DT) based on the scattering-integral (SI) method and applying the automated algorithm to iteratively improve the 3D SCEC Community Velocity Model Version 4.0 (CVM4) in Southern California. In F3DT, the starting model as well as the derived model perturbation is 3D in space and the sensitivity kernels are calculated using the full physics of 3D wave propagation. The SI implementation of F3DT is based on explicitly constructing and storing the sensitivity (Fréchet) kernels for individual misfit measurements. The sensitivity (Fréchet) kernels are constructed through the temporal convolution between the earthquake wavefield (EWF) from the source and the receiver Green tensor (RGT) from the receiver. Compared with other F3DT implementations, the primary advantages of the SI method are its high computational efficiency and the ease to incorporate 3D Earth structural models into very rapid seismic source parameter inversions. For the first iteration, we used over 3,500 phase-delay measurements from regional small to medium-sized earthquakes to invert for 3D perturbations to the 3D reference model, SCEC CVM4. The updated model, CVM4SI1, reduced the variance of the phase-delay measurements by about 29% and the synthetics generated by the updated model generally provide better fit to the observed waveforms. In the second iteration, we incorporated phase-delay measurements made on ambient noise Green's function data and additional regional earthquakes to further improve path coverage. The updated model CVM4SI1 improved waveform fittings, which allows us to pick more phases from the original waveform dataset. In this presentation we will report our recent progresses on automating the complete F3DT workflow, the second iteration velocity model, CVM4SI2, and waveform improvements produced by the updated model.

Full-wave Ambient Noise Tomography of the Northern Cascadia

SHEN, Y., University of Rhode Island, Narragansett, RI, USA, yshen@gso.uri.edu; ZHANG, W., University of Rhode Island, Narragansett, RI, USA, wzhang@gso.uri.edu

The use of ambient seismic noise to determine the crustal and upper mantle structure has become an established practice in seismology. Compared to the traditional methods that utilize surface waves from earthquakes, it has several advantages, particularly in extending usable waves to short periods and providing constraints on shallow structure. In this study, we adapt the full-wave finite-frequency method for ambient noise tomography. The phase-delay sensitivity of the impulse response between the two vertical components of a pair of stations to S-wave speed perturbations, for example, is similar to that of Rayleigh waves from earthquakes, as expected. The sensitivity reaches a local minimum value at about one eighteenth wavelength depth below the free surface and has large values on the free surface. This near surface effect should be taken into account in seismic wave simulation. We solve this problem using a non-uniform-grid finite-difference method. With a boundary-conforming grid in a non-staggered finite-difference method, we find that surface topography has strong effects on the sensitivity kernels of short-period waves. Thus in places with large surface topography, such as the Cascadia, the topographic effects should be taken into account in the use of short-period ambient noise. We have processed data collected by the USArray and the regional seismic networks in the northern Cascadia and will report the crustal structure beneath the region obtained from full-wave ambient noise tomography.

Can We Improve Q Estimates by Using a New "Geometrical Spreading" Model?

JIAKANG, X., Air Force Research Laboratory, Bedford, MA 01731, USA.

Path affects on seismic spectra are traditionally modeled as G(f,t) exp (- pi f t / Q(f)), where t is the travel time, G(f,t) the geometrical spreading term (GST); and Q(f) the quality factor. G(f,t) is estimated in a reference velocity structure and removed from data to allow Q(f) estimation. This limits the precision of Q estimates because G(f,t) only approximates the wave spreading effect in complex Earth structure. Recently a new GST has been proposed as being the product of the original G(f,t) and an exponential term, exp (- k t). When the new GST is used to estimate k and Q(f), the latter is invariably found to be frequency independent. I will show that (1) an exponential GST model lacks a physical basis, (2) data fitting using this model is effectively a curve fitting using a 1st order Taylor series expansion; (3) previous data that were fit by a power-law frequency dependence of Q(f) can also be well fit by the 1st order expansion because of the long tail of a power-law function and the limited frequency bands involved; (4) recent laboratory measurements of intrinsic Q of mantle materials at seismic frequencies show that it is often frequency dependent, which should lead to frequency-dependent total Q(f), a result that is at odds with results estimated with the new GST; (5) several recent long-period surface wave Q models used data that contradict the new GST; and (6) the traditional model already includes possible attenuation in the form of exp (- S t), which is caused by 3D scattering from large scatterers. But S is difficult to estimate because of a parameter trade-off in finite frequency bands. Therefore, while traditional Q(f) estimates are limited in their precision, uniqueness and spatial resolution, they are not grossly erroneous and cannot be improved, and are likely degraded, using the new GST model.

Eikonal Tomography: Surface Wave Tomography by Phase-Front Tracking Across a Regional Broad-Band Seismic Array

LIN, F., University of Colorado, Boulder, Colorado, fan-chi.lin@colorado.edu; RITZWOLLER, M.H., University of Colorado, Boulder, Colorado, michael.ritzwoller@colorado.edu; SNIEDER, R., Colorado School of Mines, Golden, Colorado, rsnieder@mines.edu

We present a new surface wave tomography method based on phase-front tracking across a regional array. For a seismic source, all available phase travel time measurements between that source and all stations are first used to estimate the phase travel time map across the region and determined the phase-front at each instantaneous time. Based on the eikonal equation, the gradient of the phase travel time map at each location can be used to determine the movement of the phase front and estimate both the direction of wave propagation and the local phase velocity. For each location, the directionally dependent phase velocity measurements are summarized from different sources to estimate both the isotropic and azimuthally anisotropic phase velocities and their uncertainties. The method naturally accounts for ray bending and no ad hoc choice of regularization is required. The method also provides an intuitive way to disentangle systematically the azimuthal variation of the velocity measurements from random measurement errors and allows a statistically robust measure of azimuthal anisotropy. Applications to both earthquake and ambient noise measurements across the EarthScope/USArray Transportable Array stations in the western US are used to demonstrate the method. The resulting 3D models of the isotropic and azimuthally anisotropic velocities of the crust and upper mantle are shown.

Seismic Wave Gradiometry Using the Wavelet Transform: Potential Application to Surface Wave Inversions using USArray

POPPELIERS, C., Augusta State University, Augusta, GA, USA, cpoppeli@aug.edu

This paper describes a new development in seismic wave gradiometry. This work follows previous work on time-domain wave gradiometery, but proposes applying a wavelet transform to the data prior to wave gradiometric analysis. As an illustration

of the method, we analyze data from two underwater shots that were recorded by a portion of the Glendora Array. The analysis of the data revealed the presence of typical body- and surface waves, in addition to several phases that are interpreted to be the result of vertically oriented geologic discontinuities. The analysis method presented here clearly shows that the back azimuth and vector slowness of these data are highly time- and frequency dependent on a scale of only tens of meters. Being able to observe these phenomena at this scale suggests a new paradigm of surface wave inversions: using azimuth-dependant slowness estimates derived from wavelet gradiometry to estimate anisotropic surface wave velocity structure. In this talk, I outline a method of using wavelet gradiometry to invert USArray data to derive azimuth-dependant surface wave velocity structure for a portion of the North American continent.

Influence of Velocity Anisotropy on an Accuracy of Microearthquake Locations

CHESNOKOV, E.M., University of Houston, Houston, Texas, USA, emchesno@mail.uh.edu; KRASNOVA, M.A., IFZ, Moscow, Russia, mkrasnova@ifz.ru

Precision of coordinate determination of microevents as well as of geometry and dynamics of the hydrocracking process plays a major role in seismic monitoring of hydropumping, since even minor mistakes in the resolution of the frac location can lead to serious mistakes during the planning of drilling of subsequent wells. Velocity models with isotropic layers are generally used to determine the microearthquake coordinates. At the same time it is well known that sedimentary rocks possess strong elastic anisotropy. In order to evaluate possible mistakes in the location of microearthquakes due to anisotropy, a numerical experiment was conducted.

A homogeneous anisotropic space with different symmetry types (VTI, HTI, orthorhombic)was considered. A numerical experiment was conducted according to the following scheme: (1) some "cloud" of earthquakes and perfshots was chosen, where the location of the initial cloud was assumed as the initial location; (2) a homogenous anisotropic space was considered as an alternative model; (3) body wave travel times from the initial focal points to a station in the observation system were calculated in an alternative model of medium and were used as initial calculations to determine the coordinates in the anisotropic space.

The analysis of the obtained results shows that the neglect of the anisotropic elastic behaviors of the medium: (1) strongly influence the determination precision of the coordinates of each microearthquake; (2) can shift and deform the initial earthquake "cloud" form (the most minimal distortions are observed in the case of the observation system being placed at depths close to those of the initial event "cloud").

Imaging with Scattered Teleseismic Waves: Data, Method and Application to the Hellenic Subduction Zone

PEARCE, F.D., MIT, Cambridge, MA, USA, fpearce@mit.edu; RONDENAY, S., MIT, Cambridge, MA, USA, rondenay@mit.edu

Scattered teleseismic body waves are commonly used to image sharp changes in material properties within the lithosphere and mantle. When dense broadband arrays are available, high-resolution imaging can be achieved using teleseismic migration. Such methods involve the backprojection of scattered waves by stacking their signal along diffraction hyperbolae, with their relative arrival time and amplitude providing the position and magnitude of elastic discontinuities, respectively. Here, we use a 2D, elastic teleseismic migration method based on the Generalized Radon Transform. The method provides detailed images of perturbations in elastic properties with respect to a smooth reference model. We discuss the data requirements and assumptions necessary for optimal resolution. Quasi-linear, dense seismic arrays must be oriented perpendicular to the strike of geologic structures (*e.g.* arc-perpendicular in subduction zone). Station spacing, array length, and event distribution place important constraints on dip and depth resolution. Several preprocessing steps are necessary to isolate the scattered wavefield from raw data recorded at the surface. Deviations from the assumptions of isotropy and 2D symmetry result in degraded image quality. Synthetic data are used to test the resolving power of the method and to identify potential artifacts. The 2D GRT method is applied to two dense seismic arrays across the western Hellenic subduction zone. Results clearly image a ~10 km-thick low-velocity layer consistent with subducted oceanic crust within the southern segment, and a ~20 km-thick low-velocity layer within the northern segment interpreted as subducted continental crust. Comparing the two imaged subducted crusts shows evidence for rollback of the southern segment that may be partially accommodated by slab tearing subparallel to the Cephalonia transform fault.

Investigating the Limits of Ray-Based Global Surface-Wave Tomography

HJORLEIFSDOTTIR, V., LDEO, Columbia Univ., Palisades, NY; DALTON, C.A., Boston University, Boston, MA, dalton@bu.edu; EKSTROM, G., LDEO, Columbia Univ, Palisades, NY, ekstrom@ldeo.columbia.edu

Models describing the three-dimensional variations of elastic and anelastic properties of the crust and mantle provide important constraints on the state, composition and dynamics of the Earth's interior. For the top few hundred kilometers of the Earth, such models are primarily constrained by seismic observations, and, on a large scale, by observations of seismic surface waves. In this study we investigate how the models are affected by approximations in the theoretical treatment of wave excitation and propagation in the measurement and prediction of the data. We use a spectral-element wave-propagation solver (SPECFEM3D_GLOBE) to generate accurate seismograms for an Earth model comprised of crustal model Crust 2.0 and mantle model S362ANI. Realistic distributions of 50 earthquakes and 163 seismic stations are used to mimic real conditions. We generate data sets consisting of 8150 three-component, teleseismic, seismograms, accurate at periods between 30–800 seconds. We process the waveforms using the same data-selection and measurement algorithms (Ekstrom *et al.*, 1997) used in the analysis of real data. We quantify the validity of measurement techniques that are derived within a ray-theoretical framework and that attempt to isolate the fundamental mode from other phases.

We investigate the ability of great-circle ray theory (GCRT), exact-ray theory (ERT), and finite-frequency theory (FFT), together with the true phase velocity maps for the Earth model mentioned above, to predict phase anomalies measured from the SPECFEM synthetics. We find that the differences between measured and predicted phase anomalies are much larger than the differences between predictions based on GCRT, ERT and FFT. The difference between measured anomalies and those predicted using GCRT is not larger than the difference between measured anomalies and those predicted using ERT and FFT.

Engaging Students and Teachers in Seismology: In Memory of John Lahr

Oral Session · Wednesday 4:15 PM, 21 April · Salon E
Session Chairs: John Taber and Larry Braile

John Lahr's Lasting Impact on the IRIS E&O Program

TABER, J.J., IRIS, Washington, DC, taber@iris.edu; BRAVO, T.K., IRIS, Vancouver, WA, tkb@iris.edu; HUBENTHAL, M., IRIS, Washington, DC, hubenth@iris.edu; JOHNSON, J., Volcano Video Productions, Portland, OR, jendaj@comcast.net; MCQUILLAN, P., IRIS, Washington, DC, mcquillan@iris.edu; TOIGO, M., IRIS, Washington, DC, toigo@iris.edu; WELTI, R., IRIS, Seattle, WA, russ@iris.washington.edu

John Lahr, USGS seismologist emeritus and an original member of the committee that guides the E&O agenda, was a key contributor to the IRIS E&O program over the past 10 years. John was an original member of the committee that guides the E&O program and he helped to initiate the Seismographs in Schools program that became a primary focus of his educational efforts. Through that program, he worked with teachers across the country to engage students in the recording of earthquakes. He shared his sense of wonder and curiosity about the world using simple and practical explanations, whether it was squeezing a rock to show its elasticity, breaking spaghetti to teach about faults, or recording how fast his fingernails grew to compare to tectonic plate movement.

Following John's example, IRIS E&O works to advance awareness and understanding of seismology and geophysics while inspiring careers in Earth Sciences. The focus on seismology and the use of seismic data has allowed the IRIS E&O program to develop and disseminate a unique suite of products and services for audiences ranging from the general public, to teachers, and to undergraduate students and faculty. These activities both provide services for, and rely on the volunteer involvement of IRIS Consortium members and include: an undergraduate summer internship program, professional development for teachers and college faculty, seismographs in schools and related collection and use of seismic data, IRIS/USGS museum exhibits including the new Active Earth Display, IRIS/SSA distinguished lecturers, publications including videos, animations, online recordings, teachable moments and classroom modules, and the dissemination of materials, activities, software and data via the IRIS Web site. The impact of these activities is continuously monitored via internal and external assessment to ensure effectiveness of the program.

A Decade of Earthquake Monitoring with an Educational Seismograph

BRAILE, L.W., Purdue University, West Lafayette, IN, USA, braile@purdue.edu

Since January of 2000 we have operated an educational seismograph for earthquake monitoring and support of the IRIS Seismographs in Schools program. The seismograph (AS-1, http://www.amateurseismologist.com/) consists of an inexpensive and easy to install and operate vertical component seismometer, amplifier and digitizer. The seismograph is used with the AmaSeis Windows software developed for IRIS by Alan Jones (http://bingweb.binghamton.edu/~ajones/). The IRIS Seismographs in Schools program engages K–16 students and teachers in monitoring earthquakes and in discovery learning through recording, analyzing and interpreting seismograms. Compelling aspects of the program are the use of real and relevant scientific

data, observing in real time, acquiring their own data, and the ability to analyze and obtain accurate information about earthquakes from the seismograms. In ten years of nearly continuous recording with the educational seismograph, we have recorded excellent seismograms from hundreds of local, regional and teleseismic earthquakes that display interesting wave propagation characteristics. A tool within the AmaSeis software provides the ability to easily estimate the epicenter to station distance from P and S arrivals. A calibration procedure for the seismograph was developed so that recorded seismograms can be used to determine reasonably accurate magnitudes of recorded earthquakes. Tutorials for seismograph operation and interpretation of seismograms, and suggested educational activities have been developed for use with the educational seismograph and are available online (http://www.iris.edu/hq/sis, http://web.ics.purdue.edu/~braile/edumod/as1lessons/as1lessons.htm).

The Quake-Catcher Network: Bringing Seismology to Homes and Schools

LAWRENCE, J.F., Stanford University, Stanford, CA, USA, jflawrence@stanford.edu; COCHRAN, E.S., UC Riverside, Riverside, CA, USA, escochran@ucr.edu; SALTZMAN, J., Stanford University, Stanford, CA, USA, saltzman@stanford.edu; CHRISTENSEN, C.M., Stanford University, Stanford, CA, USA, carlgt1@yahoo.com; HUBENTHAL, M., IRIS Education and Outreach, Washington D.C., USA; CHUNG, A.I., Stanford University, Stanford, CA, USA, aichung@stanford.edu

The Quake-Catcher Network (QCN) is a collaborative initiative for developing the world's largest, low-cost strong-motion seismic network by utilizing sensors in and attached to volunteer internet-connected computers. QCN is not only a research tool, but provides an educational tool for teaching earthquake science in formal and informal environments. A central mission of the Quake-Catcher Network is to provide scientific educational software and hardware so that K–12 teachers, students, and the general public can better understand and participate in the science of earthquakes and earthquake hazards. With greater understanding, teachers, students, and interested individuals can share their new knowledge, resulting in continued participation in the project, and better preparation for earthquakes in their homes, businesses, and communities.

The primary educational outreach goals are 1) to present earthquake science and earthquake hazards in a modern and exciting way, and 2) to provide teachers and educators with seismic sensors, interactive software, and educational modules to assist in earthquake education. QCNLive (our interactive educational computer software) displays recent and historic earthquake locations and 3-axis real-time acceleration measurements. This tool is useful for demonstrations and active engagement for all ages, from K-college. QCN provides subsidized sensors at $49 for the general public and $5 for K–12 teachers.

With your help, the Quake-Catcher Network can provide better understanding of earthquakes to a broader audience. Academics are taking QCN to classrooms across the United States and around the world. The next time you visit a K–12 classroom or teach a college class on interpreting seismograms, bring a QCN sensor and QCNLive software with you! To learn how, visit http://qcn.stanford.edu.

Seismological Education and Outreach at a College Football Game: An Experiment to Record Crowd-Related Seismicity

NIES, A., Boise State University, Boise, ID, andrewnies@u.boisestate.edu; HANEY, M.M., Boise State University, Boise, ID, matt@cgiss.boisestate.edu; ZOLLWEG, J., Boise State University, Boise, ID, jzollweg@hotmail.com; THE BOISE STATE FOOTBALL SEISMOLOGY TEAM, Boise State University, Boise, ID

During a 2009 home football game, the Boise State Football Seismology Team, a group of 20 undergraduate students, graduate students, and faculty, participated in a passive experiment designed to record seismicity resulting from the more than 30,000 fans in Bronco Stadium. To our knowledge, this represented only the third such experiment ever conducted: earlier football recordings had taken place at Louisiana State University and the University of Wisconsin. The deployment consisted of five broadband seismometers and, in contrast to previous recordings at football games, included a strong-motion instrument within the stadium.

The primary goal of the experiment was to provide students with experience deploying instruments and an opportunity to work with a unique data set. The response from the students was overwhelming: over a dozen students, both undergraduate and graduate, volunteered their time for the experiment. In addition, the deployment caught the attention of the local news media. The success of the experiment demonstrated the utility of deploying seismometers at football games for getting students involved in seismology and showcasing the excitement of the field to the community.

We find that the broadband instruments are able to record distinct microearthquakes (Ms = –1.5) within the frequency band from 0.5–5 Hz during the game. Comparison of these times to a field observer log shows that the microearthquakes are the clear result of crowd-related seismicity following touchdowns, kickoffs, and interceptions. We plan to further analyze the polarization of the radiated seismic waves and their horizontal-to-vertical (HV) spectral ratio, which should have implications for the earthquake hazard on campus.

Translating Seismology into Simple Animations: A Powerful Learning Tool for Earth-Science Educators

JOHNSON, J., Volcano Video Productions, Portland, OR USA, jendaj@comcast.net; BRAVO, T.K., IRIS, Vancouver, WA USA, tkb@iris.edu; BUTLER, R.F., University of Portland, Portland, OR USA, butler@up.edu

Earth-science teachers with limited geologic knowledge, as well as seasoned professors are eager to supplement existing teaching resources with computer animations of geologic processes. John Lahr recognized this and encouraged the production of a wide variety of animations and video demonstrations.

John found that unfamiliar science concepts can be more accessible when learning is supported by animations. Even step-wise illustrations require learners to mentally fill the gaps between static diagrams. The effectiveness of animations is in part because they provide an additional cognitive pathway to learning. A well-designed animation can enable learners to focus on the scientific concept and educational activity at hand thus increasing student interest and motivation. The dynamic nature of animations may better engage the current generation of students where static images alone produce frustration.

Furthermore, highly simplified cartoons that are grossly distorted can be used more effectively than realistic depictions to illustrate processes that cannot be viewed in scaled models. Graphic exaggeration attracts learner's attention to critical components or intervals of time that require special focus. We all know that the Magic School bus doesn't go to the core in near-light speed, but the lessons learned on that imaginary voyage are still valuable.

IRIS' Education and Outreach program offers cartoon & interactive-Flash animations covering a variety of seismology and Earth-science topics. Accompanying video lectures can both promote Earth-science teachers' grasp of new science content and support their classroom presentation of earthquake science. To complement these, most of the animation and video lecture sets also have links to classroom activities that promote active learning of key seismological topics.

Teachable Moments: Capturing the Power of an Earthquake to Teach about Seismology

BRAVO, T.K., IRIS, Washington DC, tkb@iris.edu; BUTLER, R.F., University of Portland, Portland, OR, butler@up.edu; JOHNSON, J., IRIS, Washington DC, jendaj@comcast.net

Real-time seismic data in the classroom can capture the attention and imagination of students. Earthquakes are dynamic, each providing a new angle for presenting seismology content. Today's K–12 classroom teachers and college faculty have an interest in presenting content related to current events, and much information is available via the Web. Instructors, however, lack the time to synthesize the material into a coherent package. IRIS Education and Outreach and the University of Portland have developed a set of 'Teachable Moments', Power Point and .pdf presentations which provide a short summary of current earthquakes that can be quickly and easily used in the classroom. The presentations, generated by seismologists and educators, are available within a few hours to one day after a significant earthquake. The presentations include a variety of content allowing educators to customize the information for their classes. Common elements include US Geological Survey earthquake and volcano information, plate tectonic and regional tectonic maps and summaries, computer animations, seismograms, photos, and other event-specific information. These timely classroom presentations serve to enhance Earth science education, by increasing the time devoted to discussing seismology concepts and providing high quality information to build student knowledge about tectonic processes.

Engaging Students and Teachers in Seismology: In Memory of John Lahr

Poster Session · Wednesday AM, 21 April · Exhibit Hall

Temblor: Simplifying Earthquake Visualization

POWERS, P.M., USGS, Pasadena, CA, pmpowers@caltech.edu

The study of earthquakes is an ideal gateway to the earth sciences, one that unifies elements of structural geology, plate-tectonics, seismology, and geodynamics. Introductory-level students, however, have not often been compelled to think in 3-D and have a difficult time grasping concepts and phenomena distilled into 2-D figures. Addition of a fourth, time dimension can further raise barriers to understanding. Software applications designed to enhance and ease this learning process, however, are commonly plagued by complex installation procedures, licensing fees, unintuitive interfaces, long and/or steep learning curves, and data format issues. Temblor is a free, 4-D visualization application that addresses these difficulties. Preconfigured Temblor 'scenes' integrate earthquake locations with other related data sets such as 3-D fault models and GPS data and allow users to easily navigate and

animate earthquake catalogs (*i.e.* to add time as the 4th dimension). By focusing specifically on crustal earthquakes, Temblor eliminates complexity involved with the development and use of a general data viewer. Likewise, the interface is tailored towards interaction and understanding rather than customization. Preliminary use by introductory-level students at the University of Southern California elicited an enthusiastic response. Many found they better understood the relationships between earthquakes and faults and between mainshocks and aftershocks after using Temblor for only a few hours. Student feedback is currently being used to improve usability prior to wide release of the application. Temblor is written in Java and is available for Windows XP+ or Mac OS X 10.5+.

Introduction to Earthquake Focal Mechanisms Using Seismographs in Schools Data

LEVASSEUR, D., Christian Brothers High School, Sacramento/CA/USA, dlevasseur@cbhs-sacramento.org; FORD, S. R., Lawrence Livermore Nat'l Lab, Livermore/CA/USA, sean@llnl.gov

High School students are introduced to the concept of focal mechanisms to describe an earthquake using a lesson that incorporates the calculation of a fault-plane solution using Seismographs in Schools (SiS) data supplemented by data from the Berkeley Digitial Seismograph Network (BDSN). The lesson begins with a faulting introduction based on material from IRIS and the USGS. The students are shown an example that uses first-motion data from the USGS database. Finally, the students download and pick P-wave first-motions from an event recorded using the AS-1 SiS data as well as data from the BDSN. Collections of focal mechanisms around California are analyzed to understand the sense of motion on faults.

Teachers Involved in Expeditionary Seismology: The TIES that bind

BOYD, D., Conrad High School, Dallas, TX USA, davidboyd828@gmail.com; DILLON, T., Chapin High School, El Paso, TX USA; ARRATIA, M., Ringgold Middle School, Rio Grande City, TX USA; WEART, C, Weslaco High School, Weslaco, TX USA; MOTE, A., Travis High School, Austin, TX USA; MYRICK, M., Wiggs Middle School, El Paso, TX USA; OHMAN, S., Coronado High School, El Paso, TX USA; THEIS, H., Tatum High School, Tatum, TX USA; PULLIAM, J., Baylor University; GRAND, S.P., UT Austin; ELLINS, K., UT Austin; OLSON, H., UT Austin

We will report on our participation in a seismological investigation of the Rio Grande Rift and ways in which this experience will affect our teaching. We are involved in many phases of the investigation, from installation to station service runs to data analysis and presentation of results. In the summer of 2008 we deployed 71 broadband seismographs in southeastern NM/western Texas. This was a major undertaking that involved a large collection of teachers, undergraduate and graduate students, principal investigators, and other helpers, plus several members of EarthScope's FlexArray support group in Socorro, NM.

Teachers bring a lot of savvy and outstanding people skills to the tasks of finding suitable station sites, identifying and contacting landowners, presenting the project and obtaining permission to install a temporary station. Service runs allow us to reconnect with each other and the project. Involvement over a period of time allows for concepts to sink in, background reading to be carried out, and results in a greater investment in the project and its goals.

Ultimately we expect our collaboration to result in a two-way transfer of knowledge. Rather than counting on university professors and researchers who are well-schooled in seismological concepts and theory but short on relevant teaching experience to produce teaching materials and lesson plans, we are experienced teachers who are learning seismological concepts and analysis techniques. We will then take the first stab at creating the teaching materials for high school and middle school students. The final products will emerge from a collaborative process that is also a two- to three-year team-building and training exercise. We also received AS-1 seismometers and trained in their use at an IRIS workshop and are engaged in creating our own regional sub-network of school-based seismographs.

Networking in Educational Seismology: The IRIS Seismographs in Schools Program

BRAVO, T.K., IRIS, Washington DC, tkb@iris.edu; BRAILE, L.W., Purdue University, West Lafayette, IN, braile@purdue.edu; HUBENTHAL, M., IRIS, Washington DC, Michael.Hubenthal@iris.edu; TABER, J., IRIS, Washington DC, taber@iris.edu; TOIGO, M., IRIS, Washington DC, toigo@iris.edu; WYATT, K., Oregon Shakes, Depoe Bay, OR, kwyatt@geocouple.com

A seismometer in the classroom promotes awareness of earthquake activity around the world and provides an opportunity to for both students and teachers to become engaged in the process of collecting, analyzing and drawing conclusions from seismic data. Central to this effort for IRIS has been the AS-1 educational seismometer. The AS-1 features an open-design to engage students in middle and high school classrooms, undergraduate programs, and public venues in the operation of the instrument while also providing educational quality data. Since the program's inception over 150 schools have received seismographs and training through the program and many more will come online as a result of the John Lahr fund, which is helping to support future hardware requests.

A recent priority for the program has been improving the connectedness of educational seismograph users. We have developed an online interface enabling educators to share and make use of seismic data while also communicating with other educational seismology users. Users can view and compare near-real-time displays of other participating schools, upload and download data, and contact nearby schools that also operate seismographs. In order to promote and maintain program participation and communication the site features a discussion forum that allows users to discuss technical issues as well as facilitating discussions in educational seismology.

There has been recent growth in a global community of educational seismograph users. IRIS has been collaborating with several international networks to develop and provide web-based tools using the web structure developed by the IRIS program. These tools allow educators around the world to easily establish an online presence for their own regional networks. Currently over 300 educational seismic stations worldwide are networked via the Seismographs in Schools web site.

Teachers on the Leading Edge: An Earth Science Teacher Professional Development Program Featuring Pacific Northwest Geologic Hazards

BUTLER, R.F., University of Portland, Portland, OR USA, butler@up.edu; GRANSHAW, F., Portland Community College, Portland, OR USA, fgransha@pcc.edu; BUTLER, R.F., University of POrtland, butler@up.edu; GROOM, R., Mt. Tabor Middle School, Portland OR USA, rgroom@pps.k12.or.us; HEDEEN, C., Oregon City High School, Portland OR USA, Chris.Hedeen@orecity.k12.or.us; JOHNSON, J., Volcano Video Productions, Portland, OR USA; MAGURA, B., Jackson Middle School, Portland OR USA, bmagura@pps.k12.or.us; PRATT-SITAULA, B., Central Washington Univdersity, Ellensburg, WA USA, psitaula@geology.cwu.edu; THOMPSON, D., Orting High School, North Orting, WA USA thompsond@orting.wednet.edu; WHITMAN, J., Pacific Lutheran University, Tacoma, WA, USA whitmaj@plu.edu

Teachers on the Leading Edge (TOTLE) is a professional development program for middle- and high-school Earth science teachers that features Pacific Northwest active continental margin geology. Training workshops and teaching resources have been developed primarily for grades 6–8, though concepts apply to introductory undergraduate coursework. Program themes include overviews of the Earth, plate tectonics, and seismology with emphasis on geologic hazards (earthquakes, liquefaction, landslides, and tsunami) as aspects of living on the "leading edge" of the N. American continent.

Fundamental concepts and observations progress from global patterns, to regional context, and then to local applications. TOTLE's master teachers and Geoscience educators have developed inquiry-based lesson plans that translate Pacific Northwest geologic-hazards research from the USGS, Oregon Department of Geology and Mineral Industries, and Washington State Department of Natural Resources. We emphasize the importance of zoning regulations, infrastructure engineering, and emergency preparedness in geologic hazard mitigation in order to: (1) demonstrate how improvements in Geoscience knowledge have led to improved engineering designs that mitigate hazards; (2) align lessons with national and state science standards that focus on science, technology, and societal connections; and (3) avoid fatalism by developing a culture of geologic-hazard awareness among future citizens of the Pacific Northwest. Participants in the week-long TOTLE–EarthScope workshops receive an extensive collection of maps, posters, and experimental apparatus that are proven tools for concept. In addition, they receive a DVD with well as over 100 animations and video lectures with accompanying PowerPoint presentations and activities. These teaching resources greatly facilitate teachers' transfer of workshop learning to their classroom

Joint Inversion of Multiple Geophysical Data Sets for Seismic Structure

Poster Session · Wednesday AM, 21 April · Exhibit Hall

A Probabilistic Framework for the Joint Inversion of Multiple Datasets

HAUSER, J., NORSAR, juerg@norsar.no; DYER, K.M., LLNL, dyer1@llnl.gov; PASYANOS, M.E., LLNL, pasyanos1@llnl.gov; BUNGUM, H., NORSAR, Hilmar.Bungum@norsar.no; FALEIDE, J.I., University of Oslo, j.i.faleide@geo.uio.no; CLARK, S.A., University of Oslo, s.a.clark@geo.uio.no

In this study we constrain Vp, Vs, density and thickness for the sediments, the crystalline crust and uppermost mantle in the European Arctic. A Monte Carlo Markov Chain is used to sample the posterior distribution, which describes the ensemble of

models that are in agreement with prior information and the datasets. An example for prior information used in this work is the extent of regions with no significant sediment coverage. The datasets we use are thickness constraints, velocity profiles, gravity data, surface wave group velocities and body wave traveltimes. The samples drawn from the posterior distribution using a Monte Carlo Markov Chain form our probabilistic model. Analyzing this ensemble of models that fit the data allows to estimate a mean model and the standard deviation for the model parameters, *i.e.* their uncertainty. It is common in joint inversions to use fixed relationships between the seismic parameters; for a given Vp there is only one specific value allowed for Vs and density. Such an approach neglects the fact that in a heterogeneous earth the relationships between seismic parameters will vary spatially and thereby makes it difficult to find models that are in agreement with the various data sets. A probabilistic approach on the other hand allows us to test plausible ranges for these relationships and thereby explore their spatial variability. Maps for the thickness of sediments and the crystalline crust of our probabilistic model are in good agreement with knowledge of the regional tectonic setting. The predicted model uncertainties, which are more important than the absolute values, correlate well with the variation in data coverage and data quality in the region. A potential practical application of our probabilistic model is to take model uncertainties into account when locating seismicity.

Testing Joint Inversion of Travel Times and Gravity Data for Imaging of Western Colombia: Trade-offs and Sensitivities.

ROWE, C.A., Los Alamos National Laboratory, Los Alamos, NM, char@lanl.gov; DIONICIO, L.V., INGEOMINAS, Bogota, Colombia, viviana.dionicio@gmail.com; MACEIRA, M., Los Alamos National Laboratory, Los Alamos, NM, mmaceira@lanl.gov; ZHANG, H., MIT, Cambridge, MA, hjzhang@mit.edu

We report on continued exploration of the sensitivities and trade-offs encountered when jointly inverting for three-dimensional seismic structure of western Colombia using seismic body wave travel times and satellite gravity. We have selected 3,609 earthquakes recorded at 33 sensors distributed throughout the country, with additional data from stations in neighboring countries to invert for structure between 72.5 to 77.5 degrees W and 2 to 7.5 degrees N.

Preliminary results recently presented demonstrated the successful joint inversion of these two distinct data types; a remaining problem has been the relative weighting to the data sets for optimal results, as well as sensitivity to the starting model and the need to groom the seismic catalog, in particular the need to decluster events from this highly heterogeneous array of source zones.

We present a refined jointly inverted model for the region and compare to an independent study for the same region using the D. Zhao tomographic method applied to body waves alone.

Tomographic Imaging of the Upper Mantle beneath the Colorado Rocky Mountains from Simultaneous Joint Inversion of Teleseismic Body Wave Residuals and Bouguer Gravity

MACCARTHY, J.K., New Mexico Tech, Socorro, NM, jkmacc@nmt.edu; ASTER, R.C., New Mexico Tech., Socorro, NM, aster@ees.nmt.edu; HANSEN, S.M., University of Wyoming, Laramie, WY, shansen1@uwyo.edu; DUEKER, K.G., University of Wyoming, Laramie, WY, dueker@uwyo.edu

We report on the 3D velocity structure of the uppermost mantle beneath the Colorado Rockies, derived from teleseismic travel time residuals and ground-based Bouguer gravity data. The CREST seismic network consisted of 59 broadband PASSCAL stations deployed in the central Colorado Rocky Mountains for ~15 months in 2008 and 2009. CREST was embedded in the time-coincident EarthScope Transportable Array (TA), producing a composite network of 167 stations with a mean spacing of ~24 km. An iterative nonlinear inversion is employed, where an assumed coupling relation that links the seismic and gravity data sets is encoded into the minimized objective function. We explore multiple data coupling relations and weighting schemes in order to evaluate the resolving power of the simultaneous joint inversion, and we apply the method toward inverting for a model of 3D velocity structure beneath the Colorado Rockies. Competing models for the anomaly are: 1) upwelling asthenosphere associated with flat-slab roll-back, 2) Laramide thickening and hydraulic weakening of lower lithosphere that promoted subsequent Rayleigh-Taylor instabilities of the lower lithosphere that are flanked by thinned lithosphere, 3) compositional variations due to hydration and or low-solidus material, and 4) a mini-plume or water pipe diapirs shed upwards from the 410 km low velocity zone.

Joint Inversion of Seismic and Magnetotelluric Data in the Parkfield Region of California Using the Cross-Gradient Constraint

BENNINGTON, N.L., University of Wisconsin-Madison, Madison/Wisconsin/USA, ninfa@geology.wisc.edu; THURBER, C.H., University of Wisconsin-Madison, Madison/Wisconsin/USA, clifft@geology.wisc.edu; BEDROSIAN, P., USGS, Menlo Park/California/USA, pbedrosian@usgs.gov; ZHANG, H., MIT, Cambridge/Massachusetts/USA, hjzhang@mit.edu

The inversion of geophysical data suffers inherent problems including imperfect resolution and model nonuniqueness. We are exploring the utility of structural constraints by employing a cross-gradient (C.G.) penalty function to improve models of fault zone structure along the San Andreas fault in the Parkfield, California area. Existing seismic and resistivity models at SAFOD show significant spatial similarity between their main features. As a first step, we capitalized on this likeness by developing an alternating inversion scheme that uses a C.G. penalty function to achieve images that fit both resistivity and seismic data adequately but are structurally more similar. The strategy involves calculating model perturbations necessary to "zero-out" the C.G. penalty function and applying these perturbations to the separately inverted resistivity and seismic models. An additional iteration of the two separate inversions, using the perturbed models, yield models that preserve the structural similarity achieved from the C.G. perturbation reasonably well.

The next step is the development of a joint inversion code, tomoDDMT, which merges the seismic inversion code, tomoDD, and the magnetotelluric (MT) inversion code, Occam2DMT. In separate inversions, the seismic and resistivity models are inverted for under varying gridding schemes due to resolution differences. This difference in gridding is overcome by projecting both models onto a regular, much finer grid, which allows the two models to be linked in a uniform way. The C.G. constraint is calculated on this "common" grid and those values are projected back to the seismic and resistivity model spaces. A simultaneous solution is then carried out for the seismic and resistivity models subject to the C.G. constraint. Occam2DMT employs Cholesky factorization to carry out inversions. However, tomoDDMT employs the LSQR algorithm for the simultaneous solution of both models in order to increase the speed of the inversion.

Joint Inversion of InSAR and Seismic Waveform Data for the Finite-fault Solution of the 21 February 2008 Wells, Nevada Earthquake

FORD, S.R., Lawrence Livermore Nat'l Lab, Livermore/CA/USA, sean@llnl.gov; DREGER, D.S., Berkeley Seismological Lab, Berkeley/CA/USA, dreger@seismo.berkeley.edu; RYDER, I., University of Liverpool, Liverpool/UK, I.Ryder@liverpool.ac.uk

The February 21, 2008, Mw 6.0 Wells, Nevada, earthquake was well recorded by the NSF EarthScope Transportable Array (TA). This event occurred in an area with historically low seismicity, and unfortunately due to its proximity to the town of Wells, it inflicted considerable damage to the unreinforced masonry buildings of the historic district. We use broadband, three-component displacement records from the TA and InSAR displacements to invert for kinematic finite source models. The seismic moment tensor analysis shows that this event occurred on a northeast striking normal fault, and preliminary finite-source analysis shows that the causative structure is the east-dipping fault plane. The rupture appears to be bilateral however slip to the southwest, in the direction of Wells, Nevada, was appreciably higher. We investigate the sensitivity of the finite-source solutions to the fault geometry, and the distribution of available data. Unfortunately there were no near-source strong motion stations, however we demonstrate that the finite-source model obtained from regional distance records may be used to effectively simulate the level of strong ground motion (peak ground velocity) in the near-fault region. Additionally, we relate simulated ground motions for the town of Wells with observations of heavy object sliding and damage patterns.

Joint Inversion of Rayleigh Wave Ellipticity and Spatial Autocorrelation Measurements

HOBIGER, M., LGIT, CNRS, Université J.Fourier, Grenoble, France, manuel.hobiger@obs.ujf-grenoble.fr; CORNOU, C., LGIT, IRD, CNRS, U. J. Fourier, Grenoble, France, cecile.cornou@obs.ujf-grenoble.fr; LE BIHAN, N., CNRS, GIPSA-Lab, Grenoble, France, nicolas.le-bihan@gipsa-lab.inpg.fr; ENDRUN, B., Inst. of Geosciences, U. Potsdam, Potsdam, Germany, endrun@geo.uni-potsdam.de; RENALIER, F., LGIT, CNRS, Université J. Fourier, Grenoble, France, florence.renalier@obs.ujf-grenoble.fr; DI GIULIO, G., INGV, ITSAK, Thessaloniki, Greece, giuseppe.digiulio@ingv.it; SAVVAIDIS, A., ITSAK, Thessaloniki, Greece, alekos@itsak.gr; WATHELET, M., LGIT, IRD, CNRS, U. J. Fourier, Grenoble, France, marc.wathelet@obs.ujf-grenoble.fr; BARD, P.-Y., LGIT, LCPC, CNRS, U. J. Fourier, Grenoble, France, pierre-yves.bard@obs.ujf-grenoble.fr

The local soil structure (*i.e.* shear and pressure wave velocities) can be obtained by inversion of dispersion curves ranging over a sufficiently large frequency band. However, measurements of such dispersion curves using ambient seismic vibrations require a large number of seismometers and a long measuring time.

As a simple alternative, we propose to invert Rayleigh wave ellipticity obtained by ambient seismic noise measurements at a single site using a method based on the random decrement technique (Hobiger *et al.*, 2009). Indeed, the fre-

quency-dependency of Rayleigh wave ellipticity is tightly related to the shear wave profile of the soil.

However, as different soil structures can result in the same ellipticity curve (*e.g.* homothetic structures in velocity and thickness), the inversion of ellipticity curves alone is ambiguous. Therefore, additional measurements fixing the shear-wave velocity in the superficial layers have to be included into the inversion process. We suggest using a small number of seismic stations to measure spatial autocorrelation curves. In this way, three seismic sensors and one hour of measurements can be sufficient to invert the local soil structure.

We will present the method to extract the Rayleigh wave ellipticity curve, show which parts of the ellipticity curve have to be included in the inversion process and demonstrate the benefit of the additional spatial autocorrelation curve measurements. Then, we will present an example application to real noise data collected within the framework of the European NERIES project at well-known European accelerometric sites and the results will be compared to the inversion of broad frequency-band dispersion curves at the same sites.

Seismic Imaging: Recent Advancement and Future Directions

Poster Session · Wednesday AM, 21 April · Exhibit Hall

Characterization of the Closely-Spaced Earthquakes along the North Anatolian Fault Zone, NW Turkey

BULUT, F., Helmholtz Centre Potsdam GFZ, Potsdam/Germany, bulut@gfz-potsdam.de; BOHNHOFF, M., Helmholtz Centre Potsdam GFZ, Potsdam/Germany, bohnhoff@gfz-potsdam.de; ELLSWORTH, W.L., U.S. Geological Survey, Menlo Park /California / USA, ellsworth@usgs.gov; DRESEN, G., Helmholtz Centre Potsdam GFZ, Potsdam/Germany, dre@gfz-potsdam.de

Investigating the location and source properties of earthquakes using relative seismological techniques reduces the influence of wave propagation and site effects on seismic data yielding significant improvement in the measurements. We search for earthquakes with similar waveforms in order to identify spatiotemporal clusters as well as repeating earthquakes along the 1999 Izmit rupture zone and its transition into the Sea of Marmara region. Earthquakes in each cluster are relocated inverting cross-correlation derived relative travel times using the double-difference method in order to characterize the spatiotemporal distribution of co-located microearthquakes with a relative location accuracy comparable to or better than the source size. High-precision relative hypocenters define the geometry of each fault patch, permitting a better understanding of fault kinematics and their role in local-scale seismotectonics along the region of interest. Earthquake source parameters are measured using the multi-window spectral ratio technique (MWSR). The technique eliminates the effect of radiation pattern and path terms for co-located events. Spectral-ratio-derived source parameters are also used to determine path-averaged Q for each cluster by finding the value of Q that restores the raw spectrum to the ω-squared model with the corner in the location determined by the MWSR method. The most developed sequence we observed represents a NNW-SSE oriented 78° SW dipping splay fault that is neighboring the northernmost segments of NAFZ in Çınarcık Basin. The failure has initiated at the junction that connects the splay fault to the main branch of NAFZ and then systematically migrated into the splay fault within 20 hours. The results show that the temporal sequences represent the failure of adjacent fault patches, and do not indicate a repetitive failure of a particular area. We observe the migration of earthquakes at rates of 0.7 to 2.3 km/day.

SORD as a Computational Platform for Earthquake Simulation, Source Imaging, and Full 3D Tomography

WANG, F., Univ. of Southern California, Los Angeles/CA/United States, fengw@usc.edu; ELY, G.P., Univ. of Southern California, Los Angeles/CA/United States, gely@usc.edu; JORDAN, T.H., Univ. of Southern California, Los Angeles/CA/United States, tjordan@usc.edu

Earthquake simulations in 3D structures are currently being used for forward prediction of ground motions, imaging of sources, and structure refinement (full-3D tomography). The computational platform for such simulations requires the accurate location of sources and receivers within the computational grid; the flexibility to represent geological complexities, such as topography, non-planar faults, and other distorted surfaces; and the facility to calculate 3D Fréchet kernels for source and structural perturbations. We are adapting the Support Operator Rupture Dynamics (SORD) code for these purposes. SORD is an efficient numerical code developed by Ely, Day, and Minster (2008), which employs a structured but distortable mesh that can handle non-planar surfaces, such as topography. We represent point sources of arbitrary location as mesh-distributed sources of finite duration that match the travel-time and amplitude centroids of radiated waves; similarly, we represent receivers as centroid-preserving summations on a distributed mesh. We compute synthetic seismograms for a 3D reference model of Southern California that includes topography and compare the travel-times and amplitudes with those computed for 3D Cartesian-mesh models, such as the "squashed topography" approximation in common use, and we show the differences can be significant in tomographic inversions. We use SORD and scattering-integral method (Chen et. al. 2007) to calculate 3D structural (Fréchet) kernels, and illustrate their use in obtaining a physical understanding of seismic wave interference, excitation, and amplification in sedimentary basins, such as Los Angeles basin.

The Crustal and Uppermost Mantle Structure of Iran from 3D Seismic Tomography

SUN, Y., MIT, Cambridge, MA, USA, youshun@mit.edu; ZENG, X., University of Science and Techno, Hefei, Anhui, China, zeng.xfang@gail.com; TOKSOZ, M.N., MIT, Cambridge, MA, USA, toksoz@mit.edu

Iran is one of the most seismically active intra-continental regions. In the north, earthquakes occur throughout the crust along the Alboz fold belt. Two nation-wide seismic networks (Iranian Seismic Telemetry Network and Iran National Seismic Networks) have been installed in recent years. In total, 97 stations routinely report arrivals of events in the country and surrounding regions. Most travel-time data are at local and regional distances so that it is possible to obtain more accurate locations of earthquakes. We combined the catalogues from ISTN and INSN and relocated more than 26,000 events using about 150,000 P-wave arrivals and 70,000 S-wave arrivals and 1D P- and S-wave velocity models. This dataset contains ten times more data than the one we previously used, and therefore improves the resolution of 3D tomography. We then employed 3D travel-time tomography to invert the crust and upper most mantle seismic structure and to improve the accuracy of earthquake location. The result reveals a clear high velocity boundary along the Zagros suture. The high velocity anomaly beneath the Caspian Sea suggests an oceanic crust. The most remarkable low velocity zone is the Lesser Caucasus, where many quaternary volcanoes are located. The central Iranian microplate appears as a low velocity zone.

Seattle Basin Shear-Velocity Model from Noise Correlation Rayleigh Waves

DELOREY, A.A., University of Washington, Seattle, WA USA, adelorey@uw.edu; VIDALE, J.E., University of Washington, Seattle, WA USA, john_vidale@mac.com

Much of Seattle, Washington lies atop a deep sedimentary basin. The Seattle Basin amplifies and distorts the seismic waves from nearby moderate and large earthquakes in ways that modulate the hazard from earthquakes. Seismic hazard assessments heavily depend upon upper crustal and near-surface S-wave velocity models, which have traditionally been constructed from P-wave models using an empirical relationship between P-wave and S-wave velocity or by interpolating across widely spaced observations of shallow geologic structures. Improving the accuracy and resolution of basin S-wave models is key to improving seismic hazard assessments and predictions for ground shaking.

Tomography, with short-period Rayleigh waves extracted using noise interferometry, can refine S-wave velocity models in urban areas with dense arrays of short period and broadband instruments. We apply this technique to the Seattle area to develop a new shallow S-wave model for use in hazard assessment. Continuous data from the Seismic Hazards in Puget Sound (SHIPS) array have inter-station distances that range from a few, to tens of kilometers. This allows us to extract Rayleigh waves between 2 and 10 seconds period that are sensitive to shallow basin structure. Our results show that shear wave velocities are about 25% lower in some regions in the upper 3 km than previous estimates and align more closely with surface geological features and gravity observations.

We validate our model using several locally recorded earthquakes and make predictions on the levels of shaking at different regions around Seattle during likely future events using a finite difference code. Our results can be used to update seismic hazard maps for Seattle and can be reproduced in other urban areas with dense arrays of short period and broadband instruments.

Testing Global 3D Travel Time Prediction for Earthquake Location

BEGNAUD, M.L., Los Alamos National Laboratory, Los Alamos, NM USA, mbegnaud@lanl.gov; BALLARD, S., Sandia National Laboratories, Albuquerque, NM USA, sballar@sandia.gov; ROWE, C., Los Alamos National Laboratory, Los Alamos, NM USA, char@lanl.gov; YOUNG, C., Sandia National Laboratories, Albuquerque, NM USA, cjyoung@sandia.gov; STECK, L., Los Alamos National Laboratory, Los Alamos, NM USA, lsteck@lanl.gov; HIPP, J., Sandia National Laboratories, Albuquerque, NM USA, jrhipp@sandia.gov

Three-dimensional (3D) velocity models are being more readily developed with the improvements to computer processing speeds and multi-core functionality.

Normally 3D models are developed to investigate global crustal and mantle structures and not to improve event location accuracy. Historically, the use of these structurally-oriented 3D models, those that have not been optimized for location improvements, have not displayed the increased location accuracy over standard one-dimensional (1D) models that would warrant the time and speed required to use them for standard relocation studies.

We have developed a 3D global tomography model using P phases specifically addressing the problem of improving event location accuracy. We describe the travel-time prediciton and location capabilities of this model over standard 1D models. We perform location tests on 42 events in Eurasia with ground truth levels of 5 km or better. These events generally posess hundreds of Pn and P phases from which we can generate different realizations of station distributions, yielding a range of azimuthal coverage and proportions of teleseismic to regional arrivals, with which we test the robustness and quality of relocation. The 3D model reduces mislocation over standard 1D ak135, especially with increasing azimuthal gap. The 3D model appears to perform best for locations based solely or dominantly on regional arrivals, which is not unexpected given that ak135 represents a global average and cannot therefore capture local and regional variations. We also plan to perform location tests on a 3D model based on the EHB global data set and compare them to the model based on our existing data.

Global 3-D P-Wave Tomography with Teleseismic and Regional Travel Time Prediction Capabilities

SIMMONS, N.A., Lawrence Livermore National Lab, Livermore, CA USA, simmons27@llnl.gov; MYERS, S.C., Lawrence Livermore National Lab, Livermore, CA USA, myers30@llnl.gov; JOHANNESSON, G., Lawrence Livermore National Lab, Livermore, CA USA, Johannesson1@llnl.gov

We are developing a global tomography model of the mantle and crust in order to accurately predict travel times for P-wave arrivals at both teleseismic and regional distances. Three-dimensional ray tracing is a requirement to achieve accurate travel time predictions necessitating characterization of discontinuous boundaries such as the Moho. We explicitly represent undulating and discontinuous velocity discontinuities within a modeling framework that allows for direct representation of such surfaces while facilitating rapid model referencing. Namely, the model space is parameterized with sets of nodes along vertices defined by triangular tessellations of a spherical surface. The tessellation-based model architecture is hierarchical in that fine node sampling is achieved by recursively subdividing a base-level tessellation. Determining the required node spacing to effectively model a given set of data is problematic, given the covariant nature of seismic data and the differing wavelengths of actual seismic heterogeneity. With this in mind, we have developed an inversion process called Progressive Multi-tier Tessellation Inversion (PMTI) that takes advantage of the hierarchical nature of the tessellation-based design. PMTI allows the data to drive model resolution by progressively solving for shorter wavelength structure, thereby robustly imaging regional trends and allowing details to emerge where resolution is sufficient. Using the PMTI approach, we have developed a global-scale P-wave model that simultaneously predicts teleseismic P wave arrivals and regional Pn arrivals throughout the Middle East. Prepared by LLNL under Contract DE-AC52-07NA27344.

Determination and Validation of Regional 3-D Crust and Upper Mantle Vp and Vs Models and Their Tectonic Implications—Case Example from the Taiwan Region

CHIU, J.M., CERI, The University of Memphis, Memphis, TN USA, jerchiu@memphis.edu; KIM, K.H., KORDI, Ansan, Korea, kwanghee@kordi.re.kr; HUANG, B.S., IES, Academia Sinica, Nankang, Taipei Taiwan, hwbs@earth.sinica.edu.tw; CHEN, K.C., IES, Academia Sinica, Nankang, Taipei Taiwan, chenkc@earth.sinica.edu.tw; LIANG, W.T., IES, Acadmia Sinica, Nankang, Taipei Taiwan, wtl@eaarth.sinica.edu.tw; YEN, H.Y., IG, National Central University, Chung-Li, Taiwan, yenhy@earth.ncu.edu.tw; PUJOL, J., DES, The University of Memphis, Memphis, TN USA, jpujol@memphis.edu

A comparison of P-wave travel time residuals between local crust and anti-pole events reveals that lateral variation of upper crust contribute to most of the observed residuals. A successful understanding and quantification of upper crust structure is essential for a reliable determination of 3D crust and upper mantle velocity structure. Synthetic P and S station corrections can be obtained from a JHD analysis of the calculated travel times from local events via 3D model to stations. Similarities between the observed and the synthetic P and S station corrections provide the first validation that the resultant 3-D models are close to the real earth. The 3-D velocity model can also be converted to a 3-D density model from which the expected gravity at sea level can be calculated. The observed and calculated Bouguer gravity anomaly can then be compared to further validate the closeness of the resultant 3-D models to the real earth. We applied the above approaches to the Taiwan region. Spatial patterns and lateral variations of gravity anomalies derived from the two independent geophysical data sets agree exceptionally well in most areas. All earthquakes in the catalog are relocated using the resultant 3-D models. Tectonic implications of the resultant 3-D models and relocated hypocenters can thus be explored. The high mountains are characterized by deep root, ~55–60 km, and brittle active upper crust and ductile aseismic mid to lower crust. The Central Range is bounded by two high angle thrust faults extending from near surface to ~30 km. The continental and oceanic crust deformed across the north-south trending collision suture in eastern Taiwan beneath which crustal thickness is relatively thin, ~23 km. Thus the excessive heat from the collision and the elevated upper mantle may play an important role in the tectonic evolution of the Taiwan region.

Ground Motion: Observations and Theory

Poster Session · Wednesday AM, 21 April · Exhibit Hall

Experimental Evidence of Inhomogeneous P Wave at Very Low Strain

MARCELLINI, A., CNR-IDPA, Milano, Italy, alberto.marcellini@idpa.cnr.it; TENTO, A., CNR-IDPA, Milano, Italy, alberto.tento@idpa.cnr.it; DAMINELLI, R., CNR-IDPA, Milano, Italy, rossella.daminelli@idpa.cnr.it

Particle motion of body waves allows to differentiate between dissipative and non dissipative soil type. Particularly relevant is to establish the strain threshold between elastic and non elastic soil behavior and, in case of the presence of anelasticity, to check the reliability of simple models. In the present paper we analyse the records of two superficial open quarry explosions of unexploded 2nd world war bombs dropped by Allies air raid, recently rescued at a few meters depth close to Milano Central station. The seismic stations located at 2.5 km and 550 m epicentral distance, respectively, show a clear separation between body waves and surface waves.

The results show: 1) despite the low strain (max strain not exceeding 10^{-7}) elastic approx is not applicable; 2) the data evidence a clear elliptical prograde P wave particle motion with g greater than 0 and less than 30 degrees (g is angle between the **P** propagation and the **A** attenuation vector, **P** precedes **A**); 3) the Homogeneous Isotropic Linear Viscoelastic model is sufficient to describe conveniently this inhomogeneous P wave motion.

Response Spectra of Probable Ground Motions for Nonlinear Analysis of Systems

MALHOTRA, P.K., FM Global, Norwood, MA, USA, Praveen.Malhotra@FMGlobal.com

In a conventional seismic analysis, the input motion is defined either by a probabilistic response spectrum or by ground motion histories whose spectra 'match' the probabilistic response spectrum. In both cases, it is implicitly assumed that the system input of certain probability will produce system output of the same probability. This assumption is not strictly valid for nonlinear systems. A more accurate way of using the response spectrum in the probabilistic analysis of nonlinear systems is presented. First, the spectra of probable ground motions at a site are generated from the site-specific hazard curves. These spectra are used to generate the probabilistic response curves corresponding to the probabilistic hazard curves for the site. It is shown that the conventional use of a 500-year mean return period (MRP) response spectrum in nonlinear analysis produces responses which have longer MRPs.

Strong Motion Recordings and Residual Displacements: What Are We Actually Recording in Strong Motion Seismology?

GRAIZER, V., US Nuclear Regulatory Commission, Washington, DC, USA, Vladimir.Graizer@nrc.gov

A number of recent publications on strong motion data processing ignore the complexities involved when calculating residual displacements by double integrating strong motion accelerograms. Double integration of equations of pendulums results in a mixture of translational displacement and double integrated tilt. It was demonstrated that tilt contributes the most "undesirable" effects on the low frequency component of ground motion and specifically residual displacement. I am presenting a summary of previous papers and a summary of the associated problems so that researchers may take into account some of the nuances involved in strong motion data processing. My aim is to show that to do justice to strong motion data processing a more in depth appreciation of some of the principles behind the instrumentation used and the data processing involved is essential. I don't intend to discourage researchers from calculating residual displacements, but to encourage thoughtful consideration, including any necessary justification (*e.g.*, additional GPS information or simultaneous recording of rotations) as an aid to reliability. To bear in mind that in the first approximation the strong motion instruments are sensitive to tilts, and that the records contain errors. In general, the best is to combine measurements of translational and rotational strong motion to recover reli-

able residual displacements based on the integration of accelerograms. To achieve reasonably reliable estimates of "true" ground displacement including residual from strong motion accelerograms one need to:

• Clean the record from tilts or demonstrate that tilts are negligible using the information obtained from rotational sensors or some other means;

• Perform a "quality" check of the record showing that it satisfies requirements to the signal-to-noise ratio;

• Integrate the record applying baseline correction, for example by using the "quiet" intervals at the beginning and at the end of the record.

'Domitoring': First Results of the Seismic Surveillance of Cologne Cathedral

HINZEN, K.-G., Cologne University, Cologne, Germany, hinzen@uni-koeln.de; FLEISCHER, C., Cologne University, Cologne, Germany, claus.fleischer@uni-koeln.de; SCHOCK-WERNER, B., Dombauverwaltung Köln, Cologne, Germany, barbara.schock.werner@dombauverwaltung-koeln.de

In 2006, a strong motion network in the Lower Rhine Embayment (LRE), NW Germany was established. The 19 free field stations were recently supplemented by five strong motion stations within Cologne Cathedral, one of the largest Gothic cathedrals in the World and a world heritage monument since 1996. One station is located in the archaeological excavation in the cathedral basement, 7 m below the floor, on natural ground. A second station has been installed on top of the vault of the nave above the chorus, and three are at the 70, 100 and 130 m levels, respectively, of the northern tower. At 157.38 m, the northern cathedral tower is the second tallest in Europe. While the main goal is the recording of local earthquake motions within the building, other phenomena are detectable with the continuous, synchronized records of the five accelerometer stations.

The largest free-swinging bell, the Petersglocke rings only on special occasions (*e.g.* Christmas, New Year, death of the Pope). The 24 t bell is located at the 55 m level in the southern tower. The motions induced by the swinging bell are recordable throughout the cathedral, including the basement and the northern tower. The period of the swinging bell is 3.6 s. In the northern tower, the spectral amplitudes of the second harmonic dominate the spectrum. With 1.2 s it is in between the first two EW-eigenperiods of 1.31 s and 1.04 s of the tower.

Since the Cathedral is located adjacent to the Cologne main train station, regularly scheduled trains can be utilized as a 'seismic control' by taking the train signals to calculate stacked transfer functions between the basement and the four other cathedral measuring locations.

Records of teleseismic and micro earthquakes show that these can be detected under and within the building even though it is founded on the sediments of the LRE and located right in the center of the city.

Seismologic Methods, Techniques, and Theory

Poster Session · Wednesday AM, 21 April · Exhibit Hall

Seismological Attenuation Coefficient and Q

MOROZOV, I.B., University of Saskatchewan, Saskatoon, SK, Canada, igor.morozov@usask.ca.

Despite its long history, broad acceptance, and widespread use in attenuation studies, quality factor Q cannot be unambiguously associated with a property of energy dissipation in propagating medium. Energy dissipation is related to multiple external factors such as fracturing, fluid content and saturation, viscosity, porosity, permeability, "tortuosity," and distributions of scatterers. All of these factors cannot be lumped in an unambiguous Q^{-1} included in the elastic moduli, as it is often assumed in visco-elastic models.

By contrast to Q, the attenuation coefficient, χ, represents a much more consistent property of energy dissipation. This quantity can be modeled and also is directly and unambiguously measured in most practical cases. The conventional transformation of χ into the apparent $Q = \pi f/\chi$ (where f is the frequency) makes Q a phenomenological attribute of the wave. and also leads to its built-in positive frequency dependence. Such strong positive $Q(f)$ is often reported, particularly for the "scattering Q," yet it may be entirely due to a frequency-independent, "geometrical" γ. Two theoretical models of such geometrical attenuation are presented here: 1) caused by ray bending in an arbitrary, smoothly varying medium, and 2) caused by plane-wave reflectivity at normal incidence.

In seismological observations, linear frequency dependencies of the attenuation coefficient $\chi(f) = \gamma + kf$ were observed for many wave types within several subbands from ~500 s to 100 Hz. The geometrical attenuation parameter γ systematically correlates with tectonic types of the lithosphere. Notably, γ is consistently positive for body and surface waves and negative for normal modes, which leads to the apparent absorption band of the Earth. Therefore, frequency-dependent in-situ Q is not required in order to explain the observations.

Wave Equations in Nonlinear Elastic Anisotropic Randomly Inhomogeneous Media

CHESNOKOV, E.M., University of Houston, Houston, TX, USA, emchesno@mail.uh.edu; KUKHARENKO, Y.A., IFZ, Moscow, Russia, emchesno@mail.uh.edu; GONCHARUK, S., Moscow University, Moscow, Russia, vya-goncharuk@yandex.ru.

This paper presents a theoretical investigation of wave propagation in randomly inhomogeneous anisotropic media with large initial stresses An exact expression for the mean value of elastic constants of a deformed medium have obtained. The Feynman diagram technique developed in quantum field theory was used for operating with diverging infinite series. The elastic body wave velocity dependency on the initial stress of the medium is also investigated in this paper.

Smoothing-Free Earthquake Source Inversion: Physically-Guided Regularization in Finite Fault Modeling

SONG, S., URS Group, Inc., Pasadena/CA/USA, seok_goo_song@urscorp.com; SOMERVILLE, P., URS Group, Inc., Pasadena/CA/USA.

Kinematic rupture models constrained by inverting geophysical data are important resources to understand many aspects of earthquake source physics. Detailed knowledge about the kinematics of the earthquake source process is critical for inferring rupture dynamics, for building source models for ground-motion simulation, and for studying earthquake mechanics in general. However, source-inversion results for past events exhibit large intra-event variability for models developed by different research teams for the same earthquake. This variation among rupture models has raised questions about their reliability. Most kinematic source inversion problems are very ill-posed because of insufficient data. Tikhonov regularization (*e.g.*, minimum norm or smoothing) is often used in order to improve the instability of the inversion. But this non-physical regularization may prevent us from performing physical interpretation of inversion results. In this study we replace the Tikhonov regularization with more physics-based regularization, such as mean and standard deviation of earthquake slip and its auto-coherence. We tested this idea with the 1999 Izmit, Turkey, event by inverting both geodetic and seismic data, and found that the stability of ill-posed inverse problems can be achieved without non-physical smoothing constraints. The strength of this new approach is that physics-based regularization enables us to do more physics-based interpretation of inversion results, avoiding contamination introduced by non-physical regularization. This new approach may help us to understand how data shape a rupture model in a more physics-based way.

Determining the Focal Mechanisms of Earthquakes in Southern California by Full Waveform Modeling

BUSFAR, H.A., MIT, Cambridge, MA, United States of America, busfarha@mit.edu

Determining the focal mechanism of earthquakes help us to better characterize reservoirs, define faults, and understand the stress and strain regime. The objective of this paper is to find the focal mechanism and depth of earthquakes. This objective is met using a full waveform modeling method in which we generate synthetic seismograms using a discrete wavenumber code to match the observed seismograms. We first calculate Green's functions given an initial estimate of the earthquake's hypocenter, the locations of the seismic recording stations, and the velocity model of the region for a series of depths with intervals of 1 km. Then, we calculate the moment tensor for 6840 different combinations of strikes, dips, and rakes for each of those depths. These are convolved with Green's function and with an assumed smooth ramp source time function to produce the different synthetic seismograms corresponding to the different strikes, dips, rakes, and depths. We use a grid search in order to find the synthetic seismogram, with the combination of depth, strike, dip, and rake, that best fits the observed seismogram. These parameters will be the focal mechanism solution of an earthquake. We tested the method using four earthquakes in Southern California. Their locations, depths, and source mechanisms were determined using data from a multitude of stations. The results show a very good match between the synthetic and observed seismograms. The main advantage of this method is that we use relatively high frequencies, which makes it possible to find the focal mechanism and depth of earthquakes using as few as two stations when the velocity structure is known.

Multiwavelet Seismic Wave Gradiometry: Application to the Glendora Array, Sullivan, IN, USA

POPPELIERS, C., Augusta State University, Augusta, GA, USA.

This poster describes new developments in seismic wave gradiometry. This work follows previous work on time-domain wave gradiometery, but proposes applying a multi-wavelet transform to the data prior to wave gradiometric analysis. The result from this approach is that we can estimate the wave's time- and frequency-dependent vector slowness and geometrical spreading as well calculating formal uncertainty

estimates at each time/frequency point. This new approach is demonstrated by analyzing two underwater shots that were recorded by a portion of the Glendora Array. The Glendora site is a former surface coal mine that has subsequently been filled by mine tailings, and as such forms an artificial sedimentary basin in which the geometry is well known. The array used for the analysis was located in a corner formed by the intersection of two vertically oriented boundaries between mine tailings and the surrounding bedrock. The analysis of the data revealed the presence of typical body waves and surface waves, in addition to several phases that are interpreted to be 1) reflections of surface waves off of the vertical tailings/bedrock boundaries, 2) surface waves generated by the interaction of direct-arrival water-born acoustic waves with the water/tailing interface (the lake shore), and 3) the interaction of other water-born acoustic waves in Glendora lake with other water/tailing interfaces. The surface waves are highly time- and frequency dependent and highlight the extreme complexity of surface wave propagation in geologically complex areas.

A Bayesian Method for Single-Station Identification of Local and Regional Earthquake

EBEL, J.E., Weston Observatory/Boston Colleg, Weston, MA USA, ebel@bc.edu

For several years, the New England Seismic Network of Weston Observatory has been using a wavelet-transform method to detect and identify earthquake waveforms in the New England region. For each detection, the time, scale (*i.e.*, predominant period) and energy of the beginning of the event detection are found, along with the time, scale and energy of the highest energy in the detection waveform and the time of the end of the detection. From these seven detection parameters, an identification from among the following event types is made based on a Bayesian probability scheme: teleseismic P wave, regional earthquake, local earthquake, quarry blast, or noise transient. From a single station detection of these parameters, the origin time, epicentral distance, coda magnitude Mc and Lg magnitude MLg of the event can be estimated. An improved method for making regional and local earthquake identifications has been developed using training data from over 150 station detections from New England and vicinity. The Bayesian probability identifications of local and regional earthquakes are based on the training-data distributions of the scales and energies of the detection beginnings and peak energies. The method also takes into account the relative values of Mc and MLg for the detections. Most local and regional earthquake detections are properly identified using this Bayesian identification method.

Toward Using Eccentric Mass Shakers for Active Seismic Monitoring

NIU, F., Rice University, Houston/Texas/USA, niu@rice.edu; SILVER, P., Carnegie Institute of Washington, Washington/DC/USA, silver@dtm.ciw.edu; NIGBOR, R., University of California at LA, Los Angeles/California/USA.

4D (Time-lapse 3D) seismic imaging using either passive or active sources is a promising technique to investigate tectonic processes. A key issue in active seismic monitoring is the selection of a low-frequency source with high repeatability and sufficient strength. We have performed two pilot studies using large eccentric mass shakers from NEES@UCLA. In a pilot experiment at Parkfield we were able to record sine sweeps from the largest shakers, ANCO MK-15's with 100,000 lb maximum force, at distances up to ten kilometers. The stacked Green's function obtained from the sweeps matches well with previous collocated shot records, suggesting a suitable source for investigating structural changes at seismogenic depths. Episodic Tremor and Slip (ETS) is arguably the most interesting phenomenon in Earthquake seismology in many years. It has been speculated that there is fluid flow at the time of ETS, which is testable with 4D seismic investigations. We conducted another pilot experiment in the Cascadia region during the 2009 ETS event, again using the NEES@UCLA shakers. We built a 15'x15'x3' cement pad on basaltic bedrock to couple the shaker, and deployed arrays of short period instruments at 30km and 90km. In addition to weeks of shaker data, we also recorded a quarry blast near our shaker source. The observed blast seismograms indicate that we can observe direct Pg, Sg as well as record and identify reflections from the oceanic Moho, PmPo and SmSo by beam forming. Preliminary results for the shaker source data indicate that the Green's function calculated with an n-th root stack of 80 hours of data at 90km agrees reasonably well with the shot data, both showed the target Moho reflections. This suggests that it may be possible to monitor deep changes associated with an ETS event seismically using a large eccentric mass shaker source.

Thermal Anomalies Identification and Analysis of Several Earthquakes in Sichuan, China

ZHAO, J., School of Geography, BNU, Beijing, China, donquixote797970@gmail.com; ZHANG, W., School of Geography, BNU, Beijing, China, wumingz@bnu.edu.cn; WANG, W., School of Geography, BNU, Beijing, China; YAN, G., School of Geography, BNU, Beijing, China; MU, X., School of Geography, Beijing, China.

In this study, meteorological data is combined with remote sensing images to detect and analyze the thermal anomalies related to earthquakes in Sichuan, China. Taking into consideration of various factors (such as seismic types and temporal availability of data), four major earthquakes are selected: Yajiang (2001, Ms5.4&6.3), Maerkang (2005, Ms5.1), Wenchuan (2008, Ms8.0) and Pingwu (2008, Ms6.1). Based on Split-Window algorithm (Beck &Li), we retrieve the long-term LST maps from thermal infrared data of polar-orbited NOAA-AVHRR (from one month before to after each earthquake). Besides, images of geostationary meteorological FY series satellites are used to obtain short-term LST maps with higher temporal resolution on seismic days. These maps clearly show the temperature changed in the vicinity of every epicenter. To ascertain that these changes were due to corresponding earthquakes instead of normal climate variation, analysis of meteorological data is conducted with HHT algorithm (Hilbert-Huang Transform). For each case, IMFs (intrinsic mode function) are extracted from daily average temperature data of six surrounding meteorological stations in a period of ten years before earthquake and the seismic year, and then Hilbert transform is applied to each IMF component. Subsequently, the energy distribution of signal is obtained. Based on the distribution contrast, signal changes caused by earthquake can be distinguished and co-analyzed with LST maps. The results indicate: 1) these large-area abnormal temperature changes relate to earthquake; 2) the period, pattern and amplitude of thermal anomalies have certain relationship with seismic depth and magnitude; 3) this method of combining ground and satellite thermal data can be applicable to other foggy area like Sichuan.

Numerical Prediction of Earthquake Ground Motion

Poster Session · Wednesday PM, 21 April · Exhibit Hall

Numerical Modeling of 3D Wave Propagation in the Grenoble Valley (French Alps) with Special Reference to the Duration Observed for Local Seismic Events

CHALJUB, E., LGIT,CNRS,J. Fourier Univ., Grenoble/France, Emmanuel.Chaljub@obs.ujf-grenoble.fr; CORNOU, C., LGIT,CNRS,IRD,J. Fourier Univ., Grenoble/France, Cecile.Cornou@obs.ujf-grenoble.fr; TSUNO, S., LGIT,CNRS,J. Fourier Univ., Grenoble/France, Seiji.Tsuno@obs.ujf-grenoble.fr

Located in a Y-shaped alpine valley filled with hundreds of meters of late quaternary deposits, the city of Grenoble is subject to important amplification and lenghtening of duration of seismic ground motion. In order to better understand these particular site effects and to predict realistic strong ground motion, we have developed a 3D numerical approach based on the Spectral Element Method.

We use a simple model of the Grenoble valley, defined by a 1D velocity model for the sediment cover and a homogeneous layered bedrock. Intrinsic attenuation is modeled by a constant shear quality factor in the sediments. The three-dimensional geometry of the model is provided by the sediment-bedrock interface and by surface topography. We simulate the low-frequency ($f<2$ Hz) response of the Grenoble valley to local seismic events with magnitude $M<3$ and compare our results to the recordings of permanent and temporary seismic networks installed in the area.

While the level of amplification between sediment and rock sites is fairly reproduced, the duration of ground motion is found to be strongly underestimated in the numerical predictions. Next, we show how the duration of ground motion is affected by changes in the attenuation model and in surficial velocities. We find that the duration of ground motion can hardly be explained without assuming an increase of the quality factor with depth. Including low velocity surficial layers does not increase the duration as much as expected because the energy trapped in the near surface is more efficiently attenuated. Our results suggest that diffracted surface waves play an essential role in the observed duration and motivate further work to constrain the variations of intrinsic attenuation.

Euroseistest Numerical Simulation Project: Comparison with Local Earthquake Recordings for Validation.

CHALJUB, E., LGIT, Grenoble / France, emmanuel.chaljub@obs.ujf-grenoble.fr; BARD, P.Y., LGIT / LCPC, Grenoble / France, bard@obs.ujf-grenoble.fr; HOLLENDER, F., CEA Cadarache, Cadarache, France, fabrice.hollender@cea.fr; THEODULIDIS, N., ITSAK, Thessaloniki, Greece, ntheo@itsak.gr; MOCZO, P., Comenius University, Bratislava, Slovakia, Peter.Moczo@fmph.uniba.sk; TSUNO, S., LGIT, Grenoble, France, seiji.tsuno@obs.ujf-grenoble.fr; KRISTEK, J., Comenius University, Bratislava, Slovakia, Jozef.Kristek@fmph.uniba.sk; CADET, H., ITSAK, Thessaloniki, Greece, kdhelo@gmail.com; BIELAK, J., Carnegie Mellon University, Pittsburgh, USA

The ultimate goal of the Euroseistest verification and validation project is to assess the capability of numerical simulation to accurately predict seismic ground motion up to relatively high frequencies . This presentation will focus on the validation step, consisting in comparing numerical predictions with actual recordings up to 4 Hz.

The exercise has been performed for 6 local, weak to moderate magnitude events, spanning various azimuths, depth and distances, and recorded by a local array of 19 surface and borehole accelerometers. In general, while the detailed waveforms do not match, the overall amplitude, duration, and spectral shape exhibit a relatively satisfactory agreement. The level of agreement is however found to be event-dependent, as a combined result of the large sensitivity of waveform details to the source location and mechanism, the geometry of the sediment-basement interface, and the internal sediment layering, and of the uncertainties in the source parameters and basin structure. The best agreement is found indeed for the largest—and thus best known- event.

In order to remove the errors due to source parameter uncertainties, the instrumental site to reference spectral ratios derived from the available recordings were compared with those derived from 1D and 3D synthetics. The best fit is obtained for 3D simulations, which do account for both the broad band amplification due to lateral reverberations, and the scatter due to the sensitivity of the diffraction pattern to the source location. There is however a trend for underestimating the actual amplification, in probable connection with incorrect estimates of damping and internal sediment layering structure.

The next challenge in view of deterministic simulation of ground motion at intermediate frequency thus consists mainly in improving the performance of shallow geophysical investigations.

High-Frequency Generation in k^{-2} Kinematic Source Model

CAUSSE, M.C., LGIT and KAUST, Grenoble / France and Thuwal / Kingdom of Sandi Arabia, mathieu.causse@obs.ujf-grenoble.fr; LAURENDEAU, A.L., LGIT, Grenoble / France, aurore.laurendeau@obs.ujf-grenoble.fr; COTTON, F.C., LGIT, Grenoble / France, fabrice.cotton@obs.ujf-grenoble.fr; MAI, M.M., KAUST, Thuwal / Kingdom of Sandi Arabia, martin.mai@kaust.edu.sa

The high-frequency content of ground-motion is strongly sensitive to the small-scale slip distribution. For realistic ground-motion simulations due to future earthquakes, it is thus imperative to properly *a priori* estimate the slip roughness distribution. We then investigate different approaches for assessing the degree of roughness of the slip distribution of future earthquakes. First, we analyze a database of slip images extracted from a suite of 152 finite-source rupture models from 80 events (Mw=4.1–8.9). This results in an empirical model defining the distribution of the slip spectrum corner wavenumbers (k_c) as a function of moment magnitude. Besides, the robustness of the empirical model rests on a reliable estimation of k_c by kinematic inversion methods. We address this issue by performing tests on synthetic data with a frequency-domain inversion method. These tests reveal that due to smoothing constraints used to stabilize the inversion process k_c tends to be underestimated. We then develop an alternative approach: (1) we establish a proportionality relationship between k_c and the Peak Ground Acceleration (PGA), using a k^{-2} kinematic source model; (2) we analyze the PGA distribution, which is believed to be better constrained than slip images. These two methods reveal that k_c follows a lognormal distribution, with similar standard deviations for both methods. High frequency finite-source simulations are also highly sensitive to the frequency dependence of the directivity effects. Following, Bernard and Herrero (1994) and Boatwright *et al.*, (2002), we then analyze the frequency dependence of the directivity effects in the available ground-motion records of recent strike slip earthquakes.

Modeling of Scattering from the Pacific Trench of Mexico Excited by Teleseismic Body Waves

DOMINGUEZ-RAMIREZ, L., UCLA, Los Angeles, CA. USA, ladominguez@ucla.edu; SANCHEZ-SESMA, F., UNAM, Mexico City. Mexico, sesma@servidor.unam.mx; DAVIS, P., UCLA, Los Angeles, CA. USA, pdavis@ess.ucla.edu

We examine the role that the local topography-bathymetry plays on the propagation of seismic waves due to the Pacific trench of Mexico. Abrupt irregularities in the topography such as the subduction of the Cocos plate generate a region where the wave propagation of body waves is clearly affected by the ragged topography. Analysis of the seismic records from the Mesoamerican Seismic Experiment suggests the presence of a scattered field induced by S, PS, and SS phases generated by events at distances > 8000 km. We observed a topography-related phase coming out from trench when low frequency body waves from events with magnitude larger than Mw=7.0 occurred in the Tonga-Fiji and Scotia Sea regions hit the trench, diffraction of the incident field radiates energy inland in the form of crustal waves that propagate with little attenuation. Detection of the field was achieved by applying the Hough Transform to the seismic records and tracking back the scattered phase. We obtained a direct correlation between the incident field (body waves) and the surface waves generated by the difference in topography-bathymetry associated with the trench. The influence of the topography is studied by means of the indirect boundary element method (IBEM). In this study, we consider a model of two layers and a simplified topography to simulate the seismic response of the trench. Modeling of the scattered field provides insight on the diffraction of seismic waves throughout the continental crust and the seismic hazards associated with the topography.

Numerical Analysis of Earthquake Ground Motion in the Mygdonian Basin, Greece: Comparison of 2D Wave Propagation in Linear and Nonlinear Media

BONILLA, L.F., IRSN, Fontenay-aux-Roses, France, fabian.bonilla@irsn.fr; GELIS, C., IRSN, Fontenay-aux-Roses, France, celine.gelis@irsn.fr; FOERSTER, E., BRGM, Orleans, France, e.foerster@brgm.fr; MARIOTTI, C., CEA, Bruyeres-le-Chatel, France, christian.mariotti@cea.fr; PECKER, A., Geodynamique & Structures, Bagneaux, France, alain.pecker@geodynamique.com; STEINITZ, B., Bagneaux, France, benoit.steinitz@geodynamique.com; BARD, P.Y., LCPC, Grenoble, France, pierre-yves.bard@obs.ujf-grenoble.fr; TSUNO, S., LGIT, Grenoble, France, seiji.tsuno@obs.ujf-grenoble.fr; HOLLENDER, F., CEA, Cadarache, France, fabrice.hollender@cea.fr; PITILAKIS, K., AUTH, Greece, kpitilak@civil.auth.gr; MAKRA, K., ITSAK, Greece, makra@itsak.gr

Local site effects have long been recognized as an important factor contributing to the characteristics of ground motion. The main effects contemplate amplification, spatial variability, and increase of the ground motion duration among others. Given the scarcity of strong-ground motion records, most of empirical site effect studies are conducted using weak ground-motion, implicitly assuming linear material behavior. However, linear wave propagation studies need to be understood before going into more complex nonlinear analyses. In the case of having strong motions striking low-strength materials, shear modulus reduction and hysteretic damping occur. Their study is known as nonlinear site response.

The EURO-SEISTEST area is located in the epicentral area of June 20th 1978 Thessaloniki earthquake (Ms 6.5). The valley lies between the lakes of Volvi and Langada, 35 km from the city of Thessaloniki, and has an approximately E-W trend (6 km wide and 10 km long). Detailed geophysical and geotechnical information is available providing a fairly good 3D description of the valley. Furthermore, given the size of the model and the strong impedance contrast (S-wave speeds of 130 m/s for the shallower layer and 2600 m/s for the bedrock, respectively), the numerical modeling is challenging both in terms of memory and computation time.

Thanks to the geophysical and geotechnical description of the Volvi basin, we present 2D linear and nonlinear numerical modeling performed along the Stivos-Profitis profile (9400 m long and 300 m depth) in order to: 1) compute 2D wave propagation up to 8 Hz; 2) compare results from finite differences, finite elements, and discrete elements schemes; 3) compare different material rheologies; 4) compare results in terms of PGA, response spectra, and maximum shear deformation for the linear and nonlinear cases; and 5) analyze the effect of basin geometry and material characteristics on the horizontal and vertical components of ground motion.

Stable Discontinuous Staggered Grid in the 4th-order Finite-difference Modeling of Seismic Ground Motion

KRISTEK, J., Comenius University Bratislava, Bratislava, Slovakia, kristek@fmph.uniba.sk; MOCZO, P., Comenius University Bratislava, Bratislava, Slovakia, moczo@fmph.uniba.sk; GALIS, M., Comenius University Bratislava, Bratislava, Slovakia, martin.galis@fmph.uniba.sk

If the minimum wave speed in an upper part of a computational model is smaller than that in a lower part of the model it may be reasonable to use a discontinuous spatial grid with a finer part, with a grid spacing h, covering the upper part of the model and a coarser part, with a grid spacing H>h, covering the lower part of the model. A total number of grid points in such a grid can be significantly smaller than that in a uniform grid. This simple idea led modelers using grid methods, mainly the finite-difference (FD) method, to implement discontinuous grids.

A number of algorithms to include discontinuous spatial grid have been developed. They mainly differ in the allowed grid ratio H/h and the way they interpolate values in the missing grid positions in the coarser grid. In general, the larger H/h, the larger possibility of inaccuracy and, mainly, instability with increasing number of time steps. The interpolation itself does not play a key role. These aspects, however, are not often explicitly addressed in the publications, and the inevitable instabilities (in most cases) are only rarely admitted.

Two basic problems are to be solved. The obvious one is that of the missing grid points: how to update particle velocity and stress at grid points of the finer grid close and at the boundary of the finer grid. The other, and apparently not so obvious, problem is how to update particle velocity and stress at grid points of the coarser grid close and at the boundary of the coarser grid, that is, at those grid points of the coarser grid which coincide with grid points of the finer grid.

We present an algorithm of a stable discontinuous staggered-grid. The grid ratio H/h can be an arbitrary odd number. We demonstrate the stability and accuracy of the algorithm for large number of time steps, and for grid ratio as large as 19.

Seismic Wavefield Generated by SH Line Sources in Two Quarter Spaces with Scatterers Distributed around the Bimaterial Interface

BENITES, R.A., GNS-Science Ltd, Wellington, New Zealand, R.Benites@gns.cri.nz; BEN-ZION, Y., University of Southern CA, Los Angeles, CA 90089-0740, benzion@usc.edu

We develop a computational framework for simulating SH waves in a fault zone model consisting of two welded quarter spaces with various distributions of cracks around the interface separating the different media. The choice of SH line sources corresponds to the assumption of a strike-slip fault with rupture direction parallel to its strike (rake zero) and observations along lines perpendicular to it. Full waveform simulations for up to 15 Hz are performed in the time-domain, and incorporate the multiple scattering among the cracks, a vertical bimaterial interface and the free-surface. We use a Boundary Integral numerical scheme based on artificial wave-source distribution around the boundaries of all cracks [1], for which both the displacement and stress Green's functions due to each source are computed exactly using a kernel analytical solution derived by the Cagniard-de Hoop method [2]. Examined case studies include several realizations of crack distribution, where the cracks can be of equal or different aspect ratios and orientations. The results show head and body waves, expected from previous related models of a bimaterial interface separating two homogeneous quarter spaces, and the multiply scattered wavefield generated by the cracks. For wavelengths much larger than the cracks size, the presence of cracks appears to slow the waves and increase the seismic attenuation compared to the properties of the hosting medium.

References
[1] R. Benites, *et al.*, J. Acoust. Soc. Am., 86 (1992).
[2] Y. Ben-Zion, Geophys. J. Int., 98 (1989).

Numerical Modeling of Earthquake Ground Motion in the Mygdonian Basin, Greece: Verification of the 3D Numerical Methods

MOCZO, P., Comenius University Bratislava, Bratislava, Slovakia, moczo@fmph.uniba.sk; KRISTEK, J., Comenius University Bratislava, Bratislava, Slovakia, kristek@fmph.uniba.sk; FRANEK, P., Geophysical Institute SAS, Bratislava, Slovakia, geofpefr@savba.sk; CHALJUB, E., LGIT UJF, Grenoble, France, Emmanuel.Chaljub@obs.ujf-grenoble.fr; BARD, P.-Y., LGIT UJF, Grenoble, France, Pierre-Yves.Bard@obs.ujf-grenoble.fr; TSUNO, S., LGIT UJF, Grenoble, France, Seiji.Tsuno@obs.ujf-grenoble.fr; IWATA, T., DPRI Kyoto University, Kyoto, Japan, iwata@egmdpri01.dpri.kyoto-u.ac.jp; IWAKI, A., DPRI Kyoto University, Kyoto, Japan, iwaki@egmdpri01.dpri.kyoto-u.ac.jp; PRIOLO, E., INOGS, Trieste, Italy, epriolo@inogs.it; KLIN, P., INOGS, Trieste, Italy, pklin@inogs.it; AOI, S., NIED, Tsukuba, Japan, aoi@bosai.go.jp; MARIOTTI, C., CEA, Arpajon, France, christian.mariotti@cea.fr; BIELAK, J., CMU, Pittsburgh PA, USA, jbielak@cmu.edu; TABORDA, R., CMU, Pittsburgh PA, USA, rtaborda@cmu.edu; KARAOGLU, H., CMU, Pittsburgh PA, USA, hkaraogl@cmu.edu; ETIENNE, V., GEOAZUR, Nice, France, Vincent.ETIENNE@unice.fr; VIRIEUX, J., LGIT UJF, Grenoble, France, Jean.Virieux@obs.ujf-grenoble.fr

The capability of numerical methods to predict earthquake ground motion is investigated through the ongoing Euroseistest verification and validation project. The project focuses on the Volvi Mygdonian basin (Greece) which has been a subject of extensive geophysical and geotechnical investigations for more than two decades.

A new detailed 3D model of the basin (5 km wide, 15 km long, with maximum sediment thickness 400 m and minimum S-wave velocity 200 m/s) as well as recordings of local earthquakes by the Euroseistest instruments provide a reasonable basis for the verification and validation of the numerical methods.

Here we present the results of the verification phase of the project for 3D numerical methods. Numerical-modeling teams from Europe, Japan and USA employ the finite-difference method (FDM), finite-element method (FEM), global pseudospectral method (GPSM), spectral- element method (SEM), discrete-element method (DEM) and discontinuous Galerkin method (DGM).

The problem configurations include elastic and viscoelastic rheologies, basin models built from smooth velocity gradients or composed of three homogeneous layers, one hypothetical event and six local events with magnitude between 3 and 5. Numerical predictions for frequencies up to 4 Hz are compared using quantitative time-frequency envelope and phase goodness-of-fit criteria computed at 288 receivers. Solutions are also analyzed with respect to rheology, geometry of the interface and source parameters, and their representations in the computational models.

In particular, it is shown that the agreement between numerical predictions of ground motion duration strongly depends on the ability of each method to model accurately the surface waves diffracted off the basin edges and propagating within the basin.

Formulation and Implementation of the Spectral Element Method (SEM) for Elastodynamic Problems

MEZA-FAJARDO, K.C., U Nacional Autónoma de Honduras, Tegucigalpa, Honduras, kcmeza@upatras.gr; PAPAGEORGIOU, A.S., University of Patras, Patras, Greece, papaga@upatras.gr

Various numerical methods have been proposed and used to investigate wave propagation in realistic earth media. Recently an innovative numerical method, known as the Spectral Element Method (SEM), has been developed and used in connection with wave propagation problems in 3D elastic media (Chaljub *et al.* 2006).

The SEM combines the flexibility of a finite element method with the accuracy of a spectral method and, thus, it can readily deal with non-flat free surface and spatially variable anelastic attenuation. The SEM is a highly accurate numerical method that has its origins in computational fluid dynamics. One uses a weak formulation of the equations of motion, which are solved on a mesh of hexahedral elements that is adapted to the free surface and to the main internal discontinuities of the model. The wavefield on the elements is discretized using high-degree Lagrange interpolants, and integration over an element is accomplished based upon the Gauss-Lobatto-Legendre integration rule. This combination of discretization and integration results in a diagonal mass matrix, which greatly simplifies the time integration algorithm and ensures minimal numerical grid dispersion and anisotropy. Furthermore, it allows an efficient parallel computer implementation.

We present the formulation of the SEM in a matrix form that can readily be implemented in a computer code (Meza-Fajardo, 2007). The key to this implementation is the use of the 'Tensor (or Kronecker) Product' of matrices. [Orszag(1980) pointed out early on that tensor-product forms were the foundation for efficient implementation of spectral methods.] The use of the tensor product allows for a very compact and clear expression of the element matrices.

We demonstrate the efficiency and effectiveness of the method by implementing the proposed formulation to study various canonical problems of elastodynamics.

Moderate Earthquake Ground Motion Validation in the San Francisco Bay Area

DREGER, D.S., UC Berkeley, dreger@seismo.berkeley.edu; KIM, A., Schlumberger, AKim9@slb.com; LARSEN, S., Lawrence Livermore National Lab, larsen8@llnl.gov

We performed 3D ground motion simulations for 10 recent small to moderate earthquakes (Mw 4.1–5.4) in the San Francisco Bay Area to evaluate two versions of the USGS 3D velocity model (Brocher, 2005; Jachens *et al.*, 2006; Brocher, 2008). Comparisons were made in terms of modeling phase arrival timing, peak ground motion amplitudes, and the seismic waveforms. In the simulations we assumed the source parameters reported in the BSL Moment Tensor Catalog. Broadband seismic data from the BDSN, and strong motion data from the USGS and the CGS strong motion arrays were used in the analysis. The comparison of peak ground velocity (PGV) for both models reveals that both 3D models predict the observed PGV well over four orders of magnitude and P and S wave timing and pseudo-spectral acceleration are well modeled by the 3D structure. While the revised model (model 8.3.0) significantly improved the timing of the first arrival, and the waveform fit is generally good, there remain discrepancies in estimated amplitudes and durations that require improvements to the structure. Nevertheless, from our low-frequency (0.5 Hz) analysis we found that the 3D model is suitable for the simulation of PGV to assess strong shaking hazard of future large earthquakes, since earthquakes larger than M6 have PGV carried by waves of 1 to several seconds period.

Nonstandard FDTD Scheme for Computation of Elastic Waves

TAKENAKA, H., Kyushu University, Fukuoka, Japan, takenaka@geo.kyushu-u.ac.jp; JAFARGANDOMI, A., The University of Edinburgh, Edinburgh, United Kingdom, arash.jafargandomi@ed.ac.uk

Finite-difference method in time-domain (FDTD) is one of the most popular techniques used for modeling of elastic wave propagation. The main drawback of the standard FDTD, especially for models that are much larger than the wavelength, is phase error due to grid dispersion. In large scale modeling, hence long propagation distances, the phase error due to the grid dispersion becomes very severe. There have been several attempts to reduce grid dispersion and anisotropy of the FDTD. Among them the nonstandard scheme which was originally proposed in computational electromagnetics (*e.g.* Cole, 1997, IEEE Trans. MTT), is one of the most successful schemes to reduce grid dispersion and anisotropy. Recently, we developed a nonstandard finite-difference time-domain (NS-FDTD) scheme (fourth-order accurate in space and second-order accurate in time) for 2D elastic (P-SV) wave computations (JafarGandomi and Takenaka, 2009, Geophys. J. Int.). The nonstandard scheme improves the accuracy and efficiently reduces numerical dispersion and grid anisotropy. However, our original scheme could not significantly reduce numerical dispersion errors of both of P and S waves at the same time. Since we focused on improvement of S wave to optimize the parameters for the nonstandard

scheme, computational errors for P wave was almost equal or a little better than those for the standard FDTD scheme. In this study we propose a new nonstandard scheme which gives highly accurate solutions both for P and S waves. The difference between this new scheme and our original scheme is only treatment of the constitutive equations, so the computational costs are almost the same. We also show an example to illustrate feasibility of the new scheme.

Studying the Effect of Fault Roughness on Strong Ground motion

SHI, Z., San Diego State University, San Diego, CA, USA, zshi@projects.sdsu.edu; DAY, S., San Diego State University, San Diego, CA, USA.

Natural faults manifest geometric complexities with a broad range of scales from large features such as big bending and segmentation that can span over tens of kilometers visible from the field to small topography variations on fault slip surface at micron scales revealed in the lab. Previous studies have indicated that the geometrical properties of the fault can have strong influence on the static stress distribution around the fault and the dynamic process of earthquake rupture. One important question here is what components and what length scales of the fault geometrical complexity are most prominent in affecting the characteristics of strong ground motion such as high-frequency content and peak values of acceleration and velocity. In an attempt to provide some insights into the answer, we perform 3-D numerical simulations of dynamic rupture along a single continuous fault plane with roughness distributions varying in style (*e.g.*, self-similar or self-affine fractal) and strength. Calculations are carried out using the Support Operator Rupture Dynamics (SORD) code by Ely *et al.* (2008, 2009) capable of handling non-planar boundaries. Having a highly scalable parallel implementation with MPI, SORD will also allow us to explore roughness models that cover an extended range of length scales by utilizing large high-performance computing clusters. Detailed analysis of our simulation results will be presented in the meeting.

A Stochastic Earthquake Ground-Motion Prediction Model for the United Kingdom

RIETBROCK, A., University of Liverpool, Liverpool/UK, A.Rietbrock@liverpool.ac.uk; STRASSER, F., Council for Geoscience, Pretoria/South Africa, fstrasser@geoscience.org.za; EDWARDS, B., ETH, Zurich/Switzerland, edwards@sed.ethz.ch

Low-seismicity regions such as the United Kingdom pose a challenge for seismic hazard analysis in view of the limited amount of local data available. In particular, ground-motion prediction is faced with the problem that most of the instrumental observations available have been recorded at large distances from small earthquakes. Direct extrapolation of the results of regression on these data to the range of magnitudes and distances relevant for the seismic hazard analysis of engineered structures generally lead to unsatisfactory predictions.

The present study presents a new ground-motion prediction equation (GMPE) for the UK in terms of peak ground acceleration (PGA), peak ground velocity (PGV) and 5%-damped pseudo-spectral acceleration (PSA), based on the results of numerical simulations using a stochastic point-source model calibrated with parameters derived from local weak-motion data. The predictions from this model are compared with those of previous GMPEs based on UK data, other GMPEs derived for stable continental regions (SCRs), as well as recent GMPEs developed for the wider European area.

The Big Ten Earthquake Scenarios for Southern California

ELY, G.P., Univ. of S. California, Los Angeles, CA, gely@usc.edu; JORDAN, T.H., Univ. of S. California, Los Angeles, CA, tjordan@usc.edu; MAECHLING, P., Univ. of S. California, Los Angeles, CA, maechlin@usc.edu; OLSEN, K.B., San Diego State Univ., San Deigo, CA, kbolsen@sciences.sdsu.edu; DAY, S.M., San Diego State Univ., San Diego, CA, day@moho.sdsu.edu; MINSTER, J.-B., UC, San Diego, San Diego, CA, jbminster@ucsd.edu; GRAVES, R.W., URC Corp., Pasadena, CA, robert_graves@urscorp.com; BIELAK, J., Carnegie Mellon Univ., Pittsburgh, PA, jbielak@cmu.edu; TABORDA, R., Carnegie Mellon Univ. Pittsburgh, PA, ricardotaborda@gmail.com; BEROZA, G., Stanford Univ., Stanford, CA, beroza@stanford.edu; MA, S., San Diego State Univ., San Diego, CA, sma@geology.sdsu.edu; CUI, Y., San Diego Supercomputer Center, La Jolla, CA, yfcui@sdsc.edu; URBANIC, J., Pittsburgh Supercomputing Center, Pittsburgh, PA, urbanic@psc.edu; CALLAGHAN, S., Univ. of S. California Los Angeles, CA, scottcal@usc.edu

The Big Ten project is generating a hierarchy of simulations for roughly ten of the most probable large (M > 7) ruptures in Southern California, with the objective of understanding how source directivity, rupture complexity, and basin effects control ground motions. The ruptures and moment-magnitudes are selected from events with relatively high probability rates in the Uniform California Earthquake Rupture Forecast, Version 2 (UCERF2) model. The event set is being used to coordinate multiple types of large-scale simulations (requiring high performance computing), as well as multiple groups of researchers, around a common set of earthquake scenarios. The geoscience goals of the Big Ten project are to: (1) Understand the roles of source directivity, rupture complexity, and basin effects on ground motions, and evaluate how these factors control hazard curves from the CyberShake project; (2) Improve simulation capabilities by incorporating new codes that can model geologic complexities including topography, geologic discontinuities, and source complexities such as irregular, dipping, and offset faults; (3) Use dynamic rupture simulations to investigate the effects of realistic friction laws, geologic heterogeneities, and near-fault stress states on seismic radiation and thereby improve pseudo-dynamic rupture models of hazardous earthquakes; and (4) Use realistic earthquake simulations to evaluate static and dynamic stress transfer and assess their effects on strain accumulation, rupture nucleation, and stress release. We present wave propagation simulation results for multiple kinematic source parameterizations of each scenario as well as rupture dynamics simulations for a selected scenarios.

2D P-SV Nonlinear Investigations of Basin-Edge Amplification

O'CONNELL, D.R.H., Fugro William Lettis+Associates, Golden, CO, USA, oconnell@lettis.com; LIU, P.C., Bureau of Reclamation, Denver, CO, USA, pliu@usbr.gov; BONILLA, L.F., IRSN, Fontenay-aux-Roses, France, fabian.bonilla@irsn.fr

Basin-edge waves constructively interfere with direct and converted intrabasinal S-waves to produce regions of strongly amplified ground shaking. To investigate how soil nonlinearity might modify basin amplification, 2D P-SV nonlinear horizontal and vertical component ground motions are simulated. The calculations focus on basin and basin-margin regions within several km of the basin-edge, where the largest short-period amplifications are likely to occur. Deep basins (4 km) exhibit strong linear and nonlinear damping of basin-edge waves and relatively small amplification near basin margins. A basin thickness of 1 km is thus used to obtain results relevant for typical shallow urban basins including the San Fernando, Sylmar, and Wasatch-fault-bounded basins. We use the IWTH25 borehole and surface strong motion recordings of the M 6.9 2008 Iwate-Miyagi earthquake to show that the 2D P-SV nonlinear model of Bonilla *et al.* (2006) reproduces the horizontal and vertical peak ground motions and acceleration response spectra of this 4g surface ground motion (Aoi *et al.*, 2008). For moderate input motions (< 0.2 g), the position of basin-edge amplifications are comparable to 2D linear estimates, indicating that 2D and 3D linear basin response calculations combined with 1D nonlinear post-processing can provide realistic estimates of basin-edge responses for distant earthquakes. However, for near-fault motions (> ~0.3–0.5 g), nonlinearity sometimes produces multiple (2–4) regions of horizontal acceleration amplification within 1–2 km of the basin edge, where linear 2D calculations predict only a single region of acceleration amplification. Nonlinear basin-edge amplification is very sensitive to basin-edge dips and plane-wave incident angles, suggesting that realistic near-fault 3D-basin ground motion simulations need to explicitly incorporate 3D soil nonlinearity.

The SCEC-USGS Rupture Dynamics Code Comparison Exercise

HARRIS, R.A., U.S. Geological Survey, Menlo Park, CA, harris@usgs.gov; BARALL, M., Invisible Software, San Jose, CA, mbinv@invisiblesoft.com; ARCHULETA, R., UC Santa Barbara, Santa Barbara, CA, ralph@crustal.ucsb.edu; ANDREWS, D.J., U.S. Geological Survey, Menlo Park, CA, jandrews@usgs.gov; DUNHAM, E., Stanford University, Stanford, CA, edunham@stanford.edu; AAGAARD, B., U.S. Geological Survey, Menlo Park, CA, baagaard@usgs.gov; AMPUERO, J.P., Caltech, Pasadena, CA, ampuero@gps.caltech.edu; CRUZ-ATIENZA, V.M., UNAM, Mexico City, Mexico, cruz.atienza@gmail.com; DALGUER, L., ETH, Zurich, Switzerland; DAY, S., SDSU, San Diego, CA; DUAN, B., TAMU, College Station, TX; ELY, G., USC, Los Angeles, CA; GABRIEL, A., ETH, Zurich, Switzerland; KANEKO, Y., UC San Diego, San Diego, CA; KASE, Y., Geological Survey of Japan, Tsukuba, Japan; LAPUSTA, N., Caltech, Pasadena, CA; MA, S., SDSU, San Diego, CA; NODA, H., Caltech, Pasadena, CA; OGLESBY, D., UC Riverside, Riverside, CA; OLSEN, K., SDSU, San Diego, CA; ROTEN, D., SDSU, San Diego, CA; SONG, S., URS Corp., Pasadena, CA

Computer simulations of earthquake source rupture physics started decades ago, with a few researchers developing and using their own methods to solve problems of mostly theoretical interest. In contrast, in current times numerous spontaneous rupture computer codes are developed and used by researchers around the world, and the results are being implemented in earthquake hazard assessments. Since most of the problems simulated using these numerical approaches have no analytic solutions, it is essential to compare, verify, and validate the various versions of this research tool. To this end, a collaborative project of the Southern California Earthquake Center has been underway. We started with the basic problem of spontaneous rupture propagation that obeys slip-weakening friction on a vertical strike-slip fault in a homogeneous material and subsequently moved on to problems with heterogeneous stresses, or with differing material properties on opposite sides of the fault, or with rate-state friction. Last fall we simulated the 3D and 2D extreme

ground motion cases of rupture on a dipping fault, with either elastic or inelastic yielding, the latter of which is relevant to Yucca Mountain fault-rupture scenarios. We have also been discussing convergence and error metrics, since most of our comparisons to date involve qualitative assessments. Our upcoming exercises will likely include the case of rupture propagation on a branching fault, our first non-planar geometry benchmarks. Our website http://scecdata.usc.edu/cvws enables easy comparisons of the results, and also supplies information about the benchmarks and codes. Our overall objective is a complete understanding of the simulation methods and their ability to faithfully implement our assumptions about earthquake rupture physics, and reliably calculate the resulting ground motions.

Long Period (T > 0.8s) Strong Ground Motion Simulations along the Wasatch Front

MOSCHETTI, M.P., USGS, Golden, CO, USA, mmoschetti@usgs.gov; RAMIREZ-GUZMAN, L., USGS, Golden, CO, USA, lramirezguzman@usgs.gov; BIELAK, J., Carnegie Mellon University, Pittsburg, PA, USA, jbielak@cmu.edu

We model earthquake ground motions in the Salt Lake Basin for scenario events using the Wasatch Community Velocity Model (W-CVM). The Wasatch Fault at the eastern boundary of Salt Lake City, UT is capable of producing M7 earthquakes. However, ground motion estimates from events of this magnitude in the Wasatch region, and therefore the associated seismic risk, are unknown because such events are rare. The longer-term objective of this work is to model the effects of large, and potentially damaging, earthquakes on the Wasatch Fault using the W-CVM, version 3c (Magistrale *et al.*, 2006) and the Hercules finite element (FE) code (Tu *et al.*, 2006). The W-CVM derives from geotechnical measurements in the Salt Lake Basin, as well as regional body-wave tomography and empirical scaling relationships for wavespeeds and density. We present here the results from initial modeling efforts in the Salt Lake Basin for three seismic event simulations. Our numerical computations are valid up to 1.25Hz and use a minimum shear wave velocity of 200 m/s. In order to identify discrepancies between the W-CVM and the true, but unknown, wavespeed structure of the region we compare the synthetic and recorded waveforms.

Effect of Some Key Parameters on Directivity of Near-fault Ground Motions Derived from a Homogeneous Strike-Slip Fault Modeling

HU, J., IEM, Harbin, Heilongjiang, China; XIE, L., IEM, Harbin, Heilongjiang, China.

The rupture directivity caused by a predominately unilateral propagating fault with similar rupture speed to the local shear-wave velocity is a key factor in characterizing the near-fault ground motions. To investigate the effect of some basic source parameters on directivity, a mass of strong ground motions were simulated by using a discrete wave number method. Through analysis of peak ground motion, response spectra and significant duration of the fault-normal, fault-parallel and vertical components of ground motions, results indicate that the rupture speed, focal depth, hypocenter location and fault dip play important roles in affecting the directivity. A typical unilateral rupture fault generates an asymmetry distribution of amplitudes, spectral ordinates and durations in the ground surface between the forward and backward direction. The uniform rupture speed increases the amplitude and spectral ordinate but decrease the duration, while the non-uniform rupture speed leads to relatively smaller amplitude and spectral ordinate, but a higher duration within the same rupture distance. Also, super-shear rupture leads to directivity but there appear some difference compared with that of the sub-shear ruptures. Both focal depth and hypocenter location have obvious effects on the directivity. The deeper the fault depth gets, the smaller the ground motions amplitude becomes. Dip angle of the fault model has a effect on the ground motion. Big dip angle generates a distinct directivity in the fault-normal component, while small dip angle leads to the distinct directivity in the vertical component.

The Dynamics of Fault Stepovers with Rate-State Friction

RYAN, K., UC Riverside, Riverside, CA, USA, kryan003@email.ucr.edu; OGLESBY, D.D., UC Riverside, Riverside, CA, USA, david.oglesby@ucr.edu

We use the two-dimensional dynamic finite element method to explore the effects of friction parameterization on the dynamics of fault systems with stepovers. In particular, we investigate how rate-state friction affects the process by which rupture may jump across the stepover. We find that for a dilational fault stepover, the time it takes for the fault to weaken from peak to sliding frictional strength is relatively constant across the nucleating fault, but this weakening time increases by almost a factor of two as rupture renucleates on the secondary fault. In addition, the effective slip-weakening distance steadily increases as the rupture propagates along the nucleating fault, but then decreases again as it renucleates on the secondary fault. We will compare our results with those of compressional stepovers, and also with those obtained from a standard slip-weakening frictional parameterization.

Magnitude Scaling and Regional Variation of Ground Motion

Poster Session · Wednesday PM, 21 April · Exhibit Hall

Accelerometer Housing as a Cause of Variation of Recorded Ground Motion: The Example of the L'Aquila (Italy) 2009 Earthquake

DITOMMASO, R., Basilicata University, Potenza PZ Italy; MUCCIARELLI, M., Basilicata University, Potenza PZ Italy.

A possible reason for deviations in statistics of ground-motion parameters is the fact that the time-histories recorded at stations placed within or near buildings could be not representative of the true free-field ground motions but instead they could be contaminated by the frequencies of the buildings . These effects are known for years for large structures, but little attentions was paid to small buldings: numerical simulation show that the effect is different on peak, spectral and integral parameters and may range from a maximum of 20% for PGA to 100% for spectral ordinates (Ditommaso *et al.*, 2010, Bull. Earthq. Eng).

Several stations of Italian Accelerometric National Network are located within the sub-stations of national electric grid. The main constructive typologies used are brick masonry, reinforced concrete and pre-cast concrete, one or two floors high. To understand the influence of housing on accelerometric recordings obtained during the L'Aquila earthquake sequence (April 2009), we set up an experimental campaign focused on the dynamic characterization of housings and analyses of accelerometric recordings. The structural dynamic identification was aimed to housings and the pillars driven into the ground on which accelerometers are fixed

We studied four stations, and for all of them the preliminary results confirm that housings contaminated the accelerometric recordings. We analyzed at least 15 earthquakes for each station in terms of rotational HVSR. For each station, in correspondence of the main frequency of vibration, we always have an amplification factor greater than 1.5, but in one cases it reaches a value is greater than 4.

In our opinion, great care should devoted when comparing strong motion recordings obtained near or close even to small buildings, or recorded on artificial surfaces (concrete slabs, pillars, etc.): part of the observed variability could be due to the influence of different types of housing.

Ground Motion in Northen Sicily (Italy)

D'AMICO, S., Saint Louis University, Saint Louis, MO, USA, sebdamico@gmail.com; MERCURI, A., INGV, Rome, Italy, alessia.mercuri@ingv.it; MALAGNINI, L., INGV, Rome, Italy, luca.malagnini@ingv.it; HERRMANN, R.B., Saint Louis University, Saint Louis, MO, USA, rbh@eas.slu.edu; AKINCI, A., INGV, Rome, Italy, aybige.akinci@ingv.it

We provide a description of the ground-motion characteristics in Sicily (southern Italy). Several ground motion studies have been performed in the Italian peninsula, but the northern part of Sicily has not yet been studied from this point of view. We used data recorded by broad band stations of the Italian national network run by the Istituto Nazionale di geofisica e Vulcanologia (INGV). We used about 10.000 records from about 200 earthquakes registered from 2004 to 2009. The magnitude of the events ranged between Mw=2.0 and Mw=4.5. We computed the source spectra in term of moment-rate spectra (Mayeda et al 2003), the crustal attenuation (Malagnini *et al.* 2000), and the absolute site response (Malagnini *et al.* 2002). The results obtained can be used for upgrading the most recent hazard map of Italy and for engineering designs as well. The results obtained in this study are also useful to implement tools like Shake Map (Wald *et al.* 2005) largely used to generate a rapid earthquake response.

Towards Regional Ground Motion Models on the Eastern North Anatolian Fault Zone

UGURHAN, B., Middle East Technical University, Ankara/Turkey, ugurhan@metu.edu.tr; ASKAN, A., Middle East Technical University, Ankara/Turkey, aaskan@metu.edu.tr

North Anatolian Fault Zone (NAFZ) is one of the major active fault zones in the world which causes earthquakes of large magnitudes. Due to the westward migrating series of earthquakes on NAFZ, a severe earthquake is being expected in the Marmara region which has recently placed the main focus on this region. However, the eastern part of the NAFZ which has produced the extremely destructive 1939 Erzincan earthquake (M~8.0) is still a major threat in eastern Turkey. We present a hybrid approach for generating scenario earthquakes in the eastern North Anatolian Fault. A deterministic model which is used for simulating the low frequency content of ground motions is combined with the stochastic finite fault method for the simulation of high frequencies. Initially the 1992 Erzincan earthquake is simulated and validated against the records. Then a series of scenario earthquakes in the magnitude range of 5.5 to 7.5 is simulated. A wide range of simulations are generated to

account for the uncertainty in the results. The resulting worst case scenario earthquakes are represented in terms of maps for peak ground acceleration and spectral acceleration corresponding to various periods. Regions that will be exposed to possible severe damage are investigated. The validity of the model is tested with the NGA and regional ground motion prediction equations. This study presents initial attempts towards hybrid ground motion prediction equations for the region that take into account both data and simulations.

Source Scaling Relationship for M4.6-M7.6 Earthquakes in Taiwan Orogenic Belt

YEN, Y.-T., Graduate Institute of Geophysics, National Central University, Taiwan, ROC, alec@eqkc.earth.ncu.edu.tw; MA, K.-F., Graduate Institute of Geophysics, National Central University, Taiwan, ROC, fong@earth.ncu.edu.tw

We investigated the source scaling of earthquakes (Mw4.6-Mw7.6) from Taiwan orogenic belt, and made the contribution to the global compilation of source parameter to discuss the self-similar and non-self-similar in scaling of small to large earthquakes. In total, 19 finite-fault inverted slip models (12 dip-slip, and 7 strike-slip events) using mainly from Taiwan dense strong motion and teleseismic data were utilized in this analysis. We considered a defined effective length and width for the scaling study. To give more constraint to the large earthquakes, four additional larger events, 2008 Wenchuan M8.0, 2004 Sumatra M8.9, 2001 Kunlun M7.8 and 2001 Bhuj M7.4 earthquakes, were included for further discussion on the source scaling of small to large events. We found a scaling of 1/2 and 1/3 for the events less and larger than the seismic moment of 10**20 nt-m, respectively. It suggests a non-self similar scaling for small to moderate events, while a self-similar scaling for large events. Our study found that the seismogenic depth is a key to control the evolution of the earthquakes. For the events ruptured within the seismogenic belt the fault width developed simultaneously with fault length. The seismogenic depth of 30km corresponds to teh fault width of an earthquake magnitude of about 6.8, and it becomes the threshold magnitude to deviate the different scaling relationship of the source parameter to the seismic moment. Our results also found an extremely large stress drops for the blind thrust M5 and M6 events in western foothill of Taiwan. These events with source dimension of only 1–2 km, but, with the slip as large as meter. This high stress drop character also gives high PGA, and, thus, provides the threat to the epicentral area regardless the size of the event. Thus, in addition to the large earthquakes, the non-self similar characters with high stress drops of these blind thrust events require special attention for seismic hazard mitigation.

Empirical Characterization of Ground Motion Processes in Japan, and Comparison to Other Regions

GHOFRANI, H., Univ. of Western Ontario, London, Ontario, Canada, hghofran@uwo.ca; ATKINSON, G.M., Univ. of Western Ontario, London, Ontario, Canada, gmatkinson@aol.com

We use a large database (>10,000 records) of ground motions in Japan to explore earthquake processes including attenuation, magnitude scaling, site effects and other factors such as event type and focal depth, for events with moment magnitude $\mathbf{M} \geq 5.5$. Regression analysis and statistical analysis are implemented to characterize, and distinguish between, different types of earthquake ground motion processes including those for crustal, in-slab and interface events (for both source characterization and attenuation). We explore site effects, and their nonlinearity, by implementing Vs30 directly into ground motion prediction equations (GMPEs) as a predictive variable. In addition to Vs30, the effect of depth to the bedrock is investigated. It is important to understand potential differences in ground-motion generation and propagation between event types within this active subduction environment to adequately assess seismic hazard. This also facilitates comparison of ground motions across regions, to better understand regional variations in ground motion processes. To this end, Japanese ground motions for crustal, in-slab and interface events are compared to the corresponding motions for shallow crustal earthquakes in active tectonic regions as established by the PEER-NGA GMPEs (Eathquake Spectra, 2008). Preliminary findings suggest that there are not large differences in ground motions between the different classes of events. In-slab motions appear higher at a given distance, but this might be captured by a focal depth term in the source characterization.

Ground Motions from the 29 September 2009 Samoa M8.0 Earthquake and Aftershocks

MCNAMARA, D., USGS, Golden, CO, USA, mcnamara@usgs.gov; MEREMONTE, M., USGS, Golden, CO, USA; LEEDS, A., USGS, Golden, CO, USA; FOX, J., USGS, Golden, CO, USA; PETERSEN, M., USGS, Golden, CO, USA; GEE, L., USGS, Albuquerque, NM, USA.

The broad-scale tectonics of the Samoa region are dominated by the convergence of the Pacific and Australian plates, with the Pacific plate subducting westward beneath the Australian plate with a velocity of about 86 mm/year at the northern Tonga trench. The 29 September 2009 M8.0 Samoan earthquake was caused by normal (tensional) faulting of the Pacific Plate near the outer rise, east of the subduction zone between the Pacific and Australian plates. The earthquake was strongly felt throughout the region's islands and resulting sea-floor displacement generated a tsunami that caused loss of life and destruction in Samoa and American Samoa. Outer rise-type earthquakes are relatively rare and ground motions are not well understood. To address this, the USGS deployed five portable strong motion seismometers (Reftek Mems seismometers, Reftek RT-130 digitizers) with the goal of recording aftershocks in and around Pago Pago, American Samoa in order to calculate local site amplifications and regional subduction zone attenuation relationships. The stations compliment an existing permanent GSN station, IU.AFI, located in the independent nation of Samoa, 180km northeast of the earthquake epicenter. IU.AFI is taken as our reference rock site as the sensor sits in a sub-surface vault with a floor of basalt bedrock of the Pleistocene Salani Volcanics. The mainshock was well recorded at IU.AFI with 3-component peak ground accelerations on the order of 60–90 cm/s/s. Subsequent aftershocks display a wide range of mechanisms, and are clearly observed at IU.AFI and the five portable strong-motion seismometers. With this dataset, we examine spectral amplitudes from the outer rise mainshock and the numerous different aftershock mechanisms, relative to established subduction zone ground motion attenuation relationships. Ground motion attenuation and local site responses are key parameters for completing the USGS seismic hazard assessment in American Samoa.

Ground-Motion Prediction Equations for Eastern North America from a Hybrid Empirical Method

PEZESHK, S., The University of Memphis, Memphis, TN, USA, spezeshk@memphis; ZANDIEH, A., The University of Memphis, Memphis, TN, USA; TAVAKOLI, B., Bechtel Corporation, Frederick, MD, USA.

In the field of earthquake engineering, ground-motion prediction models are frequently used to estimate the peak ground motion (PGA) and the pseudo spectral acceleration (PSA). In regions of the world where ground-motion recordings are plentiful (such as WNA), the ground-motion prediction equations are obtained using empirical methods. In other regions such as eastern North America (ENA), with insufficient ground-motion data, other methods must be used to develop ground-motion prediction equations. The hybrid empirical method is one such method used to develop ground-motion prediction equations in areas with sparse ground motion. This method uses the stochastic method to adjust empirical ground-motion prediction relations developed for a region with abundant strong motion recordings. It estimates strong-motion parameters in a region with a sparse database. The adjustments take into account differences in the earthquake source, wave propagation, and site-response characteristics between the two regions. The purpose of this study is to use a hybrid empirical method and to develop a new hybrid empirical ground-motion prediction equation for ENA, using five new ground-motion prediction models developed by the Pacific Earthquake Engineering Research Center (PEER) for WNA. A new functional form is defined for the ground-motion prediction relation for a magnitude range of 5 to 8 and closest distances to the fault rupture up to 1000 km. Ground-motion prediction equations are developed for the response spectra (pseudo-acceleration, 5% damped) and the peak ground acceleration (PGA) for hard-rock sites in ENA. The resulting ground-motion prediction model developed in this study is compared with recent ground-motion prediction relations developed for ENA, as well as with available observed data for ENA.

Investigating the Regional Dependence of Ground-Motion Models from an Information-Theoretic Perspective

DELAVAUD, E., University of Potsdam, Potsdam-Golm, Germany, delavaud@geo.uni-potsdam.de; SCHERBAUM, F., University of Potsdam, Potsdam-Golm, Germany, fs@geo.uni-potsdam.de; KUEHN, N., University of Potsdam, Potsdam-Golm, Germany, nico@geo.uni-potsdam.de; ALLEN, T., Geoscience Australia, Canberra, Australia, Trevor.Allen@ga.gov.au

Recently, Scherbaum *et al.* (2009) have proposed an information-theoretic method to quantitatively judge the applicability of ground-motion models for hazard studies in particular regions of interest. The subsequent study by Delavaud *et al.* (2009) using response spectra and macroseismic intensities from California has demonstrated the coherence between ranking based on information from response spectra and intensity observations, respectively. In this context, we have noticed some strongly frequency-, distance- and magnitude dependent differences of the ground-motion models (GMMs) under consideration.

In the present study we are systematically exploring this further to investigate the regional dependence of ground-motion models in general. For this, we use the global dataset which Allen and Wald (2009) have built to evaluate ground-motion modeling techniques for use in Global ShakeMap. GMMs derived from different geographical regions of active crust (Western USA, Europe, Japan, Italy, Greece, Turkey) or from a composition of regional data are ranked using response spectra,

peak ground acceleration and macroseismic intensities from the global dataset but also from regional sub-datasets. In particular, we are investigating how well GMMs developed from a set of data from various regions can predict ground motion in a specific region in comparison with GMMs which have been derived for this region. Rankings are also performed in different magnitude, frequency and distance ranges to better identify the conditions for which GMMs might be regional dependent.

A Hierarchical Global Ground Motion Model to Take into Account Regional Differences

KUEHN, N.M., IEES, University of Potsdam, Potsdam/Germany, nico@geo.uni-potsdam.de; SCHERBAUM, F., IEES, University of Potsdam, Potsdam/Germany, fs@geo.uni-potsdam.de; RIGGELSEN, C., IEES, University of Potsdam, Potsdam/Germany, riggelsen@geo.uni-potsdam.de; ALLEN, T., Geoscience Australia, Canberra/Australia, Trevor.Allen@ga.gov.au

In this work we present a hierarchical global ground motion model that includes regional differences in ground motion scaling in a principled way. For this purpose, we make the assumption that the scaling of ground motion intensity parameters with earthquake source, path and site parameters is similar, but not necessarily identical in different regions. In particular, we assume that models for individual regions are sampled from a global distribution of ground motion models. Thus, we set up a multi-level/hierarchical model, where the coefficients for each region are connected by so-called global hyperparameters. Via these hyperparameters, data from one region is also used to determine the coefficients in other regions, though with less weight. That way, it is possible to determine a model even for regions with a scarce amount of data. The global model is set up as a graphical model, which allows for an intuitive understanding. The coefficients are determined in a Bayesian setting using Markov Chain Monte Carlo simulation. This offers a systematic way to include prior knowledge and provides an estimate of the epistemic uncertainty of the parameters. It also allows to update the model once new data is available. The model is learned on a global dataset, divided into 11 regions. In the dataset, there are large differences in the amount of earthquakes and records between the regions. The analysis shows some differences in ground motion scaling between regions with a lot of data, while the scaling in other regions is closer to the global average.

New Attenuation Relationship for Far Field Earthquakes Caused by Dip Slip Mechanism

ADNAN, A.B., University Technology Malaysia, Malaysia, azelan_fka_utm@yahoo.com; HENDRIYAWAN, Institute Technology Bandung, Indonesia, h3ndri91@yahoo.com; MELDI, S., University Technology Malaysia, Malaysia, meldisht@hotmail.com; MASYHUR, I., Institute Technology Bandung, Indonesia, masyhur@bdg.centrin.net.id.

The new attenuation relationship for far field earthquakes from dip slip mechanisms is produced. The attenuation function was developed using regression analysis. The analysis was carried out using more than 850 strong motion records from about 40 worldwide earthquake events with magnitudes in the range of 5.0 < Mw < 9.3, and the epicenter distances that range from 2.0 km to 1122 km. The data include the most recent earthquakes in the South East Asian region. The analysis considered earthquakes data from dip slip events that were recorded at bedrock. The accuracy of the regression model to the actual data was described by looking at the level of adjustment between original data and regression model measured using multiple coefficient of determination, and adjusted multiple coefficient of determination. The validity of regression analysis was also tested by plotting the residuals scatter. The new attenuation has also been compared to other attenuation relationships related to the same earthquake mechanism. The result shows that standard deviation of the new attenuation is relatively lower than other attenuations which indicate better prediction of the earthquake intensity due to the far field earthquakes caused by dip slip mechanism.

Energetic and Enervated Earthquakes: Real Scatter in Apparent Stress and Implications for Ground Motion Prediction

BALTAY, A.S., Stanford University, Stanford, CA USA, abaltay@stanford.edu; PRIETO, G.A., Universidad de los Andes, Bogota, Columbia, gprieto@uniandes.edu.co; IDE, S., University of Tokyo, Tokyo, Japan, ide@eps.s.u-tokyo.ac.jp; BEROZA, G.C., Stanford University, Stanford, CA USA, beroza@stanford.edu

We estimate scaled seismic energy and apparent stress to explore the relationship between radiated seismic energy and moment. Our empirical Green's function method uses time-averaged coda spectra, to exploit the stability and averaging effects of the seismic coda. In each region, we choose events that are nearly co-located so that the path term to any station is constant. Small events are used as empirical Green's functions to correct for propagation effects. For eight sequences in the western US, Mexico and Honshu, Japan, over 8 orders of seismic moment, we find that the apparent stress averages to 1 MPa for most events, with scatter between particular events and sequences. Overall, our results support earthquake self-similarity, and are consistent with studies of radiated energy determined by other methods; however, we identify several earthquakes in the magnitude range of Mw 4.5 to Mw 5.5 in Japan that have anomalously high (10 MPa) and low (20 KPa) apparent stress. We investigate the source of these energized and enervated earthquakes, their spectra, and their acceleration records. The enervated events are depleted in high frequencies compared to regular events of similar size, while the energetic events are enhanced in higher frequencies. These earthquakes highlight the fact that real variations in apparent stress exist, even though there is no systematic variation in apparent stress with earthquake size for large populations. A better understanding of the conditions that lead to these anomalous events should aid in the understanding of the origin of high frequency ground motion and may help place constraints on levels of extreme ground motion prediction.

Surface and Borehole Estimates of Single-Station Standard Deviation

RODRIGUEZ-MAREK, A., Washington State University, Pullman, WA, USA, adrian@wsu.edu; BONILLA, L.F., IRSN, France, fabian.bonilla@irsn.fr; COTTON, F., LGIT, Université Joseph Fourier, Grenoble, France, Fabrice.Cotton@obs.ujf-grenoble.fr

The KiK-net database was used to obtain single station estimates of standard deviation both for surface records and for recordings from instruments located in boreholes at depths generally ranging from 100m to 200m below the surface. A ground motion prediction equation was first developed using records from around 600 stations from the KiKnet database. Site effects were parameterized using Vs30. In addition, for borehole records the shear wave velocity at the borehole depth was also used. The standard deviation for borehole records is on average 10 to 15% lower than surface records. While borehole records can also be affected by near-surface effects, the effect of the near-surface velocity structure is much less marked for borehole records than for surface records.

The effect of the limited parameterization of site response can be removed by considering ground motion variability at a single station. Single-station estimates were obtained from 44 stations that recorded more than 15 events. Single station estimates of standard deviation for each station were first computed (*e.g.* the standard deviation of the residuals corresponding to that station). Then mean values of standard deviation were obtained for all 44 stations. Average values of single-station standard deviation records vary from 0.61 to 0.67 (in natural log basis) as a function of spectral period. Interestingly, this range is the same for standard deviations obtained using surface and borehole records, implying that most of the difference between surface and borehole variability is due to a poor characterization of site effects. The values of single-station standard deviation agree with those of various other studies that use different datasets.

The Seismo-Acoustic Wavefield: Fusion of Seismic and Infrasound Data

Poster Session · Wednesday PM, 21 April · Exhibit Hall

Seismo-acoustic Investigation at Mt. Etna Volcano: the Case Study of November 16, 2006

SCIOTTO, M., University of Catania, Catania, Italy, sciotto@ct.ingv.it; CANNATA, A., INGV Catania, Catania, Italy, cannata@ct.ingv.it; PRIVITERA, E., INGV Catania, Catania, Italy, privitera@ct.ingv.it; DI GRAZIA, G., INGV Catania, Catania, Italy, digrazia@ct.ingv.it; GRESTA, S., University of Catania, Catania, Italy, gresta@unict.it; MONTALTO, P., INGV Catania, Catania, Italy, montalto@ct.ingv.it

On November 16, 2006, an intense strombolian activity began at Southeast summit crater of Mt. Etna volcano (Sicily). Within a few hours, this activity culminated with phreato-magmatic explosions, generating small pyroclastic flows. In order to investigate the dynamics of this eruption, infrasound and seismic signals together with visual observations (pictures and videos) were studied. After comparing visual and acoustic data, a detailed characterization of spectra and waveforms of the infrasound events was performed. Then, their source mechanisms were investigated by applying the following models: i) strombolian bubble, ii) Helmholtz resonator and iii) vibrating conduit. We also have studied the time variation of the tremor source location, in order to understand the dynamics of magma bodies at depth. Finally, the time evolution of the ratio between infrasonic and seismic energy has shown important changes, that were likely due to time variations of the eruptive dynamics.

Low Frequency Sound from Earthquakes: What Can We Uniquely Learn from Seismo-Acoustics?

ARROWSMITH, S., Los Alamos National Laboratory, Los Alamos, NM, USA, sarrowsmith@gmail.com; HARTSE, H., Los Alamos National Laboratory, Los Alamos, NM, USA, hartse@lanl.gov; WHITAKER, R., Los Alamos National

Laboratory, Los Alamos, NM, USA, rww@lanl.gov; BURLACU, R., University of Utah, Salt Lake City, Utah, USA, burlacu@seis.utah.edu

Large earthquakes can generate seismo-acoustic waves. While the seismic wavefield from earthquakes is comparatively well understood, the corresponding infrasonic wavefield is less well known. The fusion of infrasonic and seismic data has the potential to help (1) improve our understanding of the remote effects of earthquakes on surface motions, (2) provide new insights into earthquake source physics, (3) better constrain earthquake depth, and (4) identify tsunamogenic earthquakes—with a possible role in tsunami warning systems. An important but less understood problem is how efficiently small and moderate earthquakes generate infrasound. We report on the first systematic and robust study of epicentral infrasound (conversion of surface ground motions to sound pressure in the epicentral area and propagation through atmosphere to the infrasonic recording stations) from small and moderate earthquakes in the Western US. By requiring observations at multiple arrays, and applying a mining explosion filter to earthquake catalogs, we can uniquely identify epicentral infrasound from earthquakes. We then focus on a particularly efficient infrasound-generating sequence of earthquakes: the 2008 Wells, Nevada earthquake sequence. We show that secondary infrasound recorded at an infrasonic array in Utah is generated by the interaction of seismic surface waves with an isolated peak called Floating Island.

Robust Detection and Location of Infrasound and Seismo-Acoustic Events

ARROWSMITH, S., Los Alamos National Laboratory, Los Alamos, NM, USA, sarrowsmith@gmail.com; WHITAKER, R., Los Alamos National Laboratory, Los Alamos, NM, USA, rww@lanl.gov; MODRAK, R., Los Alamos National Laboratory, Los Alamos, NM, USA, rmodrak@gmail.com; ANDERSON, D., Los Alamos National Laboratory, Los Alamos, NM, USA, dand@lanl.gov

Techniques developed for the detection and location of seismic events do not export well for infrasound signal processing. Furthermore, the optimum detection and location of seismo-acoustic events must exploit the unique advantages inherent in each technology. We outline the unique considerations that must be taken into account when utilizing infrasound data. With these considerations in mind, we then present new methodologies for the detection and location of infrasound and seismo-acoustic events. An F-detector, which adaptively accounts for changes in ambient noise, reduces false alarms drastically without affecting missed detections. We demonstrate the importance of this technique for infrasound arrays, where coherent noise is common. Next, we outline the Bayesian Infrasound Source Location (BISL) method, recently developed at Los Alamos. BISL does not require atmospheric models and provides robust credibility contours for the location of infrasound events recorded at multiple arrays. Given the limitations in current atmospheric models capturing the temporal variability of the atmosphere, this approach provides a reliable way to locate infrasound events in near real-time. However, as atmospheric models are improved and validated, they can be integrated into the BISL method for enhanced source location. Finally, we outline a method for combining seismic and infrasound data for the optimum location of seismo-acoustic events.

Monitoring of Micro-Seismicity Using the Temporal Seismo-Acoustic Network in Eastern Coastal Area of the Korean Peninsula

JEON, J., KIGAM, Daejeon/Korea, jsjeon@kigam.re.kr; CHE, I., KIGAM, Daejeon/Korea, che10@kigam.re.kr

To correlate between geological structure and seismic activity, the accurate hypocenter is calculated. Because there is the limit to determine the accurate hypocenter using by a sparse permanent seismic network, the mobile and temporal network is operated for a specific area annually. If seismic activity of a study area is low, the analysis of micro seismic events is important. Where construction and mine blast is active like Korean peninsula, discrimination between artificial and natural events is essential. Although there are many techniques for discriminating a blast from an earthquake, association method between seismic and infrasound signal is applied.

The temporal network consists of several short period seismic station and one seismo-acoustic array which is located near to active blast sites. This seismo-acoustic array is consisted of 4 acoustic sensors and one 3-comp seismometer and distance between acoustic sensors of corner is about 70 meter. This distance is depend on the local condition. One advantage of operation of this array is to discriminate blast simply and immediately using the time diffence between seismic signal and infrasound signal at each site.

Comparing Coupled and Separated Finite-Difference Calculations of Seismo-Acoustic Wave Propagation

CHAEL, E.P., Sandia National Laboratories, Albuquerque, NM, epchael@sandia.gov; ALDRIDGE, D.F., Sandia National Laboratories, Albuquerque, NM, dfaldri@sandia.gov; PRESTON, L., Sandia National Laboratories, Albuquerque, NM, lpresto@sandia.gov; SYMONS, N.P., Sandia National Laboratories, Albuquerque, NM, npsymon@sandia.gov

The strong contrast, or impedance mismatch, between the elastic parameters of the solid earth and those of the atmosphere amplifies errors in finite-difference (FD) modeling of wave propagation across the interface between the two regimes. In recent years, various methods for handling this boundary have been developed, and some 'full-physics' FD routines are now available which can reliably model seismo-acoustic interactions (*e.g.*, Preston *et al.*, 2008). While effective, such codes tend to be complex and computationally intensive. A simpler approach which should be sufficient for many problems is to employ separate, conventional seismic and acoustic FD codes for waves in the earth and air, respectively. In this case, the free-surface motions resulting from an underground seismic source are used to drive the acoustic waves in the atmosphere. Conversely, the surface pressure field from an atmospheric source serves as the input for the seismic response of the ground. With the algorithms separated, the two FD grids can be optimally sized based on the wavelengths in each regime, and unnecessary calculations for shear motions are avoided in the acoustic medium. We compare the two FD approaches (coupled and separated) for some fundamental situations which can be addressed analytically using ray-theory synthetics. One example is a buried line source in a solid half-space underlying a fluid half-space, a variation of Lamb's problem. In this way we can test the accuracy of both seismo-acoustic FD methods, and determine the limits of applicability of each. These tests build confidence in the FD results for more interesting seismo-acoustic problems with significant velocity structure.

The HUMBLE REDWOOD Seismic/Acoustic Coupling Experiments: Joint Inversion for Yield Using Seismic, Acoustic and Crater Data

FOXALL, B., Lawrence Livermore National Lab, Livermore, CA, bfoxall@llnl.gov; MARRS, R., Lawrence Livermore National Lab, Livermore, CA, marrs1@llnl.gov; LENOX, E., Defense Threat Reduction Agency, Albuquerque, NM, elizabeth.lenox@dtra.mil; REINKE, R., Defense Threat Reduction Agency, Albuquerque, NM; SEASTRAND, D., NSTec, Las Vegas, NV, SeastrDR@nv.doe.gov; BONNER, J., Weston Geophysical Corp., Lexington, MA, jes_bonner@yahoo.com; MAYEDA, K., Weston Geophysical Corp., Lexington, MA, kmayeda@yahoo.com; SNELSON, C., New Mexico Tech., Socorro, NM, snelson@ees.nmt.edu

Estimation of the yield of near-surface explosions is complicated by the partitioning of blast energy between the seismic and acoustic wave fields as a result of partial coupling to the ground. The HUMBLE REDWOOD experiments were carried out in 2007 and 2009 to advance the understanding of partial seismic coupling for shallow explosions. The HUMBLE REDWOOD Phase I experiment comprised seven 1450-lb ANFO charges detonated at various heights and depths of burst. Phase II included three additional 1450-lb detonations as well as three "blind" yield shots. Both sets of experiments were conducted in and above the dry alluvium of Kirtland AFB, NM near the eastern margin of the Albuquerque Basin, and were recorded by extensive local seismic and acoustic networks. Crater parameters and permanent near-source surface displacements were derived using digital photogrammetric techniques. In addition, an extensive PASSCAL Texan network was deployed on all Phase I and Phase II events to define the subsurface structure. During Phase II, a SODAR/RASS system provided shot-time atmospheric sound velocity profiles up to 1 km above ground level. The complete HUMBLE REDWOOD data set ranges from fully contained to no-crater height of burst shots and covers almost an order of magnitude in explosive yield. As predicted by Murphy and Shah (BSSA, v78, 64–82, 1988), local surface wave amplitudes are insensitive to the height of burst of above-ground explosions; as are body-wave amplitudes and acoustic impulse. We examine the utility of various yield estimation procedures based on separate inversions of the seismic, acoustic, crater parameter and surface displacement data, and on joint inversion of different combinations of the data sets.

This work performed under the auspices of the U.S. Department of Energy by Lawrence Livermore National Laboratory under Contract DE-AC52-07NA27344.

The Utilization of Portable Seismic Stations and a Small-size Infrasound Array for Characterizing Local Seismicity along Coastal Areas in Korea

CHE, I.Y., KIGAM, Daejeon, Korea, che10@kigam.re.kr; JEON, J.S., KIGAM, Daejeon, Korea, jsjeon@kigam.re.kr

Portable seismic stations were temporarily deployed to monitor weak seismic activity and characterize its source at local coastal areas in South Korea. For the discrimination of weak seismic events generated from anthropogenic sources, especially surface blasting at local industrial mines, we designed a small-size infrasound array equipped with three acoustic gauges. The triangular array was co-located with one of the temporary seismic stations. We first identified all weak seismic events and determined their locations and magnitudes using the seismic data from the temporary seismic stations and nearby permanent seismological stations. For the infrasonic data, we applied array processing to estimate azimuth and apparent velocity for infrasound signals. Then we

identified the seismic events followed by infrasonic signals as surface explosions based on seismo-acoustic analysis associating seismic and infrasonic signals. As a result of this approach, we could monitor weak seismic activity and provide accurate locations, which could not be determined by the regional seismic network alone. In addition, we could discriminate artificial seismic activity such as mining explosions from other weak seismicity, which also could not be identified by the regional infrasound network in Korea. Finally, we use the refined natural seismicity to assess seismic hazard in local coastal areas by comparing with other geological and geophysical data.

Lessons Learned from the Design, Installation and Operation of Seismo-Acoustic Arrays

HAYWARD, C.T., Southern Methodist University, Dallas, TX, hayward@smu.edu; STUMP, B.W., Southern Methodist University, Dallas, Tx, bstump@smu.edu; KUBACKI, R., Southern Methodist University, Dallas, Tx, rkubacki@smu.edu; GOLDEN, P., Southern Methodist University, Dallas, Tx, pgolden@smu.edu

Regional array installations that incorporate both seismometers and infrasound gauges offer the opportunity to not only record and characterize local seismic activity but also to identify infrasound events and seismo-acoustic events. Typically these arrays record far more infrasound only events than seismic only events and a modest number of seismo-acoustic events. The characterization of the source whether it is a naturally occurring earthquake or a manmade explosion is facilitated by the combined data sets. A region wide analysis benefits from multiple arrays as well. The actual design and implementation of an integrated seismo-acoustic array is complicated by an order of magnitude differences in wavelength between seismic and acoustic waves, dramatic differences in the noise field for each and the time varying nature of atmospheric wave propagation and noise. With over fifteen years of practical experience in addressing these problems a number of lessons have been learned. We will highlight these lessons with practical examples from both permanent and portable field installations. Frequency content of signals, coherence of signal and noise fields, temporal variations in these noise fields will all is shown as contributors to an optimum array design. Practical issues such as power requirements, data telemetry, station spacing, digitizer utilization and lightning protection all contribute to these designs and will be documented. Finally sensor bandwidth, noise and cost issues for both seismometers and infrasound gauges also must be taken into account. This assessment requires some understanding of the expected noise and signal fields for both infrasound and seismic waves.

The Los Alamos Seismo-Acoustic Research Center

ARROWSMITH, S., Los Alamos National Laboratory, Los Alamos, NM, USA, sarrowsmith@gmail.com; ROBERTS, P., Los Alamos National Laboratory, Los Alamos, NM, USA, proberts@lanl.gov; BAKER, D., Los Alamos National Laboratory, Los Alamos, NM, USA, dfbaker@lanl.gov; STEAD, R., Los Alamos National Laboratory, Los Alamos, NM, USA, stead@lanl.gov; WHITAKER, R., Los Alamos National Laboratory, Los Alamos, NM, USA, rww@lanl.gov

The Los Alamos Seismo-acoustic Research Center (SARC) is a new initiative geared towards understanding the seismo-acoustic wavefield from small explosions (< 1 ton). Of particular interest is the characterization of the transition from non-linear to linear seismo-acoustic propagation from explosions. SARC allows us to gather experimental data, enabling us to theoretically and numerically explore the little-understood transitional regime between non-linear and linear wave propagation. SARC comprises four seismo-acoustic arrays, strategically located adjacent to ground-truth explosions in Los Alamos and Socorro, NM. Data from each seismo-acoustic array is telemetered to the Research Center in real-time. We discuss the deployment and operation of SARC, and discuss some example signals.

Operational Earthquake Forecasting

Poster Session · Wednesday PM, 21 April · Exhibit Hall

CSEP: Preliminary Results of the New Zealand Earthquake Forecast Testing Center

GERSTENBERGER, M.C., GNS Science, Lower Hutt, New Zealand, m.gerstenberger@gns.cri.nz; CHRISTOPHERSEN, A., GNS Science, Lower Hutt, New Zealand; RHOADES, D.A., GNS Science, Lower Hutt, New Zealand.

The New Zealand Earthquake Forecast Testing Center has been operational and following the Collaboratory for the Study of Earthquake Predictability (CSEP) protocol for the past two years; here we present an overview of the current status of the center. At present, researchers from around the globe have provided sixteen models for testing within the center, all of which have been retrospectively tested against portions of the NZ historical catalog and are currently undergoing preliminary prospective testing. These models are predominantly short-term forecast models (*i.e.*, 3 month or 1 day forecasts) however several models target 5 year forecasts or are capable of producing forecasts of this length; most models are being tested over multiple forecast time lengths. The models explore a range of statistically based ideas such as smoothed seismicity, earthquake clustering and long-term seismicity relations. In this presentation we show the results of retrospective testing of the individual models, retrospective comparisons within each of the model classes, and we give a status report of the current unofficial prospective testing. All prospective testing to date is preliminary and results will remain so until catalog completeness problems in 2007 are corrected.

A New Generic Model for Aftershock Decay in Earthquake Forecasting

CHRISTOPHERSEN, A., GNS Science, Avalon/Lower Hutt/ New Zealand, A.Christophersen@gns.cri.nz; GERSTENBERGER, M.C., GNS Science, Avalon/Lower Hutt/ New Zealand, M.Gerstenberger@gns.cri.nz

The Short-Term Earthquake Probability (STEP) model has provided online forecasts for the probability of ground shaking in California since 2005. Using region specific parameters, STEP is installed in CSEP testing centers in California, New Zealand and Italy; models are also planned for China and Iceland.

The STEP model relies on a generic model for aftershock decay with parameters derived by averaging the decay of individual aftershock sequences. We present a more robust generic model based on abundance: the mean number of aftershock per main shock. The new model includes main shocks with too few aftershocks to have their decay parameters fitted in the traditional approach. As a consequence the abundance and consequently the forecasted rate is smaller in the new model, in particular for small main shocks. On the other hand, we find that abundance increases faster with main shock magnitude in the new model compared to the traditional model. For Italy, the cross-over between the two models is around magnitude 6.0 and the new model forecasts on average more aftershocks per main shock larger than 6.0.

We compare model parameters for different regions and report on the retrospective results for both the new and the traditional model.

Earthquake Early Warning: Update on Prospective Users' Perspectives

SAVAGE, W.U., US Geological Survey, Las Vegas, NV, USA, wusavage@usgs.gov; NISHENKO, S.P., Pacific Gas and Electric Company, San Francisco, CA, USA, SPN3@pge.com; JOHNSON, T.B., Bay Area Rapid Transit District, Oakland, CA, USA, TJohnso@bart.gov

With more than 25 million people at risk from high hazard faults in California alone, Earthquake Early Warning (EEW) presents a promising public safety and emergency response tool. EEW represents the real-time end of an earthquake information spectrum that also includes near real-time notification of earthquake location, magnitude, and shaking levels and geographic information system (GIS)-based products for compiling and visually displaying processed earthquake data such as ShakeMap and ShakeCast.

In the transportation sector, high-speed rail systems have already demonstrated the 'proof of concept' for EEW in several countries, and more EEW systems are being installed. Recently the Bay Area Rapid Transit District (BART) began collaborating with the California Integrated Seismic Network (CISN) and others to assess the potential benefits of EEW technology to transit operations and emergency response. A key issue in this assessment is that significant earthquakes are likely to occur close to or within the BART system, limiting the available time to take preemptive measures (*i.e.*, slowing or stopping trains prior to strong ground shaking).

Pacific Gas and Electric Company (PG&E) has been a leader among utility companies in promoting improvements in rapid earthquake notifications and implementing them within its service territory. PG&E has developed response algorithms and automated GIS processes that generate lists of facilities (*e.g.*, natural gas transmission lines, dams, and substations) that have the highest risk of being impacted during an earthquake. This poster presents details of the approaches being taken by PG&E and BART in exploring how to meet each organization's needs for effective response to earthquake notifications including EEW.

An Intermediate-Term Attenuation Precursor to the 2004 Parkfield Earthquake: Was It Fluid Driven?

CHUN, K.-Y., Tongji University, Shanghai/China, kchun4650@rogers.com; YUAN, Q.-Y., Tongji University, Shanghai/China, yuanqiuyi040947@hotmail.com; HENDERSON, G. A., Tongji University, Shanghai/China, gary@core.yorku.ca

Understanding earthquake precursors is fundamental to progress in earthquake prediction research. In this study we use a recently developed method to extract temporal changes in *P*-wave attenuation operator t^*, free of the usual problems plaguing such an undertaking: namely, uncertainties in seismic source spectra and station-site effects. The method requires finding an earthquake multiplet, a tight cluster of nearly identical microearthquakes. Here we report a sharp rise in t^* along impending rupture-zone paths some 18 months before the 2004 Parkfield earthquake. The

emergence of the t^* anomaly, we note, coincided in time with a decrease both in *P*/*S* spectral ratio and in similarity among the multiplet waveforms recorded at a fixed Northern California Seismic Network station. It is generally accepted that the Earth's schizosphere can be assumed to be almost universally permeated with fluids. With this in mind, we surmise that our observations are consistent with preseismic microcracking that produced a decrease in pore-fluid saturation (which increases *P*-wave attenuation but not *S* -wave attenuation) and enhanced wave scattering (which lowers waveform cross-correlation coefficients). Our noting that the perturbations in t^*, *P*/ *S* ratio and multiplet waveform similarity were causally related is supported by the fact that their postseismic recoveries took place nearly in lock step. The perturbations largely vanished within a year after the 28 September 2004 mainshock. With earthquake multiplets now being recognized as common occurrences on major active faults in many parts of the world, it would be useful to apply this method not only to California, but also to other regions of high earthquake hazards.

Earthquakes Prediction: Proper and Non-Proper Seismicity, Their Relations with Geophysical Fields' Precursors.

KERIMOV, I.G., Scientific Center of Seismology, Baku, Azerbaijan Republic, scseismo@azdata.net; KERIMOV, S.I., Scientific Center of Seismology, Baku, Azerbaijan Republic, seymourki@web.de

The new Regularity of microseisms anomalous emissions before an earthquake with multi-stage increase in intensity, decrease of their dominant frequency, polarization in the direction of the epicenter of the future earthquake and measurable at any distance from the epicenter zone, recognized as a scientific discovery by the former USSR State Committee in March 1988, with priority from May 1979, led to significant changes in requirements to seismic networks, information analysis, on understanding of anomalous nature, behavior and relations with geophysical precursors.

We proved that their manifestations depend on the microseisms' main frequency current range and delay between their appearances could be used for determining the time and magnitude of the future earthquake.

Implementation of prediction using all complex of precursors request analyzing their reliability: they did not appear before quite a number of events. This has been promoted by analyzing world strong earthquakes for more than 20 years for studying of the seismicity relationship of different planet's regions.

We came to the obvious conclusion that if this interaction exists then everywhere must be earthquakes which reproduce non-proper seismicity of their regions, invented terms "proper" and "non-proper" seismicity and have studied their characteristics. It became clear why considerable part of long- and middle-term geophysical precursors does not appear: the earthquakes reflect non-proper processes and were induced by natural events in other regions of the world.

Conclusion: Such approach showed that a real impact of strong events reaches 90% and more and differences in times between events induced by them indicate the regions' properties: activity, dynamics, and stressed states. And the results of these researches created a base for real possibilities for earthquake prediction itself.

Multidisciplinary Approach for Atmospheric Earthquake Precursors Validation

OUZOUNOV, D.P., NASA/GSFC & Chapman University, Greenbelt, MD, USA, dimitar.p.ouzounov@nasa.gov; PULINETS, S.A., Institute of Applied Geophysics, Moscow, Russian Federation, pulse1549@gmail.com; LIU, J.Y., Institute of Space Science, NCU, Chung-Li,Taiwan, jyliu@jupiter.ss.ncu.edu.tw; HATTORI, K., Chiba University, Inage, Chiba, Japan, hattori@earth.s.chiba-u.ac.jp; PARROT, M., LPC2E/CNRS, Orléans, France, Michel.Parrot@cnrs-orleans.fr; TAYLOR, P., NASA Goddard Space Flight Center, Greenbelt, MD, USA, patrick.t.taylor@nasa.gov; KAFATOS, M., Chapman University, Orange, CA, USA, kafatos@chapman.edu.

Ground and space observations have shown that there are precursory atmospheric signals associated with several recent earthquakes. Our latest results, from several post-earthquake independent analyses of more then 100 major earthquakes, show that a multidisciplinary approach has a capability for detecting pre-earthquake atmospheric signals by combining the information from multiple sensors into a common framework. Our methodology is based on the Integrated Space—Terrestrial Framework (ISTF) approach, which is an integration analysis of several physical and environmental parameters (Rn/ ion activities, air temperature, seismicity, thermal infrared radiation and electron concentration in the ionosphere) that were found to be associated with active faulting and earthquake processes. We performed an evaluation of hind-cast detection (rate of appearance, rate of false positive/negative alarms) of several atmospheric parameters over regions mainly in Asia with high seismicity. We are using existing thermal satellite data (NASA/Aqua and NOAA/POES), in situ atmospheric data (NOAA/NCEP); and ionospheric variability data (GPS/TEC and DEMETER) over three different regions with high seismicity- Taiwan, Japan and Kamchatka for the period of 2003–2008. The first part of this validation included 43 major earthquakes (M>5.9): 10 events in Taiwan, 15 events in Japan, 15 events in Kamchatka and three most recent events for M8.0 Wenchuan earthquake (May 2008) in China; Abruzzo M6.3 (Italy, April 2008) and M7.9 Samoa earthquakes (Sep 2009). The first results suggest: (i) for a systematic appearance of atmospheric anomalies near the epicentral area, 1 to 5 days in advance to the major events and (ii) the existence of a coupling process between the lithosphere and the atmosphere, in advance of the actual earthquake.

Instrumentally Recorded Precursors for the 24 May 2006, Mw=5.4, Morelia Fault Earthquake Sequence, in Mexicali Valley, Baja California, Mexico.

SARYCHIKHINA, O., CICESE, Ensenada, Mexico, osarytch@cicese.mx; GLOWACKA, E., CICESE, Ensenada, Mexico, glowacka@cicese.mx; VÁZQUEZ, R., CICESE, Ensenada, Mexico, rvazquez@cicese.mx; MUNGUÍA, L., CICESE, Ensenada, Mexico, lmunguia@cicese.mx; FARFÁN, F., CICESE, Ensenada, Mexico, fjfarfan@cicese.mx; DÍAZ DE COSSÍO BATANI, G., CICESE, Ensenada, Mexico, gbatani@cicese.mx.

On 24 May 2006 at 04:20 (UTC) a moderate-size (Mw=5.4) earthquake occurred in the Mexicali Valley, Baja California, México, roughly 30 km to the southeast of the city of Mexicali. The earthquake had normal mechanism and ruptured the Morelia fault, at the northwestern border of the Cerro Prieto pull-apart center. Locally, this earthquake was strongly felt and caused minor damage. Numerous cracks and ruptures in the surface were also created. The earthquake was recorded by both local and regional seismic networks and by continuously recording geotechnical instruments (crackmeters and tiltmeters and well piezometers). A foreshock of Mw=4.2 occurred just one minute and 20 seconds before the main shock, which was followed by a series of moderate and low magnitude aftershocks (Lira, 2006, Suárez *et al.*, 2008, Munguía *et al.*, 2009, Sarychikhina *et al.*, 2009).

During the May 2006 earthquakes sequence 5 instruments, (2 vertical crackmeters, 2 borehole tiltmeters and 1 surface tiltmeter of the Mexicali Valley Geotechnical Instruments Network) were in operation and recorded earth surface movement and tilting at the time of the 24 May 2006 mainshock and aftershock sequence. Also 6 piezometers of Mexicali Valley Piezometric Network were in operation and recorded groundwater level changes at the time of the earthquakes.

Here, we present instrumentally recorded anomalies observed in at least 2 instruments before the main event and before one Mw=4.4 aftershock. The registered anomaly had duration of days and amplitude up to 800 μrad for a tilt and 70 cm of groundwater level change. We analyze and discuss possible explanations of observed anomalies.

Operational Earthquake Forecasting

Oral Session · Thursday 8:30 AM, 22 April · Salon A
Session Chairs: Gordon Woo, Michael Blanpied, and Warner Marzocchi

Operational Earthquake Forecasting and Risk Management

WOO, G., Risk Management Solutions, UK, Gordon.Woo@rms.com

In daily life, the general public is commonly exposed to remote uncertain hazards, which would pose a threat to life and property if they were to materialize. Hazard warnings elicit a wide range of precautionary responses, many of which involve modest cost. For example, in a post 9/11 world inured to a pervasive international terrorist threat, many measures can be taken to mitigate terrorism risk, without a population flight from city centers. Short of mandatory evacuation, which may never be justified because of the false alarm rate of earthquake forecasting, there are key operational decisions to reduce potential earthquake loss that may be taken at individual, community, corporation, and civic level. Effective risk management may entail raising public awareness; alerting civil protection agencies; increasing safety inspections; advancing retrofit schedules; and purchasing earthquake insurance. In order for risk managers to gauge which of many possible preparatory measures are commensurate with the prevailing earthquake threat, they need information on the probability gain associated with precursory information. Seismological progress in estimating the contingent probability of occurrence of a major earthquake promises to make operational earthquake forecasting an important field of applied seismological research, with practical applications greatly superseding those associated with earthquake prediction.

Prospects for Operational Earthquake Forecasting

JORDAN, T.H., So. California Earthquake Center, Los Angeles, CA 90089, tjordan@usc.edu

The public needs information about future earthquakes. Although reliable and skillful methodologies for deterministic earthquake prediction have not been achieved, probabilistic forecasting methods can convey useful information about future earthquake occurrence on time scales ranging from decades to days. The goal of operational

earthquake forecasting is the production of authoritative information about the time dependence of seismic hazard to help communities prepare for potentially destructive earthquakes. Its challenges are illustrated by the destructive L'Aquila earthquake of 6 April 2009 (Mw 6.3). The earthquake ruptured a mapped (though poorly known) normal fault in a region identified by long-term forecasting models as one of the most seismically dangerous in Italy; it was the strongest of a rich sequence that started several months earlier and included ML 4.1 event on March 30 and a ML 3.9 foreshock less than four hours prior to the mainshock. According to widely circulated news reports, earthquakes had been predicted by a local resident using unpublished radon-based techniques, provoking a public controversy prior to the event that intensified in its wake. Several weeks after the earthquake, the Italian Department of Civil Protection appointed an international commission with the mandate to report on the current state of knowledge of prediction and forecasting and guidelines for operational utilization. The commission included geoscientists with experience in earthquake forecasting and prediction from China (Y.-T. Chen), France (R. Madariaga), Germany (J. Zschau), Greece (G. Papadopoulos), Italy (P. Gasparini, W. Marzocchi), Japan (K. Yamaoka), Russia (G. Sobolev), United Kingdom (I. Main), and United States (T. Jordan, chair). In this presentation, I will use the commission's findings and recommendations as the basis for speculation on the prospects for operational earthquake forecasting in Italy, California, and elsewhere.

Development of an Official Operational Earthquake Forecast for California (UCERF3 by the ongoing WGCEP)

FIELD, E.H., USGS, Golden, Golden/CO/USA, field@usgs.gov

The Working Group on California Earthquake Probabilities (WGCEP), a joint effort by the Southern California Earthquake Center, United States Geological Survey, and California Geological Survey, is in the process of developing the next-generation Uniform California Earthquake Rupture Forecast (UCERF version 3). One of the main goals for this model is to include spatial and temporal clustering in acknowledgement that triggered events, or aftershocks, can sometimes be large and damaging. The model will make real-time changes in earthquake probabilities based on active monitoring of ongoing seismicity, and as such, UCERF3 will constitute an operational earthquake forecast. This presentation will discuss current plans with respect to the following: 1) how clustering probabilities will be calculated; 2) how this differs from previous approaches (*e.g.*, the USGS STEP model); 3) how the model will be implemented from an operational perspective; 4) how it will be interfaced to hazard and loss calculations; and 5) implications for its official use in building codes and by the California Earthquake Authority for insurance purposes.

Operational Earthquake Forecasting in Italy

MARZOCCHI, W., INGV, Rome, Italy, warner.marzocchi@ingv.it

The aim of this presentation is to show the state of the art of Operational Earthquake Forecasting (OEF) in Italy. OEF can be made at different time scales according to the specific type of planned mitigation actions. Up to last year, in Italy, as well as in many other countries, the only EOF was the national seismic hazard map. Such a forecast involves a time scale of decades that is a pertinent time frame to define suitable building codes. The recent L'Aquila earthquake pushed the Italian scientific community and the Civil Protection to face quite new challenges. For instance, for the first time INGV provided regularly daily spatio-temporal aftershock forecasts; nonetheless, it has been also recognized the impelling necessity to provide daily forecasts also before the mainshock, not only after, in particular during a seismic swarm. Daily forecasts pose a formidable challenge for Civil Protection and local authorities that have to be ready to propose "light" short-term mitigation actions to the public. The term "light" means that such mitigation actions should have a low cost/impact for society, because it is very likely that they result to be a false alarm. In fact, the most reliable short-term models available almost never provide daily probabilities of large events larger than few percents. It has been also recognized the importance to provide mid-term EOF (time scales of 1–5 years). Such forecasts may be used to speed up the survey of building vulnerability in high probability areas, and in case to reinforce sensible structures, like schools, hospitals, and so on. Last, but not least, the L'Aquila experience also raised the dramatic importance of a calibrated and incisive communication to mass-media and public. All these issues are presently under consideration at INGV and they will be the main targets of future researches and initiatives.

Development of an Earthquake Impact Scale for use with the USGS PAGER System

WALD, D.J., U.S. Geological Survey, Golden Colorado USA; MARANO, K.D., U.S. Geological Survey, Golden Colorado USA; JAISWAL, K.S., U.S. Geological Survey, Golden Colorado USA; HEARNE, M., U.S. Geological Survey, Golden Colorado USA; BAUSCH, D., FEMA, Denver Colorado USA.

With the advent of the USGS Prompt Assessment of Global Earthquakes for Response (PAGER) system, which rapidly assesses earthquake impacts, U.S. and international earthquake responders are reconsidering their automatic alert and activation levels as well as response procedures. To help facilitate rapid and appropriate earthquake response, we propose an Earthquake Impact Scale (EIS) based on two complementary criteria. One, based on the estimated cost of damage, is most suitable for domestic events; the other, based on estimated ranges of fatalities, is generally more appropriate for global events. Simple thresholds, derived from the systematic analysis of past earthquake impacts, turn out to be quite effective in communicating predicted impact and response needed after an event, characterized by alerts of green (little or no impact), yellow (regional impact and response), orange (national-scale impact and response), and red (disaster necessitating international response). Corresponding fatality thresholds for yellow, orange, and red alert levels are 1, 100, and 1000, respectively. For damage impact, yellow, orange, and red thresholds are triggered by estimated losses reaching $1M, $100M, and $1B, respectively. The dual approach to alerting stems from the recognition that relatively high fatalities, injuries, and homelessness dominate response in countries where local building practices result in high collapse and casualty rates. In contrast, it is often financial and overall societal impacts that trigger the level of response in regions or countries where prevalent earthquake resistant construction practices greatly reduce building collapse and resulting fatalities. We present both simple and intuitive color-coded alerting criteria; yet, we preserve the necessary uncertainty measures by which one can gauge the likelihood for the alert to be over- or under-estimated.

Are Mitigation Actions Warranted? The Case of the 2009 L'Aquila Earthquake

VAN STIPHOUT, T., Swiss Seismological Service, Zurich, Switzerland, vanstiphout@sed.ethz.ch; WIEMER, S., Swiss Seismological Service, Zurich, Switzerland, wiemer@sed.ethz.ch; MARZOCCHI, W., INGV, Rome, Italy, warner.marzocchi@ingv.it

The disastrous earthquake in L'Aquila Italy about one year ago (M_w6.3, 6 April 2009) highlights again the issue of potentially reducing seismic risk by releasing warnings or initiating mitigation actions. Since earthquakes cluster strongly in space and time, periods of increased seismic hazard are known. During such seismic crises, seismologists typically convey their knowledge of earthquake clustering based on past experience, basic statistics and 'gut feeling'. However, this information is often not quantitative nor reproducible and difficult for decision-makers to digest. We introduce an interdisciplinary approach that combines probabilistic seismic hazard and risk assessment with cost-benefit analysis to allow objective risk-based decision-making. We analyze the effect of uncertainties in different components of this approach. Among various examples, we also consider the 2009 L'Aquila earthquake sequence. The analysis indicates that widespread evacuation was not warranted in the L'Aquila case, supporting the decisions made by authorities in the days and hours leading up to the mainshock. These results demonstrate that the current approach to mitigation actions should be re-thought, because it will hardly ever be cost-effective. Instead, future mitigation actions must be based on the weakest buildings and the ones on the poorest soil, just as flooding evacuations are targeted to flood-prone areas only.

Tobago 2011—A Prospective Case for Operational Earthquake Forecasting

LATCHMAN, J.L., The Univ. of the West Indies, St. Augustine, Trinidad, Trinidad & Tobago, j_latchman@uwiseismic.com; ASPINALL, W.P., University of Bristol, Bristol, United Kingdom, Willy.Aspinall@Bristol.ac.uk

A temporal association has existed for over 100 years between strong earthquakes in the Vema Fracture Zone (VFZ) and significant quakes near Tobago, West Indies, about 2,000 km away. Almost all Tobago quakes above magnitude 5 have been associated with swarms that follow magnitude 6 events on the VFZ, with consistent lags of 39±4 months. A 6.9MS VFZ quake occurred recently (2008/02/08), and the postulated time lag suggests an increased probability of a moderate-strong earthquake near Tobago in mid-2011. In 2008 a cGPS station was installed in Tobago to establish a baseline reference and with a view to capturing any precursory deformation that might accompany the anticipated event. Because coseismic groundwater effects were observed in the damaging 1997 Tobago sequence, radon monitoring is planned. New swarm activity developing in early 2011 could signal an imminent damaging event and we intend to formulate a Bayesian Belief Network (BBN) for Operational Earthquake Forecasting, to assess the strength of evidence if local events start happening. The BBN will also allow us to combine, probabilistically, the seismic event likelihood ratio with any other available premonitory observations, such as accelerating crustal deformation or elevated radon emissions. Emergency management officials are aware of the historical association with VFZ quakes and of the 2008 event, and should a significant event probability gain emerge, various civil protection measures could be implemented, including a public information campaign if the probability gain is strong enough. The prospective 2011 Tobago situation could be a unique opportunity for related research.

Testing and Evaluating Operational Earthquake Forecasts

SCHORLEMMER, D., U of Southern California, Los Angeles, CA, USA, ds@usc.edu; JORDAN, T.H., U of Southern California, Los Angeles, CA, USA, tjordan@usc.edu; JACKSON, D.D., UC Los Angeles, Los Angeles, CA, USA, djackson@ucla.edu; CSEP WORKING GROUP, U of Southern California, Los Angeles, CA, USA.

Operational Earthquake Forecasting is a long-standing demand of society. Already today, short-term aftershock forecasts have become a standard procedure of after-event assessment, *e.g.* during the L'Aquila 2009 aftershock sequence. The Collaboratory for the Study of Earthquake Predictability (CSEP) is testing and evaluating short-term earthquake forecasts in 4 different testing centers around the globe. All forecasts are tested in a truly prospective sense against future observations. Earthquake forecasts should first pass rigorous evaluation tests before being used in an operational sense, in particular those forecasts which may influence public policies or invoke public actions. CSEP is striving to expand testing to operational forecasts and to provide the facilities to test and evaluate such forecasts in many different tectonic environments. We report on plans, possibilities, and experiments that cover operational earthquake forecasting within CSEP and how earthquake forecasters can participate in this large-scale testing effort.

Time-Dependent Earthquake Forecasts Based on Smoothed Seismicity and Rate-And-State Friction

HELMSTETTER, A., LGIT University Grenoble, Grenoble, France, ahelmste@obs.ujf-grenoble.fr; WERNER, M., ETH Zürich, Zürich, Switzerland, max.werner@sed.ethz.ch

We present a new method for time-dependent earthquake forecasting, based on smoothed seismicity. Past earthquakes are smoothed in space and time using adaptive Gaussian kernels. The bandwidths in space and time associated with each event are determined iteratively. Starting from uniform values, we estimate the seismicity rate at the time and location of each earthquake and then modify the kernel bandwidths using a decreasing function of seismicity rate. Compared with ETAS models, this method is much simpler because is does not require a background model. Moreover, it has only three adjustable parameters: the average smoothing time and distance, and a uniform background rate, which are estimated by maximizing the likelihood of the forecasts. We applied this method to estimate daily earthquake probabilities in California. The results are much better than our null hypothesis, chosen as the time-independent model of Werner *et al.* (2010), but not as good as the ETAS model developed by Helmstetter *et al.* (2006) and Werner *et al.* (2010). Our model simply assumes that the future seismicity rate will be proportional to the present rate. Alternatively, we can estimate the future rate from the present rate using Dieterich's (1994) model based on rate-and-state friction. This model can be used to extrapolate the seismicity rate into the future without the need for any stress calculations. It predicts that seismicity will relax toward the background rate after a time equal to the nucleation time. This method requires only one additional parameter, the nucleation time.

Automated Calculation of Post-Earthquake Damage State Exceedance Probabilities Considering the Threat of Aftershocks

GERSTENBERGER, M.C., GNS Science, Lower Hutt, New Zealand, m.gerstenberger@gns.cri.nz; LUCO, N., USGS, Golden, CO, USA; UMA, S.R., GNS Science, Lower Hutt, New Zealand; RYU, H., USGS, Golden, CO, USA.

Real-time earthquake data collection and science is rapidly advancing and provides us with new opportunities for deriving, among other things, probabilities of damage of to buildings due to main shocks and aftershocks. Here we combine the STEP aftershock hazard model (Gerstenberger, 2005), as in current use by the USGS, with risk methodologies for integrating seismic aftershock hazard and main shock-damaged building structural fragilities (Luco, et. al., 2004; Yeo, 2005; Luco, et. al., 2004). Given a scenario main shock, we are able to calculate probabilities of resulting damage states of for a structure of a particular class of structure via convolution with available undamaged building fragilities. Similarly, we can then convolve these newly-developed damaged-structure fragilities (and the main shock damage state probabilities) with probabilities of shaking from aftershocks from the STEP model, in order to derive probabilities of exceeding various damage states within some short-term time period (*e.g.*, 24 hours), for the structure. This work builds upon the aforementioned previous work by Luco, et. al. and consists of the following steps: 1) start with a main shock magnitude and location; 2) for a generic building type at a particular location, calculate the probability of exceeding each potential damage states using either observed or predicted ground motions; 3) calculate probabilities of aftershock shaking, allowing the probabilities to develop with time since the main shock; 4) calculate the probabilities of exceeding the same damage states, within a short time (*e.g.*, 24 hours), taking into account both the main shock induced building damage and possible damage due to aftershock ground shaking. Here we present a prototype tool for such calculations and illustrate its use for scenarios earthquakes in New Zealand and California.

Early Aftershocks Statistics: First Results of Prospective Test of Alarm-Based Model (EAST) and Setting a Frequency-Based Model

SHEBALIN, P., IIEPT, Moscow/Russia, shebalin@mitp.ru; NARTEAU, C., IPGP, Paris/France, narteau@ipgp.jussieu.fr; HOLSCHNEIDER, M., University of Potsdam, Potsdam/Germany, hols@math.uni-potsdam.de; SCHOLRLEMMER, D., USC, Los Angeles/USA, ds@ucs.edu

It was shown recently that the c-value systematically changes across different faulting styles and thus may reflect the state of stress (Narteau *et al.*, 2009). Hypothesizing that smaller c-values indicate places more vulnerable to moderate and large earthquakes, we suggested a simple alarm-based forecasting model, called EAST, submitted for the test in CSEP in California (3-month, M≥4 class); the official test was started on July 1, 2009. We replaced the c-value by more robust parameter, the geometric average of the aftershock elapsed times (the ea-value). We normalize the ea-value calculated for last 5 years by the value calculated for preceding 25 years. When and where the normalized ea-value exceeds a given threshold, an "alarm" is issued: an earthquake is expected to occur within the next 3 months. Retrospective tests of the model show good and stable results (even better for targets M≥5).

During the first 6 months of the prospective test 22 target earthquakes took place in the testing area. 14 of them (more than 60%) were forecasted with the alarm threshold resulting in only 1% of space-time occupied by alarms (5% if space is normalized by past earthquake frequencies). This extraordinary result was obtained mostly due to successful forecast of the sequence of 11 earthquakes near Lone Pine in 1–9 October 2009. However, if we disregard aftershocks as targets, then 4 out of 9 main shocks occurred in alarms with normalized ea-value threshold resulting in 2.5 % of normalized space-time occupied by alarms, the result is also impossible to get by chance at a significance level 1%.

To expand the evaluation of the EAST model relative to larger number of forecast models, we have developed its frequency-based version. We estimate the expected frequency of earthquakes using joint retrospective statistics of targets and the ea-value.

Using Simple Models For Fast, Robust Results

HOLLIDAY, J.R.H., University of California, Davis, Davis / CA / USA, jrholliday@ucdavis.edu; RUNDLE, J.B.R., University of California, Davis, Davis / CA / USA, jbrundle@ucdavis.edu

We are living in the onset of a golden age for operational earthquake forecasting and hazard assessment. Three factors are changing the landscape of cutting-edge research: (1) the proliferation of earthquake data, (2) the increase in computational power, and (3) the development of new theories of earthquake dynamics and seismic models. It is now possible to create simple time-dependent models for future seismicity anywhere in the world and update them in near real-time using data from global and local online earthquake catalogs. Furthermore, these models can then be fed into simple ground response models and updated continuously to aid in real-time models for loss forecasting. In this presentation, we discuss the forecasting capabilities of different models submitted to the Regional Earthquake Likelihood Models (RELM) working group (now the Collaboratory for the Study of Earthquake Predictability). We discuss methods for improving the models and creating hybrid models incorporating only their best performing features. We then discuss simple ground shaking and building response models and outline possible procedures for chaining them all together. The output of such a multi-tiered calculation would prove invaluable for real-time and scenario-based hazard assessment and for cost-benefit analysis of possible mitigation actions.

Numerical Prediction of Earthquake Ground Motion

Oral Session · Thursday 8:30 AM, 22 April · Salon E

Session Chairs: Emmanuel Chaljub, Peter Moczo, and Steven M. Day

High Frequency Ground Motion from Spontaneous Ruptures on Rough Faults

DUNHAM, E.M., Stanford University, Stanford, CA, edunham@stanford.edu; KOZDON, J.E., Stanford University, Stanford, CA, jkozdon@stanford.edu

A particularly challenging aspect of generating synthetic broadband seismograms is to accurately capture, in a single model, both the coherent low frequency wavefield and incoherent high frequency radiation. Toward this end, we seek to identify the fundamental source processes responsible for exciting high frequency waves and incorporate these processes directly into spontaneous rupture models. Our present focus is on fault roughness, which we investigate using a newly devised high-order finite difference method featuring strongly rate-weakening fault friction and off-fault plasticity. The latter tames otherwise unreasonable stress concentrations and prevents fault opening. Natural fault surfaces exhibit slight deviations from planarity with amplitude-to-wavelength ratios of roughness between 10^{-3} and 10^{-2}. Such roughness

exists at all scales, providing a means of exciting waves of all frequencies. Production of high frequency radiation depends not only on fault roughness, but also on the proximity of the prestress state to the critical conditions at which self-sustaining propagation is just barely possible. Around these conditions, even slight perturbations in the fault profile induce large fluctuations in rupture velocity and the efficient production of high frequency waves. Synthetic seismograms share numerous features with actual strong motion data: an approximately flat acceleration spectrum at high frequencies (with amplitude proportional to stress drop) and nonstationarity of frequency content as a function of time (*i.e.*, a shift toward longer periods later in the record, which we explain in terms of a Doppler shift as the rupture recedes from the station).

Accurate and Stable Treatment of Nonlinear Fault Boundary Conditions with Higher-Order Finite Difference Methods

KOZDON, J.E., Stanford University, Stanford, CA, USA, jkozdon@stanford.edu; DUNHAM, E.M., Stanford University, Stanford, CA, USA, edunham@stanford.edu; NORDSTRÖM, J., Uppsala University, Uppsala, Sweden, jan.nordstrom@it.uu.se

High-order numerical methods are ideally suited for earthquake problems since they require fewer grid points to achieve the same solution accuracy as low-order methods. Though straightforward to apply these methods in the interior of a domain, it can be challenging to maintain stability and accuracy near boundaries and faults. Despite several efforts to develop high-order fault boundary treatment, no codes have demonstrated greater than second-order accuracy for dynamic rupture problems, even on rate-and-state friction problems with smooth solutions.

In this work summation-by-parts (SBP) finite difference methods are used with a simultaneous approximation term (SAT) to achieve a stable high-order method for dynamic ruptures on faults with rate-and-state friction. SBP methods use centered spatial differences in the interior and one-sided differences near the boundary. The transition to one-sided differences is done in a particular manner that permits one to provably maintain stability as well as high-order accuracy. In many methods the boundary conditions are strongly enforced by modifying the difference operator at the boundary so that the solution there exactly satisfies the boundary condition. This approach often results in instability when combined with high-order difference schemes. In contrast, the SAT method enforces the boundary conditions in a weak manner by adding a penalty term to the spatial discretization.

Both 1- and 2-D tests of spontaneous rupture propagation on strongly velocity-weakening rate-and-state faults demonstrate the theoretical accuracy and stability of the method. Additionally, we will demonstrate how the methods can be extended, through the use of coordinate transformations, to explicitly account for fault roughness and free-surface topography, both of which may be key to realistic ground motion prediction.

Dynamic Modeling of Mw 7.0 or Larger Earthquakes on the Sierra Madre–Cucamonga Fault System in Los Angeles: Effects of Inelastic Off-Fault Response

MA, S., San Diego State University, San Diego, CA, sma@geology.sdsu.edu; DAY, S.M., San Diego State University, San Diego, CA, day@moho.sdsu.edu

Although nonlinear strong ground motions have been recognized for decades, it was until recently that inelastic off-fault response is considered in the study of earthquake rupture dynamics. Large stress concentration associated with rupture front would cause the off-fault material to yield, which reduces ground motion significantly due to the failure in transmitting large off-fault stresses.

Our previous work on dynamic-rupture simulations of Mw 7.7 events on the Sierra Madre–Cucamonga fault system by assuming elastic response (Ma and Beroza, 2009) showed that large ground motions are mostly concentrated near the fault, especially on the hanging wall (San Gabriel Mountains). Ground motion reaches as large as 3 m/s in some specific areas of the Los Angeles basin, while is in general less than 1 m/s. The rupture directivity effect on ground motion in the Los Angeles basin was found not strong.

In this work, we will focus on how the inelastic off-fault material response might affect these elastic ground motion estimates. We will use our versatile finite element code to simulate MW 7.0 or larger earthquake scenarios on the Sierra Madre–Cucamonga fault system with the pressure-dependent Drucker-Prager yield criterion and incorporate the complex fault geometry from the SCEC Community Fault Model and the 3D crustal velocity structure from the SCEC Community Velocity Model. We will consider fault roughness as a major component of source randomness and examine its effects on rupture propagation and ground motion. Our elastoplastic simulations will provide more realistic time histories of ground motions in the greater Los Angeles area.

Dynamic Ground Motion in Fault Stepovers with Material Contrasts

LOZOS, J.C., Univ. of California, Riverside, Riverside, California, USA, jlozo001@ucr.edu; OGLESBY, D.D., Univ. of California, Riverside, Riverside, California, USA, david.oglesby@ucr.edu; BRUNE, J.N., Univ. of Nevada, Reno, Reno, Nevada, USA, brune@seismo.unr.edu

Using 3D dynamic models, we investigate the effect of fault stepovers on near-source ground motion. We use the finite element method to model the rupture, slip, and ground motion of two parallel strike-slip faults with an unlinked overlapping stepover of variable width. We modeled this system as both an extensional and a compressional stepover and compared the results to those of single planar faults. We found that, overall, the presence of a stepover along the fault trace reduces the maximum ground motion when compared to the long planar fault. Whether the compressional or extensional stepover exhibits higher ground motion overall depends on the width of the separation between the faults. There is a region of reduced ground motion at the end of the first fault segment when the faults are embedded in a homogeneous material. We also experiment with placing realistic material interfaces along the faults, such as a sedimentary basin in an extensional stepover, a pressure ridge in a compressional stepover, and a damage zone around the entire fault. These configurations alter the pattern of ground motion from the homogeneous case; the peaks in ground motion for the bimaterial cases depend on the materials in question. The results may have implications for ground motion prediction in future earthquakes on geometrically complex faults.

Ground Motion from Dynamic Ruptures on the Wasatch Fault Embedded in a 3-D Velocity Structure

LIU, Q., University of California, Santa Barbara, CA, qliu@umail.ucsb.edu; ARCHULETA, R.J., University of California, Santa Barbara, CA, ralph@crustal.ucsb.edu; SMITH, R.B., University of Utah, Salt Lake City, UT, robert.b.smith@utah.edu

The Salt Lake City segment of the Wasatch Fault poses a serious threat to the nearby city and surrounding communities due to the potential of a Mw 7+ earthquake. We use a finite element method (Ma & Liu, BSSA, 2006) to study the dynamic rupture process of faulting on a dipping fault in a heterogeneous velocity structure. The dynamics are controlled by a slip-weakening friction law and the distribution of stresses. We compute the ground motion for a maximum frequency of 1.0 Hz. We use the 3D Community Velocity Model (CVM) in Salt Lake Basin; minimum shear wave velocity used is 0.5 km/s. As a baseline scenario we use a constant shear stress drop $\Delta\sigma = 3.6$MPa over the 30km x 18km dipping fault and put the hypocenter midway along strike near the bottom of the fault. This scenario produces an average slip of 2.7m. The most significant ground shaking (peak horizontal velocity (PHV) larger than 1.5m/s) occurs in the area within 5 km of the fault trace, with the largest being on the hanging wall. Next, we modify the initial stress to decrease linearly from its constant value at 2 km (and deeper) to 0 at the free surface. The general PHV pattern does not change much, but the peak value at the fault trace is about half the value in baseline scenario. Next we move the hypocenter to the south; this leads to a considerable decrease for both PHV and the area which experiences significant ground shaking near the southern end, which has less along-strike directivity. The effect of the CVM is noticeable in that amplitudes and durations west of the fault are most pronounced where the sediments are thickest. To estimate a less biased evaluation of the ground motion we will vary the parameters, *e.g.* hypocenter location, heterogeneous stress conditions and slip weakening distance.

Ground Motion Predictions from 0–10 Hz for M7 Earthquakes on the Salt Lake City Segment of the Wasatch Fault, Utah

ROTEN, D., San Diego State University, San Diego, CA, droten@sciences.sdsu.edu; OLSEN, K.B., San Diego State University, San Diego, CA, kbolsen@sciences.sdsu.edu; PECHMANN, J.C., University of Utah, Salt Lake City, UT, pechmann@seis.utah.edu; CRUZ-ATIENZA, V.M., UNAM, Mexico D.F., Mexico, cruz@geofisica.unam.mx; MAGISTRALE, H., San Diego State University, San Diego, CA, harold.magistrale@geology.sdsu.edu

We predict ground motions for M7 earthquakes on the Salt Lake City segment of the Wasatch fault (WFSLC), Utah, over the entire frequency range of engineering interest by applying four different numerical techniques in sequence. First, we generate a set of realistic source representations by simulating spontaneous rupture on a planar fault with the staggered-grid split-node finite difference method. The initial shear stress distributions include depth-dependent fault-normal stress on a 50°-dipping, normal fault. Next, the slip rate histories from the spontaneous rupture scenarios are projected onto a detailed 3-D model of the WFSLC and used to simulate 0–1 Hz wave propagation in the Salt Lake Basin area with the most recent version of the Wasatch Front Community Velocity Model. The simulated ground motions show strong along-strike directivity effects for ruptures nucleating towards the ends of the WFSLC, as well as significant amplifications by the low-velocity sediments on the hanging wall. The third step is to combine the 0–1 Hz finite difference simulations with local scattering operators to obtain broadband (BB, 0–10 Hz) synthetics and maps of average horizontal peak ground motions. Finally we use

the BB synthetics, deconvolved to 240 m depth, as input to compute fully nonlinear 1-D SH ground motion along two profiles across the Salt Lake Basin. We find that the linear (BB) synthetics exceed peak horizontal ground accelerations predicted by next generation attenuation (NGA) models by more than one standard deviation on the hanging wall side of the fault. The fully nonlinear synthetics, however, exhibit peak accelerations that are generally consistent with NGA predictions.

Calibration of Simulated Motions from Spontaneous Rupture Models Relative to NGA Ground Motion Prediction Equations

SEYHAN, E., UCLA Civil & Environmental Eng., Los Angeles/CA/USA, emel.seyhan@gmail.com; STAR, L.M., UCLA Civil & Environmental Eng., Los Angeles/CA/USA, lcoyne@ucla.edu; GRAVES, R.W., URS Corporation, Pasadena/CA/USA, Robert_Graves@URScorp.com; STEWART, J.P., UCLA Civil & Environmental Eng., Los Angeles/CA/USA, jstewart@seas.ucla.edu

Previous work by Star *et al.* (in review, *Earthquake Spectra*) has calibrated simulated ground motions from the broadband hybrid simulation methodology against NGA ground motion prediction equations for the ShakeOut event and an Mw 7.15 Puente Hills blind thrust event. The methodology evaluates several attributes of the simulated ground motion suite that are relevant to engineering predictions of ground motion intensity measures: (1) the rate of attenuation with distance; (2) the intra-event standard deviation term; and (3) the mean misfit of the ground motions, as represented by an event term. For the original broadband (0–10 Hz) ShakeOut rupture scenario, we found that the median of the simulated motions are similar to the emipircal predictions at short periods in the near fault region, but then attenuate with distance more rapidly. At longer periods, the simulated motions are generally larger than the empirical predictions, due to the high static stress drop of the scenario and the coupling of strong rupture directivity with basin response effects. Here, we apply this methodology to simulated motions produced using a spontaneous rupture model, which are referred to as ShakeOut-D (Olsen *et al.*, 2009; *Geophy. Res. Ltrs*) in order to investigate any systematic differences in the ground motion response that might be related to the source characterization, particularly in terms of the coupling between rupture directivity and basin response. Since the ShakeOut-D simulations are band limited, we must restrict our analysis to the longer periods (T > 2 sec). The calculations are ongoing and the latest results will be presented at the meeting.

Efficient Simulation of Anelastic Wave Propagation by the Octree-based Finite Element Method— An Improved Approach

BIELAK, J., Carnegie Mellon University, Pittsburgh/PA/USA, jbielak@cmu.edu; KARAOGLU, H., Carnegie Mellon University, Pittsburgh/PA/USA, hkaraogl@andrew.cmu.edu; TABORDA, R., Carnegie Mellon University, Pittsburgh/PA/USA, ricardotaborda@gmail.com

We present two recent modifications to Hercules (Tu et al, 2006), an octree-based finite element parallel code for anelastic wave propagation, which have enabled us to model constant Q over almost two decades with an error of less than 5 percent, and to speed-up the wall-clock time of ground motion simulations by 250 percent with respect to our previous version.

Hercules relies on an octree-based mesher and solves the anelastic wave equations by approximating the spatial variability of the displacements and the time evolution with tri-linear elements and central differences, respectively. The code uses a plane wave approximation of the absorbing boundary condition, and introduces a Rayleigh attenuation mechanism in the bulk. In the new version we have replaced Rayleigh damping with a viscoelastic rheological model similar to the Zener model plus viscous damping, using two auxiliary variables, and have adapted a restoring force procedure developed by Balazovjech and Halada (2006) and discussed by Moczo et al (2007) for performing the stiffness matrix-displacement vector multiplication at each time-step. The improved matrix-vector multiply procedure reduces the number of multiplications and additions per time-step by a net factor of 2.5. We illustrate the applicability of the new procedure with results of a ShakeOut simulation for a maximum frequency of 1.5 Hz.

On Accuracy of the Numerical Schemes in Media With a Large P-wave to S-wave Speed Ratio

MOCZO, P., Comenius University Bratislava, Bratislava, Slovakia, moczo@fmph.uniba.sk; KRISTEK, J., Comenius University Bratislava, Bratislava, Slovakia, kristek@fmph.uniba.sk; PAZAK, P., Geophysical Institute SAS, Bratislava, Slovakia, pazak@savba.sk; GALIS, M., Comenius University Bratislava, Bratislava, Slovakia, martin.galis@fmph.uniba.sk; CHALJUB, E., LGIT UJF, Grenoble, France, Emmanuel.Chaljub@obs.ujf-grenoble.fr

The P-wave to S-wave speed ratios (Vp/Vs) as large as 5 and even larger often have to be accounted for in numerical modeling of seismic motion in structurally and rheologically realistic models of sedimentary basins and valleys. Although sediments with large Vp/Vs usually do not make a major part of the computational region, their effect can be significant because they are at or very close to the free surface. However, the accuracy of the numerical schemes with respect to varying Vp/Vs is not often addressed in studies presenting schemes.

In order to identify the very basic inherent aspects of the numerical schemes responsible for their behavior with varying Vp/Vs ratio, we included the most basic 2nd-order 2D numerical schemes on a uniform grid in a homogeneous medium. Although basic in the specified sense, the schemes comprise the decisive features for accuracy of wide class of numerical schemes. We also included 3D higher-order schemes.

We investigated the following schemes (FD–finite-difference, FE–finite-element): FD displacement conventional grid, FD optimally-accurate displacement conventional grid, FD displacement-stress partly-staggered grid, FD displacement-stress staggered-grid, FD velocity-stress staggered-grid, FE Lobatto integration, FE Gauss integration, spectral element.

We defined and calculated local errors of the schemes in amplitude and polarization normalized for a unit time. Extensive numerical calculations for wide ranges of values of the Vp/Vs ratio, spatial sampling ratio and stability ratio, and entire range of directions of propagation with respect to the spatial grid led to interesting and surprising findings.

In parallel with the numerical results and their analysis we compare the numerical schemes themselves in terms of their inherent structures, applied approximations, and truncation errors.

Numerical Prediction of Long-Period Earthquake Ground Motion in Japan

KOKETSU, K., Earthquake Research Institute, University of Tokyo, Tokyo, Japan, koketsu@eri.u-tokyo.ac.jp; MIYAKE, H., Earthquake Research Institute, University of Tokyo, Tokyo, Japan, hiroe@eri.u-tokyo.ac.jp; HIKIMA, K., R & D Center, Tokyo Electric Power Company, Yokohama, Japan, hikima.kazuhito@tepco.co.jp; HAYAKAWA, T., Ohsaki Research Institute, Inc., Tokyo, Japan, takashi.hayakawa@shimz.co.jp; SUZUKI, H., Tokyo Technology Center, OYO Corporation, Tsukuba, Japan, suzuki-haruhiko@oyonet.oyo.co.jp; WATANABE, M., Ohsaki Research Institute, Inc., Tokyo, Japan, motofumi.watanabe@shimz.co.jp

The Japan islands are in a complex tectonic setting with various subducting plates, and most of their urban areas are located on sedimentary basins. These lead to three-dimensionally complicated velocity structures, which cause significant effects on the propagation of seismic ground motions from an earthquake to the urban areas. Accordingly, it is important for the numerical prediction of long-period ground motion and its seismic hazard to determine the three-dimensional (3D) velocity structure of a target area. We have already proposed a standard procedure for modeling a regional 3D velocity structure, simultaneously and sequentially using various kinds of datasets such as those from refraction and reflection experiments, gravity surveys, geological surveys, borehole loggings, microtremor surveys, and earthquake observations. We applied the procedure to the regions from the source areas of future megathrust earthquakes (M8.0 Tokai, M 8.1 Tonankai, and M7.5 Miyagi-oki earthquakes) to the metropolitan areas of Tokyo, Osaka, Nagoya, and Sendai for constructing 3D velocity structure models. These future earthquakes were selected because of their high occurrence probabilities within 30 years, which are 87%, 66%, and nearly 100%. As the last step of the procedure, we calibrated the models by comparison of observed and synthetic ground motions from medium-sized earthquakes. We then carried out numerical predictions of long-period ground motions from the future Tokai, Tonankai, and Miyagi-oki earthquakes using the calibrated velocity structure models and the same simulation codes as those for the calibration. We calculated the response spectra of the simulated ground motions and measured their peak ground velocities and duration times. We finally combined the results into long-period ground motion hazard maps. The above process of making long-period hazard maps will be repeated for a future M8.4 Nankai earthquake (probability 55%) in 2010.

Accurate Prediction of Ground Motion Using an hp-Adaptive Discontinuous Galerkin Finite-Element Method

ETIENNE, V., Géoazur,CNRS,UNSA, Nice-Sophia-Antipolis/France, etienne@geoazur.unice.fr; CHALJUB, E., LGIT,CNRS,OSUG,J. Fourier Univ., Grenoble/France, Emmanuel.Chaljub@obs.ujf-grenoble.fr; VIRIEUX, J., LGIT,CNRS,J. Fourier Univ., Grenoble/France, Jean.Virieux@ujf-grenoble.fr; OPERTO, S., Géoazur,CNRS,UNSA, Villefranche/France, operto@geoazur.obs-vlfr.fr

Accurate simulations of earthquake ground motion require numerical methods able to handle fine geological structures when frequencies of interest are considered. To this objective, we present a discontinuous Galerkin finite-element method (DG-FEM) formulation with Convolutional Perfectly Matched Layer (CPML) absorbing condition suitable to seismic wave modeling in large scale 3D media. The method makes use of unstructured tetrahedral meshes locally adapted to the medium properties (h-adaptivity) and of interpolation orders that can change from one element to another according to an adequate criterion (p-adaptivity). These

two features allow us to reduce significantly the numerical cost of the simulations. Moreover, we designed an efficient CPML absorbing condition, both in terms of absorption and computational cost, by combining interpolation orders in the numerical domain. A quadratic interpolation is typically used in the medium to get the required accuracy while lower interpolation orders are used in the CPMLs to reduce the whole numerical cost and to obtain a well-balanced workload over processors. While the efficiency of DG-FEM has been largely demonstrated with high interpolation orders, we favor the use of low orders more appropriate to the applications we are interested in. In particular, we address the issues of seismic modeling or seismic imaging in case of complex geological structures requiring a fine discretization. We illustrate the efficiency of our approach within the framework of the EUROSEISTEST verification project which aims at comparing high-frequency (f<4Hz) numerical predictions of ground motion in the Volvi basin (Greece). Thanks to the tetrahedral meshing, we achieve a fine discretization of the basin which appears to be a sine qua non condition for accurate computation of surface waves diffracted off the basin edges. We compare our results with other methods (SEM, FDM) and demonstrate the major benefits of DG-FEM in such cases.

Efficient Parallel Seismic Simulations Including Topography and 3-D Material Heterogeneity on Locally Refined Composite Grids

PETERSSON, N.A., Lawrence Livermore National Labs, Livermore, CA USA, andersp@llnl.gov; RODGERS, A., Lawrence Livermore National Labs, Livermore, CA USA, rodgers7@llnl.gov

The wave propagation project (WPP) code simulates ground motions due to earthquakes and other seismic events, taking into account realistic heterogeneous 3-D media and topography. The WPP code solves the time-dependent elastic wave equations using an energy conserving finite difference discretization on a composite grid consisting of a set of component meshes. The top mesh is curvilinear and follows the shape of the topography, while all underlying meshes are Cartesian with hanging nodes along the grid refinement interfaces. WPP automatically generates the composite grid based on the topography provided by the user, and the depths of the grid refinement interfaces. A kinematic source model is used to simulate earthquake ruptures on arbitrary three-dimensional fault surfaces. Point force and moment tensor source discretization formulas have been developed to allow sources to be placed anywhere on the composite grid, with special treatments near grid refinement interfaces and on curvilinear meshes.

The WPP code has been verified extensively, for example using the method of manufactured solutions, by solving Lamb's problem, by solving various layer over half-space problems and comparing to semi-analytic (FK) results, and by simulating scenario earthquakes where results from other seismic simulation codes are available. WPP has also been validated against seismographic recordings of moderate earthquakes.

WPP performs well on large parallel computers and has been run on up to 32,768 processors using about 26 Billion grid points and 41,000 time steps. During this talk we will give an overview of the WPP methodology and present simulations where WPP was used to calculate ground motions in the presence of topography and 3-D material heterogeneities, for example the Grenoble basin test cases.

This is Lawrence Livermore National Laboratory contribution LLNL-ABS-422247.

Euroseistest Verification and Validation Project: An International Effort to Evaluate Ground Motion Numerical Simulation Relevance

HOLLENDER, F., CEA, Cadarache/France, fabrice.hollender@cea.fr; MANAKOU, M., AUTH, Thessaloniki/Greece, manakou@civil.auth.gr; BARD, P.-Y., LGIT,CNRS,LCPC,J. Fourier Univ., Grenoble/France, bard@obs.ujf-grenoble.fr; CHALJUB, E., LGIT,CNRS,OSUG,J. Fourier Univ., Grenoble/France, Emmanuel.Chaljub@obs.ujf-grenoble.fr; RAPTAKIS, D., AUTH, Thessaloniki/Greece, raptakis@civil.auth.gr; PITILAKIS, K., AUTH, Thessaloniki/Greece, kpitilak@civil.auth.gr; TSUNO, S., LGIT,CNRS,J. Fourier Univ., Grenoble/France, Seiji.Tsuno@obs.ujf-grenoble.fr

Numerical simulations are often used to evaluate local ground motion amplification (site effects). Before using these approaches for civil engineering design purposes, it is necessary to evaluate their reliability.

Within the framework of this evaluation effort, an ongoing international collaborative work was organized, jointly by the Aristotle University of Thessaloniki, Greece, the Cashima research project (supported by the CEA and the Laue-Langevin institute), and the Joseph Fourier University, France.

We decided to focus the study on a site (1) where the site geometry and geotechnical properties are well known and (2) where accelerometric time histories are available. The "EuroseisTest site", located few tens of km East of Thessaloniki, was chosen since it provides a detailed 3D model of the sedimentary basin (about 5 km wide, 15 km long, sediments reach about 400 m depth) and the signals of 8 local earthquakes with magnitude from 3 to 5, recorded on 19 surface and borehole accelerometers.

The project involves more than 10 international teams from Europe, Japan and USA, employing different numerical techniques (FDM, FEM, SEM, DGM, PSM, DEM). It consists in computations of different 2D, 3D, linear or non-linear cases. Through these exercises, it is possible to evaluate (1) the accuracy of numerical methods when applied to realistic applications where no reference solution exists (verification) and (2) quantify the agreement between recorded and numerically simulated data (validation).

We will present the site, the objectives, the 3D model construction strategy, the different computing cases and main results of this project. The verification work allows us to clearly identify and understand the discrepancies between the predictions of the different simulation methods. The validation work shows surprisingly good agreement for the largest magnitude event, even at high frequencies (up to 4 Hz).

Amplification and Attenuation in Southern California Basins Extracted from Ambient Seismic Field Analysis

DENOLLE, M., Stanford, Stanford/CA/USA, mdenolle@stanford.edu; BEROZA, G., Stanford, Stanford/CA/USA, beroza@stanford.edu; PRIETO, G., Universidad de los Andes, Bogota/Colombia, gprieto@uniandes.edu.co; LAWRENCE, J.F., Stanford, Stanford/CA/USA, jflawrence@stanford.edu

One of the foremost challenges to seismic hazard analysis is properly characterizing wave propagation in the geologically complex crust. Accurate ground motion simulations are limited to our incomplete knowledge of the subsurface structure. We propose to improve this situation using a newly developed analysis of the ambient seismic field in several ways.

First, we recover the spatially variable anelastic structure in South California. We use the full 3D wave field (Rayleigh and Love waves) described by our Green's functions to extract the attenuation information. The technique applied to the first order coherency is not biased by the non-uniform directional excitation of the ambient noise sources and has been validated by comparison with surface waves tomography.

Second, we study ground motion amplification from sedimentary basins with transfer functions. Our results are validated as accurate using ground motion observed in moderate earthquakes at long periods. We compare these results with CyberShake simulations in Los Angeles area. While further improvements can be achieved by accounting for more realistic earthquake source parameters as well, our preliminary results show strong amplification in the Los Angeles basin, as is seen in long-period ground motion simulations.

Elastic Model Up-Scaling for the Elastic Wave Equation Based on Non-Periodic Homogenization

CAPDEVILLE, Y., IPGP-CNRS, Paris/France, capdevil@ipgp.fr; GUILLOT, L., IPGP-CNRS, Paris/France, guillot@ipgp.fr; MARIGO, J.-J., Ecole Polytechnique, Palaiseau/france, marigo@lms.polytechnique.fr

When considering numerical acoustic or elastic wave propagation in media containing small heterogeneities with respect to the minimum wavelength of the wavefield, being able to upscale physical properties (or homogenize them) is valuable, for mainly two reasons: first, replacing the original discontinuous and very heterogeneous media by a smooth and more simple one, is a judicious alternative to the necessary fine and difficult meshing of the original media required by many wave equation solvers; second, it helps to understand what properties of a medium are really ``seen" by the wavefield propagating through it, which is an important aspect in an inverse problem approach.

We present here a solution to solve this up-scaling problem for non-periodic complex media with rapid variations in all directions based an a non-periodic homogenization procedure. We first present a pedagogical introduction to non-periodic homogenization in 1D, allowing to find the effective wave equation and effective physical properties of the wave equation in a highly heterogeneous medium. It can be extended from 1D to a higher space dimension. This development can be seen as an extension of the classical two-scale periodic homogenization theory applied to the wave equation for non-periodic media.

To validate this development, we then present two examples of wave propagation in 2D complex elastic models: a geometrically square model with random heterogeneities, and the Marmousi2 model. A reference solution is computed with the Spectral Element Method with meshes honoring all interfaces. Furthermore, we compare the results obtained in the homogenized model and in a low-pass filtered model with respect to the reference solution.

Numerical Insights of 2D-PSV Nonlinear Basin Response Analyses

BONILLA, L.F., IRSN, Fontenay-aux-Roses, France, fabian.bonilla@irsn.fr; GELIS, C., IRSN, Fontenay-aux-Roses, France, celine.gelis@irsn.fr; LIU, P.C., USBR, Denver, Colorado, USA, pliu@usbr.gov

Common nonlinear response analyses are performed in 1D soil columns. However, in the last years the development of 2D/3D nonlinear rheologies as well as increas-

ing computational power make possible to analyze wave propagation in complex structures in multiple dimensions. Basin studies are quite interesting due to the geometry, wave conversion, and edge effects on earthquake ground motion among others.

Here we present the results of 2D-PSV wave propagation in a semi-elliptic basin over a half-space considering linear and nonlinear material properties. This study aims to show 1) the effects of the angle of incidence: 2) the effects of the type of source of the incident wavefield (*e.g.* plane wave vs point source); and 3) the effects of impedance contrast between the basin fill and the bedrock on the ground motion.

Preliminary results show that nonlinear basin response is very sensitive to the angle of incidence as well as the type of source of the incoming wavefield. The incoming energy does not trigger equal nonlinear effects for inclined angles of incidence. Furthermore, the energy coming from a plane wave is higher than from a point source, therefore increasing the nonlinear response of the media. These results suggest that full 3D wave propagation including nonlinear and near-source effects should be used to better characterize the earthquake ground motion of future earthquakes in the presence of basin structures.

Quantifying the Risk Posed to Tall Steel Frame Buildings in Southern California from Earthquakes on the San Andreas Fault

MOURHATCH, R., California Institute of Technolo, Pasadena, CA, USA, ramses@caltech.edu; SIRIKI, H., California Institute of Technolo, Pasadena, CA, USA, hemanth@caltech.edu; KRISHNAN, S., California Institute of Technolo, Pasadena, CA, USA, krishnan@caltech.edu

We have recently embarked on a project to quantify the region-wide risk to tall steel buildings in southern California over the next 30 years from earthquakes on the San Andreas fault, through end-to-end simulations. These simulations include modeling the source and rupture of a fault at one end, numerically propagating the seismic waves through the earth structure, simulating the damage to selected tall buildings, and estimating the economic impact at the other end. Using kinematic finite source inversions from past earthquakes as well as stochastically generated sources, we are simulating tens of earthquakes on the San Andreas fault with magnitudes varying between 6.0 and 8.0 (earthquakes capable of causing damage to tall buildings in the LA basin), three hypocenter locations, and two rupture directions. The long-period synthetics generated using the spectral element method in conjunction with the SCEC-CVMH velocity model are propagated through 2 soil models that are representative of the greater LA region, and then combined with highpass-filtered ground motion records from the Northridge earthquake (suitably scaled for magnitude differences) to arrive at broadband motions at 636 analysis sites, spaced at 3.5km in either direction. The simulated 3-component waveforms from each of the scenario events are used to analyze 3 steel braced frame buildings and 3 steel moment frame buildings in the 20-story class for damage. Populating the building with typical office inventory, an economic loss analysis is conducted to determine region-wide annualized losses for each building under each scenario. The results are combined with the 30-year probabilities of earthquakes on the southern San Andreas fault, recently forecast by the Working Group on California Earthquake Probabilities (WGCEP) to get the annualized loss for each building from San Andreas fault earthquakes.

Site Effects in Nonlinear Structural Performance Predictions

LI, W., Georgia Institute of Technology, Atlanta/GA/USA, wli3@mail.gatech.edu; ASSIMAKI, D., Georgia Institute of Technology, Atlanta/GA/USA, dominic.assimaki@ce.gatech.edu

Limited guidance exists both in engineering practice and seismology regarding the mathematical model that should be employed for the computationally efficient evaluation of site response in synthetic ground motion predictions. We here study the role of site response model selection for synthetic ground motions computed for implementation in structural performance predictions. More specifically, we combine downhole observations and broadband ground motion synthetics for characteristic site conditions in the Los Angeles Basin, and investigate the variability in structural performance introduced by the soil model used in site response predictions. More specifically, we conduct viscoelastic and nonlinear site response simulations for a series of rupture scenarios, and evaluate the ground surface response variability that results from the selection of the soil response model. Next, we subject a series of bilinear SDOF oscillators to the ground motions computed using the alternative site response models, and evaluate the consequent variability introduced in the structural response predictions. Results show high bias and uncertainty of the inelastic structural displacement ratio for periods near the fundamental period of the soil profile. The amount of bias and period range where the structural performance uncertainty manifests are shown to be a function of the soil stiffness. We finally derive empirical correlations between the soil shear wave velocity in the near-surface (Vs30) and the variability introduced in structural analyses using results from our simulations.

Near-Surface Deformation Associated with Active Faults

Oral Session · Thursday 8:30 AM, 22 April · Salon F
Session Chairs: Lee M. Liberty and Thomas L. Pratt

Crustal Deformation Modeling in the Central United States

BOYD, O.S., USGS, Memphis, TN, olboyd@usgs.gov; ZENG, Y., USGS, Golden, CO, zeng@usgs.gov; FRANKEL, A.D., USGS, Seattle, WA, afrankel@usgs.gov; RAMIREZ-GUZMAN, L., USGS, Golden, CO.

We explore the surface deformation and strain rate signal associated with post-earthquake effects and steady-state creep on deeply buried faults beneath the Mississippi embayment with the use of analytic, semi-analytic and numerical modeling methods. Improvements in the precision of geodetic monitoring, which indicate very low rates of surface deformation, are inconsistent with the return periods of large earthquakes in the New Madrid seismic zone. We build upon previous studies and seek to answer the following questions: How does subsurface faulting and steady-state creep, if present, translate into surface deformation? How do rates of surface deformation change during the earthquake cycle? What are the far- and near-field drivers of stress, and how do they affect surface deformation? What are the effects of the embayment and of other heterogeneities in the upper crust on surface deformation? The answers to these questions will help us to constrain and address questions significant for earthquake hazard assessments: What is the recurrence behavior of New Madrid type events? To what extent is our knowledge of New Madrid, in terms of deformation and recurrence, transferable to intraplate earthquakes in general?

We present estimates of constant and time-variable surface deformation. The former results are derived from models in which steady-state creep occurs on deeply buried faults within the New Madrid seismic zone subject to various boundary conditions, including plate boundary stresses to the sides and from below. The latter, time-variable surface deformation estimates, result from modeling the viscoelastic relaxation in the lower crust/upper mantle after an earthquake on faults within the New Madrid seismic zone. Preliminary results suggest that multiple models can accommodate significant strain at depth but be damped by 80% or more at the Earth's surface.

Recurrent Eocene and Quaternary Uplift Above the Southwestern Blytheville Arch, Arkansas: Is It Contributing to the Formation of Lake St. Francis?

WILLIAMS, R.A., U.S. Geological Survey, Golden, Colorado, rawilliams@usgs.gov; STEPHENSON, W.J., U.S. Geological Survey, Golden, Colorado, wstephens@usgs.gov; PRATT, T.L., U.S. Geological Survey, Seattle, Washington, tpratt@usgs.gov; ODUM, J.K., U.S. Geological Survey, Golden, Colorado, odum@usgs.gov

Guccione (2005; Tectonophysics) concluded that Lake St. Francis, located in the New Madrid seismic zone and northeastern Arkansas, formed by multiple subsidence events and uplift downstream along the St. Francis River. This conclusion is supported in P-wave reflection profiles that show young deformation roughly 3 km southeast of the lake and about 60 km northwest of Memphis, Tennessee. The profiles reveal Quaternary uplift of a buried anticline in the post-Paleozoic deposits near Lepanto, Arkansas; Holocene uplift of this anticline may be forming a buttress or dam on the southeast side of the lake. The anticline, which overlies a seismically active area on the eastern margin of the Blytheville arch, shows evidence of recurrent uplift beginning after the Eocene and continuing into the Quaternary. The evidence includes a change in anticline height with depth and thickening strata east of the anticline. The anticline is about 100 m high at the top of the Paleozoic section, and, upwards, the height decreases to about 20 m at the Pliocene-Pleistocene surface. The modern ground surface in the region is flat, so deformation at the surface above the anticline is not recognized. Our results are consistent with previous COCORP and industry reflection data acquired near Lepanto, which also showed the anticline, but lacked imaging of the later Tertiary or Quaternary section. Sudden uplift of this anticline during past earthquakes may have temporarily blocked or altered the southerly flow of the St. Francis River thereby contributing to the formation of Lake St. Francis. It is not clear if the current seismicity near Lepanto is related to ongoing deformation of this anticline.

Evidence for One or More Major Late-Quaternary Earthquakes and Surface Faulting in the East Tennessee Seismic Zone

VAUGHN, J.D., Keen GeoServe, LLC, Dexter, MO, geoman@newwavecomm.net; OBERMEIER, S.F., Rockport, IN; HATCHER, R.D., University of Tennessee, Knoxville, TN; HOWARD, C.W., University of Tennessee, Knoxville, TN; MILLS, H.H., TN Technological University, Cookville, TN; WHISNER, S.C., Bloomsburg University.

The East Tennessee seismic zone (ETSZ) of the southern Appalachians is the second most active intraplate region east of the U.S. Rocky Mountains. It is a ~50

km-wide, 300 km-long zone of seismicity that extends from NE AL and NW GA to just NE of Knoxville, TN. Although the ETSZ has not had historical earthquakes of M>5, other researchers have suggested recently that it may be capable of generating an "infrequent" M~7.5 shock. Earthquakes originate below the regional thrust sheets at a depth of 5–26 km within basement rocks. To help clarify the late-Quaternary earthquake history and potential of this seismic zone, we have initiated a search for paleoseismic evidence. East to NE of Knoxville, TN, we have discovered: 1) surficial faulting and fracturing of late-Pleistocene terrace alluvium and colluvium at Dandridge Point; 2) minor paleoliquefaction and prevalent fractures in several other terraces; and 3) fractured and disrupted features in terrace alluvium at three sites attributed to seismic liquefaction and forceful groundwater expulsion. A tectonic, rather than landslide, origin of the terrace faulting is indicated by a "normal" outcrop of Knox dolomite immediately north (riverward) of the terrace faulting; however, structural relations at Dandridge Point are complicated by older thrust faulting and possible fault reactivation. Along the southwest margin of the ETSZ in the Sequatchie Valley (SV), we have identified left-stepping, NNW-trending lineaments on aerial photos and many fractures in Holocene and latest-Pleistocene alluvium of river banks; these SV fractures are currently interpreted to be of possible Holocene-age paleoseismic, non-paleoliquefaction, origin. Collectively, these initial findings imply that the ETSZ has produced at least one episode of surface faulting and generated one or more strong earthquakes during the late Quaternary.

Seismic Potential of the Pishin/Mach Shear Zone in Northern Baluchistan, Pakistan

KAKAR, D.M., University of Balochistan, Quetta Pakistan, dinkakar@yahoo.co.uk; SZELIGA, W., University of Colorado, Boulder CO, bilham@colorado.edu; BILHAM, R., University of Colorado, Boulder CO.

In the past century more seismic energy has been released within 200 km of Quetta than in the Himalaya of Northern Pakistan, yet much of this energy (equivalent to a single Mw8.0) has been released, not on the Chaman Fault, the principal fault bounding the western edge of the Indian plate, but in the fold and thrust belt to the east. A dozen destructive earthquakes have occurred here since 1865, including the 1935 Mw 7.7 Quetta earthquake with a death toll of 35000. The most recent damaging earthquakes occurred in 2008 in the Pishin/Ziarat region NE of Quetta, where 300 people were killed by landslides and by the collapse of adobe structures. The deformation velocity field derived from GPS measurements before and after the earthquake indicates that earthquakes here are associated with a shear zone trending NW/SE underlying the mapped fold systems that near Pishin and Mach trend approximately eastward. The Pishin/Mach shear zone defines a transition in geological structure from the partitioned thrust/wrench fault system of the Northern Kirthar ranges to its south, to the Sulaiman lobate thin-skinned tectonics in the Quetta transverse zone to its north. The forces responsible for dextral shear are thought to originate from a 15° restraining bend on the plate boundary near Chaman. The SE extent of the shear zone is uncertain but it is possible it is responsible for the damaging earthquake of 1909 near Sukkur, > 200 km to the SE. From GPS measurements we estimate the slip rate on the Pishin/Mach shear zone is 5–10 mm/yr, a range that is consistent with the kinematics of the restraining bend geometry.

Creep on the Ornach-Nal Fault, India's Western Boundary with Asia

BILHAM, R., University of Colorado, Boulder CO 80309 USA; SZELIGA, W., University of Colorado, Boulder CO 80309 USA; LODI, S., NED University, Karachi Pakistan.

Of considerable concern to the megacity of Karachi is the absence of significant historical or recent seismicity on the nearby W. edge of the Indian plate. Does this segment of Chaman fault represent a mature seismic gap or is the plate boundary creeping aseismically. The Quetta earthquake of 1935(Mw7.7) occurred on a subsidiary fault 50 km east of Chaman. A oral tradition of historically damaging moderate earthquakes is known to villagers between Nushki and Chaman, the most recent of which occurred in 1978 in 1892 respectively. Earthquakes on the Chaman fault elsewhere are relatively modest. We report here evidence for surface or near-surface creep on the southernmost Chaman system - the Ornach Nal Fault - where it approaches the Makran triple junction. GPS measurements conducted westwards across the boundary near the town of Las Bela indicate that Bela itself, like Karachi, is essentially locked to the Indian plate. Points 10, 20 and 40 km to the west of Bela move increasingly fast to the south attaining velocities approaching 18 mm/yr, the velocity encountered along the entire Makran coastline. Dislocation models fit to these data suggest that the fault is creeping at 15.8±2mm/yr below 2±1 km. The surface fault at this location is masked by a thick package of muds that have been extruded from the fault zone and which vary in width from a few hundreds of meters to 5 km. To the south and north of the GPS line these muds vent in active mud volcanoes, accelerated production has been reported at the time of nearby large earthquakes (eg, the Makran 1945 earthquake). We conclude that the possibility of a large strike-slip earthquake on the Ornach Nal system is unlikely. We hypothesize further that imminent great earthquakes are also unlikely on the Makran coast, which is apparently locked offshore, leaving a relatively minor area presently coupled to the advancing Arabian Plate.

Probabilistic Estimates of Surface Slip including the Effects of Creep and Afterslip

AAGAARD, B.T., U.S. Geological Survey, Menlo Park, CA, USA, baagaard@usgs.gov; LIENKAEMPER, J.L., U.S. Geological Survey, Menlo Park, CA, USA, jlienk@usgs.gov; SCHWARTZ, D.P., U.S. Geological Survey, Menlo Park, CA, USA, dschwartz@usgs.gov

We develop a methodology for probabilistic estimates of coseismic and postseismic surface slip for scenario earthquakes that explicitly includes the effects of creep and afterslip. We apply Monte Carlo simulations to include uncertainty from the Hanks and Bakun (2008) magnitude-area relation, distribution of slip, and the effect of creep on coseismic slip. We extract coseismic surface slip from a suite of kinematic slip models that are constructed following the same approach we used in kinematic rupture models for ground motion modeling of scenario events on the Hayward Fault (Aagaard, *et al.*, 2008), with additional calibration for coseismic surface slip using empirical regressions and observations provided by Wells and Coppersmith (1994). The kinematic slip models include variation in earthquake magnitude, rupture length, slip distribution, and reduce the coseismic slip in creeping patches delineated by Funning *et al.* (2007). Postseismic slip in our analysis is based upon empirical regressions developed from afterslip measurements from the 1987 magnitude 6.6 Superstition Hills earthquake in southern California.

We apply this methodology to a location on the Hayward fault in the San Francisco Bay area to characterize the coseismic and postseismic slip expected for magnitude 6.5–7.1 earthquakes. We find that creep decreases the expected coseismic slip and substantial afterslip may occur in the first few days following an earthquake. This analysis provides a significantly different temporal estimate of surface slip compared with conventional probabilistic estimates that ignore the effects of creep and postseismic slip.

Slip Partitioning in Oblique Fault Systems

NUNLEY, M., Cal State Northridge, Los Angeles, CA, USA, mnttfn06@csu.fullerton.edu; OGLESBY, D.D., UC Riverside, Riverside, CA, USA, david.oglesby@ucr.edu; BOWMAN, D., Cal State Fullerton, Fullerton, CA, USA, dbowman@exchange.fullerton.edu

We use 3D dynamic spontaneous earthquake rupture models to investigate the physical origin of slip partitioning in oblique fault systems. Slip partitioning has been observed in tectonic environments characterized by oblique motion. Several recent studies have suggested that partitioning of motion into predominantly dip-slip and strike-slip fault strands can occur in individual earthquakes when a deep fault branches into two or more strands with different dips near the surface. Bowman *et al.* (2003) used static models to argue that this partitioning of slip follows from the increment in stress near the surface from slip on the basal fault. The present work continues this line of research. We model the dynamics of a branched, obliquely-slipping fault system consisting of a 70°-dipping basal fault, a vertical surface fault, and a 45°-dipping surface fault, with a branch at 5 km depth. We model this system under two regional triaxial stress fields that result in oblique-normal and oblique-thrust stresses on the system, respectively. In both cases, we find that with a homogeneous regional stress field, rupture propagates on only one of the shallow fault segments (vertical in the oblique-normal case, dipping in the oblique-thrust case). However, a barrier on one of the shallow faults can induce rupture to propagate onto the other shallow fault segment, resulting in rupture propagation to all segments. In such a case, partitioned slip automatically results between the two shallow segments, in agreement with observations. In addition, slip rake angles on the shallow fault segments can differ by up to 10 degrees from the pre-stress direction, emphasizing the role of stress interactions in producing slip partitioning. The results may have implications for estimating the amount and direction of slip in future earthquakes on branched oblique fault systems.

GPS Constraints on Deformation and Fault Slip Rates in the Back Arc of the Cascadia Subduction Zone from Northern California to Central Oregon

THATCHER, W., U. S. Geological Survey, Menlo Park, CA 94025, USA, thatcher@usgs.gov

New results from campaign GPS survey profiles that include over 100 sites surveyed between 1999 and 2009 provide unprecedented detail on block motions, slip rates and internal deformation in the Cascadia back arc between 39° and 45° N from

~300 to 900 km landward of the subduction plate boundary. Typical station spacing is ~25 km and results are sufficiently precise to determine velocity gradients of 1 mm/yr or greater across mapped active strike-slip and normal faults traversed by the GPS profiles. There is a marked transition in NE California from strike-slip faulting at rates of ~ 4 mm/yr across the northern Walker Lane zone to pure extension north of about Mt. Lassen. This distinct boundary is apparently related to the prevalence of strike-slip tractions on the San Andreas plate boundary south of the Mendocino triple junction (MTJ) to tensile stresses caused by Cascadia slab retreat north of the MTJ. A horizontal extension rate of 3 mm/yr is observed across the north-striking Hat Creek and related normal faults immediately north of Lassen, but this extension decreases to no more than 1 mm/yr in the Klamath Basin, about 150 km to the north. Extension rates could be as high as ~1 mm/yr across the Surprise Valley fault (near the California-Nevada border) and the Steens Mountain-Pueblo Mountains fault (SE Oregon). But elsewhere, such as across the Summer Lake, Abert Rim, Warner Valley, and Goose Lake normal faults in southern Oregon, extension rates are < 1 mm/yr.

Possible Late Quaternary Folding and Faulting Along Umtanum Ridge, Yakima Fold and Thrust Belt, Washington

SHERROD, B.L., U.S. Geological Survey, Seattle, WA, bsherrod@ess.washington.edu; BLAKELY, R.J., U.S. Geological Survey, Menlo Park, CA, blakely@usgs.gov; BARNETT, E.A., U.S. Geological Survey, Seattle, WA, eli@ess.washington.edu; KNEPPRATH, N., U.S. Geological Survey, Menlo Park, CA, nknepprath@usgs.gov

Constraining Quaternary fault slip in the Yakima fold and thrust belt of central Washington State is important in our understanding of regional tectonics and earthquake hazards, particularly east of the Cascade Mountains. To this aim, we focus on a possible fault scarp identified using air photos along the south side of Umtanum Ridge, an anticline in the Yakima fold and thrust belt. The Wenas Valley scarp is ~9 km long, 4 to 8 m high, and on strike with a mapped thrust fault to the east. A two-dimensional model of the NW-striking Umtanum Ridge fault zone, based on magnetic and gravity anomalies, geologic mapping, and boreholes that penetrate basement rocks, consists of three oblique thrust faults and associated folds that deform Neogene basalts and underlying basement. Umtanum Ridge is modeled as a transpressional structure, uplifted 1 to 2 km along parallel NW-striking thrust faults with opposing dip. The Wenas Valley scarp lies along a thrust fault bounding Umtanum Ridge to the south. An excavation across the scarp revealed a sequence of volcaniclastic alluvial deposits, cobble-rich debris flows, angular unconformities, and buried soils. Normal faults offset the stratigraphic sequence; angular unconformities and buried soils suggest at least three periods of faulting. The total amount of normal faulting is ~3 m while the total scarp height is ~7m, suggesting substantial deformation not accounted for by the evident faulting. Bedding in the volcaniclastic alluvium is folded and could account for the discrepancy between scarp height and observed faulting. Sample analyses for age control are pending but it appears that all of the deformation is late Quaternary or younger. We favor an interpretation that the normal faulting is due to bending moment strain in the hanging wall of an oblique thrust fault, although alternative explanations are not discounted.

Geometry and Rupture History of the Seattle Fault Zone, Washington State, from Modeling of Late Holocene Land-level Changes

PRATT, T.L., U. S. Geological Survey, Seattle, WA, tpratt@ocean.washington.edu

Coseismic uplift and subsidence along the Seattle fault, Washington State, are best explained by about 11 m of seismic slip on the fault's main south-dipping strand and minor backthrust ruptures, without need for a roof thrust or a wedge. Most of this deformation occurred during a large main-strand earthquake 1,100 years ago that raised shoreline terraces along Puget Sound. Additional, smaller earthquakes in the prior 2,000 years caused surface rupture on north-dipping backthrusts that were recently interpreted as independent sources of hazard. The presence of both main faults and backthrusts has led to controversy about the fault geometry in the upper few km. One class interprets the shallow structure to be a thrust fault with some north-dipping backthrusts, while others interpret a wedge structure in which the main, south-dipping thrust faults lie at several km depth. I used an elastic, boundary-element modeling code to test these contrasting models against coseismic land-level changes that have been inferred from a marine terrace that records widespread uplift, and from sparse stratigraphic signs of coseismic subsidence to the terrace's north. A simple wedge model, in which the main thrust flattens at depth and a wedge of material is thrust into or beneath the Seattle basin, fails to account for the coseismic subsidence because uplift above the wedge negates subsidence of the footwall. A model consisting of a thrust fault reaching shallow depths with backthrusts in the forelimb strata provides a better fit to the terrace morphology, and produces subsidence in front of the fault tip. The model suggests that about 11 m of slip on an 18 km by 60 km fault plane is needed to produce the terrace morphology and slip on the backthrusts. This corresponds to a single M7.7 earthquake; however, some slip may have occurred during the smaller events evident on the backthrusts, with accompanying minor terrace uplifts quickly eroded before the large earthquake 1100 years ago.

Active Thrusting within the Himalayan Orogenic Wedge in the Kashmiri Himalaya

GAVILLOT, Y.G., Oregon State University, Corvallis,OR, gavilloy@geo.oreognstate.edu; MEIGS, A.M., Oregon State University, Corvallis,OR, meigsa@geo.oregonstate.edu; HEBELER, A.H., California State University, Northridge, CA, hebeler.aaron@gmail.com; YULE, J.D., California State University, Northridge, CA, Doug.Yule@csun.edu; MADDEN, C., Oregon State University, Corvallis,OR, madden@earthconsultants.com; MALIK, M.M., University of Jammu, Jammu, Jammu and Kashmir, India, mamalik@jammuuniversity.in; YEATS, R.Y., Oregon State University, Corvallis,OR, yeatsr@geo.oregonstate.edu; KAERICHER, M.K., California State University, Northridge, CA, mikekaericher@gmail.com

Numerous lines of evidence indicate that significant distributed deformation occurs within the Himalayan fold-thrust belt. Active thrusts lie as much as 100km north of the deformation front. Whereas geochemical and topographical data provide evidence for internal deformation in Nepal, new mapping demonstrates that a seismically active emergent thrust fault system extends stepwise from the Balakot-Bagh fault (source of the Mw 7.6 2005 Kashmir earthquake) more than 200km to the southeast on the Riasi fault (RF). The RF with a fault length of ~70km, is a ~50° northeast-dipping reverse fault system, which sits ~40km north of the deformation front in the Kashmiri Himalaya of northwest India. Our mapping demonstrates that the Riasi fault consists of two strands. The northern strand, Main Riasi fault (MRF) strand, places Precambrian Surban Limestone on folded unconsolidated (Pleistocene?) conglomerates. Undeformed younger alluvial deposits (Holocene?) overlie the MRF, which implies no Holocene (?) surface rupture on this strand. To the south, the surface expression of the Riasi frontal fault (RFF) includes a fault scarp and offset Holocene (?) terrace deposits. Contact relationships and C-14 ages from the trench study across the RFF indicate that the last surface rupturing earthquake occurred no later than ~4 ka, and suggest a recurrence interval on a millennia timescale. A preliminary OSL age of 80±6 ka from a 350m-high Bidda terrace in the upper plate of the MRF, yields a minimum long-term slip rate of 5.7 ± 0.4 mm/yr and a shortening rate of 3.7 ± 0.3 mm/yr for the RF. Given a ~34 mm/yr India-Asia convergence rate in the NW Himalaya, our preliminary results indicate that internal deformation within the orogenic belt accounts for at least ~10% of total India-Eurasia plate convergence. Discovery of surface-rupturing reverse faults within NW Himalaya indicates that seismic sources include internal upper plate faults capable of generating moderate to great earthquakes.

Characterizing Very Slow Faults in an Active Pull-Apart Setting, Vienna Basin, Austria

DECKER, K., University of Vienna, Vienna, Austria, kurt.decker@univie.ac.at; HINTERSBERGER, E., University of Vienna, Vienna, Austria, esther.hintersberger@geo.uni-potsdam.de

The degree of activity of faults is important for the inclusion of those faults into seismic hazard assessment. In general, faults are considered active if they were seismogenic during historic times. In intraplate regions, however, displacement rates along active faults and associated seismicity are rather low. Therefore, differentiation between active and inactive faults is not easily done and gets even more complicated if they split up into several fault branches. In such cases, movement along one single fault may become so small that it seems to be seismically inactive. The question arises whether those fault branches are still seismogenic or if they are negligible for seismic hazard assessment.

Such a situation is given in the Vienna Pull-Apart Basin, where a strike-slip fault at the basin margin splits up into fault splays crossing the basin. The main fault moves slowly at ~ 2.0 mm/yr with moderate seismicity (Mmax = 5.2). The splay faults do not show any historical seismicity. Geological data, however, proof that those faults moved at velocities of ≤ 0.1 mm/yr during the Quaternary. Accurate maps of the very slowly moving faults are derived from seismic, radar, gravity, sedimentologic and morphologic data. Maps reveal a system of six normal faults which branch from releasing bends of the strike-slip fault compensating fault-normal extension in a transtensional environment. Trenches across one particular fault (Markgrafneusiedl F.) show that this splay is indeed capable of creating earthquakes with M ≥ 6 at recurrence intervals of several thousand years.

Our results, together with the fact that five splay faults strike close to the Austrian capital Vienna, indicate that these very slow faults must be included into seismic hazard assessment, even for relatively short recurrence periods used for building codes. Our data call for an extended research program in order to characterize the contribution of historically inactive, very slow faults to seismic hazard.

The Seismo-Acoustic Wavefield: Fusion of Seismic and Infrasound Data

Oral Session · Thursday 8:30 AM, 22 April · Salon G
Session Chairs: Brian Stump, Jeff Johnson, and Stephen Arrowsmith

The Seismo-Acoustic Wavefield: A New Paradigm in Studying Geophysical Phenomena

ARROWSMITH, S., Los Alamos National Laboratory, Los Alamos, NM, USA, sarrowsmith@gmail.com; STUMP, B., Southern Methodist University, Dallas, TX, USA, bstump@smu.edu; JOHNSON, J., New Mexico Tech, Socorro, NM, USA, jeff.johnson@ees.nmt.edu; DROB, D., Naval Research Laboratory, Washington, DC, USA, douglas.drob@nrl.navy.mil

The field of seismo-acoustics is emerging as an important discipline in its own right, owing to the value of co-located seismic and infrasound arrays that sample both ground- and atmosphere propagating elastic energy. The fusion of seismic and infrasonic data provides unique constraints for studying a broad range of topics including the source physics of geophysical and man-made events, interaction of Earths crust and atmosphere, source location and characterization, and inversion of atmospheric properties. This overview presentation traces the seismo-acoustic wavefield from source to receiver. Beginning at the source, we review the latest insights into the physics of geophysical sources that have arisen from the analysis of seismo-acoustic data. Next, a comparative review of 3D models of the atmosphere and solid earth, and the latest algorithms for modeling the propagation of mechanical waves through these media, provides the framework for a discussion of the seismo-acoustic path. The optimal measurement of seismic and acoustic waves, including a discussion of instrumentation, as well as of array configurations and regional networks, is then outlined. Finally, we focus on broad research applications where the analysis of seismo-acoustic data is starting to yield important new results, such as in the field of nuclear explosion monitoring.

Harmonic Tremor on Active Volcanoes: Seismo-acoustic Wavefields

LEES, J.M., University of North Carolina, Chapel Hill, NC, 27599, USA, jonathan.lees@unc.edu; JOHNSON, J.B., New Mexico Tech, Socorro, NM 87801, USA, jeff.johnson@ees.nmt.edu

Harmonic tremor is often observed on active volcanoes where seismo-acoustic arrays are deployed. In this presentation we review characteristic observational phenomena and discuss the continuum from monochromatic, oscillatory behavior through periodic acoustic pulses (*i.e.* chugging) to spasmodic drumming on numerous volcanoes world wide. Harmonic tremor can provide detailed constraints on physical parameters controlling activity in active vents through physical modeling. These include physical constraints on the vent geometry, composition and density of the multiphase fluids, and visco-elastic parameters of choked flow in the conduits. Examples will show seismic tremor with and without an associated acoustic emission, an indicator of dynamic processes occurring at the top of the active vent. While explosive activity can range widely between volcanoes, harmonic tremor often exhibits remarkably similar behavior on vents as diverse as Karymsky, Tungurahua, Reventador, and Santiaguito Volcanoes. For example, chugging activity typically has a consistent 0.7–2 Hz signal on many volcanoes world wide. Commonly observed gliding, where frequency modulates over time, suggests that conditions in the conduit are non-stationary, and must be treated with specialized time series analysis tools. We explore these phenomena and highlight possible models explaining these near surface vent emissions.

Seismo-Acoustic Signals Produced by the Rapidly Inflating Santiaguito Lava Dome, Guatemala

JOHNSON, J.B., New Mexico Tech, Socorro, NM, jeff.johnson@ees.nmt.edu; LEES, J.M., University of North Carolina, Chapel Hill, NC, jonathan.lees@unc.edu

Inflation of the Caliente lava dome at Santiaguito (Guatemala) occurs coincidentally with the onset of explosive eruptions and produces conjoint 0.5 to 2 Hz infrasound and long-period (LP) seismic energy. The inflation results in upward surface movement of the 100-m-radius dome that occurs rapidly (within ~2 s) and locally results in up to 1 meter of vertical displacement of the atmosphere. This study quantifies the time history of the dome uplift using particle image velocimetry analysis of high resolution video imagery. Through comparative analysis of signals from multiple eruptive events we model the intense infrasound (up to 5 Pa at 1 km distance) as a volumetric acceleration of the atmosphere that occurs over a finite area. Upward acceleration of the massive dome also results in a thrust response (downward force) imparted to the volcanic edifice. Peak LP displacements (on the order of mm/s at 1 km) are fit by single forces at the dome surface with amplitudes of ~109 N. Given the time history of the dome's surface movement we infer a thickness of the uplifted portion of the dome on the order of 20–80 m. Although the primary seismo-acoustic signal is attributable to the rapid dome inflation there are additional superimposed seismo-acoustic signal transients that are caused by a range of phenomena, including explosive degassing, shallow gas fluid flow, surface rock fall, internal volume changes, and potential brittle failure of dome rocks.

Probing the Atmosphere and Atmospheric Sources with the USArray

HEDLIN, M.A.H., U.C. San Diego, La Jolla, CA, USA, hedlin@ucsd.edu; DROB, D., Naval Research Lab, Washington, D.C., USA, douglas.drob@nrl.navy.mil; WALKER, K., U.C. San Diego, La Jolla, CA, USA, walker@ucsd.edu; DE GROOT-HEDLIN, C.D., U.C. San Diego, La Jolla, CA, USA, chedlin@ucsd.edu

The USArray is designed to image the subsurface structure of the United States with exceptional resolution at a continental scale and for studies of regional and teleseismic earthquakes. Although the sensors of this network directly measure ground motion, they indirectly measure other phenomenon that affect ground motion. It has been known for a long time that infrasound can be detected by seismometers through acoustic-to-seismic conversion at the ground/atmosphere interface. The USArray data archive contains recordings of several hundred large atmospheric events. One example is a bolide that burst above Oregon State on February 19, 2008 and was recorded by several hundred seismic stations and four infrasound arrays. The bolide source parameters were precisely determined by the seismic data, and the time-offset records show several phase branches corresponding to multiple arrivals. Such branches have never before been observed in such spectacular detail because infrasound arrays separated by thousands of kilometers are typically used for infrasound studies. In this presentation, we look at examples of the types of acoustic events detected by our USArray processing software and what we can learn from these events. We present results from our study of acoustic branches from events such as the 2008 bolide.

Atmospheric Measurements with the USArray Transportable Array

BUSBY, R.W., IRIS, Washington DC, busby@iris.edu; WOODWARD, R., Inc Research Inst for Seismology, Washington DC, woodward@iris.edu; HAFNER, K., Inc Research Inst for Seismology, Washington DC, hafner@iris.edu; HEDLIN, M., IGPP / Scripps UC San Diego, San Diego CA, hedlin@ucsd.edu; VERNON, F., IGPP / Scripps UC San Diego, San Diego CA, flvernon@ucsd.edu

The large number of seismic stations that comprise the EarthScope USArray Transportable Array (TA) provide opportunities for observing effects from atmospheric-to-seismic coupling. The USArray has collected seismic data from over 850 station sites, stretching from the Pacific coast to the Great Plains. The stations are deployed in a grid, with 70 km spacing and have real-time continuous data to the IRIS Data Management System.

TA stations deployed in the Central US include environmental monitoring sensors as part of the refined vault infrastructure. These channels include barometric pressure (SEED Code EP-LDM), temperature and humidity, measured inside the TA station vaults.

The barometric pressure observations are obtained from a MEMS barometer, with useful signal in the range from DC to periods of 300 seconds. The pressure channel is sampled at 1 sample/sec, and timing is synchronized with the seismic data acquisition. In addition, several stations in NE Colorado have been temporarily equipped with infrasound sensors and/or precision microbarographs. Plans are to add precision barometric pressure and high-quality infrasound sensors to every TA station. Previous research has highlighted the direct effect of atmospheric pressure fluctuations on very long period vertical seismometers. The relationship to pressure observed on horizontal seismometers is more complex. However, a large number of uniform installations may allow further progress.

We present an analysis of low frequency atmospheric pressure observations at TA stations. We examine both the coherence of the atmospheric pressure observations across the array, and the coherence between the pressure and seismic observations. We discuss plans to augment future TA stations with additional sensors that may aid our understanding of seismic-acoustic coupling and/or meso-scale atmospheric pressure observations.

Seismo-Acoustic Studies in the European Arctic

GIBBONS, S.J., NORSAR, Kjeller, Norway, steven@norsar.no; RINGDAL, F., NORSAR, Kjeller, Norway, frode@norsar.no

Industrial and military explosions in northern Fennoscandia and NW Russia generate seismic and infrasound signals observed at regional distances. Similar seismic signals constrain event origin times and hundreds of events from a small number of sites have been detected and classified using correlation detectors at the ARCES array. This has provided several superb datasets for infrasound propagation studies.

Near-surface explosions at Hukkakero in northern Finland generate infrasound signals on the seismic sensors at ARCES, 175 km to the North, near to the

edge of the classical "Zone of Silence". Many tropospheric phase observations can be predicted using ray-tracing given favourable winds at low altitudes. However, the vast majority of the observed infrasound signals - probably refracted from stratospheric heights - are not predicted by ray-tracing, warranting a re-evaluation of propagation models for these distances. In 2008, a mini-array of microbarographs, co-located with ARCES seismometers, also observed later signals probably refracted from thermospheric heights. These signals are more impulsive, and are of smaller amplitude and shorter duration, than the more frequently observed signals.

Another site near the northern coast of the Kola Peninsula is approximately 250 km from both ARCES to the West and Apatity to the South. Despite poor waveform similarity between events, multichannel correlation detectors assign confidently over 350 events over an 8 year period to this site. Infrasound is observed at ARCES for almost all events in the summer and almost no events in the winter, and is observed at Apatity for almost all events. We conclude that the direction of the zonal winds is crucial to infrasound detectability at stations to the East and West, but that the meridional winds may have less effect.

The Seismo-Acoustic Boundary Layer

LANGSTON, C.A., CERI, University of Memphis, Memphis, TN, USA, clangstn@memphis.edu

The earth's near surface is surprisingly compliant in coupling infrasonic wave fields into seismic waves. Infrasound from atmospheric acoustic sources such as thunder from lightning, pressure fluctuations from storms, bolides, explosions, and spacecraft sonic booms strongly interact with the ground in areas with thick unconsolidated sediments. P- and S-wave velocities of these near-surface sediments can be less than the acoustic air wave velocity allowing acoustic waves to strongly interact with deeper layers producing distinctive leaky mode and locked mode wave trains. These data may be used to infer earthquake shaking hazards information for wave frequencies of 5–10 Hz at particular sites. These high frequency data also show that the upper few meters of soil may have very unusual mechanical properties such as near-zero or negative Poisson's ratios. Large, lower frequency Rayleigh wave trains may result from high horizontal phase velocity acoustic waves that couple with deeper sections of sediments, such as from space shuttle reentry sonic booms. Impulsive acoustic sources can be used much like naturally occurring earthquakes and buried explosions to infer earth structure in the boundary layer. There is also intriguing evidence from a recent seismic array experiment within the Mississippi embayment of the central U.S. that high-amplitude ambient ground noise may be directly excited by atmospheric infrasound generated at the time of hurricanes rather than from propagating surface waves from the continental coast. This suggests that data from the seismo-acoustic boundary layer may yield new information about hurricane dynamics.

Seismic and Acoustic Waves Generated by an Exploding Meteoroid

EVERS, L.G., KNMI, De Bilt, the Netherlands, evers@knmi.nl; DOST, B., KNMI, De Bilt, the Netherlands, dost@knmi.nl

A meteoroid penetrated the earth's atmosphere above the Netherland on October 13, 2009. In the near-field, observations were made by the Dutch seismic borehole network and three infrasound arrays. The borehole network consists of eight stations with three-component geophone strings. Each string consists of four sensor levels separated by 50 meters down to 200 meters depth. The infrasound arrays range in aperture from 75 to 1500 meters, while the number of microbarometers varies between six and 16.

Shock waves are generated by the meteoroid upon its hypersonic entry, fragmentation events and a final thermal burst. Analysis of the infrasound signals shows several events which correspond to the meteoroid's trajectory. The infrasound waves also coupled to the solid earth and were observed at depths of 200 meters. The complex seismic signature show a variety of high and low frequent waveforms.

In this presentation, we will present the first results of our analysis and the effort in understanding the coupling of the seismic-acoustic wavefield.

Source Signature and Propagation Path Effects from Topography on Local Seismic-Acoustic (Infrasound) Data

MCKENNA, M.H., US Army ERDC, Vicksburg MS USA, mihan.h.mckenna@usace.army.mil; LESTER, A.P., US Army ERDC, Vicksburg MS USA, alanna.p.lester@usace.army.mil; MCKENNA, J.R., US Army ERDC, Vicksburg MS USA, jason.r.mckenna@usace.army.mil; ANDERSON, T.S., US Army ERDC, Hanover NH USA, thomas.s.anderson@usace.army.mil; KOPENHOEFFER, K., Altasim Technologies, Columbus OH USA, kyle@altasimtechnologies.com; GIBSON, R., BBN Technologies, Arlington VA USA, rgibson@bbn.com; MCCOMAS, S., US Army ERDC, Vicksburg MS USA, sarah.mccomas@usace.army.mil

While infrasound data traditionally have been collected at distances greater than 250 km using fixed arrays, recent research has shown that signals recorded less than 50 km from the sources are complex and robust with a wide variety of impulsive and structural sources. Predominantly consisting of cultural sources with frequencies between 2 and 20 Hz, these arrivals turn in the troposphere and lower stratosphere and are highly influenced by local weather conditions. The energy interacts with the ground surface much more than the long-range infrasound waves that turn high in the atmosphere, resulting in a strong topographic influence of propagation path and source signature. Research reflecting local infrasound will be presented for two scenarios.

First, portable seismic, infrasound, acoustic and meteorological arrays (SIAM) collected data from impulsive sources at arrays located at source-to-receiver distances of 3 to 20 km in Alaska. Complex topography affected waveform character and detectability for both seismic and infrasound arrivals. Successful modeling of infrasound arrivals for these events required accurate radiosonde weather and topographical information.

Secondly, SIAM arrays were deployed to assess the fundamental modes of motion for a rail road bridge, and the source resulting infrasonic representative source was modeled. The first three modes of the target bridge were observed at 19 and 28 km. The model structure of the bridge was then coupled to the surrounding atmosphere and topography to create an asymmetric representative source model for this bridge. Though the topographic contribution to propagation was minimal for this scenario, more extreme topography in more geophysically complex areas would likely have more impact on the representative source.

Detection of Short Time Transients From Spectrograms Using Scan Statistics

TAYLOR, S.R., Rocky Mountain Geophysics, Los Alamos, NM, srt-rmg@comcast.net; ARROWSMITH, S.J., Los Alamos National Laboratory, Los Alamos, NM, arrows@lanl.gov; ANDERSON, D.N., Los Alamos National Laboratory, Los Alamos, NM, dand@lanl.gov

We present a statistical methodology for the detection of impulsive signal transients using time-frequency spectrograms that is closely related to the emerging field of scan statistics. Impulsive signals are manifest as vertical stripes on spectrograms and are enhanced on grayscale representations using vertical detection masks. Histogram analysis of grayscale spectrograms is used to form bitmap images where pixels above a defined threshold are set to one. For the case of noise only, the ones will be randomly distributed where each pixel of the bitmap image is given by a zero or a one. In contrast, a short-duration small (large bandwidth) explosion will have a large number of illuminated bits in the column corresponding to its arrival time. We form the marginal distribution of bit counts as a function of time, ni by simply summing column wise over frequency. For each time window we perform a hypothesis test of the form H0: signal + noise by defining a background density of ones, $\rho 1$, expected when a signal is present. The density can be thought of the probability of success in a signal window assuming that ni is a Bernoulli random variable. We therefore assume that ni follows the binomial distribution and can compute a probability of detection (represented as a p-value) for a given $\rho 1$.

We apply the spectrogram detector to one hour of single-channel acoustic data containing a signal from a 1 lb surface explosion recorded at 3.1 km distance and compare performance with a standard short-term average to long-term average (STA/LTA) detector. Both detectors are optimized through an extensive grid search and successfully detect the acoustic arrival from the 1 lb explosion. However, 70% more false detections are observed for the STA/LTA detector than for the spectrogram.

Infrasound Network Design for Recovering Near-Surface Atmospheric Structure

MARCILLO, O.E., New Mexico Tech, Socorro, NM USA, omarcill@ees.nmt.edu; JOHNSON, J.B., New Mexico Tech, Socorro, NM USA, jeff.johnson@ees.nmt.edu

We investigate the design of an infrasound sensor network around an active volcano to recover the conditions of the near-surface atmosphere. In a previous experiment, we recorded volcanic infrasound signal, produced by Kilauea, on a three-microphone network and inverted the corresponding relative phase delay to recover near-surface atmospheric wind; in this inversion, we solved the system by using ground measurements of the temperature to estimate intrinsic sound velocity and assumed this estimation to be representative of the entire study area. The results agree with the two main regimes present in this part of the island (6–9 m/s westerly trade winds during the day and lower-intensity 2–5 m/s winds originating from 60° to 110° at night). However, a network with at least four microphones azimuthally spaced generates a consistent three-equation system capable of recovering horizontal wind and temperature simultaneously. Using forward models, we study the influence of noise (local wind or temperature gradients) in our system of equations. This work aims to describe the design of an infrasonic network capable of providing accurate estimations of average atmospheric conditions to be used along with gas monitoring techniques to improve modeling of plume dispersal and quantifying gas flux.

Seismo-Acoustic Signals from a Semi-Urban Environment

LEWKOWICZ, J., Weston Geophysical Corp., Lexington/MA/USA, jiml@westongeophysical.com; BONNER, J.L., Weston Geophysical Corp., Lexington/MA/USA, bonner@westongeophysical.com; LEIDIG, M., Weston Geophysical Corp., Lexington/MA/USA, mleidig@westongeophysical.com; BRITTON, J.M.

We have designed, deployed, and operated an infrasonic array near the Hanscom Air Force Base near Bedford, MA. The array consists of four (4) Chaparral 2 acoustic gauges in a 100 meter aperture with a broadband three-component Guralp CMG-3T seismic sensor at the center element. During the operation of this seismo-acoustic array (nicknamed HANS), we have collected a variety of seismic and infrasonic signals in this semi-urban setting (< 20 km from Boston, MA). The database includes seismic and acoustic waveforms from nearly co-located quarry blasts and earthquakes near the town of Littleton, MA. Additionally, we have a database of seismic and acoustic data from 16 construction explosions that includes on-site instrumentation and ground truth. The database is supplemented with blasting information as well as seismic data from additional stations in New England. We also have an extensive number of acoustic signals in the database from known (military or commercial aviation) and unknown sources. We will present the characteristics of these signals and discuss future needs for seismic-acoustic monitoring in urban environments.

Quantification and Treatment of Uncertainty and Correlations in Seismic Hazard and Risk Assessments

Oral Session · Thursday 1:30 PM, 22 April · Salon A

Session Chairs: Chris H. Cramer, Jack Baker, and Tuna Onur

Non-Stationary Path Effects in Portfolio Loss Computation

WALLING, M.A., U.S.G.S., Golden/CO/USA, mwalling@usgs.gov; LUCO, N., U.S.G.S., Golden/CO/USA, nluco@usgs.gov; RYU, H., U.S.G.S., Golden/CO/USA, hryu@usgs.gov

We present an add-on to a recently-developed direct (*i.e.*, non-simulation-based) method for calculating annual frequencies of exceeding portfolio earthquake losses, by accounting for correlations in ground motion associated with source, path and site effects. The ground motion correlation induced by each effect is accommodated through the uncertain inter- and intra-event terms in a ground motion prediction equation. In part, the inter-event term (η) represents differences in ground motion at a site that can be attributed to characteristics of the source, such as its stress-drop, mean-rise time, and rupture velocity. The intra-event term (ξ), on the other hand, partially represents ground motion differences that can be attributed to properties of the site, such as its geologic profile, and to path effects as waves travel between the source and the site. The systematic effects of source, site, and path can be estimated from data and then separated from remaining unsystematic components of ground motion. In the referenced direct method of engineering portfolio loss computation, source effects shared amongst all sites are handled by conditioning on and integrating over η. In some simulation-based approaches, shared path effects are handled by correlating ground motions as a function of the separation distance between any two sites. Any site effects are typically either treated as independent or are not separated from the path effects. The work we present here is uniquely different from approaches taken in the past in that it treats path effects as non-stationary, formulating the induced ground motion correlation not as a function of only the distance between sites but also the distances between the sites and the source. Via an example loss computation, we demonstrate the impacts on the direct method of both stationary and non-stationary treatment of path effects.

Impacts of Earthquake Hazard Uncertainties on Probabilistic Portfolio Loss Risk Assessment

MOLAS, G.L., Risk Management Solutions, Inc., Newark, CA, gilbert.molas@rms.com; ONUR, T., Risk Management Solutions, Inc., Newark, CA, tuna.onur@rms.com; BRYNGELSON, J., Risk Management Solutions, Inc., Newark, CA, jason.bryngelson@rms.com; SHOME, N., Risk Management Solutions, Inc., Newark, CA, nilesh.shome@rms.com

This paper will present results of recent work assessing the impact of seismic hazard uncertainty on probabilistic loss estimates (average annual losses and losses at different levels of annual probability of exceedance) for portfolios of buildings.

The effects of local conditions and seismic environment are also studied. The study is limited to California and includes the effect of the Next Generation Attenuation (NGA) relationships used in the 2008 USGS National Seismic Hazard Maps as representation of the epistemic uncertainty in the ground motion model.

This work is part of ongoing effort to assess and to de-aggregate uncertainties within each component of a probabilistic seismic loss model and to assess their relevance to loss estimates.

Updated Computation of Probability Distributions of Regional Annual Losses for Seismic Design Alternatives in Memphis, Tennessee

RYU, H., Stanford University, Stanford/CA/USA, dynaryu@gmail.com; LUCO, N., USGS, Golden/CO/USA, nluco@usgs.gov; KARACA, E., Swiss Re, Armonk/NY/USA, Erdem_Karaca@swissre.com; WALLING, M., USGS, Golden/CO/USA, mwalling@usgs.gov

In Memphis, Tennessee, the 2003 International Building Code (IBC) has been adopted for the design of new buildings, but it has been amended to allow the use of lower earthquake ground motion values or the seismic provisions of the previously-used model building code - *i.e.* the 1999 Southern Building Code (SBC) - for non-essential buildings. Through a regional risk assessment study for Memphis, we have evaluated the implications of adopting each of the following seismic design options: the 1) 2009 NEHRP Recommended Seismic Provisions, 2) 2006 IBC, 3) 2003 IBC, 4) amended 2003 IBC, and 5) 1999 SBC. Since these design options apply mainly to new buildings, we simulated a portfolio of buildings on currently-vacant parcels in Memphis, considering local zoning requirements and the structural characteristics of nearby existing buildings. For each building, we have derived vulnerability models representing the different design options based on both i) the simulated structural characteristics of the building and ii) the design ground motion values and corresponding seismic design or performance categories specified by the provisions (see Karaca and Luco, 2009). Then, we computed the annual frequencies of exceedance for each in a range of potential regional earthquake losses by applying the probabilistic portfolio loss estimation methodology originally proposed by Wesson *et al.* (2009) and recently amended by Walling *et al.* (2010) in order to account for correlation in ground motion associated with path effects. The results illustrate that the regional seismic risk can be significantly higher for design based on the amended 2003 IBC compared to the other design options.

A Bayesian Ground Motion Model for Estimating the Covariance Structure of Ground Motion Intensity Parameters

KUEHN, N.M., IEES, University of Potsdam, Potsdam/Germany, nico@geo.uni-potsdam.de; RIGGELSEN, C., IEES, University of Potsdam, Potsdam/Germany, riggelsen@geo.uni-potsdam.de; SCHERBAUM, F., IEES, University of Potsdam, Potsdam/Germany, fs@geo.uni-potsdam.de; ALLEN, T., Geoscience Australia, Canberra/Australia, Trevor.Allen@ga.gov.au

We present a Bayesian ground motion model that directly estimates both coefficients and the correlation between different ground motion intensity parameters. For this purpose, we set up a multivariate statistical model, embedded in a graphical framework, which mimics our insight into the data generating process, *i.e.* which includes a source, path and station term. For each term, coefficients to predict the median of the intensity parameter distribution can be estimated, together with the associated covariance structure (*i.e.* inter-event, intra-event and inter-station variability plus correlation coefficients). The graphical structure provides intuitive insight into the model. The coefficients of the model are estimated in a Bayesian framework using Markov Chain Monte Carlo simulation. Thus, prior information can be included in a principled way and an estimate of the epistemic uncertainty of the parameters can be obtained. The Bayesian approach also allows to update the model once new data is available. The parameters of the model are estimated on a global dataset using peak ground acceleration, peak ground velocity and the response spectrum at three periods as the target variables. The analysis shows that the coefficients of the model are similar to those estimated without the covariance structure. This is also true for the intra-event variability, while the inter-event variability is reduced when estimated with the covariance structure.

Spatial Correlation of Earthquake Ground Response Spectra: Measurement Techniques and Implications for Regional Infrastructure Risk

BAKER, J.W., Stanford University, Stanford/CA/USA; JAYARAM, N., Stanford University, Stanford/CA/USA.

Risk assessment of spatially distributed building portfolios or infrastructure systems requires quantification of the joint occurrence of ground-motion intensities at several sites, during the same earthquake. This presentation will present an overview of techniques to quantify the needed joint distributions using observations from past earthquakes, and describe how these distributions can be used in probabilistic seismic risk assessments of spatially-distributed lifelines. Lifeline risk assessment presents challenges related to describing ground-motion intensity over a region, and related to the computationally expensive task of repeatedly analyzing performance of a lifeline system under many damage scenarios. A simulation-

based framework will be presented that develops a small but stochastically-representative catalog of earthquake ground-motion intensity maps that can be used for lifeline risk assessment. The approach dramatically reduces required computational expense, while also maintaining a set of simulations that is consistent with all conventional probabilistic seismic hazard analysis calculations. The feasibility of the proposed approach is illustrated by using it to assess the seismic risk of a simplified model of the San Francisco Bay Area transportation network. A catalog of only 150 intensity maps is generated to represent hazard at 1,038 sites from ten regional fault segments causing earthquakes with magnitudes between five and eight.

The CyberShake Project: Full-Waveform Probabilistic Seismic Hazard Calculations for Southern California

GRAVES, R., URS Corporation, Pasadena, CA, robert_graves@urscorp.com; CALLAGHAN, S., USC/SCEC, Los Angeles, CA; SMALL, P., USC/SCEC, Los Angeles, CA; MEHTA, G., USC, Los Angeles, CA; MILNER, K., USC/SCEC, Los Angeles, CA; JUVE, G., USC/SCEC, Los Angeles, CA; VAHI, K., USC, Los Angeles, CA; FIELD, E., USGS, Golden, CO; DEELMAN, E., USC/ISI, Los Angeles, CA; OKAYA, D., USC, Los Angeles, CA; MAECHLING, P., USC/SCEC, Los Angeles, CA; JORDAN, T., USC, Los Angeles, CA

The goal of SCEC's CyberShake Project is to replace the empirical ground motion prediction equations (GMPEs) used in traditional PSHA with physics-based 3D ground motion simulations. To do this, we first expand the Uniform California Earthquake Rupture Forecast (UCERF2.0) into multiple rupture variations with differing hypocenter locations and slip distributions using a pseudo-dynamic approach, which results in about 415,000 rupture variations per site. 3D strain Green tensors are then calculated using seismic reciprocity and convolved with the rupture variations to obtain full waveform synthetic seismograms. We extract peak intensity measures (*e.g.*, spectral acceleration at frequencies up to 0.3 Hz) and combine with the original rupture probabilities to produce probabilistic seismic hazard curves for the site. CyberShake is computationally intensive; 189 million individual jobs were needed to generate hazard curves at 223 sites, requiring 5.2 million CPU hours on the TACC Ranger supercomputer and producing 176 terabytes of data. The CyberShake1.0 hazard map shows strong amplification effects in the sedimentary basins where the coupling of rupture directivity and basin response leads to hazard levels substantially larger that the traditional models. This is particularly true for sites along the basin margins where the simple basin amplification terms of the GMPEs fail to capture the basin focusing and wave guide effects that are present when using the fully 3D geological structure. Since we retain the full set of ground motion waveforms, the event-specific phenomena that contribute to the hazard at a particular site can be identified and analyzed. Moreover, the hazard map can be recomputed quickly to reflect revisions to the extended earthquake rupture forecast, including the short-term variations in event probabilities provided by operational earthquake forecasting that cannot be accommodated by standard GMPEs.

An Empirical Perspective on Uncertainty in Earthquake Ground Motions

ATKINSON, G.M., Univ. of Western Ontario, London, ON, Canada, gmatkinson@aol.com

ncertainty in the ground-motion amplitudes that will be realized from earthquakes at a given magnitude and distance plays a critical role in seismic hazard analysis. Examination of ground-motion variability from an empirical perspective can be used to characterize its epistemic and aleatory components, which are implicitly coupled, in a self-consistent manner that minimizes "double-counting" of uncertainty. This study empirically evaluates both components of uncertainty for shallow crustal earthquakes in active tectonic regions as deduced from the NGA database. The epistemic component of uncertainty is estimated to be about 0.2 log(10) units near the source, and grows with increasing distance; the growth with distance may be due to regional attenuation variability. The aleatory component (commonly referred to as 'sigma') for a specific magnitude-distance scenario is about 0.24 log(10) units at low frequencies, decreasing to about 0.19 log(10) units at high frequencies; sigma is approximately independent of magnitude and distance. The joint consideration of the epistemic and aleatory components of uncertainty, in the context of the underlying database, may be useful in reducing unintended conservatism in computed seismic hazard estimates at low probabilities.

Intra-Event Uncertainty of Long-Period Ground Motions For Large Earthquakes With Southeast-Northwest Rupture Direction on the Southern San Andreas Fault

OLSEN, K.B., San Diego State University, San Diego, CA, USA, kbolsen@sciences.sdsu.edu; DAY, S.M., San Diego State University, San Diego, CA, USA, day@moho.sdsu.edu; DALGUER, L.A., ETH-Zurich, Zurich, Switzerland, dalguer@tomo.ig.erdw.ethz.ch; CUI, Y., SDSC, La Jolla, CA, USA, yfcui@sdsc.edu; MAECHLING, P., Univ. Southern California, Los Angeles, CA USA, maechlin@usc.edu; JORDAN, T., Univ. Southern California, Los Angeles, CA, USA, tjordan@usc.edu; CHOURASIA, A., Univ. Southern California, Los Angeles, CA, USA, amit@sdsc.edu; OKAYA, D., Univ. Southern California, Los Angeles, CA, USA, okaya@usc.edu

e compute ensemble averages and variances for synthetic ground motion in southern California from 7 spontaneous rupture models of large (Mw7.8) southeast-northwest-propagating earthquakes on the southern San Andreas fault (ShakeOut-D). The ensemble averages predict entrainment by basin structure of a strong directivity pulse, with 3 sec spectral accelerations (3s-SA) in the Los Angeles and Ventura basins significantly larger than those predicted by the empirical relations. The ShakeOut-D predictions of long-period SAs within the basins of the greater Los Angeles area are lower by factors of 2–3 compared to those from a kinematically parameterized, geometrically similar, scenario rupture. The latter result agrees with the results from a previous comparison of kinematically and dynamically parameterized simulations of Mw7.7 San Andreas scenarios (TeraShake). As in the previous study, we attribute the difference to reduced forward directivity due to the less coherent wavefield excited by the spontaneous-rupture sources, caused by strong local fluctuations in the spontaneous-rupture sources but lacking in the kinematic sources. For ln(3s-SA), the ShakeOut-D rock site stds are very close to ~0.5 at all distances up to 50 km. This value compares favorably with intra-event stds of ~0.56 for two Next Generation Attenuation (NGA) empirical relations, namely Boore & Atkinson (2008) and Campbell & Bozorgnia (2008) (*i.e.*, within roughly their epistemic uncertainty). The stds for ShakeOut-D increase significantly for distances beyond 50 km, reaching ~0.7 at 100 km. The relative stability of the ShakeOut-D predictions (at a given site) suggests that simulation ensemble variances may be substantially reduced through use of sources based on spontaneous rupture simulations. Alternatively, kinematic source parameterizations should be improved to better incorporate constraints from those simulations.

Empirical Testing of Probabilistic Seismic Hazard Estimates

ALBARELLO, D., University of Siena, Siena, Italy, albarello@unisi.it; D'AMICO, V., INGV, Pisa, Italy; MUCCIARELLI, M., University of Basilicata, Potenza, Italy.

Several probabilistic procedures are presently available for seismic hazard assessment (PSHA). These result in a number of different outcomes (hazard maps), each generally compatible with available observations and supported by plausible physical models. To take into account this inherent uncertainty ("epistemic"), outcomes of these alternative procedures are combined in the frame of logic-tree approaches by scoring each procedure as a function of the respective reliability. This is deduced by evaluating ex-ante (by expert judgements) each element concurring in the relevant PSH computational procedure. This approach appears unsatisfactory also because the "value" of each procedure depends both on the reliability of each concurring element and on that of their combination: thus, checking the correctness of single elements does not allow evaluating the correctness of the procedure as a whole. An alternative approach to scoring is here presented that is based on the ex-post empirical testing of the considered PSH computational models. This is performed by comparing the probabilistic "forecasts" provided by each model with empirical evidence relative to seismic occurrences (*e.g.*, strong-motion data or macroseismic intensity evaluations) during some selected control periods of dimension comparable with the relevant exposure time. In order to take into account the inherent probabilistic character of hazard estimates, formally coherent procedures have been developed that are based on Likelihood estimates and Counting protocols. Some results obtained by the application of these testing procedures in Italy will be shortly outlined.

Uncertainty in Probabilistic Fault Displacement Hazard Analysis

MOSS, R.E.S., Cal Poly, San Luis Obispo/CA/USA, rmoss@calpoly.edu; TRAVASAROU, T., Fugro West, Oakland/CA/USA, ttravasarou@fugro.com

In recent years the computational methods used in probabilistic seismic hazard analysis (PSHA) have been scrutinized and consensus is building on; how to best carry out the complex calculations, how to properly model the input variables, and how to best capture the various forms of uncertainty. Probabilistic fault displacement hazard analysis (PFDHA) however is a relatively new field when compared to PSHA and the above issues along with new issues specific to faulting have not been evaluated. This study uses a PFDHA for the Los Osos Fault in Central California as the basis for evaluating how different assumptions and methods influence the results. Uncertainty in this analysis can be attributed to insufficient or incomplete data, data modeling assumptions, probability distribution assumptions/constraints, and differing computation techniques. These are evaluated in turn to estimate the sensitivity of PFDHA to these uncertainties. This provides guidance on where future efforts can best be focused to reduce uncertainty in PFDHA studies.

A First Attempt to Constrain Reliability and Measurement Error Associated with Expert Opinion and Judgment in Interpreting Paleoseismic Data

GRANT LUDWIG, L., University of California, Irvine, CA, lgrant@uci.edu; RUNNERSTROM, M.G., University of California, Irvine, CA, miryha@uci.edu

The state of practice for probabilistic seismic hazard assessment and calculation of earthquake probabilities to be used for policymaking requires application of the best available science and utilization of the best available data. Determination and evaluation of the best available data is a subjective process where the epistemic uncertainty of expert opinion is represented as weighted branches in logic trees. Paleoseismic data, including slip rate and average recurrence interval, are critical components of seismic hazard calculations, but contain inherently large, generally unquantified uncertainties due to irreproducibility and measurement error associated with human judgment. These uncertainties have been difficult to incorporate in seismic hazard analysis even though the epistemic uncertainty of human judgment may be significant. This problem could be addressed by constraining inter-rater reliability as a proxy for measurement error associated with expert opinion and judgment in interpreting paleoseismic data. Inter-rater reliability is commonly used to measure agreement between multiple raters in applications such as evaluations of courtroom testimony, judgment of student performance, and medical diagnoses. We present results of a first attempt, or pilot study, to constrain inter-rater reliability in reporting published paleoseismic data parameters that are important for seismic hazard analysis.

Possible Explanations for Discrepancies Between Precariously Balanced Rocks and 2008 Hazard Maps

BRUNE, J., University of Nevada, Reno, Reno, Nevada, USA, brune@seismo.unr.edu; PURVANCE, M., University of Nevada, Reno, Reno, Nevada, USA, MDP@seismo.unr.udu; ANOOSHEHPOOR, R., University of Nevada, Reno, Reno, Nevada, USA, Rasool@seismo.unr.edu; ANDERSON, J., Reno, Nevada, USA, jga@seismo.unr.edu; GRANT-LUDWIG, L., University of California, Irvine, Irvine, California, USA, lgrant@uci.edu; ROOD, D., LLNL, Livermore, California, dylan@crustal.UCSB.edu; KENDRICK, K., University of California, Rivers, kendrick@usgs.gov

Precariously balanced rocks (PBRs) which have been in place thousands of years provide upper bounds on seismic hazard at a site. At a number of sites in California and Nevada, tested and estimated toppling ground motions are inconsistent with 2008 2% in 50 yr hazard maps. There are a several possible explanations for these discrepancies. Possible global explanations include: Incorrect seismic attenuation assumptions, and incorrect assignment and division of epistemic and aleatory uncertainties. Possible local explanations include: site and path effects, incorrect assignment of random background seismicity, and incorrect assignment of activity and source parameters on nearby faults.

The observation that nearly all sites are consistent with the high probability maps (10% in 50 yr), and nearly all are inconsistent with low probability maps (1% in 50 yr) suggests that the implied increase in ground motion hazard with time period is incorrect (assigned aleatory variability is too large). Extensive data in the Mojave Desert strengthen this suggestion. PBRs also suggest that trans-tensional stepovers in strike slip faults do not generate large ground motions. In some cases PBRs indicate that nearby faults are not as active as assumed in the 2008 seismic hazard maps (*e.g.*, PBRs are essentially on the fault trace of the Cleghorn and Pinto Mountain faults). In our presentation we consider individual site discrepancies and possible explanations for each case.

Earthquake Debates

Oral Session · Thursday 1:30 PM, 22 April · Salon F
Session Chairs: Danijel Schorlemmer, David D. Jackson, Jeremy D. Zechar, and Warner Marzocchi

A Discussion of Elastic Rebound, Earthquake Recurrence and Characteristic Earthquakes

ELLSWORTH, W.L., U. S. Geological Survey, Menlo Park, CA, USA, ellsworth@usgs.gov; WELDON II, R.J., Dept. of Geological Sciences, University of Oregon, Eugene, OR, USA, ray@uoregon.edu

One hundred years have passed since H. F. Reid proposed the elastic rebound model for earthquakes, in which fault slip during an earthquake releases stored elastic strain energy. Reid, as well as G. K. Gilbert a quarter century before, well understood that substantial time was required to accumulate the elastic strain energy released in earthquakes, but it was not until the advent of plate tectonics a half-century later that the source and rate of strain accumulation driving the deformation was quantified. Today, we speak of a seismic cycle of interseismic strain accumulation, coseismic strain release and postseismic adjustments as a recurring process, and we apply the underlying concepts to forecast future earthquakes and fault system behavior. Advances in geology, seismology and geodesy over the past several decades, and the emergence of the field of paleoseismology have greatly advanced our understanding of the fault recurrence behavior.

But, do conceptual models such as the seismic cycle or the characteristic earthquake model blind us from seeing the full range of recurrence behaviors? A central question that has emerged is the relationship between one faulting event and the next. How is the strain released in one event related to the amount of strain accumulated during the interseismic period and/or the strain released in the preceding event? Are the ruptures at a point approximately periodic or random in time? If they are quasi-periodic what controls the periodicity? If they are random, what does this say about elastic rebound? In this presentation, we will turn a critical eye to these models, and discuss the state of the evidence that supports or may refute some of the well-known and widely applied descendants of Reid's elastic rebound model.

Reply to Ellsworth and Open Discussion

WELDON, II, R.J., Dept. of Geological Sciences, University of Oregon, Eugene, OR, USA, ray@uoregon.edu

A Discussion of Elastic Rebound, Earthquake Recurrence and Characteristic Earthquakes

WELDON, II, R.J., Dept. of Geological Sciences, University of Oregon, Eugene, OR, USA, ray@uoregon.edu; ELLSWORTH, W.L., U. S. Geological Survey, Menlo Park, CA, USA, ellsworth@usgs.gov

One hundred years have passed since H. F. Reid proposed the elastic rebound model for earthquakes, in which fault slip during an earthquake releases stored elastic strain energy. Today, we speak of a seismic cycle of interseismic strain accumulation, coseismic strain release and postseismic adjustments as a recurring process, and we apply the underlying concepts to forecast future earthquakes and understand fault system behavior. Advances in geology, seismology and geodesy over the past several decades, and the emergence of the field of paleoseismology have greatly advanced our understanding of fault recurrence behavior.

But, do conceptual models such as the seismic cycle or the characteristic earthquake model blind us from seeing the full range of recurrence behaviors? A central question that has emerged is the relationship between one faulting event and the next; *i.e.* how is the strain released in one event related to the amount of strain accumulated during the interseismic period and/or the strain released in the preceding event? If ruptures are not periodic or characteristic, what controls the variations in the displacement and length of time between events? How does one explain the growing paleoseismic dataset that includes clusters of earthquakes separated by hiatuses up to 5 times longer than the average interval, variable slip per event at some sites but repeated amounts of slip in others, and the fact that long intervals are not obviously preceded or followed by large displacements, any more than short intervals are always preceded or follow by smaller than average displacements. In Part 2 of this discussion we will use paleoseismological data from around the world to critically examine elastic rebound based models, and discuss the state of the evidence that supports or may refute some of the well-known and widely applied descendants of Reid's model.

Reply to Weldon and Open Discussion

ELLSWORTH, W.L., USGS, Menlo Park, CA, USA, ellsworth@usgs.gov

The Case for Gutenberg-Richter Scaling on Faults

PAGE, M.T., USGS, Pasadena, CA, USA, pagem@caltech.edu; FELZER, K.R., USGS, Pasadena, CA, USA, kfelzer@gps.caltech.edu; WELDON II, R.J., University of Oregon, Eugene, OR, USA, ray@uoregon.edu; BIASI, G.P., University of Nevada, Reno, NV, USA, glenn@seismo.unr.edu; ALDERSON, D.L., Naval Postgraduate School, Monterey, CA, USA, dlalders@nps.edu; DOYLE, J.C., CalTech, Pasadena, CA, USA, doyle@cds.caltech.edu

The Gutenberg-Richter (G-R) magnitude-frequency distribution is known to describe the distribution of earthquake sizes within large regions. There is controversy, however, as to whether this distribution also applies at the scale of individual faults. An alternative hypothesis, the characteristic earthquake hypothesis, posits that large earthquakes on major faults occur at a higher rate than a Gutenberg-Richter extrapolation from small events predicts (Wesnousky *et al.*,1983; Schwartz and Coppersmith, 1984). The primary evidence for such a scaling break is an apparent mismatch between instrumental and paleoseismic earthquakes rates for several major fault zones. This mismatch, however, can also be explained as a rate change rather than a deviation from G-R statistics.

We present the evidence for Gutenberg-Richter scaling on faults in Southern California, where there is a wealth of paleoseismic data and the characteristic earthquake hypothesis has been applied in seismic hazard analysis. We show that, 1) the instrumental catalog does not show deviations from G-R scaling near the mapped faults in Southern California, 2) each individual catalog for the Southern San Andreas is internally G-R, including a catalog of paleoseismic events, and 3) rate changes over long time periods and regions do exist.

We are able to model the observed paleoseismic and modern instrumental earthquake rates for the Southern San Andreas fault with an ETAS model that has Gutenberg-Richter scaling. This demonstrates that appeals to more exotic magnitude distributions are not needed to explain the data; rather, one magnitude-frequency distribution will do.

Reply to Page and Open Discussion
SCHWARTZ, D.P., USGS, Menlo Park, CA, USA, dschwartz@usgs.gov

Do Large Earthquakes on Faults Follow a Gutenberg-Richter or Characteristic Distribution?: A Characteristic View
SCHWARTZ, D.P., USGS, Menlo Park, CA, USA, dschwartz@usgs.gov

In 1984 Schwartz and Coppersmith published "Fault Behavior and Characteristic Earthquakes: Examples from the Wasatch and San Andreas Fault Zones." Using then-newly-available geologic recurrence and slip per event data they concluded a) individual faults and fault segments tend to produce essentially the same size or "characteristic" earthquakes (CE) having a relatively narrow range of magnitudes near the maximum and b) a linear extrapolation of the cumulative recurrence curve (Gutenberg-Richter [GR] distribution) for smaller magnitudes on a fault underestimates the frequency of large events. Explicit in the CE model is that recurrence of surface rupture reflects strain released directly on the fault plane and not in a volume of crust around it. This concept and its variations (maximum moment and uniform slip models) have come to play a major role in seismic hazard analysis.

During the past 26 years a large number of new observations of fault rupture behavior have been made worldwide: normal faults in the Basin and Range, Apennines, Andes; strike-slip faults in California, New Zealand, Asia; thrust faults in Taiwan and the Himalaya. These include paleoearthquake chronologies, successive slip at a point on a fault, and improved instrumental and historical earthquake locations. Paleoseismic slip per event data show a high degree of self-similarity from rupture to rupture as opposed to the variability expected from a GR magnitude distribution. Historically even high slip rate faults have failed to produce the number of small-moderate earthquakes expected from a GR distribution. Global observations continue to support the concept that a GR magnitude distribution is appropriate for regions only, whereas for most individual faults moment is primarily released in a limited range of large earthquakes whose magnitudes are controlled by physical properties of the fault zone.

Reply to Schwartz and Open Discussion
PAGE, M., U.S. Geological Survey, 525 S. Wilson Avenue Pasadena, CA 91106, pagem@caltech.edu.

Applications of Earthquake Simulators to Assessments of Earthquake Probabilities
DIETERICH, J., UC Riverside, Riverside, CA, USA, dieterichj@ucr.edu; RICHARDS-DINGER, K., UC Riverside, Riverside, CA, USA, keithrd@ucr.edu

Current methodologies for assessing earthquake probabilities, such as those used by successive Working Groups on California Earthquake Probabilities, rely on idealized generic probability distributions for earthquake occurrence and employ highly simplified approximations of the physical processes and interactions that determine the onset and extent of earthquake slip. These assessments have become exceedingly complex, but unfortunately remain quite uncertain, in part because site-specific recurrence statistics for infrequent large earthquakes are unknown. Recent advances in large-scale simulations of earthquakes in fault systems make it possible to accurately model earthquake rupture processes and stress interactions in high resolution representations of fault systems for large numbers of earthquakes (typically 10^5 to 10^6 events, M5.0 to M8.0). The simulations incorporate clustering processes including foreshocks and aftershocks. Possible applications of simulators in assessments of earthquake probabilities include the generation of site-specific empirical density distributions of earthquake recurrence times, characterization of stress interactions and possible clock-resets for use with conditional probability estimates, and probabilistic evaluation of the effects of segment-to-segment ruptures and fault branching.

Reply to Dieterich and Open Discussion
MICHAEL, A.J., USGS, Menlo Park, CA, USA, michael@usgs.gov

Barriers to the Use of Physics-Based Seismicity Simulators in Seismic Hazards Assessments
MICHAEL, A.J., USGS, Menlo Park, CA, USA, michael@usgs.gov

Useful physics-based simulators of seismicity require an accurate representation of the physics that governs the seismogenic process and an accurate representation of the faults and associated geologic structures. Current simulators utilize faults with temporally constant failure stresses and/or rate- and state-friction but usually do not include poroelastic effects, viscoelasticity, or dynamic triggering effects. Earthquakes may include multiple faults but we do not have sufficiently detailed structural models of fault intersections, which limits our ability to model fault-to-fault jumps. Despite failing to include all of the known physical processes or accurate fault structures, it may be possible to validate simulators based on their ability to replicate known properties of earthquakes and seismicity catalogs. Unfortunately, many of these key properties are poorly constrained. Recently improved understanding of uncertainties in finite fault slip inversions suggests that we may not accurately understand the behavior of individual events. Some properties of earthquake catalogs are controversial, such as the degree of characteristic behavior and whether or not earthquakes are semi-periodic, and thus their use in validation methods would be similarly controversial. Another problem is that Gutenberg-Richter and modified-Omori behavior may be produced by so many different models that they can not be used to differentiate between them. That the simple and intuitively appealing idea of slip-predictability has failed observational tests demonstrates the complexity of the seismogenic process and thus we should be cautious about using simulators to extrapolate our current physical understanding into earthquake hazards assessments. In fairness to the physics-based simulation methods, many of these issues also plague current statistical approaches.

Reply to Michael and Open Discussion
DIETERICH, J.H., UC Riverside, Riverside, CA 92521, USA, dieterichj@ucr.edu

Seismic Structure and Geodynamics of the High Lava Plains and Greater Pacific Northwest

Oral Session · Thursday 1:30 PM, 22 April · Salon G
Session Chairs: David E. James, G. Randy Keller, and Matthew J. Fouch

Seismic Imaging of Remnant Slabs, Slab Gaps and Problematic Plumes in the Pacific Northwest
JAMES, D.E., Carnegie Institution/DTM, Washington, DC, james@dtm.ciw.edu; FOUCH, M.J., Arizona State University, Tempe, AZ, fouch@asu.edu; ROTH, J.B., ExxonMobil Exploration, Houston, TX, jeffrey.roth@asu.edu; CARLSON, R.W., Carnegie Institution/DTM, Washington, DC, carlson@dtm.ciw.edu

olcanism in the Cascadian back arc over the past 12 Ma is concentrated along the orthogonal SRP/Yellowstone and High Lava Plains/Newberry time-progressive volcanic tracks. While both tracks originated close to the region of the Idaho/Oregon/Nevada border that marked the initiation ca. 17 Ma of the massive flood volcanism, they exhibit contrasting upper mantle structures. The HLP/Newberry volcanic terrane is underlain by low velocities confined largely to the uppermost mantle beneath the Moho, with extremely low velocities located in areas of Holocene basaltic volcanism. In contrast, the SRP/Yellowstone volcanic province is characterized by ultra-low velocities, particularly in S, that extend to a uniform depth of about 200 km along its entire length. While the SRP/Yellowstone hotspot is widely assumed to result from plate motion across an ascending deep mantle plume, new high-resolution S-wave seismic images show little evidence for a plume conduit in either upper or lower mantle. The seismic images instead reveal two prominent non-plume features: (1) a tabular "sheet" of low velocities at 300–600 km depth, parallel to the uppermost mantle anomaly beneath the SRP/Yellowstone, but offset ~100 km to the northwest and extending well into eastern Oregon; (2) the northern limb of a sub-horizontal Farallon slab remnant, lying in the transition zone beneath and parallel to the surface expression of the SRP/Y province. These images confirm prior suggestions of a "slab gap" whose southeastern boundary coincides with the SRP/Yellowstone track. The seismic observations, coupled with reconstructed subduction history for the Northwest Pacific and recent numerical studies demonstrating that plume-like behavior can be mimicked by certain kinds of subduction processes, suggest that alternative interpretations based on subduction models are possible for SRP/Yellowstone.

Seismic Evidence for Fossil Subduction and Small-Scale Convection Beneath the Northwestern U.S.

SCHMANDT, B., University of Oregon, Eugene/OR/USA, bschmand@uoregon.edu; HUMPHREYS, E., University of Oregon, Eugene/OR/USA, genehumphreys@gmail.com

ew high-resolution P and S tomography of the western U.S. upper mantle reveals strong multi-scale heterogeneity closely correlated with tectonic and magmatic activity. We invert travel-time residuals from the EarthScope TA and 1700 additional stations for 3-D velocity structure. The inversion uses frequency-dependent 3-D sensitivity kernels to interpret multiple frequency residuals and recent advances in western U.S. crust thickness and velocity models to better isolate the mantle component of residuals. In addition to VP and VS models, we jointly invert the two datasets for VP/VS perturbations. We image an arcuate high-velocity "curtain" roughly beneath the Challis-Kamloops volcanic trend that extends vertically from near the base of the lithosphere to depths of ~240 km beneath WA and ~400 km beneath central ID, which we interpret as the leading edge of Siletzia lithosphere abandoned during accretion in the Columbia embayment. Some Challis-Kamloops magmatism is attributed to melting the basaltic crust of this lithsophere. Normal-dip subduction beneath the Cascade arc was established shortly after accretion and must have become separated by a tear from the flat-subducting Laramide slab. A strong, nearly spherical high-velocity anomaly underlies the Wallowa Mountains (WM), the source region for a large fraction of the Columbia River Basalts (CRB). The high-velocity body may represent melt-depleted residuum created by extraction of the voluminous CRB from the mantle or removal of dense lithosphere beneath the WM, which have experienced ~1.5 km of uplift since the initial CRB eruptions. The presence of these structures must have a considerable impact on asthenospheric flow in the mantle wedge and may be related to differences between the WA and OR Cascades in terms of magmatic productivity and vigor of asthenospheric flow as inferred from SKS splitting.

Lithosphere-Asthenosphere Interaction Beneath the Pacific Northwest From the Integrated Analysis of Body and Surface Waves

OBREBSKI, M., UC Berkeley, Berkeley/CA/USA, obrebski@berkeley.edu; ALLEN, R., UC Berkeley, Berkeley/CA/USA, rallen@berkeley.edu; PORRITT, R., UC Berkeley, Berkeley/CA/USA, rwporritt@gmail.com; POLLITZ, F., USGS, Menlo Park/CA/USA, fpollitz@usgs.gov; HUNG, S.-H., National Taiwan University, Taipei/Taiwan, shung@ntu.edu.tw

he Pacific Northwest has undergone complex and intense tectonic and magmatic activity over the Cenozoic Era. In particular, the Neogene-Quaternary magmatic activity documented in the Yellowstone-Snake River Plain and in the High Lava Plain has drawn much attention. The relation that may link these two features to each other and to the Columbia River Basalts, the depth at which they originate, and their possible relation with the subduction of the Juan De Fuca-Farallon oceanic plate are still a theme of debate. In an effort to answer these questions, we take advantage of the growing amount of seismic data collected over the Western US to image the velocity structure of the crust and mantle beneath the Pacific Northwest. In this study we focus on the lithospheric and asthenospheric structure. The compressional (DNA10-P) and shear (DNA10-S) velocity models we present here use seismic data from the Earthscope Transportable Array, regional seismic networks and two Flexible Array experiments (Mendocino and FACES experiments) deployed on the west coast. DNA10-P is a multi-frequency model obtained using finite-frequency sensitivity kernels calculated in 4 frequency bands (0.5–1.25s, 1.25–2.5s, 2.5–10s and 10–50s). Owing to its broad range of periods, this model is characterized by a high resolution below a depth of 50km where the seismic ray paths start crossing each other. DNA10-S is a multi-phase model that includes constraints from teleseismic body waves (periods from 18 to 100s), ballistic surface waves and Green's functions extracted from noise correlation (8 to 40s). By inverting jointly these different types of data, we obtain a model with better resolution at lithospheric depth that allows investigating the possible link between density structures in the mantle and the geotectonic features observed in the Pacific Northwest.

Surface Wave Constraints on the Causes of High Lava Plains Volcanism

WAGNER, L.S., UNC-Chapel Hill, Chapel Hill, North Carolina, USA, wagner@unc.edu; FOUCH, M.J., Arizona State University, Tempe, Arizona, USA, fouch@asu.edu; LONG, M.D., Yale University, New Haven, CT, USA, maureen.long@yale.edu; JAMES, D.E., Carnegie Inst. of Washington, Washington, DC, USA, james@dtm.ciw.edu; FORSYTH, D., Brown University, Providence, RI, USA, Donald_Forsyth@brown.edu

he High Lava Plains (HLP) are a time progressive track of silicic volcanism complemented by non-time-progressive basaltic eruptions. The HLP began under the Owyhee plateau ~15 Ma and then trended to the north-west at an oblique angle to North American plate motion. The current terminus of the HLP is located beneath Newberry Volcano, just east of the Cascades. We present surface-wave tomographic images calculated with the two-plane-wave method of Forsyth and Li (2004) using data collected by the High Lava Plains broadband seismic deployment and USArray Transportable Array stations (TA). These images clearly show the track of the HLP, as well as that of the Yellowstone-Snake River Plains (YSRP). A number of interesting features are observed in our tomographic images, including an extension of the YSRP low velocity lineament past the Owyhee plateau towards Mendocino, and a distinct decrease in the depth extent and amplitude of the HLP low velocity zone located between Steens and Newberry related volcanism. The location of this decreased and shallow low velocity anomaly corresponds spatially to the location of decreased SKS splitting amplitudes. This may help explain both the causes of HLP volcanism as well as its apparent temporal progression towards the North-West.

Regional Electrical Conductivity of the Pacific Northwestern U.S. from EMScope

EGBERT, G.D., Oregon State University, Corvallis, Oregon, USA, egbert@coas.oregonstate.edu; SCHULTZ, A., Oregon State University, Corvallis, Oregon, USA, adam@coas.oregonstate.edu; FOUCH, M.J., Arizona State University, Tempe, Arizona, USA.

agnetotelluric (MT) data are being acquired in a series of transportable arrays deployed across the continental US through EMScope, a component of USArray. Deployments in 2006–2009 acquired data at 221 sites, with the same nominal spacing as the USArray seismic transportable array (~70 km), covering the Northwestern US, from the Oregon-Washington coast across the Rocky Mountains, through most of Montana and Wyoming. Electrical conductivity is particularly sensitive to the presence and connectivity of fluids (aqueous and magmatic) , so these observations provide unique constraints, which, in conjunction with other geophysical and geological data, can add significantly to our understanding of the composition and physiochemical state of Earth's interior. Three-dimensional inversion of 110 sites from the Pacific Northwest portion of the EMscope array footprint reveals extensive areas of high conductivity in the lower crust beneath the Northwest Basin and Range, inferred to result from fluids (including possibly partial melt at depth) associated with magmatic underplating, and beneath the Cascade Mountains, probably due to fluids released by the subducting Juan de Fuca slab. Initial inversion results for data from the Eastern half of the array reveal similar large-scale patterns of strong conductivity variations at depths of 20–50 km, *e.g.*, extending southwest from Yellowstone into the central Snake River Plain. Deeper conductivity anomalies are also suggested by the inversions, but the very strong contrasts in the lower crust (possibly extending into the top of the mantle) presents challenges for resolution of upper mantle structure. We will provide an overview of the MT results to date, compare them with existing images of EarthScope body wave seismic data, and discuss initial efforts at integration of these datasets.

Raytrace Models from the High Lava Plains (HLP) Controlled-source Experiment.

COX, C.M., University of Oklahoma, Norman, OK USA, cmcox@ou.edu; KELLER, G.R., University of Oklahoma, Norman, OK USA, grkeller@ou.edu; HARDER, S.H., University of Texas, El Paso, El Paso, TX USA, harder@geo.utep.edu; KLEMPERER, S., Stanford University, Stanford, CA USA, sklemp@stanford.edu

he High Lava Plains (HLP) of eastern Oregon and adjacent parts of Idaho and Nevada were the target of a very large controlled-source seismic experiment in early September 2008. A total of 67 scientists, students, 6 staff members from the PASSCAL/Earthscope Instrument Center and volunteers deployed 2612 Texan short-period seismic recorders and 120 RT-130 recorders from the PASSCAL and EarthScope instrument pools to record 15 seismic sources spaced across the High Lava Plains (HLP) region. This was the largest number of instruments deployed in an on-land controlled-source crustal scale experiment. This deployment also took advantage of the 117 seismometers in the HLP broadband array whose deployment over the past three years was led by Carnegie Institution of Washington and Arizona State University. Together, these efforts are providing a deep and three-dimensional image of the structure of this region. The seismometers were located to provide high-resolution images of the mantle and crust directly beneath the path of volcanism that dotted the High Lava Plains during the past 16 Ma. At a glance, our results show that the crustal structure across the HLP region is similar to that in the northern Basin and Range. The crust does thicken from northwest to southeast across eastern Oregon, with relatively higher velocities in the lower crust that suggest underplating in the region west of Steens Mountain. The average crustal velocity is somewhat higher than in the Basin and Range suggesting some magmatic modification of the crust. However, the full implications of our results await our team's integrated analysis with petrologic and geologic data, which is intended to reveal the complex processes that created HLP. http://www.dtm.ciw.edu/research/HLP/

P-to-S Receiver Function Imaging of the Crust Beneath the High Lava Plains of Eastern Oregon

EAGAR, K.C., Arizona State University, Tempe, AZ, keagar@asu.edu; FOUCH, M.J., Arizona State University, Tempe, AZ, fouch@asu.edu; JAMES, D.E., Carnegie Inst. of Washington, Washington, DC, james@dtm.ciw.edu; CARLSON, R.W., Carnegie Inst. of Washington, Washington, DC, rcalson@ciw.edu

We analyze teleseismic P-to-S receiver functions to image crustal structure beneath the High Lava Plains (HLP) of eastern Oregon and the surrounding Pacific Northwest region. The high-density broadband seismic array in the area provides an opportunity to constrain, in high-resolution, variations in regional bulk crustal composition, Moho depth, and crustal anisotropy by applying the *H-k* stacking method to receiver functions from 209 individual stations. Our results reveal relatively thin crust beneath the HLP and northern Great Basin that thickens dramatically below the Cascade volcanic arc and Idaho Batholith. Poisson's ratios are more scattered but generally show higher values than average continental crust throughout the HLP. Although the crust beneath HLP is generally thin everywhere, receiver functions also reveal localized small-scale complexities such as a dipping or diffuse Moho or anisotropic layers. The Owyhee Plateau seems to have a distinctive crustal signature, characterized by thick crust and receiver functions that adhere well to the *H-k* stacking assumptions of a flat-lying, isotropic, homogeneous crust. The transition from the HLP to the Owyhee Plateau occurs over short distances and coincides approximately with the Sr^{87}/Sr^{86} 0.706 line, which delineates cratonic North America to the east from younger terranes to the west. Our results suggest a fundamentally different crustal evolution of the HLP in response to widespread magmatism relative to surrounding terranes, especially the Owyhee Plateau, which seems to have escaped significant Cenozoic modification. The high Poisson's ratios of the HLP crust may suggest mafic underplating and high, near melting, temperatures in the crust, consistent with the occurrence of rhyolitic volcanism across the HLP.

An Integrated Analysis of Lithospheric Structure in the High Lava Plains region: Preliminary Observations

KELLER, G.R., University of Oklahoma, Norman, OK 73019 USA, grkeller@ou.edu; OKURE, M., University of Oklahoma, Norman, OK 73019 USA, msokure@ou.edu; WALLET, B., University of Oklahoma, Norman, OK 73019 USA, bwallet@ou.edu; COX, C., University of Oklahoma, Norman, OK 73019 USA, cmcox@ou.edu

In order to place our ongoing investigations of the High Lava Plains of Oregon in a regional context, we are analyzing the structure of the lithosphere across the Oregon region using wide-angle reflection and refraction, gravity, magnetic, and receiver function data. The various geophysical datasets were analyzed individually and then integrated considering known geology and structures. We assumed that variations lithospheric structure are most likely the result of processes related to plate subduction, terrane accretion, and associated creation and melting of crustal material, as well as, Basin and Range extension. A database of seismic constraints on crustal thickness was created by combining existing databases, new seismic results, and receiver functions that are created as an EarthScope data product. We then used gravity and elevation data a soft constraint to resolve inconsistencies before producing a crustal thickness map. The main feature on this map is a consistent west to east thinning of the crust from the Cascades all across Oregon. This pattern is surprising in the north where the accreted terranes are found.

We also applied a variety of filters to our regional gravity and magnetic data primarily to enhance upper crustal features. The resulting maps provide new insight on the origin and extent of a variety of tectonic features. For example, residual gravity and magnetic maps correlate well with recent interpretations of the position of the 87Sr/86Sr > 0.706. The significant differences in gravity magnetic signatures across this line are consistent with there being a relatively abrupt lithosphere transition between the Proterozoic-Archean Wyoming Craton and the younger regions to the west. In addition, the magnetic data reveal a circular pattern of local highs that can be interpreted as outlining a major caldera within which the Harney basin would represent a central depression and zone of sediment deposition.

Crustal Stress Indicators for Southwest British Columbia: What Controls Faulting in the Crust?

BALFOUR, N.J., University of Victoria, Victoria, BC, Canada, nbalfour@uvic.ca; CASSIDY, J., Pacific Geoscience Centre, Sidney, BC, Canada, John.Cassidy@NRCan-RNCan.gc.ca; DOSSO, S., University of Victoria, Victoria, BC, Canada, sdosso@uvic.ca

We present new stress and anisotropy results, which are combined with seismicity, local tectonics, and GPS data (velocity and strain) to determine regional stresses that control faulting in the North American crust above the Cascadia subduction zone in SW British Columbia (BC). The region experiences crustal earthquakes with recorded magnitudes up to 7.3. These events have a shorter reoccurrence interval than megathrust earthquakes and pose a significant hazard to major population centers. The North American plate in this region includes a change in margin orientation from N-S in Washington State to NW-SE in BC and involves a complex region of deformation above a bend in the subducting Juan de Fuca plate. Over 1000 focal mechanisms have been calculated to identify the dominant style of faulting and inverted to estimate the 3 principal stress orientations and stress ratio. These results are then compared with results from recent anisotropy work where over 4000 station-event pairs have been analysed for shear-wave splitting. By comparing stress orientations with fast directions we investigate whether the source of anisotropy is stress or structure related and identify any variations in the stress field. Preliminary results indicate a change in fast direction with distance from the trench from margin-parallel on Vancouver Island to margin-normal on Mainland BC. This change is also reflected in GPS velocity vectors and may suggest there is some variation in the stress with distance from the margin.

Coulomb Stress Interactions among M≥6 Earthquakes in the Gorda Deformation Zone and on the Mendocino Fracture Zone, Cascadia Megathrust and Northern San Andreas Fault

ROLLINS, J.C.R., University of Southern Californi, Los Angeles/California/USA, chrisrol@usc.edu; STEIN, R.S.S., United States Geological Survey, Menlo Park/California/USA, rstein@usgs.gov

The Gorda deformation zone, a 200 x 200 km area of rotation, subduction and diffuse shear in the southernmost Juan de Fuca plate, displays the highest rate of large earthquakes in the contiguous United States. Since 1980, sixteen M≥6 earthquakes, including four M≥7 shocks, have ruptured four different fault systems in this area, making it well suited for the study of earthquake interaction by static Coulomb stress transfer. We calculate that five of the recent M≥6 shocks occurred at sites where other earthquakes had imparted ≥0.9-bar Coulomb stress increases less than nine months beforehand, a correlation we cannot replicate in location-randomized control tests. M≥6 left-lateral earthquakes were absent for at least 14 years where the calculated Coulomb stress decreased as a result of the 1980 Mw=7.3 Eureka earthquake. Stress imparted by the 1980 earthquake to the Mendocino Fracture Zone and Cascadia megathrust explains the enigmatic triangular aftershock pattern of the 1980 quake first identified by Eaton (1987). The January 2010 M6.7 earthquake is calculated to have increased stress by >0.2 bar on the Cascadia megathrust and Mendocino Fracture Zone. From these observations, we derive generalized static stress interactions among right-lateral, left-lateral and thrust faults near triple junctions. Dynamic stress interactions may also occur, as two M>6 earthquakes occurred 21 hr and 200 km apart in 1991.

Upper Mantle Anisotropy Beneath the High Lava Plains: Linking Upper Mantle Dynamics to Surface Tectonomagmatism

LONG, M.D., Yale University, New Haven, CT USA, maureen.long@yale.edu; FOUCH, M.J., Arizona State University, Tempe, AZ USA, fouch@asu.edu; WAGNER, L.S., University of North Carolina, Chapel Hill, NC USA, lswagner@email.unc.edu; JAMES, D.E., Carnegie Institution, Washington, DC USA, james@dtm.ciw.edu

The High Lava Plains (HLP) of southeastern and central Oregon comprises a young (< 15 Ma), bimodal volcanic province that exhibits an age progression in silicic volcanism towards the northwest, along with widespread basaltic volcanic activity. A variety of models have been proposed to explain the volcanic history of the region, but consensus on which model best explains the observations remains elusive. In order to investigate the geometry of mantle flow beneath the HLP and to test models for the origin and evolution of the HLP province, we combine constraints on upper mantle anisotropy from SKS splitting and surface wave analysis using stations of the HLP broadband seismic experiment and the USArray Transportable Array (TA). Stations in the region exhibit significant SKS splitting, with average delay times at single stations ranging from ~ 1.0 sec to ~ 2.7 sec. Nearly all observed fast directions are approximately E-W, which argues for well-organized contemporary mantle flow in an E-W direction beneath the HLP. The E-W fast splitting directions are consistent with constraints on azimuthal anisotropy from surface wave analysis, but are inconsistent with models that invoke plume-driven flow along the strike of the HLP. We observe significant lateral variations in average splitting delay times, with a region of particularly large dt (> 2 sec) that delineate a region in the heart of the HLP province and another region of large delay times just to the north of Newberry Volcano. There is a notable spatial correlation between stations that exhibit large delay times and the location of Holocene volcanic activity, as well as with regions with relatively low S wavespeeds in the uppermost mantle from surface wave models. We discuss several possible models that may explain lateral variations in uppermost mantle velocities and anisotropy strength.

The Mantle Flow Field Beneath Western North America

FOUCH, M.J., Arizona State University, SESE, Tempe, AZ, USA, fouch@asu.edu; WEST, J.D., Arizona State University, SESE, Tempe, AZ, USA, john.d.west@asu.edu

The goal of this study is to image the mantle flow field beneath western North America. We utilize broadband data from regional and portable seismic arrays, with an emphasis on stations from EarthScope's USArray Transportable Array, to image seismic anisotropy and constrain deformation in the lithosphere and asthenosphere across the region.

Regional shear wave splitting parameters show clear variations with geologic terrane. In the Pacific NW, splitting times are large and fast directions are ~E-W with limited variability. Away from the Pacific-North American plate boundary, and sandwiched between broad regions of simple and strong splitting, stations within the Great Basin (GB) exhibit significant complexity. Fast directions show a clear rotation from E-W in the northern GB, to N-S in the eastern GB, to NE-SW in the southeastern GB. Splitting times reduce dramatically, approaching zero within the central GB.

While lithospheric fabric likely contributes to the shear wave splitting signal at many of the stations in this study, the broad-scale trends in both fast directions and delay times argue for a substantial asthenospheric source to the anisotropy. The regional mantle flow field therefore appears to be strongly controlled by significant and recent changes in plate boundary geometry. Assuming a North American plate reference frame, mantle flow appears to be controlled by absolute plate motion away from tectonic North America; conversely, rapid westward slab rollback of the Juan de Fuca plate dominates the Pacific NW U.S. flow field. To fill this gap in asthenospheric material, mantle flows strongly eastward S of the Juan de Fuca plate. Beneath the Great Basin, the paucity of shear wave splitting, combined with tomographic images and a range of geochemical and geologic evidence, supports a model of downward mantle flow due to a lithospheric drip.

Joyner Lecture

Thursday 5:15 AM · Salon E & F

Progress and Controversy in Seismic Hazard Mapping

FRANKEL, A., U.S. Geological Survey, Seattle, WA, afrankel@usgs.gov.

Probabilistic seismic hazard maps translate what we know about earthquake sources, faulting, crustal deformation, and strong ground motions into a form that can be used by engineers to design structures. I will discuss three examples that illustrate how seismic hazard maps are developed and applied: the production of the 1996 national seismic hazard maps, the controversy involving the seismic hazard in the New Madrid region of the central U.S., and the construction of detailed urban seismic hazard maps for Seattle using three-dimensional ground-motion simulations.

Deterministic Simulated Ground Motion Records under ASCE 7-10 as a Bridge Between Geotechnical and Structural Engineering Industry

Oral Session · Thursday 3:30 PM, 22 April · Salon E

Session Chairs: Alexander Bykovtsev and Walter Silva

Requirements for Development of Acceleration Time Histories per ASCE 7-10 Standard

CROUSE, C.B., URS Corp., Seattle, WA, cb_crouse@urscorp.com

Revisions to the provisions for the development of acceleration time histories for 3-D dynamic response analysis have been introduced in Section 16.1.3.2 of the ASCE 7-10 standard. These revisions were necessary due to the switch from the geometric mean, horizontal component, response spectral acceleration to the maximum response spectral acceleration in a 2-D horizontal plane. Consequently, the new scaling requirement is that the average square-root-sum-of-squares (SRSS) of the response spectra of the scaled horizontal-component accelerograms selected for the dynamic analysis, does not fall below the corresponding Maximum Considered Earthquake (MCE) response spectrum within the natural period band of interest. For sites within 5 km of an active fault that controls the MCE ground motion, each pair of fault-normal (FN) and fault-parallel (FP) components shall be scaled such that the average FN response spectrum is not less than the MCE response spectrum within the period band of interest. Chapter 16 of ASCE 7-10 and prior ASCE 7 standards have permitted the use of simulated ground motions when the required number of appropriate recorded accelerograms is not available. One application for which simulation methods should be given serious consideration is critical long period structures, such as high rise buildings located in areas subjected to great magnitude earthquakes that can produce large long period motions lasting several minutes. Unfortunately, relatively few geotechnical engineers or engineering seismologists that serve the structural engineering community are knowledgeable in simulation methods. Therefore, one solution would be to generate sets of simulated records applicable to various scenario earthquakes, such as M 8 San Andreas and M 9 Cascadia Subduction Zone events, and place these sets in a data center readily available to practicing engineers.

On the Sensitivity of Near-Source Ground Motions to Heterogeneity of Fault Ruptures

ROWSHANDEL, B., California Geological Survey, Sactamento, CA, badie.rowshandel@conservation.ca.gov

Performance-Based Earthquake Engineering calls for design of facilities for different levels of service. It typically requires design for three different service levels: (1) serviceability in frequent ground motions, (2) life safety in rare ground motions, and (3) collapse prevention in very rare ground motions. Many issues exist with defining and establishing design ground motions for multiple service design levels. As seismic design deviates from the traditional prescriptive approach, users need clarification and guidelines to deal with the challenges in developing design ground motions. Similarly, the existing (ASCE 7-10) procedure for the selection of time histories for seismic design is accompanied by much uncertainty. Procedures for developing scenario ground motions and design response spectra, and selecting time histories are therefore needed.

Among the factors which often contribute significantly to the variability of observed near-source ground motions and hence to the uncertainty in design ground motions, is the unpredictability of future ruptures. We have examined the sensitivity of near-source ground motions to source rupture parameters. Information on distributions of asperities and slip, reported for recent major earthquakes, are used in conjunction with Ground Motion Prediction models. Based on Monte Carlo simulations, the impact of variability in rupture parameters on the amplitude and the distribution of near-source ground motions, and on the shape of response spectra of specific seismic sources are investigated. Results show that intense ground motions in isolated areas in the vicinity of faults and also some of the features and peculiarities in the shapes of site-specific response spectra, such as reported in past earthquakes and cannot be explained by local soil effects or other ways, can be modeled by proper choices of fault rupture parameters.

A Consideration of Uncertainty when Selecting Near-Source Ground Motions for Design

OLSEN, A.H., University of Colorado, Boulder, CO, anna.olsen@colorado.edu; HEATON, T.H., Caltech, Pasadena, CA, heaton@caltech.edu

Both the seismological and engineering communities acknowledge that anticipating future ground motions at a site is fraught with uncertainty. At present, the fundamental question of site-specific ground motion selection cannot be how to accurately predict future ground motions, but rather how to account for the inherent uncertainty. Two recent studies provide insight into the latter question. In her dissertation, Olsen (2008) demonstrated that peak ground displacement and velocity (a vector intensity measure) predict failure (*i.e.*, collapse or significant permanent drift) of steel moment-resisting frames better than spectral acceleration at the frame's fundamental elastic period. Yamada, Olsen, and Heaton (2009, BSSA) collected 147 recorded strong ground motions within 15 km of 10 faults. The authors showed that the marginal distribution of PGA at these sites is log-normal and expected to remain so with the addition of future records. The marginal distribution of PGD is close to uniform on a log scale, and the current observed distribution may change significantly after the next well-recorded large earthquake. For structures whose failure is best predicted by PGA, the latter study suggests that a ground motion can be selected with a suitably large PGA (say, 2 standard deviations above the mean) since the probability of that PGA is well-defined. The probability of a future near-source PGD is not well-defined, and thus selecting ground motions for the design of structures whose failure is best predicted by PGD is problematic. In this case, we suggest that a design provide the structure least vulnerable to extreme PGD given other constraints on the project, such as budget.

Structural Effects of Earthquake Vertical Ground Motions

SPRAGUE, H.O.S., Black & Veatch Special Projects, Overland Park / Kansas / USA, spragueho@bv.com

The traditional focus of the development of methodologies to characterize and mitigate earthquake induced ground motions has been on the orthogonal horizontal ground motion components. Vertical ground motions have been ignored as a source of earthquake induced damage by traditional building codes. There is evidence that

vertical ground motions have great damage potential that warrant consideration. Some industries have developed design provisions for vertical ground shaking, most have not. There is a significant likelihood of damage due to vertical shaking, either alone or in combination with horizontal shaking. This potential should be investigated for typical building and nonbuilding structures. Building structural code provisions should be developed to formally address the effects of vertical ground motion for different types of structures and rigorously account for the combined effects of vertical and horizontal ground shaking.

Earthquake Source Statistics Including Variability of Slip for Simulation-Based Ground Motion Prediction

SONG, S., URS Group, Inc., Pasadena/CA/USA, seok_goo_song@urscorp.com; SOMERVILLE, P., URS Group, Inc., Pasadena/CA/USA; GRAVES, R., URS Group, Inc., Pasadena/CA/USA.

It is important to quantify the variability of earthquake source processes in a systematic way for accurate prediction of ground motion intensity and variability. We adopt spatial data analysis tools, commonly used in geostatistics, to extract the important features of earthquake source processes from available rupture models and to reproduce them for simulation-based ground motion prediction. The earthquake source process is described by key kinematic source parameters, such as final slip, rupture velocity, and slip duration. The heterogeneity of source parameters and their linear dependency (coupling) are characterized by two point statistics, *i.e.*, auto- and cross-coherence. One point statistics, *i.e.*, the marginal probability density function (PDF) for each source parameter can also characterize many important features of earthquake rupture dynamics, such as subshear or supershear rupture, crack- or pulse-like rupture, stick-slip or creep. The strength of our approach is that all these features can be handled systematically in the form of a single multi-variate PDF. In this study, we specifically focus on the effect of one-point statistics of earthquake slip on near-fault ground motion characteristics. There are several types of scaling laws available to define the characteristics of slip distribution, such as mean slip and correlation length as a function of earthquake size. However, one-point statistics of earthquake slip such as standard deviation or full shape of the marginal PDF of earthquake slip may also be important in determining near-fault ground motion characteristics. Our preliminary study shows that near-fault peak ground velocities are increased by 10–30% for a factor of two increase in the standard deviation of earthquake slip, keeping both the mean slip and the spectral decay rates the same. This study suggests that we need to consider scaling laws for the standard deviation of earthquake slip as well as for mean slip and correlation length.

Deterministic Simulated Ground Motion (SGM) Records under ASCE 7-10 as a Bridge between Geotechnical and Structural Engineering Industry

BYKOVTSEV, A.S., Regional Acad. Natural Sciences, 2644 Foghorn Cove, Port Hueneme, CA 93041, bykovtsev1@yahoo.com

According to new requirements of the ASCE 7-10 Chapter 21 Site-Specific Ground Motion Procedures for Seismic Design, at least five recorded or horizontal SGM acceleration time histories shall be selected from events having magnitudes and fault distances that are consistent with those that control the Maximum Considered Earthquake. In some cases (*e.g.*, from M6.0 to M8, less than 5 km from the fault zone) there may not be five sets of recorded ground motions that are appropriate, and SGM would be needed. Unfortunately, there is no official procedure to follow for near-field sites (D < 5 km from the fault). This presents a paradox: the Building Codes and Standard ASCE/SEI 7-10 requires engineers to provide SGM records (Chapter 21), but there is no official procedure for accomplishing this at near-field sites. This paradox should be resolved as soon as possible and official procedure for SGM should be created.

We are planning to discuss why Fault Segmentation and Vertical Component of SGM should be included in the proper procedure for definition of Base Ground Motions Section 21.1.1 of ASCE 7. Additionally, analyses of SGM for different distances from faults and different types of fault movement (strike slip, dip slip, and oblique slip), arrival time, period and peak for maximum impulses of ground acceleration in three components will be presented.

We will provide analysis of main existing approaches that focus on SGM and address the following aspects: 1) procedures for horizontal- and vertical- component SGM records for planar and nonplanar fault topology within 5 km of a fault zone; 2) comparisons of solutions for different deterministic models; 3) procedures for determining site-specific design ground-motion parameters for landslides and slope stability analyses with time history procedures; 4) site-specific design ground-motion parameters for bridges, high-rise buildings and essential facilities (with time history procedures) located within 5 km of a fault zone.

Characterizing the Next Cascadia Earthquake and Tsunami

Poster Session · Thursday AM, 22 April · Exhibit Hall

An Evaluation of Tsunami Evacuation Options of Padang, West Sumatra, Indonesia

CEDILLOS, V., GeoHazards International, Palo Alto, California, USA, vcedillos@gmail.com; CANNEY, N.E., Stanford University, Stanford, California, USA, canneyn@stanford.edu; DEIERLEIN, G.G., Stanford University, Stanford, California, USA, ggd@stanford.edu; HENDERSON, J.S., Tipping Mar, Berkeley, California, USA, jscotthenderson@gmail.com; ISMAIL, F.A., Andalas University, Padang, West Sumatra, Indonesia, febrin@ft.unand.ac.id; SYUKRI, A., Andalas University, Padang, West Sumatra, Indonesia, andemungo@yahoo.com.sg; TOTH, J., Stanford University, Stanford, California, USA, jtoth@stanford.edu; TUCKER, B.E., GeoHazards International, Palo Alto, California, USA, tucker@geohaz.org; WOOD, K.R., Stanford University, Stanford, California, USA, kwood4@stanford.edu

Padang, West Sumatra, Indonesia has one of the highest tsunami risks in the world. Currently, the strategy to prepare for a tsunami in Padang focuses on developing early warning systems, planning evacuation routes, conducting evacuation drills, and educating the public about its risk. These are all necessary, yet insufficient efforts. Padang is located so close to the offshore megathrust and has such flat terrain that a large portion of its populace will be unable to reach safe ground in the time—less than 30 minutes—between the earthquake and the tsunami arrival at the shore. It is estimated that over 50,000 inhabitants of Padang will be unable to evacuate in that time, even if they head for safe ground immediately following the earthquake. Given these circumstances, other means to prepare for the expected tsunami must be developed. With this motivation, GeoHazards International and Stanford University partnered with Indonesian organizations—Andalas University in Padang, the Laboratory for Earth Hazards (LIPI), and the Ministry of Marine Affairs and Fisheries (DKP)—in an effort to evaluate the need for and feasibility of developing Padang's tsunami evacuation options including horizontal and vertical evacuation. This project team designed and conducted a course at Stanford University, undertook several field investigations in Padang, and participated in a reconnaissance trip following the M7.6 September 30, 2009 earthquake. The team concluded that: 1) the tsunami-generating earthquake is still a threat despite the recent earthquake; 2) Padang's tsunami evacuation capacity is currently inadequate and evacuation structures need to be implemented as part of the evacuation plan; 3) suitable evacuation solutions are highly dependent on the natural and built environment; and 4) previous estimates of the number of people unable to evacuate in time are probably grossly low.

Reconciling Recurrence Interval Estimates, Southern Cascadia Subduction Zone

PATTON, J.R., OSU, COAS; Cascadia GeoSciences, Corvallis/OR/USA, jpatton@coas.oregonstate.edu; LEROY, T.H., PWA; Cascadia GeoSciences, Mckinleyville/CA/USA, toml@pacificwatershed.com

Earthquake and tsunami hazard for northern California and southern Oregon is dominated by estimates of recurrence for earthquakes on the Cascadia subduction zone (CSZ) and upper plate thrust faults. Site-based terrestrial paleoseismic evidence derived recurrence interval (RI) estimates (270–1,370 years) are inconsistent with the regional marine record of great earthquakes (RI = ~240 years). Reconciling these differences reveals information regarding different sources of coseismic or interseismic deformation in the southern CSZ.

Given that many earlier investigations utilized bulk peat for 14C age determinations and that these early studies were largely reconnaissance work, these existing terrestrial data sets are compiled, evaluated, ranked, and excluded according to their paleoseismic relevance. We construct an OxCal age model to evaluate the discriminated 14C based space-time relations graphically and statistically.

Not all events are observed in each region and not all events have age control. Some regions (*e.g.* South Bay) lack cores representing the complete modern tidal elevation range (biasing the paleoseismic record). New cores in these regions may help find more evidence of paleoearthquakes. For example, when individual sites in the same region (South Bay and Hookton Slough) are combined, a more complete record of coseismic subsidence can be assumed, reducing the terrestrial RI to 360±40, yet still longer than the marine RI.

We find that modifying the earthquake and tsunami hazard probabilities for northern California could be considered. This justification may be further substantiated depending on evidence from future core sites in the South Bay, Arcata Bay, and Mad River Slough regions combined with new 14C age determinations from known strata that lack good age, elevation, and biogeochemical control in the Mad River Slough and the Eel River valley regions.

Cascadia Tremor and Its Megathrust Implications

WECH, A.G., University of Washington, Seattle, WA USA; CREAGER, K.C., University of Washington, Seattle, WA USA.

The Cascadia subduction zone, extending from northern California to Vancouver Island, experiences repeated episodes of tectonic tremor associated with slow slip. As a spatially constrainable mechanism for stable strain release, these episodic tremor and slip (ETS) events provide information about the inter-plate coupling as the fault transitions from fully locked to stable sliding with increasing depth. Because tremor's associated slow slip may transfer stress to the updip seismogenic portion of the plate interface, monitoring when, where, and how much slip is occurring may serve in forecasting the threat of a megathrust earthquake. Thus mapping and continuous tremor monitoring may be important for both inferring the downdip extent of the megathrust and identifying slow slip's megathrust triggering potential (eg. an anomolous increase in activity). Recent advances in location and detection methodology make it possible to perform a detailed search of tremor activity on both a larger spatial scale and a finer time scale. We use an automated approach to detect and locate tremor combining an envelope cross-correlation location technique with spatial clustering analysis to perform a systematic search for tremor. Applying this technique to 7 overlapping networks from northern California to mid-Vancouver Island on past and real-time data, we have created an automated system for margin-wide identification of both ETS and inter-ETS tremor activity starting from 2006. The resulting 55,000+ tremor epicenters have an average width of 53 ± 9 km and are generally bounded between the 30–45 km plate interface depth contours, with some deviation in the south. They also have a distinct updip edge whose boundary may represent a physical change in plate coupling that is 10's of km further inland than current estimates of the downdip edge of the seismogenic zone.

HAZUS Analyses of 15 Earthquake Scenarios in the State of Washington

TERRA, F.M., URS Corporation, Oakland/CA/USA, fabia_terra@urscorp.com; WONG, I.G., URS Corporation, Oakland/CA/USA, Ivan_Wong@urscorp.com; FRANKEL, A., US Geological Survey, Denver/CA/USA, afrankel@usgs.gov; BAUSCH, D., FEMA Region VIII, Denver/CO/USA, douglas.bausch@dhs.gov; BIASCO, T., FEMA Region X, Bothel/WA/USA, Tamra.Biasco@dhs.gov; SCHELLING, J.D., Washington State Emergency Manag, Camp Murray/WA/USA, j.schelling@emd.wa.gov

Near-real time ShakeMaps can provide emergency personnel information on the distribution of strong ground shaking to facilitate an informed and effective emergency response in the event of a catastrophic earthquake. The addition of estimates of potential impacts including injuries, search and rescue, shelter, and building inspection needs, and essential facility and lifeline functionality after a large earthquake, will allow emergency personnel to respond more appropriately to the areas that are in immediate need. Additionally, these tools will provide planners and responders with the tools necessary to develop scientifically-grounded mitigation and response strategies as well as exercise earthquake response plans. The objective of this project was to use scenario ground motion hazard maps produced in a USGS ShakeMap format to provide much more accurate input into FEMA's risk analysis software HAZUS-MH. The USGS developed 15 Washington scenario ShakeMaps, including for example, a **M** 7.4 earthquake on the Whidbey Island fault, **M** 7.1 on the Tacoma fault and a **M** 9.0 Cascadia subduction zone event. A comprehensive summary packet was developed for each scenario that includes a set of 13 multi-risk maps which were developed from each of the scenario earthquakes. Several improvements were made to the HAZUS runs including an improved inventory for essential facilities using data from the Washington State Emergency Management Division as well as the Homeland Security Infrastructure Program. Interim-census information provided by Environmental Systems Research Institute was used to update the demographic data in HAZUS to 2005. Comparison of results from runs using HAZUS MR3 and MR4 demonstrate the improvements to the building-stock and damage calculation modules in MR4. The risk analysis mapping and summary packets will be utilized by state, regional, and local authorities to better plan and respond to future earthquakes.

The National Science Foundation American Reinvestment and Recovery Act Cascadia Initiative

JACKSON, M., UNAVCO, Boulder, CO USA, jackson@unavco.org; WOODWARD, R., IRIS, Washington, DC USA, woodward@iris.edu; TOOMEY, D., Universty of Oregon, Eugene, OR USA, drt@uoregon.edu

The National Science Foundation (NSF), through the American Reinvestment and Recovery Act (ARRA), funded land- and ocean-based infrastructure initiatives that will provide an unprecedented amount of new data on the Cascadia region, that will lead to new discoveries and insights into episodic tremor and slip and the structure of the Juan de Fuca plate and Cascadia Subduction zone. Onshore the initiative includes funding for high-rate real-time GPS upgrades at 232 EarthScope Plate Boundary Observatory stations and the deployment of 27 new EarthScope USArray Transportable Array broadband seismometers along the Cascadia forearc and back-arc. The onshore initiatives are already underway with full upgrade/deployments anticipated by September 2010 and full operations for at least 3–5 years.

Offshore, the initiative is spurring the development of a 60 new ocean bottom seismometers that can be deployed in both shallow and deep water. Instruments are being developed by Lamont-Doherty Earth Observatory, Scripps Institution of Oceanography and the Woods Hole Oceanographic Institution and will become part of the U.S. National Ocean Bottom Seismograph Instrument Pool. Cascadia offshore deployments plans are still being developed, but will likely involve both a synoptic view and focused views of plate and trench activity. All the data from the onshore and offshore NSF ARRA Cascadia Initiative will be made freely available to interested investigators as quickly as possible and without artificial delay.

Our presentation will provide an update on this multi-disciplinary effort to study the Cascadia region of North America.

The 17 November, 2009 Haida Gwaii (Queen Charlotte Islands), British Columbia, Earthquake Sequence

CASSIDY, J.F., Geological Survey of Canada, Sidney, BC, Canada, jcassidy@nrcan.gc.ca; ROGERS, G.C., Geological Survey of Canada, Sidney, BC, Canada, grogers@nrcan.gc.ca; BRILLON, C., University of Victoria, Victoria, BC, Canada; KAO, H., Geological Survey of Canada, Sidney, BC, Canada; MULDER, T., Geological Survey of Canada, Sidney, BC, Canada; DRAGERT, H., Geological Survey of Canada, Sidney, BC, Canada; BIRD, A.L., Geological Survey of Canada, Sidney, BC, Canada; BENTKOWSKI, W., Geological Survey of Canada, Sidney, BC, Canada.

On November 17, 2009, a magnitude 6.5 earthquake struck off the southern tip of Haida Gwaii (Queen Charlotte Islands). This earthquake was felt across much of north-central British Columbia to distances of nearly 500 km. Due to its remote and offshore location, no damage was reported. This region is an active transform boundary just north of the Cascadia subduction zone where the Queen Charlotte Fault (QCF) separates the Pacific and North American plates off the outer coast of Haida Gwaii. This fault has experienced earthquakes as large as magnitude 8.1 in the past. However, the 2009 event did not occur on the QCF, but rather was located about 20–30 km to the west. The predominantly strike-slip focal mechanism that we determined does not align with the QCF or relative plate motion vectors in the area, but it is rotated about 30 degrees clockwise. The earthquake was followed by an unusually rich aftershock sequence. The largest aftershock, Mw 5.5, occurred seven minutes after the mainshock. Smaller aftershocks continued for nearly two months. Early aftershocks appeared to extend in an NE-SW direction, but after several weeks a NW-SE alignment of aftershocks also became apparent. Preliminary locations of the aftershocks indicate that the majority (assuming ruptures identical to the mainshock) fit the regions of enhanced Coulomb stress from the mainshock rupture. We apply refined location techniques to improve the relative locations of these events and to better understand their relationship to the tectonic structure of this complex region.

The Evolution of Slow Slip and Tremor in Time and Space

Poster Session · Thursday AM, 22 April · Exhibit Hall

Imaging Shallow Cascadia Structure with Ambient Noise Tomography

PORRITT, R.W., UC Berkeley, Berkeley, CA USA, rob@seismo.berkeley.edu; ALLEN, R.M., UC Berkeley, Berkeley, CA USA, rallen@berkeley.edu; SHAPIRO, N.M., IPG Paris, Paris France, nshapiro@ipgp.jussieu.fr; BOYARKO, D.C., Miami University of Ohio, Oxford, OH USA, boyarkdc@muohio.edu; BRUDZINSKI, M.R., Miami University of Ohio, Oxford, OH USA, brudzmr@muohio.edu; O'DRISCOLL, L., University of Oregon, Eugene, OR USA, lodrisco@uoregon.edu; ZHAI, Y., Rice University, Houston, TX USA; HUMPHREYS, E.D., University of Oregon, Eugene, OR USA, ghump@uoregon.edu; LEVANDER, A.R., Rice University, Houston, TX, alan@esci.rice.edu

Along strike variation has been observed throughout the Cascadia Subduction Zone in multiple studies with a variety of data sets. Body-wave tomography shows a broad zone in the center of the slab with a weak high velocity signal in an atypically quiescent seismic zone (Obrebski and Allen, 2009) . Characteristics of primitive basalts found in the arc volcanoes change along strike defining four distinct magma sources or plumbing systems (Schmidt et al, 2007). However, the most striking variation is in the recurrence rate of episodic tremor and slip throughout the region (Brudzinski and Allen, 2007). These separate observations reflect lithospheric variations on a regional scale.

This study connects previous observations by analyzing a surface wave model from ambient seismic noise cross-correlations with two Flexible Array deployments. Longer period bands than typically used in ANT are recovered via a manual waveform analysis returning robust group and phase velocity maps from 7–92 seconds. Thus structure is well resolved from the surface to approximately 100km in depth allowing for simultaneous interpretation of crust and uppermost mantle structure.

Significant variations are observed along strike in this model. The high velocity mafic Siletzia terrain is observed in the lower-mid crust along the Cascadia forearc. This mafic material coincides with the region of long term tremor recurrence interval (~20 months) from Brudinzki and Allen (2007). The southern border of the Siletzia terrain is marked by a clear velocity variation along the expected Gorda-Juan de Fuca plate boundary. In this southern region, the root of the Klamath mountain is clearly compressing the subducting Gorda plate where the tremor recurrence interval is only on the order of ~10 months. Finally, there is a striking low velocity feature under the Columbia river. This feature is also hinted at in body wave studies, but ANT better resolves this anomaly.

PBO Strainmeter Measurements of Cascadia Slow Slip and Tremor Events, 2005–2010

HODGKINSON, K., UNAVCO, Boulder, CO, USA, hodgkinson@unavco.org; MENCIN, D., UNAVCO, Boulder, CO, USA, mencin@unavco.org; HENDERSON, B., UNAVCO, Boulder, CO, USA, dhenders@unavco.org; BORSA, A., UNAVCO, Boulder, CO, USA, borsa@unavco.org; GALLAHER, W., UNAVCO, Boulder, CO, USA, warreng@unavco.org; GOTTLIEB, M., UNAVCO, Boulder, CO, USA, gottlieb@unavco.org; JOHNSON, W., UNAVCO, Boulder, CO, USA, johnson@unavco.org; VAN BOSKIRK, E., UNAVCO, Boulder, CO, USA, boskirk@unavco.org; JACKSON, M., UNAVCO, Boulder, CO, USA, jackson@unavco.org

The Plate Boundary Observatory, installed and maintained by UNAVCO for the Earthscope program, includes seventy-four borehole tensor strainmeters distributed in regional arrays along the North American - Pacific Plate Boundary. Thirty-nine of the strainmeters are installed between the California-Oregon boarder and central Vancouver Island, British Columbia. These instruments' ability to measure strain transients on the level of tens of nanostrain over periods of hours to days makes them ideal for recording the evolution of slow slip and tremor events. With the first strainmeter deployment taking place in June 2005, many of the Pacific Northwest strainmeters now have several years of near continuous areal and shear strain measurements. The strainmeter at Hoko Falls on the Olympic Peninsula, for example, recorded four Slow Slip and Tremor events between June 2005 and January 2010. Almost five years after the first strainmeter installation, not only are the PBO strainmeters providing a unique temporal image of the development of the strain transients of individual slow slip events, but they are recording data which can be used to compare the relative magnitude of the strain signals and time interval between events. In this presentation we present a catalogue of slow slip and tremor events as recorded by PBO strainmeters in the Pacific Northwest with estimates of their relative magnitudes and repeat intervals for strainmeters that have recorded multiple events.

Constraints on Aseismic Slip During and Between Northern Cascadia Episodic Tremor and Slip Events from Plate Boundary Observatory Borehole Strainmeters

ROELOFFS, E.A., U.S. Geological Survey, Vancouver, WA, evelynr@usgs.gov; MCCAUSLAND, W.A., U.S. Geological Survey, Vancouver, WA, wmccausland@usgs.gov

Plate Boundary Observatory (PBO) borehole strainmeters augment continuous GPS data to constrain features of Episodic Tremor and Slip (ETS) events in northern Cascadia. During ETS events in 2007, 2008, and 2009, shear strain transients were observed as tremor activity migrated past each strainmeter along the strike of the subducting oceanic plate. The propagation direction and sense of slip can be inferred from the two shear strain components of any individual strainmeter. For all of these events, the shear strain excursions and net offsets are consistent with models inferred from the GPS time series that specify thrust displacement 35–45 km deep along the plate boundary. Strain signals coincide in time with tremor activity within a 50-km horizontal radius. At strainmeter B018, directly above the inferred slip, abrupt onsets of strain signals coincide, to within 30–60 minutes, with initiation of tremor less than 50 km away, supporting the hypothesis that the tremor and strain originate from a single underlying process. At strainmeter B004 in northern Washington, 70 km up-dip of the modeled slip zone, the time histories of the 2007, 2008, and 2009 ETS events are all consistent with slip propagating northward at constant speed, although the 2007 event propagated faster and produced strains about half as large as those during the other two events. The PBO borehole strainmeters can detect smaller slip events than GPS at periods of a few weeks or less. Between the large, recurrent ETS events in northern Cascadia, at least four tremor bursts on northern Vancouver Island or in the south Puget Sound area were accompanied by a signal on one strainmeter. Surface displacements from these inter-ETS tremor bursts were not evident in GPS time series. Strain time series associated with two of these tremor bursts have the same time history for both shear components, implying they can be explained by increasing slip over a spatially fixed source.

Cascadia Slow slip Events Found in Water Level Changes at Tidal Stations

ALBA, S.K.M., University of Oregon, Eugene, OR, salba@uoregon.edu; WELDON II, R.J., University of Oregon, Eugene, OR, ray@uoregon.edu; LIVELYBROOKS, D., University of Oregon, Eugene, OR, dlivelyb@uoregon.edu; SCHMIDT, D.A., University of Oregon, Eugene, OR, das@uoregon.edu

By analyzing hourly water level records from NOAA tide gauges, we have determined relative uplift between Port Angeles, WA, and multiple neighboring sites associated with 10 slow slip events on the Cascadia subduction zone that occurred between 1997 and 2009. The Port Angeles record was compared individually to the other sites with a transfer function to remove correlated ocean and atmospheric "noise". The average relative displacement over all 10 events, as well as that associated with some of the larger individual events, agrees with displacements inferred from modeling GPS data. Because water level steps similar in size to slow quakes occur throughout the record we tested the average displacement or step size of 10 randomly selected 'event' periods. Analysis of 10,000 such steps showed <5% probability of obtaining the same displacement value as that proposed in the model. Examination of a stack of the 9 intervals between events shows a subsidence rate approximately equal in magnitude, suggesting vertical deformation follows a sawtooth pattern with strain accumulation between slow slip events followed by release of a similar amount of strain during the events themselves. This would be unlikely if the step is a product of chance. The shape of the step appears linear, suggesting that vertical deformation is smoothly continuous over the ~16 day period, this also agrees with the model. Autocorrelation of individual denoised records and cross-correlations between the Port Angeles record denoised using different sites show peaks of higher correlation at intervals corresponding to the average interval between events, further supporting their presence in the record. Successful denoising of Port Angeles with Seattle, which has a continous record of >100 years, will allow possible identification of previously unseen past slow slip events.

On the Temporal Evolution of an ETS Event along the Northern Cascadia Margin

DRAGERT, H., Geological Survey of Canada, Sidney, BC, Canada, hdragert@nrcan.gc.ca; WANG, K., Geological Survey of Canada, Sidney, BC, Canada, kwang@nrcan.gc.ca; KAO, H., Geological Survey of Canada, Sidney, BC, Canada, hkao@nrcan.gc.ca

Episodic Tremor and Slip (ETS) has now been observed along the northern Cascadia Margin for over 15 years. More recent densification of GPS coverage and the introduction of Gladwin borehole strainmeters (BSM) under the Plate Boundary Observatory have enabled the derivation of improved slip models and allowed more detailed monitoring of the evolution of the slip surface during prolonged ETS events. For this study, we examine in detail the along-strike migration of the May 2008 ETS as determined from the GPS and BSM observations. GPS sites overlying the 30 km depth contour of the subducting plate interface show the slip to initiate west of northern Puget Sound and then propagate bi-directionally to the northwest and the south at ~8km per day. Shear strain time series at regional BSM sites confirm this steady expansion of the slip zone. The tremors observed for this ETS episode show a similar migration pattern but also show temporal gaps in activity and possible changes in migration velocity. At present, the coarser daily sampling of the GPS positions and the sensitivity of strain measurements to non-tectonic signals prevent the geodetic confirmation of this detailed tremor behaviour which could be caused by structural or stress boundaries.

Tectonic Tremor Near the Calaveras Fault Triggered by Large Teleseisms

AGUIAR, A.C., Stanford University, Stanford, CA, USA, acaguiar@stanford.edu; BROWN, J.R., Stanford University, Stanford, CA, USA, jrbrown5@stanford.edu; BEROZA, G.C., Stanford University, Stanford, CA, USA, beroza@stanford.edu

Deep, tectonic tremor accompanies large, slow slip events in subduction zones, such as Cascadia and SW Japan. It can also be triggered by surface waves from distant large earthquakes. This type of triggered tremor has been identified in several areas of California, including an area centered on the Calaveras fault. In subduction zones, studies have shown that tremor is a superposition of many small low frequency earthquakes (LFEs). Ongoing tremor near Cholame has also been shown to be comprised of LFEs. Due to the strong similarities between triggered and spontaneous tremor, we hypothesize that triggered tremor is also a superposition of LFEs.

We test this hypothesis using data from the vicinity of the Calaveras fault because it is very well instrumented. We have analyzed data from ~25 stations around the Calaveras fault for the time periods of two Mw≥8 earthquakes. So far, these data show tremor triggered by the 2002 Denali (Mw=7.9) and 2009 Samoa (Mw=8.0) earthquakes. We use a matched filter method that autocorrelates waveforms of each station across the network and have found more than a dozen signals that repeat during a period of 500 s for each event. This strongly suggests that triggered tremor is comprised of LFEs. We locate the LFEs on the downward extension of the Calaveras fault using HypoDD. Depths appear to be shallower than the 22–25 km depth found for tremor near Cholame, but deeper than background seismicity. LFE detections of the Denali event match detections of the Samoa event, which suggests that the source region of tremor is persistent over time. Identifying LFEs within triggered tremor should allow us to develop greatly improved locations, which in turn should greatly increase our understanding of this phenomenon. It will also allow us to search for tremor, or isolated low frequency earthquakes occurring at other times.

Tidal Triggering of LFEs near Parkfield, CA

THOMAS, A.T., UC-Berkeley, Berkeley,CA,USA, amthomas@berkeley.edu; BURGMANN, R.B., UC-Berkeley, Berkeley,CA,USA, burgmann@seismo.berkeley.edu; SHELLY, D.R., USGS, Menlo Park, CA, USA, dshelly@usgs.gov

Studies of nonvolcanic tremor (NVT) in Japan, Cascadia, and Parkfield, CA have established the significant impact small stress perturbations, such as the solid earth and ocean tides, have on NVT generation. Similar results irrespective of tectonic environment suggest that extremely high pore fluid pressures are required to produce NVT. Here we analyze the influence of the solid earth and ocean tides on a catalog of ~500,000 low frequency earthquakes (LFE) distributed along a 150km section of the San Andreas Fault centered at Parkfield [Shelly *et al.* this meeting]. LFEs comprising the tremor signal are grouped into "families" based on waveform similarity and precisely located using waveform cross-correlation. Analogous to repeating earthquakes, LFE families are thought to represent deformation on the same patch of fault. While the locations of repeating earthquakes are assumed to be coincident with the location of asperities in the fault zone, NVT occur below the seismogenic zone, where fault zones behave ductilely. Here we explore the sensitivity of each of these LFE families to the tidally induced shear and normal stresses on the SAF. Preliminary results show spatially smooth variations in both shear and normal stress sensitivity that could potentially be explained by along-fault variations in pore pressure. Assuming that the individual families are fault patches on which the pore pressures are locally high (*i.e.* near-lithostatic), we quantify the effective normal stress at each LFE location using rate and state friction and LFE rate differences during times when the tides are promoting (or retarding) failure. In addition to mapping pore pressures in the deep fault zone, we further explore spatiotemporal variations in triggering behavior to determine how static stress changes influence modulation, if propagating slip pulses also experience tidal triggering, and if families with quasi-periodic recurrence behaviors are more or less sensitive to tidal effects.

Investigating Low Frequency Impulsive Events at Slumgullion Landslide

MACQUEEN, P., University of Oregon, Eugene, Oregon, pmacquee@uoregon.edu; GOMBERG, J., USGS, Seattle, Washington, gomberg@usgs.gov; SCHULZ, W., USGS, Golden, Colorado, wschulz@usgs.gov; BODIN, P., University of Washington, Seattle, Washington, bodin@u.washington.edu; FOSTER, K., UC San Diego, San Diego, California, ktafoster@gmail.com; KEAN, J., USGS, Golden, Colorado, jwkean@usgs.gov; CREAGER, K., University of Washington, Seattle, Washington, kcc@ess.washington.edu

Understanding tremor will provide important constraints on the mechanics of fault slip and will improve hazard assessments. Low frequency earthquakes (LFEs) are often identified during tremor episodes and may be a key to understanding what generates tremor. The Slumgullion Landslide in the San Juan Mountains of southwest Colorado has been shown to behave similarly to fault systems that exhibit slow slip phenomena such as transient aseismic slip, LFEs, and tremor, and thus potentially provides a natural smaller scale analog model for understanding these phenomena.

In this study we deployed an array of 88 Texan seismic recorders at Slumgullion landslide from August 19–27, 2009. In addition to "slide quakes" and tremor-like signals, we also observed impulsive low frequency events seismically similar to LFEs. Preliminary analysis has shown high rates of correlation between these events, indicating that they came from the same source region and type, as well as interesting temporal clustering. This temporal clustering tends to occur in pairs with a separation of approximately 10 seconds. This is a work in progress, and further analysis should shed more light on how these landslide low frequency events relate to their plate-scale cousins.

The Seismic Story of the Nile Valley Landslide - Foreshocks, Mainshocks, and Aftershocks

ALLSTADT, K., University of Washington, Seattle, WA USA, allstadt@uw.edu; VIDALE, J., University of Washington, Seattle, WA USA, vidale@ess.washington.edu; THELEN, W., University of Washington, Seattle, WA USA, wethelen@ess.washington.edu; SARIKHAN, I., WA Dept of Natural Resources, Olympia, WA USA, isabelle.sarikhan@dnr.wa.gov; BODIN, P., University of Washington, Seattle, WA USA, bodin@uw.edu

The Nile Valley landslide of October 11th, 2010, was one of the largest in recent Washington state history. This translational slide involved a volume on the order of 10^7 cubic meters and destroyed 2 houses, a portion of highway, and partially dammed a stream causing flooding. People in the area reported noises and deformation 2 days beforehand and evacuated safely. The main sliding sequence occurred over about 6 hours and portions of it were captured by two regional seismic stations 12 and 29 km away. Distinct pops began to appear about 3 hours before a partial slope failure generated a continuous 2-minute signal with an emergent onset. After this, the pops became more frequent and evolved into the largest sliding event. This appeared as a 13-minute broadband rumble centered on 4.5Hz with an emergent onset and spindle shape. Diminishing rumbling followed for another hour.

After the landslide occurred, we installed 12 vertical geophones and 4 three-component seismic stations around the perimeter. More than 60 small events were recorded at these stations in the days after the slide and are likely due to settling and continued deformation. One particularly large movement 9 days after the main event generated a signal that also appeared on the more distant regional stations. This event had a similar shape to the main event but lasted only 15 seconds with about 25% of the amplitude. Smaller events recorded on the seismic stations at the site showed a buildup in amplitude hours before this event.

This case adds to the body of knowledge on the seismic manifestation of landslides and gives more clues as to what happens before, during, and after a landslide of this type. In addition, our observations indicate that landslides may show precursory patterns that seismic monitoring can detect, potentially saving lives.

Monitoring for Nuclear Explosions

Poster Session · Thursday AM, 22 April · Exhibit Hall

Recent Fundamental Advances in Seismic Monitoring

WILLEMANN, R.J., IRIS Consortium, Washgington, DC, ray@iris.edu

Despite continuing advances in seismological monitoring, some people to doubt that a test ban is verifiable. To contribute to good use of their science by policy makers, seismologists could write publicly about changes that go beyond incremental improvements. There are at least three distinct areas that might be described in terms that non-seismologists could readily grasp.

First, high-capability sensors have been deployed around the world. Even modestly funded researchers sometimes deploy dozens of broadband stations that operate reliably in remote sites, far from technical support and in harsh conditions. Challenges are met with carefully selected commercial systems and modest adaptations. The only continental regions that still cannot be well-monitored are where low income and low hazard limit investment.

Second, seismology has embraced use of scattered energy. Waves radiated in many directions from a source but scattered and recorded by a single seismometer are used to evaluate source properties more reliably. Near-source scattering creates makes it possible now to identify repeating earthquakes and to reliably sort explosions from different mines. Information from scattered waves contributes better earth models.

Finally, computational capabilities are near to fulfilling the long-sought goal of simulating high frequency waveforms. Various numerical methods have been tested and work well together to simulate generation of high frequency waves and propagation for thousands of miles. The best resolution at the furthest distances requires modeling the earth at a finer scale, but U.S. national laboratories already have the required computers and soon so will many universities.

Towards Continental Scale Regional Phase Amplitude Tomography

PHILLIPS, W.S., Los Alamos National Laboratory, Los Alamos NM, wsp@lanl.gov; YANG, X., Los Alamos National Laboratory, Los Alamos, NM, xyang@lanl.gov; STEAD, R.J., Los Alamos National Laboratory, Los Alamos, NM, stead@lanl.gov

Amplitude tomography provides attenuation maps of regional phases in short period bands, and is important for magnitude estimation and event identification monitoring efforts. Station distribution is typically sparse in Asia, and areas of concentration tend to be spatially and temporally limited. High quality data have

been accumulating for some time, however, and we are now beginning to reach the level of coverage needed to study large areas. Using amplitude data from permanent and temporary deployments, we invert for attenuation across central, southern and eastern Asia. Data must be limited by identifying distances over which source corrected amplitudes follow simple 1-D models, thus avoiding measurements of coda of previous phases. We combine data from different channels at each station after correcting for relative site effects. Data are inverted to obtain 2-D attenuation in each band, or 1-Hz attenuation and frequency power law coefficients, frequency dependent site terms, and frequency dependent source terms or source parameters moment and corner frequency. Lg amplitudes are best fit, followed by Sn and Pg. Pn amplitudes are poorly modeled using standard spreading coefficients, perhaps due to focusing or focal mechanism effects. We observe little fit degradation when using the more restrictive power law Q model. Solving for source parameters degrades fits somewhat, but remains acceptable. We also test the use of geophysical province polygons to model frequency dependent attenuation, using a double difference, L1 direct search method. Such models can be used for quality control, and as background models for future efforts.

Station Set Residual: Event Classification Using Historical Distribution of Observing Stations

PROCOPIO, M.J., Sandia National Laboratories, Albuquerque, NM, mjproco@sandia.gov; LEWIS, J.E., Sandia National Laboratories, Albuquerque, NM, lewisje@sandia.gov; YOUNG, C.J., Sandia National Laboratories, Albuquerque, NM, cjyoung@sandia.gov

Analysts working at the International Data Centre in support of treaty monitoring through the Comprehensive Nuclear-Test-Ban Treaty Organization spend a significant amount of time reviewing hypothesized seismic events produced by an automatic processing system. When reviewing these events to determine their legitimacy, analysts take a variety of approaches that rely heavily on training and past experience.

One method used by analysts to gauge the validity of an event involves examining the set of stations involved in the detection of an event. In particular, leveraging past experience, an analyst can say that an event located in a certain part of the world is expected to be detected by Stations A, B, and C. Implicit in this statement is that such an event would usually not be detected by Stations X, Y, or Z. For some well understood parts of the world, the absence of one or more "expected" stations—or the presence of one or more "unexpected" stations—is correlated with a hypothesized event's legitimacy and to its survival to the event bulletin.

The primary objective of this research is to formalize and quantify the difference between the observed set of stations detecting some hypothesized event, versus the expected set of stations historically associated with detecting similar nearby events close in magnitude. This Station Set Residual can be quantified in many ways, some of which are correlated with the analysts' determination of whether or not the event is valid. We propose that this Station Set Residual score can be used to screen out certain classes of "false" events produced by automatic processing with a high degree of confidence, reducing the analyst burden. Moreover, we propose that the visualization of the historically expected distribution of detecting stations can be immediately useful as an analyst aid during their review process.

IMS Seismic Stations Instrumentation Challenges

STAROVOIT, Y.O., CTBTO, IMS, Vienna, Austria, yuri.starovoit@ctbto.org; GRENARD, P., CTBTO, IMS, Vienna, Austria, patrick.grenard@ctbto.org

The IMS seismic network is a set of monitoring facilities where the primary network has worldwide distributed 50 stations and the auxiliary seismic network consists of 120 stations. Besides the difference in the mode of data transmission to the IDC the technical specifications for seismographic equipment to be installed at both primary and auxiliary stations are essentially the same.

In context of technical specifications for IMS seismic stations it was stressed that verification seismology is concerned with searching of reliable methods of signal detections at high frequencies. In the meantime MS/Mb screening criteria between earthquakes and explosions relies on reliable detection of surface waves.

The IMS requirements for instrumental noise and operational range of data acquisition system are defined as certain dB level below minimum seismic noise within the required frequency band from 0.02 to 16Hz. The type of sensors response is requested to be flat either in velocity or acceleration. The compliance with IMS specifications may therefore introduce a challenging task when low-noise conditions have been recorded at the site. It means that as a station noise power spectrum approaches the NLNM it may require a high sensitive sensor connected to a quiet digitizer which may cause a quick system clip and waste of the available dynamic range.

The experience has shown that hybrid frequency response of seismic sensors where combination of flat in velocity and flat in acceleration portions of the sensor frequency response may provide an optimal solution for utilization of available dynamic range and low digitizer noise floor.

In addition to the above IMS stations need to meet specific requirements such as data authentication, central facility data buffering, precise relative timing accuracy between data samples coming from array elements as well as more than 97% of data with less than 5 min delay in transmission to IDC.

ISC Contribution to Monitoring Research

STORCHAK, D.A., ISC, Thatcham, U.K., dmitry@isc.ac.uk; BONDÁR, I., ISC, Thatcham, U.K., istvan@isc.ac.uk; HARRIS, J., ISC, Thatcham, U.K.; GASPÀ, O., ISC, Thatcham, U.K., oriol@isc.ac.uk

The International Seismological Centre (ISC) is a non-governmental organization charged with production of the ISC Bulletin—the definitive global summary of seismicity based on reports from over 4.5 thousand seismic stations worldwide.

The ISC data have been extensively used in preparation of the Comprehensive Test Ban Treaty (CTBT). They are now used by the CTBTO Preparatory Technical Secretariat (PTS) and the State Parties as an important benchmark for assessing and monitoring detection capabilities of the International Monitoring System (IMS). The ISC also provides a valuable collection of reviewed waveform readings at academic and operational sites co-located with the IMS stations.

To improve the timeliness of its Bulletin, the ISC is making a special effort in collecting preliminary bulletins from a growing number of networks worldwide that become available soon after seismic events occur. Preliminary bulletins are later substituted with the final analysis data once these become available to the ISC from each network.

The ISC also collects and maintains data sets that are useful for monitoring research. These are the IASPEI Reference Event List of globally distributed GT0-5 events, the groomed ISC bulletin (EHB), the IDC REB, USArray phase picking data. In cooperation with the World Data Center for Seismology, Denver (USGS), the ISC also maintains the International Seismographic Station Registry that holds parameters of seismic stations used in the international data exchange.

The UK Foreign and Commonwealth Office along with partners from several Nordic countries are currently funding a project to make the ISC database securely linked with the computer facilities at PTS and National Data Centres. The ISC Bulletin data will soon be made available via a dedicated software link designed to offer the ISC data in a way convenient to monitoring community.

Comprehensive Nuclear Test Ban Treaty (CTBT) Monitoring in the Context of the National Data Centre Preparedness Exercise (NPE)

COYNE, J., CTBTO, Vienna, Austria, john.coyne@ctbto.org; KITOV, I., CTBTO, Vienna, Austria, ivan.kitov@ctbto.org; KRYSTA, M., CTBTO, Vienna, Austria, monika.krysta@ctbto.org; BECKER, A., CTBTO, Vienna, Austria, andreas.becker@ctbto.org; BRACHET, N., CTBTO, Vienna, Austria, nicolas.brachet@ctbto.org; MIALLE, P., CTBTO, Vienna, Austria, pierrick.mialle@ctbto.org

The Comprehensive Nuclear Test Ban Treaty Organization (CTBTO) is tasked with monitoring compliance with the CTBT. In order to fulfill this mission, the CTBTO is building the International Monitoring System (IMS), which consists of 337 seismic, hydroacoustic, infrasound, and radionuclide monitoring facilities. Data from the IMS are collected, processed and reviewed by the International Data Centre (IDC). The analysis results are available to State Signatories of the CTBTO. Each State Signatory may designate a National Data Centre (NDC) authorized to receive IMS data and IDC products. Under the CTBT it is the responsibility of the States to determine the origin of events, and consequently NDCs are essential to the verification regime.

To prepare for their role, the NDCs organize and conduct annual NPEs, which are an opportunity for NDCs to collaborate to assess the quality of the IMS data and IDC products and to gain a better understanding of how these products may fulfill verification needs. An NPE is initiated with an event selected from the IDC automatic event bulletins by a nominated NPE coordinator, based on criteria established by NDC participants. The event is submitted to NDCs for in-depth investigation when they may use in it their own tools and techniques, in addition to software provided by the IDC. Each NDC scrutinizes IMS data and IDC products, and may include in its review additional data, *e.g.* local or regional bulletins, radionuclide reports, ATM models.

The NPE 2009 event addressed in this presentation includes both seismic and infrasound observations. Fictitious radionuclide detections are simulated from a hypothetical release of radioactivity at the event location. Feeding the backward atmopsheric transport modeling, they allow differentiating between the events which could have and could not have been at origin of these detections.

Crust and Upper Mantle Tomography using Pn, Pg, Sn, and Lg Phases for Improved Regional Seismic Travel Time Prediction

MYERS, S.C., Lawrence Livermore National Lab, Livermore, CA 94551, smyers@llnl.gov; BEGNAUD, M.L., Los Alamos National Laboratory, Los Alamos, NM 87545, mbegnaud@lanl.gov; BALLARD, S., Sandia National Laboratories, Albuquerque, NM 87185, sballar@sandia.gov; PASYANOS, M.E., Lawrence Livermore National Lab, Livermore, CA 94551, pasyanos1@llnl.gov; PHILLIPS, W.S., Los Alamos National Laboratory, Los Alamos, NM 87545, wsp@lanl.gov; RAMIREZ, A.L., Lawrence Livermore National Lab, Livermore, CA 94551, ramirez3@llnl.gov; ANTOLIK, M.S., Quantum Technology Sciences, Inc, Cocoa Beach, FL 32930, mantolik@aftac.gov; HUTCHENSON, K.D., Quantum Technology Sciences, Inc, Cocoa Beach, FL 32930, khutchenson@qtsi.com; DWYER, J.J., Air Force Technical Applications Center, Patrick Air Force Base, FL 32925, jdwyer@aftac.gov; ROWE, C.A., Los Alamos National Laboratory, Los Alamos, NM 87545, char@lanl.gov; WAGNER, G.S., Air Force Technical Applications Center, Patrick Air Force Base, FL 32925, gwagner@aftac.gov

The need to monitor at lower event magnitude necessitates the use of regional data, including secondary phases, in seismic locations. We have developed a regional seismic travel time (RSTT) model that includes a 3-dimensional crust and an upper mantle that is characterized by laterally varying velocity and linear gradient with depth. RSTT is built on a global tessellation of nodes with node spacing of ~1°. In previous work, we conducted tomography using Pn data throughout Eurasia. The resulting model reduced median Pn-based epicenter error from ~17 km for the ak135 model down to ~9 km for RSTT. In order to further the utility of the RSTT model, we use Pg, Sn, and Lg tomography to improve travel time predictions for secondary phases. The Pg, Sn, and Lg data have ~41,000, ~107,000, and ~25,000 arrival time measurements, respectively. The secondary-phase data sets provide good coverage across Eurasia, with node hit count in the thousands throughout the Tethys collision belt. Data coverage diminishes to tens of hits in the aseismic portions of northern Eurasia, and some small regions are not sampled for the Pg and Lg data sets. Using a validation data set, we find that travel time prediction error for secondary phases at near-regional distance (~5°) is reduced from ~4 to ~5 seconds for the ak135 model to ~ 3 seconds for the RSTT model. At far-regional distance (~10°) travel time prediction error is reduced from ~7 to ~10 seconds to ~3 to ~4 seconds. We also conducted location tests using events that are known to within 1 km or to within 5 km. The results are promising, showing reduction of epicenter error from ~30 km to ~15 km for the Sn phase, a 50% reduction in error. Location improvement for Pg and Lg is approximately 20%. Prepared by LLNL under Contract DE-AC52-07NA27344, LLNL-ABS-422303.

A New Approach for Improved Epicenter Location of Regional Earthquakes Using a Sparse Remote Network

SONG, F., Massachusetts Institute of Tech., Cambridge, MA, fxsong@mit.edu; FEHLER, M.C., Massachusetts Institute of Tech., Cambridge, MA, fehler@mit.edu; TOKSÖZ, M.N., Massachusetts Institute of Tech., Cambridge, MA, toksoz@mit.edu; LEE, W., Korea Polar Research Institute, Incheon, Korea, wonsang@kopri.re.kr

Conventional earthquake epicenter location requires a good azimuthal distribution of stations, which may not be available in practice. One example where station distribution limits azimuthal coverage is a network located on an island arc where seismicity often occurs at distance from the network. Limited azimuthal coverage results in large epicenter errors for conventional travel-time based approaches. One possible solution for such situations is to use the beamforming technique which exploits inter-station waveform similarity to estimate the back-azimuth and uses S-P time to constrain the epicentral distance. Unfortunately in many places only a sparse array of stations is available. This hampers traditional waveform beamformers due to severe spatial aliasing.

In this study, we introduce an incoherent beamformer. It applies to the low-frequency phase detection data, and therefore avoids the aliasing. The method begins with regional phase detection via multi-taper spectral analysis. The obtained spectrogram is transformed to enhance phase arrival identification. The transformed spectrogram is then beamformed to obtain the event back-azimuth. The phase arrival times, determined from the beamed trace, are used to estimate epicentral distance given their travel-time models. Finally the epicenter is derived from the epicentral distance and the back-azimuth estimates. The uncertainty range of the location is also estimated. This method is validated using the Anza network and a regional earthquake dataset in California. The located epicenters compare well with high-quality catalog epicenters that were determined from a conventional travel-time inversion method with full-azimuth station coverage. The applicability of this method is further demonstrated using data from a sparse regional network in Korea.

Toward an Empirically-based Parametric Explosion Spectral Model

FORD, S.R., Lawrence Livermore Nat'l Lab, Livermore/CA/USA, sean@llnl.gov; WALTER, W.R., Lawrence Livermore Nat'l Lab, Livermore/CA/USA, bwalter@llnl.gov

Small underground nuclear explosions need to be confidently detected, identified, and characterized in regions of the world where they have never occurred. We are developing a parametric model of the nuclear explosion seismic source spectrum derived from regional phases (Pn, Pg, Sn, and Lg) that is compatible with earthquake-based geometrical spreading and attenuation. Earthquake spectra are fit with a generalized version of the Brune spectrum, which is a three-parameter model that describes the long-period level, corner-frequency, and spectral slope at high-frequencies. These parameters are then correlated with near-source geology and containment conditions. Initial results show a correlation of high gas-porosity (low strength) with increased spectral slope. However, there are trade-offs between the slope and corner-frequency, which we try to independently constrain using Mueller-Murphy relations and coda-ratio techniques. The relationship between the parametric equations and the geologic and containment conditions will assist in our physical understanding of the nuclear explosion source.

Modeling Rg from the HUMBLE REDWOOD II Experiment: A Blind Test for Yield and Depth of Burial Estimation

BONNER, J.L., Weston Geophysical Corp., Lexington, MA, bonner@westongeophysical.com; REINKE, R., DTRA/CXTTP, Kirtland AFB, NM, robert.reinke@abq.dtra.mil; LENOX, E., DTRA/CXTTP, Kirtland AFB, NM, elizabeth.lenox@ABQ.DTRA.MIL; FOXALL, B., Lawrence Livermore National Lab, Livermore, CA, bfoxall@llnl.gov; MAYEDA, K., Weston Geophysical Corp., Lexington, MA, kmayeda@yahoo.com

We examine the feasibility of using short-period surface waves (*e.g.*, Rg) to estimate the yields and depths of burial (DOB) of small chemical explosions recorded at local distances. Rg and other primary and scattered waves were recorded from a series of six chemical explosions detonated at different DOB as part of the HUMBLE REDWOOD II experiment at Kirtland Air Force Base in Albuquerque, NM. The yields and DOB were not reported to researchers in order to evaluate which seismic and/or acoustic techniques provide the best estimates for these parameters. Our seismic technique includes 1) development of a velocity model using inversion of Rg group velocity dispersion data, 2) estimation of an apparent attenuation model, 3) propagation of synthetics with isotropic moments through these models to determine the best fit to the observed Rg spectral amplitudes, and 4) estimation of a range of DOB and yields that fit these moments using the Denny and Johnson (1991) explosion source model and near-source material properties. Preliminary results from a station at 0.65 km from the explosions suggest a range of yields from 50 to 1500 lbs at DOB from 1 to 20 meters. These results represent a lower bound on the yields, and our next step will involve the estimation of depth-dependent decoupling factors to account for the venting and cratering phenomenology that accompanied several of these shots. Finally, we will incorporate additional stations that recorded the explosions into the Rg analysis. The final results from the Rg modeling and other techniques (*e.g.*, coda methodology, P-wave modeling, and non-seismic techniques such as acoustic methods) will then be compared to the actual yields and DOB by the experiment organizers.

Analysis of Repeated Explosions at Degelen Mountain in the Semipalatinsk Test Site, Kazakhstan

STROUJKOVA, A., Weston Geophysical Corp., Lexington, MA, USA, ana@westongeophysical.com; BONNER, J.L., Weston Geophysical Corp., Lexington, MA, USA, jes_bonner@yahoo.com

A number of nuclear explosions were conducted by the former Soviet Union in tunnels used repeatedly at the Degelen Mountain Testing Area in Kazakhstan. Over 50 tunnels were used two or more times. The secondary explosions (henceforth called "repeat shots") conducted in these tunnels were placed close to the damaged zones left by the previous explosions. While this practice reduced the costs of tunnel excavation in granites, it yielded a unique dataset for comparative study of seismic wave excitation in intact and damaged rocks.

We have analyzed the seismic data from the "repeat shots" recorded at the station Borovoye. Based on the limited yield information available from open sources, scientists in the former Soviet Union previously determined that the seismic amplitudes of the "repeat shots" can be significantly reduced in comparison with the first explosion. For a small number of events with reported yields we calculated spectral amplitude reduction ratios. Despite the amplitude differences between the explosions conducted in the same tunnel, their waveforms show good correlation.

Several chemical explosions with known yields conducted at Degelen confirmed the amplitude reduction in the second explosion (*e.g.*, Omega-2 and Omega-3). Analysis of the seismic data revealed that the P waveforms exhibit good correlation between events, while their S waveforms are uncorrelated. In addition, the P/S amplitude ratio for Omega-3 event computed at frequencies below 2 Hz is approximately twice as high as the ratio for Omega-2, and slightly lower above 4 Hz. These observations suggest different shear wave generating mechanisms for the two events and require additional research to quantify the differences.

Exploring the Limits of Waveform Correlation Event Detection as applied to Three Earthquake Aftershock Sequences

CARR, D.B., Sandia National Laboratories, Albuquerque, NM, USA, dbcarr@sandia.gov; RESOR, M.E., Sandia National Laboratories, Albuquerque, NM, USA, meresor@sandia.gov; YOUNG, C.J., Sandia National Laboratories, Albuquerque, NM, USA, cjyoung@sandia.gov

For nuclear explosion seismic monitoring, major aftershock sequences can be a significant problem, because each event must be treated as a possible nuclear test. Fortunately, the high degree of waveform similarity expected within aftershock sequences offers a way to more quickly and robustly process these events than is possible using traditional methods (*e.g.* STA/LTA detection).

We explore how waveform correlation can be incorporated into an automated event detection system to improve both the timeliness and the quality of the resultant bulletin. To comprehensively characterize the potential benefits and limits of waveform correlation techniques, we studied 3 aftershock sequences in different geographic areas and with different fault geometries: Northridge (1994), Pakistan (2005), and Wenchuan (2008). In each case, we first assessed the level of correlation for events in either the EDR or IDC catalogs using aggregative hierarchical cluster analysis (dendrograms) based on waveform correlation. We then processed the sequence using our own waveform correlation-based event detection system, which compares incoming waveform data to a continuously updating library of known events. Incoming waveform data that correlates above a specified threshold with a library event is marked as a repeating event. We chose thresholds to achieve a reasonable false alarm rate, and re-processed with other thresholds to explore the differences. For each sequence, we processed data at two stations to assess the dependence on path.

We analyzed 4 days of data from each aftershock sequence. The percentage of known events found to be a member of a cluster ranged from 22-60. In addition, we identified significant numbers of new events that were not in the EDR or IDC catalog without any false alarms, showing a potential to lower the detection threshold without increasing analyst workload.

Automatic Hydroacoustic Phase Identification using a Two-Stage Neural Net

SALZBERG, D., SAIC, Arlington, VA, USA, david.h.salzberg@saic.com; DYSART, P., SAIC, Arlington, VA, USA, dysartp@saic.com; LOCKWOOD, M., SAIC, Arlington, VA, USA, lockwoodm@saic.com

We demonstrate a Neural-Net based process to identify in-water explosions using hydroacoustic sensors. Signals are classified as H-phase from an in-water explosion), T-phase (from an earthquake) or N-phase (noise). The classification must be based on parameters derived from the signals. These "hydro features" quantify the energy, spectral and cepstral properties of the recorded signals.

The neural net classification is a two-stage approach: the first stage separates T vs. not T, and the second stage separates H (explosion) from N (noise). The parameters for the two stages are determined by processing a training data set: that is a data set of "known signals", and a recall set: another independent set of "known" signals. These are used to estimate the parameters of the neural nets. The developed toolkit allows us to determine the optimal parameter set by either using an arbitrary number of parameters, or preferably, by applying a threshold to the normalized distance (Mahalanobis distance) and similarities between the parameters (Covariance threshold). Since optimal values of the two thresholds are unknown, a grid search is employed to determine the optimal threshold values: that is the number of parameters that provide the optimal performance when trained on the training set, and validated on the recall set.

Analyzing the results, we are able to isolate the features that are important to the classification. In some cases, these met our *a priori* expectations: the presence of energy at higher frequencies indicates H/N rather than T, and a broad-band cepstrum indicates H rather than N. In other cases, we were surprised: the number of crossings of threshold values compared to duration was as important as the cepstrum. Analysis indicates that those were useful in separating airguns (Noise) from Explosions (H).

With these parameters, we were able to identify 98% of the H-phases in the training dataset, while missing less than 1%.

Routine Infrasound Event Detection and Location at the IDC

BRACHET, N., CTBTO, Vienna/Austria, Nicolas.Brachet@CTBTO.ORG; MIALLE, P., CTBTO, Vienna/Austria, Pierrick.Maille@CTBTO.ORG; BITTNER, P., CTBTO, Vienna/Austria, Paulina.Bittner@CTBTO.ORG; GIVEN, J., CTBTO, Vienna/Austria, Jeffrey.Given@CTBTO.ORG

In early 2010, the International Data Centre (IDC) of the CTBTO began routine automatic processing of infrasound data reviewed by interactive analysis. Since then, the detected and located events are systematically included in the Reviewed Event Bulletin (REB) available to State Signatories to the CTBT.

Each infrasound array is processed separately for signal detection. Signals are detected using a progressive multi-channel correlation method (PMCC). For each detection, signal features—onset time, amplitude, frequency, duration, azimuth, speed, and F-statistics—are measured and used to identify detections as infrasonic, seismic, or spurious. Infrasonic signals along with seismic and hydroacoustic signals are subsequently associated between stations to locate events. During association, care is taken to ensure that infrasound processing does not degrade the performance of seismic event detection.

The IDC has developed specific analysis and visualization tools for infrasound review in conjunction with seismic and hydroacoustic data. An important aide for training analysts has been the constitution of a reference database of infrasound events observed on the IMS network, which reflects its global detection capability and captures the spatial and temporal variability of the observed phenomena.

Infrasound events have been added to the REB since 2007 based on preliminary results from the development of offline automatic processes. Detection and association criteria have been implemented to reduce the false-alarm rates in the automatic processing down to a manageable level for interactive analyst review. Additional work remains to improve identification of valid signals and decrease formation of false events.

Theoretical and Experimental Developments in Ground to Ground Infrasound Propagation

WAXLER, R., University of Mississippi, Oxford, MS, USA, rwax@olemiss.edu; TALMADGE, C.L., University of Mississippi, Oxford, MS, USA, clt@olemiss.edu; DROB, D., NRL, Washington DC, douglas.drob@nrl.navy.mil; CHUNCHUZOV, I., University of Mississippi, Oxford, MS, USA, igor.chunchuzov@gmail.com; HETZER, C., University of Mississippi, Oxford, MS, USA, claus@olemiss.edu; ASSINK, J., University of Mississippi, Oxford, MS, USA, jdassink@olemiss.edu; BLOM, P., University of Mississippi, Oxford, MS, USA, psblom@olemiss.edu; DI, X., University of Mississippi, Oxford, MS, USA, xiaodi@olemiss.edu

The propagation of infrasonic signals from large explosions depends critically on the refraction of sound by winds in the troposphere, stratosphere and thermosphere. Direct measurements of the winds in the upper atmosphere are quite difficult, so that to model infrasound propagation one relies on interpolations of coarsely resolved data fused with quasi-empirical models. While propagation models based on such atmospheric specifications provide a qualitative picture of the propagated field, they fail to correctly predict the observed phases, except in special cases. In this presentation, the theory of infrasound propagation will be reviewed and compared with recent experiments. Theoretical and experimental approaches to developing improved atmospheric models will be presented.

What InSAR Can Tell Us About Underground Nuclear Explosions: A Decade of Experience

VINCENT, P., Oregon State University, Corvallis, Oregon USA, pvincent@coas.oregonstate.edu; BUCKLEY, S.M., University of Texas at Austin, Austin, Texas USA, sean.buckley@mail.utexas.edu

Beginning in late 1999 when InSAR was first used to discover subsidence signals associated with past underground nuclear tests at the Nevada Test Site, to more recent characterization of uplift discovered at China's underground nuclear test site at Lop Nor, InSAR was the first remote-sensing tool to directly measure subtle subsidence (and uplift) signals associated with underground nuclear tests. A multitude of mechanical, hydrologic, and thermal test-related phenomena have been revealed through applying standard and advanced InSAR processing techniques. Although the bulk of information has been derived from observing post-test phenomena, some dynamic information relating to local ambient stress direction, explosive energy partitioning and coupling have been derived from coseismic test signals. A synopsis of results, analysis, and implications will be presented as well a discussion of limitations of the technique as a monitoring tool. Finally, a where we go from here perspective will be presented, including the recent advantages afforded by new SAR satellite missions.

Recent Advances in Source Parameters and Earthquake Magnitude Estimations

Poster Session · Thursday AM, 22 April · Exhibit Hall

Moment Magnitudes in the Middle East from Regional Coda Wave Envelopes

GOK, R., Lawrence Livermore National Lab., Livermore, CA, gok1@llnl.gov; MAYEDA, K., Weston Geophysical, ; PASYANOS, M.E., Lawrence Livermore National Lab., Livermore, CA; MATZEL, E., Lawrence Livermore National Lab., Livermore, CA; RODGERS, A.J., Lawrence Livermore National Lab., Livermore, CA; WALTER, W.R., Lawrence Livermore National Lab., Livermore, CA.

Moment magnitude calculation for small to moderate size events in the Middle East still remains as a challenge. One critical issue is the uneven distribution of stations that can lead to large azimuthal gaps that degrade reliable moment tensor solutions from the long-period waveform modeling. A second big issue is the dramatic difference of the lithospheric structure over the paths from event to station causing significant variation in body and surface waves amplitude and phase. Moment magnitude estimation of small to moderate events that require short period signals are even more affected by these 2-D structural effects. The regional coda envelope method for moment magnitude estimation has proven to be very robust in many studies in different parts of the world. In the Middle East there has been a large increase in the availability of broad-band stations through improved national networks and the temporary deployments. We take advantage of these stations to use the regional coda envelopes to estimate moment rate source spectra and moment magnitudes of 495 regional events recorded by 67 stations. We used more than 100 independent waveform modeled moment magnitudes for absolute scaling of the source spectra. The moment rate source spectra between 0.03–8 Hz are determined using 13 separate narrow band measurements. We started with a 1-D calibration where we used the Extended Street and Herrmann (ESH) approach to calibrate the path. As expected, we obtained good Mw(coda) estimates using this 1-D path correction for larger events (Mw ≥4.5) at low frequencies (≤0.5 Hz) as determined by comparing to the independent waveform moments. We are implementing a 2-D path correction to allow us to obtain reliable moment magnitudes of smaller events by making more use of the higher frequencies by reducing the interstation scatter for each event.

Temporal and Spatial Variations of Local Magnitudes in Alaska and Aleutians and Calibration with Moment Magnitudes

RUPPERT, N.A., University of Alaska Fairbanks, Fairbanks, natasha@gi.alaska.edu; HANSEN, R.A., University of Alaska Fairbanks, Fairbanks, roger@giseis.alaska.edu

We evaluated temporal and spatial variability of local magnitudes (M_L) in the earthquake catalog of Alaska Earthquake Information Center. Regionally recorded hypocenters in the mainland Alaska are available in the catalog beginning early 1970's. No comprehensive Aleutian-wide M_L statistics exists prior to mid-1990's. We identify four time intervals with similar magnitude residual trends between M_L vs. body wave magnitude m_b: 1971–1976, 1977–1989, 1990–1999.5, 1999.5–2008. The three latter intervals are also identified in M_L vs. moment magnitude M_W residual trends. These time intervals correspond to the periods with different data processing procedures. Strong spatial variations in M_L vs. m_b and M_L vs. M_W are present in the catalog. For the pre-1990 data, the largest discrepancies are observed for the Gulf of Alaska earthquakes. For the latest time period 1999.5–2008, the largest residuals between M_L and m_b or M_W are observed for the earthquakes located within the oceanic segment of the Aleutian arc and within 100 km of the trench. We find that the latest time interval has the best correspondence between M_L and M_W values in the mainland Alaska, especially for shallow (depth <40 km) earthquakes. We calculated a set of magnitude corrections for the mainland Alaska and Aleutians that need to be applied to homogenize magnitude values in the catalog in time and space.

New Developments in Earthquake Monitoring in Switzerland

OLIVIERI, M., SED ETHZ, Zurich/Switzerland, olivieri@sed.ethz.ch; CLINTON, J., SED ETHZ, Zurich/Switzerland, clinton@sed.ethz.ch; DEICHMANN, N., SED ETHZ, Zurich/Switzerland, deichmann@sed.ethz.ch; HUSEN, S., SED ETHZ, Zurich/Switzerland, husen@sed.ethz.ch; GIARDINI, D., SED ETHZ, Zurich/Switzerland, domenico.giardini@sed.ethz.ch

The Swiss Seismological Service (SED) has an ongoing responsibility to improve the seismicity monitoring capability for Switzerland. This is a crucial issue for a country with a low background seismicity but where a large M6+ earthquake is expected in the next decades. With over 30 stations and station spacing of ~25km, the SED operate one of the densest broadband networks in the world, which is complimented by a similar number of realtime strong motion stations. In parallel to the existing in-house processing tools, SeisComp3, a state-of-the-art monitoring system, is currently being tested. We are evaluating the capability of the software to detect and identify small local (>Ml1) as well as large regional events. We are also preparing a new attenuation relation for local magnitude Ml from the broadband and strong motion data-set recorded in the last 10 years. We discuss our results in terms or location and magnitude accuracy, with particular attention to the specific improvements needed from monitoring systems for improved monitoring of small regions with high quality seismic networks.

Seismic Quality Factor and Source Parameters of the Baikal Rift System Earthquakes

DOBRYNINA, A.A., Institute of the Earth's crust, Irkutsk/Russia, dobrynina@crust.irk.ru; CHECHELNITSKY, V.V., Baikal Seismological Center, Irkutsk/Russia, chechel@crust.irk.ru; CHERNYKH, E.N., Institute of the Earth's crust, Irkutsk/Russia, cher@crust.irk.ru; SANKOV, V.A., Institute of the Earth's crust, Irkutsk/Russia, sankov@crust.irk.ru

Using S-wave spectra source parameters (seismic moment, radius, stress drop, dislocation amplitude) of 110 local Baikal rift system (BRS) earthquakes with magnitude M=3.1–4.7 were obtained. We used digital waveforms obtained by short-period seismic stations of regional network. To convert station spectrum to source one we took into account the channel response, local site-effect (LSE), geometrical spreading, attenuation and source radiation pattern. LSE was obtained by spectral ratios method. Obtained LSE are divided into three groups: (1) stable LSE independent on season; (2) LSE with daily and/or seasonal variations and (3) unstable LSE. Attenuation pattern (Q-factor) of the lithosphere in BRS was studied analyzing coda waves of 274 local events. The Q values were estimated at 6 central frequencies and for 8 lapse time windows from 20 to 90 sec for all BRS and for different tectonic blocks (Siberian craton, rift basins, uplifts, main active faults). Q value increase with increasing of lapse time window. Lateral Q variations connected with upper crust structure are observed. Comparison Q for BRS and different tectonic regions showed that Q(f) for BRS is agree with ones for tectonic active regions while Q(f) for Siberian craton is agree with ones for stable regions. The lateral Q variations are dependent on the degree of Cenozoic tectonic activity of the structures and the crust age for non active blocks. Observed changes of Q for different lapse time windows are explained by crustal vertical heterogeneity and its decreasing with depth. Maximal attenuation is observed for main active faults. Comparison of seismic moment-local magnitude relations for BRS and other rifts showed satisfactory agreement that gives evidence of existing of general pattern of lithosphere destruction and seismicity in extension zones of the crust .

A General Method to Estimate Earthquake Moment and Magnitude Using Regional Phase Amplitudes

PASYANOS, M.E., Lawrence Livermore National Lab, Livermore/CA/USA, pasyanos1@llnl.gov

Attenuation models of the crust and upper mantle are becoming increasing available. This presentation discusses a general method of estimating earthquake magnitude using regional phase amplitudes, called regional Mo or regional Mw. This method uses an earthquake source model along with an attenuation model and geometrical spreading which accounts for the propagation to utilize regional phase amplitudes of any phase and frequency. Amplitudes are corrected to yield a source term from which one can estimate the seismic moment. Moment magnitudes can then be reliably determined with sets of observed phase amplitudes rather than predetermined ones, and afterwards averaged to robustly determine this parameter. We first examine several events in detail to demonstrate the methodology. We then look at various ensembles of phases and frequencies, and compare results to existing regional methods. We find regional Mo to be a stable estimator of earthquake size that has several advantages over other methods. Because of its versatility, it is applicable to many more events, particularly smaller events. We make moment estimates for earthquakes ranging from magnitude 2 to as large as 7. Even with diverse input amplitude sources, we find magnitude estimates to be more robust than typical magnitudes and existing regional methods and might be tuned further to improve upon them. The method yields a more meaningful quantity of seismic moment, which can be recast as Mw. Lastly, it is applied here to the Middle East region using an existing calibration model, but it would be easy to transport to any region with suitable attenuation calibration.

Detailed Results and Validations of the SCARDEC Method

FERREIRA, A.M.G., University Of East Anglia, Norwich, U.K., A.Ferreira@uea.ac.uk; VALLÉE, M., Geoazur, IRD, University of Nice, France, vallee@geoazur.unice.fr; CHARLÉTY, J., Geoazur, University of Nice, France, charlety@geoazur.unice.fr

We present in a joint abstract (reference 10-083) an automated method to simultaneously retrieve the seismic moment, focal mechanism, depth and source time functions of large earthquakes. This approach, referred as the SCARDEC method, is based on

body-wave deconvolution. We detail here the results for the major subduction earthquakes of the last 20 years, with a stronger focus on the events for which our solutions differ from the Global CMT results. Because Global CMT makes use of other seismic data for large and shallow earthquakes (mostly long period surface waves), we explore the compatibility of our source parameters by forward modelling these surface waves. Two methods (full ray theory and spectral element methods) are used to simulate the long-period wavefield for the 3D Earth model S20RTS combined with the crust model CRUST2.0. We show that our solutions agree with surface waves as well as Global CMT solutions. This can be explained by the fact that most of the differences with Global CMT are linked to correlated variations of the seismic moment and dip of the earthquakes, and it is theoretically known that long-period surface waves are little sensitive to the independent effects of these two parameters for shallow earthquakes. While the SCARDEC method makes only use of body waves arriving in the 30 minutes after the earthquake origin time, this validation shows that the retrieved source parameters remain consistent with most of the subsequent parts of the seismograms. Additionally, we show that the aftershocks fault plane geometry tends to favour the earthquake dips determined by the SCARDEC method. Finally, for some well instrumented earthquakes, our results are also supported by independent studies based on local geodetic or strong motion data.

Deterministic Simulated Ground Motion Records under ASCE 7-10 as a Bridge Between Geotechnical and Structural Engineering Industry

Poster Session · Thursday AM, 22 April · Exhibit Hall

Deterministic Simulations of Nonlinear Vibration of Viscoelastic Elements in Thin-Walled Constructions with Variable Rigidity

ABDIKARIMOV, R.A., Tashkent Financial Institute, Tashkent/Uzbekistan, rabdikarimov@mail.ru

At present a quantity of computer codes for deterministic simulation and calculation of various thin-walled constructions on strength, stability and vibrations is known. However, this not mean, it is possible to solve all problems of mechanics of a deformable rigid body in structural industry. Development of new, more precise mathematical models of deformation of elements of thin-walled constructions in view of variableness of thickness, real properties of a material, under static and dynamic loadings with new, more appropriate, optimum algorithms, always will be the main goal of our research. As a result of our previous study (Bykovtsev, Abdikarimov, Hodjaev & Katz 2003), we are going to present current results of nonlinear vibrations of a viscoelastic plate with variable thickness.

The equation of movement concerning a deflection w and displacements u, v is described by system of the nonlinear integro-differential equations in partial derivatives. As a result of entered dimensionless sizes and applying Bubnov-Galerkin's procedure for definition of unknowns the system of the nonlinear integro-differential equations was obtained. Integration of the nonlinear integro-differential system of the equations was carried out with the help of the numerical method based upon using the quadrature formula. On the basis of these developed algorithms the computer codes on algorithmic language Delphi was created and used for research.

An amplitude-time dependences, deflected mode, and moment-time characteristics of vibrations of viscoelastic elements at wide ranges of changes in parameters of deformable systems were investigated. Different calculation scenarios were carried out using various changes of thin-walled constructions thickness. Results of calculations, at various physical and geometrical parameters of a viscoelastic plate, will be presented in tables and graphics.

Deterministic Calculation of Dynamic Stability of Viscoelastic Elements in Thin-Walled Constructions with Variable Rigidity

ABDIKARIMOV, R.A., Tashkent Financial Institute, Tashkent/Uzbekistan; KHODZHAEV, D.A., Irrigation and Melioration, Tashkent/Uzbekistan.

There is a number of works devoted to the decision of a problem on stability of elastic plates with variable rigidity (Bykovtsev, Abdikarimov, Hodjaev & Katz 2003). The results of deterministic simulations with geometric nonlinear statement and investigations of dynamic stability of viscoelastic thin-walled constructions with variable rigidity under dynamic compression loads will be presented. As an example the viscoelastic plate of variable rigidity with the sides a and b will be considered. We count, that the plate is hinged on all edges and is exposed to dynamic compression along the side a force $P(t) = s \bullet t$, s - loading speed.

For the set of physical and geometrical ratios the mathematical model of stability of a viscoelastic plate with variable rigidity is constructed at dynamic loading which is described by a system of the nonlinear integro-differential equations in partial derivatives concerning a deflection w and displacements u, v which decision is searched on Bubnov-Galerkin's method.

Having entered into the given system dimensionless sizes and keeping former designations, after performance of Bubnov-Galerkin's procedure, concerning unknowns we shall obtain a system of the nonlinear ordinary integro-differential equations. Integration of the obtained system of the equations was carried out with the help of the numerical method based upon the use of quadrature formula. On the basis of the developed algorithm of the decision of a problem the program on algorithmic language Delphi is created. Results are shown as schedules and tables.

Over a wide range of change of mechanical and geometrical parameters at various scenarios of change of thickness, critical time, and critical loadings are found. Also their dependences on physical-mechanical properties of a material of a plate and its geometrical characteristics are investigated.

Simulated Ground-Motion (SGM) Procedure with Time History Analysis for Bridges, High-Rise Buildings and Essential Facilities Located within 5 km of a Fault Zone

BYKOVTSEV, A.S., Region. Academy Natural Sciences, 2644 Foghorn Cove, Port Hueneme, CA-93041, USA, bykovtsev1@yahoo.com

In order to examine sensitivity of SGM to variations in seismic source parameters (SSP), for critical long period structure, investigation stability of main SSP in simulation methods should be given serious consideration. The range of variations for stable SSP should be determined from time history analyses and included in future considerations. We will provide analysis dependences of SGM from variations in stable and unstable SSP in the vicinity 5km of the fault.

An optimal approach for Next Generation Attenuation Relationships for the Central and Eastern US and prediction equations for comprehensive seismic-source model with stable SSP will be presented. Main SGM equations for near zone (within 5km of the fault) and far field also will be presented. The algorithm used to create SGMs was based on 2D-analytical solutions by Bykovtsev (1979&1986) and 3D-analytical solutions by Bykovtsev-Kramarovskii (1987&1989). Validation tests for computer codes based on these algorithms were done by V.Graizer at the Institute of Earth Physics (Moscow). Comparisons with alternative numerical procedures based on Green's functions solution (Haskell model) provided identical results. Ultimately, the algoritm is 10,000 times faster than numerical algorithms based on Green's functions. Comparisons of different algorithms will be presented. After official validation tests the computer codes were recommended by the USSR government for use in earthquake engineering and mining industries. Analyses of SGMs for different fault distances and different fault movement types (strike slip, dip slip, and oblique slip) will be presented. Maximum peak ground acceleration (PGA) in three components, arrival time and period for maximum impulses of PGA will be presented in tables. The presented approach and methods have been quite successful in generating realistic SGM compared with observations for earthquakes and explosions and has been applied to many SGM engineering and mining projects.

Site Specific Seismic Investigation (SSSI) for Large Landslides in Santa Barbara and Ventura Counties, California

BYKOVTSEV, A.S., Region. Academy Netural Sciences, 2644 Foghorn Cove, Port Hueneme, CA-93041, USA, bykovtsev1@yahoo.com

Results of SSSI performed for large landslides in Santa Barbara County and for large landslides area in Camarillo-Ventura County, CA will be presented. The sites in Santa Barbara are crossed by the Mission Ridge-Arroyo Parida active fault with maximum M=6.8. The landslide in Camarillo occupies approximately 3.5 acres and is located less than 5km from the Simi-Santa Rosa Fault (ID-332 Dip 60N,L=40km,M=6.7 with 6 segments) and the Oak Ridge-onshore Fault (ID-245 Dip 65S,L=49km,M=6.9 with 8 segments). Results of a screening analysis procedure-Special Publication 117 (SP-117) and a quantitative SSSI based on Deterministic Simulated Ground Motion (DSGM) under ASCE 7-10 will be presented for several types of large landslides. Most critical to the evaluation of the slope stability at the site is the shear strength testing of the weak clay layers in the Sespe and Saugus Formation. Optimal structural parameters for landslides areas stabilization were found.

According to ASCE 7-10 Chapter 21 probabilistic and deterministic MCE analyses are now mandatory included in SSGMP. Our preliminary study shows that probabilistic analysis (PA) based on ASCE 7-10 provides more conservative results, and as a result the seismic coefficients in slope stability analyses were overestimated by approximately 20%. The deterministic analysis (DA), including fault segmentation and analyses existing time history records from COSMOS data base, was used for control and correction of results obtained by PA. The DA provided more accurate results in near-fault zones(less than 5km). As a result of analyses we conclude, that SP-117 should be revised for proper definition of DSGM in near-fault zones. Analyses DSGM (computed using algorithm Bykovtsev-Kramarovskii-1987) for different site locations and different type of movement on fault will be presented. Analyses of obtained results show, that for several scenarios, the maximum seismic radiation will be on some distance approximately 1–3km from the fault.

Deterministic Calculation of Nonlinear Vibrations of Viscoelastic Orthotropic Cylindrical Panels with Concentrated Masses

KHODZHAEV, D.A., Irrigation and Melioration, Tashkent/Uzbekistan.

In connection with intensive development of engineering now numerous researchers are attracted with problems of strength and stability of thin-wall shell constructions from composites. By development of calculation methods of elements of constructions from composites in the relevant mathematical formulation of a problem characteristic properties of deforming of such material which can influence their lift capability essentially should be reflected. In addition real elements of constructions as shell have a number of features. In particular, refer to them complexity of geometry of a shell, presence of patch piece, substantiating ribs, etc. At calculation of similar shells it is necessary to deal with differential equations in partial derivatives with discontinuous or quickly varying coefficients. Therefore the solution of equations of the indicated type is extremely hindered even at presence of the modern computers. The given work is dedicated to problems of simulation and calculation of thin-wall constructions in view of the indicated features.

The viscoelastic orthotropic cylindrical panel from with constant thickness, carrying the concentrated masses is considered. The mathematical model of the problem is under construction on the basis of the Kirchhoff-Love hypothesis in geometrically nonlinear setting and is described by a system of nonlinear integro-differential partial equations with five different weekly singular kernels of a relaxation.

The integration of a received system was conducted with the help of the numerical method, founded on use of quadrature formulas. Calculations were conducted on programming language Delphi. For real composite material at wide range of change physical-mechanical and geometrical parameters influence of viscoelastic properties of a material and availability of concentrated masses on behavior of cylindrical panels is investigated.

Addressing Surface Faulting at Caltrans Bridges

MERRIAM, M., Caltrans, Sacramento/CA, Martha_Merriam@dot.ca.gov; YASHINSKY, M., Caltrans, Sacramento/CA, Mark_Yashinsky@dot.ca.gov

Surface faulting is not as wide-spread a seismic hazard as is ground motion; therefore the costs of losses resulting from surface faulting are not as great. However if a bridge is crossed by a fault there is potential for collapse and subsequent disruption in traffic patterns as well as possible injuries and loss of life. Caltrans is developing procedures to address surface faulting at about 50 bridges located within 100 ft of fault in a regulatory AP EFZ and at bridges near other Caltrans-active (active within late-Q) faults.

Avoidance often cannot be used as mitigation for faulting at bridges that are part of major highways with established alignments. Bridges can usually accommodate a few feet of displacement through ordinary design however. Consequently we evaluate surface fault rupture hazard at a bridge in steps. If a geologist determines that a bridge may be underlain by a fault, then a conservative value of displacement is estimated. The engineer then determines if the bridge can handle this displacement. If additional design would be needed, studies are undertaken to provide a better estimate of the location, magnitude, and orientation of displacement.

If the bridge cannot accommodate the displacement, then changes in design can be made. Lytle Creek Wash Bridge in San Bernardino, CA was designed to survive surface rupture by using catcher bents that move under the superstructure while continuing to support it. Bolu Viaduct in Turkey was retrofitted to survive offset by supporting the superstructure on large friction pendulum bearings. The Alyeska petroleum pipeline in Alaska was able to survive over 13 feet of fault offset by designing its supports on long pads that allowed the pipeline to bend and displace without breaking. Other solutions may also be envisioned that allow a bridge superstructure to be supported while the ground moves 6–7 meters.

Detection and Identification of Seismic Phases on Engineered Structures

BAKER, M.R., Geomedia Res. & Dev., El Paso, TX U.S.A., bakergrd@cs.com

Seismic evaluation of engineering structures typically relies on inducing and recording the velocity of an isolated phase such as the P, S, or surface wave, with a simplified analysis based on that single mode of energy propagation. In practice, the velocity analysis of waveforms measured in the kilohertz range on concrete structures and pavements is frequently biased by contamination of arrivals that sample the bestiary of reflected, scattered, and leaky modes. The presence of interfering arrivals is apparent in frequency-domain phase velocity analysis when the spectrum shows nulls. Time domain analysis of instantaneous amplitude and phase detect destructive interference of arrivals, and comparison with *a priori* characteristics in phase-coherent segments aids identification of the type of arrivals. Test cases sample scattering in curing concrete, gravels and asphalts where wavelengths cover the range from raypath to effective medium approximations. Additional examples demonstrate the identification of structural reflections. The phase arrival analysis is used to both screen waveforms for suitability for surface wave analysis, and to identify likely time windows for phase velocity analysis.

Quantification and Treatment of Uncertainty and Correlations in Seismic Hazard and Risk Assessments

Poster Session · Thursday AM, 22 April · Exhibit Hall

Ground Motion Uncertainty in ShakeMap Constrained by Observations, Prediction Equations, and Empirical Studies

WORDEN, C.B., Synergetics, Inc., Fort Collins, CO, cbworden@caltech.edu; WALD, D.J., USGS, Golden, CO, wald@usgs.gov; LIN, K., USGS, Golden, CO, klin@usgs.gov; CUA, G., Swiss Seismological Service, ETH, Zurich, Switzerland, georgia.cua@sed.ethz.ch

The recent release of a significant ShakeMap software upgrade (Dec 2009, V3.5) entailed substantial redevelopments. Here we focus on a new approach for incorporating multiple data sets as well as quantifying their collective contribution to the spatial variations of shaking uncertainties. ShakeMap now uses a weighted-average approach for incorporating observed peak ground motions and intensities, and estimates from ground motion prediction equations (GMPEs), into the ShakeMap ground motion and intensity estimation framework. We describe the systematic combination of data across the geographic area that weights each contribution by a spatially-varying uncertainty, and produces a total uncertainty for each point in the output. At each output point, the ground motion is calculated as the average of the (scaled) nearby observations, converted observations, and the output of one or more GMPEs, inversely weighted by each contribution's uncertainty. In the case of direct ground motion observations, the uncertainty contribution is a function of distance from the observation. For converted observations (*e.g.*, macroseismic intensity converted to peak ground acceleration), there is an additional component of uncertainty, due to the conversion process itself, that must be incorporated. For GMPE estimates, the uncertainty contribution is the combined intra- and inter-event variance. With suitable observations it is possible to use a biased GMPE (where the magnitude provided to the equation is adjusted to minimize the misfit with the data), in which case the GMPE uncertainty contribution is reduced to simply the intra-event variance. We will demonstrate improvements in the mean misfit, variance, and computed uncertainty, through the incorporation of native and converted ground motion data, and the biasing of generic GMPEs.

A Generalised Conditional Intensity Measure Approach and Holistic Ground Motion Selection

BRADLEY, B.A., University of Canterbury, Christchurch, New Zealand, brendon.bradley@canterbury.ac.nz

A generalised conditional intensity measure (GCIM) approach is proposed for use in the holistic selection of ground motions for any form of seismic response analysis. The essence of the method is the construction of the multivariate distribution of any set of ground motion intensity measures conditioned on the occurrence of a specific ground motion intensity measure (commonly obtained from probabilistic seismic hazard analysis). The approach is therefore allows any number of ground motion intensity measures, identified as important in a particular seismic response problem, to be considered. A holistic method of ground motion selection is also proposed based on the statistical comparison, for each intensity measure, of the empirical distribution of the ground motion suite with the 'target' GCIM distribution. A simple procedure to estimate the magnitude of potential bias in the results of seismic response analyses when the ground motion suite does not conform to the GCIM distribution is also demonstrated. The combination of these three features of the approach make it entirely holistic in that: any level of complexity in ground motion selection for any seismic response analysis can be exercised; users explicitly understand the simplifications made in the selected suite of ground motions; and an approximate estimate of any bias associated with such simplifications is obtained.

Estimating Epistemic Uncertainty in the Location and Magnitude of Historical Earthquakes

BAKUN, W.H., USGS, Menlo Park/CA/USA, bakun@usgs.gov; GOMEZ CAPERA, A.A., INGV, Milan/Italy, gomez@mi.ingv.it; STUCCHI, M., INGV, Mila/Italy, stucchi@mi.ingv.it

The location and magnitude of significant historical earthquakes, with objective estimates of their epistemic uncertainty, are important input in probabilistic seismic hazard assessment calculations. Bakun and Wentworth (1997), Gasperini *et al.* (1999) and Musson and Jimenez (2008) have proposed independent techniques for estimating an earthquake location and magnitude from intensity data. The three estimates obtained for a given set of intensity data are different and none of the three techniques is consistently better at matching instrumental locations and magnitudes of recent well-recorded earthquakes. Rather than attempting to select one

of the three solutions as best for an historical earthquake for which the instrumental location and magnitude are unknown, we use all three techniques to estimate the location and the magnitude and their epistemic uncertainties.

The estimates are calculated using bootstrap-resampled data sets with Monte Carlo sampling of a decision tree. The decision-tree branch weights are based on goodness-of-fit measures of location and magnitude for many recent earthquakes for which satisfactory instrumental and intensity data are available. The location estimates are based on the spatial distribution of locations calculated from the bootstrap-resampled data. The locus of the maximum location spatial density is the preferred source location. The spatial density contours enclosing 67% and 95% of the locations are the perimeters of the 67% and 95% confidence region of source location, respectively. The median of the distribution of bootstrap-resampled magnitude estimates is the preferred magnitude and the distribution of magnitudes provides the confidence intervals for magnitude.

Near-Surface Deformation Associated with Active Faults

Poster Session · Thursday PM, 22 April · Exhibit Hall

What Is the Effective Number of Parameters in a Fault Slip Model?

FUNNING, G.J., UC Riverside, Riverside, CA, USA, gareth@ucr.edu

A common problem when modelling fault slip is knowing what level of detail is plausible. This is especially important when trying to establish the robustness of features within such models—how can we be sure, for example, that the improved fit to data of one model over another is not merely the result of increasing the number of free parameters (*e.g.* increasing the number of slip patches or allowing the rake on each patch to vary)? Standard statistical tests, such as the analysis of variance (ANOVA) test, may permit us to address this question, by testing whether such an improvement in misfit could be obtained by pure chance. However, such tests require as inputs the number of independent data and number of independent model parameters, quantities that are difficult to estimate.

In this study, I concentrate on the question of model parameters. Taking a number of different approaches, such as methods based on 'nesting' of uniform-slip rectangular dislocations, ABIC-based maximum likelihood methods and principal component analyses, I quantify the number of independent model parameters for a range of models of the 1994 Northridge and 1997 Manyi earthquakes, and thus resolve the maximum detail possible in each case.

Revisiting Surface Rupture Mapping of the 2002 M7.9 Denali Fault Earthquake with LiDAR

HAEUSSLER, P.J., U.S. Geological Survey, Anchorage, Alaska, USA, pheuslr@usgs.gov; LABAY, K., U.S. Geological Survey, Anchorage, Alaska, USA, klabay@usgs.gov; SCHWARTZ, D.P., U.S. Geological Survey, Menlo Park, California, USA, dschwartz@usgs.gov; SEITZ, G.G., San Diego State University, San Diego, California, USA, seitz3@earthlink.net

New GeoEarthScope LiDAR data provide a unique opportunity to compare conventional surface-rupture mapping with that produced by LiDAR. The 2002 M7.9 Denali fault earthquake produced about 341 km of surface rupture on the Denali, Totschunda and Susitna Glacier faults. Our previously published surface-rupture map was based on mapping from vertical aerial photographs using digital photogrammatic methods, and field mapping on the ground and from the air. Digital photogrammetry yields a 3D map, which is perhaps the highest resolution surface-rupture map that can be produced economically with conventional methods over a large area. GeoEarthScope acquired LiDAR data in 2008 centered on the intersection between the Denali and Totschunda faults.

The new LiDAR-based bare earth, 0.5 m, DEM reveals many previously unidentified features, including additional fault strands, sackungen, ground cracks, and offsets. However, not all of these features were active in 2002, such as a prominent 2.5 km-long scarp at the southern edge of the Denali-Totschunda transfer zone. Since 2002, we flew over this scarp several times, landed on it, walked on it, but never found evidence for 2002 surface rupture. This example demonstrates that LiDAR excels at showing the cumulative deformation of surfaces over their lifetime, which often encompasses several seismic cycles. In contrast, conventional methods allow a confident determination of fresh ground rupture. Although the LiDAR was generally excellent for fault mapping, the conventional aerial photographs were particularly useful for identifying the 2002 rupture in some low-lying, swampy areas where a swath of tilted and downed trees revealed the fault trace. However, because vertical relief was small it was difficult to identify on LiDAR. Our study highlights how these methods are complimentary and when used together result in better overall maps.

Spatial and Temporal Variability of Submarine Landslide Deposits Triggered by Megathrust Earthquakes at Port Valdez, Alaska

RYAN, H.F., USGS, Menlo Park, CA, hryan@usgs.gov; HAEUSSLER, P.J., USGS, Anchorage, AK, pheuslr@usgs.gov; LEE, H.J., USGS, Menlo Park, CA, hjlee@usgs.gov; PARSONS, T., USGS, Menlo Park, CA, tparsons@usgs.gov; SLITER, R.W., USGS, Menlo Park, CA, rsliter@usgs.gov

Submarine slope failures at Port Valdez triggered by the 1964 M9.2 great Alaskan earthquake generated some of the highest tsunami wave heights observed in Alaska (> 50 m). Debris flow deposits from the slope failures are imaged on high-resolution mini-sparker sub-bottom profiles. We imaged fields of relatively intact blocks greater than 60 m tall off the Shoup Glacier moraine, in addition to an acoustically chaotic to transparent unit as thick as 40 m that extends over much of Port Valdez just beneath the seafloor. At least 5 similar acoustically chaotic units are intercalated with layer-parallel reflectors below the 1964 deposits. We interpret these units as debris lobe deposits from paleo-submarine landslides that were triggered by prior earthquakes on the Alaskan megathrust. Based on time-averaged sedimentation rates calculated for Port Valdez, debris lobe 2 is assigned to the timing of the penultimate earthquake (913–808 yrs B.P., Carver and Plafker, 2008). Debris lobe 2 has a similar spatial distribution as the 1964 deposit and also includes large blocks off the Shoup Glacier moraine. However, along the northeast margin of Port Valdez, debris lobe 2 deposits are thicker and record additional block-like failures. The older debris lobes are thinner, less extensive, and did not involve the failure of large, intact blocks. We postulate that variations in the thickness and spatial extent of the debris flows are related to differences in the recurrence interval between and/or magnitude of megathrust earthquakes, modulated by variations in climatic conditions. The retreat of Shoup Glacier from its terminal moraine in the 1700s and also perhaps during the Medieval Warm Period (ca. 850–1200 A.D.) may have facilitated failure of the Shoup Glacier moraine during the more recent megathrust earthquakes.

A Tunnel Runs through It—An inside View of the Thrust-Faulted Portland Hills, Oregon

WELLS, R., U.S. Geological Survey, Menlo Park, CA, rwells@usgs.gov; WALSH, K., Portland State University, Portland, OR, (deceased); PETERSON, G., Shannon and Wilson, Inc., Lake Oswego, OR, glp@shanwil.com; FLECK, R., U.S. Geological Survey, Menlo Park, CA, fleck@usgs.gov; BEESON, M., Portland State University, Portland, OR, (deceased); EVARTS, R., U.S. Geological Survey, Menlo Park, CA, revarts@usgs.gov; BURNS, S., Portland State University, Portland, OR, BurnsS@pdx.edu; BLAKELY, R., U.S. Geological Survey, Menlo Park, CA, blakely@usgs.gov; DUVALL, A. University of Michigan duvall@umich.edu

Construction of a 3-mile-long (4.5 km) light rail tunnel in 1993–98 provided a unique view of faults and folds in the Portland Hills. We have compiled unpublished geologic mapping of the tunnel and interpretation from tunnel design borings with new Ar/Ar ages to document Quaternary faulting and folding of the Portland Hills. Three units are recognized in the tunnel: 1) folded 15–16 Ma flows of the Columbia River Basalt Group (CRBG) forming the Portland Hills anticline; 2) faulted 1.4 Ma to 120 ka Boring basalt flows in the western third of the tunnel; and 3) loess and fluvial strata interbedded with the Boring basalts. CRBG flows are offset by a west dipping thrust fault at Sylvan, 1.6 km from the west portal, which thrusts Winter Water Member at least 500 m eastward over Sentinel Bluffs Member. The thrust dips toward the Tualatin basin, but no offset is observed in deep wells to the SW. We interpret this fault as a roof thrust to a NE dipping master thrust at depth, consistent with east-side-up faulting along strike to the NW. Boring flows above the Sylvan thrust have been tilted SW, presumably as a result of continued slip on the master thrust at about 0.09 mm/yr. Near vertical strands of the NW-trending Sylvan Creek-Oatfield fault cut Boring lavas 550–700 m from the west portal. Flows and mudstone along the Oatfield strand are vertical, with tops to the west, and 15 Ma Grande Ronde Basalt is thrust eastward over a 1.1 Ma Boring basalt flow. A 120 ka flow forming the west portal is also cut by shear zones near the Sylvan Creek fault. These faults are interpreted to root into the NE dipping master thrust at depth, giving a post-1 Ma vertical slip rate of 0.2 mm/yr. Slip rates are slow, and the faults may be blind. The Sylvan-Oatfield fault is reflected in aeromagnetic anomalies, but no fault scarps have been recognized on Lidar images of the Portland Hills.

Shallow Crustal Structure in the South Georgia Rift near the Epicenter of the 1886 Charleston, South Carolina Earthquake

BEALE, J.N., Virginia Tech, Blacksburg, Virginia, USA; BUCKNER, J.C., Virginia Tech, Blacksburg, Virginia, USA; CHAPMAN, M.C., Virginia Tech, Blacksburg, Virginia, USA.

Reprocessing of reflection data collected near Summerville, South Carolina has revealed Cenozoic faulting associated with Mesozoic structure at the epicenter of the 1886 Charleston earthquake (Chapman and Beale, BSSA, 2009; Chapman and

Beale, BSSA, in review, 2010). The area is in the South Georgia Rift that includes parts of South Carolina, Georgia, Florida and Alabama. The data near Summerville image Cenozoic faulting along the northwestern margin and within the interior of an early Mesozoic extensional basin that extends approximately 25 km along the Ashley River between Summerville and Charleston. The basin is associated with positive potential field anomalies. Our modeling indicates that mafic rocks comprise the shallow crust within the basin to a depth of at least 4.5 km. Modern seismicity is spatially associated with the Mesozoic-Cenozoic faulting imaged along the northwestern boundary of the feature near Summerville and within the interior along the Ashley River.

The basin structure was initially interpreted from a series of short seismic reflection profiles to the north and west of Summerville and along the Ashley River. Here we show the reprocessed data that define the geometry of the basin, and focus in particular on the longest profile in the study area that crosses the feature approximately 17 km to the south of the Ashley River. The extent and geometry of the basin to the south of the Ashley River is an important issue for seismic hazard assessment. Major deformation of the Mesozoic basement is evident along this southern profile, further constraining the geometry of the extensional basin. Few shocks have been instrumentally located near the profile, but contemporary investigators noted severe deformation of the ground surface, including long-wavelength bending of railroad track, in this area in 1886.

Determining Earthquake Recurrence Over the Past 3 - 4 Events on the Southern Santa Cruz Mountains Section of the San Andreas Fault

STREIG, A.R., University of Oregon, Eugene, OR, USA, streig@uoregon.edu; DAWSON, T.E., California Geological Survey, Menlo Park, CA, USA.

The Santa Cruz Mountains section (SAS) of the San Andreas fault last ruptured during the 1906 earthquake, an event that produced continuous surface rupture across multiple interpreted fault sections from Point Arena to San Juan Bautista. Paleoseismic studies on the SAS at the Grizzly Flat (GF) and Arano Flat (AF-MC) sites provide evidence of 1906 surface deformation, but have yielded differing records of prehistoric surface-fault ruptures. GF is located 14 km northwest of the AF-MC site and records one prehistoric earthquake between AD 1632–1659 (Schwartz *et al.*, 1996). The record at AF-MC sites record a younger penultimate earthquake between AD 1720–1790, with a third event between AD 1600–1680 (Fumal *et al.*, 2003). The AF-MC sites suggest nine earthquakes in the past ~1000 years, and an average recurrence interval of 105 years over the past 1,000 years (Fumal *et al.*, 2003).

The Hazel Dell site is located approximately 9.5 km north of AF-MC, near the mid-point between the AF-MC and GF sites. Three trenches revealed evidence of 1906 and as many as three pre-historic surface fault ruptures. Preliminary age dates suggest the average of the last three measured intervals is roughly 200 years, and the penultimate earthquake occurred sometime after AD 1482–1627 and before ~1770, the approximate timing in which non-native pollen from *erodium cicutarium* appears regionally in the stratigraphic record. The age range for the penultimate event at GF and Hazel Dell sites and the third event at AF-MC overlap suggesting that, if these events are the same, then this earthquake ruptured at minimum 14 km of the fault. In contrast, the penultimate event observed at AF-MC appears to be restricted to the southernmost part of the SAS. These preliminary results combined with the paleoseismic record for the GF and AF-MC sites suggests earthquakes decrease in frequency from south to north.

Late Quaternary Shortening and Earthquake Chronology of an Active Fault in the Kashmir Basin, Northwest Himalaya

MADDEN, C., Oregon State University, Corvallis, Oregon, USA, madden@earthconsultants.com; TRENCH, D., Oregon State University, Corvallis, Oregon, USA, david.trench@gmail.com; MEIGS, A., Oregon State University, Corvallis, Oregon, USA, meigsa@geo.oregonstate.edu; AHMAD, B., University of Kashmir, Srinagar, J & K, India, shabir79@rediffmail.com; BHAT, M.I., University of Kashmir, Srinagar, J & K, India, bhatmi@hotmail.com; YULE, J.D., CSU Northridge, Northridge, California, USA.

In contrast to the central Himalaya, where shortening from the collision of India with Asia is localized at the Himalayan frontal thrust (HFT), distributed deformation characterizes convergence across the northwest Himalaya (NWH). Evidence for distributed deformation in the NWH includes active shortening on a fault system over 40 km northeast of the HFT that includes the Riasi fault zone (Hebeler *et al.*; Gavillot *et al.*, this meeting), and the Balakot-Bagh fault, source of the Mw 7.6, 2005 Kashmir earthquake. New mapping and paleoseismic data indicate that active faulting also occurs within the Kashmir Valley (KV), an intermontane basin ~100 km north of the NWH deformation front. The 40-km-long Balapora fault (BF) is the longest of three northeast-dipping reverse faults that cut Quaternary terraces on the southwest side of the KV. Outcrops and artificial trenches demonstrate that the base of overbank deposits in a low fill terrace of the Rambira River exhibits ~13 m of vertical separation across the BF. Weakly developed soils and the lack of loess suggest these deposits postdate the last glacial maximum (22–17 ka) and may be as young as 10–6 ka, the last period of enhanced monsoon and regional aggradation in the NWH. These crude age constraints, 13 m of vertical separation, and a 60 degree average fault dip yield a preliminary shortening rate of 0.3 to 1.3 mm/yr for the BF. Paleoseismic trenches across the BF near Shupiyan reveal growth strata and colluvial wedges that record 2–4 surface rupturing events in the latest Quaternary. These preliminary results indicate that the BF is a low slip rate fault and poses a seismic hazard to the people of the nearby city of Srinagar and the KV. Determining the percentage of Indo-Asian convergence across the KV requires dating of terrace deposits and additional mapping of the BP and other active faults in the KV.

Middle Holocene Surface Rupture of the Riasi Fault, Kashmir, India

HEBELER, A., CSU Northridge, Northridge/Ca/USA, hebeler.aaron@gmail.com; YULE, J.D., CSU Northridge, Northridge/Ca/USA, Doug.Yule@csun.edu; MADDEN, C., Oregon State University, Corvallis/Or/USA, madden@earthconsultants.com; MALIK, M., University of Jammu, Jammu/Kashmir/India; MEIGS, A., Oregon State University, Corvallis/Or/USA, meigsa@geo.oregonstate.edu; GAVILLOT, Y., Oregon State University, Corvallis/Or/USA, gavilloy@science.oregonstate.edu; KAERICHER, M., CSU Northridge, Northridge/Ca/USA.

The Mw 7.6 Kashmir earthquake and its surface rupture of the Balakot-Bagh fault, considered by many to be inactive prior to 2005, underscored the need to better understand the active tectonics of the northwest Himalaya and raised concern that other unrecognized active faults may occur in the region. The Riasi fault, by all accounts a close relative to the Balakot-Bagh fault, occurs ~150 km along strike to the southeast of the 2005 rupture. Both are reverse faults that place tightly folded Precambrian limestone over Pliocene and younger non-marine strata. Folded fluvial strath terraces occur in the hanging walls of both faults, which cut Quaternary alluvium locally. This study focuses on a site ~10 km to the north of Riasi, India where the Riasi fault consists of two splays. The northern splay places Precambrian limestone over a well-indurated limestone-clast conglomerate of late Pleistocene(?) age (Unit 3). One of two paleoseismic trenches (T1) across the southern splay exposed a distinct angular unconformity separating ~25° south-dipping, polylithic cobble and boulder alluvium (Unit 2) from unconsolidated limestone-clast conglomerate and breccia (Unit 1) with ~5° S depositional dips. Calibrated calendar C-14 ages from detrital charcoal constrain the age of this unconformity to ~4,500 yrs old. Relations at the bottom of T1 suggest that the tip of the southern splay occurs a few m below the maximum depth of our excavator. Steeply dipping strata of Unit 3 cut by low-angle thrusts and unconformably overlain by relatively undeformed Unit 2 strata were revealed in Trench T2. The trench relations can be explained by surface rupture of the Riasi fault ~4,500 yrs ago. It is intriguing to consider the 2005 Kashmir earthquake and its ~2,000 yr recurrence (Kondo *et al.*, 2008) as an analog for earthquake size and recurrence on the Riasi fault.

Timing and Magnitude of Late Quaternary Paleoearthquakes on the South Kochkor Thrust fault, central Tien Shan, Kyrgyz Republic

WELDON, L.M., Dept. of Geological Sciences, University of Oregon, Eugene, OR, USA, lili@uoregon.edu; DJUMABAEVA, A., Kyrgyz Institute of Seismology, Bishkek, Kyrgyz Republic; ABDRAKHMATOV, K., Kyrgyz Institute of Seismology, Bishkek, Kyrgyz Republic; WELDON, II, R.J., Dept. of Geological Sciences, University of Oregon, Eugene, OR, USA; BEMIS, S., Dept. of Geological Sciences, University of Oregon, Eugene, OR, USA.

This study presents the results of work done in conjunction with an NSF-funded international field camp in 2006 and 2007. The South Kochkor fault is the eastern trace of the north-vergent Kochkor Thrust fault zone that extends ~60 kms along the south side of Kochkor Valley between the Kyrgyz Range to the north and the Terskey Ala-Too Range to the south. Previous work indicates that the Kochkor fault zone has ~7.5 km of total slip and has a late Quaternary slip rate of 2–4 mm/yr.

A paleoseismic study site was chosen along a well-defined fault scarp cutting a late Quaternary fan associated with the Ukok River emanating from the north flank of the Terskey Range near the village of Karasash. Logging of a hand dug excavation (expanded over two years), topographic profiling, and Be-10 and C-14 dating of surfaces and deposits across the fault yielded a history of four paleoseismic events in the past ~60,000 Be-10 dated years, and one event in the past ~10,000 C-14 dated years. The most recent Holocene event had ~2 meters of dip slip displacement and the total dip slip displacement of the fan surface by what is inferred to be 4 events is ~8 meters. Deflected streams and an offset boulder in the excavation suggest a component of left lateral slip as well.

Tracing Active Faulting in the Inner Continental Borderland, Southern California, Using New High-Resolution Seismic Reflection and Bathymetric Data

CONRAD, J.E., U.S. Geological Survey, Menlo Park, CA, jconrad@usgs.gov; RYAN, H.F., U.S. Geological Survey, Menlo Park, CA, hryan@usgs.gov; SLITER, R.W., U.S. Geological Survey, Menlo Park, CA, rsliter@usgs.gov

New high-resolution seismic and bathymetric surveys offshore southern California reveal a complicated network of active faults and associated deformation. Major active faults in the inner Continental Borderland include the Palos Verdes (PV), Coronado Bank (CB), San Diego Trough (SDT), and San Pedro Basin (SPB) faults. Smaller faults, including the Avalon Knolls (AK) fault and several other unnamed faults also show evidence of recent offset. Combined, these faults are thought to accommodate about 5–8 mm/yr of slip between the North American and Pacific plates, but it is not clear how slip on these faults is distributed across the inner Borderland. For example, high-resolution seismic reflection data show that the PV and CB faults, considered linked in recent seismic hazard assessments, are separated by a zone at least 20 km wide that shows no recent near-surface deformation. West of this area, new high-resolution bathymetric data around Santa Catalina Island show a series of prominent submerged paleoshorelines that indicate that the island is subsiding. This suggests that the SDT fault does not form a restraining bend by connecting to the Catalina fault (which appears inactive), but instead continues northward along strike into a complicated zone where it appears to link with the SPB fault and/or with the AK fault. Between the SPB and AK faults, a series of west-trending folds deforms young sediment in eastern San Pedro Basin. In central San Pedro Basin, the SPB fault can be traced in deep penetration seismic reflection profiles, but near-surface expression of this fault is not apparent in high-resolution reflection data, though it has clear seafloor offset to the northwest in Santa Monica Basin. These observations suggest that right lateral slip in the inner Borderland has involved both spatially and temporally variable slip transfers across multiple fault strands.

The San Andreas Fault Zone Directly Offshore Pacifica and Daly City, California: Complex Deformation and Previously Unmapped Structures

ROSS, S.L., U.S. Geological Survey, Menlo Park, CA, sross@usgs.gov; RYAN, H.F., U.S. Geological Survey, Menlo Park, CA, hryan@usgs.gov; CHIN, J.L., U.S. Geological Survey, Menlo Park, CA, jchin@usgs.gov; SLITER, R.W., U.S. Geological Survey, Menlo Park, CA, rsliter@usgs.gov; CONRAD, J.E., U.S. Geological Survey, Menlo Park, CA, jconrad@usgs.gov; DARTNELL, P., U.S. Geological Survey, Menlo Park, CA, pdartnell@usgs.gov; EDWARDS, B.E., U.S. Geological Survey, Menlo Park, CA, bedwards@usgs.gov; PHILLIPS, E.L., U.S. Geological Survey, Menlo Park, CA, ephillips@usgs.gov; WONG, F.L., U.S. Geological Survey Menlo Park, CA, fwong@usgs.gov

High-resolution seismic reflection profiles acquired in 2006 and 2007 reveal previously unmapped folds and a possible associated fault, which may have a reverse component, near where the San Andreas fault (SAF) heads offshore at Daly City, California. Based on local seismicity and other geophysical data, the Golden Gate area is widely considered transtensional; a fault with reverse motion would provide unexpected evidence for compressive deformation associated with the northern part of the SAF's Peninsula segment.

North of where the SAF intersects the coastline, newly mapped folds suggest shortening between the SAF and the coastline. South of this intersection, offshore of Pacifica and Daly City, a 7-km-long fold and a possible associated high angle fault lie about 3 km west of the SAF; these newly mapped features strike generally north-northwest but at their northern end they bend north-northeast towards the SAF. The strata above the possible fault show increasing vertical offset with depth, suggesting multiple episodes of deformation. There appears to be no surface expression of either the fold or fault in either the multi-beam bathymetry or high-resolution seismic reflection data. It is not clear what the relationship is between the new features and other structures in the area, including the Pilarcitos and San Pedro faults. A map of Holocene sediment thickness shows the sediments thinning by at least 6 m between San Pedro Point and Lake Merced, possibly suggesting relative uplift.

The high-resolution seismic reflection data were collected with a single-channel mini-sparker system operated between 160 and 500 joules. Depth of penetration averaged about 80 m. Line spacing ranged from about 1 to 1.5 km. Further seismic reflection data collection with a similar system but closer line spacing is planned this summer to help resolve these seismotectonic issues.

Measurement of Apparent Offset and Interpretation of Paleoslip: A Case Study from the San Andreas Fault in the Carrizo Plain

AKCIZ, S.O., University of California, Irvine, CA, sakciz@uci.edu; GRANT LUDWIG, L., University of California, Irvine, CA, lgrant@uci.edu; ZIELKE, O., Arizona State University, Tempe, AZ, olaf.zielke@asu.edu; ARROWSMITH, J.R., Arizona State University, Tempe, AZ, ramon.arrowsmith@asu.edu

LIDAR topographic data can provide unprecedented representation of faulting-related surface features and an opportunity to analyze and model their evolution through time quantitatively and reproducibly. New high resolution topographic data from the southern San Andreas fault show that the average slip along the Carrizo section during the 1857 earthquake was ~5 m. Here we present the results from >20 field-reviewed, shallow excavations surrounding a ~20 cm deep channel which was initially interpreted to be offset by ~5 m at the Bidart site along the SAF in the Carrizo Plain. Our observations show: 1) sharp bend in the channel coincides with the trace of the 1857 fault rupture. 2) A mud flow deposit is the oldest unit to bury the surface deformed in 1857. The shallow channel is either younger than or likely contemporaneous with deposition of a pea gravel unit which sporadically overlays the post-1857 mud flow unit. 3) Pea gravel and mudflow deposits show no evidence of intense deformation compared to the underlying units which were interpreted to have deformed significantly (moletracks, fissures, apparent offsets, unit thickness changes, etc.) during 1857. 4) Sharp bend in the channel trace, clearly observed in field and LIDAR images, is younger than the 1857 offset and is now interpreted as a deflection. Pea gravel deposit could have been deflected around a ~5 m offset structure, but the deposition setting is not appropriate to confirm this interpretation. 5) Subtle deformational features within the pea gravel are similar to the evidence previously documented at the Phelan Fan and LY4 paleoseismic sites (3 km and 35 km NW of Bidart), which may collectively suggest a post-1857 aftershock or moderate Cholame/Carrizo earthquake. New technologies and numerical methods provide novel opportunities for understanding processes that shape the surface of the earth. However, validation and 4-dimensional (depth and time) stratigraphic investigations are still warranted.

A Re-evaluation and Comparison of Paleoseismic Earthquake Dates for the Pallett Creek Site on the Southern San Andreas Fault

BIASI, G.P., University of Nevada Reno, Reno, NV, USA, glenn@seismo.unr.edu; SCHARER, K.M., Appalachian State University, Boone, NC, USA, scharerkm@appstate.edu

The seminal work (Sieh, 1978, 1984, Sieh *et al.*, 1989) on at the Pallett Creek paleoseismic site on the southern San Andreas fault predated the development of AMS as a primary radiocarbon dating method. Samples containing several grams of carbon were required for a date, leading to a greater use of bulk samples and less certainty about carbon provenance. Given the importance of the site for seismic hazard estimation in southern California, and the opportunity to apply new methods to clear up dating questions, an independent re-sampling and re-dating of the Pallett Creek site was undertaken. Photographic and descriptive evidence allowed confident identification of layers and event horizons in natural and developed exposures of the geologic section. In most cases the carbon source could be identified under the microscope. The site carbon content is dominated by charcoal. Sixty-two new dates were developed for the reassessment. Earthquake dating methodologies have also evolved, from ad hoc association of all or part of nearby dates with earthquakes to two versions of Bayesian event dating (OxCal - Bronk-Ramsey, 1995; Shaver - Biasi *et al.*, 2002). Earthquake dates from new AMS sampling generally agrees with the Bayesian analysis (Biasi *et al.*, 2002) using the older combined data set. We are also able to compare between Bayesian methods using the new sample set. Two differences are suggested. First, OxCal event dates tend to be younger by one to four decades. Second, where dates differ, the discrepancy traces to a conceptual difference between programs. Shaver applies the layer ordering constraint first, then in a serial step dates the event from proximal layer dates only. OxCal seems in cases to weight to layers away from the event horizon. Neither analysis lends much support for temporal clustering of earthquakes.

Insights into Active Deformation of Southern Prince William Sound, Alaska from New High-Resolution Seismic Data

FINN, S.P., Boise State University, Boise/ID/USA, sfinn@cgiss.boisestate.edu; LIBERTY, L.M., Boise State University, Boise/ID/USA, lml@cgiss.boisestate.edu; HAEUSSLER, P.J., USGS, Anchorage/AK/USA, pheuslr@usgs.gov; PRATT, T.L., USGS, School of Oceanography, UW, Seattle/WA/USA, tpratt@ocean.washington.edu

We collected ~400km of multi-channel seismic data in August 2009 in eastern and southern Prince William Sound, Alaska, for identifying and characterizing active faults. Preliminary processing show at least three seismic facies that we infer are late Quaternary and younger sediments, which are less than a few hundred meters thick. We found numerous high-angle faults, particularly in the southern part of the Sound. Beneath Montague Strait, we observe a zone of uplift and faulting broader than what occurred in the 1964 M9.2 earthquake. Additionally, growth faulting and the shallow depth to Tertiary rocks suggest reactivation of older struc-

tures and long-term regional uplift. Within eastern Prince William Sound, lineations mapped on land and sea floor are also related to active faulting, suggesting significantly greater deformation related to megathrust earthquakes in the area than previously published. Additional analyses of newly acquired data, in combination with existing surveys should help improve seismic hazard assessments and tectonic models for the area.

PFLOW: A 3-D Numerical Modeling Tool for Calculating Fluid-Pressure Diffusion from Coulomb Strain

WOLF, L.W., Auburn University, Auburn, AL, USA, wolflor@auburn.edu; LEE, M.-K., Auburn University, Auburn, AL, USA, leeming@auburn.edu; MEIR, A.J., Auburn University, Auburn, AL, USA, ajm@cam.auburn.edu; DYER, G., Auburn University, Auburn, AL, USA, gbd0001@auburn.edu

A new 3D time-dependent pore-pressure diffusion model PFLOW is developed to investigate the response of pore fluids to the crustal deformation generated by strong earthquakes in heterogeneous geologic media. Given crustal strain generated by changes in Coulomb stress, this MATLAB-based code uses Skempton's coefficient to calculate resulting changes fluid pressure. Pore-pressure diffusion can be tracked over time in a user-defined model space with user-prescribed Neumann or Dirchilet boundary conditions and with spatially variable values of permeability. PFLOW employs linear or quadratic finite elements for spatial discretization and first order or second order, explicit or implicit finite difference discretization in time. PFLOW is easily interfaced with output from deformation modeling programs such as Coulomb (Toda *et al.*, 2007) or 3D-DEF (Gomberg and Ellis, 1994). The code is useful for investigating to first-order the evolution of pore pressure changes induced by changes in Coulomb stress and their possible relation to water-level changes in wells or changes in stream discharge. It can also be used for student research and classroom instruction. We present two example applications in which we utilize the codes to study predicted coseismic pore pressure changes resulting from volumetric strain. The first explores pore pressure changes and diffusion induced by the 1999 Chi-Chi earthquake (Mw = 7.6) in Taiwan. The second focuses on the poroelastic response associated with the Loma Prieta, California, earthquake. In both cases, strain is calculated using a published fault rupture model and the deformation modeling code, Coulomb 3.1 (Toda *et al.*, 2007).

Advances in Seismic Hazard Mapping

Poster Session · Thursday PM, 22 April · Exhibit Hall

Preliminary Geological Site Condition Map of Korea

KANG, S., Korea Ocean Res. & Dvlp. Inst, Ansan, Gyeonggi-do, Republic of Korea, sukang@kordi.re.kr; KIM, K.-H., Korea Ocean Res. & Dvlp. Inst, Ansan, Gyeonggi-do, Republic of Korea, kwanghee@kordi.re.kr

The average shear wave velocity in the upper 30 m defined from borehole data is routinely used for classifying the site conditions. However, nation-wide information of site conditions is not available in Korea because it is difficult to classify the site condition using the limited borehole data. Also, it requires considerable financial investment and time to acquire and to analyze the necessary geological and geotechnical data obtained from borehole data. Hazards and risk assessments are known to highly dependent on geologic site conditions. Therefore, it is desirable to explore alternative methods to provide the general site conditions on a regional scale. Fortunately, comprehensive information of geologic units and geomorphology of Korean Peninsula is available in digital maps for GIS users. We used geologic units and rock type information from the geologic map, and slope and elevation information from the geomorphologic data to classify the sites. The results reveal Class B sites (mainly rock) are predominant, although softer sediments at sites located near rivers or on landfills are often found. We compared our results to the borehole data which includes locations and ground conditions. There are some differences between the results. The discrepancy is attributed to the relatively large scale geologic map (1:250000) which may not include accurate site condition of the regions. These results provide useful information for the further study of regional hazard estimation, risk management, and other seismological and geotechnical applications or land use planning in developing areas.

Assessment of Seismic Hazard for Jordan: A Sensitivity Study with Respect to Different Seismic Source and Magnitude Recurrence Models

YILMAZ, N., Disaster & Emergency Man. Pres., Ankara/ 06530/ Turkey, nazany@deprem.gov.tr; YUCEMEN, M.S., Middle East Technical University, Ankara/ 06530/ Turkey, yucemen@metu.edu.tr

Many studies have been carried out for the understanding of earthquake phenomenon and its effects since the first introduction of probabilistic seismic hazard analysis methodology in late sixties. Accordingly, various models have been developed to describe location, magnitude, probability of future earthquake occurrences and the spatial distributions of their effects. This study focuses on alternative models for seismic sources and magnitude distribution. A case study is carried out for Jordan in order to examine the sensitivity of seismic hazard results to seismic source modeling and various assumptions with respect to magnitude distribution. Four cases, in which different seismic source models (*i.e.* area and line (fault) models) are combined with different magnitude distributions (*i.e.* exponential distribution, characteristic earthquake model proposed by Youngs and Coppersmith (1985) and pure characteristic earthquake model), are considered to assess seismic hazard for Jordan. In order to compare seismic hazard results obtained from these cases, difference maps, which show the spatial variation of the difference in peak ground acceleration (PGA) values, are constructed for return periods of 475 and 2475 years. Seismic hazard results of these four cases are combined through the use of logic tree method and best estimate seismic hazard maps are drawn for PGA and spectral acceleration (SA) at 0.2 sec and 1.0 sec corresponding to return periods of 475, 1000 and 2475 years.

Field Reconnaissance and Response to the M=7.6 Padang, Indonesia Earthquake

MCGARR, A., US Geological Survey, Menlo Park, CA USA, mcgarr@usgs.gov; MOONEY, W.D., US Geological Survey, Menlo Park, CA USA, mooney@usgs.gov

On September 30, 2009, a M=7.6 earthquake struck the city of Padang, Indonesia. The earthquake was located on the west coast of Sumatra (between the Sumatra fault and the Sunda Trench fault) and affected an area with a population of about 1.2M people, including 900,000 in Padang. The earthquake caused 1,195 deaths and significant damage to about 140,000 houses and 4,000 other buildings. The casualties in Padang were mostly due to building damage and collapse. Additionally, landslides in the outlying rural mountain areas buried several villages, damaged roads, and caused over 600 deaths. These numbers would likely have been higher had the earthquake struck earlier, when schools and offices were in session.

In response to this event, three time-sensitive activities that were explicitly requested of the US Geological Survey: (1) providing the Government of Indonesia with high-resolution optical imagery for ongoing emergency response, and assisting in the identification of landslides that have isolated villages and created hazards by damming major river drainages; (2) providing technical assistance in the assessment of earthquake damage in Padang and neighboring regions; (3) providing in-the-field capacity building to Indonesian scientists in modern practices of urban hazard assessment. All three tasks were successfully completed between Oct. 8 and Dec. 9, 2009. The role of the USGS was to provide this requested technical assistance on a Government-to-Government basis, however activities were undertaken in cooperation with US civilian engineering professionals organized by the Earthquake Engineering Research Institute (EERI) program "Learning from Earthquakes" and NOAA (for tsunami preparedness).

Seismic Hazard Assessment of Georgia, Taking into Account Local Site Conditions with Emphasis on Tbilisi Urban Area

ELASHVILI, M., Seismic Monitoring Centre, Ilia State University, Nutsubidze Str. 77, 0177 Tbilisi, Georgia, m.elashvili@seismo.ge; JAVAKHISHVILI, Z., Seismic Monitoring Centre, Ilia State University, Nutsubidze Str. 77, 0177 Tbilisi, Georgia, z.javakh@seismo.ge; GODOLADZE, T., Seismic Monitoring Centre, Ilia State University, Nutsubidze Str. 77, 0177 Tbilisi, Georgia, tea@seismo.ge; JORJIASHVILI, N., Seismic Monitoring Centre, Ilia State University, Nutsubidze Str. 77, 0177 Tbilisi, Georgia, nato@seismo.ge

Caucasus is one of the most seismically active regions in the Alpine-Himalayan collision belt. Strong earthquakes with magnitude up to 7 have occurred here. Modern seismic hazard and risk assessment represents an indispensable condition for sustainable development of Caucasus region in whole and Georgia itself.

So called seismic zonation maps of Georgia have been compiled in 1937, 1957, 1968 and 1978 a part of USSR seismic maps. Maps were mainly based on observed seismicity, in later versions some seismotectonic elements were also used, but all of them had serious drawbacks. These maps were changing after each strong earthquakes, which occurred in the area of "lower" seismic hazard, in some cases the difference between predicted and experienced intensities reached 2–3 units on MSK scale.

Present work aimed assessment of seismic hazard related risks of Georgia and especially Tbilisi area by means of modern technologies and methods. It includes latest results from latest international activities held in Georgia. Namely development and implementation of modern GIS technologies for Seismicity Analysis, Seismic Hazard and Risk Assessment, Calculation of Possible loses. Seismic hazard of Georgia was calculated using logic three approach, 50 years period and 1, 2, 5 and 10 % probabilities of accidence. Commonly used SIESRISKIII code was integrated in GIS and used for hazard calculations. Special GIS database was created,

integrating all the basic information needed for seismic hazard and risk assessment: such layers as Seismic sources, Observed earthquake effects, Soil categories, Terrain model and Social-Economical-demographic infrastructure. Program codes and necessary interface in GIS for the editing and handling prepared database, multipurpose analysis of collected data, assessment of seismic hazard and risk and visualization of derived results were prepared.

Dissemination and Visualization of Digital Geotechnical Data Associated with the 1995 Hyogo-ken Nanbu Earthquake in Kobe, Japan

THOMPSON, E.M., Tufts University, Medford/MA/USA, eric.thompson@tufts.edu; TANAKA, H., Tufts University, Medford/MA/USA, hajime.tanaka@tufts.edu; BAISE, L.G., Tufts University, Medford/MA/USA, laurie.baise@tufts.edu; TANAKA, Y., Kobe University, Kobe/Japan, ytgeotec@tiger.kobe-u.ac.jp; KAYEN, R., United States Geologic Survey, Menlo Park/CA/USA, rkayen@usgs.gov

We have recently developed a web-based data management tool to disseminate, explore, and visualize a rich dataset associated with the 17 January 1995 Hyogo-ken Nanbu earthquake ($M = 6.9$). The amount of damage caused by the event far exceeded what would be expected for a typical event of this magnitude and the event has become one of the most studied earthquakes in history. The damage from the earthquake can be attributed to "basin-edge" effects, widespread liquefaction, site amplification, as well as structural effects. Extensive geotechnical and damage data were collected after the event but have remained generally unavailable to the wider research community. The website employs only free and open-source software, such as OpenLayers, MapServer, MySQL, R, Plone, and others for managing, visualizing, and exploring the data in one and two dimensions. The data include geotechnical, geographic, geological, and earthquake damage data. The geotechnical data include the Jibankun database which includes over 7000 borings with stratigraphic descriptions, related in-situ and laboratory tests, and velocity profiles. The geographic and geologic data include a digital elevation map, shoreline and water bodies, and a regional geologic map. The earthquake damage data include building damage, infrastructure damage, and liquefaction surface effects, which can be used to link the seismic and geotechnical information to economic losses. The website allows users to explore, query, and download data for education and research purposes. The research potential of the dataset is demonstrated for the study of the spatial extent of liquefaction by comparing liquefaction potential predicted from the SPT N-values and that observed during the earthquake. The spatial resolution of the dataset allows for interpolation between points and a comparison of spatial extent of liquefaction surface effects.

A Kinematic Fault Network Model of Crustal Deformation for California and Its Application to the Seismic Hazard Analysis

ZENG, Y., US Geological Survey, Golden, Colorado, USA, zeng@usgs.gov; SHEN, Z.-K., Univ California, Los Angeles, Los Angeles, California, USA, zshen@noah.ess.ucla.edu; PETERSEN, M.D., US Geological Survey, Golden, Colorado, USA.

We invert GPS observations to determine the slip rates on major faults in California based on a kinematic fault model of crustal deformation with geological slip rate constraints. Assuming an elastic half-space, we interpret secular surface deformation using a kinematic fault network model with each fault segment slipping beneath a locking depth. This model simulates both block-like deformation and elastic strain accumulation within each bounding block. Each fault segment is linked to its adjacent elements with slip continuity imposed at fault nodes or intersections. The GPS observations across California and its neighbors are obtained from the SCEC WGCEP project of California Crustal Motion Map version 1.0 and SCEC Crustal Motion Map 4.0. Our fault models are based on the SCEC UCERF 2.0 fault database, a previous southern California block model by Shen and Jackson, and the San Francisco Bay area block model by d'Alessio *et al.* Our inversion shows a slip rate ranging from 20 to 26 mm/yr for the northern San Andreas from the Santa Cruz Mountain to the Peninsula segment. Slip rates vary from 8 to 14 mm/yr along the Hayward to the Maacama segment, and from 17 to 6 mm/yr along the central Calaveras to West Napa. For the central California creeping section, we find a depth dependent slip rate with an average slip rate of 23 mm/yr across the upper 5 km and 30 mm/yr underneath. Slip rates range from 30 mm/yr along the Parkfield and central California creeping section of the San Andres to an average of 6 mm/yr on the San Bernardino Mountain segment. On the southern San Andreas, slip rates vary from 21 to 30 mm/yr from the Cochella Valley to the Imperial Valley, and from 7 to 16 mm/yr along the San Jacinto segments. The shortening rate across the greater Los Angeles agrees with the regional tectonics and crustal thickening in the area. We are applying the result to seismic hazard evaluation. The overall geodetic and geological derived hazard models are consistent with the current USGS hazard model for California.

The Importance of Detailed Geologic Mapping in Regional Seismic Slope Stability Assessment

ABRAMSONWARD, H., AMEC Geomatrix, Inc., Oakland, CA, hans.abramsonward@amec.com; APEL, T., AMEC Geomatrix, Inc., Oakland, CA, trey.apel@amec.com; GRAY, B.T., AMEC Geomatrix, Inc., Oakland, CA, brian.gray@amec.com; BOZKURT, S.B., AMEC Geomatrix, Inc., Oakland, CA, serkan.bozkurt@amec.com

The recent availability of a wide range of spatial data sets such as digital elevation models (DEMs), probabilistic earthquake ground motion maps, GIS-based landslide inventories, and geology maps, has facilitated regional slope instability hazard assessment based on statistical correlations between various data sets. While these approaches are useful for first-order screening of broad regions for potential seismically induced landslide hazard, the reliability of these assessments depends largely on the accuracy of the landslide inventories and geologic mapping used.

This poster will present a comparison of earthquake-induced landslide hazard maps from western Oregon based on landslide inventories and geologic maps of variable resolutions, illustrating the value of detailed landslide mapping and geologic mapping in regional landslide hazard assessments. Key datasets used in the assessments include freely available DEMs, aerial photographs, the Statewide Landslide Information Database of Oregon (SLIDO), the GIS-based statewide geologic map of Oregon (OGDC v.5), historical rainfall data, and probabilistic peak ground acceleration (PGA) estimated by the USGS in their 2008 National Seismic Hazard Maps.

Estimating 5% Damped Response Spectra at Shallow Soil Sites in the Central United States

WOOLERY, E., University of Kentucky, Lexington, Kentucky USA, woolery@uky.edu; STREET, R., Hermosa, South Dakota USA, bhrstreet@yahoo.com; PASCHALL, A., University of Kentucky, Lexington, Kentucky USA, Anthony.Paschall@uky.edu

Ground motion estimations in the central United States have been generally focused on deep (> 30 m) alluvial sites such as those found in the Mississippi Embayment; however, this study considered an area more typical of those outside of the embayment in order to test how well site-specific linear ground motions can be predicted using current attenuation relations and 1-D modeling. The study is located in a 0.4 x 0.4 degree area northeast of Evansville in southwestern Indiana. The region has no major river valleys and the soil/sediment overburden varies from a few meters to approximately 30 m.

During the last two decades, approximately 150 high-resolution (512 to 1024 sps) velocity records have been acquired from earthquakes with magnitudes ranging between M3 and M5.23. The bulk of these observations are from the M4.96 and M5.23 southeastern Illinois earthquakes of 10Jun87 and 28Apr08, respectively, as well as the M4.5 SW Indiana earthquake of 18Jun02. The shear-wave velocities of the sediment and bedrock, as well as sediment thickness and depth to the bedrock have been determined at all of the 2002 and 2008 earthquake observation sites and at some of the 1987 sites.

A comparison of the ground motions corrected for spreading and attenuation at a reference distance of 50 km with the same ground motions corrected for spreading, attenuation, and 1-D site effects at 50 km show that the overall 5% damped response spectra for frequencies greater than 2 Hz are reduced from a factor of nearly 25 to approximately 6 when 1-D site effects are included. This suggests that current ground-motion models and linear site-effect corrections still miscalculate response spectra by a factor of 3 for a given frequency, however.

Key Science Issues in the Intermountain West for the Next Version of the U.S. National Seismic Hazard Maps

HARMSEN, S.C., U. S. Geological Survey, Denver, CO, USA, harmsen@usgs.gov; PETERSEN, M.D., U. S. Geological Survey, Denver, CO, USA, mpetersen@usgs.gov; HALLER, K.M., U. S. Geological Survey, Denver, CO, USA, haller@usgs.gov; LUND, W.R., Utah Geological Survey, Salt Lake City, UT, USA, billlund@utah.gov

Every six years the U.S. National Seismic Hazard Maps (NSHMs) are updated by including newly vetted science. The 2008 hazard maps for the Intermountain West (IMW) include results from: 1) models of alternate dips on normal faults; 2) hazard from intersecting faults; 3) revised weights on alternate models for Wasatch ruptures; 4) consensus input parameters from the Utah Quaternary Fault Parameters Working Group; 5) NGA ground-motion models with new details on hanging-wall site amplification, soil-site amplification and long-period (greater than 2 s) response; and 6) an updated seismicity catalog. Inclusion of this information results in spatially and spectral-period dependent changes in the maps of up to 40% over dipping faults. The NSHMs have been adopted as the basis for building code maps in the 2009 NEHRP Recommended Provisions, 2010 ASCE Standard,

and 2012 IBC. The USGS is now planning the next version of the seismic hazard maps to be released in 2014. Science issues for the 2014 update include: 1) the relation of geodetic, seismic (*e.g.*, catalog-extrapolated) and geologic (surface faulting) strain rates, 2) linking or clustering of neighboring fault ruptures, 3), review of the 40-50-60 degree normal-fault dip uncertainty distribution and possible inclusion of corresponding strike-slip-fault dip uncertainty, 4) new soil models for the IMW, and 5) new ground-motion models for rock and soil sites. The IMW workshop will be held in 2011 or 2012 to discuss these and other potential issues.

Constraints on Ground Accelerations Inferred from Unfractured Hoodoos near the Garlock Fault, California

ANOOSHEHPOOR, R., University of Nevada, Reno, NV, rasool@seismo.unr.edu; BRUNE, J.N., University of Nevada, Reno, NV, brune@seismo.unr.edu; PURVANCE, M.D., University of Nevada, Reno, NV, mdp@seismo.unr.edu; DAEMEN, J.K., University of Nevada, Reno, NV, daemen@mines.unr.edu

There are numerous fragile geological features located in Red Rock Canyon State Park, California, within a few kilometers of a trans-tensional step-over on the Garlock Fault. These hoodoos consist of relatively easily eroded sandstones lying beneath a more weather-resistant volcanic cap rock. The weakly cemented shafts of these hoodoos have not been fractured and thus can be used to constrain ground motions from recent events on the Garlock Fault. Evidence from trenching on the central section of the Garlock Fault suggests that one of the most recent events (within the last 550 years) produced up to 7 m of slip along the central portion of the Fault (McGill and Rockwell, 1998; McGill *et al.*, 2009).

Using the accurate shapes of the hoodoos, determined via photogrammetry, and the flexural relation for failure of a rectangular beam, one can estimate peak ground accelerations leading to fracture of the hoodoo shafts. Accurate bending test in laboratory on a relatively large sample similar to the weakly cemented segments of the hoodoos provide tensile strength of about 7 bars. Previous results from point-load tests had indicated tensile strengths up to 3 bars. For the bending strength estimate a minimum of 0.56 g of ground acceleration could lead to fracture of one of the two hoodoos near its contact with the ground.

The 2008 US NSHM predict 2%, 5%, and 10% probability of exceedence in 50 year ground accelerations near the hoodoos of 0.526 g, 0.359 g and 0.254 g, respectively. Therefore whether or not this hoodoo is inconsistent with the 2% probability of exceedence in 50 year ground accelerations depends on its age. Should the hoodoos be older than 1000 years, they could have been exposed to a major earthquake with 7 meters of slip on a fault within a few kilometers without fracture.

Dating Precariously Balanced Rocks Using Be-10 With Numerical Models

ROOD, D.H., Lawrence Livermore National Lab, Livermore, CA, rood5@llnl.gov; BALCO, G., Berkeley Geochronology Center, Berkeley, CA, balcs@bgc.org; PURVANCE, M., University of Nevada, Reno, NV, mdp@seismo.unr.edu; ANOOSHEHPOOR, R., University of Nevada, Reno, NV, rasool@seismo.unr.edu; BRUNE, J., University of Nevada, Reno, NV, brune@seismo.unr.edu; GRANT LUDWIG, L., University of California, Irvine, CA, lgrant@uci.edu; KENDRICK, K., US Geological Survey, Pasadena, CA, kendrick@usgs.gov

Surface exposure dating of precariously balanced rocks (PBRs) is a powerful tool for constraining unexceeded ground motions, but can only be successful if the geomorphic history of the rock is known. Our approach is to 1) collect profile samples of the PBRs and pedestals at various heights above the ground surface and 2) sample saprolite and stream sediment to constrain surface denudation rates. We measured Be-10 concentrations in 30 samples from 8 corestone PBRs along a 150-km transect near the San Andreas, San Jacinto, and Elsinore faults in southern California. To constrain the exhumation history of the PBR, we use a forward model and compare our Be-10 data to predicted profiles for a range of surface denudation rates and exposure times, with different ratios of pre- and post-exhumation erosion rates yielding different nuclide concentrations as a function of depth.

Using simplified shielding corrections and assuming rapid exhumation, our model predicts surface exposure ages for 4 PBRs that range from 23-16 ka, consistent with minimum exposure ages from varnish microlamination dating results. However, because the cosmic ray flux is only partly attenuated by the rock, to accurately interpret PBR profiles requires that the model include a shielding correction that accounts for the shape of the PBR. Three-dimensional models for PBRs were constructed using photogrammetric and terrestrial LiDAR scanning (TLS) data. Using a model with a more realistic shielding correction, one PBR near the San Andreas Fault at Grass Valley gives best-fit parameters that indicate that the rock, including the pedestal, was exhumed rapidly (within 1 ka) at 18.0 ± 2.5 ka (including Be-10 production by neutrons and muons). To further refine our model and exposure ages, ongoing work will focus on applying our model to additional PBRs and constraining PBR rock erosion rates using in-situ C-14.

Volcanic Plumbing Systems: Results, Interpretations and Implications for Monitoring

Oral Session · Friday 8:30 AM, 23 April · Salon A
Session Chairs: Gregory Waite and Weston Thelen

Seismic Monitoring at Cascade Range Volcanoes: What We've Learned, Where We Are, Where We Need To Be

MORAN, S.C., U.S. Geological Survey, Vancouver, WA USA, smoran@usgs.gov; MALONE, S.D., University of Washington, Seattle, WA, steve@ess.washington.edu; MURRAY, T.L., U.S. Geological Survey, Anchorage, AK USA, steve@ess.washington.edu; OPPENHEIMER, D.H., U.S. Geological Survey, Menlo Park, CA USA, oppen@usgs.gov; THELEN, W.A., University of Washington, Seattle, WA USA, wethelen@ess.washington.edu

The Cascade Range includes 13 volcanoes considered to have the potential to erupt at any time, including two that have erupted in the last 100 years (Mount St. Helens (MSH) and Lassen Peak). Seismic monitoring of these volcanoes has been the joint responsibility of the Pacific Northwest Seismic Network and the U.S. Geological Survey. Monitoring began in the early 1970s with the installation of stations near Mount Baker, Mount Rainier, MSH, Lassen Peak and Mount Shasta. By 2009 the network had grown to 60 stations in operation within 20 km of a volcanic center. Although only two eruptions have been captured by this network (both at MSH), anomalous seismicity and episodes of seismic unrest have been detected at or near most volcanoes, including volcano-tectonic earthquake swarms (Rainier, MSH, Hood, Three Sisters, Medicine Lake, Lassen), shallow low-frequency events (Baker, Hood, Three Sisters, Lassen), and deep long-period events (Baker, Glacier Peak, Rainier, MSH, Lassen). Such anomalous seismicity occurs several times per year across the Cascades, underlining the fact that each Cascade volcano is a dynamic system requiring a modern real-time seismic monitoring network to accurately characterize and interpret these episodes as well as to prepare for the next eruption. A proposal in development by the U.S. Geological Survey to create a National Volcano Early Warning System (NVEWS) would more than double the total number of seismic stations in operation near Cascade volcanoes. Such networks would allow determination of reasonably accurate hypocenters with potential for detecting sub-km-scale hypocenter migrations in time, well-constrained fault-plane solutions and shear-wave splitting directions for stress-field monitoring, and time-varying tomographic models for detecting changes in material properties that might, for example, be associated with intruding magma.

Real-Time Tracking of Earthquake Swarms at Redoubt Volcano, 2009

WEST, M.E., Geophys. Inst./AVO, UAF, Fairbanks AK 99775, mewest@alaska.edu; THOMPSON, G., Geophys. Inst./AVO, UAF, Fairbanks AK 99775, gthompson@alaska.edu

We have designed a real-time earthquake swarm monitoring system that can provide on the fly metrics to quantify volcano-seismic swarms. These metrics provide a quantitative perspective of the swarm's activity relative to comparable sequences elsewhere. This system also identifies the start and end of an earthquake swarm, and also significant escalations in a swarm. Our system consists of a real-time event catalog, a swarm tracking system and a generic alarm management system. The tracking system continuously measures mean event rate, median event rate, mean magnitude and cumulative magnitude. These are compared with (configurable) swarm start, escalation and end thresholds that define the levels at which alarms are declared. The alarm management system dispatches alarms to a call-down list, allowing observatory scientists to be notified in sequence until someone acknowledges the alarm via a confirmation web page.

Swarm tracking has proven to be an effective way to characterize the conduit processes as they unfold. By serving parameters that describe seismic swarms while the processes are still unfolding, systems such as the one described here provide an ability to quantify the seismic behavior within the conduit system and provide tools for on the fly comparisons to similar events elsewhere and/or earlier in the same volcanic sequence.

Precursory Seismicity to the November 21, 2008 Eruption at Nevado Del Huila Volcano, Colombia

MCCAUSLAND, W.A., Cascades Volcano Observatory, Vancouver, WA USA, wmccausland@usgs.gov; CARDONA, C.E., INGEOMINAS, Popayan, Colombia, cecardona@ingeominas.gov.co; WHITE, R.A., U.S. Geological Survey, Menlo Park, CA USA, rwhite@usgs.gov; SANTACOLOMA, C., INGEOMINAS, Popayan, Colombia, csantacoloma@ingeominas.gov.co

The first historical eruption at Nevado del Huila, Colombia, began with two phreatic explosions in February and April 2007, both accompanied by an expulsion of water and the opening of several km-long cracks at the summit. A magmatic eruption began on November 21, 2008, and was accompanied by the largest known

historical lahar. Precursory seismicity started as early as 1997 with isolated swarms of volcano tectonic (VT) earthquakes at 2 -10 km depths within 10 km of the edifice. Seismicity preceding the 2007 explosions lasted 12 - 24 hours and consisted of spasmodic bursts of mainly VT and a mixture of VT and long period (LP) earthquakes, respectively. Seismicity between April 2007 and November 2008 evolved from randomly spaced LP, hybrid and VT earthquakes into spasmodic bursts of LPs and hybrids and finally into self-similar, equally-spaced, equal-amplitude LP and hybrid earthquakes. These self-similar swarms began in early to mid-October 2008, marking a significant increase in seismicity at the volcano. Another swarm occurred in the 12 days leading up to the November 21 eruption, when over 18,000 seismic events were recorded. During this swarm, the events became very frequent and regular in time, occurring at a rate of ~4 events per minute in the hours prior to the eruption. Cross correlation of the events shows that this regularity became most pronounced on November 20, when there were two time intervals of recurrence, 10 s and 40 s, and the development of two characteristic event types, one of smaller amplitude than the other. In the 5 hours before the eruption, time intervals between small amplitude repeaters condensed to one interval, 40 s, and then systematically decreased to 10 s leading into the eruption. In contrast large amplitude repeaters did not show any clear change in their occurrence rate or amplitude.

Investigating Volcanic Plumbing Systems through "Inversion" of Seismologically-Determined Crustal Stress Fields

ROMAN, D.C., University of South Florida, Tampa, Florida, USA, droman@cas.usf.edu

Inversion of geodetically-determined crustal strain field measurements has long been used to constrain the location, shape, and dynamics of volcanic plumbing systems. However, because they are based only on observations at Earth's surface, geodetic inversion results are often nonunique, and geodetic monitoring may not detect subtle and/or deep deformations produced during the initial phase of magmatic unrest. Thus, inversion of the 3D crustal stress field, which may be measured using fault-plane solutions for VT earthquakes and/or split S-waves in local or regional earthquakes, is an important, though underdeveloped, complement to the geodetic modeling approach. Here, I examine the results of four preliminary attempts to "invert" crustal stress fields through forward modeling of stresses induced by dike inflation. Two of the data sets represent episodes of unrest which did not proceed to eruption, at Iliamna Volcano, in 1996 and at Mt. Spurr, Alaska, in 2004. In both cases, forward models of local crustal stresses provide strong evidence for mid-crustal magma intrusion and illuminate the relationship between intruded magma and local seismicity. The remaining two data sets represent episodes of unrest preceding eruptions at Crater Peak, Alaska in 1992 and at the Soufriere Hills Volcano, Montserrat, in 1999. In both cases, forward models of local crustal stresses confirm dike inflation months prior to the eruption onsets, highlighting the ability of volcanic stress field monitoring to detect early, subtle signals of precursory magma pressurization. Major challenges in volcanic stress field inversion include accounting for regional stresses and determining precise locations for stress field measurements; however initial results, combined with the possibility of joint inversion of surface strain fields and 3D stress fields, demonstrate the potential of this new approach.

Inflation and Rheology of the Submarine Campi Flegrei Magma Systems Using Long Water Pipe Tiltmeters

BILHAM, R., University of Colorado, Boulder, bilham@colorado.edu; ROMANO, P., Universita de Salerno, Fisciano Italy, pierom@sa.infn.it; SCARPA, R., Universita de Salerno, Fisciano Italy, roberto.scarpa@sa.infn.it

The Campi Flegrei volcanic region west of Naples, Italy, has a several thousand year history of vertical deformation recorded both by marine terraces and by the submergence and emergence of archaeological structures. Between 1982 and 1985 peak uplift of 1.7 m occurred which was associated with local microseismicity, since which time the region has been slowly subsiding. In the past decade subsidence has been been replaced with intermittent episodes of inflation of one or more submarine magma chambers. Of considerable interest concerns the geometry and gas/liquid ratio of these partially offshore magma chambers. We report here the installation of an array of water-pipe tiltmeters with lengths between 28 m and 278 m in tunnels on the flanks of the region of maximum inflation. The tiltmeters record inflation rates of 0.1–1 mm/week, upon which are superimposed local load tides, wth amplitudes roughly an order of magnitude greater than the solid Earth body tides. In addition to the tides, the tiltmeters record a line spectrum of seiches in the Bay of Naples and in the Tyrrenium sea. Since the tiltmeters are calibrated to within 1% we are able to determine the precise admittance between the measured seiches and tides and their resulting onshore tilts. Of particular interest are a group of seiche periods between 20 minutes and 56 minutes since these have no astronomical counterpart, and constitute local loading frequencies recorded clearly by tide gauges and tiltmeters. We describe here initial results from three tide gauges and two tunnel-based tiltmeter arrays beneath the town of Pozzuoli that suggest that accuracies of 1% for nanoradian tilts in the period range 10 minutes to 10 hours can be obtained, with a long term tilt stability of approximately 0.1 μradian/yr.

Evolution of the Lateral Conduit System at Kilauea Volcano during the Early Stages of the Pu'u O'o Eruption

COLELLA, H.V., UC Riverside, Riverside, CA 92521, USA, hcole001@ucr.edu; DIETERICH, J.H., UC Riverside, Riverside, CA 92521, USA, dieterichj@ucr.edu

The early stages of the Pu'u O'o-Kupaianaha eruption allows for observation of the evolution of a lateral conduit system. During this time the Kilauea summit experienced 47 inflation-deflation events. The periods of inflation were characterized by accelerating rates of shallow tectonic earthquakes, or short period events, punctuated by rapid deflation of the summit, a spike in volcanic earthquakes, or long period events, and a fountaining episode and Pu'u O'o. The cumulative number of short period events observed during this period reveals three distinct earthquake rates, which coincidently, correlate with increases in deflation rates. We assume magma flow rates are proportional to the pressure difference between the primary summit reservoir and magma stored elsewhere in the rift and invoke the Dvorak and Okamura (1987) hydraulic model to explain the tilt rate variation during inflation-deflation episodes. The increase in deflation rates, or magma withdrawal, at the summit suggests that magma begins to move more freely through the lateral conduit connecting Kilauea's summit to the Pu'u O'o-Kupaianaha eruption site. We propose the increase in earthquake rates represents the breakdown or clearing of obstructions near the summit, while the increase in deflation rates represents a shift from a "clogged" conduit to a more "free flowing" conduit.

Volcano Monitoring with Continuous Seismic Correlations: Examples Using Ambient Noise and Volcanic Tremor

HANEY, M.M., Boise State University, Boise, ID, matt@cgiss.boisestate.edu

Recently, the possibility of using continuous seismic energy, in particular ambient ocean-related noise, to monitor volcanoes has shown tremendous promise. The ability to sense internal structure and stress within a volcano, independent of traditional volcanic seismicity, has implications for the prediction of so-called "blue sky" eruptions that occur without precursory phenomena. Ambient noise techniques rely on the principle that useful seismic signals can be generated "at will" by cross-correlating pairs of continuous recordings. However, several issues regarding continuous seismic correlations remain, for instance: Over what range of time-scales can predictions be made? Does the technique perform better at particular types of volcanoes? How can the methodology be applied during eruptions, when the ambient noise may be overwhelmed by local volcanic seismicity?

To address these issues, I focus on examples from the recent eruptions of Redoubt and Okmok volcanoes in Alaska. Whereas continuous seismic correlations changed over a month prior to the eruption of Redoubt, no significant changes were observed at Okmok. Furthermore, once the eruption of Okmok was underway, unusual low-frequency continuous tremor in the VLP band (0.2–0.4 Hz) dominated the ocean-generated ambient noise. I show how to partially overcome the inability to measure ocean-related noise during an eruption by extending the ambient noise methodology to monitor the location and mechanism of volcanic tremor. From continuous seismic correlations, I find evidence for the VLP tremor source at 2 km depth BSL due to a CLVD mechanism. This is consistent with a model of a magma reservoir emptying into a shallow NW-SE trending dyke. Due to the continuous nature of the tremor, its location and mechanism can be tracked over time.

Noise Tomography and Green's Function Estimates on Erebus Volcano, Antarctica

CHAPUT, A.J., New Mexico Tech, Socorro, NM, USA, jchaput@ees.nmt.edu; ASTER, R.C., New Mexico Tech, Socorro, NM, USA, aster@ees.nmt.edu; KYLE, P.R., New Mexico Tech, Socorro, NM, USA, kyle@nmt.edu

Passive imaging in volcanic media has garnered much attention over the past few years with the development of methodologies pertaining to seismic noise and multiply scattered wavefields. In the simplest case, ambient seismic noise may be used to recover direct inter-station Rayleigh waves and infer a pseudo-3D velocity model of the volcanic edifice. In the case of particularly active volcanoes, it is also possible to make use of seismic coda as a novel and higher frequency noise source in order to recover higher resolution information about the medium of interest. Here, we make use of over 2000 Strombolian eruptions spanning 2003–2008 recorded in seismic and infrasound data from the Mount Erebus Volcano Observatory (MEVO), alongside several months of continuous ambient noise recorded on the much denser 2007–2009 broadband seismic deployment in order to infer both general velocity characteristics and more precise strong scatterer locations within Mt Erebus. Eruption coda with a hypothesized diffuse field character were bandpass filtered, aligned, and autocorrelated on 5 MEVO permanent stations, yielding high frequency Green's function estimates and a probable magma chamber location at ~600m below the lava lake.

The structural validity of small-scale variations in these Green's function estimates is bolstered by a lack of correlation with source wander within the lava lake, as inferred by infrasound-based source-semblance, and by its often anticorrelated character with respect to the variation in VLP-SP lag times (Knox et al). Rayleigh wave tomography utilizing one hour segments of ambient noise spanning several months further helps constrain the shape and location of this magmatic system, and may yield clues as to the origin of much later arrivals in the body wave Green's function estimates. This study aims at combining multiple passive approaches in a volcanic medium in order to better constrain the shape and behavior of the magmatic system.

Pulsatile Loading of Redoubt Volcano, Alaska

DENLINGER, R.P., USGS, Vancouver, Wa, USA, roger@usgs.gov; WEST, M.E., U Alaska Fairbanks, Fairbanks, AK, USA, mewest@alaska.edu; DIEFENBACH, A., USGS, Vancouver, WA, USA.

Seismicity associated with the 2009 eruption of Redoubt volcano, located near Cook Inlet, Alaska, increased markedly above background levels 20 days prior to explosive activity and continued until after extrusion of a new summit dome was complete. The frequency of earthquakes during this eruptive period often correlated to ocean tidal range. Given the volcano's close proximity to Cook Inlet and the width of the inlet, ocean tides impose a body force on the crust beneath Redoubt 100 times larger than earth tidal forces. This body force is applied over the entire crust and opposes flow of melt to the surface. After the first explosion on March 22nd, dome extrusion began. When extrusion rates were high, seismicity was 'clustered' in time: seismicity increased following each tidal-range minimum, then abruptly declined as dome growth and tidal range increased.

Seismicity clearly delineates the period during which lava extrusion occurred. Deformation data show a volume loss at depth in concert with lava extrusion, consistent with a reduction in stress at depth. Continued seismicity during extrusion is responding either to this stress drop or to flow of melt in the conduit. This seismicity correlates to ocean tides, which impose a pulsatile modulation of the pressure gradients driving melt to the surface. Such a juxtaposition of seismicity, dome growth, and pulsating load may be explained by some strain-weakening or strain-rate weakening process. We examined shear heating, melt stress relaxation, and gouge formation. Of these, gouge formation along the conduit walls exhibits strain weakening in the correct range of probable shear rates and shear strengths for existing loading conditions, and we infer this to be the most likely mechanism behind the observed relation between seismicity and ocean tides at Redoubt volcano.

Initial Results from a Temporary Seismic Array in Katmai National Park, Alaska: Velocity and Attenuation Models

MURPHY, R.A., University of Wisconsin-Madison, Madison, WI, rmurphy@geology.wisc.edu; THURBER, C.H., University of Wisconsin-Madison, Madison, WI, clifft@geology.wisc.edu; PREJEAN, S.G., USGS Alaska Volcano Observatory, Anchorage, AK, sprejean@usgs.gov

We invert data from local earthquakes occurring between August 2008 and March 2009 to determine the three dimensional (3D) P wave velocity (Vp) and attenuation structures in the Katmai volcanic region. Arrival information and waveforms for the study come from an array of 11 three-component broadband instruments deployed in the area between Mageik volcano and Katmai caldera and from the Alaska Volcano Observatory (AVO) permanent network of 20 seismometers in the region, which are predominantly single-component, short period instruments. Absolute and relative arrival times are used in a double-difference seismic tomography inversion to solve for an improved velocity model for the main volcanic centers. We use the resulting 3D velocity model to relocate catalog earthquakes in Katmai between January 1996 and August 2009. Inversions for the quality factor Q are completed using a spectral decay approach to determine source parameters, t*, and site response with a nonlinear inversion; the effect of removing instrument response is also investigated. Using the final 3D velocity model to define the ray paths, t* values are then inverted to determine frequency-independent Q models. Our previous work using only data from the AVO permanent network revealed a low velocity and low Q zone from the surface to ~7 km depth centered on the volcanic axis and extending ~25 km between Martin and Katmai volcanoes. Relocated hypocenters also provided insight into the geometry of seismogenic structures in the area. The more densely spaced temporary array data allow us to develop higher resolution Vp models that will better image the shallow magma storage areas and plumbing systems beneath Trident, Novarupta, and Katmai. We hope to identify seismic features that shed light on the magma pathways utilized or formed during the 1912 eruption.

Crustal Structure and Magma Plumbing of Newberry Volcano: A P-Wave Tomography Study

BEACHLY, M.W., University of Oregon, Eugene, OR, beachly@uoregon.edu; HOOFT, E.E.E., University of Oregon, Eugene, OR, emilie@uoregon.edu; TOOMEY, D.R., University of Oregon, Eugene, OR, drt@uoregon.edu; WAITE, G.P., Michigan Tech University, Houghton, MI, gpwaite@mtu.edu; DURANT, D.T., University of Oregon, Eugene, OR, ddurant@uoregon.edu

Newberry is a lone shield volcano in central Oregon, located ~40 km east of the Cascade axis. Newberry eruptions are silicic within the central caldera and mafic on its periphery suggesting a central silicic magma storage system, possibly located at upper crustal depths. The system may still be active with a recent eruption, ~1300 ka. Understanding the volcanic structure is important to assessing hazard and geothermal potential. A low-velocity anomaly previously imaged at 3–5 km beneath the caldera indicates either a magma body (Achauer *et al.*, 1988) or a hot pluton (Zucca and Evans, 1992).

In 2008 the University of Oregon and the USGS recorded a shot from the High Lava Plains experiment on 81 three-component seismometers along a 40 km SW-NE refraction profile across the volcano. Teleseismic events were also recorded for 14 days. We present a P-wave tomography study combining this data with (1) a 1983 USGS study that recorded 7 shots on 120 vertical-component seismometers along a 60 km E-W profile, and (2) a 1984 USGS study that recorded 12 shots on a 2 dimensional array of 120 vertical-component seismometers distributed over the top of the volcano. These combined data sets provide abundant sampling of the volcano, over a region roughly 60 km E-W, 15 km N-S, and 10 km deep.

Preliminary results from the 2008 refraction profile reveal a P-wave reflector beneath the caldera that appears to coincide with the top of the low-velocity anomaly at 3–5 km depth. The new velocity model will allow us to accurately locate this reflector as well as model its amplitude. The seismic properties of the reflector may help differentiate between an upper crustal magma body and a hot pluton. We will also obtain detailed resolution of (i) the shallow velocity structure of the caldera and (ii) a previously observed high-velocity anomaly associated with an intrusive zone west of the caldera.

Two-dimensional P-wave Velocity Model of Ross Island, Antarctica: Preliminary Results

MARAJ, S., New Mexico Tech, Socorro, NM, smaraj@nmt.edu; SNELSON, C.M., New Mexico Tech, Socorro, NM, snelson@ees.nmt.edu; KYLE, P., New Mexico Tech, Socorro, NM, kyle@nmt.edu; ASTER, R.C., New Mexico Tech, Socorro, NM, aster@ees.nmt.edu

A controlled-source seismic refraction experiment (Tomo-Erebus, TE) was undertaken during the 2008–09 Austral summer field season to examine the magmatic system beneath the active Erebus volcano (TE-3D) and the crustal structure beneath Ross Island (TE-2D). Previous geophysical studies north of Ross Island have determined the north-south trending Terror Rift within the broader Victoria Land Basin, which are part of the intraplate West Antarctic Rift System. The location of the Terror Rift near to Ross Island is unknown, as is the effect of the rift and its thin (~20 km) crust on the evolution of Ross Island volcanism.

For TE-2D, 21 seismic recorders (Ref Tek 130) with three-component 4.5 Hz geophones (Sercel L-28-3D) were deployed along a 77-km east-west line between Capes Royds and Crozier. For TE-3D, 79 similar instruments were deployed in a 3 x 3 km grid around the crater of Erebus, an array of 8 permanent short period and broadband sensors and 23 three-component sensors (Guralp CMG-40T, 30s-100 Hz) were positioned around the flanks and summit of Erebus. Fifteen chemical sources ranging from 75 to 600 kg of ANFO were used. An additional shot was detonated in the sea (McMurdo Sound) using 200 kg of dynamite. Although the station spacing is ~5 km, the data have a high signal to noise ratio with clear first arrivals and wide-angle reflections across the array. A raytracing program, MacR1D, was used to develop 1-D P-wave velocity models by matching layers of known velocities with the P-wave first arrival times. 1-D velocity models were developed for 3 sources and show ~3 layers with a velocity of ~7 km/s below 6–8 km depth. The 1-D models were used as the starting model for the P-wave tomographic velocity model. These results will be used to ascertain the role of Ross Island within the Terror Rift.

Recent Advances in Source Parameters and Earthquake Magnitude Estimations

Oral Session · Friday 8:30 AM, 23 April · Salon E
Session Chairs: Domenico Di Giacomo and George L. Choy

IASPEI Standard Magnitudes At The U.S. Geological Survey/National Earthquake Information Center

DEWEY, J.W., U.S. Geological Survey, Denver, CO, dewey@usgs.gov; BRYAN, C.J., Bryan Geophysical LLC, Vancouver, WA, cj_bryan@hotmail.com; BULAND,

R.P., U.S. Geological Survey, Denver, CO, buland@usgs.gov; BENZ, H.M., U.S. Geological Survey, Denver, CO, benz@usgs.gov

The U.S. Geological Survey/National Earthquake Information Center (USGS/NEIC) is testing algorithms for automatic computation of earthquake magnitudes following standard procedures that have been adopted by the IASPEI Commission on Seismological Observations and Interpretation. The USGS/NEIC will calculate short-period body-wave magnitude *mb* using P-wave amplitudes and periods measured through a short-period filter that replicates WWSSN-SP response and that is slightly different than the short-period filter currently in use at the USGS/NEIC. *mb(IASPEI)* computed in these USGS/NEIC tests are on average larger by about 0.1 magnitude units than the *mb* computed with the currently used filter. The IASPEI procedure for determining *Ms_20*, *Ms* measured from teleseismic Rayleigh waves having periods within a few seconds of 20s, is identical with the procedure currently used by the USGS/NEIC to compute *Ms*. New for the USGS/NEIC are two magnitudes determined from maximum velocities recorded on velocity proportional seismographs: *mB_BB*, measured from phases with periods of 0.2s–30s in the P-wavetrain, and *Ms_BB*, measured from phases with periods of 3s–60s in the Rayleigh wavetrain at regional and teleseismic distances. *mB_BB* shows promise as a rapid estimator of moment-magnitude (*Mw*) that does not require inversion for source-mechanism and that is less prone than *mb* to saturation at high *Mw*. *Ms_BB* is of interest as an estimator of *Ms* from observations at regional distances. Also new for the USGS/NEIC data base will be inclusion of measurement times of the maximum amplitudes used in magnitude calculations. The magnitudes and associated amplitudes, periods, and measurement-times jointly provide multi-faceted perspectives of earthquake sources that supplement descriptions of the sources that are based on waveform modeling.

Estimating Source Parameters of Small-To-Medium Sized Earthquakes Using a Multi-Objective Optimisation Approach

HEYBURN, R., AWE Blacknest, Brimpton Common, Reading, Berkshire, U.K., ross@blacknest.gov.uk; BOWERS, D., AWE Blacknest, Brimpton Common, Reading, Berkshire, U.K., bowers@blacknest.gov.uk; FOX, B., AWE Blacknest, Brimpton Common, Reading, Berkshire, U.K., ben.fox@rms.com

In detailed seismological studies of small-to-medium sized ($4 < mb < 5.5$) earthquakes of special interest, observations from several different types of seismic data can be analysed to obtain reliable estimates of the source parameters (*e.g.* source depth, source mechanism, M_0). The advantages of using several different data types are that the source parameters can be better constrained, and potential trade-offs between source parameters can be resolved. A method of source parameter estimation by joint inversion of surface-wave data and teleseismic body-wave data has been developed and is tested on several earthquakes located in a range of tectonic settings. Teleseismic body-wave data are inverted using the Gaussian relative amplitude method, and the surface-wave data are either inverted by modeling surface-wave amplitude spectra, or by modeling waveform data at a near-regional station. Results from the inversion of each individual data set are combined using a multi-objective optimisation approach. Source parameters obtained using this approach are evaluated by calculating and comparing synthetic seismograms with the observed data. The good fit of the synthetic seismograms to the observed seismograms for many of the earthquakes analysed suggests that the method is a useful way of estimating the source parameters of small-to-medium sized earthquakes. The method is also useful for resolving the well-known trade-off between depth and M_0 from inversions of surface wave data.

Application of Regional Body-Wave Magnitude Scales to Earthquakes in a Continental Margin

HONG, T.K., Yonsei University, Seoul, South Korea, tkhong@yonsei.ac.k.r; LEE, K., Yonsei University, Seoul, South Korea.

Continental margins are encompassed by plate boundaries that naturally accompany high seismicity due to plate collision and subduction. Offshore events occur frequently around the continental margins. The offshore events are potential generators of destructive tsunamis. Accurate measurement of magnitudes of such events is highly demanded for prompt responses to potential tsunamis. However, the continental margins accompany complex crustal structures due to active tectonics. Body-wave magnitudes are widely used to quantify the sizes of regional and teleseismic earthquakes. Regional body-wave magnitudes are typically based on Pn and Lg waves. Regional body waves are significantly influenced by complex crustal structures. For instance, Lg waves are strongly attenuated in such laterally-varying crusts. The region around the Korean Peninsula and Japanese islands belong to a eastern margin of the Eurasian Plate. A paleo-rifted backarc region is located between the Korean Peninsula and Japanese islands. Earthquakes in the region are well observed in dense seismic networks in Korea and Japan. We investigate mb(Pn) and mb(Lg) for the events in the region. We examine the limitation and applicability of the regional body-wave scalings by comparing the magnitude estimates with reported magnitudes of local institutes. The mb(Lg) scaling yields reasonable estimates even for offshore events. The mb(Pn) magnitudes appear to be influenced by local geology in station sites.

Automatic Computation of Moment Magnitudes for Small Earthquakes and the Scaling of Local to Moment Magnitude

EDWARDS, B., Swiss Seismological Service, Zurich, Switzerland, edwards@sed.ethz.ch; ALLMANN, B., Swiss Seismological Service, Zurich, Switzerland, allmann@sed.ethz.ch; CLINTON, J., Swiss Seismological Service, Zurich, Switzerland, clinton@sed.ethz.ch; FAEH, D., Swiss Seismological Service, Zurich, Switzerland, faeh@sed.ethz.ch

Moment magnitudes are computed for small and moderate earthquakes using a spectral fitting method. The resulting MW are compared with those from broadband moment tensor solutions and found to match with negligible offset and scatter for available MW values of between 2.8 and 5.0. Using the presented method MW are computed for earthquakes in Switzerland with a minimum ML = 1.3. A combined bootstrap and orthogonal L1 minimization is then used to produce a scaling relation between ML and MW. The scaling relation has a polynomial form and is shown to reduce the dependence of the predicted MW residual on magnitude relative to an existing linear scaling relation. The computation of MW using the presented spectral technique is fully automated at the Swiss Seismological Service, providing real-time solutions within a few minutes of an event through a web based XML database. The scaling between ML and MW is explored using synthetic data computed with a stochastic simulation method. It is shown that the scaling relation can be described by the interaction of Q, the stress drop and the Wood-Anderson filter. Furthermore, it is shown that the stress drop controls the saturation of the ML scale, with low-stress drops (*e.g.*, 0.1–1.0MPa), characteristic of Swiss earthquakes, leading to saturation at magnitudes as low as ML = 3–4. It is found that a high stress-drop or one that increases with seismic moment is required in order to scale ML and MW in Switzerland.

Regional Variations in Apparent Stress Scaling From Coda Envelopes

MAYEDA, K., Weston Geophysical, Lexington, MA, USA, kmayeda@yahoo.com; MALAGNINI, L., INGV, Rome, Italy, malagna@ingv.it

Within broad regions it is likely that apparent stress varies with location due to lateral variations in regional stress field, rheology, and degree of tectonic activity. A new, state-of-the-art coda ratio methodology has been applied to a variety of tectonic regions and we find clear distinctions between each of them. The methodology outlined in Mayeda *et al.* (2007) has been successfully applied to a number of moderate-to-large earthquake sequences in Japan (*e.g.*, Fukuoka, Iwate, Niigata, Miyagi, Tottori), Chi-Chi, Taiwan; Hector Mine, CA; San Giuliano, Italy; Colfiorito, Italy; and Wells, Nevada. An increase in scaling with increasing moment is observed for all sequences and the absolute levels appear to correlate with the degree of fault maturity. The coda methodology allows for very precise average estimates of both Brune stress drop as well as apparent stress that are free of radiation pattern, directivity, path, and site response effects. Due to the large numbers of broadband data for each of the sequences, we have ample redundancy.

Comparisons of Different Teleseismic Magnitude Estimates from Global Earthquake Datasets and Assessment of Influence of Site and Propagation Effects

DI GIACOMO, D., GFZ Potsdam, Potsdam, Germany, domenico@gfz-potsdam.de; PAROLAI, S., GFZ Potsdam, Potsdam, Germany, parolai@gfz-potsdam.de; BORMANN, P., GFZ Potsdam, Potsdam, Germany, pb65@gmx.net; SAUL, J., GFZ Potsdam, Potsdam, Germany, saul@gfz-potsdam.de; BINDI, D., INGV Milano-Pavia, Milano, Itlay, bindi@mi.ingv.it; WANG, R., GFZ Potsdam, Potsdam, Germany, wang@gfz-potsdam.de; GROSSER, H., GFZ Potsdam, Potsdam, Germany, gros@gfz-potsdam.de

The magnitude of an earthquake is one of the most used parameters to evaluate the earthquake's damage potential. Moreover, rapid and sufficiently accurate earthquake magnitude determinations are required by disaster management organizations to guide postseismic emergency actions. However, many magnitude scales have been developed over years and each magnitude scale has its own meaning. This contribution shows the comparisons for a global dataset (about 770 earthquakes) among some of the classical magnitude scales (*Ms*, *mb* and *mB*) and the modern and non-saturating moment and energy magnitude (*Mw* and *Me*, respectively) determinations. One of the main focus is the comparisons of our rapid *Me* determinations with both *Mw* obtained by the well-established procedure of the Global Centroid Moment Tensor project and other magnitude estimations. Our procedure is based on the correction for the various propagation effects by pre-calculated spectral amplitude decay functions. The latter are computed from numerical simulations of Green's func-

tions of P-waves in the distance range 20°–98° given the average global Earth model AK135Q. As our procedure is intended to work without knowledge of the source geometry, we will discuss our results by dividing the analyzed earthquakes in different fault plane solution classes. In addition, the need and the importance of complementing the information provided by different magnitude estimates (with special emphasis to *Mw* and *Me*) is outlined with representative case studies. Finally, we show the results of the analyses based on the random effect model of our *Me* residuals for about 40000 single station *Me* determinations. Such analyses allow us to quantify the effect of the station site on teleseismic P-waves signals in the period range 1–80 s, and also to identify source-to-receiver paths with distinct residual patterns.

A Report Card on Real-Time Estimators of Seismic Sources

OKAL, E.A., Northwestern University, Evanston, IL USA.

In the framework of real-time tsunami warning, we analyze critically a number of simple, yet robust, algorithms quantifying various properties of the seismic source of large- to mega-earthquakes. These include (i) the mantle magnitude M sub m, introduced by Okal and Talandier in 1988; (ii) the energy-to-moment ratio and slowness parameter THETA introduced by Newman and Okal in 1998, in the footsteps of the work of Boatwright and Choy [1986]; and the parameter Tau-1/3 [Reymond *et al.*, 2006], characterizing the duration of very high-frequency P-waves.

We also examine independent algorithms such as Mwp pioneered by Tsuboi, and widely used at the warning centers, and W-phase inversion, as developed by Kanamori and Rivera, and for which we propose a magnitude approach, WMm. We also investigate a duration test by combining Tau-1/3 to an energy estimate. We use a dataset of about 70 earthquakes recorded digitally in the past 20 years to address several questions: What is the general level of performance of such methods? Can we identify systematic shortcomings and can they be explained theoretically? Are truly gigantic earthquakes (*e.g.*, Sumatra 2004) correctly assessed? Are anomalous events (such as the so-called "tsunami earthquakes"— Nicaragua, 1992; Java 1994, 2006) routinely identifiable?

In particular, we document a systematic bias between results of the Mwp algorithm and source slowness, and question several aspects of the implementation of that algorithm, especially in the time domain. Among the remaining challenges faced in field of real-time assessment of seismic sources, we earmark the case of "delayed" sources, whose source time history picks up after a significant delay, such as during the earthquakes of 2001 in Peru, and to a lesser extent 2006 in the Kuril Islands.

Developing Real-Time Magnitude Estimation Using a Damped Predominant Period Function, Tpd, Applied to Data from the Hellenic Seismological Broadband Network (Operated by the Institute of Geodynamics, National Observatory of Athens, NOA)

LODGE, A., University of Liverpool, Liverpool/UK, a.lodge@liverpool.ac.uk; BOUKOURAS, K., Institute of Geodynamics, NOA, Athens/Greece, kbouk@gein.noa.gr; RIETBROCK, A., University of Liverpool, Liverpool/UK, A.Rietbrock@liverpool.ac.uk; MELIS, N., Institute of geodynamics, NOA, Athens/Greece, nmelis@gein.noa.gr

For the earliest possible measures of earthquake magnitudes after the occurence of large earthquakes, methods must concentrate on information in the first P-wave arrivals. In recent years a great deal of interest has been stimulated by attempts to use a time-domain estimate of the predominant period of a waveform, to estimate seismic magnitude from the very first P-wave arrivals in seismograms. Using an aftershock dataset of over 1500 events (ML = 0.7–5.8), Hildyard and Rietbrock (in press), study the relationship between magnitude and the damped predominant period calculated from the inital P-wave arrival. Initially they investigate previously published techniques, specifically Tpmax (Nakamura, 1988; Allen and Kanamori, 2003) and tc (Kanamori, 2005). However, for this dataset, neither of these functions show a strong trend. Thus they develop a modified, damped version of the Tp function, which they call Tpd. The performance of Tpdmax is demonstrated to be superior to that of both Tpmax and tc. Here we apply the Tpd magnitude estimation technique to data from Greece (NOA). Initially we use data from 2001–2008 to determine the trend between Tpdmax and magnitude. We then use the playback function of SeisComP3 on selected events from 2009 over magnitude 3.4 to estimate the magnitude of these events in 'real-time' from the NOA data.

Rapid Centroid Moment Tensor (CMT) Inversion in 3D Earth Structure Model for Earthquakes in Southern California

LEE, E., Dept. of Geology and Geophysics, Laramie, WY, U.S.A., elee8@uwyo.edu; CHEN, P., Dept. of Geology and Geophysics, Laramie, WY, U.S.A.; JORDAN, T.H., Dept. of Earth Sciences, Los Angeles, CA, U.S.A.; MAECHLING, P.J., Dept. of Earth Sciences, Los Angeles, CA, U.S.A.

Accurate and rapid CMT inversion is important for seismic hazard analysis. We have developed an algorithm for very rapid CMT inversions in a 3D Earth structure model and applied it on small to medium-sized earthquakes recorded by the Southern California Seismic Network (SCSN). Our CMT inversion algorithm is an integral component of the scattering-integral (SI) method for full-3D waveform tomography (F3DT). In the SI method for F3DT, the sensitivity (Fréchet) kernels are constructed through the temporal convolution between the earthquake wavefield (EWF) from the source and the receiver Green tensor (RGT) from the receiver. In this study, our RGTs were computed in a 3D seismic structure model for Southern California (CVM4SI1) using the finite-difference method, which allows us to account for 3D path effects in our source inversion. By storing the RGTs, synthetic seismograms for any source in our modeling volume could be generated rapidly by applying the reciprocity principle. An automated waveform-picking algorithm based on continuous wavelet transform is applied on observed waveforms to pick P, S and surface waves. A grid-searching algorithm is then applied on the picked waveforms to find an optimal focal mechanism that minimizes the amplitude misfit and maximize the weighted correlation coefficient. The grid-search result is then used as the initial solution in a gradient-based optimization algorithm that minimizes the L2 norm of the generalized seismological data functionals (GSDF), which quantifies waveform differences between observed and synthetic seismograms using frequencies-dependent phase-delay and amplitude anomalies. In general, our CMT solutions agree with solutions inverted using other methods and provide better fit to the observed waveforms.

Characteristics of the Earthquake Environment Inferred from Global Variations in Modern Magnitudes

CHOY, G.L., U. S. Geological Survey, Denver, CO 80225, USA, choy@usgs.gov; KIRBY, S.H., U. S. Geological Survey, Menlo Park, CA 94025, skirby@usgs.gov

In the pre-digital era, measures of earthquake size were often derived by first computing a magnitude and then applying an empirical formula. In contrast, modern methods first measure earthquake size which is then used to derive a magnitude. Mw (moment magnitude), for instance, is derived from the low-frequency asymptote of displacement while Me (energy magnitude) is computed directly from the broadband velocity spectrum. A teleseismic study of more than 1500 shallow earthquakes (Me > 5.5 and depth < 70 km) that occurred from 1987 to 2008 found considerable variability between Me and Mw. The global distributions of anomalously energetic and enervated events turn out to be non-random and may provide insight into variation of seismogenic conditions. Energetic earthquakes (radiating anomalous high energy as measured by Mw-Me < –0.2 or apparent stress > 1.0 MPa) are intraplate and intraslab earthquakes largely confined to specific high-deformation tectonic settings, an observation which can lead to improving estimates of seismic hazard potential. Along subduction-plate boundaries, energetic events occur in high-deformation regimes such as marine collision zones, submerged continent-continent collisions, and regions of slab distortion. Enervated earthquakes, those radiating anomalously low energy as measured by Mw-Me > 0.5, are found in three regimes not all of which are tsunamigenic. Class I are large (M > 7.5) located near sediment poor trench axes and have been associated with tsunami earthquakes involving slow rupture. Class II are smaller events deeper and further from the trench axis at sediment rich subduction zones. Class III are events downdip of subducted fracture zones and ridges which may provide the mechanism to transport sediments down the plate interface.

Toward a Moment Magnitude Catalog for Earthquake Hazard Assessment in Eastern Canada

BENT, A.L., Geological Survey of Canada, Ottawa, Ontario, Canada, bent@seismo.nrcan.gc.ca

Several earthquake magnitude scales are reported in the Canadian National Earthquake Database (CNDB) with the preferred magnitude generally being a function of earthquake size and location. Because magnitude recurrence rates are the primary parameter used in earthquake hazard assessment, using a variety of magnitude scales leads to the possibility that hazard estimates are dependent on the choice of scale and may not be uniform across the country. Using a single magnitude scale for all earthquakes ensures the uniformity of the hazard estimates with Mw being the preferred scale. Work has been undertaken to determine reliable Mw's for earthquakes in eastern Canada. The largest 150 earthquakes in the CNDB that met the criteria for completeness for use in hazard assessment were evaluated on an individual basis using all available data to determine Mw. For the smaller earthquakes conversion relations for m_N and M_L were established. The m_N-Mw conversion was established by collecting information for all eastern Canadian earthquakes for which both were available. A simple conversion applying a constant was found to be acceptable. More complex relations were explored but not found to be a statistically significant improvement. A complexity stemmed from the observation that the conversion appears to be time dependent changing by 0.1 magnitude units (from 0.4 to 0.5) around 1995. This date had previously been noted as a time when several factors (station numbers, instrument types, average frequency, analysis package)

which could affect magnitude changed and is being studied in more depth. There were few earthquakes for which both M_L and Mw were available but enough data to establish an M_L-m_b conversion. Again, a constant (0.45) was found to be as good as more complex relations. The m_b's are then converted to MW using global relations.

Tsunami Early Warning Using Earthquake Rupture Duration and Predominant Period: The Importance of Length and Depth of Faulting

LOMAX, A., ALomax Scientific, Mouans-Sartoux, France, anthony@alomax.net; MICHELINI, A., Istituto Nazionale di Geofisica, Rome, Italy, michelini@ingv.it

After an earthquake, rapid assessment of hazards such as tsunami potential is important for early warning and emergency response. Tsunami potential depends on sea floor displacement, which is related to the length, L, width, W, mean slip, D, and depth, z, of earthquake rupture. Currently, the primary discriminant for tsunami potential is the centroid-moment tensor magnitude, MwCMT, representing the product LWD, estimated through an indirect, inversion procedure. The obtained MwCMT and implied LWD value vary with rupture depth, earth model and other factors, and is only available 30 min or more after an earthquake. The use of more direct procedures for hazard assessment could avoid these problems and aid in effective early warning.

We present a direct procedure for rapid assessment of earthquake tsunami potential using two, simple measures on P-wave seismograms—the predominant period on velocity records, TauC, and the likelihood that the high-frequency, apparent rupture-duration, T0, exceeds 50–55 sec. TauC and T0 are related to the critical parameters L, W, D and z. For a set of large earthquakes, the period-duration product TauC.T0 gives more information on tsunami impact and size than MwCMT and other current discriminants. All discriminants have difficulty in assessing the tsunami potential for strike-slip and back-arc, intraplate earthquakes. Our results suggest that tsunami potential is not directly related to the product LWD from the "seismic" faulting model, as is assumed with the use of the MwCMT discriminant. Instead, knowledge of rupture length, L, and depth, z, alone can constrain well the tsunami potential of an earthquake, with explicit determination of fault width, W, and slip, D, being of secondary importance. With available real-time seismogram data, rapid calculation of the direct, period-duration discriminant can be completed within 6–10 min after an earthquake occurs and thus can aid in effective and reliable tsunami early warning.

Recent Developments in Source Inversion by Using the W-phase

RIVERA, L., IPGS - UdS/CNRS, Strasbourg, France, luis.rivera@unistra.fr; DUPUTEL, Z., IPGS - UdS/CNRS, Strasbourg, France, zacharie.duputel@eost.u-strasbg.fr; KANAMORI, H., Seismological Lab., California I, Pasadena, California, U.S.A., hiroo@gps.caltech.edu

Rapid estimation of the source parameters of large earthquakes is a growing field of interest. It is useful for both emergency response and rapid scientific study and it has been recently boosted by the increasing volume of real time seismological data.

Robust estimation of the source of large earthquakes is mainly limited by data saturation, time and space complexity of the source process and overlapping of different phases.

We have recently developed a source inversion algorithm using W-phase at regional and/or teleseismic distances. W-phase is a very long period phase (100s–1000s) arriving at the same time as the P-wave. When the displacement seismograms are filtered between 100s and 1000s, it is conspicuous between the P wave and the surface waves. Because of its long period nature and because it precedes the large amplitude surface-wave arrivals, the W-phase has a high potential to provide rapid and reliable estimates of the overall source parameters of large events.

In the last two years, several international collaborations have been established to use the algorithm online either at global or at regional scale. Examples of such implementations are at NEIC, ERI (Japan), PTWC (Hawaii), UNAM (Mexico), BATS (Taiwan), and Geosciences Australia.

Recent developments lead to the use of the three components of displacement. Also, to maximize the S/N ratio while dealing with the background noise which typically increases with period, we use an adaptive filter depending on the preliminary magnitude. The screening of data was also refined by measuring the ambient seismic noise level of each trace within a few hours preceding the earthquake.

Besides the standard application, the simplicity and versatility of the algorithm make it suitable for diverse applications ranging from routine data quality control to the study of earthquakes with complex source process.

Rapid Determination of Large Earthquakes Moment Magnitude, Focal Mechanism, and Source Time Functions Inferred from Body-Wave Deconvolution

VALLÉE, M., Geoazur,IRD, University of Nice, France, vallee@geoazur.unice.fr; CHARLÉTY, J., Geoazur, University of Nice, France, charlety@geoazur.unice.fr; FERREIRA, A.M.G., University of East Anglia, Norwich, U.K., A.Ferreira@uea.ac.uk; DELOUIS, B., Geoazur, University of Nice, France, delouis@geoazur.unice.fr; VERGOZ, J., LDG-CEA, Paris, France, Julien.VERGOZ@CEA.FR

Accurate and fast magnitude determination of large superficial earthquakes is an important information for postseismic response and tsumami alert purposes. When no local real-time data is available - which is today the case of most subduction earthquakes -, the first information comes from teleseismic body waves. Standard body-wave methods give accurate magnitudes for earthquakes up to Mw=7–7.5. For larger earthquakes, the analysis is more complex, because of the non-validity of the point-source approximation. We propose here an automated deconvolutive approach, which does not impose the simplicity of the rupture process, and is therefore well adapted to large earthquakes. First we determine the source duration based on the length of the high frequency (1–3Hz) signal content. The deconvolution of the synthetic double-couple point source signals - depending on the four parameters strike, dip, rake, depth - from the windowed body-wave signals (including P, PcP, PP, SH and ScS waves) gives the apparent source time function. We search the optimal combination of these four parameters able to respect the physical features of any source time function: causality, positivity and stability of the seismic moment at all stations. Once retrieved this combination, the integration of the source time functions directly gives the moment magnitude. The present approach, referred as the SCARDEC method, has been applied to most of the major subduction earthquakes in the period 1990–2009. Magnitude difference between Global CMT and SCARDEC method may reach 0.2, but values are found consistent if we take into account that large earthquakes Global CMT solutions suffer from a known trade-off between dip and seismic moment. We show by forward modelling that the source parameters retrieved by body waves explain the surface waves as well as the Global CMT parameters.

Ms vs. Mw for Italian Earthquakes: Focus on the L'aquila Earthquake Series

BONNER, J.L., Weston Geophysical Corp., Lexington, MA, bonner@westongeophysical.com; HERRMANN, R.B., St. Louis University, St. Louis, MO, rbh@eas.slu.edu; MALAGNINI, L., INGV, Rome, Italy, malagnini@ingv.it; STROUJKOVA, A., Weston Geophysical Corp., Lexington, MA, ana@westongeophysical.com

We derive a relationship between moment magnitude (Mw) and surface wave magnitude (Ms) for earthquakes occurring in Italy, with a primary focus on the L'Aquila earthquake (6 April 2009 Mw 6.1) and its aftershocks. We used the Russell (2006; Bonner *et al.*, 2006) variable-period surface wave magnitude formula, henceforth called Ms(VX), to estimate the Ms for 125 Italian earthquakes with 2.8 < Mw < 6.1 at distances ranging from 50 to 414 km. We applied the technique to Rayleigh and Love waves, resulting in 1449 and 1142 magnitude estimates, respectively. The network-averaged magnitudes show that most of the events (80%) had a Love-wave Ms that was larger (average 0.2 m.u.) than the Rayleigh-wave estimate. The larger Love-wave magnitudes are somewhat unexpected for the normal fault focal mechanisms (Herrmann and Malagnini, 2009) of the L'Aquila sequence. We observe larger interstation standard deviation for the Love-wave magnitudes (0.2 m.u.) than for Rayleigh waves (0.17 m.u). Residual Ms(VX) estimates (*e.g.*, station minus network average) show no significant distance dependence on the magnitudes; however, there is a clear azimuthal effect on the Rayleigh-wave station residuals. The largest residuals are observed at azimuths parallel and perpendicular to the predominant strike (~330°) of the events. An azimuthal effect on the Love waves is less obvious. The interstation standard deviations can be reduced by ~15% by correcting for azimuthal effects.

Mw estimated from broadband waveform modeling were regressed against Ms(VX). Mw can be estimated from Ms(VX) and Rayleigh waves using the relationship: Mw=1.79 + 0.67*Ms(VX) for 2< Ms <6, while for Love waves, the relationship is Mw=1.66 + 0.68*Ms(VX). These relationships are similar to the Rayleigh-wave equation for North America [Mw=1.95 + 0.65*Ms(VX)] derived by Bonner *et al.* (2008) for many different focal mechanisms.

Source Parameters of Nanoseismicity Recorded at Mponeng Deep Gold Mine, South Africa: Implications for Scaling Relationships

KWIATEK, G., GFZ Potsdam, Potsdam, Germany, kwiatek@gfz-potsdam.de; PLENKERS, K., GFZ Potsdam, Potsdam, Germany, plenkers@gfz-potsdam.de; DRESEN, G., GFZ Potsdam, Potsdam, Germany, dre@gfz-potsdam.de; JAGUARS GROUP.

We investigate the source parameters of nanoseismic events (M_W>−3.0) recorded with a high-sensitivity seismic network at Mponeng gold mine, South Africa. The network, composed of one 3-component accelerometer (50Hz to 25kHz) and 8 acoustic emission sensors (700Hz to 200kHz) is located at a depth of 3543m and covers the limited volume of approx. 300x300x300m. The acoustic emission sensors are calibrated relative to the 3-component accelerometer in the lower frequency band (f<25kHz). The waveform data is used to analyze the source characteristics

of two datasets: (1) post-blasting activity recorded during working days, located more than 80m from the network at the stope level and (2) aftershock sequence of a M_W1.9 event that occurred approx. 30 m from our network. The calculated values of M_W ranged from −0.5 to −4.0 with corner frequencies 0.5–15kHz (source sizes from 10m to a few centimeters). We observe high static stress drop release ranging 1–100MPa with apparent stress 0.5MPa–50MPa. We search for differences in seismic source characteristics between the two datasets by comparing the calculated seismic moments, source radii, S-to-P energy ratios, dynamic and static stress drops and other derived source parameters. The study aims to give new insights into the ongoing discussion if a breakdown of scaling is present for seismic events with small magnitude.

Empirical Relations Between Radiated Seismic Energy and Source Dimension

CHESNOKOV, E.M., University of Houston, Houston, TX, USA, emchesno@mail.uh.edu; KING, J., University of Houston, Houston, TX, USA, jdking@uh.edu; ABASEYEV, S.S., University of Houston, Houston, TX, USA, s_abaseyev@yahoo.com

Scaling between small and large earthquakes is an unanswered question of mechanics. The self-similarity of earthquakes with respect to size has been recently considered in numerous empirical studies. We examine the self similarity of earthquakes using radiated seismic energy and rupture size to develop empirical functions relating large and small events. The source parameters of a large number of microseismic events observed during hydraulic stimulation of north Texas gas shale reservoirs were studied. These data are compared to published empirical results to determine empirical relations between radiated seismic energy and source dimension. Energy was calculated using maximum P and S wave amplitudes normalized to perforation shot radiated energy. Source dimension was calculated following the corner frequency method of Brune [1970].These results suggest that the apparent stress drop is not self consistent between the smallest of the induced events and those events with magnitude larger than zero. There is however a clear trend linking the smallest events (1E−2 Joules) to the largest (1E18 Joules) from previous studies.

Further Development of the Cepstral Stacking Method (CSM) for Accurate Determinations of Focal Depths for Earthquakes and Explosions

ALEXANDER, S.S., Penn State University, University Park, PA 16801, shel@geosc.psu.edu; CAKIR, R., WA State Dept. of Nat'l. Res., Olympia, WA 98501, recep.cakir@dnr.wa.gov

The Cepstral Stacking Method (CSM) that was developed initially by one of the authors (Alexander) has been shown to give focal depths accurate typically to within 1 km for earthquakes and explosions observed at regional distances. Only one regional station with good frequency bandwidth and good S/N in the P to S signal interval is required. CSM estimates can be made in near-realtime for active monitoring or anytime for past events. Examples will be presented from past applications for discriminating earthquakes from explosions, determining minimum depth vs magnitude for eastern North America where no surface faulting is observed, identifying active faults and their surface projection when focal mechanisms are available, and constraining active fault geometry and dynamics by comparing mainshock focal depths with their aftershocks' depths.

Given the growing number of regional networks and local arrays in operation globally, the CSM has been extended to take advantage of either or both of these types of additional regional observations of earthquakes and explosions. Network stacking of individual station CSM outputs can improve the ability to obtain accurate pP and sP delay times and both network stacking and array stacking allow reliable depths to be determined for small events with marginal S/N levels. Examples showing the improvements from these additional CSM approaches will be presented.

Subsurface Imaging for Urban Seismic Hazards at the Engineering Scale

Oral Session · Friday 8:30 AM, 23 April · Salon F
Session Chairs: John N. Louie and William J. Stephenson

New Technique to Invert 1-D Soil Structure Based on the Site Information with Similar Amplification Characteristics

KAWASE, H., DPRI, Kyoto University, Uji/Kyoto/Japan, kawase@zeisei.dpri.kyoto-u.ac.jp; KURIBAYASHI, K., Japan Eng. Consultants Co. Ltd., Tokyo/Japan, kuribayashi-ke@ej-hds.co.jp

To predict strong ground motions for future scenario earthquakes, we need to characterize three factors, namely, source spectra, path attenuation, and local site amplification. For local site amplification we would like to have an S-wave velocity structure at a target site. In this study we first try to separate the so-called source spectra, attenuation coefficient, and site amplification factors from K-Net, KiK-net, and JMA records observed throughout Japan. As a reference site we use one very hard rock (Vs=3.45 km/s) station of KiK-net. Once we obtain linear site amplification factors for weak to moderate ground motions less than 200 Gals in terms of PGA, we use site amplification factors to invert one-dimensional S-wave velocity structures below each site based on the initial models of available boring data and a GA inversion technique. We found at about 55% of the K-Net and KiK-net sites we can successfully invert S-wave velocity structures from the surface to the seismological bedrock. Since JMA sites do not have any geological information, for JMA sites as well as for the remaining 45% of K-Net and KiK-net sites with not-so-good matching we introduce a new technique. First we find three sites among the sites with good matching where the derived site amplification factors are similar to each other. Then by using the 1-D structures of these similar sites as initial models we perform S-wave velocity inversion for the target site. As a result, we find good matching at about 80% of JMA sites and 75% of the K-Net and KiK-net sites with not-so-good matching in the first place. Thus we can conclude that the proposed technique can derive 1-D structures that can explain observed site amplification factors with high probability. The proposed technique may succeed because additional constraints from similar sites contribute to stabilize the inversion. However, still we need to prove that our inverted structure be surely the structure at the site.

Shear-wave Velocity Model of the Santiago de Chile Basin Derived from Ambient Noise Measurements for Simulations of Ground Motion

PILZ, M., Helmholtzzentrum Potsdam - GFZ, Potsdam, Germany, pilz@gfz-potsdam.de; PAROLAI, S., Helmholtzzentrum Potsdam - GFZ, Potsdam, Germany, parolai@gfz-potsdam.de; PICOZZI, M., Helmholtzzentrum Potsdam - GFZ, Potsdam, Germany, picoz@gfz-potsdam.de; ZSCHAU, J., Helmholtzzentrum Potsdam - GFZ, Potsdam, Germany, zschau@gfz-potsdam.de; additional affiliation of author 1: Institution: University Potsdam, Department for Geosciences City/State/Country: Potsdam, Germany

Although the most intense shaking during an earthquake generally occurs near the rupture fault the shaking at one site can easily be several times stronger than at another site, even when their distance from the rupture fault is the same. Such site effects are mainly caused by the softness of the soil near the surface and by the thickness of the sediments above hard rock.

Measurements of seismic noise at 146 sites have been carried out in the northern part of Santiago de Chile first to determine the fundamental resonance frequency of the sites and then to invert the horizontal-to-vertical (H/V) spectra individually, considering additional geological and geophysical information as constraints, for estimating local S-wave velocity profiles which were found to vary substantially over short distances in the investigated area. The resulting 3D model was derived for a 26 km x 12 km area by interpolation between the single S-wave velocity profiles and shows good agreement with the few existing velocity profiles but allows to image the entire area as well as deeper parts of the basin in much more detail than before.

Using the highly variable S-wave velocity-depth gradient and the high-resolution surface and bedrock topography of the investigated area, we simulated 3D seismic wave propagation by means of a spectral element method. For the scenario events, we focus on the San Ramón fault, a multi-kilometric frontal thrust, crossing the eastern outskirts of the city. A conservative estimate of the rupture with well-constrained hypocenters down to 15 km depth under the Principal Cordillera yields events of magnitude Mw 6.9 to Mw 7.4. Our results indicate that peak ground velocity can vary significantly on small scale due to site and topographic effects, hence allowing identifying areas which are particularly endangered.

Estimating Dynamic Strain Amplitudes Beneath Mobile Shakers

MENQ, F.-Y., The University of Texas @ Austin, Austin, TX, USA, fymenq@mail.utexas.edu; COX, B., The University of Arkansas, Fayetteville, AR, USA, brcox@uark.edu; STOKOE, K.H., The University of Texas @ Austin, Austin, TX, USA, k.stokoe@mail.utexas.edu

With the large-scale mobile shakers available at the Network for Earthquake Engineering Simulation (NEES) Texas Equipment Site, nonlinear shear modulus measurements of soil and cyclic loading tests leading to liquefaction can be conducted in-situ. Prior to performing these types of tests in the field, it is desirable to estimate the shear strain amplitude the shakers can induce as a function of depth. Rigorous numerical methods may be used for estimating the strain distribution beneath the shakers. However, these methods require a significant number of parameters not known in advance of field work. A simplified prediction method has been developed in this work and verified with data from previous field measurements. There are five steps in this method: (1) determine the stress at the depth of interest using a vertical-to-horizontal ratio of 2-to-1 to distribute the force applied

at the ground surface, (2) estimate the small-strain shear modulus of the soil at the depth of interest, (3) calculate shear strain from the estimated shear stress and shear modulus, (4) update the shear modulus for the shear strain calculated in the previous step using a nonlinear soil model in an equivalent-linear fashion, and (5) repeat steps 3 and 4 until convergence. This method for predicting strain amplitude beneath the base plate of a mobile shaker has been evaluated using a series of in-situ nonlinear tests conducted on sandy soil in a manner similar to the procedures described in Cox *et al.* (2009a and 2009b). The model proposed by Menq (2003) was used to estimate the shear moduli of the sand. Using the steps described above, it was found that the estimated shear strains were within a factor of two from the measured shear strains. Considering that shear strain is typically displayed on a log scale, this level of accuracy is adequate in the design stage of field studies.

Earthquakes in Southern Nevada Project: A Summary of Findings to Date

SNELSON, C.M., Dept of Earth and Env Sci, NMT, Socorro, NM 87801, snelson@ees.nmt.edu; TAYLOR, W.J., Applied Geophysics Center, UNLV, Las Vegas, NV 89154, wanda.taylor@unlv.edu; LUKE, B., Applied Geophysics Center, UNLV, Las Vegas, NV 89154, barbara.luke@unlv.edu; SAID, A., Dept of Civil and Env Eng, UNLV, Las Vegas, NV 89154, aly.said@unlv.edu

Unprecedented population growth in southern Nevada in recent decades has added urgency to and also led to challenges in characterizing the seismic hazard of this tectonically active urban area. The Earthquakes in Southern Nevada (ESN) project has spent the last 5 years acquiring and integrating geologic, geophysical, geotechnical, and structural engineering data to asses the seismic hazard and develop a better understand of the seismic risk for the region. This region has several basins (*e.g.*, Las Vegas Valley, Eldorado Valley, Pahrump Valley) that are cut by active normal (dominant on the east) and/or strike-slip faults (dominant on the west), which have the potential of producing M6+ earthquakes within the region. These basins can be deep (up to several km) and amplify energy from strong ground motions. The various data sets have been acquired to better understand the depth, lithologies, and location of these faults; potential focusing effects of the basin and the basin-fill sediments; and anticipated response of buildings and bridges that are key to public safety. As a result, the ESN project has been able to (1) confirm the location at depth of many of the active faults, determine that there have been multiple episodes of faulting over time, and in some cases determine slip rates on these faults; (2) develop a 3D geologic model, a 3D map of shear wave velocities in the upper 100 m, and a general ground-shaking hazard map; and (3) characterize dynamic response of critical structures, with particular attention paid to bridges. The joint analysis of these data sets has led us to assess the seismic hazard potential with more accuracy. We have found a lower ground-shaking hazard along the Stateline fault, a higher hazard within the Las Vegas Valley fault system, and some of the structures studied show lower risk than previously thought.

Analysis of High-Resolution P-Wave Seismic Imaging Profiles Acquired through Reno, Nevada, for Earthquake Hazards Assessment

FRARY, R.N., U.S. Geological Survey, Golden, CO, USA, rfrary@usgs.gov; STEPHENSON, W.J., U.S. Geological Survey, Golden, CO, USA, wstephens@usgs.gov; LOUIE, J.N., University of Nevada-Reno, Reno, NV, USA, louie@seismo.unr.edu; ODUM, J.K., U.S. Geological Survey, Golden, CO, USA, odum@usgs.gov; MAHARREY, J.Z., U.S. Geological Survey, Golden, CO, USA, jzmaharrey@usgs.gov; DHAR, M.S., University of Nevada-Reno, Reno, NV, USA, dharm@unr.nevada.edu; KENT, R.L., University of Texas-NEES, Austin, TX, USA, rkent@mail.utexas.edu; HOFFPAUIR, C.G., University of Texas-NEES, Austin, TX, USA, cghoffpauir@mail.utexas.edu

In support of the Western Basin and Range Community Velocity Model and the proposed Reno-Carson City Urban Hazard Maps, the U.S. Geological Survey, University of Nevada, Reno, and nees@UTexas, Austin collaborated on a high-resolution seismic imaging study of the Truckee Meadows basin in Reno and Sparks, Nevada, during June 2009. We acquired two seismic reflection profiles to determine basin structure and fault locations in this area. We used the nees@UTexas minivib I vibrator source with a 12-second linear sweep from 15–120 Hz each, and recorded 2-second records on 144 channels with 5-m geophone intervals. One 6.72-km profile followed the Truckee River through downtown Reno east to Rock Boulevard, and a second 3.84-km profile followed Manzanita Lane, about 4.5 km south of the Truckee River. The second profile crossed several previously-mapped faults, including the Virginia lake fault. The seismic processing was catered to the urban environment and included pre-correlation automatic gain correction and frequency-offset (FX) spatial filtering to mitigate ambient noise. Additionally both post-stack time and pre-stack depth migrations were conducted for comparison. Final depth images of these profiles reveal strong reflections between about 0.2 km and 1.0 km depth. Preliminary interpretation of the Truckee River profile suggests the presence of several possible faults and an eastward-dipping reflection sequence. The Manzanita Lane profile shows reflections across a fault zone with multiple steeply-dipping strands.

Seismic, Geotechnical, and Earthquake Engineering Site Characterization

YILMAZ, O., Anatolian Geophysical, Istanbul, Turkey, oz@anatoliangeo.com; ESER, M., Anatolian Geophysical, Istanbul, Turkey, oz@anatoliangeo.com; BERILGEN, M., Yildiz Technical University, Istanbul, Turkey, berilgen@yildiz.edu.tr

We conducted a shallow seismic survey and determined the seismic model of the soil column within a residential project site in Istanbul, Turkey, approximately 40 acres in size. At each of the 20 locations within the project site, we deployed a receiver spread with 48 4.5-Hz vertical geophones at 2-m intervals. We used a buffalo gun at the bottom of a charge hole and acquired three shot records with source locations at each end of the spread and at the center of the spread. By applying a nonlinear traveltime tomography to the first-arrival times picked from the three shot records, we estimated a near-surface P-wave velocity-depth model along the receiver spread at each of the 20 locations. By applying lateral averaging after the inversion, we then obtained a P-wave velocity-depth profile down to a depth of 30 m representative of each location. Next, we identified the off-end shot record with the most pronounced dispersive surface-wave pattern and performed plane-wave decomposition to transform the data from offset-time to phase-velocity versus frequency domain. A dispersion curve associated with the fundamental mode of Rayleigh-type surface waves was picked in the transform domain and inverted to estimate an S-wave velocity-depth profile. We then combined the seismic velocities with the geotechnical borehole information regarding the lithology of the soil column and determined the site-specific geotechnical earnthquake engineering parameters—maximum soil amplification ratio, maximum surface-bedrock acceleration ratio, depth interval of significant acceleration, maximum soil-rock response ratio, and design spectrum periods. Finally, we obtained seismic images of the near-surface along selected traverses from the analysis of reflected waves to delineate landslide failure surfaces, fault geometry and geometry of layers within the soil column.

A Case Study for Seismic Zonation in Municipal Areas

YILMAZ, O., Anatolian Geophysical, Istanbul, Turkey, oz@anatoliangeo.com; ESER, M., Anatolian Geophysical, Istanbul, Turkey, murat@egejeofizik.com; BERILGEN, M., Yildiz Technical University, Istanbul, Turkey, berilgen@yildiz.edu.tr

Following the August 1999 earthquake with 7.4 magnitude, the Municipal Government of Izmit, Turkey, decided to conduct a pilot seismic zonation project to determine whether the cause of the damage was poor construction materials and methods or weak soil conditions. At each of the 16 locations within the municipal area, we conducted shallow seismic survey and acquired three shot records. We performed traveltime tomography to estimate a near-surface P-wave velocity-depth model and Rayleigh-wave inversion to estimate an S-wave velocity-depth profile down to a depth of 30 m. We then combined the seismic velocities with the geotechnical borehole information and determined the geotechnical earnthquake engineering parameters for each district—soil amplification and its effective depth range, design spectrum periods, and liquefaction probability and depth range. We diagnosed that the cause of the severe damage by the August 1999 earthquake within the municipal area of Izmit is soil amplification and localized liquefaction.

In addition to geotechnical characterization of the soil column in each district, we also conducted shallow reflection seismic survey at 10 locations within the municipal area along line traverses with an average length of 450 m primarily in the EW direction and derived seismic images down to a depth of 100 m. From the interpretation of the seismic sections, we delineated several faults most of which reach the surface and cause significant lateral velocity variations within the near-surface. These are most likely the active auxiliary faults associated with and oblique to the North Anatolian right-lateral strike-slip fault which traverses the muncipal area in the EW direction. We conclude that the neotectonic model of the area is represented by pull-apart tectonism rather than pure strike-slip fault mechanism.

Interferometric Multichannel Analysis of Surface Waves (IMASW)

O'CONNELL, D.R.H., Fugro William Lettis+Associates, Golden, CO, USA, oconnell@lettis.com; TURNER, J.P., Fugro William Lettis+Associates, Golden, CO, USA, j.turner@fugro.com

IMASW uses a non-stationary noise-correlation approach to produce deterministic seismograms from background noise, and split-spread vibratory and impact sources. Rayleigh-wave group and phase slownesses are estimated using time- and frequency-domain analyses. Compared to MASW or ReMi processing using only phase slownesses, the combination of Rayleigh-wave phase and group slowness data provide improved resolution of shallow S-wave velocity structure. Monte Carlo inversion is used to estimate P- and S-wave velocities and uncertainties. Several

IMASW results follow: 1) IMASW inversions using Santa Clara Valley passive (ReMi) data indicates good resolution of the shallowest several low-velocity zones indicated in borehole logs (Stephenson *et al.*, 2005) and good resolution of shear-wave velocities to 100–150 m depths. 2) In the northern San Fernando Valley, a PS suspension log was sited at the center point of an IMASW line in the LADWP Van Norman Complex located in steeply-dipping units to evaluate the performance of IMASW using active sources off both ends of the line. The line-averaged dispersion IMASW inversion resolved a 70-degree dipping high-velocity zone at 25 m depth and velocities in the low-velocity zone at 40 m depth, in agreement with the PS suspension log. 3) Comparison of six PS-suspension log-IMASW profile pairs across the Van Norman Complex showed that on average Vs30 estimates between the two methods differed by < 1%. 4) An IMASW profile on the hanging wall of the Mission Hills fault resolves a strong velocity contrast from 1200–1500 m/s Tertiary hangingwall rocks to 800–900 m/s Quaternary Saugus Formation in the footwall across the 62-degree dipping reverse fault at a depth of 150 m. 5) Drilling logs confirmed that IMASW Rayleigh group slowness dispersion helped resolve a 20-m-thick basalt flow embedded in alluvium at 50 m depth in southwestern Utah.

Constraints on the Near Surface Seismic Velocity Structure of the Wasatch Front Region, Utah, from Sonic Log Analyses

PECHMANN, J.C., University of Utah, Salt Lake City, UT, pechmann@seis.utah.edu; JENSEN, K.J., University of Utah, Salt Lake City, UT, kevin.j.jensen@utah.edu; MAGISTRALE, H., FM Global, Norwood, MA, harold.magistrale@fmglobal.com

We constructed generalized P-wave velocity profiles from 24 sonic logs from the seismically hazardous Wasatch Front region, Utah, in order to better constrain the near surface velocity structure of this region and thereby enable improved earthquake ground motion predictions. The maximum depths of the logs range from 0.9 to 5.3 km with a median penetration of ~2 km. Seven of the sonic logs are from wells located on bedrock and 17 are from wells drilled in fault-bounded Quaternary basins. The profiles show that the lateral variability of the measured P-wave velocities in the bedrock is comparable to that in the basins. The geometric mean P-wave velocity in the bedrock increases from ~3.0 km/s near the surface to ~5.8 km/s at 5 km depth. The sonic logs from the basins are generally consistent with the basic basin model developed by Hill *et al.* (1990, BSSA 80, 23-42) using two sonic logs and a seismic reflection profile from the northern Salt Lake Basin. This model consists of four layers separated by impedance contrasts interpreted as the boundaries between unconsolidated and semiconsolidated sediments (R1), between semiconsolidated sediments and Tertiary sedimentary rocks (R2), and between Tertiary sedimentary rocks and older basement rocks (R3). R2 is clearly the largest of these impedance contrasts, as previously reported, and is the only one that is easily identifiable without lithologic information. The basin P-wave velocities that we determined just below R2 are typically ~1 km/s lower than those reported by Hill *et al.* (1990). Exceptions occur in places where it appears that R2 is coincident with R3, *i.e.*, semiconsolidated sediments directly overlie basement. The results of this study have been incorporated into the latest version of the Wasatch Front Community Velocity Model, which is being used to predict ground motions from large Wasatch Front earthquakes.

Preliminary Results from a Multi-Method Approach for Acquiring Shear-Wave Velocity Data in the Portland and Tualatin Basins, Oregon

ODUM, J.K., U.S. Geological Survey, Golden, CO, USA, odum@usgs.gov; STEPHENSON, W.J., U.S. Geological Survey, Golden, CO, USA, wstephens@usgs.gov; MAHARREY, J.Z., U.S. Geological Survey, Golden, CO, USA, jzmaharrey@usgs.gov; FRARY, R.N., U.S. Geological Survey, Golden, CO, USA, rfrary@usgs.gov; DART, R.L., U.S. Geological Survey, Golden, CO, USA, dart@usgs.gov

The use of site-specific shallow shear-wave velocity (Vs) to assess site response is an important parameter in urban seismic hazard investigations, building codes (IBC 2006) and in design applications by the earthquake engineering community. As such, the need for rapid, accurate, and inexpensive collection of shallow Vs over large urban sedimentary basins and within heavily developed cities is becoming critical for future urban hazard mapping and earthquake-effects studies. As part of a continuing project to evaluate the strengths and weaknesses of Vs acquisition methodologies in various geologic and environmental settings the USGS used a multi-method approach to acquire Vs data at 19 sites in the Portland, Oregon area in 2009. These included the active-source (4-kg sledgehammer) P- and S-wave seismic refraction/reflection and both passive-source refraction microtremor (ReMi) and spatial auto-correlation (SPAC) methods. Challenges to acquiring high-quality Vs data to depths greater than 30 m in urbanized areas come in part from both the inherent logistical constraints of the spatial area available for sensor arrays and the signal-to-noise degradation related to buildings, infra-structure and cultural noise. While it was not possible to acquire data using all methods at every site, we typically were able to acquire data using at least three methods at 14 sites. Two of the sites selected for this multi-method survey are in the proximity of preexisting Vs-logged boreholes; thus allowing a comparison of up to four different acquisition methods at those sites. We present Vs-versus-depth profiles from sites in different geologic environments. These profiles are used to compare the similarities and differences in resulting Vs structure derived from the collocated multi-method data sets.

Optimized Velocities and PSDM in the Reno basin

KELL-HILLS, A.M., Seismological Lab., U. of Nevada, Reno, NV, USA, Kell@seismo.unr.edu; PULLAMMANAPPALLIL, S., Optim, Inc., Reno, NV, USA, satish@optimsoftware.com; LOUIE, J.N., Seismological Lab., U. of Nevada, Reno, NV, USA, Louie@seismo.unr.edu; CASHMAN, P., Geol. Sci. & Eng., U. of Nevada, Reno, NV, USA, pcashman@mines.unr.edu; TREXLER, J., Geol. Sci. & Eng., U. of Nevada, Reno, NV, USA, trexler@unr.edu

We collected seismic reflection profiles in the Reno, Nevada basin in collaboration with the USGS and nees@UTexas during June 2009. Stratigraphic horizons and vertical offsets associated with faulting appear along a 6.72 km Truckee River profile while strong, horizontally propagating body waves are seen in shot gathers from the southern 3.84 km Manzanita Lane profile. Reno-area basin fill overlies Miocene andesitic volcanic rocks and consists of Neogene sedimentary rocks and Quaternary outwash deposits. Using the seismic shot records, we seek to create an optimized velocity model of the Reno basin using commercial SeisOpt®@2D™ software. The refracted P-wave arrivals provide inputs for a global velocity model over the length of the profiles and to a depth proportional to the source offset distances, expected to be 150–200 m. Within this basin most of the lateral velocity heterogeneity should be within 200 m of the surface. Comparing this velocity model to stacked sections produced by the USGS will add confidence to the interpretations of strong reflection boundaries seen in the seismic sections. Boundaries in the velocity model should coincide with prominent reflection boundaries as well as with known depths of volcanic fill and other deposits, constraining their depths and velocities. The tomographic velocity sections will then be used as input with the shot records to a Kirchhoff pre-stack depth migration (PSDM) imaging steeply dipping structure and further constraining current interpretations and fault/basin geometry. The PSDM will help to resolve the cause of the horizontally propagating waves seen along Manzanita Lane possibly as sidewall reflections from a vertical fault. A confident depth section will also reveal the lateral extent of unconformities and fanning of bedding dips, which are observed where rocks are exposed at the basin margins, identifying a record of syndepositional tectonism.

Mt. Rose Fan Failure Plane: Low Angle Normal Fault or Landslide?

KELL-HILLS, A.M., Seismological Lab., U. of Nevada, Reno, NV, USA, Kell@seismo.unr.edu; SARMIENTO, A., Cent. of Neotectonic, U. Nevada, Reno, NV, USA; ASHCROFT, T., Geol. Sci. & Eng., U. of Nevada, Reno, NV, USA, ashcrof2@unr.nevada.edu; LOUIE, J.N., Seismological Lab., U. of Nevada, Reno, NV, USA, louie@seismo.unr.edu; KENT, G., Seismological Lab., U. of Nevada, Reno, NV, USA, gkent@seismo.unr.edu; WESNOUSKY, S., Cent. of Neotectonic, U. Nevada, Reno, NV, USA, stevew@seismo.unr.edu; PULLAMMANAPPALLIL, S., Optim, Inc., Reno, NV, USA, satish@optimsoftware.com

The Reno-area basin, sited at the western limit of the Basin and Range province within the Walker Lane, borders the Carson Range of the Sierra Nevada Mountains on the east. Triangular facets observed along an abrupt range front of the Carson Range indicate active faulting, motivating research in a rapidly urbanized area. Within the Mt. Rose fan complex, we trace a continuous ~1.4 mile long, north-northeasterly striking scarp offsetting both pediment surfaces and young alluvium at fan heads. A paleoseismic trench excavated across the scarp north of Thomas Creek at ~39.4° N latitude reveals a sharp, planar, low angle contact presumed to be a low angle normal fault (LANF). The interface dips at ~33°, parallel to bedding, and is capped by a well-developed soil greater than 50,000 years old. An alternative to the LANF working hypothesis allows for the sharp, low angle contact exposed in the trench to be a landslide. This trench study alone does not allow for conclusive evidence supporting either a LANF or landslide, suggesting additional trenching studies in the future, and the collection of a high-resolution shallow seismic reflection profile in November. Initial processing of the 250-m-long, hammer source profile does not reveal as prominent a seismic image of a LANF as did the alluvium-to-granite interface of the 1954 Dixie Valley rupture. However, the application of advanced seismic processing will characterize the structure. Commercial SeisOpt®@2D™ software and P-wave arrival times provide an optimized velocity model, which will show the locations of velocity gradients. The velocity section and survey shot gathers provide input for a Kirchoff pre-stack depth migration (PSDM), an imaging technique that will confidently show the structure to a depth of 75–100 m and test the working hypotheses. This integration of a paleoseismic trench and geophysical techniques will help to characterize fault structure and earthquake hazard within the populated urban basin.

State of Stress in Intraplate Regions

Oral Session · Friday 8:30 AM, 23 April · Salon G
Session Chairs: Charles Langston and Christine Powell

State of Stress in Central and Eastern North America Seismic Zones

MAZZOTTI, S., Geological Survey of Canada, Sidney, BC, Canada, smazzotti@nrcan.gc.ca; TOWNEND, J., Victoria University Wellington, Wellington, New-Zealand.

We use a Bayesian analysis to determine the state of stress from focal mechanisms in ten seismic zones in central and eastern North America, and compare it with regional stress inferred from borehole measurements. Comparison of the seismologically-determined azimuth of the maximum horizontal compressive stress (SHS) with that determined from boreholes (SHB) exhibit a bimodal pattern: In four zones, the SHS and regional SHB orientations are closely parallel, whereas in the Charlevoix, Lower St. Lawrence and Central Virginia zones, the SHS azimuth shows a statistically significant 30–50° clockwise rotation relative to the regional SHB azimuth. This pattern is exemplified by the northwest and southeast seismicity clusters in Charlevoix, which yield SHS orientations respectively strictly parallel and strongly oblique to the regional SHB trend. Similar ~30° clockwise rotations are found for the North Appalachian zone and for the 2003 Bardwell earthquake sequence north of the New Madrid zone. The SHB/SHS rotations occur over 20–100 km in each seismic zone, but are observed in zones separated by distances of up to 1500 km. A possible mechanism for the stress rotations may be the interaction between a long-wavelength stress perturbation source, such as postglacial rebound (PGR), and local stress concentrators, such as low-friction faults. The latter would allow low-magnitude (<10 MPa) PGR stresses to locally perturb the pre-existing stress field in some seismic zones, whereas PGR stresses have little effect on intraplate state of stress in general.

Seismogenic Yield Stresses in an Intraplate Region Estimated Using Laboratory Friction Experiments to Interpret Earthquake source Parameters

MCGARR, A., U.S. Geological Survey, Menlo Park/CA/USA, mcgarr@usgs.gov; BOATWRIGHT, J., U.S. Geological Survey, Menlo Park/CA/USA, boat@usgs.gov

"Stick-slip often accompanies frictional sliding in laboratory experiments with geologic materials. Shallow focus earthquakes may represent stick-slip during sliding along old or newly-formed faults in the earth." (Brace and Byerlee, Science, 1966) We pursue this hypothesis, proposed 44 years ago, by applying two techniques, based on laboratory stick-slip friction results, to investigate the crustal yield strength within earthquake rupture zones in the stable continental region of North America. The first approach (McGarr *et al.*, Bull. Seismol. Soc. Am., 2009) uses the maximum slip within the rupture zone of an earthquake and its seismic moment, in conjunction with results from laboratory friction experiments, to estimate the yield stress. The second approach is based on the observation that for stick-slip friction experiments, the apparent stress is about 5 % of the yield stress. We applied these two methods to nine earthquakes with reverse or thrust fault mechanisms, and moment magnitudes from 4 to 6.8, to sample seismogenic yield stresses over depths between 1 and 26 km. The resulting yield stresses range from about 30 to 300 MPa, increase approximately linearly with depth, and are generally consistent with the deepest available in situ stress measurements. Nearly all of the yield stresses suggest that these earthquakes are the result of frictional sliding involving pre-existing faults with pore pressures that are close to hydrostatic. The yield stress at the shallowest depth, however, is too high to be consistent with frictional sliding and may indicate fresh rock fracture. Applying the same analyses to three earthquakes in California, with thrust or reverse mechanisms and moment magnitudes between 6.5 and 7, revealed no significant differences in yield stress as a function of depth compared to their counterparts in the intraplate region.

Passive Margin Earthquakes as Indicators of Intraplate Deformation

WOLIN, E., Northwestern University, Evanston, IL, emilyw@earth.northwestern.edu; STEIN, S., Northwestern University, Evanston, IL, seth@earth.northwestern.edu

Mysterious large earthquakes occur at passive continental margins. The continent and neighboring seafloor are part of the same plate, so these earthquakes reflect deformation within the plate. The most plausible mechanism is reactivation of faults remaining from continental rifting by the modern stress field. As a result, the nature and distribution of passive margin earthquakes is a primary constraint on the stress field.

A crucial question is whether all such earthquakes reflect tectonic faulting. For example, the 1929 M 7.2 earthquake on the Grand Banks of Newfoundland triggered a landslide of thick continental slope sediments, resulting in a tsunami. However, investigators differ as to whether a tectonic earthquake nucleated the landslide, or whether it resulted from slope instability but released enough energy to appear as an earthquake. We approach this issue using a new result that aftershocks following a large (M~7) earthquake in this tectonic setting should continue for a very long time due to the slow deformation rate. Because large landslides should not be followed by a long aftershock sequence, it is possible to distinguish landslides that result from tectonic activity from those that result from slope instability. We find that both the Grand Banks earthquake and the analogous M 7.3 event in Baffin Bay in 1933 have similar aftershock sequences that continue today, suggesting that both were tectonic earthquakes.

The location of these events suggests that the primary influence is flexural stresses produced by removal of the Laurentide glacial load. Recent GPS data showing that the primary deformation within eastern North America results from deglaciation support this hypothesis. To assess this issue we compare the seismic moment release in earthquakes on the deglaciated portion of the coast to that on the remainder of the coast and on other passive margins.

Reservoir-Triggered Seismicity in the Canadian Shield

LAMONTAGNE, M., Natural Resources Canada, Ottawa, ON, Canada, malamont@nrcan.gc.ca; MANESCU, D., Hydro-Québec, Montreal, Qc, Canada, Manescu.Dan@hydro.qc.ca

The International Commission on Large Dams (ICOLD) has recently published a Bulletin on Reservoir-Triggered Seismicity (RTS). The Bulletin, in its rough draft stage, reviews the state of knowledge on this phenomenon, and suggests a methodology to assess its likelihood in various tectonic contexts. In light of future development of hydro-electric reservoirs, we examine how this Bulletin applies to the Canadian Shield environment, *i.e.* a mostly seismically quiescent region that contains some active areas and five documented cases of RTS. We find that some generalizations contained in the Bulletin should be refined in light of the known RTS history in the Canadian Shield. According to the Bulletin, for example, the thrust faulting environment and the quasi absence of background seismicity make RTS unlikely in the Canadian Shield, in contradiction to the known RTS history. Another example is that the Bulletin describes reservoir-triggered earthquakes as tectonic events that occur prematurely because of the increase in pore-fluid pressure. Based on this, one could consider the regional earthquake activity representative of the potential for RTS, even though tectonic earthquakes in the Canadian Shield generally occur much deeper (5–30 km depth) than RTS (upper 1–2 km depth). We present some preliminary ideas on the assessment of RTS potential in the Canadian Shield, keeping in mind the difficulty in forecasting the impact of increased pore fluid pressures on faults that are generally unmapped, have an unknown neotectonic history and lack sufficient knowledge of their permeability. The problem of defining a representative RTS event (location, magnitude, depth) for the design of dams and appurtenant structures is also examined. We also present some shallow earthquakes near reservoirs in Quebec that are now recognized as small magnitude RTS.

On the New Madrid Strain Rate/Release Discrepancy: Reexamining the Observational Underpinnings of Sacred Exotic COws

HOUGH, S.E., U.S. Geological Survey, 525 S. Wilson Avenue Pasadena, CA 91106, hough@usgs.gov; PAGE, M., U.S. Geological Survey, 525 S. Wilson Avenue Pasadena, CA 91106, pagem@caltech.edu

At the heart of the conundrum of seismogenesis in the New Madrid Seismic Zone is the apparently substantial discrepancy between low strain rate and high recent seismic moment release. GPS data reveal a strain rate not resolvably different from zero. Previous modeling of post-glacial rebound predicts a strain rate of ~10–9yr^{-1} over a region of ~20,000 km^2, with the rate predicted to remain nearly constant for the next few millennia. Along the St. Lawrence Seaway, where the strain rate associated with rebound is stronger, previous studies have shown that post-glacial rebound can plausibly account for the historic seismic moment release rate. In the New Madrid region, post-glacial rebound provides sufficient strain to produce a sequence with the moment release of one Mmax6.7–6.9 every 500 years, a value that is lower than most published estimates but at the low end of the range inferred from a recent analysis of consensus intensities. One can also construct a range of consistent models that permit a higher Mmax, with a longer average recurrence rate. For example, post-glacial strain rate can produce one Mmax6.9–7.1 event every 1000 years. If one assumes this mean rate and with a coefficient of variation of 0.5, the observed historic/prehistoric clustering has a 10–20% probability. The probability of recent clustering is higher if we assume a Poissonian rate. It is thus possible to reconcile predicted strain and seismic moment release rates with alternative models: one in which 1811–1812 sequences occur every 500 years, with the largest events being ~Mmax6.8, or one in which sequences will occur on average less frequently, but with Mmax close to or slightly higher than 7.0. Both models assume that seismicity follows standard statistics given a strain signal controlled by post-glacial rebound, with magnitude values on the low end of recently derived estimates. Neither model predicts that New Madrid sequences will shut off any time soon.

Earthquake Focal Mechanisms and Stress Estimates in the New Madrid Seismic Zone

HORTON, S.P., University of Memphis, Memphis,TN, shorton@memphis.edu; JOHNSON, G., Quantum Technology Sciences, Inc, Cocoa Beach, Fl, gjohnson@qtsi.com

P- and SH- wave polarities from data recorded by the Cooperative New Madrid Seismic Network between 2000–2007 were used to determine 290 focal mechanisms. Rose diagrams derived from the nodal planes reveal two dominant fault orientations for strike-slip earthquakes. These fault orientations match the dominate trends in seismicity and/or structural trends in the northern Mississippi Embayment. Nodal planes oriented ~50° are parallel to the orientation of both the southwest-segment seismicity and to the Reelfoot Rift. Nodal planes oriented ~30° are parallel to the northern-segment seismicity and to the Mississippi Embayment axis. Rose diagrams for reverse faults in the central segment show two major trends. One trend, oriented about 147°, is parallel to the average trend of the central-segment seismicity. The other trend is oriented north-south. North-south striking secondary reverse faults are predicted for through-going strike-slip faults oriented about 50°. Normal faults concentrate in the central segment, and they show a variety of nodal plane orientations. An inversion of all focal mechanisms for the regional stress field shows an overall horizontal maximum compressive stress oriented 79° ±30° in the NMSZ. When inverted separately, the outer fringes of seismicity (the southern half of the southwest segment, the northern segment, and the northwest arm) show orientations more comparable to stable North America (~N65E). Rotation of the compressive stress direction toward east-west occurs chiefly in the center of the NMSZ (*i.e.* the northern part of the southwest segment and the central segment).

The Relationship Between Intrusions and Earthquakes in the New Madrid Seismic Zone as an Indicator of Stress Concentration

POWELL, C.A., CERI, University of Memphis, Memphis/TN, capowell@memphis.edu; LANGSTON, C.A., CERI, University of Memphis, Memphis/TN, clangstn@memphis.edu

An often-quoted mechanism for the generation of intraplate earthquakes is stress concentration within rocks surrounding intrusions. We examine this relationship for the New Madrid seismic zone (NMSZ) and find that earthquakes tend to lie outside of mafic intrusions located along the borders of the Reefoot rift but inside intrusions located along the rift axis. Most notably, a recent inversion of magnetic data demonstrates that seismicity delineating the Reelfoot fault, the most seismogenic arm of the NMSZ, occurs within an axial intrusion. We suggest that the presence of intrusions plays an important role in facilitating NMSZ seismicity but that the relationship between earthquakes and intrusions is more complicated than stress concentration in surrounding host rocks. Analytic solutions for stresses near intrusions suggest that if the rigidity of the intrusion exceeds that of the surrounding rock, stress will be concentrated within the intrusion and in the region just outside the intrusion. In the case of relatively homogeneous mafic intrusions in felsic rock, the felsic rock usually fails, producing earthquakes. However, in the case of more complicated intrusions, failure can initiate within the intrusion itself. This appears to be the case for the intrusion hosting the Reelfoot fault. This axial intrusion has a similar potential field signature as the Osceola Igneous Complex that lies further south near the Blytheville Arch. Like the Osceola complex, the Reelfoot intrusion may consist of several igneous dikes, sills, and plugs intruded into the Precambrian upper crust and may be highly fractured. We suggest that the heterogeneous nature of the Reelfoot intrusion facilitates generation of microseismic activity in response to stress concentration. This mechanism may explain seismic activity in the enigmatic southern portion of the Reelfoot fault.

Seismicity and Crustal Structure of the Eastern Tennessee Seismic Zone from Gravity and Magnetic Data Modeling

ARROUCAU, P., NCCU, Durham, NC, United States, parroucau@nccu.edu; VLAHOVIC, G., NCCU, Durham, NC, United States, parroucau@nccu.edu; POWELL, C.A., University of Memphis, Memphis, TN, United States, capowell@memphis.edu

The seismicity of intraplate interiors, although accounting for only 0.5% of the energy released by earthquakes, raises challenging questions regarding its relationships with inherited geological structures as well as the respective roles played by local stress sources and far-field forces generated by global tectonics. The earthquakes of the Eastern Tennessee Seismic Zone (ETSZ), in the eastern part of North America, form a NE-trending, 300 km long and 100 km wide, belt of diffuse seismicity. These earthquakes occur at mid-crustal depths and their magnitudes never exceed 5.0, so that the associated rupture never propagates up to the ground surface. Thus, no obvious relationship seems to exist between their distribution and the faults known from geological mapping. On the other hand, that distribution appears to be significantly correlated with seismic velocity variations inferred from body-wave tomography and with observed potential field anomalies, thus suggesting some control of the seismicity by geological contrasts at depth. In this work, we attempt to investigate the possible links between the seismic activity of the ETSZ and its crustal structure by means of potential field data modeling. We use the gravity and magnetic databases provided by USGS to invert for density and magnetic susceptibility variations within the crust. Information compiled from surface geology, available seismic profiles and well-log data, as well as recent 3D body-wave tomographic imaging results, is used to constrain the models prior to the inversion.

Mesozoic-Cenozoic Structure at the Epicenter of the 1886 Charleston, South Carolina Earthquake

CHAPMAN, M.C., Virginia Tech, Blacksburg, Virginia USA, mcc@vt.edu; BEALE, J.N., Virginia Tech, Blacksburg, Virginia USA, jabeale@vt.edu

The study focuses on evidence of Cenozoic faulting in the epicentral area of the 1886 Charleston, South Carolina earthquake and its connection with Mesozoic structure. The seismic data consist of several reflection profiles collected near Summerville, South Carolina in the period 1975–1983. Reprocessing of the data reveals an extensive early Mesozoic extensional basin, approximately 20 km in width, lying between Summerville and Charleston. The basin is delineated by the geometry of reflections that image early Mesozoic volcanic and sedimentary rocks, and by positive magnetic and gravity anomalies. Cenozoic compressional reactivation of Mesozoic extensional faults is imaged in the interior of the basin. The northwestern boundary of the basin is marked by a sharp gradient in the magnetic field. Folded Cretaceous and Tertiary Atlantic Coastal Plain sediments in association with diffractions and truncated reflections from the early Mesozoic section at four locations along this magnetic gradient indicate that the northwestern basin boundary is faulted. Instrumentally located earthquakes are clustered at the location of the faults imaged in the interior of the basin, and in proximity to the northwestern basin margin. Modeling of magnetic and gravity data indicates that the upper crust beneath the seismically imaged structural basin is composed largely of mafic rocks to a depth of at least 4 km. We propose that the Charleston earthquake occurred due to compressional reactivation of a Mesozoic fault in a localized zone of intense early Mesozoic continental rifting.

The Mt Narryer Fault: the Source of Australia's Largest Earthquake?

HENGESH, J.V., University of Western Australia, Crawley, WA, Australia, Hengesh@civil.uwa.edu.au; WHITNEY, B.B., University of Western Australia, Crawley, WA, Australia.

The Mt. Narryer fault zone in west central Australia is a Quaternary active structure that may have produced the 1885 ML 6.6 Mt. Narryer and the 1941 ML 6.8 to 7.2 Meeberrie earthquakes. The fault zone is a 120-km long north-trending structure that includes at least four left-stepping en echelon fault segments. The two southern segments of the fault zone are expressed by west-side up displacement of the Roderick and Sanford alluvial valley deposits. Analysis of imagery and digital terrane models indicate that the scarps across the Sanford and Roderick Rivers have captured and diverted active stream flow, formed sag ponds, and impounded Lake Wooleen. The alluvial surface in both valleys is uplifted, warped and incised. Scarp heights of 3 to 8 meters suggest formation during multiple surface deformation events. The northern fault segments are expressed by strong vegetation alignments and fault scarps on the order of 1 to 1.5 meters. The linear nature of the northern scarps suggests a significant strike slip component of motion, while the two southern scarps appear to have a significant reverse component of motion. Preliminary analysis of drainage patterns west of the Mt Narryer fault zone suggest that additional fault scarps may be present.

Regional tilting, and local folding and faulting indicate that parts of Western Australia are being actively deformed. North-trending reverse faults such as the Mt Narryer structure suggest deformation as a result of east-west directed shortening. However, north-south directed convergence of the Australian Plate with the Timor Arc is causing down to the north flexure of the continental lithosphere in response to the collision. The competing styles of deformation suggest that active tectonic processes in this stable continental region are being driving by far-field plate boundary forces.

A Seismic Investigation of the Rio Grande Rift: the Role of Edge-Driven Convection in Continental Rifting

ROCKETT, C.V., Baylor University, Waco, TX, carrie_rockett@baylor.edu; PULLIAM, J., Baylor University, Waco, TX, jay_pulliam@baylor.edu; GRAND, S.P., University of Texas at Austin, Austin, TX, steveg@maestro.geo.utexas.edu

Much of the tectonic activity in the southwestern United States can be attributed to the foundering of the Farallon slab, which occurred ~40 Ma. However, a tectonic lull in the region followed the slab's foundering; active rifting of the Rio Grande Rift and the Southern Rockies dates to just ~10 Ma. The process of "edge-driven convection" may explain the pattern and timing of recent tectonic activity and such

convection would be expected to produce both mantle downwelling and crustal thinning. A fast seismic velocity anomaly can be seen in the mantle beneath the eastern flank of the Rio Grande Rift in the results from the linear La Ristra seismic deployment (Gao *et al.*, 2004) and the crust appears to thin above this anomaly (Wilson *et al.*, 2003). These results suggest that a closer look at the 3D geometry of the crust and upper mantle beneath the eastern flank of the Rio Grande Rift is warranted. In 2008, as part of a "Seismic Investigation of Edge Driven Convection Associated with the Rio Grande Rift" (SIEDCAR), investigators deployed a two-dimensional array that interspersed stations between EarthScope's Transportable Array (TA) stations in southeastern New Mexico and west Texas. Results from analyses of SIEDCAR and TA data show the anomalous region, which coincides with a topographic low, is larger than originally believed and extends southward from Artesia, NM to Mexico. We will present tomographic seismic velocity models for P and S waves produced with these data and will thus obtain quantitative constraints on the geometry, location, and amplitude of the anomaly. Ultimately these constraints will serve as inputs to geodynamic modeling, which will answer the question about whether edge-driven convection plays a significant role in rifting.

Seismic Anisotropy and Crustal Thickness of Eastern Flank of the Rio Grande Rift

PULLIAM, J., Baylor University, Waco, TX USA, jay_pulliam@baylor.edu; BARRINGTON, T., Baylor University, Waco, TX USA; XIA, Y., University of Texas at Austin, Austin, TX USA; GRAND, S.P., University of Texas at Austin, Austin, TX USA; BOYD, D., Chapman High School, Dallas, TX USA; DILLON, T., Chapin High School, El Paso, TX USA; ARRATIA, M., Ringgold Middle School, Rio Grande City, TX USA; WEART, C., Weslaco High School, Weslaco, TX USA

The Rio Grande Rift, located between the Colorado Plateau and the Great Plains, has a complex tectonic history comprised of two distinct phases in the Cenozoic era. An early stage of rifting began in the mid-Oligocene (~30 Ma) and lasted until the early Miocene (~18 Ma), followed by a lull and then an apparent reactivation along previous zones of weakness during an extension event in the late Miocene (~10 Ma), which continues today. The rift now extends more than 1000 km in length, trending north-south from Southern Colorado through New Mexico and Western Texas and into Chihuahua, Mexico.

In 2008 71 EarthScope FlexArray stations were installed between Transportable Array stations to form a broad 2D deployment on the eastern flank of the RGR in southeastern New Mexico and western Texas as part of the SIEDCAR (Seismic Investigation of Edge Driven Convection Associated with the Rio Grande Rift) study. SKS splitting measurements from these, as well as from TA stations in the vicinity, show a more complex 2D pattern, but one which conforms with variations in crustal thickness and inferred velocity anomalies in the uppermost mantle. We will report on these measurements and their implications for the style of convection associated with the RGR.

Specifically, a topographic low that extends from Artesia, NM to the southeast through Pecos, TX to Ft. Stockton, TX is characterized by short time lags between the fast and slow polarization directions, although the fast polarization directions are consistently northeasterly. On the rift flank proper, closer to the rift valley, time lags are larger and oriented more toward east-northeast. Receiver function modeling generally confirms that there is a significant increase in crustal thickness across the transition from the Rift province to the Great Plains, but the transition is not consistent in its location or abruptness.

Statistics of Earthquakes

Oral Session · Friday 1:30 PM, 23 April · Salon A
Session Chairs: Donald Turcotte, James Holliday, John Rundle, and Mark Yoder

Evaluating Earthquake Predictions on Laboratory Experiments and Resulting Strategies for Predicting Natural Earthquake Recurrence

KILGORE, B., US Geological Survery, Menlo Park, California; BEELER, N.M., US Geological Survery, Vancouver, Washington.

We study earthquake recurrence on a 2 m. long laboratory fault surface between granite blocks. In the experiments earthquake occurrence follows a period of controlled, constant rate shear stress increase, analogous to tectonic loading. Precursory slip initiates and accumulates within a limited area of the fault surface while the surrounding fault remains locked. Dynamic rupture propagation and eventual slip of the entire fault surface occurs spontaneously when slip in the nucleating zone becomes sufficiently large. The experiment produces repeating events of ~M–2. For a catalog of recurring events, the prior recurrence times, precursory slip and slip rate can be used to predict the next event. We develop retrospective prediction strategies and evaluate the success of the various approaches.

Our generic approach to event prediction is to first construct a hazard function; for example for recurrence time, the cumulative probability from the maximum likelihood fit to the first few recurrences is a useful function. An alarm is declared at some threshold value. Two approaches were studied; in the first case the alarm continues until the next event (single parameter), in the second case following the threshold the alarm sounds for a fixed duration (two parameter). Similar strategies can be applied to prior slip and slip rate data. We evaluate the predictions using the methods of Molchan (1991) and Zechar and Jordan (2008). If parameters are chosen wisely the two parameter alarms can be successful with area skill scores approaching 1.0. The single parameter alarms are generally skillful. We will apply our most successful recurrence time strategies to retrospectively predict natural recurrence of selected earthquakes near Parkfield California, small repeating events (less than M3) and the M6 Parkfield earthquake.

The Effect of Censored Time, Space and Magnitude Data on Earthquake Clustering Statistics

WANG, Q., UCLA, Los Angeles, CA, USA, qiwang@ucla.edu; JACKSON, D., UCLA, Los Angeles, CA, USA, david.d.jackson@ucla.edu

The Epidemic-type Aftershock Sequence (ETAS) model is widely used in seismic studies. The observations used for estimating the ETAS parameters will always be limited in space, time, and magnitude, yet unobserved ("censored") earthquakes affect the probabilities of events in the observable region. The effect of the censoring window will affect the pair statistics to which the ETAS model will be fit, so the effects of this window must be incorporated in parameter estimation. Moreover, the Log-likelihood values of the ETAS model contributed by each pair of earthquakes are affected by the censored data. Real earthquake data in California and simulations based on the ETAS model are used in this study to explore how significant the effect of censoring is in ETAS parameter estimations. This effects are so significant, especially those of time and mangitute, that they should not be ignored. One parameter, the spontaneous rate (also called the "background rate") is important for understanding the underlying physics of tectonic loading, but its estimate is strongly biased by the censored data. A larger time, space and magnitude window should be used to get better estimates of the parameters in the ETAS model. The size of the larger window is discussed in this study.

Activation vs. Quiescence: Which is the Precursory Signal for the Next Large Earthquake?

RUNDLE, J.B., University of California, Davis, CA, USA, jbrundle@ucdavis.edu; HOLLIDAY, J.R., University of California, Davis, CA, USA, jrholliday@ucdavis.edu; TURCOTTE, D.L., University of California, Davis, CA, USA, dlturcotte@ucdavis.edu; TIAMPO, K.F., University of Western Ontario, London, Ontario, Canada, ktiampo@uwo.ca; KLEIN, W., Boston University, Boston, MA, USA, klein@bu.edu

Many years ago, Gardner and Knopoff (1974) asked the question: "Is the sequence of large earthquakes, with aftershocks removed, Poissonian?". The one-word abstract was "Yes". They came to this answer by removing earthquakes from the Southern California catalog until the remaining event occurrences were consistent with Poisson statistics. Since that time, there has been a vigorous debate as to whether the probability for earthquake occurrence is highest during periods of smaller-event activation, or highest during periods of smaller-event quiescence.

The physics of the activation model are based on an idea from the theory of nucleation—that a small event has a finite probability of growing into a large earthquake, so that more small events imply a larger probability for occurrence of a large earthquake. An objection to this model has been stated as: "the greatest probability for a large earthquake is the moment after it occurs". Examples of this type of model are the ETAS and STEP models, which are statistical models utilizing the Omori and Gutenberg-Richter laws.

The physics of the quiescence model is based on the idea that the occurrence of smaller earthquakes may be due to a mechanism such as critical slowing down, in which fluctuations in systems with long range interactions tend to be suppressed prior to large nucleation events. An example of such a model is the seismic gap model. Other models include both, such as the Pattern Informatics model which looks only for deviations (activation or quiescence) and weights both equally.

In this talk we use this background to discuss both previous and new models that illustrate these points. We also discuss the question of whether time since the last large earthquake should play a role in earthquake probabilities (such as in the elastic rebound model).

Regional Seismicity as a Flow of Clusters: A Case Study in California

ZALIAPIN, I., U of Nevada Reno, USA; BAUTISTA, J., U of Nevada Reno, USA.

This study further develops and applies the seismic cluster analysis of Zaliapin *et al.* [PRL 101, 018501, 2008] to identify earthquake clusters in seismicity of California

and analyze their various statistical properties in time-space-energy domain. As one expects, the most prominent clustering correspond to aftershock sequences. At the same time, we identify and study other important types of clusters including foreshocks and swarms. Our analysis allows one to objectively represent the observed seismicity as a flow of clusters of different types; it thus provides a novel approach to describe the dynamics of regional seismicity and study its possible relations with the physical properties of a region.

Parkfield Repeating Earthquakes Are Neither Time- nor Slip-Predictable

RUBINSTEIN, J.L., USGS, Menlo Park, CA, USA, jrubinstein@usgs.gov; ELLSWORTH, W.L., USGS, Menlo Park, CA, USA, ellsworth@usgs.gov

We examine 28 repeating micro-earthquake sequences near Parkfield, California to test whether simple models of earthquake recurrence can explain their behavior. Repeating micro-earthquakes represent the ideal dataset with which earthquake recurrence models can be tested, in that they repeatedly rupture the same fault patch producing nearly identical waveforms. Using precise measurements of relative moment from a newly developed SVD-based method, we show that time- and slip-predictability do a poorer job predicting the time(slip) of the next earthquake than a much simpler, single-parameter renewal model. Additionally, we find that time- and slip-predictability typically work better for randomly reshuffled catalogs of repeating earthquakes than they do for the time/slip pairings from the true catalog. These two tests taken together strongly suggest that the time- and slip-predictable models of earthquake recurrence offer no predictive power for these repeating earthquake sequences. These models likely fail because their assumptions are incorrect, *i.e.*: 1) the loading rate is probably variable; 2) there can be variable stress drop; and 3) there is not a specific failure threshold. An additional possibility is that these fault patches are accommodating slip both seismically and aseismically (creep). Closer examination of the repeating earthquake data strongly supports this possibility, in that we commonly find an inverse relationship between recurrence time and earthquake size, *i.e.* the largest events occur after the shortest interval. Our preferred explanation for this observation is a fault patch that accommodates slip both seismically and aseismically where either: 1) creep rate accelerates with time following a repeat of the earthquake or 2) creep is delayed for a period of time following the earthquake. This type of behavior can be explained by the numerical model for repeating earthquakes by Chen and Lapusta [2009].

When Geomorphology Discriminates Between Occurrence Probability Models.

FITZENZ, D.D., University of Evora (CGE), Evora, Portugal, delphine@uevora.pt; FERRY, M.A., University of Evora (CGE), Evora, Portugal, matthieu@uevora.pt; JALOBEANU, A., University of Evora (CGE), Evora, Portugal, jalobeanu@uevora.pt

In seismic hazard assessment, the recurrence of large earthquakes is classically either included in a Gutenberg-Richter cum Poisson model, or addressed by a characteristic earthquake model. While the former is largely conditioned by recent instrumental (and often smaller) events, the latter is mostly unconstrained. We propose a methodology to assess how much earthquake geology and geomorphology can actually constrain the recurrence of full-segment ruptures. We study the Jordan Valley Fault, a 110 km-long segment of the Dead Sea Fault system for which an exceptional wealth of historical, archeological, paleo-seismological, and geomorphological data are available. We use the segment geometry and the characteristics of the past known ruptures to design an algorithm to build synthetic earthquake catalogs (slip and time) using alternatively the uniform, exponential, lognormal, BPT, or Weibul inter-event time distributions. For each law, we generate tens of thousands of catalogs for the duration of the geomorphological record, *i.e.*, 7 markers spanning 47,000 yrs. We then compute the likelihood of the model parameters explaining the geomorphological data with their uncertainties. The lognormal, BPT and Weibul can all generate catalogs of more than 60 events each, featuring rapid changes in slip rates and match the long-term trend in the morphological data. Around the optimum of the probability of the parameters given the data, the mean recurrence time is around 680 years. Further, the Bayesian theory ensures that the relative probability of each model can then be obtained by integration over its parameter space.

Epistemic Uncertainty in California-Wide Synthetic Seismicity Simulations

POLLITZ, F.F., U.S. Geological Survey, Menlo Park, CA USA, fpollitz@usgs.gov

Seismicity catalogs on synthetic fault networks hold promise for providing key inputs into probabilistic seismic hazard analysis, *e.g.* coefficient of variation (COV), mean recurrence time as a function of magnitude, probability of fault-to-fault ruptures, and conditional probabilities for foreshock-mainshock triggering. I present a seismicity simulator that includes the following ingredients: static stress transfer, viscoelastic relaxation of the lower crust and mantle, and vertical stratification of elastic and viscoelastic material properties. A cascade mechanism (which includes a proxy parameter for dynamic weakening), combined with a simple Coulomb failure criterion, is used to determine the initiation, propagation, and termination of synthetic ruptures. It is employed on a 3D fault network provided by Steve Ward in June, 2009 for the SCEC Earthquake Simulators Group. This all-California fault network.

initially consisting of 8000 patches, each of ~12 square km size, has been re-discretized into ~100000 patches, each of ~1 square km size, in order to simulate the evolution of California seismicity and crustal stress at magnitude M4 - 8. The fault network includes both vertical and dipping faults. Numerical efficiency is gained by employing joint Fast Multipole Method (FMM) and Mean Field Approximation in the spatial domain for all stress interactions, plus a temporal FMM for all non-static stress interactions. Resulting synthetic seismicity catalogs spanning ~ 100000 years and about one million events are evaluated with magnitude-frequency and magnitude-area statistics. For a-priori choices of fault slip rates and mean stress drops, I explore the sensitivity of various constructs (COV, etc.) on input parameters such as mantle viscosity and the dynamic weakening parameter. These simulations are intended as a guide for understanding the epistemic uncertainty to be expected when simulators are applied to large fault networks (*e.g.* the ongoing UCERF3 effort).

Earthquake Statistics of Synthetic Seismicity for Northern California Using Virtual California

YIKILMAZ, M.B., UC Davis, Davis, CA, USA, mbyikilmaz@ucdavis.edu; TURCOTTE, D.L., UC Davis, Davis, CA, USA, dlturcotte@ucdavis.edu; YAKOVLEV, G., UC Davis, Davis, CA, USA, glebos@gmail.com; RUNDLE, J.B., UC Davis, Davis, CA, USA, jbrundle@ucdavis.edu; KELLOGG, L.H., UC Davis, Davis, CA, USA, kellogg@ucdavis.edu

We present earthquake statistics for northern California using a synthetic earthquake catalogue generated by the Virtual California (VC) earthquake simulation. VC is a three-dimensional earthquake simulation code that includes static interactions of stress between fault segments using dislocation theory. Our model consists of 552 x 4 elements, each 3 km x 3 km in size and includes all major strike-slip faults in northern California. We ran our model for 100,000 simulation years and studied the frequency-magnitude statistics of all of northern California and at points on specified faults. We also investigated recurrence interval statistics at these points. As a specific example, we analyzed San Francisco and found the mean recurrence interval of 218.07 years, the standard deviation of 35.92 years and the coefficient of variation of 0.16 for this site. We further studied correlation of activity and interaction between faults by sub-sampling various faults in the model. Our preliminary results indicate that the Calaveras Fault controls rupture segmentation along the San Andreas and San Gregorio faults.

Distinguishing Tectonic Categories of Earthquakes in the EEPAS Forecasting Model

RHOADES, D.A., GNS Science, Lower Hutt, New Zealand, d.rhoades@gns.cri.nz; SOMERVILLE, P.G., Risk Frontiers, Sydney, Australia, psomervi@els.mq.edu.au; DIMER DE OLIVEIRA, F., Risk Frontiers, Sydney, Australia, fdimer@els.mq.edu.au; THIO, H.K., URS Corp, Pasadena, CA, Hong_Kie_Thio@URSCorp.com

The EEPAS model, which regards Every Earthquake as a Precursor, According to Scale, of larger earthquakes to follow it in the long-term, is a long-range earthquake forecasting method which is demonstrably informative in several seismically active regions, including California, Japan, New Zealand and Greece. In previous applications of the model, all earthquakes have been treated uniformly regardless of their tectonic setting. In this study however, we distinguish crustal, plate interface and slab earthquakes and apply the model to the SEIS-PC earthquake catalogue of Japan for magnitude M ≥ 4. The tectonic type of each earthquake was assigned using a definition of the plate boundaries by Gudmundsson and Sambridge. The period from 1966–1995 was used as a learning set, and 1996–2005 as a testing set for confirmation of the results, with the target earthquakes being those with magnitude M ≥ 6. Fitting of the EEPAS model to the learning set, targeting the earthquakes of particular tectonic types separately, showed it is optimal to use slab and interface events as precursors to major slab earthquakes, interface events only as precursors to major interface events, and crustal events only as precursors to major crustal events. Applying these restrictions gives an average probability gain per earthquake of about 1.5. The gain is higher for earthquakes in the slab and on the interface than for crustal earthquakes. In the independent testing period, a similar average probability gain is obtained, but the probability gain is higher for crustal earthquakes, and lower for slab and interface earthquakes, than in the learning period. Overall, the results support the hypothesis that earthquake interactions involved in long-term seismogenesis are stronger between earthquakes of similar tectonic types than between those of different types.

Numerical Models of Aftershocks, with 3D Heterogeneous Stress, Rate-State Friction, and Coulomb Stress: Comparisons with the Landers, Denali, and Loma Prieta Earthquakes

SMITH, D.E., U.C. Riverside, Riverside/CA/USA, desmith@ucr.edu; DIETERICH, J.H., U.C. Riverside, Riverside/CA/USA, dieterichj@cur.edu

We have implemented simulations of seismicity that integrate 3D spatially heterogeneous stress on geometrically complex faults with rate-state seismicity equations and Coulomb stress to simulate different parts of the seismic cycle, especially aftershock sequences. The model generates both temporal and spatial characteristic of real aftershocks, including scattered aftershocks in traditional Coulomb "stress shadow" zones, and it produces a focal mechanism orientation for each simulated event. Significantly, rotations of failure orientations in the aftershocks sequences are biased by the stress perturbation of the mainshock. This bias can lead to underestimates of crustal stress based on stress rotations. We model several seismic events and their associated aftershock sequences. Specifically, we compare two primarily strike-slip events, Landers and Denali, with Loma Prieta, which had a significant thrust component to the slip. Some key observables we are investigating include: 1) the percentage of events in Coulomb stress increase vs. decrease area, 2) stress heterogeneity based on seismicity statistics 3) spatial and temporal rotation of focal mechanisms. Comparisons of observed and simulated focal mechanism data will be used to evaluate biasing effects in the focal mechanism rotations, which will permit estimates of average crustal stress.

Forecasts of Repeating Microearthquakes near Parkfield, California

ZECHAR, J.D., ETH Zurich, Zurich, SWITZERLAND, jeremy.zechar@sed.ethz.ch; NADEAU, R.M., Berkeley Seismological Lab, Berkeley, CA, USA, nadeau@seismo.berkeley.edu

Using cross-correlation based pattern matching scans of continuous data from the Parkfield High-Resolution Seismic Network (HRSN), we identified 34 sequences of repeating microearthquakes-co-located events of approximately the same size that are inferred to break the same fault patch. These sequences are comprised of 837 earthquakes with moment magnitudes ranging from –0.6 to 2.1 that occurred between January 1987 and November 2009. We analyzed the inter-event times for each sequence and constructed two types of prospective forecasts: one giving the probability of a repeat between the most recent event in the sequence and the SSA meeting in April 2010, and another that ranks the sequences in terms of the relative likelihood of a repeat before the SSA meeting. The former set of forecasts is based on finding a best-fit recurrence model from several candidates (exponential, Weibull, lognormal, and Brownian Passage Time), and the latter set is based on comparing the time since the last event in each sequence with all previous intervals. Before the abstract submission deadline, we archived these forecasts at http://earth.usc.edu/~zechar/ssa2010.htm. In this presentation, we report the results of this prospective experiment and the merits of each forecast approach. We present results from additional retrospective predictability experiments using these and other microrepeater sequences; we discuss the process of repeat identification and catalog curation in light of data quality gaps; and we consider the effects of the 2004 M6.0 Parkfield earthquake.

Analysis of Spatial Variations in Magnitude of Completeness of JAGUARS Catalog (–5 < M < –1) Recorded in the Mponeng Deep Gold Mine in South Africa

PLENKERS, K., GFZ Potsdam, Potsdam, Germany, plenkers@gfz-potsdam.de; SCHORLEMMER, D., USC, Los Angeles, CA, ds@usc.edu; KWIATEK, G., GFZ Potsdam, Potsdam, Germany, kwiatek@gfz-potsdam.de; JAGUARS-GROUP.

We apply the approach of a probability-based magnitude of completeness, M_P, to a three-dimensional, in-mine network. The network is located at 3.5km depth in a complex observational volume with geological heterogeneities and cavities. The recording of events is directly influenced by the surrounding heterogeneities. Therefore the direction of recording must be carefully taken into account. For the analysis of the JAGUARS network, we extend the approach of Schorlemmer and Woessner (2008) and take into account these complexities. By doing so we find that the heterogeneities that are well known for the JAGUARS network, are reflected strongly in the detection probabilities. For example low detection probabilities are found near tunnels and geological boundaries. As the completeness depends directly on the recording, M_P varies in space and ranges from –2.9 to –4.7. Lowest M_P are found as expected in the center of the network. For comparison, we calculate completeness magnitudes based on frequency-magnitude analyses. Values of both methods agree if appropriate subsets for the frequency-magnitude analyses are chosen. We conclude that the extended approach to calculate the probability-based M_P is able to analyze correctly spatial variations in completeness even in the presence of strong heterogeneities. Analysis of detection probabilities gives insights into the networks performance as it points out areas of poor recording coverage. We used the JAGUARS (Japanese-German Underground Acoustic emission and microseismicity Research in South Africa)-project network and catalog, which contains seismic events in a magnitude range from $-5 < M_W < -1$. Magnitudes were calculated using recordings of a 3C-accelerometer and acoustic emission-sensors in a frequency range from 700Hz to 180kHz. A total of about 20,000 events were used.

Seismology of the Atmosphere, Oceans, and Cryosphere

Oral Session · Friday 1:30 PM, 23 April · Salon F

Session Chairs: Daniel McNamara, Keith Koper, and Richard Aster

Storms, Infragravity Waves and Possible Sources of the Earth's Vertical and Horizontal Hum

ROMANOWICZ, B.A., Berkeley Seismological Lab., Berkeley, CA, USA, barbara@seismo.berkeley.edu; DOLENC, D., Large Lakes Observatory, Duluth, MN, USA, ddolenc@d.umn.edu; RHIE, J., Seoul University, Seoul, Korea, junkee.rhie@gmail.com

The fundamental spheroidal modes of the Earth are continuously excited by processes that involve non-linear interactions between the atmosphere, oceans and the seafloor. Wind driven ocean waves interact with each other to produce infragravity waves, which are a likely source of this vertical hum. Recently, the hum has also been observed on horizontal components, with similar energy and from similar azimuths, strongest in the direction of the ocean-continent borders. Here we review our previous analysis of ocean floor noise in the infragravity wave band (20–500 s) at two broadband ocean floor stations, MOBB (California) and KEBB (offshore Washington State). We also compare the long-period noise observed at MOBB and FARB, located on a small island nearby. During a storm, long-period noise observed on the vertical component at KEBB increases not when the storm passes over KEBB, but when it reaches the coast, 300 km further east, indicating that coupling with the seafloor occurs near the coast. Similar long-period noise is observed on the vertical and horizontal components at FARB and MOBB, but not on nearby mainland stations. The energy in the infragravity wave band at FARB is, as at MOBB, modulated in phase with local tides, suggesting that infragravity waves are locally generated. Analysis of this signal following the arrival of a dispersed swell shows that it is generated in the near shore region from ocean waves with periods shorter than 23 s. The comparison of the incoming swell dispersion and the frequency of the resulting infragravity waves further shows that nonlinear interaction between a pair of swell components with frequencies f1 and f2 results in infragravity wave with frequency (f2-f1). The observation of strong tilting of the island due to the passing of infragravity waves suggests that swaying of the islands and underwater mounds, driven by tilting due to infragravity waves, is a possible source of the Earth's horizontal hum.

Atmosphere -> Ocean Waves -> Seismic Signals: Solid Earth–Climate Connections

BROMIRSKI, P.D., Scripps Inst. of Oceanography, La Jolla, CA, USA, pbromirski@ucsd.edu

Continuous seismometer recordings over extended periods describe wave climate variability. Intense storms having steep atmospheric pressure gradients cause strong winds that generate high waves. Wave energy is coupled into ambient seismic noise by wave-wave interactions in the open ocean and along coasts, and by direct pressure fluctuations at the ocean bottom in nearshore shallow water, generating double- and single-frequency microseisms, respectively. Some of the ocean swell energy is transformed into very long period infragravity (IG) wave energy along coasts, generating the Earth's "hum". The spatial and temporal distribution of storms and their associated wave energy controls the locations where high amplitude ambient seismic noise is generated. Changes in climate-related broad-scale atmospheric patterns that affect storm track and intensity have a corresponding affect on the spatial ambient noise distribution. Because storm activity is seasonal, winters produce the highest ambient noise levels in each hemisphere. And because ocean gravity waves propagate long distances, seismometers in both hemispheres detect signals produced by winter waves generated in the opposite hemisphere. Microseism and hum Rayleigh waves can propagate long distances, and are detected at locations far from their generation region. Although seismometers detect ambient noise signals generated simultaneously along long stretches of coastline, the nearest coastlines tend to produce the dominant signal. The integrative character of ambient noise observations provides an assessment of the amount of wave energy reaching particular coasts that is complementary to point oceanographic measurements. Increasing wave energy along coasts is of particular concern under rising sea levels, which allows more energy to reach farther shoreward.

Global Trends in Microseism Intensity from the 1970s to Present

ASTER, R.C., New Mexico Tech, Socorro, NM, USA, aster@ees.nmt.edu; MCNAMARA, D.E., US Geological Survey, Golden, CO, USA, mcnamara@usgs.gov; BROMIRSKI, P.D., Scripps Inst. of Oceanography, La Jolla, CA USA, pbromirski@ucsd.edu

Unbiased assessments of regional and global extreme storm frequency are needed to assess variability in the spatiotemporal distribution and intensity of large extratropical storms. Two globally prominent seismic ambient noise peaks near 7 and 14 s period are generated via distinct mechanisms involving the transfer of storm energy from ocean gravity waves to the solid Earth, and provide relevant spatially integrative proxies for assessing wave conditions. Because most land-observed microseism energy in this period band is coastally or near-coastally generated, microseism-derived metrics are especially appropriate for assessing coastal wave events. Continuous digital data from the Global Seismographic Network and precursor networks chronicle Earth's microseism activity from the early 1970s. Metrics of extreme microseism events at stations worldwide show significant regional connections to the El Nino Southern Oscillation (ENSO) as well as large oscillations in wave intensity that do not obviously follow recognized climate indices. We note generally increasing trends in extreme microseism hours per year, particularly in the northern hemisphere, from the early 1970's through the early 2000s, capped by recent downturn beginning around 2005.

Probing Microseism Origin and Earth Structure via Array Analysis of *P* Waves from Storms

ZHANG, J., Scripps Inst. of Oceanography, La Jolla / California / USA, jianz@ucsd.edu; GERSTOFT, P., Scripps Inst. of Oceanography, La Jolla / California / USA, gerstoft@ucsd.edu; SHEARER, P.M., Scripps Inst. of Oceanography, La Jolla / California / USA, pshearer@ucsd.edu; BROMIRSKI, P.D., Scripps Inst. of Oceanography, La Jolla / California / USA, pbromirski@ucsd.edu

Storms over deep oceans can generate microseismic *P* waves. Using array beamforming of the data from the Southern California Seismic Network (SCSN) and the Hi-net in Japan respectively, we show for Super Typhoon Ioke that a tropical cyclone can be traced seismologically via *P*-wave backprojection. Our results confirm deep ocean origin of double-frequency (DF) microseisms due to nonlinear wave-wave interactions, yet perhaps efficient for *P* waves only as deep water surface-wave microseisms are not observed. Spectral analysis shows two *P*-wave arrivals. In the short-period DF band above about 0.16 Hz, significant *P* waves are generated near the wake of Ioke by local wind seas. We also see *P* waves in the long-period DF band from about 0.1 to 0.15 Hz, generated at distances closer to the Japan shoreline by opposing swells. Microseismic *P* waves may contribute to imaging Earth structure. We demonstrate that travel-time anomalies beneath an array can be obtained from storm-generated *P* waves via noise cross-correlation across the array stations, suggesting using tropical cyclones as additional sources in seismic tomography.

On the Composition of Earth's Short-Period Seismic Noise Field

KOPER, K.D., Saint Louis University, Dept. of Earth and Atmospheric Sciences 3642 Lindell Blvd, St. Louis, MO 63108, USA, koper@eas.slu.edu; SEATS, K., Saint Louis University, Dept. of Earth and Atmospheric Sciences 3642 Lindell Blvd, St. Louis, MO 63108, USA; BENZ, H.M., United States Geological Survey, Box 25046, MS966, Denver, CO 80225, USA.

In the classic microseismic band of 5–20 s seismic noise consists mainly of fundamental mode Rayleigh and Love waves; however, at shorter periods seismic noise also contains a significant amount of body wave energy and higher-mode surface waves. In this study we perform a global survey of Earth's short period seismic noise field with the goal of quantifying the relative contributions of these propagation modes. We examined a year's worth of vertical component data from 18 seismic arrays of the International Monitoring System that were sited in a variety of geologic environments. The apertures of the arrays varied from 2–28 km, constraining the periods we analyzed to 0.25–2.5 s. Using frequency-wavenumber analysis we identified the apparent velocity for each sample of noise and classified its mode of propagation. The dominant component was found to be Lg, occurring in about 50% of the noise windows. Since Lg does not propagate across ocean-continent boundaries this energy is most likely created in shallow water areas near coastlines. The next most common component was P wave energy, which accounted for about 28% of the noise windows. These were split between regional P waves (Pn/Pg at 6%), mantle bottoming P waves (14%), and core sensitive waves (PKP, 8%). This energy is mostly generated in deep water away from coastlines, with a region of the north Pacific centered at 165W and 40N being especially prolific. The remainder of the energy arriving in the noise consisted of Rg waves (28%), a large fraction of which may have a cultural origin. Hence, in contrast to the classic microseismic band of 5–20 s, at shorter periods fundamental-mode Rayleigh waves are the least significant component.

Seismic Observations of Seasonal Sea-Ice Cycles in Alaska

MCNAMARA, D., USGS, Golden, CO, USA; KOPER, K., St. Louis University, St. Louis, MO, USA.

Traditionally the microseism band is composed of two prominent peaks in the global seismic background noise spectrum, near 7 and 14 s period, that arise from distinct coupling processes between ocean gravity waves and the solid Earth. Microseism power spectral density (PSD) is dominated by a primary peak, also called the single-frequency microseism (SFM) (10–20 s), that is generated by waves breaking on coastlines. The generally much stronger secondary peak, also known as the double-frequency microseism (DFM) centered near 5–10 s is generated by the half-period periodic variation of sea bottom pressure due to standing wave components of the ocean gravity wave field. In this study, we present evidence that PSD amplitudes in the short-period portion of the DFM (~0.5–2 s) are strongly correlated with local wave activity for stations located within a few kilometers of a coastline. Similar to the longer-period portions of the microseism band, the short-period portion displays a strong seasonal amplitude variation with low power in the northern hemisphere summer and high power in the winter. However, in late fall, when sea-ice forms in the vicinity of the station, short-period microseism PSD amplitudes decrease significantly. We compare PSD amplitudes with National Oceanographic Atmospheric Administration (NOAA) meteorological data including: water and air temperature, wave height and ice cover. In addition, eigen-decomposition of the Hermitian spectral matrix is applied to determine polarization attributes of the signal as a function of time and frequency. We observe that the dominant source of energy in the 0.5–2 s band is from local wave activity at nearby coastlines and the seasonal freeze/thaw cycle of sea ice in the Cook Inlet and the Bering Sea explains the seasonal amplitude variation in our dataset. These observations present a possible new passive-seismic method for sea-ice monitoring.

At the Interface Between Earthquake Sciences and Earthquake Engineering in the Pacific Northwest

Oral Session · Friday 1:30 PM, 23 April · Salon G
Session Chairs: Arthur D. Frankel and Ivan G. Wong

A SSHAC Level 3 Probabilistic Seismic Hazard Analysis for British Columbia

MCCANN JR, M.W., Jack R. Benjamin & Assoc., Inc., Menlo Park, California USA, mccann@jbaslc.best.vwh.net; ADDO, K., BC Hydro, Burnaby, British Columbia Canada.

As part of its dam safety program, BC Hydro has undertaken and is completing a comprehensive probabilistic seismic hazard analysis (PSHA) for the province of BC. The PSHA is being carried out in accordance with the SSHAC (1997) guidelines as a Level 3 analysis. As defined by the SSHAC, the goal of the PSHA is to develop inputs that represent the composite distribution of the informed scientific community. In conducting a study of this magnitude, it is BC Hydro's objective to have an up-to-date, and technically sound assessment of the seismic hazard in its service area. In addition, BC Hydro desires to achieve scientific stability with respect to the inputs to the PSHA over a period of time. While it is anticipated that new information (data, studies, and alternative interpretations) will become available in the future, experience suggests that most PSHAs that have been performed in a manner that achieves the SSHAC goal, do remain stable.

In both the seismic source characterization and ground motion modeling of the PSHA, new evaluations and models have been developed. The seismic source characterization process has evaluated and explored the use of turbidite datasets to develop a Cascadia recurrence model, currently available geodetic data to estimate recurrence for crustal sources, and new seismic source modeling concepts have been introduced. On ground motion, a new subduction ground motion prediction model was developed based on an updated and expanded dataset from subduction zones around the world.

Seismic Hazard in Western Canada from Global Positioning System vs. Earthquake Catalogue Data

MAZZOTTI, S., Geological Survey of Canada, Sidney, BC, Canada, smazzotti@nrcan.gc.ca; LEONARD, L.J., Geological Survey of Canada, Sidney, BC, Canada; CASSIDY, J.C., Geological Survey of Canada, Sidney, BC, Canada; ROGERS, G., Geological Survey of Canada, Sidney, BC, Canada; HALCHUK, S., Geological Survey of Canada, Ottawa, ON, Canada.

Probabilistic seismic hazard analyses are principally based on frequency-magnitude statistics of historical and instrumental earthquake catalogues. This method assumes that return periods of large damaging earthquakes (100s–1000s yr) can be extrapolated from 50–100 yr statistics of small and medium earthquakes. The method has obvious limitations when applied to areas of low-level seismicity where the earthquake statistics may be poorly constrained. In this study, we test an alternative

approach to assess seismic hazard in Western Canada. We use horizontal velocities at ~250 Global Positioning System (GPS) sites in BC and Alberta to calculate strain rates and earthquake statistics within seismic source zones. GPS-based strain rates are converted to seismic moment, earthquake frequency-magnitude statistics, and seismic hazard using a logic-tree method. The GPS-based earthquake statistics and seismic hazard are then compared to those derived from the earthquake catalogue. In one zone (Puget Sound), the GPS seismic hazard estimates are in good agreement with those from earthquake statistics. In nearly all other zones (*e.g.*, most of BC and Alberta), the GPS seismic hazard estimates are significantly larger than those from the earthquake catalogue by one or two orders of magnitude. This discrepancy could indicate that the earthquake catalogue significantly under predicts long-term seismic hazard in areas of low-level seismicity. Alternatively, significant aseismic deformation may occur over long time-scales, which would imply that the GPS strain rates over predict the true seismic hazard. We discuss the nature and limitations of both methods in light of our results for Western Canada, with the goal of defining a methodology to incorporate GPS strain rate data into probabilistic seismic hazard assessments.

Key scientific issues in the Pacific Northwest for the next version of the U.S. National Seismic Hazard Maps

PETERSEN, M.D., U.S. Geological Survey, Golden, CO USA, mpetersen@usgs.gov; FRANKEL, A.D., U.S. Geological Survey, Seattle, WA USA, afrankel@usgs.gov

The U.S. National Seismic Hazard Maps are updated every six years by incorporating newly vetted science on earthquake sources and ground motions. The 2008 hazard maps for the Pacific Northwest region include source models for three additional crustal faults, an updated seismicity catalog, a revised model for the magnitude-frequency distribution of the Cascadia Subduction Zone, a source zone to account for deep intraslab earthquakes near Portland, NGA ground motion prediction equations for crustal earthquakes, and new ground motion prediction equations for subduction interface events. The new models result in significant changes at 5 and 1 hz compared with the 2002 version; the highest changes are near the coast. These maps have been incorporated into the 2009 NEHRP Recommended Provisions, 2010 ASCE - Standard, and the 2012 IBC. The USGS is now planning the next version of the seismic hazard maps for 2014. The science issues for the Pacific Northwest that are being considered include:1) magnitude-frequency distributions and spatial and temporal cluster models for faults, including the Cascadia Subduction Zone, 2) improved models for the width of the seismogenic portion of the Cascadia Subduction Zone based on modeling of GPS data and the locations of Episodic Tremor and Slip events, 3) new models of crustal strain from GPS data, 4) new information on crustal faults, such as the Tacoma fault and eastern Washington faults, and 5) new ground motion prediction equations for subduction interface, deep intraslab, and crustal earthquakes. A Pacific NW workshop will be held in 2011 or 2012 to discuss these and other potential issues that will affect the seismic hazard evaluation.

Site Response and Sedimentary Basin Effects in the Portland, Oregon Region

FRANKEL, A.D., U.S. Geological Survey, Seattle, WA, afrankel@usgs.gov; CARVER, D.L., U.S. Geological Survey, Denver, CO, carver@usgs.gov; NORRIS, R.D., U.S. Geological Survey, Seattle, WA, norris@usgs.gov

We analyzed seismograms of local and regional earthquakes collected by an array of 12 portable accelerographs we deployed in the Portland, Oregon region starting in 2005. The main purpose of this network is to quantify the effects of the shallow soils and the Portland and Tualatin sedimentary basins on ground motions. This study represents the first step toward constructing urban seismic hazard maps for the area. Ten local earthquakes with magnitudes between 2.6 and 3.8 have been recorded to date, along with several regional earthquakes up to M6.3. We inverted spectra of a subset of the local earthquakes to determine site response and stress drop. Stations on soft soils (fill and young alluvium) near the Willamette and Columbia rivers show amplifications of a factor of 2–4 around 1 Hz, relative to a reference rock site. Seismograms from these stations generally have longer durations of ground motions at frequencies around 1 Hz compared to stations on rock or stiff soil. Two stations on thin soil over basalt in the Portland Hills have strong resonant peaks around 4–5 Hz. The site in Beaverton displays a long-period arrival after the S-wave for an earthquake to the north. This arrival is likely a basin surface wave produced along the northeast margin of the Tualatin basin. A stiff-soil site over the deepest part of the Tualatin basin does not show high response around 1 Hz, but exhibits substantial amplification at lower frequencies.

Impacts to Oregon's Critical Energy Infrastructure Hub

WANG, Y., Oregon Dept of Geology-DOGAMI, Portland/OR/USA, yumei.wang@dogami.state.or.us

The Pacific Northwest's extreme disaster is a giant earthquake on the Cascadia subduction zone, which would produce minutes of strong ground shaking, coastal subsidence, landslides, liquefaction, lateral spreads, and a near-field tsunami. The entire state of Oregon relies on a single critical energy infrastructure hub that includes co-located fuel pipelines, petroleum tank farms, ports and river front facilities, and high voltage electricity transmission, all which are concentrated along the lower reach of the Willamette River in northwest Portland. Much of this energy infrastructure has been constructed many decades ago, has severe seismic design deficiencies, and high seismic vulnerability. The fuel transmission pipelines that operate in this energy hub cross several major rivers and lack geographic redundancy. The energy hub is located on very poor soils that are highly susceptible to earthquake-induced liquefaction, lateral spreading, and permanent ground deformation. Direct damage will likely lead to impaired infrastructure, fires, hazardous materials spills, severe reduction in available fuel, upstream and downstream economic effects, and slow regional recovery. Possible impacts due to ground shaking and seismic hazards from a magnitude 8.5 earthquake, associated with landslides, lateral spreads, sloshing within tanks, foundation failures, un-navigable waterways, and other damages, will be presented. To minimize extensive direct earthquake damage, indirect losses and untold ripple effects, improved resiliency of the hub is needed. Short, medium, and long range risk management solutions involve the public and private sectors.

Seismic Source Characterization of the Yakima Fold Belt and its Implications to Seismic Hazard

WONG, I., URS Corporation, Oakland, CA USA, ivan_wong@urscorp.com; ZACHARIASEN, J., URS Corporation, Oakland, CA USA; THOMAS, P., URS Corporation, Oakland, CA USA; YOUNGS, R., AMEC Geomatrix, Oakland, CA USA; HANSON, K., AMEC Geomatrix, Oakland, CA USA; SWAN, B., AMEC Geomatrix, Oakland, CA USA; PERKINS, B., Shannon & Wilson, Inc., Seattle, WA USA; MCCANN, M., Jack Benjamin & Associates, Menlo Park, CA USA.

We performed a regional probabilistic seismic hazard analysis (PSHA) of the Mid-Columbia River region in central Washington to assess the hazard at several damsites operated by the Chelan, Douglas, and Grant Counties Public Utility Districts. Several dams are located within the Yakima Fold Belt (YFB), which comprises a suite of east-west-striking, predominantly north-verging anticlines. The YFB folds and faults deform the Columbia River basalts and are largely confined to regions where the basalt is present.

Notable seismicity within the Mid-Columbia region includes the 1872 **M** 6.8 North Cascades earthquake and the Entiat-Chelan seismic zone, a pronounced cluster of microseismicity near the southern end of Lake Chelan. Several investigators (*e.g.*, Crosson and Creager, 2003), have suggested that this zone could be associated with the 1872 earthquake.

Two alternative structural models, representing thick-skinned and thin-skinned deformation, have been suggested for the YFB. In a previous major PSHA of the region, the thin-skinned model was assigned the highest weight, and most of the YFB faults were assigned low probabilities of being seismogenic. We favor the thick-skinned model in which the YFB faults penetrate the basement and are seismogenic.

Twelve YFB faults, including the Saddle Mountains and Toppenish Ridge faults and two faults near Lake Chelan, the Entiat-Chelan seismic zone, and background seismicity are included in the seismic source model as crustal fault sources. Maximum magnitudes for the 50 to 160-km-long YFB faults range from **M** 6.7 to 7.6. There are no direct measurements of paleoseismic displacements on most of the faults, hence slip rates are inferred from long-term deformation rates, observed geodetic rates, and limited paleoseismic data from secondary faults. Estimated rates span more than an order of magnitude and range from about 0.01 to 0.3 mm/yr.

Seismicity and Seismotectonics

Oral Session · Friday 3:30 PM, 23 April · Lower Level
Session Chairs: Diane Doser and Jeanne Hardebeck

Finite Fault Kinematic Rupture Model of the 2009 Mw 6.3 L'Aquila Earthquake from Joint-Inversion of Strong Motion, GPS and InSAR Data

YANO, T., UC Santa Barbara, Santa Barbara/CA/U.S.A., tomoko_yano@umail.ucsb.edu; SHAO, G., UC Santa Barbara, Santa Barbara/CA/U.S.A., shao@umail.ucsb.edu; LIU, Q., UC Santa Barbara, Santa Barbara/CA/U.S.A., qliu@umail.ucsb.edu; JI, C., UC Santa Barbara, Santa Barbara/CA/U.S.A., ji@geol.ucsb.edu; ARCHULETA, R.J., UC Santa Barbara, Santa Barbara/CA/U.S.A., ralph@crustal.ucsb.edu

The 6 April 2009 Mw 6.3 L'Aquila earthquake is the best-recorded normal faulting event for near-fault strong motion and static field measurements. The highest accelerations occur for five stations on the hanging wall directly above the fault with peak horizontal accelerations in the range of 347- 662 cm/s^2 and peak velocities in the range of 32–42 cm/s. To understand what led to the distribution of ground

motions, we have jointly inverted the strong motion data and static field data. We used 14 strong motion accelerograms within 50 km. The accelerograms are integrated to velocity with a passband of 0.2–0.6 Hz. We have used both GPS and InSAR data to constrain the static field. In our initial model we assume a single, planar fault that has a strike of 140° and a dip of 45°. We use nonlinear inversion method (Ji *et al.*, 2002) to constrain the kinematic rupture history. First, we inverted each data set separately. In the static only inversion the maximum slip is about 100 cm with some slip located near the surface. For seismic only inversion the maximum slip is about 80 cm with no slip at the surface. The joint-inversion produces maximum slip about 100 cm in a patch that is about 6 km southeast of the hypocenter, and some slip located near the surface. The rupture propagation is primarily updip and to the southeast. The rupture velocity is relatively slow, about 2 km/s. These preliminary models will be re-examined to determine if the fit between the data and synthetics can be improved. We will also use isochrones to check for consistency between the synthetics and the arrival of phases at frequencies higher than we can resolve in the inversion.

Pronounced sP Phases Recorded at Regional Distances in Southwestern Japan: Modeling and Implications

HAYASHIDA, T., EPSS, Hiroshima University, Hiroshima, Japan, hayasida@geol.sci.hiroshima-u.ac.jp; TAJIMA, F., Ludwig-Maximilians University, Munich, Germany, tajima@geophysik.uni-muenchen.de; MORI, J., DPRI, Kyoto University, Kyoto, Japan, mori@eqh.dpri.kyoto-u.ac.jp

The Japan islands are located in the northwestern Pacific where two oceanic plates (Pacific and Philippine Sea plates) subduct beneath the Eurasian plate. Reflecting this complex tectonic environment, the configuration of the slab and crustal structure vary from region to region. In southwestern Japan, *sP* phases are clearly observed at the epicentral distances of 60 km or further while the phases are less visible in other regions of Japan. The amplitudes of *sP* phases are sometimes larger than those of direct S-waves, especially at a distance of 130 km or further. We found that subsurface sedimentary layers are critical for *SV-P* conversion at the ground surface and subsequent propagation to observation stations. The strong *sP* phase arrivals in southwestern Japan can be explained by the shallow crustal structure of the Chugoku area. Thus, we used *sP* phases to refine the slab and crustal models in this region. The a greement between the synthetic seismograms calculated with an existing regional 1D model and the data is reasonable in general. However, the agreement between the synthetics and the data has some significant differences for the *sP* phase amplitudes and the travel times of the *sP*- and *S*-waves at many of the stations. The synthetics calculated with our improved 1D model match the observed waveform data better. For stations where the travel times in the synthetics calculated with the improved 1D model still show large discrepancies, we constructed a 2D/3D model considering the configuration of the slab and the variation of the velocity discontinuity depths. The synthetics calculated with the 2D/3D model can better account for the travel times of *sP*- and *S*-waves. Our improved structural model indicates a deeper Moho beneath the central and southern part of Chugoku region that corresponds to the recent receiver function images.

Spatial Distribution of Stress along the Interplate Boundary in Hokkaido Northern Japan

GHIMIRE, S., Hokkaido University, Sapporo, Japan, ghimire@mail.sci.hokudai.ac.jp; TANIOKA, Y., Hokkaido University, Sapporo, Japan, tanioka@mail.sci.hokdai.ac.jp

We analyzed earthquake focal mechanism data to infer the spatial distribution of stress and to check the effect of large earthquakes in stress field along the interplate boundary in Hokkaido region, northern Japan. The interplate boundary in this work is inferred as the surface defining the upper boundary of the double seismogenic zone and is estimated from the earthquake catalog from the Hokkaido University after compensating the location errors.

To estimate stress states we compiled focal mechanism data from different sources. The entire study area is first divided into small squares (100km^2) then for each area data is selected from the catalog. The inversion estimates four parameters of the stress tensor: three principal stress directions and a parameter 'R' defined as the ratio of the maximum and minimum deviatoric stresses.

Our result unveils many features showing spatial variation in stress state. The dominant strike slip regime in the deeper part (<55km) across the Kurile trench, comparatively high angle (>75°) between the maximum horizontal stress and the subducting slab and small R-values (between 0.1 and 0.3) suggest a dominant tectonic stress along the trench axis most probably supplied by the arc-arc collision in this region. Across the Japan trench the scenario is similar to that in the Kurile but the maximum horizontal stress is parallel to the subducting slab. A dominant thrust regime at the depths between 25 and 55km with higher R-values (between 0.8 and 1.0) advocates for the uniaxial compression. In the shallower part the stress condition is significantly dependent of that in the nearby deeper parts indicating mechanically weak interplate boundary at shallow depths. The effects of large interplate earthquakes in the stress conditions are dynamic and significant in the shallower parts and the system reverses to initial conditions as time passes.

Investigating the Source of Seismic Swarms Along the Eastern End of the Puerto Rico Trench

MINTZ, H.E., Baylor University, Waco, TX, USA, hallie_mintz@baylor.edu; PULLIAM, J., Baylor University, Waco, TX, USA, jay_pulliam@baylor.edu; LOPEZ VENEGAS, A.M., University of Puerto Rico, Mayaguez, PR, USA, alberto.lopez3@upr.edu; TEN BRINK, U., Woods Hole Science Center, USGS, Woods Hole, MA, USA, utenbrink@usgs.gov; VON HILLEBRANDT-ANDRADE, C., University of Puerto Rico, Mayaguez, PR, USA, christa@prsn.uprm.edu

Over the last thirty years seismic swarm activity has frequently occurred offshore in the Sombrero Seismic Zone, located off the Northeastern corner of Puerto Rico. Seismic swarms have been recorded lasting from one day up to several weeks with magnitudes commonly no more than Ms 4. Causes of these swarms have yet to be determined; however, some have proposed a tear in the subducting North American Plate would cause such energy to be released. Tearing is suggested because it would accommodate the reactivation of faults and relieve stress buildup within the sharp curvature of the subducting slab and subducting ridges. Swarm hypocenters were commonly determined using data collected only from land-based stations of the Puerto Rico Seismic Network (PRSN), which lacks the necessary distribution of seismic azimuths to generate accurate focal depths. Ocean bottom seismographs were temporarily deployed in 2007 in and around the Sombrero Seismic Zone, providing full azimuthal coverage and recorded two seismic swarms in a six month window. This new dataset combined with data from the PRSN provides stronger constraints on earthquake hypocenters and focal mechanisms. Both the source of these swarms and their associated faulting mechanisms can now be ascertained with the addition of seismic data from the ocean bottom seismographs.

A New Method for Identifying Triggered Seismicity

MAGEE, A.C., Arizona State University, SESE, Tempe, AZ, United States, angela.magee@asu.edu; FOUCH, M.J., Arizona State University, SESE, Tempe, AZ, United States, Fouch@asu.edu; CLARKE, A.B., Arizona State University, SESE, Tempe, AZ, United States, Amanda.Clarke@asu.edu

Remotely triggered seismicity, events triggered more than a few fault lengths away from large events, has been documented in several places (*e.g.*, Yellowstone and Long Valley) for some large earthquakes (*e.g.*, the 2002 Denali and 1992 Landers earthquakes). Previous studies have identified examples of triggered seismicity by counting individual events using filtered seismograms in order to distinguish local events from the large remote earthquakes which may have triggered them.

Here we investigate potentially triggered seismicity in the western U.S. associated with the M_W 7.8 November 3, 2002 Denali fault earthquake, and the M_W 6.5 February 12, 2008 Oaxaca, Mexico earthquake. We use two different methods to identify apparently triggered local seismicity. In the first method, we identify local seismic events on high-pass filtered waveforms occurring within eight hours before and after the arrival of P-waves from the Denali mainshock. Our results are consistent with those of Gomberg *et al.* (2004). In the second method, we create a proxy for local seismic energy, computing moving time window envelopes of the high-pass filtered waveforms for eight hours before and after the arrival of mainshock P-waves. This method is simpler, faster, less subjective, and produces similar results as the first method for the Denali event.

We find that more areas of the western U.S. experienced increases in integrated ground motion after the Oaxaca earthquake than after the Denali earthquake. The difference may be associated with higher instrument density during the Oaxaca event. In order to better understand mechanisms by which seismicity is triggered, we qualitatively compare regions of significant triggered seismicity with maps of both recent (<10 Ma) volcanism and Quaternary faults, and find a strong correlation between triggered seismicity and regions of young volcanism.

Asymmetric Properties of Early Aftershocks on Faults in California

ZALIAPIN, I., U of Nevada Reno, NV, USA, zal@unr.edu; BEN-ZION, Y., U of Southern California, Los Angeles, CA, USA, benzion@usc.edu

We examine the relations between spatial symmetry properties of earthquake patterns along faults in California (CA) and local velocity structure images, to test the hypothesis that ruptures on bimaterial faults have statistically preferred propagation directions (*e.g.*, Ben-Zion, 2001). The analysis employs the catalogs of Power and Jordan (2009) for twenty five predominantly-linear fault-zones in CA. We distinguish between clustered and homogeneous parts of each earthquake catalog, using the earthquake clustering technique of Zaliapin *et al.* (2008) that employs the Baiesi-Paczuski (2004) distance between earthquakes, and calculate an asymmetry

index for the clustered portion of each catalog. The results indicate strongly asymmetric patterns in early times of close aftershocks along large faults with prominent bimaterial interfaces (*e.g.*, sections of the San Andreas fault), with enhanced activity in the directions predicted for the local velocity contrasts, and absence of significant asymmetry along most other faults which separate similar rock bodies. Assuming that the symmetry properties of offspring events reflect symmetry properties of the parent earthquake ruptures, the results can be used to develop refined estimates of seismic shaking hazard associated with individual fault zones.

Time Reversal in Geophysics

Oral Session · Friday 3:30 PM, 23 April · Salon I
Session Chairs: Carene Larmat, Jean-Paul Montagner, and Kees Wapenaar

Time Reversal Source Localization of Long-Duration Signals in a Laboratory Sample with Implications to Earth Processes

ANDERSON, B.E., Brigham Young University, Acoustics Research Group, Dept. of Physics & Astron., Provo, UT, bea@byu.edu; ULRICH, T.J., Los Alamos National Laboratory, Los Alamos, NM, tju@lanl.gov; GUYER, R.A., Los Alamos National Laboratory, Los Alamos, NM, guyer@physics.umass.edu; JOHNSON, P.A., Los Alamos National Laboratory, Los Alamos, NM, paj@lanl.gov

Time reversal is a robust technique that may be used for source localization. Traditional time reversal experiments in the laboratory have been performed with pulse like signals in numerous studies. Study of continuous-wave source signal localization in solids is a new finding.

Here we report experimental observations of spatial focusing of single-frequency, continuous-wave, steady-state elastic waves in a reverberant elastic cavity using time reversal. Spatially localized focusing is achieved when multiple receiver channels are employed, while a single channel receiver does not yield such focusing. The amplitude of the energy at the focal location increases as the square of the number of channels used, while the amplitude elsewhere in the medium increases proportionally with the number of channels used, as expected for time reversal focusing. The observation is important in the context of imaging in solid laboratory samples. While boundary conditions are different from Earth, the result also has import to problems involving localization of continuous-wave like signals in Earth, such as tremor and Earth hum.

Time Reverse Modeling of Low-Frequency Tremor Signals

STEINER, B., Spectraseis AG, Zurich, Switzerland, brian.steiner@spectraseis.com; SAENGER, E.H., ETH Zurich & Spectraseis AG, Zurich, Switzerland, erik.saenger@erdw.ethz.ch; ARTMAN, B., Spectraseis AG, Zurich, Switzerland, brad.artman@spectraseis.com; WITTEN, B., Spectraseis AG, Zurich, Switzerland, ben.witten@spectraseis.com; SCHMALHOLZ, S.M., ETH Zurich, Zurich, Switzerland, stefan.schmalholz@erdw.ethz.ch

Time Reverse Modeling (TRM) of passively acquired seismic signals is a promising complementary exploration method for active seismic. It detects weak seismic events which are quasi continuous in time, for example tremors, which are usually difficult to locate with current procedures. The passively measured seismograms from several synchronous sensors of a seismic network at the Earth's surface are reversed in time and are then used as source signals for TRM. Synthetic seismic wave propagation studies using a parallelized numerical explicit finite-difference method demonstrate that TRM is able to locate the source of tremor-like signals. We apply imaging conditions to collapse the time axis to visualize possible source locations. An example is the maximum absolute particle velocity at each point of the numerical grid. Furthermore, wave-field decomposition into P- and S-wave fields is applied to characterize the source type. Real examples of tremor-like signals include volcanic tremors or waves emitted by events in connection with subduction zones. Additionally, several field surveys have shown that hydrocarbon reservoirs may act as a secondary source of low-frequency (*i.e.* 1 Hz - 6 Hz) seismic waves. These signals are sometimes termed hydrocarbon tremors. Applications of TRM on data passively acquired above hydrocarbon reservoirs support the hypothesis that there are tremor-like signals originating from the location of hydrocarbon reservoirs. We perform some case studies on several problems like uncertainty in the velocity model, resolution in space, length of modeling or other parameters. We compare results from synthetic studies and field measurements and discuss the feasibility and pitfalls of TRM to detect source locations of seismic tremors. The results show the potential of TRM to be developed toward an effective tool for seismic source localization.

Time Reversal Applied to Location of San Andreas Triggered Tremor

LARMAT, C., Los Alamos National Laboratory, Los Alamos, NM, USA, carene@lanl.gov; JOHNSON, P.A., Los Alamos National Laboratory, Los Alamos, NM, USA, paj@lanl.gov; GUYER, R.A., Los Alamos National Laboratory, Los Alamos, NM, USA, guyer@physics.umass.edu

Non-volcanic tremor (tremor) is recognized in seismic record as coherent and consistent amplitude variations of the envelope of the signal on several stations. The nature and exact location of tremor source remains under investigation because of the difficulty of using classical source location methods. This difficulty comes from the long-duration nature of tremor signals which have no identifiable features such as P and S arrivals. We have applied Time Reversal (TR) to a number of source location problems (Larmat *et al.*, 2008) and propose to apply TR to triggered tremor along the San Andreas fault by the passage of Love waves associated with the 2002 Denali fault earthquake (2,400 miles away!) (Gomberg *et al.*, 2008). In principle, time reversal is ideal for obtaining source location, due to the robust, source focusing of the process: each phase contained in the signal automatically converges back to the source point. In particular, long-duration signals such as tremor pose no problem for source location (*e.g.*, see Anderson *et al.*, this session). In this paper we describe progress in applying TR to location of a tremor source near the town of Hemet (South California). We face inherent difficulties. Back-propagation is done numerically in an "open" 65 x 80 x 50 km volume of the Los Angeles basin. Much of the seismic energy leaves the volume without encountering the 10 stations of the Anza network that recorded tremor signals. These signals are in the 5 to 15 Hz frequency range. Full waveform modeling up to 8 Hz would requires 6,500 CPU-hrs using the spectral element package SPECFEM3D. This is beyond our current computational power. To overcome this limitation, we back-propagate a clipped envelope of the tremor signal, *i.e.*, a "down-shifted" frequency version. We obtain a focus 7 km S-W off the fault scarp and with no clear depth location. Further study is needed to determine the uncertainty of the location. Twosource of biases are investigated: (a) the velocity model, (b) the effect of using clipped envelope of the original signal in a TR process.

Time Reversal Source Imaging and GRiD MT Monitoring with W-Phase

TSURUOKA, T., ERI, Univ. Tokyo, Tokyo/Japan, tsuru@eri.u-tokyo.ac.jp; KAWAKATSU, K., ERI, Univ. Tokyo, Tokyo/Japan, hitosi@eri.u-tokyo.ac.jp; RIVERA, R., Université de Strasbourg, Strasbourg/France, luis.rivera@eost.u-strasbg.fr

Kawakatsu and Montagner (GJI, 2008) demonstrated the essential equivalence of the time reversal source imaging advocated by Larmat *et al.* (GRL, 2006) and the GRiD MT moment tensor inversion algorithm (Tsuruoka *et al.*, PEPI, 2009; Kawakatsu, BERI, 1998), while the former gives an approximate solution to the latter through the happy approximation underlined by Claerbout (2001). Considering the absence of technical difficulty in solving the inverse of moment tensors in real time, we prefer the GRiD MT algorithm for most of seismic monitoring purposes of earth's activities.

For tsunami early warning purposes we have implemented a W-phase source inversion algorithm (Kanamori and Rivera, GJI, 2008) into the GRiD MT system which had been developed earlier at the ERI (http://wwweic.eri.u-tokyo.ac.jp/GRiD_MT/). W-phase is a very long-period (200–1000s) phase starting right after the P-wave arrival, and is suitable for fast source parameter retrieval. The GRiD MT system continuously monitors seismic wavefield at a period of 20–50s and automatically and simultaneously determines the origin time, location and seismic moment tensors within 3min of the event occurrence. The new system using W-phase works at a much longer-period band and consists of modules that continuously perform the following tasks: (1) receiving data, (2) decimation, deconvolution and filtering, (3) moment tensor inversion, (4) detection of seismic events. When broad-band seismograms are available at regional distances (*i.e.* delta ≤ 12deg), we can detect seismic events and determine satisfactory solutions within 6 min after the earthquake occurrence. We performed a systematic test on several recent Japanese events to investigate the performance of the system. We will discuss several examples (*e.g.*, Ibaraki-oki, 2008; Iwate-oki, 2008) in detail. The preliminary results suggest that this system provides rapid and robust source parameters. And examples of test applications may be presented.

The Gap between Theory and Practice for Seismic Interferometry for the Earth

SNIEDER, R., Colorado School of Mines, Golden, Colorado, USA, rsnieder@mines.edu; SLOB, E., Delft University of Technology, Delft, Netherlands, E.C.Slob@CiTG.TUDelft.NL; WAPENAAR, K., Delft University of Technology, Delft, Netherlands, C.P.A.Wapenaar@TUDelft.NL

The field of seismic interferometry has grown spectacularly over recent years. Despite the flurry of theoretical derivations, the applications of this technique to passive data has mostly, but not exclusively, been limited to the retrieval of surface

waves. Seismic interferometry is often justified using concepts such as "equipartitioning" and "time-reversal". These concepts are indeed important, but we often fail to verify to what degree these assumptions really hold for the earth. We review three formulations of seismic interferometry.

One formulation is based on a radiation boundary condition at a bounding surface. This theory requires only sources of field fluctuations at the boundary. For the earth, having sources near the surface is indeed most realistic, but the assumption of a radiation boundary condition is inconsistent with the surface of the earth being a stress-free. Alternatively one can consider an attenuating earth with a free surface. Theory predicts that noise generated by sources throughout the volume proportional to the attenuation, will produce the Green's function after cross-correlation. According to the fluctuation-dissipation theorem, such noise is indeed generated, but the thermal energy involved (kT) is much too small to be observable. Another derivation of Green's function is based on equipartitioning of normal modes. Since most noise is generated near the surface of the earth, the energy of earth's normal modes cannot be expected to be equipartitioned. But there is a more fundamental problem with this approach as well; the assumption of stationary modal coefficient is for non-attenuating systems inconsistent with a random forcing.

Observational studies of cross-correlation of noise typically lead to estimates of the Green's function in which the body waves are under-represented. This is likely to be caused by the inconsistency of the requirements of the conditions for Green's function extraction and the conditions in the earth.

Earthquake Source Modeling using Time-Reversal or Adjoint Methods

HJORLEIFSDOTTIR, V., LDEO, Columbia Univ., Palisades, NY, vala@ldeo.columbia.edu; LIU, Q., University of Toronto, Toronto, Canada, liuqy@physics.utoronto.ca; TROMP, J., Princeton Univ., Princeton, NJ, jtromp@princeton.edu

In recent years there have been great advances in earthquake source modeling. Despite the effort, many questions about earthquake source physics remain unanswered. In order to address some of these questions, it is useful to reconstruct what happens on the fault during an event, or determining the slip distribution on a fault plane as a function of time and space. This is a difficult process involving many tradeoffs between model parameters.

Here we use a technique that uses synthetic seismograms computed for a 3D Earth model to invert for the slip on a fault plane during rupture. By including 3D seismograms we can use parts of the waveforms that are often discarded, as they are altered by structural effects in ways that cannot be accurately predicted using 1D Earth models. However, generating 3D synthetic is computationally expensive. Therefore we turn to an adjoint method (Tarantola Geoph. 1984, Tromp *et al.* GJI 2005), that reduces the computational cost relative to methods that use Green's function libraries. In its simplest form an adjoint method for inverting for source parameters can be viewed as a time-reversal experiment performed with a wave-propagation code (McMechan GJRAS 1982, Larmat *et al.* GRL 2006). The recorded seismograms are inserted as simultaneous sources at the location of the receiver and the computed wavefield (which we call the adjoint wavefield) is recorded on an array around the earthquake location.

Here we show, mathematically, that for source inversions for a moment tensor (distributed) source, the time integral of the adjoint strain is the quantity to monitor and that by preconditioning good results are obtained in few iterations. We present the results of time-reversal experiments using synthetic seismograms computed for point sources and finite sources. We also show an example for a real event.

Seismic Hazard Mitigation Policy Development and Implementation

Oral Session · Friday 3:30 PM, 23 April · Salon G
Session Chairs: Yumei Wang and Zhenming Wang

Seismic Policy Development and Implementation in Kentucky

COBB, J., Kentucky Geological Survey, Lexington, Kentucky, USA, cobb@uky.edu

In the United States, seismic policy is typically developed at the national level by a federal agency or non-governmental organization, then revised and adopted by an individual state, and implemented at the state and local levels. The National Earthquake Hazard Reduction Program (NEHRP) provisions for seismic hazard mitigation were developed by the Building Seismic Safety Council (BSSC). The NEHRP provisions were then endorsed by the Federal Emergency Management Agency (FEMA) and became the recommended provisions (policies) for seismic regulations for new buildings and other structures in the U. S. The provisions also become design standards (policies) when they are referred to or adopted by other organizations such as the International Code Council (ICC). ICC developed the 2000 International Building and Residential Codes (IBC-2000 and IRC-2000) based on the 1997 edition of the NEHRP recommended provisions. The provisions become state policies when they are referred to or adopted by state government agencies. For example, the provisions were referred to by the Kentucky Emergency Management Division and therefore became Kentucky policy on seismic safety regulations. The 2000 International Building and Residential Codes (IBC-2000 and IRC-2000) were adopted by the Kentucky Department of Housing, Buildings, and Construction and became the 2002 Kentucky Building and Residential Codes (KBC-2002 and KRC-2002).

Developing and implementing sound seismic policy is complicated and challenging. The policy development, however, begins with earthquake sciences. For example, the development of the NEHRP provisions began with the national seismic hazard maps by the United States Geological Survey (USGS) that require inputs from earthquake sciences. Therefore, it is critical for seismologists to clearly define, quantify, and communicate seismic hazards to stakeholders. It is also important for engineers and stakeholders to understand seismic hazards being provided.

What Earthquake Engineers need Seismologists to Contribute

POLAND, C.D.P., Degenkolb Engineers, San Francisco/CA/USA, CPoland@Degenkolb.com

Robust, comprehensive and cost effective seismic mitigation policies will yield a resilient built environment that protects life and supports quick recovery. Such policies have eluded communities exposed to significant seismic risk because of expected high costs, competing priorities, and misunderstanding that has led them to believe they are doing all they can and need to do. Earthquake Professionals, engineers and scientists, need to work in harmony to deliver clarity about what will happen and what needs to be done to achieve community resilience. Engineers need to design the infrastructure to protect people from harm and assure recovery within a few years. Power, water, and communication networks need to begin to operate shortly after a disaster, and people need to be able stay in their homes, travel to where they need to be, and resume a fairly normal living routine within weeks so they can participate in the recovery activities. Seismologists hold the keys to understanding the hazard and characterizing it in terms that will form the basis for proper policy and be used for the evaluation and design of facilities and systems. For policy making, communities need to understand the extreme events they face and use those as the basis of their emergency response planning. They also need to know the events that are expected in the useful life of their buildings and lifelines that can be used as the basis for design. To be useful, earthquake engineers need these various events characterized in terms of expected intensity, frequency content, duration, and uncertainty so that appropriate parameters, procedures, and standards can be developed and used for evaluation, design, and rehabilitation.

New "Courtney Grants" to Seismically Strengthen Community Infrastructure in Oregon: What about Other States?

WANG, Y., Oregon Dept of Geology (DOGAMI), Portland/Oregon/USA, yumei.wang@dogami.state.or.us

The state of Oregon established the nation's first state-funded seismic rehabilitation grant program in 2009. This program was created to eliminate collapse-prone, public schools to avoid mass student fatalities in future major earthquakes, as well as to promote community preparedness across the state. The formation of this grant program took place over 10 years and involved diverse stakeholders and public policy discussions on a wide variety of issues, such as the probability of a Cascadia subduction zone earthquake, seismic ground motions specific to great subduction zone earthquakes, the role of state government, use of state funds, and more. This 10-year effort was led by Senator Peter Courtney, Oregon Seismic Safety Policy Advisory Commission (OSSPAC), and by Oregon Department of Geology and Mineral Industries (DOGAMI). Under the leadership of Senate President Courtney, the 75th Oregon Legislature (2009–2011) authorized the first seismic bond sales of $15 million for public schools and $15 million for emergency facilities. The first "Courtney grants" to provide state bond funds to help strengthen public school and emergency service buildings will be issued in 2010. Seismic vulnerability scores for about 3,500 schools and emergency service buildings across the state are publicly available on www.oregongeology.org/sub/projects/rvs/default.htm and www.ode.state.or.us/go/quakesafeschools. The Oregon seismic rehabilitation grant program is administered by the Oregon Emergency Management (www.oregon.gov/OMD/OEM/). U.S. Congressperson David Wu is taking a lead role to request a Government Accountability Office (GAO) study on seismic safety of schools across the nation.

History of Seismic Provisions in the Building Code of Arkansas

AUSBROOKS, S.M., Arkansas Geological Survey, Little Rock, Arkansas, United States of America.

The New Madrid seismic zone (NMSZ) is one of the most seismically active zones in the central-eastern U.S. and extends into northeast Arkansas. The NMSZ was the location of three ($7.4 < m < 7.8$) earthquakes in 1811–1812. In 1991, only two years

after the Loma Prieta earthquake in California, sufficient awareness and concerns were raised that the 78th General Assembly of the State of Arkansas passed Act 1100 establishing the Arkansas Earthquake Code (AEC). The purpose of the code was to safeguard life, health and property by requiring earthquake resistant design for all public structures with certain exemptions for farm buildings, parks, and bridges. The Act tied the AEC to the minimum seismic requirements found in the Arkansas Building Code which is embedded within the Arkansas Fire Prevention Code (AFPC). It also established design criteria based on zones of anticipated damage with respect to the NMSZ. In 1999, the 82nd General Assembly amended various sections of the AEC to include provisions that tied the previously established zones of anticipated damage to Av and Aa values and expanded the number of exempt structures. In 2006, the state of Arkansas began the process to adopt the 2007 Edition of AFPC which includes seismic provisions found in the 2006 Edition of the International Building Code (IBC). Though the seismic provisions in the 2006 IBC differ only slightly from the 2000 IBC that Arkansas currently used, it sparked at times a heated debate among engineers, scientists, emergency planners, and economic developers and lead to additional exemptions in the code. In April of 2008 the 2007 AFPC was adopted and the revised code does contain Appendix L which allows for alternative seismic design standards. It is very important to note that the use of Appendix L is allowed only if the local jurisdiction has adopted it by ordinance.

Impacts of the 2009 Samoa Tsunami and Earthquake

DENGLER, L.A., Humboldt State University, Arcata,CA,USA, lori.dengler@humboldt.edu; BRANDT, J., CA Dept. Fish and Game, Ontario, CA, USA, jbrandt@dfg.ca.gov; EWING, L., CA Coastal Commission, San Francisco, CA, USA, lewing@coastal.ca.gov; IRISH, J., Texas A & M University, College Station, TX, USA, jirish@civil.tamu.edu; JONES, C., Jones Engineering, Durham,NC, USA, chris.jones@earthlink.net; LAZRUS, H., University of Oklahoma, Norman, OK, USA, lazrus@ou.edu

An interdisciplinary team visited Samoa and American Samoa in late October and November, 2009. The team, sponsored by ASCE/COPRI, EERI, and the NTHMP focused on identifying the factors which effected the impacts of the September 29, 2009 tsunami. Factors that reduced impacts included time of day, the first significant surge being a drawdown, minimal ground shaking damage, tsunami awareness and preparedness programs, drills, informal community warning systems, local heroes who went out of their ways to help others, shore protection, well-built structures that provided vertical evacuation in some cases, and a village structure that provided shelter to displaced people. Factors that increased vulnerability included little time between ground shaking and the arrival of the first surges, failure to respond to ground shaking as a natural warning sign, embarrassment that others would perceive evacuating as silly, reliance on automobiles for evacuation, confusion about evacuation routes and safe areas, lack of awareness of multiple waves, barriers to evacuation such as mangrove swamps, rivers and fences, and weak structures. The team identified a number of issues to reduce tsunami vulnerability including development of tsunami evacuation routes and maps, assessment of village vulnerability that includes exposure and access to higher ground, examining informal tsunami warning systems and developing criteria to support them in near-source tsunami events, and memorializing the 2009 event to institutionalize tsunami awareness.

Statistics of Earthquakes

Poster Session · Friday AM, 23 April · Exhibit Hall

Darned Lies and Circular Statistics?

ANDERSON, D.N., Los Alamos National Laboratory, Los Alamos, NM, USA, dand@lanl.gov; ARROWSMITH, M.D., Los Alamos National Laboratory, Los Alamos, NM, USA; TAYLOR, S.R., Rocky Mountain Geophysics, Los Alamos, NM, USA.

This presentation is stimulated by the recent interesting article entitled "Lies, Damned Lies and Statistics (in Geology)" by P. Vermeesch that recently appeared in the American Geophysical Union publication Eos. In the article, Pearson's chi-square test is applied to a large catalog of earthquakes to infer that earthquakes are unevenly distributed by weekday with seismic activity being particularly high on Sunday. The conclusion is made that the strong dependence on p-values with sample size makes them uninterpretable. A possible problem with the analysis is that more powerful statistical procedures could have been made to test the null hypothesis of a uniform distribution of earthquakes versus day of week. For example, circular statistics is more amenable to testing uniformity as a function of day of week using the Rayleigh test of uniformity.

We will show applications of circular statistics to reinvestigate the uniformity of earthquake seismicity with day-of-week and with time-of-day. Inclusion of model error into the standard error estimates will also help alleviate the problem caused by large data sample sizes. Time-of-day represents a common application by seismic network operators to exclude manmade seismicity from local earthquake catalogs. Typically, daytime and nighttime hours are defined, and subsequently analyzed using linear histograms. Because the starting point is non-arbitrary, it is difficult to adequately assess trends in data. We show the results of performing basic statistics on traditional time-of-day histograms and compare to circular distributions using a dataset of earthquakes and mining explosions from the Western United States. We additionally illustrate improvements to standard errors used in classical hypothesis testing that ameliorate the unrealistic influence of large sample sizes on the power of a hypothesis test.

Separating Aftershocks from Background Seismicity Using Record-Breaking Intervals

YODER, M.R., University of California, Davis, Davis, CA, USA, yoder@physics.ucdavis.edu; TURCOTTE, D.L., University of California, Davis, Davis, CA, USA, dlturcotte@ucdavis.edu; RUNDLE, J.B., University of California, Davis, Davis, CA, USA, rundle@physics.ucdavis.edu

A major challenge in seismology is to separate aftershock sequences from background earthquakes. We suggest a test, based on record-breaking statistics of inter-occurrence times between successive earthquakes, which might contribute to a solution to this long standing problem. A record-breaking inter-occurrence time is a time that is longer (or shorter) than any previous time interval observed in a sequence. Background seismicity may have temporal correlations, but temporal trends are expected to be weak. Aftershock seismicity is characterized by a clear trend, in which the inter-occurrence times systematically increase as a function of time according to Omori's law. Record-breaking statistics of time-series data are sensitive to temporal trends, and so may be used to distinguish an aftershock sequence from stationary background seismicity. For a stationary Poisson process, the number of record-breaking inter-occurrence times is proportional to the logarithm of the number of variables in the sequence. We show that inter-occurrence times of global seismicity show good agreement with this behavior. In an aftershock sequence, where interval times are systematically increasing with time, it is expected that there will be many more record-breaking long intervals (inter-occurrence times) than record-breaking short times. We show that for aftershock sequences, the number of record-breaking long inter-occurrence times has a power-law dependence on the number of intervals in the sequence. In this paper, we carry out systematic studies of the inter-occurrence times in California and suggest tests whereby a sequence of inter-occurrence earthquakes can be considered to be part of an aftershock sequence or belong to the background seismic activity.

Initiation and Propagation of Earthquake Rupture

GRAN, J.D., University of California, Davis, Davis, CA, USA, gran@student.physics.ucdavis.edu; YAKOVLEV, G., University of California, Davis, Davis, CA, USA, glebos@gmail.com; TURCOTTE, D.L., University of California, Davis, Davis, CA, USA, dlturcotte@ucdavis.edu; RUNDLE, J.B., University of California, Davis, Davis, CA, USA, rundle@physics.ucdavis.edu

In most cases there are no precursory slip or creep events before an earthquake rupture initiates. In order to study theis problem we utilize a modified fiber-bundle model. The fibers are considered to be analogous to asperities on a fault. Time to failure for each fiber is specified from a Poissonian distribution. The hazard rate is assummed to have a power-law dependence on stress. When a fiber fails the stress on the fiber is redistributed to a specified number of adjacent fibers. Our initial studies assume a constant applied stress at t =0. This problem is applicable to the time delays associated with aftershocks. A primary objective is to assess precursory damage. Damage is defined to be the fractuion of fibers that have failed. Results are sensitive to the hazard-rate exponent and the range of stress transfer. In general a power-law increase in damage is followed by a catastrophic rupture. We quantify this transition.

Seismology of the Atmosphere, Oceans, and Cryosphere

Poster Session · Friday AM, 23 April · Exhibit Hall

First Observations From the NEPTUNE Canada Seismograph Network

ROGERS, G.C., Geological Survey of Canada, Sidney, BC, Canada, grogers@nrcan.gc.ca; MELDRUM, R.D., Geological Survey of Canada, Sidney, BC, Canada; MULDER, T.L., Geological Survey of Canada, Sidney, BC, Canada; BALDWIN, R., Geological Survey of Canada, Sidney, BC, Canada; ROSENBERGER, A., Geological Survey of Canada, Sidney, BC, Canada.

NEPTUNE Canada is the world's first large regional cable-linked, multi-disciplinary scientific seafloor observatory. In the fall of 2007 an 800 kilometer ring of powered fiber optic cable was laid on the seafloor over the northern part of the Juan de

Fuca plate and connected to a shore facility near Port Alberni on Vancouver Island. Five nodes were attached to the cable early in the summer of 2009 paving the way for junction boxes and scientific instruments installed in the late summer and fall. In September 2009, three broadband OBS packages were deployed in the form of a large triangle with apexes at ODP 1027 (mid plate) and two sites on the continental slope, ODP 889 and Barkley Canyon. The broadband systems comprise a broadband seismometer and strong motion accelerometer in a surficially buried spherical titanium case. Noise levels observed are as expected with the spectra being similar to coastal seismograph stations, making the instruments suitable for local earthquake locations and regional moment tensor calculations. In summer 2010 an additional broadband package will be installed on the Endeavour segment of the Juan de Fuca Ridge, and four short period instruments will be installed nearby forming a small array, 6 km in maximum dimension, to record earthquake activity in the vicinity of the many multi-disciplinary ridge experiments. The ridge installations will complete the initial phase of the NEPTUNE Canada Seismograph Network which will consist of four broadband and four short period seismic systems. The NEPTUNE Canada Seismograph Network relies heavily on knowledge gained and equipment and techniques developed during previous temporary deployments of autonomous OBS instruments in the region by MBARI and the University of Washington. NEPTUNE Canada will re-occupy their broadband site and two of their short period sites at the ridge. NEPTUNE Canada seismic data is archived by, and available from, both the Geological Survey of Canada and IRIS.

Investigating Source Locations for Body Wave Energy in Ambient Seismic Noise

PYLE, M.L., Saint Louis University, St. Louis, MO USA, mpyle1@slu.edu; KOPER, K.D., Saint Louis University, St. Louis, MO USA, kkoper@gmail.com

The microseismic frequency band contains a large amount of coherent energy which has generated much interest recently because of its use in surface wave tomography as well as its apparent link to temporal changes in ocean wave behavior. The dominant component of this energy travels as surface waves, but body waves also contribute a significant portion at slightly higher frequencies. However, while surface wave noise appears to be generated by ocean wave interaction along the coastline, several studies have indicated that the body wave energy may originate from the deep ocean suggesting the possibility of different mechanisms for the generation of surface and body wave noise. Further investigation of the nature of body wave noise is necessary to better understand how and where it is generated. Seismic arrays are useful in this investigation since array analysis provides a powerful tool for placing constraints on the direction and mode of incoming coherent energy. We back-project the noise from the array to a grid of potential source locations, in a manner similar to a technique recently used to study earthquake rupture properties. The use of small aperture arrays of the International Monitoring System allows for comparison of the back projection results with traditional frequency waveform analysis and provides the additional ability to use data from several arrays at the same time in order to place tighter constraints on noise source locations in the Pacific Ocean. Preliminary results project one month of noise in January 2009 to an area in the middle of the Northern Pacific suggesting the possibility of a persistent deep ocean generation for microseismic P-waves. Future work will examine noise locations over time and compare with significant wave height data to see if sources are stationary or rely on meteorological conditions such as oceanic storms.

Seismic Noise Polarization at Stations in the Central United States

HAWLEY, V., Saint Louis University, St. Louis, MO 63108, USA, vhawley@slu.edu; KOPER, K.D., Saint Louis University, St. Louis, MO 63108, USA.

Saint Louis University possesses a century-long archive of seismic data from seismometers deployed in and around St. Louis, MO. Although the seismic equipment evolved significantly over this time span, meticulous records of instrument response were kept. Therefore, the microseisms present in these seismograms provide a homogeneous proxy of ocean-wave activity over the last century. In this study, we document the current microseism properties near St. Louis, MO using modern digital data. This will provide a baseline for comparison with the older historic data. Using the IRIS DMC, we obtained continuous seismic data for 2007 and 2008 from four broadband, three-component stations in the Midwest (SLM, CCM, USIN, UTMT). Polarization analysis was done using a technique based on the work of Samson (1983), as described by Park *et al.* (1987). Essentially, eigen decomposition of the 3-by-3 Hermitian spectral matrix associated with a sliding window of data is applied to yield various polarization attributes as a function of time and frequency. For each hour of data we determined the amplitude, degree of polarization, angle of incidence, phase difference between horizontal components, phase difference between horizontal and vertical components, and back azimuth, all as a function of frequency. We found that microseisms arrive from the direction of the north Atlantic Ocean and are polarized mainly as Rayleigh waves in the band of 5–20 s. A clear seasonality also exists in this frequency band, with the microseisms being much stronger in northern hemisphere winter.

An Explicit Relationship Between Time-Domain Noise Correlation and Spatial Autocorrelation (SPAC) Results and Application to Microseism Directionality

TSAI, V.C., U.S. Geological Survey, Golden, CO, vtsai@post.harvard.edu; MOSCHETTI, M.P., U.S. Geological Survey, Golden, CO, mmoschetti@usgs.gov; MCNAMARA, D.E., U.S. Geological Survey, Golden, CO, mcnamara@usgs.gov

The success of recent ambient noise tomographic studies is now understood to arise due to cross-correlation properties documented in the acoustics community since the 1950s. However, despite the fact that Aki's 1957 spatial autocorrelation (SPAC) work yields identical analytical results, the precise relationship between SPAC and time-domain cross-correlation remains not entirely transparent. Here, we present an explicit comparison of the two approaches and clarify that SPAC theory is indeed equivalent to the cross correlation theory used for recent noise tomography studies. This equivalence allows theoretical work from each field to be applied to the other, and we illustrate a few examples of this. Using the approach taken, in addition to determining phase velocities, we find it possible to quantify the directionality of noise sources in a new framework. This technique may allow for more accurate location and characterization of microseism energy than is possible with other techniques.

Temporal Icequake Investigation and Location at Mount Erebus, Antarctica

KNOX, H.A., New Mexico Tech, Socorro, NM, USA, hunter@ees.nmt.edu; ASTER, R.C., New Mexico Tech, Socorro, NM, USA, aster@ees.nmt.edu; KYLE, P.R., New Mexico Tech, Socorro, NM, USA, kyle@nmt.edu

Erebus volcano constitutes an accessible natural laboratory for long-term monitoring and investigation of Strombolian eruptive behavior and other interesting seismic phenomena, such as icequakes. Specifically, it has been previously noted that swarms of icequakes have been recorded on the long running permanent seismic network and that these swarms appear to have seasonal dependence. In this investigation, we examine broadband seismograms of these events spanning seven years (2003-present) with the intention of determining the event frequency, event magnitude, seasonal dependence, event mechanism, and the distribution of locations. These types of studies are fundamentally important on several fronts, including the possibility that icequakes may be used in a similar fashion as local earthquakes for tomographic imaging. This part of the study focuses on the location, distribution, and magnitude of icequakes recorded on two dense temporary networks deployed during 2008 and 2009. These temporary networks consisted of 24 broadband stations arranged in two concentric rings around the volcano, as well as 99 short period stations deployed both on the summit of Erebus volcano and along the Terror-Erebus axis of Ross Island, Antarctica. Another interesting aspect of this investigation is a temporal study, both on a yearly scale and an approximately decadal scale, which may yield insight not only into the presumably shallow mechanism of these events but also to what extent their frequency of occurrence may be correlated with seasonal temperature variations and corresponding glacial surface stresses. This research is conducted with events recorded on the long running permanent Mount Erebus Volcano Observatory (MEVO) network, which consists of six broadband stations. http://erebus.nmt.edu

Hydro Acoustics in Tsunami Warning

SALZBERG, D., SAIC, Arlington, VA, david.h.salzberg@saic.com

For the past several years, we have been investigating the use of hydroacoustic data for tsunami warning, using the IMS stations as the data source. Through this research, we have demonstrated that the spectral characteristics of hydroacoustic signals from earthquakes (T-phases) primarily results from anaelastic attenuation within the solid earth portion of the propagation. As the attenuation is a fractional energy loss per wavelength, that means that means that the depth of energy release can be determined very precisely. Using that determined depth coupled with the water depth, we are then able to predict the spectral content of the excited tsunami. Because of the way the tsunami propagates in the ocean, the short wavelength (high frequency) component of the tsunami is particularly dangerous in the near field (local), whereas the longer wavelength tsunami is primarily responsible for the far field tsunami. Analysis of IMS hydroacoustic data from the Northern Sumatra (Dec 26, 2004), Nias Island (March 28, 2005), Java (July 17, 2006), Southern Sumatra (Sep 12, 2007), Peru (Aug 12, 2007) and the most recent Tonga (March 19, 2009) earthquakes demonstrates the relationship between T-wave (hydroacoustic) spectral content and the amplitudes of the near and far field tsunamis: Events with shallow spectral slopes have larger near field tsunamis than is expected. However, factoring in shallow rupture (indicated by the T-phase spectrum), the observed near-field tsunami amplitude can be attributed to a short wavelength tsunami that is non-dispersive in shallow (near-field) waters; the shorter wavelength tsunami, when

propagating to the far-field, disperses as the long-wave approximation is not valid in the deeper ocean. We are also have compared the tsunami spectrum predicted by the spectral slope to that observed by the tsunami buoys (DART), and find that in the cases exampled, the predicted spectrum is close to the observed spectrum.

Time Reversal in Geophysics

Poster Session · Friday AM, 23 April · Exhibit Hall

Time Reversal and Cross-Correlations Techniques—the Normal Mode Approach

MONTAGNER, J.-P., Institut de Physique du Globe, Paris/France, jpm@ipgp.fr; LARMAT, C., LANL, Los Alamos/New Mexico/USA, carene@lanl.gov; PHUNG, H., Institut de Physique du Globe, Paris/France, nguyen@ipgp.fr

Time-reversal methods (hereafter referred as TR) were successfully applied in the past to acoustic waves in many fields such as medical imaging, underwater acoustics, non destructive testing and recently to seismic waves in seismology for earthquake imaging. Different studies have explored the TR method to locate and characterize seismic sources in elastic media.

But few authors have proposed an analytical analysis of the method, especially in the case of an elastic medium and for a finite body such as the Earth.

We show how to use a normal mode approach to investigate the convergence property of time reversal.

Generalizing the scalar approach of Draeger & Fink (1999) and Weaver & Lobkis (2002), the theoretical understanding of time-reversal method is addressed for the 3D- elastic Earth by using normal mode theory. TR methods are related with auto-correlation of seismograms for source imaging. We show as well how TR problem relates to the retrieval of Green's function with a multiple source cross-correlation, with its application to structural imaging.

In the case of source imaging, automatic location in time and space of earthquakes and unknown sources is obtained by TR technique. In the case of big earthquakes such as the Sumatra-Andaman earthquake of december 2004, we were able to reconstruct the spatio-temporal history of the rupture. We present here some new applications of these techniques to environmental sources such as glacial earthquakes.

Revealing Source and Path Sensitivities of Basin Guided Waves by Time-Reversed Simulations

ROTEN, D., San Diego State University, San Diego, CA, droten@sciences.sdsu.edu; DAY, S.M., San Diego State University, San Diego, CA, day@moho.sdsu.edu; OLSEN, K.B., San Diego State University, San Diego, CA, kbolsen@sciences.sdsu.edu

Simulations of earthquake rupture on the southern San Andreas fault (SAF) predict large excitation in the San Gabriel/Los Angeles (SGB/LAB) and Ventura (VTB) basins, with amplitudes strongly depending upon source details (slip distribution, direction and rupture velocity). Clearly there is a need to better understand how interaction between source directivity and basin effects leads to these high amplitudes.

We propose a method for rapid calculation of the sensitivity of such predicted wavefield features (*i.e.* excitation in the SGB/LAB) to perturbations of the source kinematics and to details of the velocity structure. The method is based on isolating the wavefield feature of interest and calculating its pullback onto the source by means of a single time-reversed (*i.e.* adjoint) simulation. This allows calculation of the feature excitation resulting from any source perturbation without running a forward simulation. The same time-reversed calculation also yields path-sensitivity kernels which reveal how the energy is propagating from the source (SAF) to the feature excitation (SGB/LAB or VTB).

Path sensitivity-kernels computed for the SGB/LAB and VTB confirm our earlier interpretation that this excitation is caused by long-range channeling along a sedimentary waveguide. For a given amount of slip on the SAF, excitation in the SGB/LAB is greatest for rupture concentrated between the northern Coachella Valley and the Transverse Ranges and propagating to the NE, while excitation in the VTB is mostly sensitive to rupture on the northern segment of the SAF. Basin amplitudes are especially high for super-shear rupture velocities (between 3750 and 4000 m/s) along that fault segment, and even higher for energetically forbidden rupture speeds between the Rayleigh and S-wave velocities. This emphasizes the need for imposing physical constraints on source parameterizations.

Looking inside a Subducting Slab Using Source-Side Seismic Interferometry

MATZEL, E.M., Lawrence Livermore National Lab, Livermore, CA, matzel1@llnl.gov

In a fundamentally new technique for studying Earth structure, Campillo and Paul (2003) used the cross correlation of the diffuse coda recorded at different seismic stations to obtain the Green's function of the Earth between them. Since then, the field of noise correlation has rapidly expanded and resulted in sharp images of the crust and upper mantle. To date, most noise correlation work has focused on using the ambient noise field to obtain estimates of structure between pairs of stations. However, with the proliferation of dense arrays consisting of 10's to 100's of seismometers, it is straightforward to flip the geometry used by Campillo and Paul and focus instead on the structure between pairs of sources. Our method, similar to that of Curtis *et al.* (2009), involves correlating the coda of pairs of events recorded at individual stations and then stacking the results over all stations to obtain the final waveform.

By effectively replacing each earthquake with a "virtual station" recording all the others, the technique isolates the portion of the data that is sensitive to the source region and has the potential to dramatically increase the resolution of tectonically active areas where seismic stations either can't or haven't been located. Here, we apply the methodology to 40 small and moderate magnitude earthquakes located within and around the Central American slab and recorded by the USArray and other seismic networks. This results in estimates of the Green's function for 780 paths within the slab region. We demonstrate these estimates match closely with those predicted by large-scale 3D models. Finally, the envelope of each waveform is inverted to obtain the best 1D structure between each source pair and these models are then combined to create an image of the slab itself.

Imaging the Rupture of the September 2009 M8.1 Samoan Outer Rise Earthquake and a Triggered Aftershock on the Plate Interface

HUTKO, A., IRIS, Seattle, WA, USA, alex@iris.washington.edu; LAY, T., University of California, Santa Cruz, CA, USA, thorne@pmc.ucsc.edu; KOPER, K., St Louis University, St Louis, MO, USA, koper@eas.slu.edu

Applications of teleseismic P-wave back-projection to image gross characteristics of large earthquake finite-source ruptures have been enabled by ready availability of large digital data sets. Imaging with short-period data from dense arrays or broadband data from regional and global networks can place constraints on rupture attributes that otherwise have to be treated parametrically in conventional modeling and inversion procedures. Back-projection imaging may constrain choice of fault plane and rupture direction, velocity, duration and length for large earthquakes, and can robustly locate early aftershocks embedded in mainshock surface waves. Back-projection methods seek locations of coherent energy release from the source region, ideally associated with down-going P wave energy. We apply broadband P-wave back-projection imaging to the 29 September 2009 Samoa (Mw8.1) earthquake using data from global and large regional arrays in Japan, Australia, and NAmerica and compare data results with results using synthetic seismograms generated from finite fault modeling. Combining results from regional large-aperture arrays, however, is not straightforward, due to gross smearing as a result of the limited receiver geometries. We attempt to handle this problem by deconvolving the point-spread function, which takes into account the exact receiver geometries, from each regional array (similar to empirical greens function decon.). The deconvolution results, free of smearing artifacts, are then averaged. Results indicate a bilateral mainshock rupture consistent with finite-fault modeling. Results from different regional arrays indicate a later burst of energy about 80 seconds and 220 km to the SW of the mainshock centroid, consistent with a triggered aftershock. This feature is later and father from the epicenter than a second ~M7.8 thrust event that occurred on the about 60 seconds after origin time and on the plate interface about 70 km west of the outer-rise mainshock

Rupture Imaging of Recent Large Earthquakes in South America via Backprojection of Teleseismic P-waves

SUFRI, O., Saint Louis University, St. Louis, MO, USA, oner.sufri@gmail.com; XU, Y., Saint Louis University, St. Louis, MO, USA; KOPER, K.D., Saint Louis University, St. Louis, MO, USA.

It is becoming increasingly popular to image the ruptures of large earthquakes by backprojecting teleseismic P waves. Although cruder than traditional finite-fault modeling, this approach can constrain important source properties such as rupture velocity, rupture directivity, the relative location of subevents, and the approximate duration of the source time function. This approach can also detect the very earliest aftershocks that appear in the coda of the main event. Importantly, it can be carried out very quickly because it relies on first-arriving seismic energy and does not require the geometry of the fault plane to be known. In this work, we backproject teleseismic P waves to investigate the source properties of the Mw 7.7 Peru earthquake of 12 November 1996, the Mw 8.4 southern Peru earthquake of 23 June, 2001, and its Mw 7.6 aftershock of 7 July, 2001. We download data from the IRIS DMC, align the P waves using a multi-channel cross-correlation algorithm, and map beam energy as a function of time back to the source region. In particular, we examine the effect of different array geometries and stacking methods on the rupture images. Initial results indicate that the three earthquakes have complex rupture

patterns and that the rupture for the Mw 7.7 1996 and Mw 8.4 2001 events initially propagated down-dip. This was also observed in our previous analysis of the 2007 Mw 8.1 Pisco earthquake. We compare our backprojection results to the detailed finite fault models that have been produced by inverting geodetic data and seismic waveforms, and find reasonable agreement.

Seismic Structure and Geodynamics of the High Lava Plains and Greater Pacific Northwest

Poster Session · Friday AM, 23 April · Exhibit Hall

Rayleigh Wave Phase Velocity Dispersion Analysis in the High Lava Plains, Oregon

FENG, H.S., UCLA Dept of Earth and Space Sci, Los Angeles, CA, USA, helenxxfeng@gmail.com; BEGHEIN, C., UCLA Dept of Earth and Space Sci, Los Angeles, CA, USA, cbeghein@ucla.edu

The High Lava Plains (HLP) region in Oregon is the most volcanically active area in the continental United States, but does not conform to conventional models of magmatism and crustal formation. Our goal is to gain a better understanding of the three-dimensional (3-D) variations in upper mantle seismic velocities in relation to the surface tectonics, as well as the cause of the large volume of continental intraplate volcanism. Previous results from shear-wave splitting measurements (Long *et al.*, 2009) showed a predominantly E-W fast direction of propagation, with an unusually large splitting time of about 2 s. They concluded that this signal originates from active flow in the asthenosphere. Here, we analyze Rayleigh wave dispersion in the HLP region, which will enable us to put tighter constraints on the depth of origin of the anisotropy. We are processing data collected by two dense arrays of seismic stations (HLP and USArray) to measure Rayleigh wave phase velocities between periods of 16 s and 100 s, using a traditional inter-station method. This will allow us to constrain 3-D variations in seismic wave velocities and azimuthal anisotropy in the upper ~200 km of the mantle, and therefore gain insight on the deformation processes taking place under the study region.

Crustal and Lithosphere Structure of the Pacific Northwest with Ambient Noise Tompgraphy

GAO, H., University of Oregon, Eugene/OR/USA, hgao@uoregon.edu; HUMPHREYS, E., University of Oregon, Eugene/OR/USA, genehumphreys@gmail.com; YAO, H., MIT, Cambridge/MA/USA, hjyao@mit.edu; HILST, R., MIT, Cambridge/MA/USA, hilst@mit.edu

Ambient noise Rayleigh wave tomography is used to image the crust and upper mantle structures in the Pacific Northwest of western U.S., with a focus of the structure near NE Oregon. This is the source area of the ~16 Ma Columbia River flood basalt eruptions, and includes the ~50 Ma suture between oceanic Siletzia and continental North America lithosphere. Anisotropic surface wave tomography is applied to test ideas about crust and mantle modification in the region affected by the Columbia River flood basalt eruptions and Siletzia accretion. Very complicated structures have been found beneath NE Oregon using ambiant noise tomography (Yang *et al.*, 2008), receiver functions and SKS-splitting. Our study includes two years of data (2007–2009) recorded by >300 seismometers (from EarthScope's Transportable array and the High Lava Plains, Wallowa flex-array studies, and 7 permanent stations) producing ~55,000 cross correlations. Our initial results are similar to those of Yang *et al.*, although we image greater detail and velocity contrast. The shear wave velocity is abnormally slow in the crust beneath the Pasco basin while high around the Wallowa Mountains in NE Oregon. The western Snake River Plain (SRP) is relatively slower compared to the eastern part in the shallow depth. With depth increasing, the central and eastern SRP become slower. Generally, central and southern Oregon is slow in the crust and upper mantle beneath the High Lava Plain.

Preliminary model of the Juan de Fuca slab

CHU, R., Caltech, Pasadena, California, USA, chur@gps.caltech.edu; SUN, D., Caltech, Pasadena, California, USA, sdy@gps.caltech.edu; HELMBERGER, D.V., Caltech, Pasadena, California, USA, helm@gps.caltech.edu

Tomographic images of the structure beneath the Pacific Northwestern United States display a maze of dipping blobs. Many of these features produce diffraction patterns evident in the USArray observations indicative of sharp edges. We use this complexity in multipathing, ranging from 3.0 to 6.0 sec in *S* and 0.5 to 2.0 sec in *P* waveforms to define the edge of the slab. The locations of these mapped out features agree quite well with existing contour lines defining the plate's upper interface (McCrory *et al.*, 2006) with a step-over to the east near Seattle. This feature is particularly obvious in two recent tomographic models, Xue and Allen (2007) and Schmandt and Humphreys (2009). Synthetics from these two models fit the timing quite well and even some of the complexity where the velocity jumps from fast to slow producing up to a 10% contrast in *S* and 4% in *P*. After examining many regional events, we found four events to be the most useful, 2 events in the Gulf of Mexico, the Well's event in Nevada and a reversed profile from the Queen Charlotte earthquake. Distortions in the triplication data with rapid changes in differential timing validate the multipathing features. The sharpest edges occur at the southern boundary beneath Northern California near Eureka and near the Seattle step-over where the seismicity is the strongest. A hybrid model satisfying the waveform data, the modified tomographic images and conventional slab wisdom will be presented.

The 2006–2010 Maupin, Oregon Earthquake Swarm

BRAUNMILLER, J., Oregon State University, Corvallis, Oregon, USA, jbraunmiller@coas.oregonstate.edu; WILLIAMS, M., Oregon State University, Corvallis, Oregon, USA, mwilliams@coas.oregonstate.edu; TREHU, A.M., Oregon State University, Corvallis, Oregon, USA, trehu@coas.oregonstate.edu; NABELEK, J., Oregon State University, Corvallis, Oregon, USA, nabelek@coas.oregonstate.edu

Seismicity in the Pacific Northwest east of the Cascades is characterized by sporadic bursts of clustered seismicity with occasional M=6 earthquakes. The Maupin area had experienced two previous swarm episodes—in 1976, with the largest instrumentally recorded earthquake of M_w = 4.6, and in 1987—before a new burst of activity started in December 2006. Since then, more than 420 earthquakes have been recorded by the Pacific Northwest Seismic Network about 10 km SE of Maupin and 50 km E-SE of Mount Hood. The current sequence lacks a distinct main shock, with the largest events (M_w = 3.8 and 3.9) on March 1, 2007 and July 14, 2008, more than one year apart; 17 additional events had M≥3, with the most recent on January 2, 2010. During the first year, USArray-TA stations surrounded the swarm providing good resolution. The closest TA-site G06A has been adopted and is now permanent site KENT. We also use data from the 2006–2009 High Lava Plains Broadband experiment. HypoDD relocation of 41 M≥2.5 events indicates a NNW-SSE trending source volume of <1 km^3 at 16–17 km depth. Moment tensor inversion of the six largest events shows pure double-couple strike-slip mechanisms, forming two groups with slightly rotated nodal planes relative to each other. The three largest 2007 events and the July 2008 event have a ~15° NW trending nodal plane while the April 2008 and 2009 M_w = 3.3 events are rotated ~10° clockwise. Rotation is consistent with slight waveform changes at G06A, and all larger events belong to one of the two groups. In general, the first group is comprised of earlier events slightly south of the second group indicating a slight fault bend and a possible northward propagation. The swarm is ongoing, but has slowed down since mid-2008. The swarm's longevity suggests it is driven by repeated fluid injection into a small volume locally relieving stress.

Seismicity and Seismotectonics

Poster Session · Friday AM, 23 April · Exhibit Hall

Broadband Source Mechanism Modeling of Recent Earthquakes in Calabria, Southern Italy

D'AMICO, S., Saint Louis University, St. Louis, Missouri, USA, sebdamico@gmail.com; ORECCHIO, B., Univ. Calabria-Univ.Messina, Messina, Italy, orecchio@unime.it; PRESTI, D., Università di Messina, Messina, Italy, dpresti@unime.it; GERVASI, A., Ist. Naz. Geofis. e Vulc., Cosenza, Italy, gervasi@ingv.it; GUERRA, I., Università della Calabria, Cosenza, Italy, guerra@unical.it; NERI, G., Università di Messina, Messina, Italy, geoforum@unime.it; ZHU, L., Saint Louis University, St. Louis, Missouri, USA, lupei @eas.slu.edu; HERRMANN, R., Saint Louis University, St. Louis, Missouri, USA, rbh@eas.slu.edu.

The aim of this study is to provide moment tensor solutions for recent events occurred in the Calabrian area. The data set consists of waveforms from more than 100 earthquakes recorded by the national seismic network of Istituto Nazionale di Geofisica e Vulcanologia (INGV), the regional stations of Calabria University and the temporary network of CATSCAN project (Calabria Apennine Tyrrhenian–Subduction Collision Accretion Network). Under the CATSCAN project, 40 portable digital broadband seismographs were deployed throughout southern Italy by Lamont-Doherty Earth Observatory, INGV and University of Calabria. The magnitude of the events ranged between M=2.5 and M=4.7, whereas the path lengths ranged between a few kilometers and about 280 km. We computed the moment tensor solutions using the Cut And Paste (CAP) method proposed by Zhu and Helmerger (BSSA, 1996) and the inversion technique proposed by Herrmann (SRL, 2008). Both methods determine the source depth, moment magnitude and focal mechanisms using a grid search technique. They allow time shifts between synthetics and observed data in order to reduce dependence of the solution on the

assumed velocity model and on earthquake locations. For the earthquakes investigated we tried different station distributions (for example using only the nearest, the farthest stations or combinations of both). We also changed the azimuthal station distribution and the epicentral parameters of the event. The final solution is robustly determined. The methods provide a good-quality solutions in the area in a magnitude range (2.5–4.5) not properly represented in the Italian national catalogues. In addition the solutions estimated from P-onset polarities are often poorly constrained in this magnitude range.

Crustal Structure of the Iranian Plateau and Surounding Region

PRIESTLEY, K., University of Cambridge, Bullard Labs, Madingley Rise, Madingley Road, Cambridge, United Kingdom, kfp10@cam.ac.uk; RHAM, D., University of Cambridge, Bullard Labs, Madingley Rise, Madingley Road, Cambridge, United Kingdom, dr291@cam.ac.uk; ACTON, C., University of Cambridge, Bullard Labs, Madingley Rise, Madingley Road, Cambridge, United Kingdom, c.e.acton.00@cantabgold.net

We have determined the variation in crustal structure of the Iranian Plateau and surrounding region using receiver functions and surface wave dispersion data. P-wave receiver functions have been determined at over 100 sites on the Iranian Plateau. Fundamental mode Rayleigh and Love wave group velocities have been determined from over 5000 regional seismograms for paths crossing the plateau and these measurements combined it tomographic group velocity maps for periods between 10 and 70 seconds. The combined analysis of the receiver function and surface wave dispersion data gives a 3D image of the crust of the Iranian Plateau and surrounding region. The crust is ~40 km thick beneath the Mesopotamian Foredeep increasing to 55–60 km beneath the Zagros Mountains, then thinning to 40–45 km beneath the central plateau. The crustal thickness remains 40–45 km beneath the Kopet Dagh Mountains of northeastern Iran then thins to ~30 km beneath the Tuan Shield in southern Turkmenistan. Despite earlier gravity studies suggesting that the Alborz Mountains of northern Iran were not supported by a crustal root, our analysis shows a thickening of the crust from ~48 km beneath the northern part of the Central Iranian Plateau to 55–58~km below the central part of the Alborz Mountains, then a thinning of the crust to ~46 km north of the Alborz Mountains beneath the coastal region of the South Caspian Sea. Thus, the Alborz Mountains do have a crustal root but of insufficient thickness to compensate the elevation of the range. The crust of the South Caspian Basin is 45–50 km thick and contains 20–25 km of sediment. The crust beneath the coast of the Makran in southern Iran is ~ 25 km thick but rapidly increases to ~45 km thick 200 km north of the coast.

Modeling of Three-Dimensional Regional Velocity Structure Using Wide-Angle Seismic Data from the Hi-CLIMB Experiment in Tibet

GRIFFIN, J.D., Purdue University, West Lafayette, Indiana, griffijd@purdue.edu; NOWACK, R.L., Purdue University, West Lafayette, Indiana, nowack@purdue.edu; TSENG, T.L., Tawain National University, Taipei, Taiwan, tailintseng@ntu.edu.tw; CHEN, W.P., University of Illinois, Urbana, Illinois.

Using data from local and regional events recorded by the Hi-CLIMB array in Tibet, we utilize P-wave arrival times to constrain a three-dimensional velocity structure in the crust and the upper mantle in western China. We construct more than 30 high-quality, regional seismic profiles, and select 8 of these, which show excellent crustal and Pn arrivals, for further analysis. Travel-times from four close-in events provide details on crustal velocities, and four events at regional distances provide further constraint on Moho structure and mantle lid velocities. We use the 3-D ray tracer, CRT, to model the travel-times. Initial results indicate that the Moho beneath the Lhasa terrane of southern Tibet is over 73 km deep with a high Pn speed of about 8.2 km/s. In contrast, the Qiangtang terrane farther north shows a thinner crust, by up to 10 km, and a low Pn speed of 7.8–7.9 km/s. Preliminary estimates of upper mantle velocity gradients are between .003 and .004 km/s per km, consistent with previous results by Phillips *et al.* (2007). Travel-times from events to the west and east of the array indicate that both Moho structure and mantle-lid velocities in the region are highly three-dimensional and share a general trend with surface topography.

Seismotectonic Environment of Some Enervated Earthquakes Along the Sumatra Subduction Zone

MCCANN, W.R., Earth Scientific Consultants, Westminster, Colorado USA, wrmccann@comcast.net; CHOY, G.L., U.S. Geological Survey, Denver, Colorado USA, choy@usgs.gov

Teleseismic studies have found that, for a given seismic moment Mo, the radiated energy Es for an earthquake can vary considerably. We characterize as enervated those earthquakes (EE's) radiating anomalously low energy as measured by Mw–Me > 0.5, where Me and Mw are energy and moment magnitudes, respectively. Large (M > 7.5) interplate EE's have been associated with anomalously large tsunami. However, we have found 270 smaller earthquakes in the past 20 years that are also enervated that are not necessarily confined to the accretionary prism. They may occur updip as well as downdip of the nominal seismogenic zones of the plate interface. In the Sumatra subduction zone many of these EE's occur non-randomly near rupture areas of the 2000 Enggano, 2004 Sumatra and 2005 Nias earthquakes. The location of EE's may be related to fine slab structure, as refined with multichannel seismic reflection and teleseismic seismic cross-sections, bathymetry and satellite gravity. Local slab relief of 1–3 km over a horizontal distance of 10–20 km may arise from differential properties on opposite sides of obliquely subducting fracture zones or represent subducted seafloor relief. Locations of EE's on the periphery of low-slip regions of rupture of the main shock suggest that they occur at transitions on the plate interface from predominately stick-slip to stable sliding. EE's also locate along the updip edge of the main region of coseismic slip in 2005. We suggest that the locations of these EE's are evidence of the updip location of a transition from stable sliding to stick slip. Finally, some EE's locate relatively deep along the plate interface, where geodetic and thermal models estimate the deeper edge of stick-stick to stable sliding. We propose that these EE's are evidence of the lower limit of the interplate stick-slip regime.

A Study of Seismicity, Earthquake Source Processes, and Fault Interactions in the Region Between the Denali and Fairweather-St. Elias Fault Systems, Southeast Alaska and Northwest Canada

DOSER, D.I., Univ. Texas at El Paso, El Paso, TX, doser@utep.edu; ESCUDERO, C.R., Univ. Texas at El Paso, El Paso, TX, frogsrain@gmail.com; RODRIGUEZ, H., Univ. Texas at El Paso, El Paso, TX, hugor@miners.utep.edu

We have relocated historical (1899–1971) and recent (post-1971) seismicity and examined source properties of moderate magnitude (Mw 4.5–6) earthquakes in the region of southeastern Alaska-northwestern Canada where strike-slip and thrust faults interact in a complicated fashion to transfer plate motion between the Fairweather-Queen Charlotte transform boundary and the oblique plate convergence of the St. Elias region. Relocations of historical events indicate that most plate bounding fault systems have ruptured since 1899. Moderate magnitude events have occurred with regularity between the northern Fairweather and southern Denali faults and along the Duke River-Totschunda fault system. Recent seismicity in the northern Fairweather region appears to have a relationship to regions of rapid uplift following glacial unloading and also clusters around the edges of gravity highs. Stress drop analysis of moderate events using empirical greens function techniques indicates events along the Fairweather-Queen Charlotte system show the lowest stress release, with events along the Totschunda fault having moderate stress release and events occurring off major fault systems in the Glacier Bay and Yakutat Bay regions showing the highest stress release. We are continuing to evaluate space-time seismicity patterns, stress variation, and the relationship of seismicity to other geophysical data (*e.g.* gravity, magnetics) within the region to determine how these fault systems interconnect.

Seismic Reflection Images of the Central California Coast Ranges and the Tremor Region around Cholame from Reprocessing of Industry Seismic Reflection Profile "SJ-6"

GUTJAHR, S., Freie Universitaet Berlin, Berlin, Germany, stine@geophysik.fu-berlin.de; BUSKE, S., Freie Universitaet Berlin, Berlin, Germany, buske@geophysik.fu-berlin.de

The SJ-6 seismic reflection profile was acquired in 1981 over a distance of about 180 km from Morro Bay to the Sierra Nevada foothills in South Central California.

The profile runs across several prominent fault systems, *e.g.* the Riconada Fault (RF) in the western part as well as the San Andreas Fault (SAF) in its central part. The latter includes the region of increased tremor activity near Cholame, as reported recently by several authors.

We have recorrelated the original field data to 26 seconds two-way traveltime which allows us to image the crust and uppermost mantle down to approximately 40 km depth. A 3D tomographic velocity model derived from local earthquake data (Thurber *et al.*, 2006) was used and Kirchhoff prestack depth migration as well as Fresnel-Volume-Migration were applied to the data set.

Both imaging techniques were implemented in 3D by taking into account the true shot and receiver locations. The imaged subsurface volume itself was divided into three separate parts to correctly account for the significant kink in the profile line near the SAF.

The most prominent features in the resulting images are areas of high reflectivity down to 30 km depth in particular in the central western part of the profile corresponding to the Salinian Block between the RF and the SAF. In the southwestern part strong reflectors can be identified that are dipping slightly to the northeast at depths of around 15–25 km. The eastern part consists of west dipping sediments at depths of 2–10 km that form a syncline structure in the west of the eastern part.

The resulting images are compared to existing interpretations (Trehu and Wheeler, 1987; Wentworth and Zoback, 1989; Bloch *et al.*, 1993) and discussed in the frame of the suggested tremor locations in that area.

Finite-Source Parameters and Scaling of Micro-Repeating Earthquakes at Parkfield

DREGER, D.S., Univ. of California, Berkeley, Berkeley, California, USA, dreger@seismo.berkeley.edu; NADEAU, R.M., Univ. of California, Berkeley, Berkeley, California, USA, nadeau@seismo.berkeley.edu; KIM, A., Univ. of California, Berkeley, Berkeley, California, USA; STATZ-BOYER, P., Univ. of California, Berkeley, Berkeley, California, USA, psb@berkeley.edu; ACEVEDO-CABRERA, A., Univ. of California, Berkeley, Berkeley, California, USA.

We compare source parameters over a range of event magnitudes for repeating and non-repeating earthquakes along the Parkfield segment of the San Andreas Fault. Seismic moment rate functions obtained from empirical Green's function deconvolutions using the Berkeley Seismological Laboratory High Resolution borehole Seismic Network (HRSN) are inverted for the kinematic rupture processes of the events. With this method it is assumed that if a suitable empirical Green's function (eGf) can be found, namely a collocated smaller event with the same radiation pattern as the targeted larger event, the shared propagation, attenuation and site effects can be effectively removed by the deconvolution process leaving the moment rate function of the target event. The obtained moment rate functions are then inverted for the spatial distribution of moment release, the rupture speed and possibly the slip velocity. We update our analysis of the SAFOD target repeaters using the recent December 2008 observations of the Mw2 events from the borehole instrumentation deployed at 2.5 km depth in the SAFOD mainhole. S minus P times indicate that the events are occurring approximately 300m from the downhole sensors. In addition, we present finite-source models and related parametric scaling for Parkfield events from Mw 1.8 to 6.0. In particular we will be examining the scaling of stress drop and apparent stress (both average values), as well as the parameters related to the finite-source analysis such as the dimensions and heterogeneity of slip and stress, and kinematic parameters such as slip rise time and rupture velocity.

Landers Off-Fault Aftershocks are Well-Aligned with the Background Stress Field, Contradicting the Hypothesis of Highly-Heterogeneous Crustal Stress

HARDEBECK, J.L., US Geological Survey, Menlo Park, CA, jhardebeck@usgs.gov

It has been proposed that the crustal stress field contains small-length-scale heterogeneity of larger amplitude than the uniform background stress. This model predicts that small earthquake focal mechanisms reflect the loading stress, rather than the uniform background stress, because earthquakes preferentially occur in volumes of crust where the local stress field is aligned with the loading. The loading stress is usually the tectonic loading, but for aftershocks the loading stress is the mainshock stress perturbation. So, if the heterogeneous stress hypothesis is correct, the focal mechanisms of background seismicity and aftershocks should align with different loading stresses. However, I show that the focal mechanisms of off-fault triggered aftershocks of the Landers earthquake align with the same stress field as the pre-Landers mechanisms. Post-Landers events in regions experiencing a 0.05–5 MPa coseismic differential stress change (too small to rotate the background stress) align with the modeled static stress changes, implying that they were triggered by the stress perturbation. These triggered aftershocks are also well-aligned with the pre-Landers stress field obtained from inverting the pre-Landers focal mechanisms. The alignment of the aftershock focal mechanisms with the pre-Landers stress is inconsistent with the prediction of the heterogeneous stress model that the pre-Landers events and triggered aftershocks should sample crustal volumes with different stress orientations. The inverted pre-Landers stress must be the persistent background stress field. The aftershocks occurred on faults that were well-oriented for failure in the background stress field and then loaded by the Landers-induced static stress change. Therefore, at least at Landers, earthquake focal mechanisms provide an unbiased sample of the spatially-coherent crustal stress field.

The Earthquakes of August 3, 2009 in the Canal de Ballenas Region, in the Gulf of California, Mexico

CASTRO, R.R., CICESE, Dep. Sismologia, Ensenada, Baja California, Mexico, raul@cicese.mx; VALDES, C.M., Instituto de Geofisica, UNAM, Mexico, D.F., Mexico, carlosv@ollin.igeofcu.unam.mx; SHEARER, P., IGPP, SIO, UCSD, La Jolla, California, U.S.A., pshearer@ucsd.edu; WONG, V.M., CICESE, Dep. Sismologia, Ensenada, Baja California, Mexico, vwong@cicese.mx; ASTIZ, L., IGPP, SIO, UCSD, La Jolla, California, U.S.A., lastiz@ucsd.edu; VERNON, F., IGPP, SIO, UCSD, La Jolla, California, U.S.A., flvernon@ucsd.edu; PEREZ-VERTTI, A., CICESE, Dep. Sismologia, Ensenada, Baja California, Mexico, aperez@cicese.mx; MENDOZA, A., CICESE, Dep. Sismologia, Ensenada, Baja California, Mexico, antonio@cicese.mx

On 3 August 2009 the National Seismological Service of Mexico (SSN) reported an earthquake of magnitude *Mw* 6.9 that occurred near Canal de Ballenas (28.48N, 112.24W), in the central region of the Gulf of California. The initial location reported by the SSN and IRIS suggested that the epicenter was on the North American plate near a fault that is considered inactive. This earthquake was preceded by a magnitude 5.8 event that occurred about 5 minutes before. In the next 40 minutes after the main event two aftershocks with magnitudes 4.9 and 5.9 occurred, and on 5 August a third aftershock of *M* 5.5 was located in the Canal de Ballenas region. The transform fault of Canal de Ballenas has been the site of other important events in the past. For instance on July 8, 1975 an earthquake with *Ms* 6.5 occurred west of Angel de la Guarda island. Other earthquakes of moderate magnitude have occurred in this region, more recently to the north, in the lower Delfin basin, on November 26, 1997 (*M* 5.5) and south of Angel de la Guarda island on November 12, 2003 (*Mw* 5.4) and September 24, 2004 (*Mw* 5.8). The events of August 2009 were recorded by the regional stations of the broadband network RESBAN that CICESE operates and by stations of the SSN also located in the region of the Gulf of California (in La Paz, Hermosillo, Santa Rosalia, San Pedro Martir and Mexicali). The focal mechanism of the main event, reported in the CMT Harvard catalog, is right lateral strike-slip with a strike of 216 deg and a dip of 78 deg. The regional records of the broadband stations permit the determination of precise locations and estimates of the rupture area of this important sequence of earthquakes. The resulting hypocentral coordinates indicate that the main events of this sequence occurred along the Canal de Ballenas transform fault.

Foreshock Sequence of the 2008 Mw 5.0 Mogul-Somersett, Nevada, Earthquake

SMITH, K.D., Seismo. Lab., U. Nevada Reno, Reno, Nevada, USA, ken@seismo.unr.edu; VON SEGGERN, D.H., Seismo. Lab. U. Nevada Reno, Reno, Nevada, USA, vonseg@seismo.unr.edu; ANDERSON, J.G., Seismo. Lab., U. Nevada Reno, Reno, Nevada, USA, jga@seismo.unr.edu

The 2008 Mogul-Somersett west urban Reno, Nevada earthquake sequence captured the attention of the Reno-Tahoe area community through much of 2008. The earthquake sequence began in late February with a number of small magnitude felt events in the communities in west urban Reno. A portable real-time instrument, installed on a home PC at a local residence, confirmed the shallow event depths (S-P times < 0.5 sec), improved regional network locations, and provided an accounting of small magnitude activity (M < 0.0). Through much or early 2008 the sequence produced a regular rate of M ~1–2 earthquakes along a NW striking vertical shallow fault. This behavior abruptly changed on April 15, 2008, with four M 3+ earthquakes and initiation a second shallow vertical structure east and parallel to earlier activity. Over the next 10 days three M 4+ events culminated in the Mw 5.0 April 26, 2008 mainshock (11:45 PM local time). The mainshock and early sequence show predominately drextral slip on NW striking structures. Ten portable instruments, including IRIS Ramp systems, were ultimately in operation in the Mogul source area. Here we investigate the foreshock sequence, estimate source parameters of the mainshock, and isolate the immediate aftershocks of the main event. The Mogul-Somersett sequence appears to be defining a more extensive NW striking source region forming one of three primary intersecting zones of seismicity in the Reno-Tahoe area; 1) a NW striking zone of seismicity west of Reno along the northern Sierran front, 2) a NE striking zone of activity in the North Tahoe area extending into south Reno, and 3) the NW trending 2008 Mogul sequence including historical seismicity NW of urban Reno. Complexities observed in the seismicity in NW Nevada are not well reflected in local tectonic models used in assessing the seismic hazard for the Reno-Tahoe area.

P-Wave Slowness Anomalies across USArray Determined by Limited-Aperture Beam Forming

SAWYER, R.L., Augusta State University, Augusta, GA USA, rsawyer@aug.edu; POPPELIERS, C., Augusta State University, Augusta, GA USA, cpoppeli@aug.edu

We analyzed eleven teleseismic earthquakes recorded by USArray for P-wave back azimuth perturbations. There were two groups of events: the first group originated in South America and the second group originated in northeastern Asia. We formed virtual arrays by searching around geographic points on a uniform grid that superimposed the USArray stations. For each virtual array we performed conventional beam forming analysis on the first arrival P-waves. For the eastern portion of the array, our analysis shows that for earthquakes originating from the south, the back azimuths resolved from beam forming deviate to the east of the great-circle back azimuths. For the same eastern portion of the array our analysis shows that for earthquakes originating from the north, the resolved back azimuths deviate to the

west of the great-circle back azimuths. The opposite pattern exists for the northern portion of the array; earthquakes that originate from the south arrive at a back azimuth that deviates to the west of the great circle back azimuths, whereas for the earthquakes originating from the north the arrival back azimuths deviate to the east of the great circle back azimuths. These observations are consistent with a near surface velocity gradient across the array. We hypothesize that the near-surface velocity is lower in the middle of the array, with an increase in velocity on the eastern and western portions of the array.

Lateral Crustal Velocity Variations across the Andean Foreland in San Juan, Argentina from the JHD Analysis.

ASMEROM, B.B., University of Memphis, Memphis,TN, bbasmerm@memphis.edu; CHIU, J.M, University of Memphis, Memphis,TN, jerchiu@memphis.edu; PUJOL, J., University of Memphis, Memphis,TN, jpujol@memphis.edu; SMALLEY, R., University of Memphis, Memphis,TN, rsmalley@memphis.edu

P and S wave station corrections obtained from JHD re-analysis of local earthquakes recorded by PANDA network (1987–1988) show significant lateral crustal velocity variations across the Andean foreland near San Juan, Argentina. This study uses six times more events around Pie de Palo, a basement uplift surrounded by thick sedimentary basins, than the previous study (Pujol *et al.*, 1991). Crustal events beneath the Pie de Palo are grouped into three clusters. Station corrections obtained from these clusters show similar but slightly different spatial patterns. Except for one station directly above thick valley sediment, all stations surrounding Pie de Palo show prominent negative station corrections using cluster-1 events that are directly underneath Pie de Palo. However, positive station corrections are observed for stations across the southeastern edge of Pie de Palo when cluster-2 events are used. The magnitude and distribution of these positive station corrections become even more pronounced from cluster-3, extending further east of Pie de Palo. The patterns of station corrections strongly imply the existence of a localized low velocity zone that may extend more to the south in the upper crust beneath the southeastern edge of Pie de Palo. The area between this low velocity region and eastern Precordillera shows a consistent negative station correction that reveals the existence of high velocity material in the upper crust. Station corrections also reveal that upper crustal velocities are low immediately to the west of eastern Precordillera. A well-defined west-dipping fault is apparent from cross-sectional views of seismicity across the northern Pie de Palo, while poorly defined, gently west- as well as east-dipping faults are observed in the southern part. Moreover, the spatial patterns of station corrections help to set up important priori information to be implemented in the initial model of upper crust for 3-D velocity inversion.

Seismic Networks, Analysis Tools, and Instrumentation

Poster Session · Friday AM, 23 April · Exhibit Hall

A Software Toolbox for Systematic Evaluation of Seismometer-Digitizer System Responses

BONNER, J.L., Weston Geophysical Corp., Lexington, MA, bonner@westongeophysical.com; BULAND, R., USGS NEIC, Golden, CO, buland@usgs.gov; HERRMANN, R.B., St. Louis University, St. Louis, MO; STROUJKOVA, A., Weston Geophysical Corp., Lexington, MA, ana@westongeophysical.com; LEIDIG, M.R., Weston Geophysical Corp., Lexington, MA, mleidig@westongeophysical.com; FERRIS, A., Weston Geophysical Corp., Lexington, MA, aferris@westongeophysical.com

Absolute amplitudes of seismic waveforms are required for body- and surface-wave magnitudes, moment estimation, multi-station source characterization, and attenuation model development. In order to measure these amplitudes, seismic data must be corrected for the multiple components of a digital seismic system (*e.g.*, the seismometer, digitizer, and FIR filters). When the response of the digital seismic system is known, deconvolution of the digital system response is a relatively straightforward process. However, when, for various reasons, the seismic data are transmitted to a data center with little or no knowledge of the system response, the data may be discarded or used only for seismological tasks that do not require absolute amplitude measurements.

We are developing a software toolbox that will recover the seismometer response for recorded seismic data. The toolbox includes 1) a database of known seismometer and digitizer responses with possible sensitivities and FIR filter responses, 2) methods for estimating response "transfer" functions between stations with and without known responses using noise power density functions and broadband signal characterization, 3) techniques for using synthetic seismograms for response validation, and 4) advanced methods for quality control. We have validated these techniques using networks with well-calibrated digital system responses, and are currently using the methods on additional networks with suspect or unknown responses. We plan to implement the tools in an easy-to-use Graphical User Interface (GUI) that can provide seismologists with improved quality control for their data.

Guidelines for Standardized Testing of Broadband Seismometers and Accelerometers

HUTT, C.R., USGS, Albuquerque/NM/USA, bhutt@usgs.gov; EVANS, J.R., USGS, Menlo Park/CA/USA, jrevans@usgs.gov; FOLLOWILL, F., Consultant, Livermore/CA/USA, ffollowill@hotmail.com; NIGBOR, R.L., UCLA, Los Angeles/CA/USA, nigbor@ucla.edu; WIELANDT, E., Stuttgart University, Stuttgart/Germany, E.Wielandt@t-online.de

In July 1989, and again in May 2005, the U.S. Geological Survey hosted international public/private workshops with the goal of defining widely accepted guidelines for the testing of seismological inertial sensors, seismometers, and accelerometers. The second workshop recommended development of guidelines for such testing. Through an open consensus process, formal guidance for testing of broadband seismometers and accelerometers has been developed and was recently published as USGS Open File Report 2009–1285. These guidelines address the long-standing need for standardization in the testing and specification of seismic and earthquake-engineering sensors and recorders.

This presentation outlines the Guidelines and presents details of specific sensor parameters and their measurements procedures. These parameters include Power Demand, Sensitivity, Offset, Frequency Response, Clip Level, Self Noise and Dynamic Range, and Linearity. Sample test reports are provided to foster discussion of Guideline implementation.

NetQuakes—A New Approach to Urban Strong Motion Seismology

LUETGERT, J.H., USGS, Menlo Park, CA, luetgert@usgs.gov; HAMILTON, J.C., USGS, Menlo Park, CA, jhamilton@usgs.gov; OPPENHEIMER, D.H., USGS, Menlo Park, CA, oppen@usgs.gov

More densely sampled strong ground motion recordings are needed in urban areas to provide more accurate ShakeMaps for post-earthquake disaster assessment and to provide data for structural engineers to improve design standards. Ideally, urban areas would have strong ground motion recorders every 1–2 km to adequately sample varied geology and built environment. This would require the addition of thousands of instruments to existing networks. There are several fiscal and logistical constraints that prevent us from doing this with traditional strong motion instrumentation and telemetry. In addition to the initial expense of instruments and their installation, there are recurring costs of telemetry and maintenance.

The USGS has implemented the NetQuakes project to install small, relatively inexpensive seismographs in 1–2 story structures that utilize the host's Internet connection. The 18 bit recorder uses ±3g internal tri-axial MEMS accelerometers. 200 sps data are recorded to a 1–2 week ringbuffer. When triggered, a data file is sent to USGS servers via the Internet. A connection to the host's LAN, and thence to the public Internet, can be made using WiFi to minimize cabling. Timing is maintained by NTP discipline of an internal clock, achieving accuracy generally better than a sample interval.

An innovative data acquisition strategy maximizes data return while minimizing false triggers. The instruments level trigger at 0.25%g. When events are located by the regional network, we determine if a seismic arrival is expected at each instrument. If so, a data request is automatically posted to the instrument.

In 2009, we installed 68 NetQuakes instruments in the San Francisco Bay Area and have integrated their data into the near real time data stream of the Northern California Seismic System. 90 more will be installed in northern California and an additional 90 will be installed by other regional seismic networks in 2010.

How Low Can You Go? Exploring the Capabilities of Low-Cost Accelerometers

CHUNG, A.I., Stanford University, Stanford/CA/USA, aichung@stanford.edu; LAWRENCE, J.F., Stanford University, Stanford/CA/USA, jflawrence@stanford.edu; PRIETO, G.A., Universidad de los Andes, Bogota/Colombia, gprieto@uniandes.edu.co; KOHLER, M.D., UCLA, Los Angeles/CA/USA, kohler@ess.ucla.edu; COCHRAN, E.S., UCR, Riverside/CA/USA, cochran@ucr.edu

For this study, we make use of the ever-advancing micro electro-mechanical systems (MEMS) accelerometer technology to discover what exciting results can be obtained using low-cost accelerometers. Costing roughly $50–150, these compact three-dimensional USB accelerometers are dramatically less expensive than both the three-component seismometers used in seismic studies and the uniaxial accelerometers that are traditionally used in building studies.

We explore the applicability of these sensors in both ambient noise and traditional seismic studies. Although the use of ambient noise recordings to determine structural qualities of buildings is not new, we will ascertain the feasibility of

obtaining building responses using these compact, low-cost accelerometers in place of traditional accelerometers.

Using smaller and cheaper accelerometers has exciting consequences. In the future, it may be possible to perform minimally invasive campaign-style state-of-health monitoring of buildings that provide more useful and dependable results than those from the current methods.

In addition, we analyze data recorded by the Stanford Campus network, an inexpensive but dense seismic network comprised of roughly 50 USB sensors.

ShakeNet: A Tiered Wireless Accelerometer Network for Rapid Deployment in Civil Structures

MISHRA, N., USC, Los Angeles, CA, nmishra@usc.edu; HAO, S., USC, Los Angeles, CA, shuaihao@usc.edu; KOHLER, M., UCLA, Los Angeles, CA, kohler@ess.ucla.edu; GOVINDAN, R., USC, Los Angeles, CA, ramesh@usc.edu; NIGBOR, R., UCLA, Los Angeles, CA, nigbor@ucla.edu

ShakeNet is a portable wireless sensor network for instrumenting large civil structures such as buildings and bridges. It will consist of about 30 sensor nodes each equipped with a 24-bit analog-to-digital conversion board supporting triaxial MEMS accelerometers suitable for vibration sensing, an imote2 CPU board for wireless communication, and battery (ShakeBoxes). The system comes preloaded with sensing software as well as deployment tools that will enable civil engineers to rapidly deploy the network. In addition to the sensors, the system contains 5 to 10 master-tier nodes that provide increased communications capacity. The ShakeNet software subsystem is built upon Tenet, a programmable wireless sensing software architecture designed for tiered sensor networks. ShakeNet will be field tested in a variety of structures including steel moment-frame and reinforced concrete buildings, a dam, and a steel truss bridge. ShakeNet delivers wireless structural health monitoring capability to the structural and earthquake research communities while providing the same level of fidelity and stringent data requirements as those given by the high-end wired sensors. Small form factor and portable design make the ShakeBox easy to rapidly deploy. The modular design of Tenet allows application developers to choose among various wireless sensor network data routing and transportation protocols according to application requirements. Two prototype ShakeBoxes running the Tenet software have been developed and tested using an electrodynamic shake table. ShakeBox performance has been further validated by comparing with state-of-the-art wired sensors collecting building response data from a reinforced concrete building subjected to forced vibrations caused by a mechanical shaker installed on the roof.

The Central U.S. Seismic Observatory (CUSSO)

WANG, Z., Kentucky Geological Survey, Lexington, Ky. United States of America; MCINTYRE, J., Kentucky Geological Survey, Lexington, Ky. United States of America; WOOLERY, E.W., University of Kentucky, Lexington, Ky. United States of America.

A combination of strong-motion accelerometers and medium-period seismometers are currently installed at varying depths within the 1,950-foot (594 meter) borehole comprising the Central U.S. Seismic Observatory (CUSSO) in Fulton County, KY. The borehole penetrated the entire soil/sediment overburden (586 m) and was terminated 8 meters into limestone bedrock. Prior to casing the hole, electrical, sonic velocity (P- and S-wave) and deviation logs were acquired in addition to other site characterizations. The installation of strong-motion accelerometers at CUSSO will give us the ability to measure strong-motions from the bedrock through the soil column to the surface and measure how the soil column changes the characteristics of strong motions as they propagate to the ground surface. The installation of medium period seismometers, (0.06 - 50 Hz) at CUSSO will also provide real records for studying the effect by the sediments on seismic wave propagation. CUSSO will be a tool for evaluation of current analytical models for deep soil sites. Several analytical models are currently being used to predict the seismic response of deep soil sites; however, these analytical procedures have not been validated for sites deeper than 100 m. Earthquakes are now being recorded by CUSSO and data from these earthquakes are being analyzed including data from a small ($M < 2.0$), local event on November 3, 2009 and the November 17, 2009 Queen Charlotte Islands (Mw 6.6) earthquake. CUSSO is the only seismic station in the region with the ability to record bedrock ground-motions, soil column ground-motions, and free-field ground-motions from a site with >100m thick soil/sediment deposits. CUSSO, in combination with other instrumentations of the Kentucky Seismic and Strong-motion Network, as well as other networks in the region, will provide a better constrain on seismic hazard and risk assessments in the central United States.

Arizona Integrated Seismic Network: a new era in seismology for Arizona

BRUMBAUGH, D.S., Northern Arizona University, Flagstaff/Arizona/United States, david.brumbaugh@nau.edu; ARROWSMITH, J.R., Arizona State University, Tempe/Arizona/United States, ramon.arrowsmith@asu.edu; BECK, S.L., University of Arizona, Tucson/Arizona/United States, slbeck@email.arizona.edu; DIAZ, M., Arizona Geological Survey, Phoenix/Arizona/United States, mimi.diaz@azgs.az.gov; FOUCH, M.J., Arizona State University, Tempe/Arizona/United States, fouch@asu.edu; HODGE, B.E., Northern Arizona University, Flagstaff/Arizona/United States, brendan.hodge@nau.edu; ZANDT, G., University of Arizona, Tucson/Arizona/United States, gzandt@email.arizona.edu

July 1,2008 saw the start of a new era in earthquake science in Arizona with the acquisition of eight geoscope stations from the transportable array by means of a grant from FEMA. This was a cooperative grant submitted by the Arizona Geological Survey and the geoscientists at the three state universities. The eight stations obtained served as a "glue" to bring together the seismology community in the state as a working body. As in any new multi-partner effort the challenge was to evolve in a way to produce an effective unit. Following the model in California, the first step was to bring together the monitoring capabilities in the state into the new Arizona Integrated Seismic Network (AISN). This combines the new broadband geoscope stations with existing analogue and broadband stations. The extended coverage gives the state of Arizona a truly statewide network for the first time. All stations are now being monitored on a daily basis at the Arizona Earthquake Information Center. The quarterly meetings of the geoscientists involved in the grant has seen progress and products based on the monitoring of the integrated network:

- The archives and lab of the Arizona Earthquake Information Center have been reorganized for increased efficiency/usability that results in improved capabilities of data collection/release of critical information of the enlarged data stream.
- The University of Arizona group has been involved in focal mechanisms for Arizona earthquakes. Notable are solutions for the 5-09-09 M3.1 and 9-4-09 M3.5 events.
- The Northern Arizona University group has been conducting analysis of a 10-31-09 swarm near Sunset Crater.
- The research group at Arizona State University has been creating a new high-resolution Arizona seismicity catalogue and working on hazards analysis of the new AISN data.

ANSS Quake Monitoring System (AQMS) at the Pacific Northwest Seismic Network

HARTOG, R., University of Washington, PNSN, Seattle/WA/USA, renate@ess.washington.edu; KRESS, V., University of Washington, PNSN, Seattle/WA/USA, kress@ess.washington.edu; BARTLETT, T., University of Washington, PNSN, Seattle/WA/USA, bartlett@ess.washington.edu; BODIN, P., University of Washington, PNSN, Seattle/WA/USA, pbodin@ess.washington.edu

The ANSS Quake Monitoring System (AQMS) is an earthquake monitoring software system developed by the California Integrated Seismic Network (CISN), a collaborative effort by several institutes in California (see http://www.cisn.org). AQMS' real-time processing is built on earthworm v.7 and hypoinverse, however, its real power comes from the storage of information in an Oracle database system. Seismic analysts interact with the database through a Java program called Jiggle. It is the intention of ANSS that all tier 1 regional networks will adopt AQMS as their primary processing system.

At the Pacific Northwest Seismic Network (PNSN) we have been running earthworm and a "home-grown" post-processing system. During the installation, configuration, and testing of AQMS we are maintaining the old system as our primary monitoring and alarming system. Preparation for the installation of AQMS included transitioning to include Location codes in addition to Station Channel, and Network codes (SCNL vs. SCN) in our channel descriptions. We also created dataless SEED files for each station and developed a tool to insert the metadata into the AQMS database schema, based on a proC code written by Stephane Zuzlewski of UC Berkeley.

Paul Friberg of ISTI installed AQMS early in 2009. In April 2009, ISTI visited the PNSN to provide training. We have spent the next year configuring and testing the system, and developing tools to interact with the system. Meanwhile, our seismic analyst and duty seismologists practice locating earthquakes and generating magnitudes using Jiggle. We have developed a graphical tool to compare earthquake parameters generated by our old system and AQMS. At the time of writing this abstract, we have not finished a quantitative comparison between the two catalogs; however, we hope to present some preliminary results at the meeting.

EMERALD: Software for Managing Large Seismic Data Sets

WEST, J.D., Arizona State University, Tempe, AZ, john.d.west@asu.edu; FOUCH, M.J., Arizona State University, Tempe, AZ, fouch@asu.edu; ARROWSMITH, J.R., Arizona State University, Tempe, AZ, ramon.arrowsmith@asu.edu

The geosciences are currently producing an unparalleled quantity of new public broadband seismic data, generating significant new data management challenges for

the seismological community. One such challenge is the maintenance and updating of seismic metadata, including information such as station location, sensor orientation, and instrument response. Metadata changes occur at unknown intervals and are not generally communicated to data users. A second basic challenge is handling massive seismic datasets consisting of millions of waveforms. A third long-standing challenge is the difficulty of exchanging seismic processing codes between researchers, as each scientist typically develops a unique directory structure and file naming convention, making code reuse by other researchers difficult and inefficient.

To address these challenges, we are developing **EMERALD** (**E**xplore, **M**anage, **E**dit, **R**educe, & **A**nalyze **L**arge **D**atasets). The goal of the EMERALD project is to enable more efficient and effective use of massive seismic datasets, leading to higher quality data and enabling faster, more efficient analyses.
EMERALD is an integrated, extensible, standalone database server system, based on the open-source PostgreSQL database engine and designed for a small workgroup. The intuitive web browser interface, compatible with a wide range of computing clients, allows users to quickly and easily preprocess, search, review, revise, and export large seismic datasets. EMERALD can retrieve and store station metadata and automatically alert the user to metadata changes. The system also provides many methods to visualize data, analyze dataset statistics, and track the processing history of individual datasets. EMERALD integrates existing programs such as Taup and GMT, and allows development and sharing of add-on visualization and processing methods using any of 12 programming languages.

The New Data Product Development Effort within the IRIS DMS

BAHAVAR, M., IRIS, Seattle/Washington/USA, manoch@iris.washington.edu; HUTKO, A.R., IRIS, Seattle/Washington/USA, alex@iris.washington.edu; TRABANT, C., IRIS, Seattle/Washington/USA, chad@iris.washington.edu

The research supported by the raw data from the observatories of NSF's EarthScope projects are having tremendous impact on our understanding of the structure and geologic history of North America, how and why earthquakes occur and many other areas of modern seismology. The IRIS Data Management System (DMS) has embarked on a new effort to produce higher-level data products beyond raw data in order to assist the community in extracting the highest value possible from these data. These new products will serve many purposes: stepping-stones for future research projects, data visualizations, research result comparisons and compilation of unique data sets as well as outreach material. The requirements and priorities for new IRIS DMS data products are reviewed and approved by the IRIS Data Products Working Group (DPWG) in consultation with the research community. The IRIS Data Management Center (DMC) is currently working on three new data products. These are: 1) USArray Ground Motion Visualizations, routinely generated animations showing the seismic wavefield sweeping across the USArray Transportable Array from earthquakes in North America and around the world, 2) Tomoserver, a new web interface for visualization and extraction of community-supplied regional and global tomography models and 3) re-homing of EARS, the EarthScope Automated Receiver Survey, from its birthplace at University of South Carolina to its permanent home at the IRIS DMC. EARS aims to calculate crustal thickness and bulk crustal properties beneath USArray stations as well as many other broadband stations whose data are archived at the IRIS DMC. Other data products are also under consideration and will be moved to the development pipeline once approved by the IRIS DPWG.

Real-Time Double-Difference Location and Monitoring of Fine-Scale Seismic Properties

WALDHAUSER, F., LDEO, Columbia University, Palisades, NY, felixw@ldeo.columbia.edu; SCHAFF, D., LDEO, Columbia University, Palisades, NY, dschaff@ldeo.columbia.edu

The availability of precise event locations in near real-time has considerable social and economic impact in the evaluation and mitigation of seismic hazards, for example. We present a real-time procedure that uses cross-correlation (CC) and double-difference (DD) methods to rapidly relocate new seismic events with high precision relative to past events with accurately known locations. Waveforms of new events are automatically cross-correlated with those archived for nearby past events to measure accurate differential phase arrival-times. Correlation and pick delay times are subsequently inverted for the vector connecting the new event to its neighboring events. The DD monitoring tool is currently processing near real-time data feeds from the NCEDC for earthquakes recorded at the CISN in Northern California. New events are relocated within minutes or less relative to a recently developed and continuously updated high-resolution DD earthquake catalog. Back-testing results indicate that the real-time DD locations are on average accurate to within 0.07 km laterally and 0.20 km vertically. The new platform allows for monitoring spatio-temporal changes in seismogenic properties at unprecedented resolution. New events can now be rapidly associated with previously active faults, or located within previously active seismic patterns such as streaks or repeating events. Changes in recurrence intervals of repeating events can be monitored to infer changes in the loading rate, or the short-term evolution of stress concentrations can be tracked in near real-time to better assess the potential occurrence of future events. In addition to results from California we present initial results from applying the real-time DD algorithm to data recorded at global seismic networks and routinely processed at the NEIC.

Chasing Aftershocks with Subspace Detectors

HARRIS, D. B., Lawrence Livermore National Lab, Livermore, CA USA, oregondsp@gmail.com; DODGE, D. A., Lawrence Livermore National Lab, Livermore, CA USA.

We describe a prototype detection framework that automatically clusters events in real time from a rapidly unfolding aftershock sequence. This system was developed to pursue research on efficient network operations to alleviate processing bottlenecks following a major earthquake. We use the fact that many aftershocks are repetitive, producing similar waveforms. By clustering events based on waveform similarity, the number of independent event instances that must be examined in detail by analysts may be reduced. Out system processes array data and acquires waveform templates with an STA/LTA detector operating on a beam directed at the P phases of the aftershock sequence. The templates are used to add subspace detectors to the detection framework that sweep the subsequent data stream of later occurrences of the same waveform pattern. Events are clustered by association with a particular detector.

Hundreds of subspace detectors can run in our detection framework at speeds up to a hundred times faster than real time. Nonetheless, to check the growth in the number of detectors, the framework pauses periodically and reclusters detections to define more compact event groups. These groups define new subspace detectors which replace the older generation of detectors. Because low-magnitude occurrences of a particular signal template may be missed by the STA/LTA detector, we advocate restarting the framework from the beginning of the sequence periodically to reprocess the entire data stream with the existing detectors. Since the framework operates O(100 times) faster than real time, this is a viable near-real-time strategy.

We tested the framework on 10 days of data from the NVAR array covering the 2003 San Simeon earthquake. 184 detectors produced 676 detections resulting in a factor of 3.7 potential reduction in analyst workload.

At the Interface Between Earthquake Sciences and Earthquake Engineering in the Pacific Northwest

Poster Session · Friday AM, 23 April · Exhibit Hall

Development of Ground Motions for Scoggins Dam Seismic Retrofit

ZAFIR, Z., Kleinfelder, Sacramento, CA, USA, zzafir@kleinfelder.com

Built in 1975, the 151-foot high zoned earthfill Scoggins Dam is located about 25 miles west of Portland, Oregon, governed by the Cascadia subduction zone tectonic environment and a few shallow crustal faults. For the proposed seismic upgrade, ground motion criteria in terms of design uniform hazard spectra (UHS) and associated time histories were developed by US Bureau of Reclamation (Reclamation) for earthquakes having return periods of 5,000, 10,000, and 50,000 years. To be consistent with the Reclamation's risk studies, 10,000-year return period was established as the design criteria for the upgrade. However, a review of the 10,000-year UHS showed that the probabilistic spectrum does not represent any realistic seismic event which may result from any of the two distinct seismic sources for this site: a closer moderate earthquake from the Gales Creek fault and a distant subduction earthquake with magnitude greater than 9. This presentation will provide the details about a relatively new and novel method to develop ground motion criteria in terms of scenario earthquakes and associated time histories based on the results of deaggregation and conditional mean spectral (CMS) analyses. The use of these scenario events was approved by a Seismic Hazard Review Board, which was convened exclusively for this project. The revised criteria were used to analyze several different retrofit alternatives including raising of the dam and replacing the dam. The results of our analyses show that these scenario earthquakes represent more realistic events and result in more realistic expected seismic deformations of the embankment.

Vertical Escape Options Needed to Transform Tsunami Safety

WANG, Y., Oregon Dept of Geology-DOGAMI, Portland/OR/USA, yumei.wang@dogami.state.or.us; RASKIN, J., Ecola Architects, PC, Cannon Beach/OR/USA; BOYER, M.M., Chinook GeoServices Inc, Vancouver/WA/USA; MONCADA, J., Berger/ABAM Engineers, Portland/OR/USA; STRAUS, S., Glumac, Portland/OR/USA; YEH, H., Oregon State University, Corvallis/OR/USA; YU, K., Degenkolb Engineers, Portland/OR/USA.

To revolutionize tsunami safety in the U.S., a few dozen strategically located, well-designed and constructed tsunami vertical refuges are needed in extensive low-lying

coastal communities. Our ad hoc design team has developed a conceptual design for a proposed tsunami evacuation building (TEB) in Cannon Beach, Oregon, where almost 50% of residents and over 75% of businesses are in the tsunami zone. The proposed TEB is a state-of-the-art 2-story earthquake and tsunami resistant city hall that would replace the existing, collapse-prone, city hall. This TEB will be constructed within the tsunami inundation zone and meet an immediate occupancy performance level when subjected to long duration, large magnitude, Cascadia subduction zone earthquakes. In addition, it would withstand a variety of tsunami loads, including hydrodynamic stresses, debris impacts and scouring. The design includes the local architectural style, a 150-yr design life, sustainable development, and addresses regional educational, social and recovery issues. It includes on-site wave deflection walls, a pile and grade beam foundation, a post-tensioning structural system, and green technologies involving photo-voltaics, small wind turbines, net metering and battery storage for electricity, and geothermal heating of the building from the pile foundation as a ground source. Many possible design options exist, such as incorporating an eco-roof and rooftop café, public space for ocean views and special events, heliport, or tsunami history museum and education center. Reliable lifeline services for emergency response and recovery for Cannon Beach and nearby coastal communities will be achieved using water tanks and advance telecommunications. The 10,000-sq ft building will accommodate 1,000 evacuees including residents, business community and visitors and serve as a prototype.

Seismic Monitoring at the Alaskan Way Viaduct in Seattle, Washington

DELOREY, A.A., University of Washington, Seattle, WA USA, adelorey@uw.edu; VIDALE, J.E., University of Washington, Seattle, WA USA, john_vidale@mac.com

Starting in September 2008, we have been continuously monitoring a section of the Alaskan Way Viaduct, a double-decker elevated highway located along the waterfront in Seattle, Washington, with a 6-component accelerometer. Three components are located at the top of a column on the upper-deck and the other three are located on the sidewalk at the base of the same column. Our goals are two-fold, to measure the structure's response to ambient conditions, and to attempt capture the structure's response to a moderate or larger earthquake.

During ambient conditions, we found that variations in the structure's free oscillations are most sensitive to the amount of traffic-induced shaking and are able to rule out temperature and weather-related parameters as important factors. The frequencies are reduced by 1–2% during periods of high traffic versus periods of low traffic. We recorded a 4.5 magnitude earthquake located about 28 km away near Kingston, Washington on January 30, 2009. During this event, most of the energy was concentrated in the in-line and transverse fundamental modes, which collapsed to the single frequency of 1.7Hz, in stark contrast to ambient conditions where energy is distributed across many different modes. This is likely due to differences in the frequency content and point of application of the forcing between these two sources. Since the frequencies of the free oscillations remained the same before and after this event, there is no evidence for a softening of the structure due to damage. If the structure is subject to shaking at greater amplitudes and sustains damage, we expect to observe a permanent reduction of the frequencies of the free oscillations. Monitoring of bridges and buildings with accelerometers can assist in a quick assessment of the structure's health and aid in a manual or automated decision to evacuate during an earthquake.

Seismic Hazard Mitigation Policy Development and Implementation

Poster Session · Friday AM, 23 April · Exhibit Hall

Developing Seismic Hazard Maps for Policy Applications in Kentucky

WANG, Z., Kentucky Geological Survey, Lexington, Kentucky, USA, zmwang@uky.edu

Although the causes are still not fully understood, earthquakes continue to occur and will pose certain hazards to the built environment in Kentucky. There is an urgent need to develop seismic hazard maps that can be used for mitigation policy development because the current hazard maps being used are not consistent with modern earthquake sciences and difficult to understand. Three sets of maps, depicting peak ground acceleration and short period (0.2 s) and long period (1.0 s) response accelerations with 5 percent damping, associated with three earthquake scenarios, the expected earthquakes (EE), probable earthquakes (PE), and maximum considered earthquakes (MCE), have been developed in Kentucky, based on the current scientific understanding of earthquakes. EE is defined as the earthquakes that could be expected to occur any time in the bridge lifetime of 50 to 75 years. PE is defined as the earthquakes that could be expected to occur in the next 250 years. MCE is defined as the maximum event considered likely in a reasonable amount of time, varying from 500 to 1,000 years in the New Madrid Seismic Zone, 2,000 to 5,000 years in the Wabash Valley Seismic Zone, to a much longer recurrence intervals in other zones. The associated time histories have also been developed using the composite source model from individual earthquakes. The composite source model takes into account the source effects, including directivity and asperity, and three-dimensional wave propagation. These maps provide bases for performance-based seismic design and analysis of bridges and highways in Kentucky. These maps have also been used for a variety of purposes in Kentucky, including landfill design and industrial facility sitting.

Earthquake Safety Initiative for Rural Communities in Western China

YUAN, Z.X., Lanzhou Institute of Seismology, Lanzhou, Gansu, China, zhongxiayuan@yahoo.com; WANG, L.M., Lanzhou Institute of Seismology, Lanzhou, Gansu, China, wanglm@gssb.gov.cn; WANG, Z.M., Kentucky Geological Survey, Lexington, Kentucky, USA, zmwang@uky.edu

Earthquakes are major natural disaster threatening rural communities in western China. For example, many rural communities were completely or severely damaged by the May 12, 2008, Wenchuan Earthquake (M8.0). One important lesson learned from the Wenchuan earthquake is that besides economic affordability and site conditions, proper scientific input, necessary technological guidance, and public awareness are important for rural communities. Hence, it is imperative to devise an elastic and educational framework that is more suitable for improving earthquake safety for rural communities in western China through strengthening buildings.

Lanzhou Institute of Seismology initiated a new program of earthquake safety for the rural communities in Gansu Province starting in 2004. First, the technologies and guidelines for strengthening buildings in rural communities were developed with a wide range of options in terms of costs and measures, and that are also ease to apply. At the same time, the local architectural elements were incorporated to take advantage of available material, cultural concerns of residents, and local suitability. Then, booklets with good illustrations and general guidelines with empirical design parameters were compiled to provide information that is both easy to be understood and easy to be applied. In some case, lectures on earthquake safety of rural buildings were given to local officials overseeing implementation of these safety guidelines. A Web-based technical service for earthquake safety of rural buildings was also developed to provide friendly and easier-to-access service through service centers, local schools and other public facilities. This service consists of modules such as seismic hazard information, earthquake safety guide, education materials and technical illustrations.

This initiative reduced the economic losses and casualties in the rural communities of southeastern Gansu during the Wenchuan earthquake.

State of Stress in Intraplate Regions

Poster Session · Friday PM, 23 April · Exhibit Hall

Are Recent Earthquakes near Greenbrier, Arkansas Induced by Waste-Water Injection?

HORTON, S.P., University of Memphis, Memphis,TN, shorton@memphis.edu; AUSBROOKS, S.M., Arkansas Geological Survey, Little Rock,AR, scott.ausbrooks@arkansas.gov

During October and November, 2009, NEIC located eight earthquakes ($2.4 < m < 3.0$) in the vicinity of Greenbrier, Arkansas. The earthquake activity generated public concern that a recent increase in "hydro-fracking" operations to stimulate natural-gas well production in the area was the cause. Shallow source depths (0–2.5km) combined with proximity (<5km) of the epicenters to an active waste-water injection well encouraged the University of Memphis and the Arkansas Geological Survey to deploy three seismometers in the local area. Preliminary analysis of the local network indicates the occurrence of hundreds of small earthquakes located about 2km south of the waste-water injection well with source depths ranging between 6.7 and 7.6 km. While a relationship between the earthquake activity and waste-water injection at depths around 2.4 km is possible, a causal relationship has not been substantiated. Moreover, this region of Arkansas has a history (since 1976) of scattered and episodic earthquake activity. Indeed in the early 1980s and again in 2001, there were swarms of tens of thousands of small "natural" earthquakes (largest M4.5) in Enola only 20 km east-southeast. These earthquakes occurred at depths between 3 to 7 km and were clustered in a highly fractured zone within the bend of a Mississippian age graben. This graben is part of a system of steeply dipping normal faults that trend EW then turn ENE across the region. Seismic reflection profiles indicate similar structural patterns underlie both the Enola and Greenbrier areas.

Preliminary Results for the Detection of Non-volcanic Tremor in the New Madrid Seismic Zone Using a Phased Array

LANGSTON, C.A., CERI, Univ. of Memphis, Memphis/TN/USA, clangston@memphis.edu; DESHON, H.R., CERI, Univ. of Memphis, Memphis/TN/USA, hdeshon@memphis.edu; HORTON, S., CERI, Univ. of Memphis, Memphis/TN/USA, shorton@memphis.edu; WITHERS, M., CERI, Univ. of Memphis, Memphis/TN/USA, mwithers@memphis.edu

One of the most exciting discoveries to be made within the New Madrid Seismic Zone (NMSZ) in recent years is the possibility that non-volcanic tremor may be occurring within this intraplate fault system. A reflection/refraction experiment near Mooring, TN, in November 2006 recorded a sequence of high frequency signals that moved across the linear array at 3–25 km/s. The signals were reminiscent of the packets of energy reported for non-volcanic tremor (NVT) in subduction and strike-slip fault environments. We hypothesize that NVT consists of temporally-energetic swarms of micro-earthquakes at the ML –1 to –2 level occurring at mid-crustal levels in the NMSZ. To test this hypothesis a 19-station phased array was deployed in November 2009 over the Reelfoot reverse fault, near the original reflection experiment, and will be collecting continuous data for one year. The array should allow signal detection at ground motion levels equivalent to ML –2. Array analysis will increase signal-to-noise ratios and yield wave azimuth and slowness information that can be used to estimate locations for small events. The temporal and spatial characteristics of NVT within the New Madrid fault system are critical parameters that potentially relate a seismic observable to strain within the fault zone. NVT occurring at deep levels in this intraplate fault zone may be related to ductile processes similar to those postulated for NVT in subduction zones and at deep levels of the San Andreas fault. NVT within shallower parts of the fault where typical microseismicity now occurs may reflect unusual brittle failure processes associated with stress heterogeneity or anomalous pore pressure states. Here, we present preliminary data from the array and report on initial findings.

Analysis of Recent Earthquakes in Cleburne, Texas

HOWE, A.M., Southern Methodist University, Dallas, Tx, amhowe@smu.edu; HAYWARD, C.T., Southern Methodist University, Dallas, Tx; STUMP, B.W., Southern Methodist University, Dallas, Tx; FROHLICH, C., University of Texas at Austin, Austin, Tx.

On 2 June 2009, the USGS reported a magnitude 2.8 earthquake located 1.6 km northwest of Cleburne, TX, in a region of active gas development. The town has no historical seismicity, and has no known active faults. Felt earthquakes reoccurred approximately weekly in June and July with six reported by the USGS between magnitude 2.0–3.0. The most recent USGS earthquake on 10 August was a magnitude 2.0. Beginning on 15 June, SMU deployed a local network of four PASSCAL supplied Quanterra Q330 digitizers and Guralp CMG–40T seismometers. The four station initial locations were based on felt reports and had an aperture less than 10 km. Analysis of initial network events led to redeploying one station southwest of Cleburne and the installing a fifth southeast of the city, yielding a network surrounding the activity. Ten earthquakes in the sequence were analyzed (two reported by USGS) and share almost identical waveforms suggesting tightly clustered hypocenters Due to anisotropy, P and S wave arrivals were picked on the vertical channel. Event locations were determined using a 3-layer velocity model based on a logged well in the same general geology but displaced from the earthquakes. The estimated locations are centered at 32.312+.005 N and 97.381+.001 W and fall along a 2 km north-south line. Small events have continued and are being recorded locally but have not been reported by the USGS.

Observation of Microearthquake Sequences in the Haicheng, Liaoning, China

KIM, G.Y., KIGAM, Gwahang-no 92, Yuseong-gu, Daejeon Republic of Korea, gandalf@kigam.re.kr; SHIN, J.-S., KIGAM, Gwahang-no 92, Yuseong-gu, Daejeon Republic of Korea, jinsoo@kigam.re.kr

We estimated the source paramater of 30 microearthquake sequqences following earthquake of ML 4.2 November, 2, 2008 at Haicheng, Liaoning,of China. The Microearthquake sequences are remarkably similar, implying consistently similar location and source mechanism. We measured spectral ratios by stacking the ratios which were calculated through taking moving windows along direct waves. We modeled the spectral ratios to calculate seismic moments and corner frequencies using omeage square model.

Relocation of the 20 January 2007 ML 4.8 Odaesan Earthquake Sequence

KIM, K.-H., Korea Ocean Res. & Dvlp. Inst., Ansan, Gyeonggi-do, Republic of Korea, kwanghee@kordi.re.kr; KANG, S., Korea Ocean Res. & Dvlp. Inst., Ansan, Gyeonggi-do, Republic of Korea, sukang@kordi.re.kr; PARK, Y., Korea Polar Res. Inst., Incheon, Republic of Korea, ypark@kopri.re.kr

A moderate-sized earthquake (ML 4.8) occurred in the mid-east Korea Peninsula on 20 January 2007. It was the largest inland earthquake to occur in South Korea since the installation of the Korea National Seismic Network in 1998. The earthquake caused minor damage to adjacent structures and temporary failure of the electrical power supply. Although only four aftershocks were noticed in previous studies, a careful review of continuous data revealed that the main event was accompanied by at least 74 micro foreshocks and aftershocks. A subset of 25 events was selected for further analysis to determine precise earthquake locations, focal mechanism solutions, and the current status of regional tectonic stress, as well as to answer questions raised about the sequence. The results of the precise earthquake relocation reveal that the Odaesan earthquake occurred on a vertical and circular fault plane. Although the Woljeongsa Fault is noticed from the local geological map, the relocated hypocenters indicate that the Odaesan earthquake and its aftershocks did not relate to the Woljeongsa Fault. We also observed an unusual lack of large-magnitude aftershocks, a relatively large stress drop during the main event, and no previous earthquake record in the region. Observations made in the study consistently indicate the sequence is resulted from the activation of a new small-scale fault or the reactivation of a previously unmapped fault as a consequence of long-term regional tectonic loading. Focal mechanism solutions of this and other events in Korea indicate that the Odaesan earthquake was a typical consequence of crustal deformation due to current tectonics reflecting ENE–WSW compression and NNW–SSE extension near South Korea in the stable Eurasian continent.

Seismicity of Stable Continental Regions (SCRs): Correlation of Earthquake Locations, Magnitudes, and Mmax with Deep Lithospheric Structure

RITSEMA, J., University of Michigan, Ann Arbor, MI, USA, jritsema@umich.edu; MOONEY, W.D., US Geological Survey, Menlo Park, CA, USA, mooney@usgs.gov

We further demonstrate the validity of our approach to estimating the seismic potential of continental intraplate regions based on the deep seismic properties of the lithosphere. For more than a year, we have explored the hypothesis that greater integrative lithospheric strength correlates with lower rates of continental crustal seismicity and with lower maximum earthquake magnitudes, also known as Mmax. Integrative lithospheric strength is controlled by lithospheric composition and the geotherm, which is correlated with S-wave velocity. High lithospheric S-wave velocities, typical of cratonic lithosphere, correspond to high integrative lithospheric strength. We have created new global maps of S-wave velocity anomalies (δVs) at a depth of 175 km. We find that δVs ranges from +5% to –5%. We compare the values of these mantle S-wave anomalies with the moment magnitudes of intraplate earthquakes in the overlying crust. We find that only 10% of 460 events with moment magnitudes between 5 to 6; 15% of 110 events with moment magnitudes between 6 to 7; and none of the 14 intraplate events with moment magnitudes greater than 7 occur above mantle lithosphere with δVs greater than 3.5% (cratonic lithopshere). We conclude therefore that integrated lithospheric strength, as indicated by S-wave velocity anomalies, correlates with crustal seismicity. Mmax appears to be M7 for cratonic continental regions underlain by δVs greater than 3.5% at 175 km depth. This includes a large portion of the Precambrian continental interior of North America of Archean and Neoproterozoic age.

The North American Upper Mantle: Density, Composition, and Evolution

MOONEY, W.D., US Geological Survey, Menlo Park, CA, USA, mooney@usgs.gov; KABAN, M.K., GeoForschungsZentrum, Potsdam, Germany, kaban@gfz-potsdam.de

We investigate the density structure of the North American (NA) upper mantle based on the integrative use of the gravity field and seismic data. The basis of our study is the removal of the gravitational effect of the crust to determine the mantle gravity anomalies. This is accomplished by subtracting the gravitational contributions of: (1) topography and bathymetry; (2) low-density sedimentary accumulations; and (3) the 3D density structure of the crystalline crust as determined by seismic observations. Information regarding sedimentary accumulations is taken from published maps and summaries of borehole measurements of densities; the seismic structure of the crust is based on a recent compilation, with layer densities estimated from P-wave velocities. The resultant mantle gravity anomaly map shows a pronounced negative anomaly (–50 to –400 mgal) beneath western NA and the adjacent oceanic region, and positive anomalies (+50 to +350 mgal) east of the NA Cordillera. This correlates with the stable eastern region and the tectonically active western region. The close correlation of large scale features of the mantle anomaly map with the topographic map confirms that a significant amount of the topographic uplift in western NA is likely due to buoyancy in the hot upper mantle. In order to separate the contributions of temperature anomalies from compositional anomalies, we apply

an additional correction to the mantle anomaly map for the thermal structure of the uppermost mantle. The thermally-corrected mantle density map reveals density anomalies that are chiefly due to compositional variations and have a magnitude of ±250 mgal. Based on these geophysical results, the evolution of the NA upper mantle is depicted in a series of maps which display the primary processes that have formed and modified the North American crust and lithospheric upper mantle.

Source Parameters of the April 18, 2008 (Mw 5.2) Mount Carmel, Illinois Earthquake Sequence

AYELE, S.T., University of Memphis, Memphis, TN, USA, stayele@memphis.edu; HORTON, S., University of Memphis, Memphis, TN, USA, shorton@memphis.edu; POWELL, C., University of Memphis, Memphis, TN, USA, capowell@memphis.edu

The April 18, 2008 (Mw 5.2) Mount Carmel, Illinois earthquake is the largest event in the central United States in the previous 40 years. Approximately 180 aftershocks (0.8 < Mw <4.6) were located using a combination of regional network stations and temporary broadband seismometers deployed in the epicentral area by the University of Memphis and Indiana University. To help constrain earthquake source mechanisms, the orientation of faults and the tectonic processes of the area, we will perform moment tensor inversion of these aftershocks. We have tested a moment tensor inversion technique using synthetic data in the presence of realistic noise levels to establish a minimum magnitude threshold that can be reliably resolved. For the test we assume a focal mechanism and magnitude and then produce synthetics having the same station distribution (distances and azimuths) as a recorded aftershock. We obtain simulated seismograms by adding real noise from each station to the synthetics. The resulting simulated seismogram are then inverted for the moment tensor. By varying the assumed magnitude, we determined that source parameters for aftershocks with Mw<1.8 cannot be resolved.

Volcanic Plumbing Systems: Results, Interpretations and Implications for Monitoring

Poster Session · Friday PM, 23 April · Exhibit Hall

An Integrated Analysis of Low-Frequency Seismicity at Fuego Volcano, Guatemala

WAITE, G.P., Michigan Tech, Houghton, MI, gpwaite@mtu.edu; LYONS, J.J., Michigan Tech, Houghton, MI, jlyons@mtu.edu; NADEAU, P.A., Michigan Tech, Houghton, MI, panadeau@mtu.edu

Fuego volcano, Guatemala, is a basaltic-andesite stratovolcano characterized by varied low-level eruptive activity since 1999. In January 2008, we deployed arrays of broadband seismic and acoustic sensors to investigate the source of explosions and low-frequency seismicity. There was no lava effusion during the deployment, but explosions were recorded approximately once per hour, with varied amounts of ash, and with durations from 20–150 s. In addition to the explosions, our seismic arrays recorded narrow-band nonharmonic tremor with dominant frequencies of 1.6 to 1.9 Hz, very-long-period events (up to 40 s period) that are associated with puffing from a subsidiary vent, and discrete long-period events. The present work focuses on the dominant class of these LP events, which repeated approximately 10–15 times per hour, had an impulsive onset with first motion toward the vent, a short duration of <5 s, and dominant frequencies from 1–3 Hz. Their similarity suggests a nondestructive source process. While waveforms are similar from event to event when viewed on the same channel, the large variation in waveforms across the array yields a large uncertainty in slowness parameter estimates. We take advantage of the high degree of similarity between events to determine relative slowness estimates with respect to a master event. The results indicate a stationary source. By forward modeling the source location and mechanism we find it is consistent with a dipping north-south-oriented crack ~150 m beneath the crater. When integrated with gas-emission data, acoustic infrasound, and other seismic signals, the detailed analysis of this class of the LP events suggests they may be related to pressurization of the main vent prior to explosions. This work underscores the importance of multidisciplinary monitoring of open-vent volcanoes.

Return to Lo`ihi: Cross-correlation Analysis of the 1996 Earthquake Swarm at Lo`ihi Submarine Volcano, Hawai`i

CAPLAN-AUERBACH, J., Western Washington University, Bellingham, WA, USA, jackie@geol.wwu.edu; THURBER, C.H., University of Wisconsin-Madison, Madison, WI, USA, thurber@geology.wisc.edu

In July and August 1996, Lo`ihi submarine volcano experienced one of the largest earthquake swarms in Hawai`i's recorded history. Although the nearest permanent seismometer was over 35 km from Lo`ihi, >1100 events were located, >100 of which were larger than M4. The cumulative moment of the swarm exceeds that of a M6 earthquake. Preliminary studies of the event broke the swarm into two major phases, the first of which was thought to be associated with slip within Lo`ihi's southwestern flank, and the second of which was associated with the formation of a 300-m deep pit crater on Lo`ihi's summit. An eruption of the volcano was known to be ongoing throughout the time frame of the swarm. In this re-examination of the 1996 swarm we use cross-correlation analysis to further investigate the relationship between the swarm and the eruption and pit crater formation. Our investigation supports the observation that there were two phases of activity, as correlation analysis show little to no similarity between events in the two phases. Phase 2 events are generally similar to one another, with some clusters exhibiting very strong correlation. These clusters occur throughout phase 2, suggesting the presence of several broadly similar sources rather than a single evolving source. In general, events occurring in phase 1 or during the early part of phase 2 are less similar to one another than those occurring later in the swarm; events become more strongly repetitive in the later stages of activity. Phase 2 seismograms recorded on coastal stations exhibit strong T-phases that show some similarity in time series but also evolve with time. Cross-correlating clusters within the swarm allows us to relocate Lo`ihi earthquakes using a relative location technique in order to further investigate the relationship between the swarm and processes associated with the eruption and pit crater formation.

Halloween 2009 Earthquake Swarm Near Sunset Crater National Monument, Arizona

HODGE, B.E., Northern Arizona University, Flagstaff, AZ USA, brendan.hodge@nau.edu; BRUMBAUGH, D.S., Northern Arizona University, Flagstaff, AZ USA, david.brumbaugh@nau.edu

An earthquake swarm on Halloween, 2009, occurred within the San Francisco Volcanic Field of Arizona, adjacent to the 990 yr old Sunset Crater cinder cone. Seismic stations of the Arizona Integrated Seismic Network recorded 120 earthquakes occurring over a six hour time period. 73 earthquakes were of duration magnitude 2.0 or greater, and 31 of these earthquakes where well located by four or more stations. Several events of largest magnitude 2.9 occurred throughout the time span of the swarm and no events less than magnitude 1.5 were identifiable. The earthquakes predominantly occurred within the mid-crust at an average depth of 18 km. A magnitude 2.6 event marked the onset of the earthquake swarm, which was subsequently fallowed by periodic events every five to ten minutes for approximately two hours. The rate of events then increased to one event every one to five minutes before finally culminating in a magnitude 2.9 event near the end of the swarm. The locations of the earthquakes linearly cluster within a northeast trending zone and show a distinct shallowing trend toward the southwest.

Historically, tectonic activity in this area is characterized by normal faulting along predominately northwest-trending fault zones, which is in apparent conflict with this swarm. However, numerous northeast trending surface lineations are evident and commonly interpreted as inherited structure from reactivated proterozoic basement faults. Lack of an apparent mainshock-aftershock sequence, depth of events, and periodicity of event occurrence suggests the source mechanism for the swarm may be volcanogenic. Statistical analysis of the swarm catalog is consistent with this interpretation. This result would suggest a mid-crust fluid intrusion in the San Francisco Volcanic Field controlled by prefractured basement and may be an initial stage of cinder cone development.

Tracking Long Period Earthquakes Beneath Mammoth Mountain, California

SHELLY, D.R., U.S. Geological Survey, Menlo Park, CA 94305, dshelly@usgs.gov; HILL, D.P., U.S. Geological Survey, Menlo Park, CA 94305, hill@usgs.gov; PITT, A.M., U.S. Geological Survey, Menlo Park, CA 94305, pitt@usgs.gov

Mammoth Mountain, located at the southwestern edge of the Long Valley caldera in eastern California, has exhibited episodic unrest at least since 1979. Among the signs of unrest are long period (LP) earthquakes, which typically exhibit dominant energy around 1–2 Hz, substantially lower than that for "typical" brittle failure events. LP earthquakes are incompletely understood but are generally thought to reflect fluid transport in the subsurface. Given this, these events represent an important target for monitoring the inner workings of the volcano.

Like many types of volcanic earthquakes, LP events beneath Mammoth sometimes occur in temporal clusters. Most LP events are deep (~15–20 km), but they can occur substantially shallower, such as a swarm in July 2008 with catalog depths of 2–8 km. Around 100 LP events have been identified and cataloged near Mammoth in the past decade, using a specialized detection algorithm and visual inspection. Once identified, these events provide powerful templates for detecting similar activity, via cross–correlation with continuously recorded waveforms.

Preliminary analysis of the relatively shallow July 2008 LP sequence suggests that cross-correlation can successfully identify new events near the noise level or within the coda of other events. In fact, multiple events are sometimes detected in close temporal proximity to those events previously identified, revealing a rapid–

fire burst of LPs with similar waveform shape. We plan to gradually expand the scope of this study, scanning multiple years of seismic data and relocating detected events using waveform cross–correlation, with the goal of utilizing the temporal and spatial patterns of LP activity to further constrain the dynamics of the volcano.

Analysis of a "New" Seismic Dataset from the 1980 Eruption of Mount St. Helens

THELEN, W.A., Cascade Volcano Observatory, Vancouver, WA, USA, thelenwes@gmail.com; MALONE, S.D., University of Washington, Seattle, WA, USA, steve@ess.washington.edu

The 1980 eruption of Mount St. Helens represents an iconic event within the historical eruptive record. Previous studies were restricted to using the triggered record of seismicity, which contains a small percentage of the total seismicity that occurred. Between March and May of 1980, several temporary seismometers were installed to supplement the existing network, which were recorded on magnetic tapes. 5-day tapes from three stations were recovered and combined to create a nearly continuous record of seismicity from March 24 to May 20, 1980. All three stations had high-gain and low-gain vertical channels and were located at distances between 8 and 12 km from the vent. This allowed for on-scale recording of much of the strong seismicity occurring at the volcano (on the low-gain channels) and the detection of smaller events not in the triggered record (on the high-gain channels). A continuous record of seismicity allows us to use more modern seismic methods than previously available in 1980 to better understand the process of emplacing a cryptodome. We initially describe this process using an automated frequency analysis, which classifies events into low-frequency, hybrid and high-frequency events. We may also look for subtle seismic precursors to explosion or eruptions that cannot be determined from analysis of the triggered record. We characterize these explosive periods using pseudo-spectrograms, multiplet occurrence, and event character. Lastly we compare the results from analysis of the continuous record to that of the triggered record and helicorder event counts so to highlight the utility of continuous records in a monitoring environment.

Statistical Analysis of Seismicity Beneath Alaskan Volcanoes

JUNEK, W.N., University of Central Florida, Orlando, Florida, United States, wjunek@knights.ucf.edu

Over 56,000 earthquakes, cataloged by United States Geological Survey Alaska Volcano Observatory (AVO) between 2002 and 2009, are used to study the frequency-magnitude distribution of seismicity beneath active volcanoes residing along the Aleutian Arc, Alaskan Peninsula, and the Cook Inlet region. The spatial and temporal variation of seismicity patterns and b-values associated with the selected volcanoes are examined to identify trends that may provide insight into their magma supply systems and internal geophysical processes. Initial estimates for the overall b-value at each volcano range from 1.63 ± 0.03 at Gareloi to 0.87 ± 0.04 at Okmok. Variable temporal fluctuations of b are observed at each volcano, where rapid changes occur at Spurr and Augustine and relatively stable trends are found at Makushin and Okmok. Significant spatial variation of b, as a function of horizontal position and depth, is observed at numerous volcanoes, which include Gareloi ($1.0 < b < 3.0$), Shishaldin ($1.3 < b < 3.5$), Augustine ($0.5 < b < 2.0$), Katmai ($0.5 < b < 2.0$), and Okmok ($0.5 < b < 2.0$).

Oscillation of Fluid-filled Cracks Triggered by Degassing of CO2 due to Leakage Along Wellbores: Field Observations of a Single Force Source Process

BOHNHOFF, M., GFZ Potsdam, Potsdam/Germany, bohnhoff@gfz-potsdam.de; ZOBACK, M.D., Stanford University, Stanford/CA/USA, zoback@stanford.edu

We present evidence for a seismic source associated with degassing CO2 during leakage along two wellbores instrumented with arrays of downhole seismometers. More than 200 microseismic events were detected in direct vicinity of the monitoring wells. The observed seismic waves are dominantly P waves and tube waves, with no (or extremely weak S) shear waves. The waveforms of these events indicate extremely rapid amplitude decays with distance across the arrays, consistent with the seismometers being in the near field of the seismic source. The frequency characteristics, first-motion polarities and S to P amplitude ratios suggest a single force source mechanism. Because the seismic arrays were located at the depth where the density of ascending CO2 changes most rapidly, it appears that the transition of CO2 from supercritical fluid to gas triggers an oscillation of fluid-filled cavities and fractures very close to the wellbores in which the monitoring arrays were deployed. In many aspects, the observed waveforms show a striking similarity to those modeled for degassing processes below volcanoes. We suggest that the single force represents bubble growth and resulting oscillations in cement cavities between the steel casing of the well and the rock adjacent to the wellbores and/or within fractures in the rock just outside the wellbores.

Subsurface Imaging for Urban Seismic Hazards at the Engineering Scale

Poster Session · Friday PM, 23 April · Exhibit Hall

Superficial 3-D Basin Structural Model in Grenoble, France, Evaluated by Geophysical and Geological Data

TSUNO, S., LGIT, Grenoble/Isère/France, Seiji.TSUNO@obs.ujf-grenoble.fr; CORNOU, C., LGIT, Grenoble/Isère/France, Cecile.Cornou@obs.ujf-grenoble.fr; COLLOMBET, M., GEOLITHE, Crolles/Isère/France, marielle.collombet@geolithe.com; MENARD, G., LGCA, Chambéry/Savoie/France, gilles.menard@univ-avoie.fr; BARD, P.-Y., LGIT, Grenoble/Isère/France, pierre-yves.bard@obs.ujf-grenoble.fr

In order to predict earthquake ground motions including high frequency contents, we need to evaluate a superficial S-wave velocity structure. In the Grenoble Basin which is a Y-shaped valley located in the French Alps, geotechnical and geophysical surveys were already performed for estimating deep velocity structures. However, superficial velocity profiles were not available with enough detail to allow reliable numerical predictions of ground motion at frequencies above 1 Hz. Therefore, we applied the MASW technique using the High-Resolution method to estimate S-wave velocity profiles for the uppermost 50 meters of sedimentary layers. The estimated S-wave velocity structure indicates that the soft soil sediment (less than Vs 400–500 m/s) is more deeply deposit in the middle-east of Grenoble than in other areas. We made a 3D S-wave velocity model for the uppermost layers that will be used for high frequency ground motion predictions in the Grenoble sedimentary basin.

And also, we also comprehended geological profiles by integrating borehole data sets in the Grenoble Basin. These geological results are in good agreement with the geophysical results, in terms of a boundary of layers at a site and a heterogeneous soil distribution on a surface. Finally, we categorized site conditions in the Grenoble Basin through these geo-technical and geological aspects.

Cross-Constraints between Station Delays, Gravity, and Reflection for the Reno-area Basin Floor, Nevada

DHAR, M.S., University of Nevada, Reno, NV, mahesh@seismo.unr.edu; THOMPSON, M., University of Nevada, Reno, NV, thomp518@unr.nevada.edu; KELL-HILLS, A., University of Nevada, Reno, NV, annie.kell@gmail.com; LOUIE, J.N., University of Nevada, Reno, NV, louie@seismo.unr.edu; SMITH, K.D., University of Nevada, Reno, NV, ken@seismo.unr.edu; WIDMER, M.C., Washoe County Water Reso. Dept., Reno, NV, mwidmer@washoecounty.us

We have gathered data that reflect the depth of the Reno-area basin using three different techniques. From gravity modeling by the Washoe County Water Resources Department, the basin is thickest in the west Reno-area. The U.S. Geological Survey, University of Nevada, and nees@UTexas conducted high-resolution seismic imaging study in Reno and Sparks, Nevada in June 2009. From this study, we take one-half the two-way travel time for the basin-floor reflection. From the Reno Basin Volunteer Deployment conducted by the Nevada Seismological Lab with ninety USArray Flexible Array (FA) recorders borrowed from PASSCAL, we take the average station delays and station-mode-delays in the basin. The volunteer deployment placed the FA recorders at a total of 106 locations across Reno and Sparks from May 15 to July 15, 2008.

We compared basin depth, reflection time, station delays, and mode-station delays along two different profiles: one 6.72-km profile along the Truckee River through downtown Reno east to Rock Boulevard; and a second 3.84-km profile along Manzanita Lane, about 4.5 km south of Truckee River. Both profiles show good correlation between basin depth from gravity, reflection times, and the average station delays. We saw a weaker correlation of mode-station-delay with basin depth from gravity. These correlations show that interference of a low-density diatomite in west Reno on the gravity analysis is minimal. As well, the correlation shows that the USGS interpretation of basin-floor reflections is sound.

Surface Geophysics for Emergency Microzonation: The L'Aquila Earthquake Example

GALLIPOLI, M.R., CNR-IMAA, Tito Scalo PZ ITALY, gallipoli@imaa.cnr.it; MUCCIARELLI, M., Basilicata University, Potenza PZ Italy, marco.mucciarelli@unibas.it; ALBARELLO, D., Siena University, Siena SI Italy, albarello@unisi.it

The recent L'Aquila earthquake (Italy, April 2009) provided the opportunity to test extensively several shallow geophysical techniques for emergency microzonation. In the first two weeks after the mainshock more than 200 ambient noise recordings were performed. Other techniques employed included geo-electrical tomography, ReMi and ESAC. It was thus possible to identify the zones subjected to seismic amplification. The availability of a long series of recorded aftershock as well as boreholes that were drilled in the following months allowed for validation of the results.

The main outcomes of the back-analysis of the data are:

1)The HVSR obtained from noise always matches the HSVR and often the SSR from earthquakes.

2)Simple classification approaches, like outcrop lithology or Vs30, in most cases fail to identify the amplification-prone areas, due to the extensive presence of velocity inversions (cemented breccias over lacustrine clays).

3)Some cases claim for "nanozonation", because the difference in observed damage and recorded amplification varies dramatically over few tens of meters.

4)Constrained noise HVSR inversion (Castellaro and Mulargia, BSSA 2009) provided average Vs estimate in agreement with down-hole measurements.

5)The inexpensive noise HVSR technique may help geologists when preparing detailed maps and section and also to drive further, more expensive in-situ investigations.

Seismic Characterization of the Sites of the Italian Accelerometric Network

FOTI, S., Politecnico di Torino, Turin, Italy, sebastiano.foti@polito.it; PAROLAI, S., Helmholtzzentrum Potsdam—GFZ, Potsdam, Germany, parolai@gfz-potsdam.de; ALBARELLO, D., University of Siena, Siena, Italy, albarello@unisi.it; MILANA, G., INGV Rome, Rome, Italy, milana@ingv.it; MUCCIARELLI, M., University of Basilicata, Potenza, Italy, mucciarelli@unibas.it; PUGLIA, R., INGV Milan, Milan, Italy, puglia@mi.ingv.it; MARASCHINI, M., Politecnico di Torino, Turin, Italy, maraschini@polito.it; BERGAMO, P., Politecnico di Torino, Turin, Italy, bergamo@polito.it; COMINA, C., Politecnico di Torino, Turin, Italy, cesare.comina@polito.it; TOKESHI, K., Politecnico di Torino, Turin, Italy, ken.tokeshi@polito.it; PICOZZI, M., Helmholtzzentrum Potsdam—GFZ, Potsdam, Germany, picoz@gfz-potsdam.de; DI GIACOMO, D., Helmholtzzentrum Potsdam—GFZ, Potsdam, Germany, and University of Potsdam, Potsdam, Germany, domenico@gfz-potsdam.de; STROLLO, A., Helmholtzzentrum Potsdam—GFZ, Potsdam, Germany, and University of Potsdam, Potsdam, Germany, strollo@gfz-potsdam.de; PILZ, M., Helmholtzzentrum Potsdam—GFZ, Potsdam, Germany, and University of Potsdam, Potsdam, Germany, pilz@gfz-potsdam.de; MILKEREIT, R., Helmholtzzentrum Potsdam—GFZ, Potsdam, Germany, regi@gfz-potsdam.de; BAUZ, R., Helmholtzzentrum Potsdam—GFZ, Potsdam, Germany, bauz@gfz-potsdam.de; LUNEDEI, E., University of Siena, Siena, Italy, lunedei@unisi.it; PILEGGI, D., INGV Rome, Rome, Italy, pileggi@yahoo.it; BINDI, D., Helmholtzzentrum Potsdam—GFZ, Potsdam, Germany, bindi@gfz-potsdam.de.

Task 3 of project S4 "Seismic Characterization of the Sites of the Italian Accelerometric Network" financed by the Italian Civil Protection is devoted to improve the knowledge of the sites of the Italian Accelerometric Network (RAN), mainly by providing a reference shear wave velocity profile for each station. Surface wave tests have been selected as the primary tool for the characterization, due to their flexibility and cost effectiveness. The attention for site selection was pointed in particular to stations that recorded interesting events in the past and to the recently installed digital stations, also trying to obtain a good coverage for the whole Italian territory. Sites with complicated topography and with no sufficient space for performing surface wave measurements were excluded. Finally, considering the geological characteristics and the thickness of the soft sediments of the selected sites (thin, *i.e.* meters/tens of meters, or thick, *i.e.* hundreds of meters) it was decided to assign them amongst the different teams by considering their expertise. In particular, sites with thin sedimentary covers have been assigned mainly to UR with large experience in active methods and with appropriate instruments (multi-channel acquisition systems with high frequency geophones) while the deep basins were assigned to teams with large experience in passive source methods and equipped with short period seismometers. In intermediate situations, a combination of active and passive methods was used to guarantee adequate depth of exploration and good resolution at shallow depth. A benchmark test of different techniques was carried out in Bevagna. Furthermore, selected rock sites have been thoroughly investigated to assess the effects of faulting, jointing and weathering with a combination of surface wave surveys, NHV measurements and classical geomechanical approaches.

Shallow-Seismic Site Characterizations of Near-Surface Geology at 20 Strong-Motion Stations in Washington State

CAKIR, R., WA State Dept. of Nat'l. Res, Olympia, WA, USA, recep.cakir@dnr.wa.gov; WALSH, T.J., WA State Dept. of Nat'l. Res, Olympia, WA, USA, tim.walsh@dnr.wa.gov; MAFFUCCI, C.M., Pacific Northwest Seis. Network, Seattle, WA, USA, cmaffucc@u.washington.edu; PERREAULT, J., University of Washington, Seattle, WA, USA, jmp34@u.washington.edu; BURTON, K., University of Washington, Seattle, WA, USA, kaeleb@u.washington.edu

Shallow seismic surveys have been conducted including multi-channel analysis of surface waves (MASW), microtremor array measurements (MAM) and S- and P-wave refraction profiles to determine near-surface S- and P-wave velocity profiles at selected 20 Advanced National Seismic System (ANSS) station sites in Washington. These stations are located on various soil and rock sites. Determination of the S- and P-wave velocity profiles at each strongmotion site was followed by calculation of shear-wave velocities based on the National Earthquake Hazards Reduction Program (NEHRP) recommendation of average shear-wave velocity for 30 meters (Vs30) of the soil column. This study improves our understanding of; 1) shallow site effects which can be incorporated into the seismic hazard assessment in the Pacific Northwest (PNW), 2) effects of soil and rocks sites on recorded ground motion amplitudes, 3) ground motion attenuation curves in PNW, and 4) level of shaking and liquefaction potential in Washington. Specifically, at stations GNW and ALKI designated as reference sites, shear-wave velocities were determined by using both shallow seismic refraction and MASW+MAM survey techniques. The same seismic characterization methods were used for stations SFER and KCAM, which have a very little amplitude information and poor phase determination of P- and S-wave arrivals; for stations WISH, ERW, LON, UWFH, BABE, SBES, LTY and LYNC, which have lower-than-average short period amplitudes; and for stations KNJH, ATES, SMNR, PAYL, KNEL, HART, SVTR and BSFP, which have higher-than-average short period amplitudes. These results directly contribute to a better seismic hazard assessment and representation of ground motions for the USGS-ShakeMap and FEMA-HAZUS software products used for the rapid emergency response and mitigation efforts in the Pacific Northwest region.

Characterization of Shallow Seismic Velocity Structure in Southwestern Utah Using Spatial Autocoherence

HUANG, S., University of Utah, Salt Lake City/UT/USA, huang.simin@utah.edu; PANKOW, K.L., University of Utah, Salt Lake City/UT/USA, pankow@seis.utah.edu; THORNE, M.S., University of Utah, Salt Lake City/UT/USA, michael.thorne@utah.edu

The University of Utah Seismograph Stations recently installed 12 strong-motion instruments in the southwest corner of Utah, predominantly near the rapidly growing urban areas of St. George and Cedar City. At present there are no geotechnical data available to characterize the site response conditions near these instruments. In order to determine the shallow shear-wave velocity structure at the locations of these strong-motion instruments, we collected microtremor data using an array of four (3-component) broadband seismometers. At each location the broadband instruments were installed in an array with three of the instruments placed at the corners of an equilateral triangle and one in the center. At each location approximately 30 minutes of data from three different sized arrays (radii: 10-, 30-, and 90-m) were collected. The instruments were placed directly on concrete or on paving stones if a sidewalk was unavailable. We are processing these data using the method originally developed by Aki (1957). The basis of this technique is to analyze the spatial autocoherence of the microtremor data between pairs of stations in our array. From the observed autocoherence functions we are able to determine Rayleigh wave phase velocity curves, utilizing the vertical component data, and Love wave phase velocity curves from the horizontal component data. We determine velocity profiles by inverting these phase velocity data and by forward modeling using the multi-mode spatial autocorrelation (MMSPAC; Asten, 2004) method. Our models will be further constrained by comparison to horizontal-to-vertical spectral ratios. While the emphasis presented in this study is on the vertical component data, we also examine the frequency domain coherency curves for the horizontal component data.

Site Characterization in Northwestern Turkey Based on Spatial Autocorrelation Technique: A Comparative Study on Site Hazard Estimation

ASTEN, M., Monash University, Melbourne/Vic. 3800/ Australia, michael.asten@sci.monash.edu.au; ASKAN, A., Middle East Technical University, Ankara/Turkey, aaskan@metu.edu.tr; EKINCIOGLU, E.E., Ankara University, Ankara/Turkey, ezgi.ekincioglu@eng.ankara.edu.tr; SISMAN, F.N., Middle East Technical University, Ankara/Turkey, f.nurtensisman@gmail.com; UGURHAN, B., Middle East Technical University, Ankara/Turkey, ugurhan@metu.edu.tr

The geology of the Northwestern Anatolia (Turkey) ranges from hard Mesozoic bedrock in mountain ranges to large sediment-filled, pull-apart basins formed by the North Anatolian Fault zone system. Düzce and Bolu city centers are located in major alluvial basins in the region, both of which have suffered severe building damage during the 12 November 1999 Düzce earthquake (Mw=7.1). In this study, as an initial attempt to perform site characterization in the region, we employ microtremor survey technique at two strong motion stations (DZC and BOL sites) in Düzce and Bolu. Microtremor analysis is a well-known passive seismic tool to estimate the properties of sedimentary overburden. We perform inversions for a horizontally layered velocity structure based on surface wave dispersion curve analysis using the Spatial Autocorrelation (SPAC) technique. We also use horizontal to vertical spectral ratio (HVSR) to estimate the resonance period at BOL and DZC sites. Finally, for comparisons of the resonance period and peaks of HVSR, we perform a one-dimensional site response analysis using horizontal velocity structure obtained from the SPAC technique. We present our results in the form of one dimensional velocity structure and comparison of frequency-dependent site amplifications at the selected sites.

Site Effect Assessment in Bishkek (Kyrgyzstan) Using Earthquake and Noise Recording Data

PAROLAI, S., GFZ Potsdam, Potsdam, Germany, parolai@gfz-potsdam.de; ORUNBAYEV, S., Central Asian Institute for Appl, Bishkek, Kyrgyzstan, s.orunbaev@caiag.kg; BINDI, D., INGV Milano-Pavia, Milano, Italy, bindi@mi.ingv.it; STROLLO, A., GFZ Potsdam, Potsdam, Germany, strollo@gfz-potsdam.de; USUPAYEV, S., Central Asian Institute for Appl, Bishkek, Kyrgyzstan, sh.usupaev@caiag.kg; PICOZZI, M., GFZ Potsdam, Potsdam, Germany, picoz@gfz-potsdam.de; DI GIACOMO, D., GFZ Potsdam, Potsdam, Germany, domenico@gfz-potsdam.de; AUGLIERA, P., INGV Milano-Pavia, Milano, Italy, augliera@mi.ingv.it; D'ALEMA, E., INGV Milano-Pavia, Milano, Italy dalema@ingv.it; MILKEREIT, C., GFZ Potsdam, Potsdam, Germany, online@gfz-potsdam.de; MOLDOBEKOV, B., Central Asian Institute for Applied Geosciences, Bishkek, Kyrgyzstan, b.moldobekov@caiag.kg; ZSCHAU, J., GFZ Potsdam, Potsdam, Germany, zschau@gfz-potsdam.de

Kyrgyzstan, which is located in the collision zone between the Eurasian and Indo-Australian lithosphere plates, is prone to large earthquakes as shown by its historical seismicity. Hence, an increase in knowledge and awareness of local authorities and decision makers of the possible consequence of a large earthquake is mandatory to mitigate the effects of an earthquake and can only be based on improved seismic hazard assessments and realistic earthquake risk scenarios. To this regard, the Cross-Border Natural Disaster Prevention in Central Asia (CASCADE) project, financed by the German Federal Foreign Office, aimed at the installation of a cross-border seismological and strong motion network in Central Asia and at triggering microzonation activities for the capitals of Kyrgyzstan, Uzbekistan, Kazakhstan, Tajikistan and Turkmenistan. During the first phase of the project, a temporary seismological network of 19 stations was installed in the city of Bishkek, the capital of Kyrgyzstan. Moreover, noise recordings were collected by means of nearly 200 single station noise measurements as well as in array configuration. In this study, we analyse the earthquake and noise data. A broad band amplification (starting at low frequencies) is shown by the Standard Spectral Ratio (SSR) results of the stations located within the basin. The reliability of the observed low frequency amplification was validated through a time-frequency analysis of the seismograms opportunely de-noised. Discrepancies between Horizontal-to-Vertical Spectral Ratio (HVSR) and SSR results are due to large amplification of the vertical component of ground motion, probably due to the effect of converted waves. The single station noise results, once their reliability was verified by the comparison with the earthquake data, have been used to produce the first fundamental resonance frequency map for Bishkek.

Shallow Seismic and Geotechnical Site Surveys at the Turkish National Grid for Strong-Motion Seismograph Stations

YILMAZ, O., Anatolian Geophysical, Istanbul, Turkey, oz@anatoliangeo.com; SAVASKAN, E., Bilgi2000 Soil Investigations, Istanbul, Turkey, erdogdu@bilgi2000.com; BAKIR, S., Middle East Technical University, Ankara, Turkey, bakir@metu.edu.tr; YILMAZ, T., Middle East Technical University, Ankara, Turkey, mtyilmaz@metu.edu.tr; ESER, M., Anatolian Geophysical, Istanbul, Turkey, murat@egejeofizik.com; AKKAR, S., Middle East Technical University, Ankara, Turkey, sakkar@metu.edu.tr; TUZEL, B., Earthquake Research Center, Anakara, Turkey, tuzel@deprem.gov.tr

We conducted shallow seismic site survey at 161 strong-motion stations of the national grid in order to estimate P- and S-wave velocities down to a depth of 30 m. At each station site, we also drilled a geotechnical borehole down to 30-m depth. The P- and S-wave velocities were then correlated with geotechnical borehole data. A data acquisition system that includes an accelerated 50-kg impact source, a 48-channel receiver cable with 2-m geophone interval and 4.5-Hz vertical geophones, and two 24-channel, 24-bit Geode recording units was deployed to acquire three shallow seismic records at each of the station sites using the common-spread recording geometry. By applying nonlinear traveltime tomography to the first-arrival times picked from the shot records, we estimated a near-surface P-wave velocity-depth model for the site along the receiver spread. By applying Rayleigh-wave inversion to the surface waves isolated from the shot records, we estimated an S-wave velocity-depth profile for the site. In the borehole at each station site, we performed standart penetration tests (SPT) at 1.5-m depth interval, determined core recovery and rock quality, and measured the ground-water level. We then conducted geotechnical laboratory measurements and determined the soil profile for each station site.

The ultimate objective is to use shallow seismic velocities and geotechnical soil profiles to correct recorded seismograms for the local site effects, and determine geotechnical earthquake engineering parameters for each station, including site-dependent response spectrum, short- and long-corner periods of design spectrum, change of maximum ground acceleration with depth, soil amplification, susceptibility to liquefaction, and derive ground-motion prediction equations that account for the shear-wave velocity dependent site influence.

Comparison of Shear-Wave Velocity Depth Profiles from Downhole and Surface Seismic Experiments

YILMAZ, O., Anatolian Geophysical, Istanbul, Turkey, oz@anatoliangeo.com; ESER, M., Anatolian Geophysical, Istanbul, Turkey, murat@egejeofizik.com; SANDIKKAYA, A., Middle East Technical University, Ankara, Turkey, askaya@metu.edu.tr; AKKAR, S., Middle East Technical University, Ankara, Turkey, sakkar@metu.edu.tr; BAKIR, S., Middle East Technical University, Ankara, Turkey, bakir@metu.edu.tr; YILMAZ, T., Middle East Technical University, Ankara, Turkey, mtyilmaz@metu.edu.tr

We conducted shallow seismic survey at 10 strong-motion stations in Turkey and estimated shear-wave velocities down to a depth of 30 m using the method of multichannel analysis of surface waves (MASW). At each station site, we also drilled a borehole with casing down to 30-m depth and determined a downhole shear-wave velocity-depth profile. We then compared the shear-wave velocity-depth profiles estimated by the MASW and those determined by the downhole seismic survey. We also had the opportunity to compare both sets of profiles with the estimates from the spectral analysis of surface waves (SASW) previously reported. An acquisition system with an accelerated 50-kg impact source, a 48-channel receiver cable with 2-m geophone interval and 4.5-Hz vertical geophones, and two 24-channel, 24-bit Geode recording units was deployed to record two 48-channel shallow seismic records at each of the station sites using the common-spread recording geometry. By applying Rayleigh-wave inversion to the surface waves isolated from the shot records, we estimated an S-wave velocity-depth profile for the site. For the downhole seismic survey, we used a three-component 14-Hz borehole geophone and a shear-wave impact source at the surface, and recorded data at 1-m depth intervals.

The surface-wave method yields a spatially averaged velocity-depth profile along the line traverse coincident with the geophone spread, whereas the downhole seismic method yields a velocity-depth profile that is pertinent to the borehole location, only. We find a 10–15% difference between the velocities determined by the surface-wave and downhole seismic methods—consistent with the previously reported results. Since downhole measurements can be adversely affected by the borehole conditions, the velocities estimated by the surface-wave methods may be more desirable for site characterization.

Absolute site response from L'Aquila earthquake

MERCURI, A., INGV, Rome-Italy, alessia.mercuri@ingv.it; MALAGNINI, L., INGV, Rome-Italy, luca.malagnini@ingv.it; HERRMANN, R.B., SLU Dep of Earth and Atmosphe, St. Louis, MO, rbh@eas.slu.edu

The absolute site terms are calculated for the broad band stations of the Italian National Seismic Network using the L'Aquila earthquake sequence records (main shock April 6 2009 3.33 AM, Mw=6.3). The whole dataset is composed of 170 events of Mw>3.0, recorded between 30 March and 31 August.

To compute the absolute site terms we have applied the methodology proposed by Malagnini *et al.* (2004), where the site responses are obtined deconvolving source and crustal attenuation terms from recorded data. For the events we have estimated the source spectra coda according to Mayeda *et al.* (1996, 2003) and the regional attenuation parameters derived by Malagnini *et al.* (2008). The method provides the amplitude of the absolute site terms, for the three components, as a function of frequency.

The accurate knowledge of the site response, together with the topography and superficial geology information, allows to determine a generic site response. The latter is obtained averaging the site response of stations located on similar geological contexts.

This work provides the opportunity to compare the results obtained by strong-motion data with those obtained using weak-motion data recorded by a local network in the same region (Mercuri *et al.* 2009).

The January 2010 Earthquakes in Haiti and Offshore Northern California: Origins, Impacts and Lessons Learned

Oral Session · Friday AM, 23 April · Salon E

Field Observations of the Mw 7.0 Haiti Earthqauke of January 12, 2010

MOONEY, W.D. USGS, Earthquake Science Team, 345 Middlefield Rd., Menlo Park, CA. 94025

The deadly Haiti earthquake of January 12, 2010, occurred after an extended period of seismic quiescence in Haiti. Studies of historical seismicity have established that several large earthquakes have occurred near Port-au-Prince (PaP) in the past. The 1770 earthquake appears to be the closest match to the 2010 event, and similarly resulted in the destruction of essentially all the buildings in PaP and the city of

Leogane (35km west of PaP). The 2010 event occurred at 04:53 PM local time with an epicenter 30 km WSW of PaP and a focal mechanism indicating left-lateral oblique-slip motion on an east-west oriented fault. The USGS finite fault model shows a maximum slip of 5 m updip from the hypocenter and a compact source, with a down-dip dimension of approximately 30 km and an along-strike dimension of 15 km. The model also shows that the rupture was very abrupt and of short duration, with maximum moment release occurring in the first 3 to 7 s. This seismological determination was confirmed by eyewitnesses, interviewed by a 5-person USGS/EERI team that visited Haiti Jan.26 - Feb. 3, who reported 5-9 seconds of intense shaking in the epicentral zone accompanied by the immediate collapse of countless structures. Remarkably, a thorough search at the epicentral zone found no evidence for ground rupture. Extensive rock slides and landslides were triggered by severe ground shaking, and liquefaction features in the form of sand boils with a dimension of 5 m are locally evident. In addition, we received reports of river waters disappearing into the ground during the earthquake and then erupting out as geysers once the shaking stopped and the ground settled. The percentage of buildings destroyed in communities located within the sedimentary basins of PaP and Leogane was as high as 70-80%. However, communities located on hard rock (limestone) generally fared much better.

The January 2010 Earthquakes in Haiti and Offshore Northern California: Origins, Impacts and Lessons Learned

Poster Session · Friday PM, 23 April · Exhibit Hall

Shaking, Ground Effects, and Human Response to the Mw 6.5 Northern California Earthquake of January 10, 2010

DENGLER, L.A., Humboldt State University, Arcata, California, USA, lori.dengler@humboldt.edu; BAZARD, D., College of the Redwoods, Eureka, California, USA, dave-bazard@redwoods.edu; CASHMAN, S.M., Humboldt State University, Arcata, California, USA, smc1@humboldt.edu; HEMPHILL-HALEY, E., Pacific Watershed Associates, Arcata, California, USA, Eileen.Hemphill-Haley@humboldt.edu; HEMPHILL-HALEY, M., Humboldt State University, Eileen.Hemphill-Haley@humboldt.edu, Mark.Hemphill-Haley@humboldt.edu; KELSEY, H., Humboldt State University, Eileen.Hemphill-Haley@humboldt.edu, Harvey.Kelsey@humboldt.edu; MCPHERSON, R., Humboldt State University, Harvey.Kelsey@humboldt.edu, rm4@humboldt.edu; TILLINGHAST, S., Humboldt State University, Arcata, California, USA, sft1@humboldt.edu

On January 10, 2010 (4:27 PM January 9 PST), a M 6.5 earthquake occurred 30 km off the coast of Humboldt County in Northern California. Left-lateral strike-slip movement ruptured a N47E trending 25 kilometer-long unnamed fault within the Gorda plate, the deformation zone in the southernmost portion of the Juan de Fuca plate. The earthquake produced strong ground shaking in much of coastal Humboldt County. Peak ground accelerations of 46% of gravity were recorded in Ferndale and 33% in Eureka, the largest population center in the region. This was the strongest earthquake to impact Eureka since 1954. We present an isoseismal map, an overview of shaking effects, and a description of human response to the event. Damage, concentrated near the coast from Ferndale to Eureka, appears to be the result of both distance from the hypocenter and guided energy along the strike of the fault. Over 200 structures were damaged in Eureka and property losses (as of January 14) were estimated at over $40 million. Small scale liquefaction features including spread failures at King Salmon and along the Eel River and sand boils at Centerville Beach and along the Eel River were documented. About 20 percent of the vertical monuments at the Ferndale cemetery were translated, rotated, or toppled. Cemetery monuments in Eureka, Loleta and Table Bluff show similar, but smaller amounts of movement. Security camera films shows that the majority of people responded to the shaking by walking or running out of buildings. Many people recognized ground shaking as a natural tsunami warning sign and evacuated, but few went by foot and most attempted to drive to higher areas, creating significant traffic jams.

Index of Authors

SSA 2010
Abstracts for Special Session

Only the abstracts for this session are printed here. The abstracts for all other sessions can be found in the March/April issue of the *Seismological Research Letters*. All abstracts appear on the SSA website at www.seismosoc.org/meetings/2010/abstracts/.

The January/February 2010 Earthquakes in Haiti, Offshore Northern California, and Chile: Origins, Impacts and Lessons Learned

Poster Session · Friday PM, 23 April · Exhibit Hall

A Field Reconnaissance Following the MW 7.0 Haiti Earthquake of January 12, 2010

EBERHARD, M., Department of Civil Engineering, University of Washington, Seattle, WA, eberhard@u.washington.edu; BALDRIDGE, S., Baldridge & Associates, Honolulu, HI, sb@baseengr.com; MARSHALL, J., Dept. of Civil Engineering, Auburn University, Auburn, AL, jdmarshall@auburn.edu; MOONEY, W.D., U.S. Geological Survey, Menlo Park, CA, mooney@usgs.gov; RIX, G., Dept. of Civil Engineering, Georgia Institute of Technology, Atlanta, GA, glenn.rix@ce.gatech.edu

A field reconnaissance was conducted in Haiti during January 26 through February 3, 2010, by a five member team with expertise in seismology and earthquake engineering. This study has revealed a number of factors that led to catastrophic losses of life and property. Soil liquefaction, ground motion amplification, triggered landslides and rockslide, and soil embankment failures were observed to be significant factors contributing to extensive damage in Port-au-Prince and elsewhere. The earthquake caused extensive damage to buildings throughout the region, with the worst performance seen for construction based on reinforced concrete columns and slabs with infill concrete blocks. Several characteristics contributed to the weakness of such structures: poor construction material, especially the concrete; insufficient strength in columns; and low shear force capacity in walls. The massive human losses from this earthquake can be attributed to a lack of attention to designing and constructing building in Haiti that are earthquake resistant. The historic pattern of prior earthquakes in Haiti indicates that a strong earthquake with magnitude 7 or larger could strike southern Haiti near Port-au-Prince at any time.

Shaking, Ground Effects, and Human Response to the Mw 6.5 Northern California Earthquake of January 10, 2010

DENGLER, L.A., Humboldt State University, Arcata, California, USA, lori.dengler@humboldt.edu; BAZARD, D., College of the Redwoods, Eureka, California, USA, dave-bazard@redwoods.edu; CASHMAN, S.M., Humboldt State University, Arcata, California, USA, smc1@humboldt.edu; HEMPHILL-HALEY, E., Pacific Watershed Associates, Arcata, California, USA, Eileen.Hemphill-Haley@humboldt.edu; HEMPHILL-HALEY, M., Humboldt State University, Eileen.Hemphill-Haley@humboldt.edu, Mark.Hemphill-Haley@humboldt.edu; KELSEY, H., Humboldt State University, Eileen.Hemphill-Haley@humboldt.edu, Harvey.Kelsey@humboldt.edu; MCPHERSON, R., Humboldt State University, Harvey.Kelsey@humboldt.edu, rm4@humboldt.edu; TILLINGHAST, S., Humboldt State University, Arcata, California, USA, sft1@humboldt.edu

On January 10, 2010 (4:27 PM January 9 PST), a M 6.5 earthquake occurred 30 km off the coast of Humboldt County in Northern California. Left-lateral strike-slip movement ruptured a N47E trending 25 kilometer-long unnamed fault within the Gorda plate, the deformation zone in the southernmost portion of the Juan de Fuca plate. The earthquake produced strong ground shaking in much of coastal Humboldt County. Peak ground accelerations of 46% of gravity were recorded in Ferndale and 33% in Eureka, the largest population center in the region. This was the strongest earthquake to impact Eureka since 1954. We present an isoseismal map, an overview of shaking effects, and a description of human response to the event. Damage, concentrated near the coast from Ferndale to Eureka, appears to be the result of both distance from the hypocenter and guided energy along the strike of the fault. Over 200 structures were damaged in Eureka and property losses (as of January 14) were estimated at over $40 million. Small scale liquefaction features including spread failures at King Salmon and along the Eel River and sand boils at Centerville Beach and along the Eel River were documented. About 20 percent of the vertical monuments at the Ferndale cemetery were translated, rotated, or toppled. Cemetery monuments in Eureka, Loleta and Table Bluff show similar, but smaller amounts of movement. Security camera films shows that the majority of people responded to the shaking by walking or running out of buildings. Many people recognized ground shaking as a natural tsunami warning sign and evacuated, but few went by foot and most attempted to drive to higher areas, creating significant traffic jams.

Quantifying Strong Ground Shaking in Sparsely Instrumented Regions

MCPHERSON, B.C., Geology Department, Humboldt State University, Arcata,CA,USA, bob.mcpherson@humboldt.edu; HEMPHILL-HALEY, M.A., Geology Department, Humboldt State University, Arcata,Ca,USA, mark.hemphill-haley@humboldt.edu; DENGLER, L.A., Geology Department, Humboldt State University, Arcata,Ca,USA, lori.dengler@humboldt.edu; WILLIAMS, T.B., Geology Department, Humboldt State University, Arcata,Ca,USA, todd.brian.williams@gmail.com; ERICKSON, G.J., Geology Department, Humboldt State University, Arcata,Ca,USA, gwendolynerickson@hotmail.com; BAZARD, D., Math and Science Department, College of the Redwoods, Eureka,Ca,USA, dave-bazard@redwoods.edu

Following the 4:27 p.m., January 9th, 2010 Mw 6.5 Northern California earthquake, a reconnaissance team from Humboldt State University and College of the Redwoods compiled and photographed the distribution and type of land-based strong-shaking features caused by this offshore, intraplate Gorda earthquake. We documented features associated with liquefaction, lateral spreading, landslides, damaged buildings, fallen chimneys, fallen merchandise in stores, and displaced cemetery monuments as indicators for strong ground motion. The goal of this effort is to construct an isoseismal map to quantify shaking effects. We compare our results with two isoseismal maps constructed by using different data sets, one using strong motion instruments, and the second using an intensity survey of the region conducted by one of the authors (L. D.). Using this comparison, we revisit and revise the "Rural Scale" proposed by Dengler and McPherson (1993) for areas of sparse strong motion instrumentation. This rural scale can be applied to further understand shaking in other regions with poorly instrumented coverage, such as in Haiti, with the January 12th, 2010 Mw 7.0 event.

Geodetic and Seismologic Evidence for a Locked Southern Margin of the Cascadia Subduction Zone

MCPHERSON, B.C., Geology Department, Humboldt State University, Arcata, CA, USA, bob.mcpherson@humboldt.edu; HEMPHILL-HALEY, M.A., Geology Department, Humboldt State University, Arcata, CA, USA, mark.hemphill-haley@humboldt.edu; DREGER, D., Berkeley Seismological Labratory, Berkeley, CA, USA, dreger@seismo.berkeley.edu; HELLWEG, P., Berkeley Seismological Labratory, Berkeley, CA, USA, peggy@seismo.berkeley.edu; ROLLINS, J.C., Earth Sciences, University of Southern California, Los Angeles, CA,USA, john.c.rollins@gmail.com

Offshore intraplate earthquakes near the subduction zone and well-located three-dimensional seismicity provide evidence that the southern Cascadia subduction zone megathrust is presently locked. Displacements within the Gorda plate caused by events in 1994, 2005, and 2010 coseismically moved GPS stations in the overriding North American plate, demonstrating strong coupling (Williams and McPherson, 2006, McPherson *et al.*, 2007). For example, during the 9 January 2010 M 6.5 offshore event, Earthscope-PBO continuous GPS stations located between 41°N and 40.3°N, along the coast, moved eastward by as much as 20 mm. Meanwhile, to the north, GPS stations moved slightly toward the W. This motion is consistent with the northeast-striking left-lateral motion seismically derived for this earthquake. Strong coupling between the Gorda and North American plates also has long been recognized by the concomitant seismicity in both plates (TERA, 1980). Seismicity patterns help constrain the E-W dimensions of the locked zone. Combining the observations of GPS coseismic movements and four decades of seismicity, we define the locked zone as extending from Cape Blanco (N430) to the Mendocino fault (N40.30) dipping 10-12 degrees to the east, and being approxi-

mately 85 km wide. Unlike the actively deforming Gorda plate, the Juan de Fuca plate, north of Cape Blanco, is seismically quiet.

The 2010 M 6.5 and M 5.9 Offshore Ferndale Earthquakes: Seismicity, Seismic History and Stress

HELLWEG, M., Berkeley Seismological Lab, Berkeley, CA, USA, peggy@seismo.berkeley.edu; MCPHERSON, R., Humboldt State University, Arcata, CA, USA, ; DREGER, D.S., Berkeley Seismological Lab, Berkeley, CA, USA, dreger@seismo.berkeley.edu; DENGLER, L., Humboldt State University, Arcata, CA, USA, lori.dengler@humboldt.edu; ROLLINS, J.C., Univ of Southern California, Los Angeles, CA, USA, john.c.rollins@gmail.com; STEIN, R.S., United States Geological Survey, Menlo Park, CA, USA, rstein@usgs.gov

Two large earthquakes occurred offshore of Ferndale, CA on 10 Jan 2010 and 4 Feb 2010, with magnitudes of 6.5 and 5.9 respectively. The area on- and offshore of California north of Cape Mendocino is the State's most seismically active region, having produced 27 damaging earthquakes since 1900. Both 2010 events had relatively deep hypocenters (~24 km) and were widely felt, although neither ruptured the faults known from previous large quakes. Moment tensor mechanisms for both temblors indicate strike-slip faulting on essentially vertically oriented faults. The mechanisms are consistent with events within the Gorda plate, but not along the Mendocino Transform Fault. The finite fault inversion for the M 6.5 indicates that it ruptured unilaterally to the southwest from the hypocenter for 20-30 km, along the NE-SW trending fault plane, with peak slip of ~ 2 m. The M 5.9 event was too small for a finite fault solution. We show the locations of the 2010 event sequences, as well as their stress interactions with the Mendocino fault and the nearby Cascadia subduction surface. We also show their relationship to large, historical earthquakes, to the complex of known faults in the region, and to the ongoing seismicity, including mechanisms from the UCB moment tensor catalog for many quakes with M>3.5 since the mid 1990s.

Slip-Distribution and Kinematic Rupture Process of the January 9, 2010 Mw6.5 Gorda Plate Event

DREGER, D.S., Berkeley Seismological Laboratory, Berkeley, California, USA, dreger@seismo.berkeley.edu; MURRAY-MORALEDA, J., USGS, Menlo Park, CA, USA, jrmurray@usgs.gov; SVARC, J., USGS, Menlo Park, CA, USA, jsvarc@usgs.gov

The January 10, 2010 (UTC) Mw6.5 Gorda Plate event, despite its offshore location, was well recorded by broadband and strong motion seismic networks (BDSN, CREST, CGS, and NSMP) and PBO Global Positioning System (GPS) stations. This event nucleated 29.3 km deep in the thickened Gorda Plate. The seismic moment tensor solution from low-frequency (0.02 to 0.05 Hz) displacement seismograms resulted in a predominantly strike-slip focal mechanism with either SW left-lateral or NW right-lateral planes. In order to identify the causative fault plane we invert broadband seismic waveform data (0.02 to 5Hz) and GPS static deformation data for the slip distribution and kinematic rupture history. The best fitting orientation is found to be the SW-striking nodal plane assuming a rupture velocity of 2.2 km/s, where the slip extends unilaterally to the SW approximately 20 km. The peak slip in this model is 1.9 meters with a scalar seismic moment of 7.25e25 dyne cm (Mw6.5). The average stress drop is 3.2 MPa. On February 4, 2010 the largest (Mw5.9) aftershock occurred approximately 20 km south-southwest of the mainshock epicenter. A preliminary finite-source model for this event was not able to resolve the fault plane, however one model shows that it may be a 10km extension of the SW-striking mainshock fault plane, although its epicenter is not collinear with the mainshock plane. We will present sensitivity analyses to refine the orientation of the fault planes of the mainshock and aftershock by simultaneously fitting broadband and strong-motion seismic waveform and GPS static deformation data for the fault orientation, slip distribution, and kinematic rupture parameters.

Historic Earthquakes Along Southern Hispaniola, and Comparison of the Effects of the 1770 and 2010 Haiti Events.

MCCANN, W.R., , Westminster, CO 80021, wrmccann@comcast.net; MORA, S., Engineering Geologists, , ; sergiomo@geologos.or.cr

On October 18, 1751 (1751a) the whole southern coast of the Dominican Republic from Azua to El Seibo was shaken by an 8.0Mw earthquake. There are several reasons to place this event on the Muertos Trough megathrust. On November 21, 1751 (1751b), another event (7.5Mw) shook from Azua reaching into the Enriquillo valley towards Port-A-Prince, Haiti. Given the intensity of shaking along the Enriquillo valley, it seems reasonable to assign this earthquake to the easternmost section of the Enriquillo-Plantain Garden Fault. In 1770 Haiti was once again shaking by a 7.5Mw earthquake. Eyewitness reports clearly show that damage and shaking effects continue to more to the west along the southern peninsula of Haiti. This event is believed to be the predecessor to the January 12th, 2010 quake, at least in terms of its longitudinal position on the Enquillo Valley-Plantain Garden Fault Zone. That event has a magnitude of 7.0Mw, but 7.6Me. We propose that it is Me which is most comparable with magnitudes estimated from intensity reports as is it a measure of the energy radiated by the earthquake, which ground shaking is most strongly related to. It is likely that the 1751b and 1770 ruptures abut near the Haiti-Dominican Republic Border. We collected intensities for the January 12th, 2010 event for Hispaniola and adjoining islands, using personal interviews, newspaper, radio, and television reports, and DYFI of the USGS. Higher intensities are found in regions with soft or thick sediments such as near the fault rupture at Port-A-Prince and in the Cibao valley, Dominican Republic 200 kilometers from the epicenter. Also, major geologic structures may influence the decay of intensities across the island. A 40 m high local tsunami, and liquefaction? at Croix des Bouquet in 1770 suggest that the effects of two events are not the same, with the 1770 being stronger and more widespread.

New Observations of Earthquake Site Response and Seismic Attenuation in Haiti

CASSIDY, J.F., Geological Survey of Canada, Sidney, BC, Canada, jcassidy@nrcan.gc.ca; AL-KHOUBBI, I., Geological Survey of Canada, Sidney, BC, Canada, ; ROGERS, G.C., Geological Survey of Canada, Sidney, BC, Canada, ; BENT, A., Geological Survey of Canada, Ottawa, ON, Canada, ; MCCORMACK, D., Geological Survey of Canada, Ottawa, ON, Canada, ; ANDREWS, C., Geological Survey of Canada, Ottawa, ON, Canada,

On January 12, 2010, a devastating magnitude 7 earthquake struck near Port au Prince, Haiti. This earthquake caused widespread destruction, killing more than 200,000 people. Some of the key questions to be addressed in the coming months and years are: what contributed to the damage distribution? What was the role of local site response? What was the role of seismic attenuation? What was the role of earthquake source effects? In this study we utilise three-component broadband data, and strong motion recordings from three recently-deployed Canadian seismograph stations in Haiti to examine the potential contributions of local site effects and seismic attenuation. H/V ratios computed for more than 25 earthquakes of magnitude 1 to 5 show consistent site response. At Leogane, closest to the mainshock and on young, soft, Quaternary soils (and one of the hardest hit areas), several significant resonant peaks are observed in H/V ratios at frequencies between 1 and 5 Hz. In contrast, a bedrock (thin-soil) site on a hillside near Port au Prince shows relatively flat response. In Jacmel, resonant peaks are observed at higher frequencies (7-10 Hz). A preliminary comparison with damage patterns shows that the amplification peaks at lower frequencies may be associated with higher damage. Preliminary comparisons of ground shaking as a function of distance suggests that attenuation relationships derived for the nearby islands of Jamaica and Puerto Rico are applicable to Haiti.

Rapid, Multiresolution Mapping of Damage and Rupture from the 2010 Haiti Earthquake

YIKILMAZ, M.B., University of California, Davis, CA USA, mbyikilmaz@ucdavis.edu; BERNARDIN, T., University of California, Davis, CA USA, tbernardin@ucdavis.edu; BISHOP, M.S., University of California, Davis, CA USA, bishopm@cs.ucdavis.edu; BOWLES, C., University of California, Davis, CA USA, cjbowles@ucdavis.edu; ELLIOTT, A., University of California, Davis, CA USA, ajelliott@ucdavis.edu; MORELAN, A., University of California, Davis, CA USA, aemorelan@ucdavis.edu; COWGILL, E.S., University of California, Davis, CA USA, escowgill@ucdavis.edu; KELLOGG, L.H., University of California, Davis, CA USA, kellogg@ucdavis.edu; KREYLOS, O., University of California, Davis, CA USA, kreylos@cs.ucdavis.edu; OSKIN, M., University of California, Davis, CA USA, meoskin@ucdavis.edu

The 2010 magnitude 7.0 Haiti earthquake was followed by rapid collection of very large LiDAR and satellite imagery data for emergency and scientific response. We used two cyberinfrastructure tools developed by the UC Davis KeckCAVES to map the trace of the Enriquiilo fault and assess the data for ground rupture, liquifaction, landslides, and damage. The tools we are using are (1) Crusta: a virtual globe with the capability to render 3-D terrain at LIDAR resolution and conduct mapping on the terrain, and (2) LidarViewer: a point-based LIDAR visualization platform. We find no ground rupture along the fault from the 2010 earthquake, consistent with reports from the field. However, we have identified several sites where detailed field investigations may yield Holocene slip rates for the Enriquillo fault, which has yet to be determined. Specifically, at 18.477188N/72.430650W, a point bar appears to be displaced ~30 m and at 18.508445N/72.229377W, a fluvial terrace riser appears to be displaced ~6 m. We are currently mapping other active structures in southern Haiti that are broadly part of the Enriquillo fault zone and that will help to understand the structural context of the 2010, 1770 and 1751 events. Using these results, we are preparing a 3D model of the fault for use in forward simulations of fault system dynamics. Using methods that we have developed for automated feature extrac-

tion and surface characterization, we are analyzing LIDAR and other remote sensing data for the extent and scope of damage and the presence of damaged features. The scale and pace of remote sensing data collection in Haiti has been unprecedented. The scientific workflow enabled by tools like Crusta and LidarViewer is preparing us to respond to other major geologic events. Movies and additional information are available at http://haiti.geology.ucdavis.edu/ and at www.keckcaves.org.

Real Time Seismic Monitoring in Haiti

MCCORMACK, D.A., Geological Survey of Canada, Ottawa, ON, Canada, dmccorma@nrcan.gc.ca; AL-KHOUBBI, I., Geological Survey of Canada, Sidney, BC, Canada, ialkhoub@nrcan.gc.ca; ANDREWS, C., Geological Survey of Canada, Ottawa, ON, Canada, candrews@nrcan.gc.ca; LAMONTAGNE, M., Geological Survey of Canada, Ottawa, ON, Canada, malamont@nrcan.gc.ca; ASUDEH, I., Geological Survey of Canada, Ottawa, ON, Canada, iasudeh@nrcan.gc.ca; BENT, A.L., Geological Survey of Canada, Ottawa, ON, Canada, bent@seismo.nrcan.gc.ca; GREENE, H., Geological Survey of Canada, Ottawa, ON, Canada, hegreene@nrcan.gc.ca; HALCHUK, S., Geological Survey of Canada, Ottawa, ON, Canada, shalchuk@nrcan.gc.ca; DRYSDALE, J., Geological Survey of Canada, Ottawa On Canada jdrysdal@nrcan.gc.ca; WOODGOLD, C., Geological Survey of Canada, Ottawa, ON Canada, cwoodgol@nrcan.gc.ca; ADAMS, J., Geological Survey of Canada, Ottawa ON Canada, jadams@nrcan.gc.ca

Following the devastating earthquake in Haiti of 12 January 2010, the need for improved local monitoring of the seismic activity in that country has become very apparent. The Geological Survey of Canada, Natural Resources Canada has installed what is believed to be the first continuously transmitting seismograph network in Haiti. Three semi-permanent stations are installed at Port-au-Prince, Jacmel and Leogane. Each station consists of a three component broadband seismograph and a three component strong motion instrument. Continuous data are transmitted by satellite in real time to Ottawa for analysis. Data is also forwarded to the USGS. Early analysis of the data has focused primarily on locating aftershocks with the expectation that longer term monitoring will result in improved seismic hazard assessments for Haiti. The strong motion instruments have proven useful in providing clear records in cases where some of the largest aftershocks were clipped on the weak motion channels. While in Haiti, the field team presented a number of general talks on earthquake hazards and preparedness to address misconceptions and rumors within the diplomatic and aid communities.

The January 12, 2010 Mw. 7.0 Haiti Earthquake Recorded at Strong Motion Stations of the Puerto Rico Strong Motion Program

UPEGUI BOTERO, F.M., University of Puerto Rico at Mayaguez, Mayaguez PR U.S.A 00680, fabio.upegui@upr.edu; CARO CORTES, J.A., University of Puerto Rico at Mayaguez, Mayaguez PR U.S.A 00680, andres.caro@upr.edu; HUERTA LOPEZ, C.I., University of Puerto Rico at Mayaguez -Home institution: CICESE, Mayaguez PR U.S.A 00680 Ensenada Mexico, carlos.huerta@upr.edu; MARTINEZ CRUZADO, J.A., University of Puerto Rico at Mayaguez, Mayaguez PR U.S.A 00680, jose.martinez44@upr.edu; SUAREZ, L.E., University of Puerto Rico at Mayaguez, Mayaguez PR U.S.A 00680, luis.suarez3@upr.edu; PANDO, M.A., University of Puerto Rico at Mayaguez, Mayaguez PR U.S.A 00680, miguel.pando@upr.edu; Department of Civil Engineering and Surveying; Puerto Rico Strong Motion Program.

The Puerto Rico Strong Motion Program (PRSMP) is dedicated to obtain reliable and precise strong motion records produced by earthquakes affecting the Puerto Rico region. The PRSMP has 101 free-field stations, and 15 instrumented structures and dams. Among the free-field stations 27 are stand alone, 48 have telephone dial-up communication, 14 are connected through the internet and 12 shared with the Puerto Rico Seismic Network. Regarding the stations at instrumented structures, 11 are stand alone, and 4 have internet communication. All these strong motion are distributed around Puerto Rico, the US and British Virgin Islands, and the Dominican Republic. All PRSMP stations are equipped with triaxial accelerometers and digital 24 bits recorders, all set to record the ground motions with sampling frequency of 100 Hz.The January 12, 2010 Mw 7.0 Haiti earthquake occurred at 21:53 UTC and its epicenter was located by the US Geological Survey (USGS) 25 km to the southwest of the city of Port-au-Prince, Haiti. The earthquake was recorded at 6 PRSMP stations located at epicentral distances ranging from 570 to 690 km. The recorded accelerograms were processed for obtaining the respective outputs of volume (v1, v2, and v3). After the data was corrected to account for instrument response, it was successively integrated to get ground velocity and displacement. The peak ground accelerations recorded at these 6 PRSMP stations were all less than 2 cm/s2. Response spectral in terms of acceleration, velocity and displacement were calculated for all 6 records using a 5% damping. The power spectral densities calculated showed low predominant frequencies. Fourier spectral ratios of horizontal to vertical (H/V) of shear wave were also computed to quantify the amplification of the horizontal ground motions. An analysis and comparison of these seismic records and results is discussed herein.

Ground Deformation Effects of the 12 January 2010 Earthquake in Haiti

WELLS, D.L., AMEC Geomatrix, Oakland, CA, USA, donald.wells@amec.com; RATHJE, E., University of Texas, Austin, Austin, TX, USA, e.rathje@mail.utexas.edu; BACHHUBER, J., Fugro/William Lettis & Associates, Walnut Creek, CA, USA, j.bachhuber@fugro.com; COX, B., University of Arkansas, Fayetteville, AR, USA, brcox@uark.edu; FRENCH, J., AMEC Geomatrix, Oakland, CA, USA, jim.french@amec.com; GREEN, R., Virginia Tech, Blacksburg, VA, USA, rugreen@vt.edu; OLSON, S., University of Illinois, Urbana-Champaign, IL,USA, olsons@uiuc.edu; RIX, G., Georgia Tech, Atlanta, GA, USA, glenn.rix@ce.gatech.edu; SUNCAR, O., University of Texas, Austin, Austin, TX, USA, osuncar@gmail.com; PENA, L., Pontificia Universidad Catolica Madre y Maestra, Santo Domingo, DR; MUNDARAY, T., Proyectos Especiales, Santo Domingo, DR

The 12 January, 2010 MW 7.0 earthquake in southwestern Hispanola resulted in widespread damage and destruction in Port-au-Prince and across the southern Peninsula of Haiti. The meizoseismal zone extends roughly from the Port-au-Prince alluvial valley in the south-central part of the country westward to Petite Goave along the north coast of the Haitian southern peninsula. The National Science Foundation-sponsored Geo-Engineering Extreme Event Reconnaissance (GEER) Association fielded a reconnaissance team of geotechnical engineers and engineering geologists from the U.S. and the Dominican Republic. The team focused on documenting ground failure and geotechnical/geologic aspects of the earthquake, including liquefaction, settlement, lateral spreading, surface fault rupture (lack of), coastal uplift, and landsliding. The team also conducted surveys to assess whether damage and shaking intensity could be correlated to site conditions or site effects. Significant findings include: 1) Liquefaction and lateral spreading was widespread along the coast in filled ground and in young fine-grained deltaic and beach deposits, but not in coarser fluvial deposits; 2) the earthquake epicenter, focal mechanism, and distribution of aftershocks indicate that the rupture likely occurred on the Enriquillo fault, however, reconnaissance conducted along the fault in the epicentral area and the area of aftershocks showed that the rupture did not reach the ground surface; 3) an area along the coast extending at least 8 km north of the fault apparently was uplifted during the earthquake based on observations of living coral above the low tide level; 4) landsliding was not extensive, but concentrations of failures in natural slopes (including landslide dams) and in over-steepened road cuts were observed; and 5) amplified shaking apparently occurred due to soil conditions and topographic features/geologic structures.

Haiti Earthquake Magnitude 7.0 January 12th 2010 and Aftershock as Located by ISU/UASD

PUJOLS, R.A., Instituto Sismologico Universitario (ISU)/(UASD), Santo Domingo/Distrito Nacional/Dominican Republic, rafaelpujols@hotmail.com; POLANCO, E., Instituto Sismologico Universitario (ISU)/(UASD), Santo Domingo/Distrito Nacional/Dominican Republic, eugenio_polanco_rivera@msn.com; ARIAS, J., Instituto Sismologico Universitario (ISU)/(UASD), Santo Domingo/Distrito Nacional/Dominican Republic, j_ariasf@hotmail.com; DELGADO, J.R., Instituto Sismologico Universitario (ISU)/(UASD), Santo Domingo/Distrito Nacional/Dominican Republic, jdncore@hotmail.com; MARTINEZ, F., Instituto Sismologico Universitario (ISU)/(UASD), Santo Domingo/Distrito Nacional/Dominican Republic, fmpolancog@hotmail.com; RAMIREZ, N., Instituto Sismologico Universitario (ISU)/(UASD), Santo Domingo/Distrito Nacional/Dominican Republic, tramirez9@hotmail.com; GARCIA, F., Instituto Sismologico Universitario (ISU)/(UASD), Santo Domingo/Distrito Nacional/Dominican Republic, ; PEREZ, S., Instituto Sismologico Universitario (ISU)/(UASD), Santo Domingo/Distrito Nacional/Dominican Republic, stalinpp@hotmail.com

The Instituto Sismologico Universitario (ISU) at the Universidad Autonoma de Santo Domingo (UASD) is the agency responsible for monitoring the seismicity in the Dominican Republic (DR). Its area of responsibility is within the rectangle that includes the latitudes from 17 to 20.5 north and longitudes from -68 to -72.5 west. The ISU operates and maintains twelve stations, five of them are broadbands and the others are short period's seismic station. Four of the broadband have been installed with the collaboration of external Institutions like the USGS, PRSN, and UTIG. Haiti and The DR share the Hispaniola Island. In this Poster, there is a map which presents the faults system in the Hispaniola where most of these faults are actives and have historical seismicity of big events, for example, the most recent damaging earthquakes ocurred in September 22th 2003, there was a 6.5 magnitude in Puerto Plata which caused many buildings to collapsed in this city and two people died by heart attack, in August 4th 1946, an event of magnitude 8.1 caused big damage in the northestearn and produced a tsunami in the community of Matancitas that killed more than 2000 peoples. Also this poster shows the earth-

quake location by our automatic system which use earlybird, our automatic location differ a little bit with the NEIC location. The magnitude was very similar, located only by ML and Mwp and the latitude and longitude varys a few too. There is a figure that shows the seismogram view with seisgram of all of our stations. The poster shows a map with all the locations made by the ISU. This is the institution that has more events located for the aftershock of Haiti's earthquake, this poster shows a map with more than 250 earthquakes and the minumum magnitude located was 3.3 Md, shows a frecuency distribution and the daily seismicity of the aftershock located, there is a map with the main event and aftershock felted in the DR.

Preliminary Report on Aftershock Recording and Site Characterization in Haiti

HOUGH, S.E., U.S. Geological Survey, Pasadena, California, hough@usgs.gov; ANGLADE, D., Bureau des Mines et de l'Energie, Port au Prince, Haiti, ; BENZ, H., U.S. Geological Survey, Golden, Colorado, ; ELLSWORTH, W., U.S. Geological Survey, Menlo Park, California, ; GIVEN, D., U.S. Geological Survey, Pasadena, California, ; HARDEBECK, J., U.S. Geological Survey, Menlo Park, California, ; JANVIER, M.G., Bureau des Mines et de l'Energie, Port au Prince, Haiti, ; MAHERREY, J.Z., U.S. Geological Survey, Golden, CO, ; MAZABRAUD, Y., Université des Antilles et de la Guyane and IUFM de la Guadeloupe; MCNAMARA, D., US Geological Survey, Golden, Colorado; MERCIER DE LEPINAY, B., Univerite de Nice-Sophia Antipolis, France; MEREMONTE, M., US Geological Survey, Golden, Colorado; MILDOR, B.S-L., Bureau des Mines et de l'Energie, Port au Prince, Haiti; PREPETIT, C., Bureau des Mines et de l'Energie, Port au Prince, Haiti; YONG, A., US Geological Survey, Pasadena, California

Following the devastating M7.0 Port au Prince earthquake of 12 January 2010, we deployed strong motion instruments within Port au Prince to explore the variability of shaking as well as weak and strong-motion instruments around the Enriquillo-Plaintain Garden fault, primarily to improve aftershock locations and to lower the magnitude threshold of aftershock recording. Four K2 accelerometers were deployed in late January; two of these were in operation for five days, two have remained in operation since that time. In addition, four stations with broadband and strong-motion sensors were deployed along the Enriquillo Plaintain Garden fault in late January. A second phase of installation, including additional broadband stations to improve aftershock locations and additional K2s within Port au Prince to investigate site response, will be deployed in early March. All of the stations are operating in triggered mode, with on-site recording. We are further using remote-sensing (ASTER) imagery to develop a first-order map of geotechnical site characterization for Port au Prince, as a basis of comparison with the observed damage distribution and observed variability of shaking. We will report preliminary results.

Post-Earthquake Health Monitoring of Critical Infrastructure at Haiti to Assist Rapid Relief Efforts

OOMMEN, T., Tufts University, Medford/MA/USA, thomas.oommen@tufts.edu; BAISE, L.G., Tufts University, Medford/MA/USA, laurie.baise@tufts.edu; GENS, R., University of Alaska Fairbanks, Fairbanks/AK/USA, rgens@alaska.edu; PRAKASH, A., University of Alaska Fairbanks, Fairbanks/AK/USA, anupmaprakash@gmail.com

On January 12, 2010 a magnitude Mw 7.0 earthquake struck the Port-au-Prince region of Haiti. With recent technological advances, this earthquake has become a test-case for using technology in post-earthquake health monitoring and rapid relief efforts. Within days of the earthquake, several sets of satellite and aerial imagery were taken and made available for emergency response efforts. The high resolution imagery provided up to 15 cm resolution allowing the user to "see" damage on the ground. In another example of technology use in relief efforts, students at the Tufts Fletcher School of Diplomacy together with USHAHIDI provided real time mapping portal for reporting crisis (*i.e.* crisis mapping). This portal provided people in Haiti the ability to text message a request for aid and these requests were mapped to create a "crisis map" and sent to the appropriate relief agencies in real time. In this work, we link the human based data acquired by USHAHIDI with the physical data acquired through remote imagery and engineering field reconnaissance to analyze the health of critical infrastructure and improve technology based rapid relief efforts. This integration of broad spatially available remote data with sparse detailed engineering reports and pervasive personal reports through text messaging provides a richer picture of damage and relief needs than any one data set can provide alone. We use Differential Synthetic Aperture Radar Interferometry (DInSAR) to map the subsidence and displacements that have occurred to the transportation network in Port-au-Prince. This information is then used to characterize the health of the road network. Geographic Information System (GIS) network analysis tools are used to find optimal routes. Finally we use the crisis mapping data paired with field reconnaissance reports to validate the satellite imagery analysis.

Co-Seismic Landsliding and Local Tsunami Generation on the Haitian Peninsula from the January 2010 Mw 7.1 Earthquake

GOLDFINGER, C., Oregon State University, Corvallis, OR, gold@coas.oregonstate.edu; MCADOO, B.G., Vassar College, Poughkeepsie, NY, brmcadoo@vassar.edu

The Mw 7.1 Haiti earthquake caused a number of ground failures along the northern shore of the Haitian peninsula. Satellite imagery acquired post-earthquake reveals evidence of several probably co-seismic rockslides along seacliffs 4.5 km west of Grand Goave. These slides continued into the bay, possibly becoming submarine debris flows and or turbidity currents. Four failures occurred at (1) Petit Paradis, 1.2 km east of Grand Goave, (2) 0.9 km east of Fouche, (3) 3 km northeast of Grand Trout and 0.5 km south of Ca Ira. A fifth possible failure is located 1.8 km NW of La Salle. The failures all occurred at the prograding fronts of small river deltas where the frontal part of the delta collapsed as a lateral spread or partially submarine slide, transporting the delta front sediments into deeper water in Baie de Port au Prince, and Baie de Grand Goave. One of the slides, near the village of Petit Paradis, apparently generated a local tsunami. The tsunami, reportedly 2 m in height, was responsible for 7 deaths according to press reports. The upper part of this slide included trees along the shoreline which can be observed standing in ~ 2 m of water, and now 68 m offshore. Further delta front failures may occur as destabilized slopes fail in headward fashion, with or without the influence of aftershocks. The coastline in the area of failures west of Port au Prince appears to be an amalgam of similar past events, evidenced by multiple arcuate scallops and partially healed arcuate slide scars. The delta front failures have drawn attention to the rapid outbuilding of these deltas in Haiti, which are likely the result of denudation of the island over recent decades, and although the slides and tsunami were co-seismic events, the tsunami may be considered partly anthropogenic in nature.

Project REPONS: Offshore Fault Mapping and Turbidite Record Reconnaissance in Response to the January 12 2010 Earthquake, Haiti

MCHUGH, C., Queens College, CUNY, Flushing/NY/USA, cmchugh@qc.cuny.edu; GULICK, S., University of Texas, Institute for Geophysics at Austin, Austin/Texas/USA, sean@utig.ig.utexas.edu; CORMIER, M.-H., University of Missouri, Columbia, Columbia/Missouri/USA, cormierm@missouri.edu; DIEBOLD, J., Lamont-Doherty Earth Observatory of Columbia University, Palisades/NY/USA, johnd@ldeo.columbia.edu; DIEUDONNE, N., Bureau of Mines, Port au Prince/Haiti, nidie75@hotmail.com; HORNBACH, M., University of Texas, Institute for Geophysics at Austin, Austin/TX/USA, matth@utig.ig.utexas.edu; SEEBER, L., Lamont-Doherty Earth Observatory of Columbia University, Palisades/NY/USA, nano@ldeo.columbia.edu; STECKLER, M., Lamont-Doherty Earth Observatory of Columbia University, Palisades/NY/USA, steckler@ldeo.columbia.edu; Braudy, N., Queens College, CUNY, Flushing/NY/USA, nbraudy@gmail.com; DE BOW, S., University of Rhode Island, Graduate School of Oceanography, Narragansett/RI/USA, sam.debow@gso.uri.edu; DEMING, J., Seafloor Systems Inc, jdeming@seafloorsystems.com; DOUILLY, R. Universite d'Etat de Haiti, Port au Prince/Haiti, robydouilly@yahoo.fr; JOHNSON, H., University of Missouri, Columbia, Columbia/MO/USA, hej9000@yahoo.com; MISHKIN, K., Queens College, CUNY, Flushing/NY/USA, Katie.e.ryan@gmail.com; SORLIEN, C., University of Santa Barbara, Santa Barbara/CA/USA, chris@crustal.ucsb.edu; SYMITHE, S., Universite d'Etat de Haiti, Port au Prince/Haiti, symithesteevej@yahoo.com; TEMPLETON, J., Lamont-Doherty Earth Observatory of Columbia University, Palisades/NY/USA, johnt@ldeo.columbia.edu; WILSON, R., pwreader@aol.com

As part of an NSF RAPID response to the January 12, 2010 earthquake near Léogâne, Haiti, we mapped the underwater continuation of the Enriquillo-Plantain Garden fault zone, from Baie de Grand Goâve to Baie de Petit Goâve, where it resurfaces onto land. Multibeam bathymetry, sidescan sonar, chirp subbottom profiler (deep-tow and ship-based), and sediment sampling were conducted in water depths of 4 m to 1750 m from the R/V Endeavor and from a small zodiac.

The submerged traces of several faults offshore the Baie de Grand Goâve and the Baie de Petit Goâve near the epicenter is expressed by a series of en echelon linear ridges that, in places, offset both the surface and the subsurface features. The most recent expression of sea-floor faulting near Grand Goâve are small scarps with high reflectivity on the side-scan sonar. The submarine fault trace joins to the onshore trace of the Enriquillo-Plantain Garden fault to the east via a releasing bend and implies that there is a constricting bend towards the west perhaps causing the Tapion ridge. Within the Baies de Petit Goâve and Grand Goâve, river outlets are correlated with lateral spreading and/or subsidence. This subsidence may be related to locally reported small tsunamis. Twenty seven gravity cores and 5 multicores were recovered seeking turbidity currents that may have been generated by past earthquakes, including the last one. Turbidites with coral debris were sampled in the upper slope (100-300 m) adjacent to the fault-related ridges. Clear turbidites with dark-colored sands and occasional wood fragments were found at intermediate water depths (1000 m to 1100m), A thick layer (30 cm) of water saturated

sediment was recovered from the deepest basin within the Canal du Sud (1750 m). CTD measurements of turbidity in the water column show an anomalous increase for 600 m above the seafloor, almost two months after the earthquake. Sediments will be dated with short-lived radioisotopes and radiocarbon.

Caribbean Tsunami Warning Program

VON HILLEBRANDT-ANDRADE, C.G., NOAA NWS Caribbean Tsunami Warning Programs, Mayaguez, Puerto Rico, USA, christa.vonh@noaa.gov; PROENZA, X.W., NOAA National Weather Service Southern Region Headquarters, Fort Worth, Texas, USA, bill.proenza@noaa.gov

The National Geophysical Data Center of NOAA reports that over the past 500 years almost 100 tsunamis have been observed in the Caribbean. The most recent tsunami was generated as a result of the January 12, 2012 Mw 7.0 Haiti earthquake; at least seven lives were claimed. On May 28, 2009, an earthquake M 7.3 struck off Honduras. Local surveys demonstrated that a small tsunami was generated, flooding some low-lying areas. In total, just since 1842, 3510 lives have been lost to tsunami events; this is 2924 more than in the northeastern Pacific in the same time period. With growth of residents, tourists and infrastructure more lives and property are at risk to tsunami than ever before. Considering this elevated tsunami hazard and risk in the and recognizing the need for an early warning system, the Intergovernmental Coordination Group for the Tsunami and other Coastal Hazards Warning System for the Caribbean and Adjacent Regions was established in 2005 as a subsidiary body of the IOC-UNESCO. Its main objective is to identify and mitigate the tsunami hazards. The goal is to create a fully integrated end-to-end warning system. The West Coast and Alaska Tsunami Warning Center is providing tsunami warning service for the USA territories in the Caribbean while the Pacific Tsunami Warning Center in Hawaii is the interim tsunami warning service provider for the rest of the region. In 2010 NOAA established the Caribbean Tsunami Warning Program, collocated with the Puerto Rico Seismic Network at the University of Puerto Rico in Mayagüez. The main responsibilities of this center will be improving tsunami warning and forecasting capabilities as well as supporting education and preparedness efforts throughout the Caribbean. This is the first step of the U.S. phased deployment of the recommended Caribbean Tsunami Warning Center.

Surface Deformation of the January 12th, 2010 Haiti Earthquake from ALOS-PALSAR Interferometry

FUNNING, G.J., University of California, Riverside, CA 92521, USA, gareth@ucr.edu

The 12 January 2010 Haiti earthquake struck the southern portion of the country, close to the capital city of Port-au-Prince. The mapped Enriquillo-Plantain Garden fault, whose mapped trace passes through the epicentral region, and which was thought responsible for previous large earthquakes in the same region in 1751 and 1770, is the most likely structure to have supported the event, although no surface rupture was identified in post-earthquake reconnaissance. I present here preliminary results of analysis of coseismic interferograms constructed from data from the PALSAR instrument on the Japanese ALOS satellite. Data from three separate satellite tracks, two ascending and one descending, covering the epicentral region are used. Interferogram coherence is satisfactory in the region of interest, and a continuous pattern of deformation fringes can be seen in each case, consistent with the lack of an observed surface rupture. A maximum of ~80 cm of peak-trough line-of-sight displacement can be observed approximately 30 km WSW of Port-au-Prince; the 50 km-long deformation pattern that is observed is consistent with the estimated seismic Mw of 7.0. Difficulties with phase unwrapping, and the offshore location of a portion of the fault complicate the modelling of these measured displacements; through digitising of fringes and a simple linear inversion, a preliminary model involving up to 1.8 m of left-lateral fault slip is obtained. A discrepancy in the moment magnitude predicted by this model (M~6.8) and seismology (M~7.0) remains to be investigated.

Source Mechanisms of the January 12, 2010, M_w 7.1 Haiti Earthquake and its Aftershocks

HJÖRLEIFSDÓTTIR, V., Lamont-Doherty Earth Observatory of Columbia University, Palisades, NY, USA, vala@ldeo.columbia.edu; NETTLES, M., Lamont-Doherty Earth Observatory of Columbia University, Palisades, NY, USA, nettles@ldeo.columbia.edu

The focal mechanism of the devastating Haiti earthquake indicates that the rupture occurred as primarily strike-slip motion on a steeply dipping fault, with a smaller component of reverse motion. The aftershock sequence includes 75 earthquakes of magnitude 4.0 and larger in the first 10 days after the event (NEIC). Two of the aftershocks, of M_w 5.8 and 5.9, were analyzed in near-real time for distribution as 'quick CMTs', as part of the Global CMT project. Contrary to the main event, they indicate slip on NW-SE striking reverse faults. In this study, we determine the focal mechanisms of several more of the aftershocks, with magnitudes in the range M_w 4.5-6.1. We find that all events for which we have been able to determine mechanisms to date, except for one M_w 4.5 event, have thrust mechanisms similar to those determined for the large aftershocks. This finding indicates that the vast majority of aftershocks in this sequence are not occurring on the same fault structure as the main shock. With the possible exception of events that may be hidden in the waveforms of larger events occurring very close in time, there are no aftershocks larger than M_w 4.5 occurring on the main-shock fault plane within the first 10 days after the event, indicating very low aftershock activity on the main fault plane. The large number of thrust events and near absence of strike-slip events raises many questions on fault interaction and triggering of earthquakes.

The January 2010 Haiti Mainshock-Aftershock Discrepancy: Structural and Stress Interactions Between Faults in Strain Partitioned Transpression

SEEBER, N., Lamont-Doherty Earth Observatory, Columbia University, Palisades, NY, USA, nano@ldeo.columbia.edu; WALDHAUSER, F., Lamont-Doherty Earth Observatory, Columbia University, Palisades, NY, USA, felixw@ldeo.columbia.edu

Caribbean-North America plate motion across the eastern Hispaniola segment of the boundary is transpressive and is partitioned to a pair of sinistral E-W striking transform faults and a set of NW-SE striking thrust-folds. The January 12 M7.1 earthquake sequence in Haiti is an expression of this partitioning. While the CMT solution for the mainshock yields left-lateral slip on a steeply north-dipping, WSW-striking segment of the Enriquillo-Plantain Garden Fault (EPGF), most of the aftershocks are clustered at the west end of the rupture and show instead thrusting on a WNW striking fault. Our relocations of 55 aftershocks by double-difference analysis of NEIC bulletin data define a short SSW-dipping segment of a thrust fault, which reaches the surface at a push-up on the EPGF. We recognize this seismogenic segment as the northernmost part of a regional thrust fault traversing obliquely the southern peninsula of Haiti and intersecting the EPGF from the south. Motion of this fault, named the Jacmel thrust, is expected to warp the EPGF in a constricting bend dipping west. We speculate that the westward propagating sinistral mainshock rupture stopped at this bend because of increasing compression across that steep fault. This compression, however, triggered slip on the 45° dipping thrust fault near the intersection. The Jacmel thrust is expressed by a NE-verging anticline-syncline pair associated with Quaternary uplift. A similar structure intersecting the EPGF 130 km to the west develops another constricting bend and related push-up. The partitioning of oblique motion into a master strike-slip fault and distributed thrust faults, may therefore segment the master fault. This may enhance shortening on neighboring segments of the thrust fault and thus thicken the crust in the typical linear structural and topographic highs that accompany transpressive continental transforms.

The January 12, 2010 Haiti Earthquake : Indications for a Long Duration Event with a Spatially Concentrated Rupture.

VALLÉE, M., IRD - Geoazur - University of Nice, France, vallee@geoazur.unice.fr

We combine two techniques using teleseismic data to image the rupture process of the Haiti earthquake. First, we use body-wave deconvolution to extract the characteristics of the source time functions. This approach indicates that the earthquake rupture is not limited to an impulsive stage lasting 10s. In fact, coherent source phases are retrieved later in the signals, with the clearest one occurring 55-60s after rupture initiation. The second technique is based on array analyses, using a subset of the USArray on the one hand and a subset of the European array on the other hand. The source-array geometry is more favourable with the USArray, but both analyses reveal the similar seismic source behaviour : a long source duration - of about 60s, consistent with the body-wave deconvolution -, combined with a small rupture extension. Considering the uncertainty of the array analyses, it appears that the rupture did not travel more than 30-40km during the 60s-long source activity. These peculiar characteristics of the source process could be interpreted in terms of complex rupture process or in terms of very early aftershocks following the main shock. In all cases, such a long source activity confined in a small fault area is expected to increase the damages in the immediate vicinity of the earthquake.

Source Properties of the January 2010 M7 Haiti Earthquake Estimated by Back Projection of Waves Recorded by the National Seismic Network of Venezuela

MENG, L., Caltech Seismo Lab, Pasadena, CA, USA, lsmeng@caltech.edu; AMPUERO, J.P., Caltech Seismo Lab, Pasadena, CA, USA, ampuero@caltech.edu; RENDON, H., FUNVISIS, Caracas, Venezuela, hrendon@funvisis.gob.ve

Back projection of teleseismic waves based on array processing has become a popular technique for earthquake source inversion. By tracking the moving source of high frequency waves, areas of the rupture front radiating the strongest energies can be imaged. The technique has been applied to track the rupture process of the Sumatra

earthquake, and the supershear rupture of the Kunlun and Denali earthquakes. The challenge with the Haiti event is its very compact source region (<30km). Preliminary results from back projection using US-array or the European network reveal little about the rupture process. In this study, we made an effort towards imaging the 2010 M7.0 Haiti earthquake using multiple seismic array networks, including the IMS array in Texas and the National Seismic Network of Venezuela run by FUNVISIS. The FUNVISIS network is composed of 22 broad-band stations with an east-west oriented geometry, and is located approximately 12 degrees away from Haiti in the perpendicular direction to the Enriquillo fault strike. This is the first opportunity to exploit the privileged position of the FUNVISIS network to study large earthquake ruptures in the Caribbean. We applied back projection methods based on both traditional stacking and signal subspace techniques. The preliminary result is encouraging: we observe an east to west energy movement along the fault, consistent with a compact source and rupture propagation towards the west at subshear speed. We will report on our efforts to quantify confidence limits on inferred rupture parameters. These efforts could lead the FUNVISIS seismic network data to play a prominent role in the timely characterization of the rupture process of large earthquakes in the Caribbean, including the future ruptures along the yet unbroken segments of the Enriquillo fault east from the January 2010 Haiti earthquake.

12 January 2010 M=7.0 Haiti Earthquake Calculated to Increase Failure Stress on Adjacent Segments of the Enriquillo Fault and Other Fault Systems

LIN, J., Woods Hole Oceanographic Institu, Woods Hole, MA, USA, jlin@whoi.edu; STEIN, R.S., U.S. Geological Survey, Menlo Park, CA, USA, rstein@usgs.gov; SEVILGEN, V., U.S. Geological Survey, Menlo Park, CA, USA, vsevilgen@usgs.gov; TODA, S., Disaster Prevention Research Ins, Kyoto, Japan, toda@rcep.dpri.kyoto-u.ac.jp

A fundamental problem of earthquake occurrences is the predictability of space, magniude and time. Present predictability science is a very hard problem, although the place is to some extent possible to be predicted. Large and very large earthquakes, such as 2010 Central Chile, Mw8.8, present complicate difficulties regarding their future rupture zone and size, fundamentally necessary for defining the seismic cyles of the above size classes. Purcaru (1982, 1985) introduced a model of seismic cycles with connections, separating the magnitude classes of the cycles, which it is different from the Fedotov model (1965). Later we advanced (Purcaru, 2001) the first model by including a level of the critical failures of the asperities of past "subearthquakes" that will be ruptured during a future very large earthquake. This is case of the 2010 earthquake (aftershocks area 700km x 150-200km) which covers three past large earthquakes. We found that the size of the 2010 Chile confirms well our model with variable stress-drops and near levels of the failure stresses. This is useful in the finding of the cycles of the repeat of such very large earthquakes, and it provides an important necessary condition for the predictability of earthquakes. Finally, folowing the 2001 model, first multiple analyzes of seismicity patterns (1965-2010 main shock) lead to a seismic gap (about 33.5°S- 37°S), tangent at the rupture area of the giant 1960 eq.(Mw9.5), as the place of a next great earthquake, but no time prediction was made.

USGS PAGER Information for the 2010 Mw 7.0 Haiti and Mw 8.8 Chile Earthquakes

MARANO, K.D., U.S. Geological Survey, Golden, CO, kmarano@usgs.gov; WALD, D.J., U.S. Geological Survey, Golden, CO, wald@usgs.gov; JAISWAL, K.S., U.S. Geological Survey, Golden, CO, kjaiswal@usgs.gov; HEARNE, M.G., U.S. Geological Survey, Golden, CO, mhearne@usgs.gov; LIN, K., U.S. Geological Survey, Golden, CO, klin@usgs.gov; HAYES, G.P., U.S. Geological Survey, Golden, CO, ghayes@usgs.gov

Within 30 minutes of both the Jan 12, 2010 Mw 7.0 Haiti and the Feb 27, 2010 Mw 8.8 Chile earthquake, the USGS PAGER system produced estimates of the population exposed to shaking. In addition to the publicly available PAGER results, the soon-to-be released lossPAGER system postulated alert levels for both events using an Earthquake Impact Scale, with levels of Red (international response) and Orange (national response), respectively; the alert level for Chile was raised to Red once fault dimensions were constrained. These alert levels provide an estimate of the response needed quickly after an earthquake, allowing mobilization of aid and support long before media-based or ground-truth damage assessments are available. For both events, PAGER alerts and products guided initial response activities and were widely circulated via email, web, and the media. Given the catastrophic nature of the Haitian earthquake and the enormity of the Chilean event, refinements to our loss models, fault dimensions, and Vs30 maps were explored. We also describe additional products created for these earthquakes, including probabilistic landslide maps and the comparison with preliminary observed landslide distributions ascertained from aerial surveys. Scenarios earthquakes, examining the potential shaking and impact of rupture extensions to the recent Haiti earthquake rupture area were examined, and these results are presented. In addition, due to the high magnitudes and the significant number of people affected by both events, along with their temporal proximity, the public and media have raised many questions as to why the much lower magnitude Haiti event was so much more destructive. Using ShakeMap and PAGER products, we contrast these two events for educational and risk communication purposes, in terms of significant differences in the relative populations experiencing high intensity levels, fault dimensions, impacted areas, and building stock vulnerabilities.

The USGS National Earthquake Information Center Response to Recent Large Earthquakes

HAYES, G.P., USGS National Eathquake Information Center, Golden, CO, ghayes@usgs.gov; WALD, D.J., USGS National Eathquake Information Center, Golden, CO, wald@usgs.gov; EARLE, P.S., USGS National Eathquake Information Center, Golden, CO, pearle@usgs.gov; BENZ, H.M., USGS National Eathquake Information Center, Golden, CO, benz@usgs.gov; BRIGGS, R.W., USGS National Eathquake Information Center, Golden, CO, rbriggs@usgs.gov; SIPKIN, S.A., USGS National Eathquake Information Center, Golden, CO, spikin@usgs.gov; DEWEY, J.W., USGS National Eathquake Information Center, Golden, CO, dewey@usgs.gov; CHOY, G., USGS National Eathquake Information Center, Golden, CO, choy@usgs.gov; JAISWAL, K., USGS National Eathquake Information Center, Golden, CO; LIN, K., USGS National Eathquake Information Center, Golden, CO; MARANO, K.D., USGS National Eathquake Information Center, Golden, CO; HEARNE, M., USGS National Eathquake Information Center, Golden, CO

In the first two months of 2010, the USGS National Earthquake Information Center (NEIC) led a rapid response to two major global earthquakes - the January 12th Mw7.0 Haiti, and the February 27th Mw8.8 Chile earthquakes. Within minutes both events had been detected, and the NEIC began assessing their detailed seismological characteristics, tectonic setting and societal impacts. The release of initial estimates of location and magnitude triggered a collection of products that inform governments, aid agencies, the public and media of each earthquakes' occurrence (Earthquake Notification System), its estimated shaking hazards (ShakeMap) and population exposure (Prompt Assessment of Global Earthquakes for Response - PAGER). In Haiti, PAGER showed 3 million people were exposed to severe-extreme shaking (Modified Mercalli Intensity VIII+), indicating a large-scale disaster had occurred; in Chile, 5.5 million were exposed to severe shaking, signifying the necessity for a similarly extensive response. Rapid W-phase, surface-wave and body-wave moment tensor solutions allowed confirmation/updates of magnitudes, identified mechanisms and facilitated early assessments of the tectonic setting of each event, interpretations that have been supported by subsequent research efforts. Modeling of mainshock rupture processes was completed within several hours, and used to update ShakeMap and PAGER exposure estimates to provide more accurate assessments of the scale and spatial extent of each disaster. All products were distributed through the USGS Earthquake Hazards Program web pages, where they were viewed over 10 million times within 24 hours of each earthquake, and reproduced by many media outlets. Here we summarize these products, what they reveal about the earthquakes, and how they have been used to communicate population exposure in addition to standard reports of earthquake location and size - a major step in increasing awareness of vulnerability to earthquake shaking hazards.

High-Resolution Aftershock Relocations and Focal Mechanisms of the 2010 Mw7.0 Haiti and Mw8.8 Chile Earthquakes

WALDHAUSER, F., Lamont-Doherty Earth Observatory, Palisades, NY, USA, felixw@ldeo.columbia.edu; DIEHL, T, Lamont-Doherty Earth Observatory, Palisades, NY, USA, tdiehl@ldeo.columbia.edu; SEEBER, N, Lamont-Doherty Earth Observatory, Palisades, NY, USA, nano@ldeo.columbia.edu; HJORLEIFSDOTTIR, V, Lamont-Doherty Earth Observatory, Palisades, NY, USA, vala@ldeo.columbia.edu; NETTLES, M, Lamont-Doherty Earth Observatory, Palisades, NY, USA, nettles@ldeo.columbia.edu

We relocated 55 aftershocks (Mw 4.0-5.9) that occurred within 6 weeks of the January 2010 M7.0 Haiti earthquake by applying a teleseismic double-difference (DD) algorithm to P- and S- first and later arriving phase arrival-times routinely reported by the NEIC. The residual RMS was reduced from ~1s before to 0.57 s after relocation. Bootstrap error ellipses at the 90% confidence level have, on average, major horizontal axis of 1.9 km, minor axis of 1.2 km, and vertical axis of 1.3 km. Differences between NEIC and DD epicenters are 5 km on average (max=16 km). Depths are typically not resolved by routine location procedures at the NEIC. The majority of the aftershocks, including the three largest ones, cluster about 20 km west of the mainshock epicenter, near the inferred western termination of the left-lateral, steeply north-dipping, main rupture along the Enriquillo-Plantain Garden Fault (EPGF). This cluster has remarkably consistent moment tensor solutions and the 3D distribution of these hypocenters, particularly the three largest ones (Mw 5.8-5.9), is consistent with the common nodal plane dipping SSW at

intermediate angle. We conclude, therefore, that the aftershocks originated from the thrust fault represented by the nodal plane. Smaller aftershocks may originate from imbricate secondary faults at the intersection between the EPGF and the thrust fault, as indicated by both distributed locations and small variations in CMT solutions for these events. Approximate rupture areas calculated for the largest aftershocks show that most of the seismogenic thrust fault failed and that this short fault segment is now mostly de-stressed.

We also present and discuss results from teleseismic DD relocation of the Mw8.8 Maule earthquake of February 2010 and its aftershocks, using NEIC bulletin picks, complemented by automatic P-wave picks and cross-correlation differential times.

Preliminary Source Model of the 2010 Mw 8.9 Maule Chile Earthquake Constrained by Teleseismic Data

SHAO, G., University of California, Santa, Santa Barbara,CA, shao@umail.ucsb.edu; LIU, Q., University of California, Santa, Santa Barbara,CA, qliu@umail.ucsb.edu; LI, X., University of California, Santa, Santa Barbara,CA, xiangyuli@umail.ucsb.edu; ZHAO, X., China Earthquake Networks Center, Beijing, China, zhaox@seis.ac.cn; YANO, T., University of California, Santa, Santa Barbara,CA, tomoyano@gmail.com; JI., C., University of California, Santa, Santa Barbara,CA, ji@geol.ucsb.edu; ARCHULETA, R.J., University of California, Santa, Santa Barbara,CA, ralph@crustal.ucsb.edu

Recent Feb 27, 2010 Mw 8.9 Maule, Chile earthquake was studied using both teleseismic body and surface waves. Thirty-five body waves and 35 long period surfaces were selected for good azimuth coverage. Our preliminary model adopts a fault plane striking N18° E and dipping 17.5° E, inferred from the Global CMT. The complex rupture process was first modeled as multiple point sources. A simulated annealing algorithm is applied to invert for the strike, dip, rake, moment, centroid time, half-duration, and centroid location of each point source by matching the long period surface waves. We have gradually increased the number of point sources until no significant improvement in term of the waveform fits. Our result reveals that this earthquake included two major asperities, separated by about 220 km. The first asperity located at the south of the epicenter with a deeper centroid depth of 30 km. It ruptured earlier with a centroid time of 48 s. The second asperity located at the north of the epicenter with a shallower centroid depth of 16 km. It ruptured later with a centroid time of 84 s. The total seismic moment of entire rupture was $2.1x10^{22}$Nm. The fault plane was then divided into 30 km by 17 km subfaults. The slip, rake, rupture initiation time, and rise time of every subfault are then inverted simultaneously using both teleseismic body and surface waves. The jointed model has slightly larger seismic moment $2.6x10^{22}$ Nm. The inverted rupture first propagated southwestward during first 60 s in an average speed of 2 km/s, and then propagated to the north of hypocenter. The south and north high slip regions remarkably well matched the estimated slip areas of the historic earthquakes in 1835 and 1928 respectively.

Global Long-Period Seismic Wavefield of the February 27, 2010 Chile Earthquake

ASTER, R.C., New Mexico Tech, Socorro NM, USA, aster@ees.nmt.edu

The February 28, 2010 Chile Earthquake generated a seismic wavefield with peak-to-peak vertical surface wave displacements of approximately 1 cm or larger everywhere on Earth. Integrated long-period (LH) data from the Global Seismographic Network and other stations present a remarkable realization of global seismic wave propagation that valuably demonstrates the global reach of great earthquakes and fundamentals of global seismic wave propagation. Rayleigh wave amplitudes from the Chile earthquake were approximately 50% the size of those from the 2004 Sumatra-Andaman Islands earthquake, as expected from approximate long-period band moment scaling (*e.g.*, 2 x 10^22 versus 4 x 10^22 N-m) for these two megathrust events.

The Accellerogram Recorded in Buenos Aires, Argentina, During the Mw=8.8 February 27, 2010 Great Chilean Seismic Event

SABBIONE, N.C., Department of Seismology, Universidad Nacional de La Plata, 1900 La Plata, Argentina, nora@fcaglp.unlp.edu.ar; CARMONA, J.S., Universidad Nacional de San Juan,, 5400 San Juan, Argentina, jcarmona@unsj.edu.ar

The ground motion acceleration due to the Mw=8.8 February 27, 2010 great Chilean seismic event has been recorded in one broadband seismograph installed at the Seismological Station of Universidad Nacional de La Plata, at an epicentral distance of 1300 km. The maximum value in the N-S component is 2.0 gal. It is nearly 3 times higher than the maximum value of 0.75 gal, which was recorded by the same instrument during the Mw = 7.1 October 15, 1997 Chilean seismic event at the same epicentral distance.

The instrument has been in operation since 1996 in La Plata city, 50 km away from Buenos Aires. It is installed on the same type of subsoil than that of Buenos Aires city, consisting of quaternary loess with a thickness of approximately 500 m. Both 2010 and 1997 horizontal acceleration records show outstanding waves with periods around 1.2 and 2.9 sec. Moreover, the measured fundamental horizontal period values of the buildings with more than 20 floors in Buenos Aires city are larger than 1 sec. This period reaches about 3 sec in the tallest one, which is 170 m high. The distant and large magnitude seismic events, like that of February 27, 2010, have been well perceived - at times with alarm - on the uppermost floors of those tall buildings, without any structural damage.

The Very Large Central Chile Earthquake of 27 February 2010 and the Predictability

PURCARU, G., Univ. of Frankfurt, Inst. of Geosciences, Frankfurt/Main, Germany, Purcaru@geophysik.uni-frankfurt.de

A fundamental problem of earthquake ocurrences is the predictability of space, magniude and time. Present predictability science is a very hard problem, although the place is to some extent possible to be predicted. Large and very large earthquakes, such as 2010 Central Chile, Mw8.8, have complicate difficulties in finding the future rupture zone and size. These are fundamentally necessary for seismic cyles of the above size classes. Purcaru (1982, 1985) introduced a model of seismic cicyles with connections, separating the magnitude classes, thus is different from the Fedotov model (1965). Later we advanced (2001) the first model including critical failures of asperities of "sub-earthquakes" of very large earthquakes. This is case of the 2010 earthquake (aftershocks area 700km x 150-200km) which covers three past large earthquakes. We found that the size of the 2010 Chile confirms well our model with variable stress-drops and near levels of the failure stresses. This is useful in the finding of the cycles of the repeat of such very large earthquakes, and it provides an important necessary condition for the predictability of earthquakes.

W-Phase: Lessons from the February 27, 2010 Chilean Earthquake

DUPUTEL, Z., Institut de Physique du Globe de Strasbourg (CNRS, UdS/EOST), Strasbourg France, zacharie.duputel@unistra.fr; RIVERA, L., Institut de Physique du Globe de Strasbourg (CNRS, UdS/EOST), Strasbourg France, luis.rivera@unistra.fr; KANAMORI, H., Seismological Laboratory, Caltech, Pasadena, CA USA, hiroo@gps.caltech.edu

A source inversion algorithm using the W-phase was developed in 2008 (Kanamori and Rivera, 2008) and has been tested since in different operational environments (NEIC-USGS, PTWC, Taiwan, etc.). Although potentially useful down to M_w 6-7, this method targets more specifically very large earthquakes like the 1960 Chilean (M_w 9.5) or the 2004 Sumatra (M_w 9.3) events. Fast and robust methods for estimation of magnitude and focal mechanism for such large events were not available. The recent Chilean event (M_w 8.8), being the largest since the algorithm was put in operation, is of particular interest for evaluating the performance of the method. Although our preliminary analysis indicates a very successful operation, we address here the question in a more formal way by performing an a-posteriori confidence estimation through sensitivity and bootstrap analyses. We are particularly interested in the reliability of the fault dip and the seismic moment as a function of the preliminary parameters of the event (latitude, longitude, depth, initial magnitude) and the used dataset (number of phases, used channels, *i.e.* only verticals or three components), etc. It is well known that these two parameters are often unstable for shallow events. Another key question is what will happen if, instead of a clean-cut M_w 8.8 event, we had an event with large foreshocks, like the 1960 great Chilean earthquake for which 5 foreshocks larger than M 6.5 occurred, including an M 7.9 on the day before and an M 7.8, 15 minutes before the main shock. For such an event, the present W-phase algorithm would have been in great trouble mainly due to the saturation of the seismograms caused by the foreshock's surface waves. This is far from being a unrealistic hypothesis and we should explore ideas to cope with such a difficult situation.

The W-Phase and PTWC's Response to the Mw 8.8 Chile Earthquake of February 27, 2010.

DUPUTEL, Z., Université de Strasbourg, Strasbourg/France, zacharie.duputel@eost.u-strasbg.fr; RIVERA, L., Université de Strasbourg, Strasbourg/France, luis.rivera@eost.u-strasbg.fr; KANAMORI, H., Caltech, Pasadena/California/USA, ; WEINSTEIN, S., NOAA NWS Pacific Tsunami Warning, Ewa Beach/HI/USA, Stuart.Weinstein@noaa.gov; HIRSHORN, B., NOAA NWS Pacific Tsunami Warning, Ewa Beach/HI/USA, hirshorn@ptwc.noaa.gov; HSU, V., NOAA NWS Pacific Tsunami Warning, Ewa Beach/HI/USA, Vindell.Hsu@noaa.gov

We have been testing the W-phase source inversion (Kanamori and Rivera, 2008) algorithm since early January, 2010 at the the Pacific Tsunami Warning Center (PTWC). Our initial hypocentral location and origin time message automatically

triggers the W-phase software to begin its calculations at 25 minutes after the earthquake origin time. We use only vertical, broadband data streams from the IRIS and USGS global seismic networks for the inversion. For the Mw 8.8 Chile Earthquake of 2/27/2010, this initial message was sent 11 minutes after initiation of rupture at the hypocenter. At To+45 minutes, a complete W-phase solution including centroid location grid search yielded a static Mw value of 8.62 (based on 16 channels of seismic data). An updated solution at To+78 minutes gave an Mw value of 8.66 (based on 52 channels). As the Mw 8.66 value compares well with the final Mw 8.8 value, and because this is the first time in the history of the US Tsunami Warning Program that a reliable CMT was available within 45 minutes of Origin time, this is a good preliminary performance for the W-phase at the PTWC. We used the WCMT solution to drive PTWC's real time model. Although the magnitude 8.66 was lower than then eventual M8.8 and the model solution was not the best that we obtained during the event, the results did indicate early on that this EQ would generate a significant basin- crossing tsunami.Because the current impediment to a faster result is data collection and processing latencies, we will have to modify the algorithm to wait for more data to improve our results. After we are able to collect and process the real time data closer to the origin time, we will then look at decreasing the reporting time for the results down to 30 minutes after earthquake origin time. This incompressible delay is related to the propagation of W-phase to remote stations.

NOAA West Coast/Alaska Tsunami Warning Center Operations During the 2010 Chilean Tsunami

HUANG, P, NOAA, West Coast and Alaska Tsunami Warning Center, Palmer, Alaska, USA, paul.huang@noaa.gov; NYLAND, D, NOAA, West Coast and Alaska Tsunami Warning Center, Palmer, Alaska, USA, david.Nyland@noaa.gov; WHITMORE, P, NOAA, West Coast and Alaska Tsunami Warning Center, Palmer, Alaska, USA, paul.whitmore@noaa.gov

An earthquake with magnitude 8.8 occurred offshore of Maule, Chile at 0643 UTC on February 27, 2010. The NOAA West Coast and Alaska Tsunami Warning Center (WCATWC) responded to the alarm in less than 3 minutes from the earthquake origin time (o-time), and determined a stable initial magnitude and well constrained location 5 minutes after o-time. The WCATWC issued an observatory message to alert seismic monitoring agencies 7 minutes after the o-time. This earthquake is one of the largest recorded, and spawned a trans-oceanic tsunami.

WCATWC initially issued tsunami information statements that subsequently were upgraded to an advisory for California as well as areas of Alaska from Kodiak to Attu based on initial forecast amplitudes 4.5 hours after the origin. The Advisory was expanded to the entire west coast from the California-Mexico border to Attu, Alaska 7.5 hours after the origin based on updated forecasts.

The Center conducted a series of teleconferences with NWS Weather Forecast Offices and state warning points along the West Coast and Alaska throughout the event. The teleconferences allowed WCATWC to provide amplifying information to primary customers not in the official bulletins.

The tsunami impacted coastal areas under advisory, with a maximum recorded rise above normal sea level of 91cm measured at Santa Barbara, California. No inundation was observed, though damage was reported at several locations in southern California.

In order to illustrate the WCATWC's real time operation environment, we will provide timelines of tsunami warning operations during the Chile earthquake and tsunami. The timeline highlights the key parameters and observations that guide tsunami warning operations. The timeline chronicles the sequence of events from initial alarm to earthquake analysis, to initial messages, to sea level observation and tsunami forecasting, and then to supplemental messages. An evaluation of forecast model accuracy will also be provided.

Dispersion of the Feb 27, 2010 Tsunami or Why the Tsunami Was Smaller Than Predicted

SALZBERG, D., SAIC, Arlington, VA, USA, david.h.salzberg@saic.com; FRYER, G., PTWC, Ewa Beach, Hi, USA, Gerard.Fryer@noaa.gov

The February 27, 2010 Mw 8.8 Chile Earthquake resulted in an evacuation of coastal Hawaii for a non-damaging tsunami. The evacuation was ordered after the SIFT model, adjusted to match deep-ocean measurements, predicted runup significantly over the one meter danger threshold. Dispersion, which is not included in the model, may explains the over prediction. Preliminary analysis of the Hilo tide gauge record shows dispersion at all observable periods, enough to reduce peak amplitude there by 30%-the difference between evacuation and no evacuation. Hawaii was put into a warning (along with the rest of the Pacific) when DART 32412, southwest of Peru, recorded a 24 cm tsunami. When source components and slip were adjusted by the SIFT algorithm to match the DART record, the code predicted runups between 0.5 to 3 m in Hawaii. More DART data (from 32411 off Panama and 51406 near the Marquesas) were later incorporated into the model, reducing predicted runup to 1.3m, but that was still too large to allow cancellation of the warning. When the tsunami did arrive, the maximum runup in Hawaii was 0.98m. Since the source is empirically adjusted to satisfy the DART records, it must be reasonably accurate (provided that the source assumption are approximately satisfied). If the source is reasonably good, then mismatch with observation implies that some aspect of the propagation is missing from the model. One factor missing is dispersion. While the SIFT model assumes long-wave phase velocities, actual phase velocities near the observed 20-minute period are 1-2% less. Phase velocity variation near this period is low, but on a body the size of the Earth it can reduce peak amplitude by up to 50%, and significantly lengthen the wave train. The overestimates of wave height made by SIFT and other models of the Chile tsunami are consistent with dispersion. It seems likely that the non-modeled dispersion caused the over-prediction of the tsunami and led to the unnecessary evacuation.

Seismic Recordings of the Maule, Chile Tsunami of 27 Feb 2010

OKAL, E.A., Northwestern University, Evanston, IL USA, emile@earth.northwestern.edu

As discovered by Yuan *et al.* [2005] following the 2004 Sumatra event, tsunamis can be recorded by horizontal coastal seismometers deployed on land. The great Maule earthquake of 27 February 2010 was similarly recorded at a number of stations in the Pacific basin, with most remarkable records visible on raw seismograms notably at Pitcairn and Raoul Islands. We will present a quantification of these records, using the formalism developed in Okal [2007].

Plate Boundary Observatory Strain Recordings of the February 27, 2010, M8.8 Chile Tsunami

HODGKINSON, K., UNAVCO, Socorro, NM, USA, hodgkinson@unavco.org; MENCIN, D., UNAVCO, Boulder, CO, USA, mencin@unavco.org; BORSA, A., UNAVCO, Boulder, CO, USA, borsa@unavco.org; JACKSON, M., UNAVCO, Boulder, CO, USA, Jackson@unavco.org

In the 24 hours that followed the February 27, 06:34:14 UTC, 2010, M8.8 Chile earthquake a tsunami swept across the Pacific Ocean causing warnings to be issued from Antarctica to Alaska. Three PBO strainmeters, Ucluelet, Bamfield and Port Alberni, on Vancouver Island, recorded the arrival of the tsunami on the British Columbia coast as it propagated northwards along the Pacific coastline. The Ucluelet and Bamfield strainmeters, on the west coast of Vancouver Island, recorded the first arriving waves at ~23:00UTC which is consistent with tide gauge measurements at Tofino, 30 km north of Ucluelet. Maximum areal strain amplitudes of 15 and 19 nanostrain were observed about 8 hours after the initial waves at these sites. The Port Alberni strainmeter, on the northeast end of Alberni Inlet, a 1-2 km wide and 40 km long fjord, recorded areal strains of up to 4 nanostrain, the largest strains being measured 55 minutes after the largest strains at Ucluelet. While a maximum amplitude of 19 nanostrain at Ucluelet is similar to that observed for the 2009 M8.1 Samoa tsunami, the strains at Port Alberni were four times larger. In this presentation we document the arrival times, nature and frequency content of the tsunami as recorded by PBO strainmeters and compare these strain measurements with the crustal loading signature predicted by water height changes at nearby tide gauges. The ability of the strainmeters to record the tsunami signals both for the 2010 M8.8 Chile and 2009 M8.1 Samoa event suggest they could be used as a land-based instrument to record tsunami arrival times and estimates of wave heights.

Field Survey and Preliminary Simulation of the 2010 Maule, Chile Tsunami in French Polynesia

REYMOND, D., Laboratoire de Geophysique, CEA, Papeete, Tahiti, French Polynesia, reymond.d@labogeo.pf; HYVERNAUD, O., Laboratoire de Geophysique, CEA, Papeete, Tahiti, French Polynesia, hyvernaud@labogeo.pf; HEBERT, H., DASE, Commiss. Energie Atom., Bruyeres-le-Chatel, Essonne, France, helene.hebert@cea.fr; OKAL, E.A., Northwestern University, Evanston, IL, USA, emile@earth.northwestern.edu; JAMELOT, A., DASE, Commiss. Energie Atom., Bruyeres-le-Chatel, Essonne, France, anthony.jamelot@cea.fr; ALLGEYER, S., DASE, Commiss. Energie Atom., Bruyeres-le-Chatel, Essonne, France, sebastien.allgeyer@cea.fr

The 2010 Chilean tsunami impacted Polynesia with amplitudes unparalleled since the great 1960 event. Preliminary reports indicate run-up of up to 4 m on Nuku Hiva, Marquesas. All coastal areas in Polynesia were evacuated starting 03:00 Tahiti time (GMT-10), three to five hours ahead of the arrival of the first waves, thus preventing any casualties. We will present the results of field surveys scheduled for the second week in March, as well as preliminary simulations of the inundation at selected locations on Polynesian islands.

The 2010 Chilean Tsunami on the California Coastline

WILSON, R.I., California Geological Survey, Sacramento, CA USA, rick.wilson@conservation.ca.gov; DENGLER, L.A., Humboldt State University, Arcata, CA

USA, Lori.Dengler@humboldt.edu; LEGG, M.R., Legg Geophysical, Huntington Beach, CA USA, mrlegg@verizon.net; LONG, K., California Emergency Management Agency, Pasadena, CA USA, Kate.Long@calema.ca.gov; MILLER, K.M., California Emergency Management Agency, Oakland, CA USA, Kevin.Miller@calema.ca.gov

The California coast was placed in a Tsunami Advisory by the West Coast Alaska Tsunami Warning Center at 2:55 AM PST, a little over 4 hours after the earthquake origin time. The advisory forecast tsunami amplitudes ranging from approximately 0.3 to 1.4 meters and strong currents in bays and harbors. Hourly conference calls were held with the county operational areas and most counties cleared beaches and limited access to harbor areas. The highest amplitudes were predicted for San Luis Obispo County and areas south. The tsunami initially struck San Diego at 12:02pm on February 27, and moved progressively up the coast over the next hour and a half. Peak amplitudes at tide gauge locations in the state ranges from 0.12 meters to a high of 0.91 meters at Santa Barbara. At most locations, the strongest surges were recorded within the first two hours but Crescent City near the Oregon border, the largest surge occurred 6 hours after the initial onset. At many locations, the tsunami activity lasted for more than a day, and in some areas exacerbated ambient flooding from severe storm activity. Harbors in southern and central California were impacted the most by estimated tsunami currents ranging from five to 15 knots, with minor to moderate damage occurring in several areas. Damage estimates for the state could climb to over several million dollars. Estimated (from videos, eyewitness accounts) and recorded (instrumented) tsunami current velocities could provide an important validation and/or calibration tool for numerical tsunami modeling methods and databases of existing model runs.

Index of Authors